Lecture Notes
in Geoinformation and Cartography

LNG&C

Igor Ivan
Jiří Horák
Tomáš Inspektor *Editors*

Dynamics in GIscience

Springer

Lecture Notes in Geoinformation and Cartography

The Lecture Notes in Geoinformation and Cartography series provides a contemporary view of current research and development in Geoinformation and Cartography, including GIS and Geographic Information Science. Publications with associated electronic media examine areas of development and current technology. Editors from multiple continents, in association with national and international organizations and societies bring together the most comprehensive forum for Geoinformation and Cartography.

The scope of Lecture Notes in Geoinformation and Cartography spans the range of interdisciplinary topics in a variety of research and application fields. The type of material published traditionally includes:

- proceedings that are peer-reviewed and published in association with a conference;
- post-proceedings consisting of thoroughly revised final papers; and
- research monographs that may be based on individual research projects.

The Lecture Notes in Geoinformation and Cartography series also includes various other publications, including:

- tutorials or collections of lectures for advanced courses;
- contemporary surveys that offer an objective summary of a current topic of interest; and
- emerging areas of research directed at a broad community of practitioners.

More information about this series at http://www.springer.com/series/7418

Igor Ivan · Jiří Horák · Tomáš Inspektor
Editors

Dynamics in GIscience

Springer

Editors
Igor Ivan
Institute of Geoinformatics
VŠB - Technical University of Ostrava
Ostrava - Poruba
Czech Republic

Tomáš Inspektor
Institute of Geoinformatics
VŠB - Technical University of Ostrava
Ostrava - Poruba
Czech Republic

Jiří Horák
Institute of Geoinformatics
VŠB - Technical University of Ostrava
Ostrava - Poruba
Czech Republic

ISSN 1863-2246 ISSN 1863-2351 (electronic)
Lecture Notes in Geoinformation and Cartography
ISBN 978-3-319-61296-6 ISBN 978-3-319-61297-3 (eBook)
DOI 10.1007/978-3-319-61297-3

Library of Congress Control Number: 2017946055

Printed on acid-free paper

This Springer imprint is published by Springer Nature
The registered company is Springer International Publishing AG
The registered company address is: Gewerbestrasse 11, 6330 Cham, Switzerland

Preface

Still, a majority of GI systems persist to be static. We are focused on a precise and accurate description of 2D or 3D reality, but many applications disregard temporal development and continuous changes in system, data, models, and relationships. Even for capturing reality in time series, inefficient forms of storage, retrieval, processing, analysing, modelling, and visualisation are still frequently applied.

Time is the key element of contemporary GIS. Mobile and wearable electronics, sensor networks, UAVs and other mobile snoopers, IoT, and many other resources produce a massive amount of data every minute, which is naturally located in space as well as in time. While we are observers of usually mild improvement of spatial resolution of our data, we face substantial improvement of its temporal resolution. More frequent remotely sensed imagery, statistical data, or environmental measurements change our view of the world. Data time series are transformed into almost (from the human perspective) continuous data streams, which require changing of the concept of spatial data recording, storage, and manipulation.

However, dynamics is not bound only by sometimes elusive human mobility data. The long tradition of environmental monitoring, statistical surveys, or business records has produced series of scenes, each valid only for some shorter or longer time interval. The analysis and modelling of the dynamics have to overcome a stepwise approach. The temporal dimension is required to become an integral part of the system; otherwise, it is unable to fully understand the dynamics of human–environment interactions, to generate sophisticated predictions and to take appropriate measures.

Although time geography was established 50 years ago, the transformation from visual language into a full spatio-temporal information system is still limited. Dynamic spatial systems require solutions to many issues, such as efficient dealing with repeated spatial data; the archiving of historical data sets and retrieving data from archives; matching various spatial data snapshots to create a time-consistent model; quality conceptualisation and reproduction of spatio-temporal processes; detection of spatio-temporal patterns and spatio-temporal hot spots with appropriate inclusion of mutual interaction of space and time; analysis of individual group dynamics; distinguishing global and local changes; detection of changes in spatial

patterns over time; measurement of interactions between moving objects; visual exploration of large spatio-temporal datasets; and/or predictions of data movement.

Issues of dynamics do not stand alone. Extension of spatio-temporal systems and applications is accompanied by acquisition of usually heterogeneous and inconsistent resources, sometimes also influenced (highly determined) by social characteristics of the local context. The fundamental question is how to protect the privacy of sensitive spatio-temporal data from human monitoring. The large societal impact may be made through the release of Open Spatio-Temporal Data to support wide-scale research and public participation.

Ostrava, Czech Republic

Igor Ivan
Jiří Horák

Acknowledgements

The editors of this book would like to thank all the people who have been directly or indirectly involved in the development of this proceedings. First of all, we would like to thank all the authors who submitted papers. Special thanks go to all the authors whose work was finally included in this book. Next, we would like to thank the scientific committee members and all the reviewers who worked hard to read all the submitted papers, provided suggestions, and helped with the selection process. Each chapter was reviewed by at least two scientific committee members or other reviewers.

As a final note, we would like to thank European Spatial Data Research Organisation (EuroSDR), International Society for Photogrammetry and Remote Sensing (ISPRS), European Association of Geographers (EUROGEO), Czech Association for Geoinformation (CAGI), Slovak Association for Geoinformatics (SAGI), Ivo Vondrák the President of the Moravian-Silesian Region, and Tomáš Macura the Mayor of the City of Ostrava for their support.

Igor Ivan
Jiří Horák
Tomáš Inspektor

Programme Committee

Igor Ivan, VŠB-Technical University of Ostrava, CZE—chair
Tao Cheng, University College London, GB
Urska Demsar, University of St Andrews, GB
Hrvoje Gold, University of Zagreb, HR
Marcin Stępniak, Polish Academy of Sciences, PL
Martin Raubal, ETH Zurich, CHE
Gennady Andrienko, Fraunhofer Institute for Intelligent Analysis and Information Systems, GE
Natalia Andrienko, Fraunhofer Institute for Intelligent Analysis and Information Systems, GE
Bin Jiang, University of Gävle, SWE
Jiří Horák, VŠB-Technical University of Ostrava, CZE
Hassan Karimi, University of Pittsburgh, USA
David W. Wong, George Mason University, USA
Ákos Jakobi, Eötvös Loránd University, Budapest, HUN
Juan Carlos García Palomares, Universidad Complutense de Madrid, ESP
Vít Voženílek, Palacký University, CZE
Harry J.P. Timmermans, Eindhoven University of Technology, NLD
Mei-Po Kwan, University of Illinois, USA
Juha Oksanen, Finnish Geospatial Research Institute, FI
Jaroslav Hofierka, Pavol Jozef Safarik University in Kosice, SVK
Soora Rasouli, Eindhoven University of Technology, NLD
Alex Singleton, Liverpool University, GBR
Katarzyna Sila-Nowicka, University of Glasgow, GB
Simon Scheider, Utrecht University, NLD
Jed A. Long, University of St Andrews, GB
Elena Moltchanova, University of Canterbury, NZL
Daniel Arribas-Bel, University of Liverpool, GBR
Lex Comber, University of Leicester, GBR
Maorong Ge, GFZ Potsdam, GE
Joep Crompvoets, University of Leuven, BE

James Haworth, University College London, GBR
David O'Sullivan, Berkeley, University of California, USA
Maria Salonen, University of Helsinki, FI
Dominik Ziemke, Technische Universität Berlin, GE
Petr Lukeš, Czechgloge, CZ

Contents

Comparison with the Reference Value on the Example of GIS-Based Applications

Dalibor Bartoněk, Stanislava Dermeková and Ján Škurla

Abstract The article gives a new approach to the assessment of objects in terms of various criteria which by its nature belong to the issue of multi-criteria decision making and analysis. The proposed variant of multi-criteria decision-making is based on a comparison of the real considered object model that is created according to user's requirements with the reference value. The geographic object means a real object in this case the object is stored in digital geo-database in the geographic information system (GIS). The reference value represents optimal geographic object which is the most suitable for user's purposes. The comparison of the values of individual criteria is based on the theory of tolerance and metric spaces. Supplementary GIS-based application to calculate the weights of the criteria, which have served to comparison was used. The proposed procedure for the evaluation of various criteria has been validated on a pilot project "SMART Regions" in the city Brno district of Nový Lískovec neighbourhood in the Czech Republic. Around the city district known by its typical of prefabricated blocks of flats it is necessary to compare the different options for renewal urban housing development. Urbanization city prefabricated housing estates using GIS opportunities will be ready to quick respond to the call of various changes in the field of energy sustainability. Therefore, it is important to utilize the available environmental resources for energy sustainability.

D. Bartoněk (✉)
Faculty of Civil Engineering, Institute of Geodesy, Brno University of Technology, Veveří 330/95, 602 00 Brno, Czech Republic
e-mail: bartonek.d@fce.vutbr.cz

D. Bartoněk
European Polytechnic Institute, Osvobození 899, 686 04 Kunovice, Czech Republic

S. Dermeková · J. Škurla
Faculty of Civil Engineering, AdMaS Center, Brno University of Technology, Purkyňova 139, 602 00 Brno, Czech Republic
e-mail: dermekova.s@fce.vutbr.cz

J. Škurla
e-mail: skurla.j@fce.vutbr.cz

I. Ivan et al. (eds.), *Dynamics in GIscience*, Lecture Notes in Geoinformation and Cartography, DOI 10.1007/978-3-319-61297-3_1

Keywords Multi criteria analysis · GIS-based application · SMART regions

Introduction

Methods using multi-criteria analysis are applied in various areas of the real world that are valuated in terms of various criteria. These methods are widely-used in regional economics and economic geography, and could lead to different predictions that help to determine the spatial component of economic activity. The article will focus on the use of GIS-based applications for spatial analyses of SMART Regions.

The concept of SMART Regions is now primarily associated with the Europe 2020 strategy and the objectives that are set out by 2020 in the European Union. This means in particular a reduction in energy consumption and CO_2 emissions. The result would be a better living environment and support for innovation related to it. SMART Regions make the same assumptions as SMART Cities, with the only difference being that the focus is on the broader context and takes more account of the environment of cities and their complexes in order to find the maximum amount of synergies usable for the stated goals (European Innovation Partnership on Smart Cities and Communities. Strategic Implementation Plan 2013).

SMART Regions solve the problem of deployment and the use of intelligent technology. This issue contains a huge potential for increase of the efficiency of the strategic development of cities, their functionality and interconnection in all areas of sustainable development (the development of transport infrastructure, alternative energy, public transport, energy efficiency in buildings and residential areas, increasing the share of renewable energy, waste management, achieved savings, improved service quality and operation of cities and regions) (Wawerka et al. 2015). Therefore it needs using multi-criteria method for this multidisciplinary method of decision for the SMART regions. The diversity of individual areas of interest require this approach. This paper aims to use a multi-criteria methods for the purposes of issue of SMART regions. SMART Regions idea implementation in the Czech Republic would address the issue of housing estates that are perceptible threat in connection with the huge consumption of energy in these prefab housing estates. Intelligent technologies incorporate greater transparency and accountability, efficient management of resources (energy consumption, production and waste disposal, reducing the consumption of various resources and the related costs).

The use of available environmental resources become less costly. This prevents degradation of the environment. Decision-making processes are important for understanding the environmental impacts associated with energy production from renewable sources such as wind, solar, geothermal, biomass or hydropower. Due to implementation of the decision-making processes in GIS it will be possible to measure and compare different scenarios planning stakeholders (urbanists, city leaders, citizens, etc.) according to defined indicators for the use of environment, transport, natural resources, employment, etc.

Until now, many methods have been developed to merge diverse parameters criteria into common categories and the results then assign the appropriate value. Overview of currently used methods is given in the publication (Wang et al. 2009). This article describes an alternative approach to multi-criteria analysis based on the comparison of the real considered object with an idealized model—called the reference value. The reference value is determined by the price the Bulletin valid according to the current Valuation Decree under which the property appreciate. The decree sets the prices, coefficients, price increases and reductions of prices and procedures for the application of principles of valuation assets, rights and other assets. It is an attempt for a new approach at the multi-criteria analysis, where the user pre-determined values of the criteria according to their intentions concerning the further exploitation of the assessed object. So far used methods of multi-criteria analysis are used in its calculation of the criteria weights (linear relationship). The proposed solution differs from current methods in that instead of the weighting coefficients are used functional relationships that transform diverse criteria to a single comparable platform. The proposed multi-criteria method is derived from the assumptions of AHP (Analytical Hierarchical Process) and OWA (Ordered Weighted Averaging) method. The main idea is a modelling of decision-making strategy for the localization of the smart activities in the space for the different options of renewal urban housing development. The proposed method has been validated on the pilot project SMART Regions in a selected city district Brno Nový Lískovec in the Czech Republic. Applications have been developed for academic and public organizations through GIS-based platform for data integration, system for geospatial analysis and collection models for visualization and decision making. The decision-making process is carried out using spatial analysis in the form of 3D analysis, modelling environment, multidimensional data, urban planning, geo-statistics, etc. This was created with financial support Technology Agency of the Czech Republic Competence Centres No. TE02000077 and under the project No. FAST-S-15-2723.

Related Works

Multi-criteria analysis is the topic of many research projects and scientific papers. They are given only the most important studies that are closely related to our article from an extensive list of publications. They can be divided into these groups in terms of application methods:

- The optimization methods in computer technology (Thiele et al. 2009; Popov 1999). These methods using multi-objective optimization problem for improving the response time in data warehouse or updates data quality. The article (Oliviera et al. 2013) is devoted issue which describes analysis of three versions of an evolutionary algorithm for determining preference using ELECTRE TRI method. Another article deals with the implementation decision analysis with

visual basic to check the validity and reliability flood-affected areas (Oztuk and Batuk 2011).

- Pre-processing of data in GIS projects which leads to the optimization of spatial analysis (Tirelli and Pessani 2011; Sureg and Vasselman 2004; Nath et al. 2000; Lee 2004; Vahidnia et al. 2009). The method of pre-processing contributes to evaluation of effectiveness for inducing artificial neural networks and decision trees (Tirelli and Pessani 2011).
- Multi-criteria analysis as a supporting tool for the solution of general optimization problems such as knapsack problem. The DSS is aimed on supporting decision-making concerning bi-criteria location models which deal with current questions of environmental impacts (Mikhalevich et al. 1993).
- The use of multi-criteria analysis in the control and management level (Mikhalevich et al. 1993; Bryzgalin et al. 1983; Rabinabitch 1994; Avdagie and Karabegovic 2008). These studies develop information system for LandScape using different ways of managing urban landscape information and solution related to visual impacts of proposed development projects (Oh 2001). Another way is the possibility to identify and quantify alternatives at the level of managerial decision making, provide information to decision making of stakeholders (Avdagie and Karabegovic 2008). The article deals with the issue of decision making for areas in the watershed for rehabilitation and enhancement projects (Malchewski et al. 2003). Support Systems for environmental management (Massei et al. 2014). The paper describes methodology to evaluate the urban built space under different perspectives. It integrates a data base management module which consider heterogeneous criteria with the influence of various factors (Natividade et al. 2007).
- Special applications such as the use in computer support in the archaeology (Bartoněk and Bureš 2012), in the construction industry (Bureš and Bartoněk 2012) or in the CAD systems (Bartoněk and Opatřilová 2014), FuzzyCell system (Yanar and Akyurek 2006), criteria evaluation for land slide susceptibility mapping (Feizizadeh et al. 2014a), spatially-explicit sensitivity and uncertainty analysis (Feizizadeh et al. 2014b), multi-criteria spatial decision support system for planning urban infrastructures, land-use suitability assessment (Dermeková 2013; Joerin et al. 2001), analysis for the identification of spatial land-use conflicts (Ioja et al. 2014), integration of multi-criteria decision analysis in GIS to develop land suitability for agriculture (Mendas and Delali 2012). The purpose of this article is to improve uncertainty cases occurring in the decision-making process for a better interpretation of alternatives (Meng et al. 2011).
- The proposed method has the closest relationship to the methods of TOPSIS (Technique for Order Preference by Similarity to Ideal Solution), OWA and ELECTRE (ELimination and Choice Expressing Reality) (Wang et al. 2009). The authors were inspired mainly of publication (Peters and Wasilewski 2012) where metric spaces and the theory of tolerance have been discussed. On this theoretical core is based the method for comparison of the criteria between geographic objects and optimally generated model.

Theoretical Foundations

The implementation itself preceded by determination of the mathematical model and determining the input parameters for the development and programming of the particular application.

Let the non-empty set $U \neq \varnothing$ be the universe of discourse and $A \subseteq U$. In our case represents the set U of the modelled area and the subset A is a geographic object (GO). GO can be structure, land, allotment and other object of our interest. It is defined the relation of tolerance $\tau \subseteq (A \times A)$ on the set A. This tolerance is a reflexive and symmetric relation. Then $\langle A, \tau \rangle$ is the space of tolerance. Let B denote set of relevant parameters of geographical objects and let $\varphi: B \rightarrow \mathfrak{R}$. For $x \in B$, $\varphi(x)$ is evaluation of given GO according to some multi-criterial method.

Consider the tolerance space $(B, \cong_{\phi,\varepsilon})$ with the relation $(\cong_{\varphi,\varepsilon})$:

$$\cong_{\varphi,\varepsilon} = \{(x, y) \in B \times B || \varphi(x) - \varphi(y)| \leq \varepsilon\} \tag{1}$$

In our case $y \in B$, $\varphi(y)$ is the reference value that means evaluation of optimal GO that is most suitable for the user's purposes.

Furthermore is defined a function p at the non-empty set A: $p: A \times A \rightarrow [0, +\infty) \subseteq \mathfrak{R}$ which is called pseudometric (it differs from the metrics by the launch requirement to close to zero distance between two different points) if it satisfies for an arbitrary $x, y, z \in A$ the following conditions:

$$p(x, x) = 0,\ p(x, y) = p(y, x), p(x, y) + p(y, z) \geq p(x, z) \tag{2}$$

Let $\langle p, A \rangle$ be a pseudometric space and $\varepsilon \in (0, +\infty)$. There is defined the relation of tolerance metrics $\tau_{p,\varepsilon}$ by relationship:

$$(x, y) \in \tau_{\rho,\varepsilon} \Leftrightarrow p(x, y) < \varepsilon \tag{3}$$

Each pseudometric space can actually be seen as a topological space which is a very important in GIS issue and spatial expression of the real object. Relations (1) and (2) are then used to compare of geographic objects (GO) in the area represented by a set A with the reference value.

Let us have a system $\langle B, F \rangle$ where O is the set GO and F is a non-empty set of real functions: $F := \{\varphi | \varphi : B \rightarrow \Re\}$. It is possible assessment GO to represent by the set of parameters from our point of view, $G \subseteq A$. Then for each parameter $g \in G$ is possible to assign function $\varphi(g) - \varphi \in F$, which transforms the given parameter for our needs i.e. to compare with another object (in our case the reference value). Each GO G can be described as a vector of real functions in the space $\mathfrak{R}^n$:

$$\overrightarrow{\varphi}(G) = (\varphi_1(g_1), \varphi_2(g_2), \ldots, \varphi_n(g_n)) \tag{4}$$

If we apply a metric space into two different GO G, M and measurable distance d at the O between them, then you get the relationship:

$$p(G,M) := d(\overrightarrow{\varphi}(G), \overrightarrow{\varphi}(M)) = \sqrt{\sum_{i=1}^{n} (\varphi_i(g_i) - \varphi_i(m_i))^2} \tag{5}$$

for each $g_i \in G$ and $m_i \in M$.

When the Eq. (5) is substituted into Eq. (3) it gets:

$$(G,M) \in \tau_{p,\varepsilon} \Leftrightarrow \sqrt{\sum_{i=1}^{n} (\varphi_i(g_i) - \varphi_i(m_i))^2} \leq \varepsilon \tag{6}$$

This means that the pair GO (*G, M*) (*M* is in our case reference value) belongs to the pseudometric space with a tolerance metrics $\tau_{p,\varepsilon}$ just when it satisfies the condition (5). At this relationship is based comparison of criteria values for real GO with the reference value. Reference ranges are then defined by individual tables valuation decree. Reference ranges are designed for individual criteria arising out of conditions valuation areas.

Materials and Methods

SMART Regions solve the problem of deployment and use of intelligent technology. This issue contains a huge potential for increasing the efficiency of the strategic development of the cities, their functionality and interconnection in all areas of sustainable development (the development of transport infrastructure, alternative energy, public transport, energy efficiency in buildings and residential areas, increasing the share of renewable energy, waste management, and others), achieved savings, improved service quality and operation of cities and regions. Mentioned various areas have a great potential for mutual assessment, diversity requires a multi-criteria approach. For this reason we decided to use multi-criteria decision-making methods. The aim is to assess the various criteria that must be considered against the background with the issue of SMART Regions for housing estate.

The user selects criteria from the database according to the usage purpose of the object and determines the parameters of the model. This defines a model expressing the values belonging to the reference range or close to the reference value. It results in definition of the model (etalon). In case study will consider the criteria that describe the socio-economic determinants influencing the spatial location of areas of smart activities for sustainability and reduce energy consumption. Specifically,

the determinants of social (interaction of man and society, e.g. settlements), economic (e.g. Localization problems of industry, agriculture, services, tourism), communication problems (transport services, infrastructure, etc.), determinants of expressing complex problems studying determination of man's environment and vice versa (e.g. the problems of sustainable development, renewable sources, environmental protection, etc.). Potential GO in the given locality are analysed in GIS. Each GO is analysed and then quantified the relevant criteria according to user requirements. The values of these criteria are compared with the criteria of the etalon in comparative block which works on the basis of Eq. (5). For each criterion it is necessary to determine the appropriate function (Eq. 5), which transforms the criterion on a common platform and represents the user's accent due to this criterion. The result of comparison goes to the output block where it is decided whether a given geographic object meets or does not meet the requirements of users for a particular purpose. If that result does not satisfy the user's ideas then user has the possibility to correct the parameters of the etalon and the whole evaluation process can be repeated. Selection of functions for individual criteria is based on empirical knowledge.

Application "AHP-MCA"

Part of the activities related to the methodology of strategic decision making is a tool for strategic decision making. Implementation of tool is carried out by means add-on applications in an environment of ArcGIS software. The reason for choosing this software is the display of spatial information (both vector and raster data in a GIS environment) for the purpose of SMART region spatial modelling. This application leverages the capabilities of multi-criteria decision-making system. It was determined AHP method (Analytical Method hierarchical process). We can generate criteria matrix using Saaty method calculations where variants "divide" the weight of the relevant criteria. Value weights are called preferential indexes. AHP method is used for determining the size preferences for each pair of criteria. It is a method of criteria quantitative paired comparison.

Weights (preferential indexes) were calculated using add-on applications. It developed a desktop application (the plugin) for MCA (Multi-Criteria Analysis) in GIS—"AHP-MCA". Plugin extends the functionality of ArcMap. It allows to create data in raster format. Plugin has extensions using the Add-In Manager—components without registration Specific applications of various multi-criteria methods for decision in a GIS environment have been developed in Java Desktop SDK ArcObjects. Plugin has been programmed in Java, in development environment Eclipse. The application is shown in Fig. 1. Applications in ArcGIS is able to process only raster data for now. The intention will be for the processing of both raster and vector data within the development of applications in ArcGIS.

Part of the spatial analytical functions was to determine the main factors which can be defined as criteria containing the socioeconomic determinants. It is possible

Fig. 1 Application of multi-criteria analysis—"AHP-MCA"

to determine the main determinants in strategic decision-making areas for the purpose of SMART Region spatial modelling: geographic, environmental, socio-economic and territorial administrative determinants. Determinants based on predetermined coefficients which are contained in the Valuation Decree. These are the values determined from the base price building plot where there are individual coefficients. These are coefficients of the size of the community, economic and administrative importance of the municipality, the municipality location, technical infrastructure in the municipality, transport needs or civic amenities in the municipality. SMART regions can be identified by the following main factors of sustainability: economic, social, environment, governance, services.

Furthermore, it is necessary to consider also the indexes by price comparing, through which it is also possible accurately determine the criteria for multi-criteria decision-making in relation to the areas for SMART management and intelligent planning of cities. Specifically, it represents the index of the real energy sustainability, the index of the renewable sources and the index of position. Another source for determining criteria from the Valuation Decree are qualitative zones (C1–C12) that are listed in the following text as specific criteria decision-making process.

Transport accessibility is one of the key criteria for the SMART region spatial modelling (transport network, such as highway, expressway and first class roads) and its associated transportation system and access to the lot. Within the territorial administrative determinant are crucial the urban and suburban studies, the characteristics of the surrounding objects and the areas typology. The following are important relationships of the locality to the surrounding infrastructure in relation to the availability of utility networks (electricity supply, gas, heating networks, sewerage, water supply and telecommunications).

Individual areas of criteria were determined according to the needs of the target users who were civil servants working in the process of strategic decision making for the regional development (urban development areas for the purposes of competitiveness in the region around the city of Brno. For the purpose of the functional definition of the criteria in locating areas were observed mainly these characteristics of the qualitative zones (environmental, social and economic objectives of cities).

Set intervals of the availability were solved by the method of metric spaces. It is assumed the maximized character of the criteria. Not all of the criteria were maximized therefore it was necessary to convert them to the maximization. It is assumed that higher value of the criterion is desired. All the values are normalized to the interval for easy comparison of specific parameters <0, 1>.

Experimental Results

The proposed procedure for the evaluation of various criteria has been validated on a case study in the municipality of city district Brno—Nový Lískovec in the Czech Republic. Processing was carried out in software ArcGIS 10.2. according to the proposed mathematical methods. The aim was to select a suitable location in the specified area for the establishment of zones for the SMART region energy sustainability spatial modelling. First, was selected the appropriate criteria for analysis. For each criterion was determined reference range values and defined the corresponding function φ (Eq. 4). All criteria values were normalized (standardized) for better comparison, i.e. presented to the interval <0, 1>. Calculation of the selected criteria was carried out according to the Eq. (5).

In the case study were compared the real assessed areas with reference established under the tabulated data of the Valuation Decree. They were assessed different alternative with consideration of all the criteria that influence the decision-making process. They were selected 4 alternatives cooperation with a panel of expert system (civil servant and experts important for strategic decision making in cities).

Individual alternatives incorporate all the values that are listed in the valuation decree. Table values represent different ranges of values that are listed in the tables for built-up areas or specified for buildings. These are mainly land and buildings used primarily for prefabricated housing estates. These areas and buildings are determined by the Classification CZ-CC which includes locally and spatially coherent civil engineering works to such equipment or device so that it can perform the functions for which they are intended (Figs. 2, 3, 4 and 5).

Alternatives were chosen according to the results shown in the Table 1. These signs then belonged qualitative range that voted by solved region. Then they were assigned to the recommended values for these qualitative ranges which represented for our model reference value. According to the reference values 4 different range of values represented alternatives are voted.

Alternatives are reference values—the appropriate allowable values (corresponding to the restriction on the Valuation Decree), which were derived from 4 different levels and were adjusted according to the FAO system. These levels are divided into: highly suitable (A1) relatively suitable (A2), slightly suitable (A3) and unsuitable and (A4).

Criteria values for the various alternatives were compared with a reference tabulated values and have been shown using a spider graph. Differences from the

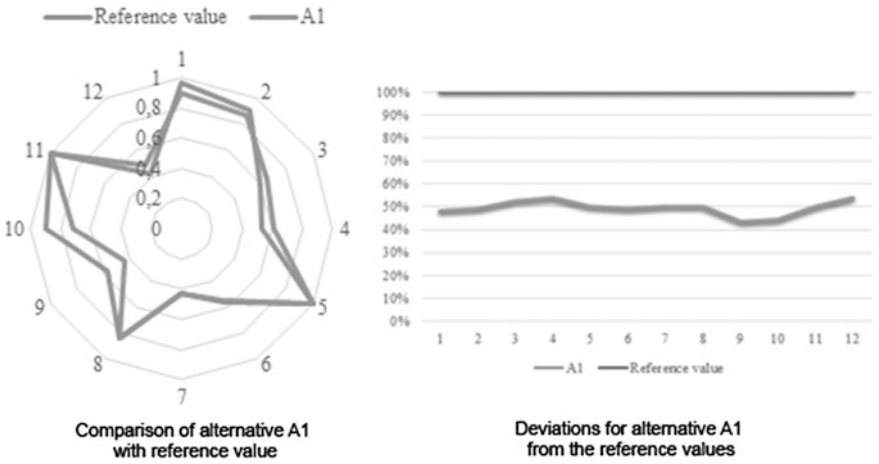

Fig. 2 Alternative A1 (highly suitable)

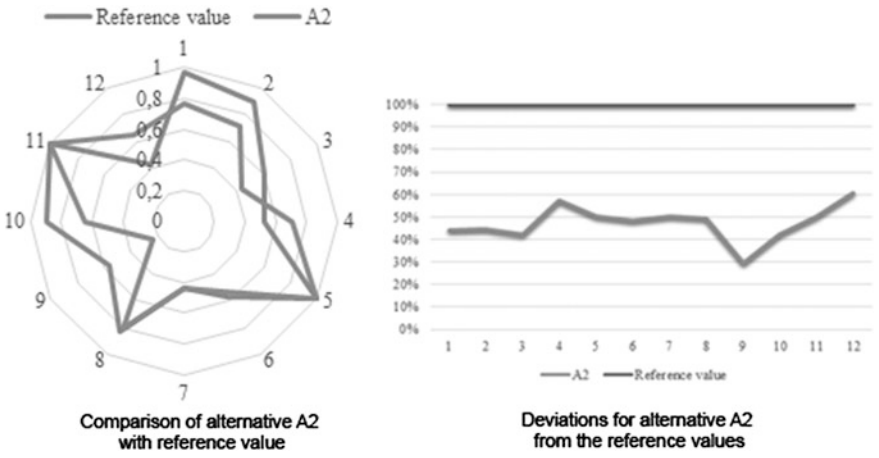

Fig. 3 Alternative A2 (relatively suitable)

reference values were reviewed and discussed with stakeholders. Alternative A1 was as expected, chosen it as the correct one. For the purposes of decision-making targets and strategies of the city it is always necessary to make several variants, which in itself include the risky variant. Management of the city needs to rethink as well as the unfavourable variants on the basis of which it is then degraded risk implications for positive alternatives. Further option appears to be admissible alternative A2, which allows certain deviations from the reference value. For this variant is necessary to develop risk analysis and impact considering the influence of the individual criteria.

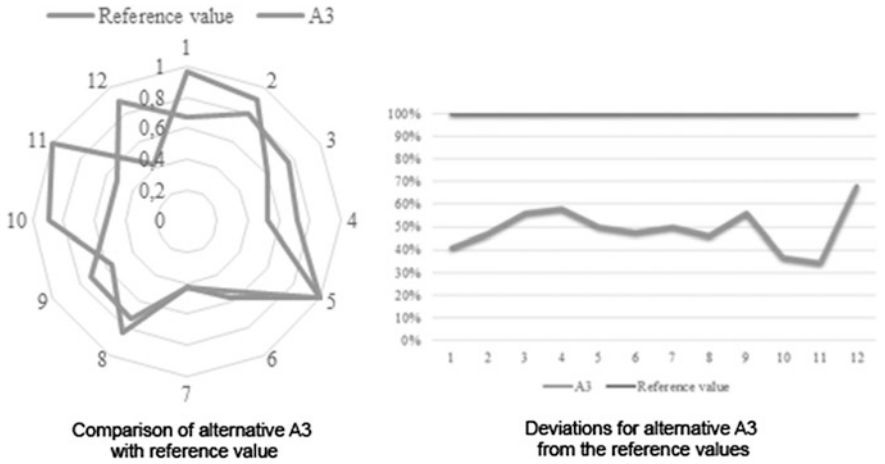

Fig. 4 Alternative A3 (slightly suitable)

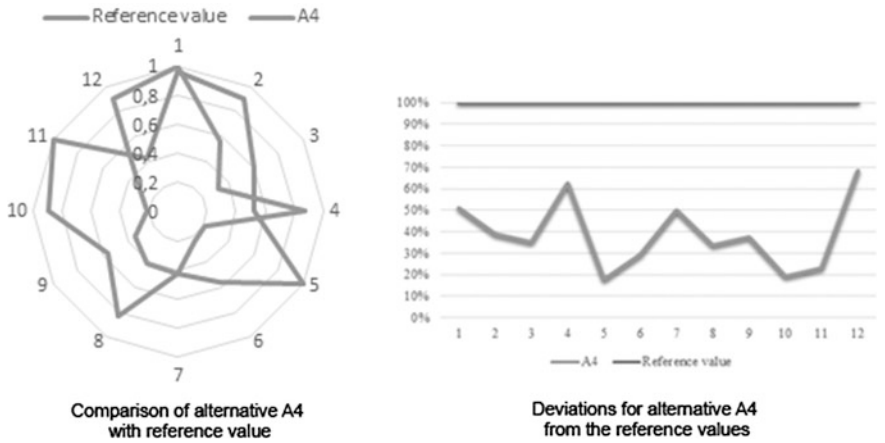

Fig. 5 Alternative A4 (unsuitable)

Alternatives A3 and A4 are examples of unsuitable placement of areas for SMART activities of energy sustainability. These alternatives are solved and submitted as areas for further assessment for land use within urban planning. Individual deviations from the reference values are shown in the following charts. As satisfactory alternatives were chosen alternative A1 and alternative A2 were chosen as substitute variants. The result of variant A1 is shown on Fig. 6.

Table 1 Mainly these characteristics of the qualitative zones

Zone signification	Characteristics of criteria
C1	Wider relations related to the development of the residential structure
C2	The concept of residential development functions
C3	Surrounding production and employment activities—investment, jobs, innovation
C4	Availability of transport infrastructure
C5	Healthcare and social care
C6	Public safety
C7	Availability of the research institutions and universities
C8	Geographical conditions
C9	The level of technical infrastructure
C10	Nature and landscape protection, pollution
C11	Energy efficiency
C12	Renewable resources

Fig. 6 Map of selected objects of alternative A1

Conclusions

This article describes a method for multi-criteria analysis the main difference of which, compared with the existing methods is that instead of weighting coefficients of the individual criteria there are used general functions. These functions transform various criteria on a common comparable platform. The aim is to assess the various criteria that must be compared with each other relative to the reference values in relation to the issue SMART regions for housing estate. The paper describes the use of multi-criteria method for determination of the evaluated criteria and for the comparison a sensitive method and reference values is used.

By combining the different results of multi-criteria analysis it was discovered the need to compare the real considered object or property (the available environmental resources for energy sustainability) with a model that is designed according to the requirements of the users who have decision-making power for strategy in the area of sustainable development and competitiveness of the region. This conclusion was confirmed by the spatial localization of areas for energy sustainability of a specific pilot project in the city district Nový Lískovec. After examining the socio-economic determinants, which resulted in the formation of spatial localization, a completely new approach, which allowed the comparison of the values of individual criteria based on the theory of tolerance and metric spaces was used.

The proposed multi-criteria analysis provided complete arrangement sets of all resulting variants and the possibility of choosing the best variant for purposes of strategic decision for localization of areas for sustainable development. The proposed method can be used for developers, for strategic planning of regional development or as a supporting method to compile the land use plan of the municipality.

Acknowledgements This was created with financial support Technology Agency of the Czech Republic Competence Centres No. TE02000077 and under the Project No. FAST-S-15-2723.

References

Avdagic, Z., & Karabegovic, A. (2008). Fuzzy Logic and Genetic Algorithm Application for Multi Criteria Land Valorization in Spatial Planning. *Artificial Intelligence Techniques for Computer*, 175–198.

Bartoněk, D., & Bureš, J. (2012). Expert GIS for locating of archaeological sites. In *4th International Conference on Cartography & GIS*. ISSN 1314-0604. Albena, Bulgaria: Bulgarian Cartographic Association.

Bartoněk, D., & Opatřilová, I. (2014). Design of man-machine interface for mobile mapping. *Advanced Science Letters, 20*(2), 501–504(4).

Bureš, J., & Bartoněk, D. (2012). Application of GIS in civil engineering. In *4th International Conference on Cartography & GIS*. ISSN 1314-0604. Albena, Bulgaria: Bulgarian Cartographic Association.

Bryzgalin, G. I., Bagmutov, V. P., & Kopeikin, S. D. (1983). Analysis and optimization of laws governing composite media on the basis of the multi-criterial approach. *Mechanics of Composite Materials, 19*(2), 154–162.

Dermekova, S. (2013). Evaluation of the criteria in real estate engineering using the GIS Support. *Geodetický a kartografický obzor, 9*(101), 235–244. ISSN: 1805-7446. (In Czech).

European Innovation Partnership on Smart Cities and Communities. Strategic Implementation Plan. 2013. http://ec.europa.eu/eip/smartcities/

Feizizadeh, B., Roodposhti, M. S., Jankowski, P., & Blaschke, T. (2014a). A GIS-based extended fuzzy multi-criteria evaluation for land slide susceptibility mapping. *Computers & Geosciences, 73,* 208–221.

Feizizadeh, B., Jankowski, P., & Blaschke, T. (2014b). A GIS based spatially-explicit sensitivity and uncertainty analysis approach for multi-criteria decision analysis. *Computers & Geosciences, 64,* 81–95.

Ioja, C. I., Razvan, Nita M., Vânau, G. O., Onose, D. A., & Gavrilidis, A. A. (2014). Using multi-criteria analysis for the identification of spatial land-use conflicts in the Bucharest Metropolitan Area. *Ecological Indicators, 42,* 112–121.

Joerin, F., Thériault, M., & Musy, A. (2001). Using GIS and outranking multi-criteria analysis for land-use suitability assessment. *Geographical Information Science, 15*(2), 153–174.

Lee, I. (2004). Mining multivariate associations within GIS environments. *Innovations in Applied Artificial Intelligence*, 1062–1071

Malczewski, J., Chapman, T., Flegel, C., Walters, D., Shrubsole, D., & Healy, M. (2003). GIS—multi-criteria evaluation with ordered weighted averaging (OWA): Case study of developing watershed management strategies. *Environment and Planning, 35,* 1769–1784.

Massei, G., Rocchi, L., Paolotti, L., Greco, S., & Boggia, A. (2014). Decision Support Systems for environmental management: A case study on wastewater from agriculture. *Journal of Environmental Management, 146,* 491–504.

Mendas, A., & Delali, A. (2012). Integration of multi-criteria decision analysis in GIS to develop land suitability for agriculture: Application to durum wheat cultivation in the region of Mleta in Algeria. *Computers and Electronics in Agriculture, 83,* 117–126.

Meng, Y., Malczewski, J., & Boroushaki, S. (2011). A GIS-based multi-criteria decision analysis approach for mapping accessibility patterns of housing development sites: A case study in Canmore, Alberta. *Journal of Geographic Information System, 3,* 50–61.

Mikhalevich, V. S., Volkovich, V. L., & Yatsenko, Y. P. (1993). Multi-criterial analysis of industry conversion rates using integral models. *Cybernetics and Systems Analysis, 29*(1), 26–34

Nath, S. S., Bolte, J. P., Ross, L. G., & Aguilar-Manjarrez, J. (2000). Applications of geographical information systems (GIS) for spatial decision support in aquaculture. *Aquacultural Engineering, 23*, 233–278.

Natividade-Jesus, E., Coutinho-Rodrigues, J., & Antunes, C. H. (2007). A multi-criteria decision support system for housing evaluation. *Decision Support Systems, 43,* 779–790.

Oh, K. (2001). Landscape information system: A GIS approach to managing urban development. *Landscape and Urban Planning, 54,* 79–89.

Oliviera, E., Antunes, C. H., & Gomes, A. (2013). A comparative study of different approaches using an outranking relation in a multi-objective evolutionary algorithm. *Computers & Operations Research, 40,* 1602–1615.

Ozturk, D., & Batuk, F. (2011). Implementation of GIS-based multi-criteria decision analysis with VB in ArcGIS. *International Journal of Information Technology & Decision Making, 10*(6), 1023–1042.

Peters, J. F., & Wasilewski, P. (2012). Tolerance spaces: Origins, theoretical aspects and applications. *Information Sciences, 195*, 211–225.

Popov, N. M. (1999). On some optimality principles in multi-criterial problems. *Computational Mathematics and Modeling, 10*(2), 178–183.

Rabinovitch, M. (1994). Multi-criterial optimization in production and management. *Operations Research '93*, 405–407.

Suveg, I., & Vosselman, G. (2004). Reconstruction of 3D building models from aerial images and maps. *ISPRS Journal of Photogrammetry & Remote Sensing, 58,* 202–224.

Thiele, M., Bader, A., & Lehner, W. (2009). *Multi-objective scheduling for real-time data warehouses* (pp. 137–151). Berlin: Springer.

Tirelli, T., & Pessani, D. (2011). Importance of feature selection in decision-tree and artificial-neural-network ecological applications. Alburnus alburnus alborella: A practical example. *Ecological Informatics, 6*, 309–315 (Elsevier).

Vahidnia, M. H., Alesheikh, A. A., & Alimohammadi, A. (2009). Hospital site selection using fuzzy AHP and its derivatives. *Journal of Environmental Management, 90,* 3048–3056.

Wang, J., Jing, Y., Zhang, Ch., & Zhao, J. (2009). Review on multi-criteria decision analysis aid in sustainable energy decision-making. *Renewable and Sustainable Energy Reviews, 13*(9), 2263–2278.

Wawetka, R., Volařík, T., & Dermeková, S. (2015). Smart housing estate: Implementation of ICT user friendly application to raise inhabitant' s sustainability awareness. In *15th International Multidisciplinary Scientific Geoconference SGEM 2015. International multidisciplinary geoconference SGEM. Informatics, Geoinformatics and Remote Sensing, Cenference proceedings, Volume I*. Sofia, Bulgaria: STEF92 Technology Ltd., 51 "Alexander Malinov" Blvd., 1712 Sofia, Bulgaria, 2015. s. 793–799. ISBN: 978-619-7105-34- 6. ISSN: 1314- 2704.

Yanar, T. A., & Akyurek, Z. (2006). The enhancement of the cell-based GIS analyses with fuzzy processing capabilities. *Information Sciences, 176,* 1067–1085.

Representing Buildings for Visibility Analyses in Urban Spaces

Jan Caha

Abstract The availability of detailed and precise digital surface models based on LiDaR data allows accurate calculation of visibility analysis even in urban areas. Lately, the viewshed analysis, which is implemented in geographical information systems, is often used to determine the visibility of buildings or other structures in both natural and urban environments. Such utilization of viewshed tool, which is originally designed to assess visibility from point to its neighbourhood, however, brings issues regarding partial visibility of the target that are usually neglected. The core of the problem here is that the target building is often represented as a single point in the viewshed analysis. This simplification can lead to an incorrect assessment of the visibility as the specific point of the building can be invisible for the observer while other parts of the building are visible. To properly analyse visibility of a building it is necessary to consider partial visibility of the target. To allow the assessment of partial visibility more than one point that represents the building needs to be defined. In this contribution, the theoretical aspects of reverse viewshed, an area from which a target point is visible, are considered with a focus on the proper representation of target building in the reverse visibility analysis. A practical study of building visibility is conducted with the building represented as single and multiple points. The results are compared and the differences are explored.

Keywords Viewshed · Reverse viewshed · Visibility · Digital surface model

J. Caha (✉)
Department of Regional Development and Public Administration, Faculty of Regional Development and International Studies, Mendel University in Brno, Zemědělská 1, 613 00 Brno, Czech Republic
e-mail: jan.caha@mendelu.cz

I. Ivan et al. (eds.), *Dynamics in GIscience*, Lecture Notes in Geoinformation and Cartography, DOI 10.1007/978-3-319-61297-3_2

Introduction

Visibility analysis is a theme of interest for landscape and urban planning since the late 70s of the 20th century (Felleman 1979). Since the early 90s, the analysis became a topic for geographical information science (Fisher 1993). The earliest studies were calculated on digital terrain models (DTM) with relatively small precision and large spatial resolution which had significant impacts on the precision of obtained viewsheds (Maloy and Dean 2001). However, availability of more accurate datasets with better spatial resolution has improved drastically with the introduction of LiDaR (Light Detection and Ranging) based surface models. Visibility analysis calculated on surface models constructed from LiDaR data have been proven to provide better and more realistic estimates of visibility (Klouček et al. 2015) than surface models based on other sources. The main reason why LiDaR datasets provide better results of visibility analyses is the fact that these models naturally contain terrain as well as features above terrain that affect visibility such are buildings and vegetation. The models that include other features besides terrain are labeled as digital surface models (DSM). Even though it is possible to construct DSM by adding features to DTM, it is better to use DSM that were directly sensed as these are more accurate than DSM that were built from DSM and additional data (Klouček et al. 2015). Precise DSM allowed more specific applications of visibility analysis—i.e. visibility of wind turbines (Klouček et al. 2015) or buildings (Rød and van der Meer 2009; Garnero and Fabrizio 2015).

Visibility of man-made structures within urban space, be it a city or cultural landscape, requires precise DSM with raster resolution at most 2 × 2 m (Hlavatá and Oťaheľ 2010) but finer resolution—e.g. 0.5 × 0.5 m—are used as well (Rød and van der Meer 2009; Garnero and Fabrizio 2015). With these spatial resolutions of the DSM, it is possible to appropriately capture details of buildings (mainly roof shapes) as well as vegetation (separate trees in parks, etc.). However, there is one aspect arising from the implementation of viewshed analysis in GIS that is neglected and can negatively affect the result of the visibility analysis. The viewshed is implemented as a tool which determines which parts of the surface are visible from a single location. The application can be reversed; the viewshed tool can be used to determine from which area of the surface a target point can be seen. Fisher (1996) referred to this variant as reverse (inverse) viewshed to highlight the difference amongst two types of analysis. The issue that we would like to discuss in this paper is related to the representation of the target in reverse viewshed. The target building (or another structure) is often represented as a single point (see for example Rød and van der Meer (2009) or Garnero and Fabrizio (2015)). Even though that a footprint of a building can be spatially significant and a single point does not have to be a suitable representation of the target structure. Unfortunately, with detailed DSM this simplification of the target to a single point can cause omission of places from which the target is at least partially visible. For practical applications, such are urban planning or archaeology even the partial visibility of the target is important as it has consequences for the observer. The problem here is

that this type of error is systemic so it will affect every visibility analysis to a specific degree and that the problem is not discussed in the literature. Since a significant number of visibility analyses is done by users that do not have formal GIS education—e.g. archaeologists, urban planners, architects or environmentalists, it is quite likely they are unaware of this issue at all. So it is important to discuss the topic and raise the awareness amongst users. The described issue affects binary (classic) viewshed as well as extended viewsheds (visibility indices) (Fisher 1996; Caha and Rášová 2015).

In this paper, we would like to discuss how simplification of target building to a single point can affect the outcomes of reverse viewshed analysis and compare the results with reverse viewshed calculated for target represented by several points. Firstly, some theoretical background regarding the visibility determination will be given, and then a case study of building visibility will be presented. The case study will focus on assessment of building visibility in urban space. The last section of the paper will provide conclusion and recommendations for visibility analyses of buildings.

Reversed Viewshed Analysis

As mentioned previously, it is necessary to differentiate between viewshed, an area visible from a point, and reverse viewshed, an area from which a point is visible, to properly describe visibility analysis that should be performed. In studies where visibility of a building is assessed the reverse viewshed is always calculated, as the question in these studies is: "From which locations the target point can be seen?" Unfortunately, since both viewshed and reverse viewshed are determined using the same tool (viewshed—ArcGIS, r.viewshed—GRASS GIS) with different settings (interchanged values of observer's and target's offset) the authors commonly make no distinction between these types of visibility analysis. Examples of such studies are Rød and van der Meer (2009), Hlavatá and Oťahel' (2010) and Garnero and Fabrizio (2015). This lack of distinction is unfortunate as the interchangeability only applies for binary viewshed. If extended viewshed (visibility indices), such is for example difference of viewing angle between the target point and local horizon (Caha and Rášová 2015), are determined then it is no longer possible to use the same tool to calculate extended viewshed and reversed extended viewshed as these characteristics of visibility are not reciprocal.

The extended viewsheds provide supplementary information about visibility beyond the boolean information visible/invisible (Fisher 1996) and provide answers to questions such as: "How well is the target visible?" The unfortunate fact is that the extended viewshed are not implemented in widely available software, and the same applies for extended reverse viewsheds (Fisher 1996). The situation has not changed during the 20 years that passed since Fisher's article, neither the extended viewshed or the reverse extended viewsheds are still implemented in common GIS.

Representation of Target in Visibility Analysis

Originally, the viewshed is an analysis designed to assess which parts of a surface are visible from a specific observing location on the surface. The analysis as it was proposed was never focused on the visibility of specific target location. The visibility of the target (e.g. building) can be evaluated based on viewshed values in the site of the target. In such case, the outcomes of the analysis are still valid as the visibility is calculated from single point to several points forming the target. The number of points that are used to evaluate target's visibility depends, of course, on the size of the target and cell size of a surface model. However, if viewshed tool is used to determine the reverse viewshed, the logic behind the analysis shifts significantly. The analysis assesses visibility of single point for observers located in individual cells of a raster. The questing arising here is whether a single point is a faithful representation of the target and when a target should be considered visible. While the single point can be a proper representation of small building on DTM with cell size 30 $\times$ 30 m, the same will not be true for a large building on DSM with cell size 1 $\times$ 1 m. The DSM surface will contain significantly more features that will affect the visibility and partial visibility of the target structure is more likely in such situation. For most urban and landscape planning situations, even partial visibility of target is interesting because the target affects the observer and its perception of the environment.

The problematics of partial visibility was firstly mentioned by Fisher (1993) who proposed variants of viewshed algorithm for assessment of partial visibility of a target cell. The proposed algorithm used five points as a representation of a cell (cell's centre point plus its four corners) and was able to identify the situation when only part of a cell was visible to the observer. However, because visibility analysis is relatively computationally demanding and that the determination of partial visibility is even more demanding the algorithms were never more significantly tested except the original study (Fisher 1993). Nevertheless, the results obtained by Fisher (1993) showed that the utilization of more than one point as a representation of the target leads to increase of visible area. Obviously, if the representation of target cell in the visibility analysis can affect the outcomes of the analysis, it is necessary to consider effects of target representation in reversed viewshed, where the target is usually significantly larger than one cell.

Figure 1 shows a simple demonstration of the issues related to an assessment of building visibility. Visibility of target building (represented as a very light grey rectangle) is evaluated from two viewpoints (vp1, vp2). If the target building is represented by single point (tp1), which is located in a centre of the target polygon, then it is invisible from both viewpoints due to obstacles (grey rectangle and circle). However, if two more points (tp2, tp3) are used to evaluate visibility, the target becomes partially visible for both observers. From viewpoint vp1 the observer can see both target points located on sides of the target but can not see the middle point. From viewpoint vp2 the user can see one side of the building but not the other side nor the middle point. The target, however, is still visible for the observer, even

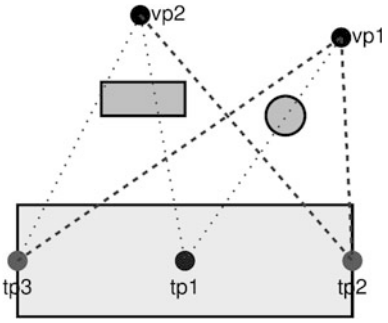

Fig. 1 Visibility of target object (*very light grey rectangle*) from two points (*vp1*, *vp2*) in situation when the target object is represented by three points (*tp1*, *tp2*, *tp3*). LoS where target point is visible are shown as *dashed lines*, LoS where the target is not visible are displayed as *dotted lines*

though, it is relatively small part of the target. This example illustrates the issue which should be considered for reversed viewshed analyses as the situation similar to Fig. 1 will occur quite often especially on precise DSM in urban spaces. The reason why reversed visibility of target in urban spaces are affected more likely by this phenomenon than reversed visibility in natural landscape is that urban space form a significant number of vistas, street canyons and often contain isolated trees or vertical structures that will lead to a partial visibility of target. Another factor that is likely to cause partial visibility is a size of the target. If the visibility of radio tower or lookout tower should be assessed then the horizontal dimension of the target is unlikely to be significant. However, buildings can have significant horizontal dimensions, ranging from tens to hundreds of meters, which makes them more likely to be partially visible especially in urban spaces.

The situations of partial visibility that were discussed previously were focused on boolean visibility, but extended viewsheds (visibility indices) are affected as well. Let us consider the difference of viewing angle between the target point and local horizon (Caha and Rášová 2015) as an example of extended viewshed. It is rather obvious that there will be a different value of extended viewshed for every point that represents the target. There is no universal approach how to evaluate the resulting extended viewsheds; the solution depends on the exact question that the analysis should answer.

Selection of Points Representing the Target

The selection of points that will be used as an approximation of the target for reverse viewshed analysis is a crucial step. There is need to balance the number of points, as the number of points will affect the computational loads and time necessary to obtain the results, and adequacy of representation. Hlavatá and Oťahel' (2010) mention representing specific buildings by more than one point for their study, but unfortunately provide no details regarding this matter.

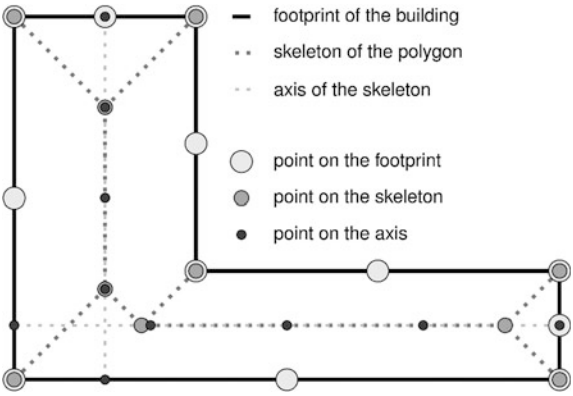

Fig. 2 Different sampling strategies for selection of points representing the target

There are several possible strategies for selection of the points (Fig. 2):

- important points or equal distance sampling of building's footprint,
- important points or equal distance sampling of building's main and/or minor axis,
- important points or equal distance sampling of a straight skeleton (Aichholzer et al. 1995) from building's footprint,
- important points selected by the user based on his expert opinion.

Each of these approaches has its advantages and disadvantages and is suitable for different types of targets. For example, the selection of points from building's footprint is only suitable for buildings that have a relatively flat roof because the inner part of the structure is not considered. However, the strategy works fine for modern buildings, especially high-rise buildings, as they tend to have flat roofs (Yu et al. 2016). For most applications, the combination of one of the first three methods with the fourth method will most likely be the optimal solution.

In Fig. 2 different sampling strategies are used for every approach. The points on the footprint of the building are placed in every corner and in the middle of every edge. The points on the skeleton of the polygon are placed on every vertex of the straight skeleton. The points on the axis are located at the start, end of the axis and every 25% of the length of the axis, which means that five points are used for every axis.

Case Study

The case study if focused on the visibility of National Monument in Vitov, Prague, Czech Republic. The structure was chosen due to its vertical dominancy with respect to surrounding areas and the diversity of neighbourhood which consists of densely built-up areas as well as parks and other recreation grounds. The National

Monument consist of an equestrian statue and a building. The size of the complex is roughly 140 × 50 m. The dimensions of the complex are considerable primarily due to its longitudinal nature.

The viewshed analysis is done in an area of size 1 km around the target building. The area of interest is shown in Fig. 3. The datasets used for this study are provided by "© IPR Praha" (www.geoportalpraha.cz) as open source data with licence CC BY-SA 4.0. The necessary datasets for the case study are DSM and DTM, both datasets have the spatial resolution of 1 × 1 m and are based on LiDaR data. All the visibility analyses calculated for this case study are done with observer's offset 1.5 m and target's offset 0 m.

Figure 4 shows DSM of the building with the representative point highlighted, a single point that could be used for reversed visibility analysis, and additional points that will be used for visibility analyses to represent the building adequately. The single representative point is selected as centre of the polygon delimiting the building (without considering the statue). The 8 points representing the National Monument are located on the main axis of the structure and are selected with respect to significant features of the building as well as the distance amongst them. One point is located on the statue in front of the main building, five points are located on the main section of the building (highest part), and two are located in the rear part of the building which is lower than the main section. The distance amongst points on the main section of the building is on average 15 m, the points on rear section are on average 20 m apart, and the point on the statue is 32 m from the first point on the building. The width of the building is not considered as important as its length for the purpose of this study and with respect to the geomorphological location of the building. However, different shapes of buildings would require different spatial layout of the points.

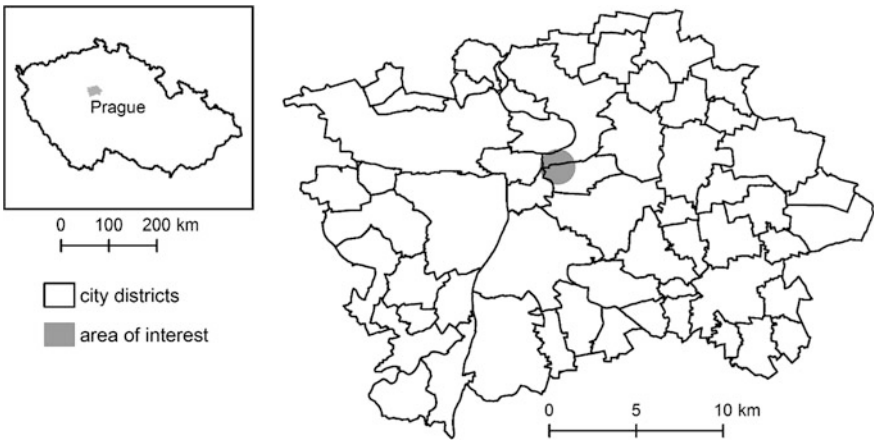

Fig. 3 Location of area of interest in Prague

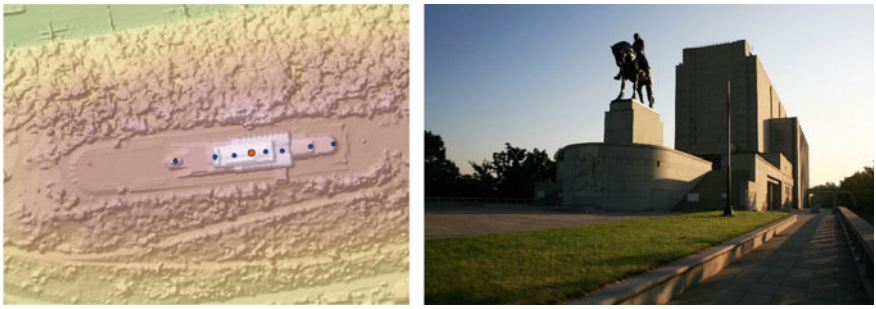

Fig. 4 National Monument in Vitkov. *Left* shaded digital surface model with representative point (*orange*) and additional points (*blue*). *Right* photography of the monument (*Source* Ondřej Kořínek [CC BY-SA 3.0 (http://creativecommons.org/licenses/by-sa/3.0)], via Wikimedia Commons)

The number of points representing the target structure is selected as a compromise between a proper representation of the target and computational time necessary to obtain the result. The computational time rises linearly with increasing number of points. Since it is not usually necessary to calculate this type of analysis in real time, the time demands are not a significant issue for this type of analysis.

Prior to visibility analysis of the building, three preprocessing steps need to be performed. Firstly, the points representing the building need to obtain the elevation information from DSM. The second phase is to remove the building itself from DSM and replace the area with values from DTM (Hlavatá and Oťaheľ 2010). This step is necessary otherwise parts of the building can overshadow the target points which would result in an incorrect assessment of building visibility. Since reverse viewshed will be determined it is reasonable to remove areas that are inaccessible for the observer from the area of interest. Such areas are roofs of buildings and places with notable vegetation (Bartie et al. 2011), both types can be identified from the difference of DSM and DTM. In our case, if the absolute value of difference between DSM and DTM is higher than 2 m the area is marked as inaccessible for the observer. The threshold (2 m) is selected as borderline that separates smaller trees and shrub from regular sized trees.

The reverse visibility analyses of the national monument are calculated for the representative point, which serves as an example of simple visibility analysis, and for eight points that properly represent the whole building. The representation of structure by a single point is used in several studies (Rød and van der Meer 2009; Garnero and Fabrizio 2015) but the representation by several points was also mentioned previously (Hlavatá and Oťaheľ 2010). For both variants, boolean viewshed and one extended viewshed (viewing angle between the target point and local horizon) were calculated. To generate a single outcome for the multipoint variant of the analysis the resulting grids were merged using the maximal value of visibility for every cell. This answers questions “From which locations is at least one target point visible?” and “How well is visible the most notable part of the

building?" It would be possible to answer different questions as well but for the purpose of this study these question we considered as sufficient.

An initial comparison of visibility of representative point and visibility of at least one point is in Fig. 5. The representative point is visible from 201,986 cells of the raster. At least one of the points representing the target building is visible from 264,917 cells, which is 31.16% increase from the visibility of the representative point. As visible from the Fig. 5, the additional areas, from which other points than the representative point are visible, are located mainly in long straight streets, behind vertically significant structures and near edges of buildings. Figure 6 shows a 3D representation of views from viewpoints (location of viewpoints is in Fig. 5). For each of these viewpoints, the representative point is hidden either by a structure (A) or by vegetation (B and C), but significant part of the building is still visible for the observer. These 3D visualizations perhaps most appropriately explain the essence of the issue of proper representation of the target in reverse viewshed analyses.

The extended reverse viewshed calculated for the national monument is viewing angle between the target point and local horizon which describes how high above the horizon the target points raises. The comparison is then made as the difference between extended reversed viewshed calculated for 8 target points and the representative point. Figure 7 shows the difference between values of extended reverse viewsheds in degrees. The highest differences are close to the target building

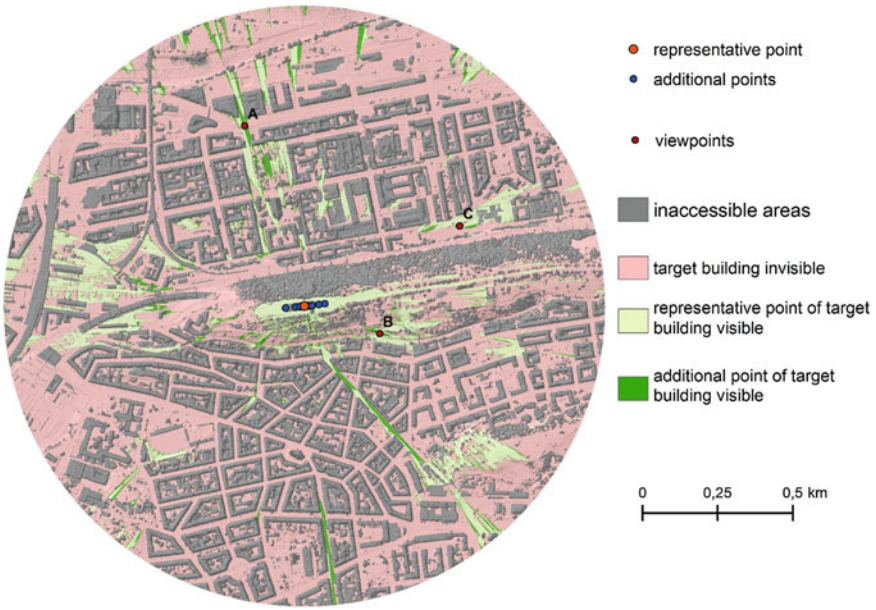

Fig. 5 The difference between reversed viewshed determined for representative point and all the points

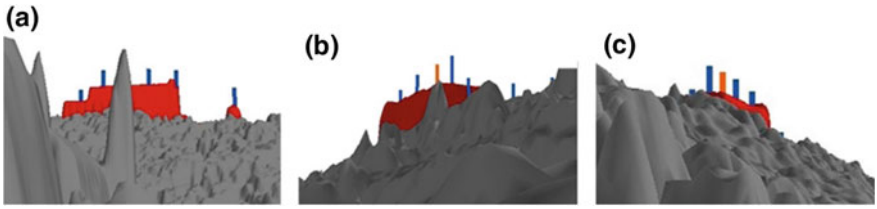

Fig. 6 3D visualization of DSM with the target building highlighted and the *points* representing the building exaggerated. The three examples represent viewpoints from the previous figure. In all three cases the representative point is invisible but the building as a whole is visible

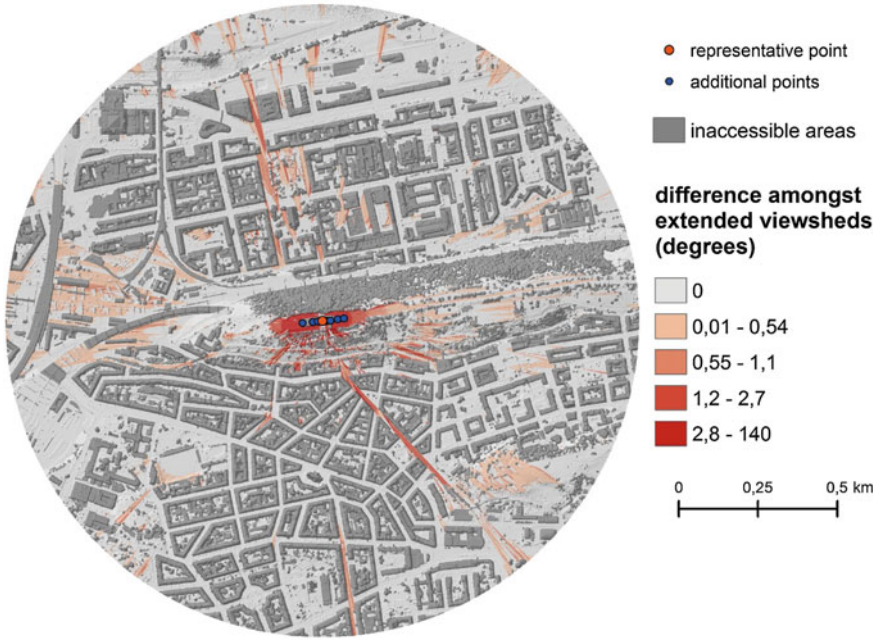

Fig. 7 The difference between extended reverse viewshed—the difference of viewing angle between the target point and local horizon—determined for representative point and all the points

because in these cases the value of extended reverse viewshed is affected by the distance from the target point. However, even points located further from the target point show some amount of difference caused by the fact that the representative point does not have to be the most prominent point representing target building. The differences for the cells located more than 150 m from the representative point are summarized as a histogram in Fig. 8. The minimum distance is chosen to filter out high values of differences which are caused by other reasons than the different visibility of points representing the target building. The results show that even

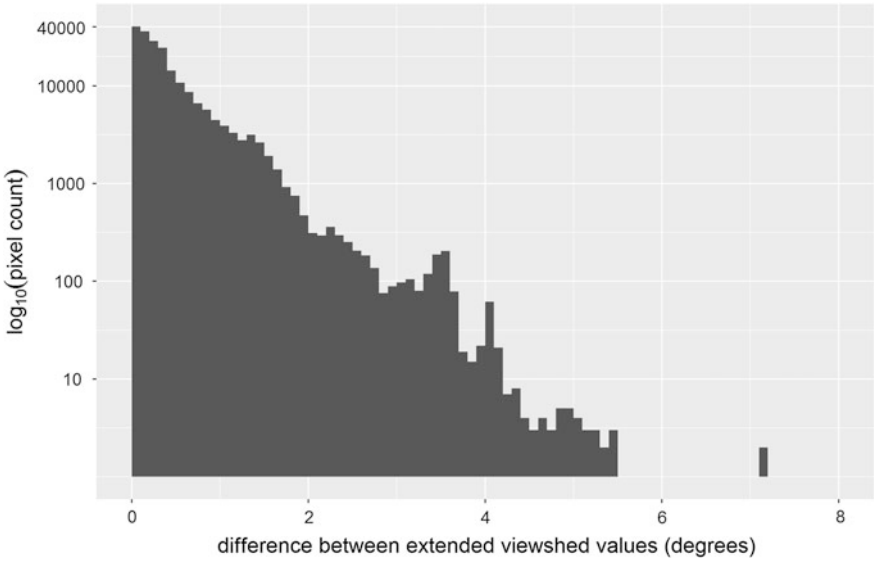

Fig. 8 Histogram of the extended reverse viewshed differences for cells located more than 150 m from the representative point

though, the number of cells with zero or minimal difference is the highest (Fig. 8), 97% of cells have difference higher than 0.016 degree, which could be considered as significant difference based on Ogburn's (2006) research which identifies the value of 1' as a threshold for resolution acuity. With difference higher than the threshold of resolution acuity the observer should be able to distinguish that specific part of the target is more distinctive that other part. In this particular case, it means that some sections of the building are higher above the local horizon than the representative point.

Conclusions

The presented research focus on the importance of target representation for reverse viewshed analysis. With the growing number of studies that assess visibility of buildings, it is necessary to point out and study factors that can affect the credibility of obtained results. This paper describes that the common approach of representing the target building (or other man-made structure) by a single point for visibility analysis can cause the results of the analysis to be incomplete. The incompleteness is a product of the determination of visibility of specific point representing the target building while neglecting possible partial visibility of the building or in other words visibility of other points that can represent the target. The issue of results omission will more likely affect visibility analysis on detailed and precise surface models

especially in urban spaces where visibility obstacles have significantly higher variability (in terms of both height and dimensions). The reasons for these omissions are theoretically described and practically demonstrated on a case study of the National monument in Vitkov, Prague.

The case study revealed that if eight points are used to represent the National monument, the reverse viewshed area will be bigger by 31% than if the building is represented by a single point. These results confirm the findings presented by Fisher (1993), who reported up to 50% rise in the area for viewshed analysis if the partial visibility of raster cells was considered. The exact value of the disparity is, however, always case specifics and depends on many factors (e.g. geomorphology of the terrain, structure of DSM) so no general conclusions about the causes can be done. The most influential factors that will affect the difference between results obtained for single and multiple point representations are dimensions and shape of the object, type of neighbourhood around the target and spatial configuration of visibility obstacles. In the case study, we identified few situations that caused the biggest area differences between the results for different target representations. Amongst them three were the most prominent—straight long streets that offer view only on the part of the target, locations were vertically significant structures with relatively small footprint (towers) hide the representative point while the rest of the target is visible and vegetation causing the same issue.

The issue described in this contribution is significant as a building visibility is one of the factors for urban and environmental planners to consider when authorizing new construction. The results of our research show that single point reverse visibility is likely to provide a smaller area from which the target is visible. For proper assessment of the visibility, the entire spatial extent of the building has to be considered to provide an exact result. The result of visibility analysis should cover even the situations in which the target is only partially visible as even the partial visibility of the target affects the observer. This is especially true in the case of assessment of building visibility in urban space.

The further research should focus on identification of the optimal number of points that should represent a target based on its size and shape. For the purpose of this research the number of points was estimated based on expert knowledge, but some general guidelines are necessary for practical implementations. The influence of partial target visibility on extended reverse viewshed is another topic that deserves attention as it helps with an assessment of how well the target is visible.

Acknowledgements This article was prepared within the project IGA FRDIS Mendel University in Brno No. 022/2017 “Visibility analysis of high-rise buildings as tool for urban and landscape planning” (FRRMS_IGA_2017/022).

References

Aichholzer, O., Aurenhammer, F., Alberts, D., & Gärtner, B. (1995). A novel type of skeleton for polygons. *Journal of Universal Computer Science, 1*(12), 752–761.

Bartie, P., Reitsma, F., Kingham, S., & Mills, S. (2011). Incorporating vegetation into visual exposure modelling in urban environments. *International Journal of Geographical Information Science, 25*(5), 851–868.

Caha, J., & Rášová, A. (2015). Line-of-sight derived indices: Viewing angle difference to a local horizon and the difference of viewing angle and the slope of line of sight. In K. Růžičková & T. Inspektor (Eds.), *Surface models for geosciences SE—6* (pp. 61–72). Ostrava: Springer International Publishing.

Felleman, J. P. (1979). *Landscape visibility mapping: Theory and practice*. New York: Syracuse.

Fisher, P. F. (1993). Algorithm and implementation uncertainty in viewshed analysis. *International Journal of Geographical Information Systems, 7*(4), 331–347.

Fisher, P. F. (1996). Extending the applicability of viewsheds in landscape planning. *Photogrammetric Engineering and Remote Sensing, 62*(11), 1297–1302.

Garnero, G., & Fabrizio, E. (2015). Visibility analysis in urban spaces: A raster-based approach and case studies. *Environment and Planning B: Planning and Design, 42,* 688–707.

Hlavatá, Z., & Oťaheľ, J. (2010). Vizuálna analýza vybraných historických dominánt Bratislavy. *Geografický Časopis, 62*(4), 293–311.

Klouček, T., Lagner, O., & Šímová, P. (2015). How does data accuracy influence the reliability of digital viewshed models? A case study with wind turbines. *Applied Geography, 64,* 46–54.

Maloy, M. A., & Dean, D. J. (2001). An accuracy assessment of various GIS-based viewshed delineation techniques. *Photogrammetric Engineering & Remote Sensing, 67*(11), 1293–1298.

Ogburn, D. E. (2006). Assessing the level of visibility of cultural objects in past landscapes. *Journal of Archaeological Science, 33*(3), 405–413.

Rød, J. K., & van der Meer, D. (2009). Visibility and dominance analysis: Assessing a high-rise building project in Trondheim. *Environment and Planning B: Planning and Design, 36*(4), 698–710.

Yu, S., Yu, B., Song, W., Wu, B., Zhou, J., & Huang, Y. (2016). Landscape and urban planning view-based greenery: A three-dimensional assessment of city buildings' green visibility using floor green view index. *Landscape and Urban Planning, 152,* 13–26.

Comparison of Fuzzy AHP Algorithms for Land Suitability Assessment

Jan Caha and Jaroslav Burian

Abstract Weighted Linear Combination (WLC) is one of the most popular methods for Multiple Criteria Decision-making (MCDM) in the field of geoinformatics. A typical utilization of WLC is in land suitability assessment and optimal location detection. The application of WLC requires the determination of weights for each criterion used in the MCDM problem. In this paper, we focus on a fuzzy Analytical Hierarchy Process (AHP) which is based on pairwise comparisons of criterion importance and, unlike the classic (crisp) AHP, it can contain uncertainty. This allows the user to include imprecise or incomplete knowledge in an MCDM problem. The theoretical part of the paper briefly describes fuzzy AHP and provides the necessary mathematical background. The practical part of the contribution is focused on testing two algorithms for weight determination in fuzzy AHP—the extent analysis method and a method based on constrained fuzzy arithmetic. The methods are described in terms of the amount of uncertainty in the result, the resulting value, and overall appropriateness. A four level fuzzy AHP problem containing one main goal, three criteria and twenty-four subcriteria is solved as a case study using both methods. Based on the results obtained, the recommendations for fuzzy AHP utilization in spatial suitability assessment are made.

Keywords Fuzzy AHP · Analytical hierarchy process · Multiple criteria Decision-making · Land suitability

J. Caha (✉)
Department of Regional Development and Public Administration,
Faculty of Regional Development and International Studies,
Mendel University in Brno, Zemědělská 1, 613 00 Brno, Czech Republic
e-mail: jan.caha@mendelu.cz

J. Burian
Department of Geoinformatics, Faculty of Science, Palacký University
in Olomouc, 17. listopadu 50, 771 46 Olomouc, Czech Republic
e-mail: jaroslav.burian@upol.cz

I. Ivan et al. (eds.), *Dynamics in GIscience*, Lecture Notes in Geoinformation and Cartography, DOI 10.1007/978-3-319-61297-3_3

Introduction

Multiple Criteria Decision-making (MCMD) was a field in the study of land and urban planning before GIS became a widespread technology (Hopkins 1977). However, the utilization of GIS made the whole process much faster and significantly simpler. The main goal of land suitability assessment is to produce suitability maps and detect optimal locations for specific developments (housing, industry, commercial areas, etc.). Firstly, the criteria of the MCMD are defined and their relationships specified with respect to the decision-making problem. This model of the decision-making problem is used to define the combination of spatial data that will solve the problem. One of these models is Weighted Linear Combination (WLC), which is generally used for spatial MCMD as it allows the user to specify the importance of each criterion in the result (Elaalem et al. 2011). The use of WLC naturally leads to the problematic of the objective specification of weights.

Even though there is a large set of techniques, not only for the specification of weights, but for the whole MCMD (Jankowski 1995), one technique used more often than others is AHP (Analytical Hierarchy Process). AHP is an MCDM tool based on the hierarchical structure of a decision-making problem and pairwise comparisons of criteria importance, in order to obtain criteria weights. The criteria are compared in pairs using a predefined scale (Krejčí et al. 2016). The scale is composed of values 1 (equal importance to compared criteria) to 9 (first element extremely more important than second) and their reciprocals. The method is commonly used within GIS (Chandio et al. 2013) and it provides better results than other methods used for weight estimation (Feizizadeh and Blaschke 2013). The typical structure of an AHP problem is shown in Fig. 1. Typically, there is one main goal in the MCDM problem that consists of several evaluation criteria. Each of these criteria can be composed of subcriteria. This approach creates the typical hierarchical structure of AHP. Because AHP is well described in the literature, we

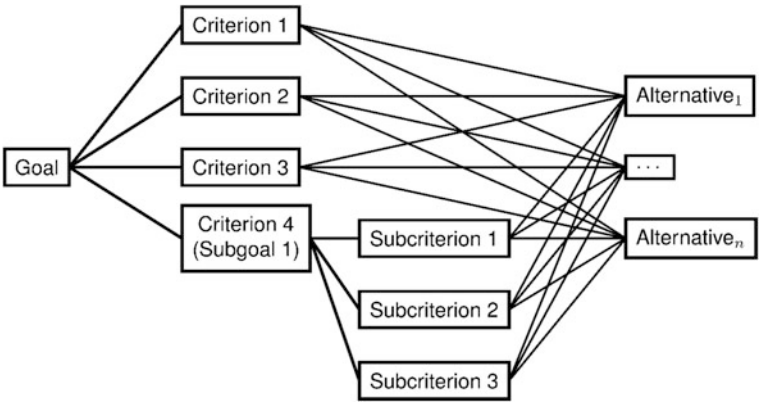

Fig. 1 The typical structure of AHP problem

refer to publications by Chandio et al. (2013), Jankowski (1995) and Feizizadeh and Blaschke (2013) for detailed descriptions of the method.

There is one important issue related to AHP. This concerns the situation in which the decision maker cannot exactly specify the pairwise comparison amongst criteria (or subcriteria), either due to a lack of knowledge or the uncertainty of the comparison itself. However, this issue is solved by the introduction of fuzzy AHP (Laarhoven and Pedrycz 1983), which allows imprecise pairwise comparisons to be made.

In this paper, we would like to compare two approaches to the determination of criterion weights in fuzzy AHP—the Extent analysis method introduced by Chang (1996) and the method based on constrained fuzzy arithmetic as described recently by Krejčí et al. (2016). The methods will be compared in terms of uncertainty amount in the result, resulting value, and overall appropriateness.

Fuzzy AHP

Due to the scope of this article, it is not possible to review the whole theory of fuzzy AHP. Only the most crucial information is mentioned. For detailed descriptions, see Laarhoven and Pedrycz (1983), Chang (1996), Wang et al. (2008) and Krejčí et al. (2016).

Fuzzy AHP is a variant of classic AHP, where the user defines the pairwise comparisons of criteria or subcriteria as fuzzy numbers (Laarhoven and Pedrycz 1983). Fuzzy numbers represent vague or uncertain values that the user cannot specify precisely. Fuzzy AHP allows the user to even utilize imprecise and uncertain knowledge about the importance of the criteria in the MCDM (Krejčí et al. 2016). The uncertainty regarding the criteria's importance is then propagated through the calculation and provides results that comprise the uncertainty of the users' knowledge about the decision-making problem. For example, the user might not be sure if criterion 1 is preferred over criterion 2 slightly or moderately. In fuzzy AHP it is possible to define a comparison using both these terms at the same time. The concept of fuzzy AHP has been criticized several times, most notably by Saaty and Tran (2007). However, Krejčí et al. (2016) argue that situations exist where the pairwise comparisons can be vague, and thus there is a reason for the utilization of fuzzy AHP.

The main goal of fuzzy AHP is to determine the suitability value of alternative A_l from the set of p alternatives $A = \{A_1, \ldots, A_p\}$ with respect to the set of n criteria $C = \{C_1, \ldots, C_n\}$. The value $A_{lj}, l \in \{1, \ldots, p\}, j \in \{1, \ldots, n\}$ is then a valuation of alternative A_l with respect to criterion j. Within GIS the values A_{lj} are usually stored in layers, and the whole calculation of AHP is performed as a weighted overlay of layers (Banai 1993). The main challenge for AHP calculation in GIS is the determination of weights w_i for every criterion C_i, so that the weighted overlay can be calculated.

Fuzzy AHP is based on the utilization of fuzzy numbers and fuzzy arithmetic, so before solving fuzzy AHP to obtain the uncertain criteria weights, some rudiments about fuzzy numbers needs to be defined. The triangular fuzzy number $\tilde{f}$ is a triplet of values $[f1, f2, f3]$ that satisfy the condition $f1 \leq f2 \leq f3$. The values are denoted as lower, middle and upper significant values; generally the significant value of a fuzzy number can be denoted as fx where $x = 1, 2, 3$. Classic (crisp) number g is then a special case of fuzzy number ($\tilde{g}$) where $g1 = g2 = g3$. The basic mathematical operations necessary to solve fuzzy AHP are addition, multiplication, division, n th root (for integer n higher or equal to 2) and reciprocal value of fuzzy number (Krejčí et al. 2016):

$$\tilde{f} + \tilde{e} = [f1, f2, f3] + [e1, e2, e3] = [f1 + e1, f2 + e2, f3 + e3], \tag{1}$$

$$\tilde{f} \times \tilde{e} = [f1, f2, f3] \times [e1, e2, e3] = [f1 \times e1, f2 \times e2, f3 \times e3], \tag{2}$$

$$\tilde{f} / \tilde{e} = [f1, f2, f3] / [e1, e2, e3] = [f1/e3, f2/e2, f3/e1], \tag{3}$$

$$\sqrt[n]{\tilde{f}} = \left[\sqrt[n]{f1}, \sqrt[n]{f2}, \sqrt[n]{f3}\right], \tag{4}$$

$$\frac{1}{\tilde{f}} = \left[\frac{1}{f3}, \frac{1}{f2}, \frac{1}{f1}\right]. \tag{5}$$

Equations (1–5) are only valid if the variables $\tilde{f}$ and $\tilde{e}$ are independent. If the variables are reliant on each other then the constraint has to be considered, otherwise, the resulting uncertainty will be inflated (Klir and Pan 1998). The problem with overestimation of uncertainty is well known in the literature (Hanss 2005). The solution is the utilization of constrained fuzzy arithmetic which can take relation amongst variables into account (Klir and Pan 1998). The use of constrained arithmetic usually requires modification of calculation procedure to acknowledge the mutual relations of the variables.

Another operation with the fuzzy number that needs to be defined is the defuzzification of fuzzy number. For the purpose of this article we will use following equation to defuzzify fuzzy numbers:

$$f = \frac{f1 + f2 + f3}{3}. \tag{6}$$

The main step in fuzzy AHP is the construction of a pairwise comparison matrix for every goal (and sub-goal). The matrix compares the importance of each criterion that belongs to a given goal (or sub-goal), against all other criterions. The element of the pairwise comparison matrix is denoted as m_{ij} where $i, j = 1, \ldots, n$, significant values of the fuzzy matrix are denoted as $m_{ij}x$ where $x = 1, 2, 3$. Based on these fuzzy pairwise comparison matrices, the weights of each criterion can be calculated. The pairwise comparison matrices used in fuzzy AHP can either use a fuzzified

Table 1 Example of fuzzy pairwise comparison matrix

	Subcriterion 1	**Subcriterion 2**	**Subcriterion** 3
Subcriterion 1	[1,1,1]	[1/3,1/2,1]	[1/6,1/4,1/3]
Subcriterion 2	[1,2,3]	[1,1,1]	[1/3,1/2,1/1]
Subcriterion 3	[3,4,6]	[1,2,3]	[1,1,1]

scale (that is based on ranking scale of classic AHP), as shown in Krejčí et al. (2016), or the decision maker can specify each comparison based on his/her knowledge. The fuzzy pairwise comparison matrix still has to be reciprocal; the main diagonal elements have to be [1,1,1], and its consistency needs to be verified prior to any calculations. There are several ways to verify the consistency of fuzzy pairwise comparison matrices (Krejčí et al. 2016), but for most applications it is sufficient if the pairwise comparison matrix of middle significant values is consistent in the same way as a crisp pairwise comparison matrix. The consistency is checked by calculating the consistency ratio (Chandio et al. 2013). An example of fuzzy pairwise comparison for Sub-goal 1 from Fig. 1 is in Table 1.

Based on the fuzzy pairwise comparison matrix (e.g. Table 1) the weights of criteria can be calculated. The algorithm used to derive the weights is a crucial step in fuzzy AHP. For classic AHP there are four main methods to calculate weights and the method based on the geometric mean is usually accepted as the best (Ishizaka and Lusti 2006). The same situation exists for fuzzy AHP. In the following subsections, we will describe two algorithms for the determination of weights in fuzzy AHP. The first algorithm is one of the oldest and has been used in a significant number of studies, although it has been heavily criticized. The second is very recent and aims to significantly improve the estimated weights in terms of uncertainty amount.

If the weight w_i of criterion C_i is calculated for all criteria, then the overall value of A_l can be calculated as:

$$A_l = \sum_{i=1}^{n} \tilde{w}_i A_{li}. \tag{7}$$

For this calculation, it is relatively unimportant if $\tilde{w}_i$ is a crisp or fuzzy number. However, the difference is significant for the results obtained, so we will denote fuzzy weights as $\tilde{w}_i$ and classic weights as w_i.

Extent Analysis Method

The Extent Analysis Method (EAM) was first described by Chang (1996). Since then it has been used is various fields, including GIS (Feizizadeh et al. 2014; Nazari

et al. 2012; Du et al. 2016). The method obtains weights in two main steps. The first step is a calculation of important values, based on the equation:

$$w_i e = \frac{\sum_{j=1}^{n} m_{ij} x}{\sum_{i=1}^{n} \sum_{j=1}^{n} m_{ij} x}; \quad x = 1, 2, 3. \tag{8}$$

And the fuzzy weight is then constructed as $\tilde{w}_i = [w_i 1, w_i 2, w_i 3]$. Even though this would be sufficient, the extent method does not end at this point and constructs a so-called weight vector from fuzzy weights. The weight vector is constructed according to a possibility degree of $\tilde{w}_i \geq \tilde{w}_j$, which is calculated as:

$$V\left(\tilde{w}_i \geq \tilde{w}_j\right) = \begin{cases} 1 & \text{if } w_i 2 \geq w_j 2, \\ \frac{w_i 3 - w_j 1}{(w_i 3 - w_i 2) + \left(w_j 2 - w_j 1\right)} & \text{if } w_j 1 \leq w_i 3, . \\ 0 & \text{otherwise.} \end{cases} \tag{9}$$

Then the dominance of w_i with respect to all other weights is determined as:

$$w_i^{nn} = min\left(V\left(w_i \geq w_j\right)\right); \quad j = 1, \ldots, n; \; j \neq i. \tag{10}$$

And finally, the weight is calculated as:

$$w_i = \frac{w_i^{nn}}{\sum_{j=1}^{n} w_j^{nn}}. \tag{11}$$

It is evident from the Eqs. (8–11) that the resulting values of the weights obtained by this method are not fuzzy numbers but crisp values. This is one of the issues concerned with this approach; that uncertainty is not propagated through the whole process of AHP but used only in one part. Other problems related to this method were pointed out by Wang et al. (2008). Two of those problems are very problematic for practical applications. The first issue is that the amount of uncertainty within $\tilde{w}_i$ ($w_i 3 - w_i 1$) is higher than it should be. This false uncertainty is the result of the utilization of fuzzy arithmetic in Eq. (8), instead of constrained fuzzy arithmetic. Wang et al. (2008) propose an optimization of Eq. (8) to solve this issue, as did Tesfamariam and Sadiq (2006). However, neither of those approaches solved the issue completely. The second issue, unfortunately, is more problematic. The process of weight vector calculation can assign the weight 0 to some elements, even though those elements should have a weight higher than zero (Wang et al. 2008). The zero weight causes criteria to be completely left out of the MCDM problem, which is a significant issue. A detailed analysis of both these issues is provided in Wang et al. (2008), who showed that this issue could lead to the selection of unsuitable alternatives and thus to the acceptance of a wrong decision. Another minor issue is that the estimation of fuzzy weights' importance values is based on the arithmetic mean method. However, the geometric mean method is regarded as the most suitable method for the estimation of weights in AHP (Barziali 1997).

Method Based on Constrained Fuzzy Arithmetic

First introduced by Krejčí et al. (2016), this method is based on the utilization of constrained fuzzy arithmetic (MCFA) in the geometric mean method for the calculation of AHP weights. MCFA considers all the relationships amongst pairwise comparisons in the fuzzy pairwise comparison matrix, and provides more precise estimates of fuzzy weights (Krejčí et al. 2016). The fuzzy weights are obtained using the following equations:

$$w_i 1 = \frac{\sqrt[n]{\prod_{j=1}^{n} m_{ij}1}}{\sqrt[n]{\prod_{j=1}^{n} m_{ij}1} + max\left\{ \begin{matrix} \sum_{\substack{k=1 \\ k \neq i}}^{n} \sqrt[n]{m_{ki}3 \prod_{\substack{l=1 \\ l \neq i}}^{k-1} \frac{1}{m_{lk}} \prod_{\substack{l=k+1 \\ l \neq i}}^{n} m_{kl}}; & \begin{matrix} m_{rs} \in [m_{rs}1, m_{rs}3], \\ r, s = 1, \ldots, n, \\ r < s; r, s \neq i \end{matrix} \end{matrix} \right\}}, \tag{12}$$

$$w_i 2 = \frac{\sqrt[n]{\prod_{j=1}^{n} m_{ij}2}}{\sum_{k=1}^{n} \sqrt[n]{\prod_{j=1}^{n} m_{kj}2}}, \tag{13}$$

$$w_i 3 = \frac{\sqrt[n]{\prod_{j=1}^{n} m_{ij}3}}{\sqrt[n]{\prod_{j=1}^{n} m_{ij}3} + min\left\{ \begin{matrix} \sum_{\substack{k=1 \\ k \neq i}}^{n} \sqrt[n]{m_{ki}1 \prod_{\substack{l=1 \\ l \neq i}}^{k-1} \frac{1}{m_{lk}} \prod_{\substack{l=k+1 \\ l \neq i}}^{n} m_{kl}}; & \begin{matrix} m_{rs} \in [m_{rs}1, m_{rs}3], \\ r, s = 1, \ldots, n, \\ r < s; r, s \neq i \end{matrix} \end{matrix} \right\}}. \tag{14}$$

The weights obtained $\tilde{w}_i = [w_i 1, w_i 2, w_i 3]$ have a middle important value equal to the weights calculated from crisp AHP by the geometric mean method. The amount of uncertainty $w_i 3 - w_i 1$ is significantly smaller than the amount of uncertainty obtained from the methods presented by Chang (1996), Wang et al. (2008), and Tesfamariam and Sadiq (2006) (Krejčí et al. 2016). The amount of uncertainty in fuzzy weights substantially affects the amount of uncertainty in the results. Obviously, the amount of uncertainty in the results should be as low as possible.

The differences between the EAM method and MCFA is obvious if we compare Eqs. (8–11) to Eqs. (12–14). The process of determination of fuzzy weights is more complex in the case of MCFA, because it utilizes constrained fuzzy arithmetic. The process takes into account the relationships amongst fuzzy values in a pairwise comparison matrix and thus allows more precise determination of fuzzy weights which contain a significantly smaller amount of uncertainty (Krejčí et al. 2016).

Case Study

In the case study, the decision-making problem focused on land suitability assessment, composed of three main criteria, each with its set of subcriteria, is to be solved. The calculation follows the method of Urban Planner model for land suitability assessment introduced by Burian et al. (2015). The criteria are social (denoted A), economic (B) and ecological (C). The subcriteria are:

- surface aspect ($A1$), distance from nursery ($A2$), distance from primary school ($A3$), distance from health facilities ($A4$), distance from public spaces ($A5$), distance from bus stop ($A6$), distance from train stop ($A7$), air quality ($A8$), noiselessness ($A9$), radon risk ($A10$),
- surface slope ($B1$), distance from power supply ($B2$), distance from water supply ($B3$), distance from gas pipeline ($B4$), distance from sewer system ($B5$), distance from roads ($B6$), flooded areas ($B7$), geological risks ($B8$), protection of transport infrastructure ($B9$), protection of technical infrastructure ($B10$),
- water protection ($C1$), nature and landscape protection ($C2$), mineral resources protection ($C3$), farmland and forest protection ($C4$).

Altogether, these criteria, subcriteria and the main goal form a four-level fuzzy AHP problem that has one main goal (optimal land use). There are three criteria on the second level of fuzzy AHP, 27 subcriteria on the third level and the alternatives are on level four. The pairwise comparison matrices are shown in Tables 2, 3 and 4.

For the testing calculations, data from analytical material used for planning (Burian et al. 2016) by the city of Olomouc (The Czech Republic) were used. The data were in raster format with each layer representing the evaluation of alternatives (cells) for one subcriteria. The data was on a scale from 0 (absolute unsuitability), through 5 (average suitability) to 9 (the highest suitability). Every raster layer has 2,502,330 cells (1745 × 1434) with cell size 10 m.

All the calculations in this chapter were performed using a fuzzyAHP package for R (Caha and Drážná 2016). The package provides methods for the representation of fuzzy pairwise comparison matrices, consistency validation and weights determination, using several algorithms: Chang (1996), Tesfamariam and Sadiq (2006), Wang et al. (2008) and Krejčí et al. (2016) and also overall fuzzy AHP calculations.

Based on pairwise comparison matrices, the weights of each criterion and subcriterion were calculated. To show the differences in the methods, the values of fuzzy weights and weights vectors obtained from EAM, and fuzzy weights from MCFA were compared.

The resulting weights, as calculated using both methods, are shown in Table 5. The issues mentioned previously are clearly visible in the outcomes. For some subcriteria of social and economic criteria, the weight vector determined by EAM is

Table 2 Fuzzy pairwise comparison matrix of social subcriteria (consistency ratio 0.079)

	A1	A2	A3	A4	A5	A6	A7	A8	A9	A10
A1	[1;1;1]	[1/5;1/2;1/2]	[1/5;1/2;1/2]	[1/6;1/2;1/2]	[2;4;4]	[1;3;3]	[1;3;3]	[1/4;1/3;1/2]	[1/7;1/6;1/5]	[1/4;1/3;1/2]
A2		[1;1;1]	[1/3;1/2;1]	[1;3;4]	[1;4;4]	[2;2;3]	[2;3;4]	[1/6;1/4;1/2]	[1/7;1/6;1/5]	[1/5;1/4;1/3]
A3			[1;1;1]	[2;4;4]	[2;4;4]	[2;3;4]	[2;3;4]	[1/4;1/3;1/2]	[1/7;1/6;1/5]	[1/4;1/3;1/3]
A4				[1;1;1]	[1/4;1/3;3]	[1/4;1/2;2]	[1/3;1/2;2]	[1/7;1/3;1]	[1/9;1/7;1/3]	[1/8;1/7;1/6]
A5					[1;1;1]	[1/4;1/3;1/2]	[1/3;1/2;1]	[1/5;1/4;1/4]	[1/8;1/7;1/6]	[1/5;1/4;1/3]
A6						[1;1;1]	[1/2;1;2]	[1/6;1/5;1/4]	[1/9;1/8;1/7]	[1/6;1/5;1/4]
A7							[1;1;1]	[1/6;1/5;1/4]	[1/9;1/8;1/7]	[1/6;1/5;1/4]
A8								[1;1;1]	[1/3;1/2;1]	[1/2;1;2]
A9									[1;1;1]	[1/2;1;2]
A10										[1;1;1]

Table 3 Fuzzy pairwise comparison matrix of economical subcriteria (consistency ration 0.051)

	B1	**B2**	**B3**	**B4**	**B5**	**B6**	**B7**	**B8**	**B9**	**B10**
B1	[1;1;1]	[1/7;1/6;1/5]	[1/8;1/6;1/6]	[1/4;1/3;1/2]	[1/5;1/4;1/3]	[1/8;1/7;1/6]	[1/9;1/8;1/8]	[1/8;1/7;1/5]	[1/5;1/3;1/3]	[1/8;1/7;1/6]
B2		[1;1;1]	[1/2;1;1]	[3;4;5]	[1;2;3]	[1/3;1/2;1/2]	[1/7;1/5;1/5]	[1/4;1/3;1/2]	[1;2;3]	[1/4;1/3;1/2]
B3			[1;1;1]	[4;4;5]	[2;3;5]	[1/3;1/2;1]	[1/7;1/5;1/5]	[1/4;1/3;1/3]	[1;2;3]	[1/4;1/3;1/2]
B4				[1;1;1]	[1/3;1/2;1]	[1/5;1/4;1/3]	[1/7;1/7;1/5]	[1/7;1/6;1/5]	[1/3;1/2;1]	[1/7;1/6;1/5]
B5					[1;1;1]	[1/4;1/3;1/2]	[1/8;1/7;1/6]	[1/6;1/5;1/4]	[1/2;1;2]	[1/6;1/5;1/4]
B6						[1;1;1]	[1/8;1/6;1/4]	[1/4;1/3;1/2]	[2;3;4]	[1/4;1/3;1/2]
B7							[1;1;1]	[1;2;5]	[6;7;8]	[1;2;3]
B8								[1;1;1]	[4;5;6]	[1/2;1;2]
B9									[1;1;1]	[1/2;1;2]
B10										[1;1;1]

Table 4 Fuzzy pairwise comparison matrices of ecological subcriteria (left) and criteria (right) (consistency ratios 0.045 and 0.000)

	C1	C2	C3	C4		A	B	C
C1	[1;1;1]	[1/2;2;3]	[1/2;1;2]	[1/2;1;3]	**A**	[1;1;1]	[1/2;1;2]	[1/2;1;2]
C2		[1;1;1]	[1/2;1;2]	[1;1;3]	**B**		[1;1;1]	[1/2;1;2]
C3			[1;1;1]	[1/5;2;3]	**C**			[1;1;1]
C4				[1;1;1]				

zero, meaning that these elements will have no impact on the result whatsoever. The issue is problematic, even if the influence of these subcriteria is small, as their weight is low, they should still contribute to the result. It is not possible to leave those subcriteria out of the MCDM problem. Wang et al. (2008) clearly showed that the application of a weight vector calculated by EAM might lead to wrong decisions being made and they warned about the misapplication of the method. Despite that, studies have been conducted that are affected by this problem, such as Nazari et al. (2012) and Pazand et al. (2014). The second issue is related to the amount of uncertainty in estimated fuzzy weights. If we look at fuzzy weights estimated by EAM and compare them with weights calculated using MCFA, we can see that the EAM weights are significantly wider. The difference between $w_i3 - w_i1$ is always smaller for MCFA. The narrower fuzzy weights are the preferable solution as they contain less uncertainty (Krejčí et al. 2016), e.g. the weight of social criterion. The $w_A3 - w_A1$ for EAM is 0.7 while it is only 0.2976 for MCFA, which is less than half the size. The difference is caused by the utilization of constraint arithmetic in MCFA and it is the appropriate solution for the estimation of weights in fuzzy AHP (Krejčí et al. 2016).

With the weights calculated, it is possible to calculate the results of the fuzzy AHP using Eg. (7). For the defuzzification, Eq. (6) was used. The results are summarized in graphs in Fig. 2. The graphs clearly show the differences in the results. The violin plots describe how fuzzy weights from the EAM method overestimate the amount of uncertainty in the outcome and because of that, even the defuzzified values are shifted towards higher values. This change in the resulting suitability values is highly undesirable as it does not allow comparison with other methods. The differences between MCFA and EAM (weight vector) are also clearly visible from Fig. 2. MFCA have more values relatively close to the modal value and few values on both extremes. EAM on the other hand, has more equally distributed values that are smaller than MCFA values. Figure 3 shows the difference in the spatial arrangement of values. The detailed image clearly shows the differences caused by weighted vector zero values determined by EAM. Even though the general spatial patterns are relatively similar if we consider the scale of the whole city, there are significant differences in bigger scales. Figure 3 shows significantly lower suitability values around streets for the result obtained by EAM.

Table 5 Weights for all criteria and subcriteria determined by both methods

	EAM—fuzzy weights	EAM—weight vector	MCFA—fuzzy weights
A	[0.1333;0.3333;0.8333]	0.3333	[0.1958;0.3333;0.4934]
B	[0.1333;0.3333;0.8333]	0.3333	[0.1958;0.3333;0.4934]
C	[0.1333;0.3333;0.8333]	0.3333	[0.1958;0.3333;0.4934]
A1	[0.0238;0.0692;0.1018]	0	[0.0268;0.0556;0.0666]
A2	[0.0377;0.0838;0.1712]	0.0323	[0.0428;0.0692;0.109]
A3	[0.0484;0.1029;0.1935]	0.0756	[0.0586;0.0903;0.1248]
A4	[0.018;0.0287;0.1263]	0	[0.0194;0.0282;0.0833]
A5	[0.0122;0.0323;0.0687]	0	[0.0178;0.0274;0.0479]
A6	[0.0205;0.0451;0.1014]	0	[0.0241;0.0376;0.0599]
A7	[0.0164;0.039;0.0865]	0	[0.0218;0.0347;0.0567]
A8	[0.0797;0.153;0.3121]	0.2314	[0.1088;0.1683;0.2482]
A9	[0.155;0.2697;0.4607]	0.4034	[0.2106;0.2924;0.3602]
A10	[0.1033;0.1763;0.3195]	0.2573	[0.1389;0.1963;0.2704]
B1	[0.0091;0.0139;0.0201]	0	[0.0121;0.0156;0.0187]
B2	[0.0474;0.086;0.1363]	0	[0.0455;0.0709;0.089]
B3	[0.0607;0.0909;0.1636]	0.0112	[0.0549;0.0739;0.1045]
B4	[0.0178;0.0308;0.0535]	0	[0.0197;0.026;0.036]
B5	[0.0256;0.0481;0.0859]	0	[0.026;0.0388;0.0565]
B6	[0.0669;0.113;0.1838]	0.0683	[0.068;0.0944;0.1287]
B7	[0.1595;0.2475;0.3958]	0.4468	[0.2271;0.2949;0.3738]
B8	[0.1014;0.1708;0.2702]	0.2638	[0.1244;0.1833;0.246]
B9	[0.0274;0.0479;0.1]	0	[0.0302;0.0461;0.0753]
B10	[0.0886;0.151;0.245]	0.2099	[0.1051;0.1561;0.2189]
C1	[0.0735;0.2941;0.9441]	0.2628	[0.1334;0.2929;0.4574]
C2	[0.0833;0.2059;0.8392]	0.2357	[0.1391;0.2071;0.4158]
C3	[0.0647;0.2941;0.8392]	0.2628	[0.1031;0.2929;0.4269]
C4	[0.0588;0.2059;0.9441]	0.2386	[0.095;0.2071;0.4118]

The MCFA method described by Krejčí et al. (2016) clearly provides more suitable outcomes that reflect all the input data. The same cannot be said of the EAM method, as this method assigned zero value to the weight vector for ten subcriteria, effectively leaving these criteria out of the analysis. Not only are some criteria left out, but the weights of some other criteria are overestimated when the weight vector values are normalized. This may cause severe problems, as some solutions will obtain a high valuation due to good scores in only a few criteria. Based on these findings, the Extent Analysis Method should be considered unreliable and should not be used for solving AHP, not only within GIS but also in other fields. The problems seen in the case study correspond to the problems with the EAM method described by Wang et al. (2008).

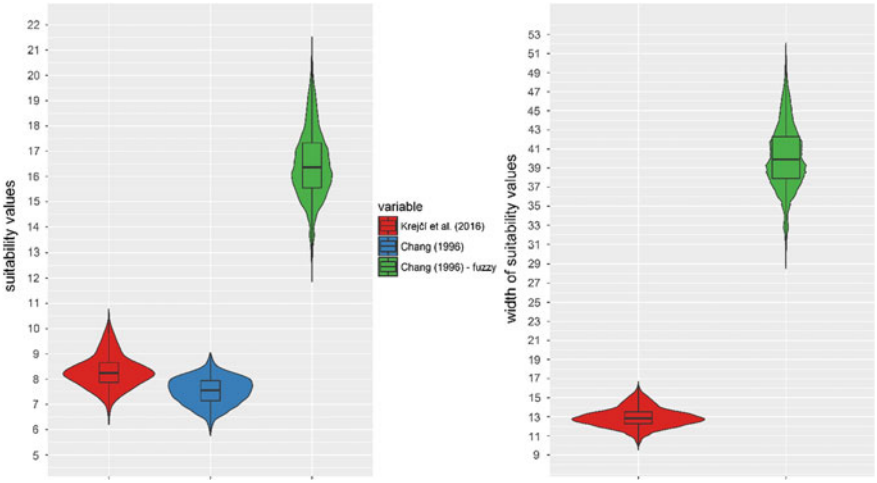

Fig. 2 Violin plots combined with box plots of calculated defuzzified suitability values (*left*) and width of fuzzy suitability values (*right*)

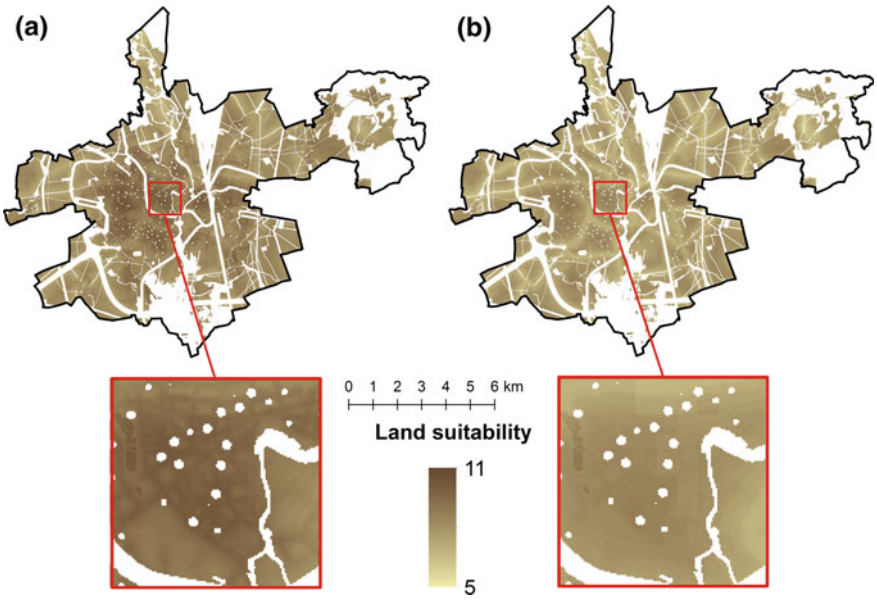

Fig. 3 Defuzzified result of MFCA (**a**) and weight vector result of EAM (**b**)

Conclusions

In this paper, we compared two methods for the calculation of criteria weights in fuzzy AHP. The Extent Analysis Method (EAM) is often used in practical studies, but it has several serious issues that have been described by Wang et al. (2008). We managed to verify the problems that can occur with the use of EAM as in the spatial fuzzy AHP problem that was used to assess the suitability of land for development. Besides testing the well-known method, we also tested a new method based on constrained fuzzy arithmetic (MCFA). The results of the case study calculated by those two methods were compared and analysed.

Unlike EAM which, by design, does not propagate the uncertainty of pairwise comparison matrices to the result of fuzzy AHP, as it provides a crisp weight vector, MCFA provides results in the form of fuzzy numbers that contain uncertainty. So it is up to the user to decide how to process the uncertainty of results. For example, the user can analyse the amount of uncertainty and select the appropriate defuzzification method, etc. While it is possible to obtain fuzzy results from the EAM method we have shown that the outcomes are unsuitable for any processing because the method significantly overestimates the amount of uncertainty in criterion weights. The overestimation of weight uncertainty occurs when one ignores the fact that fuzzy pairwise comparisons are dependent variables, and that constrained fuzzy arithmetic needs to be used to obtain the proper estimation of fuzzy weights (Krejčí et al. 2016). Based on those arguments the MCFA method proposed by Krejčí et al. (2016) can be recommended for spatial problems which should be solved using fuzzy AHP.

We tried to find why the EAM method proposed by Chang (1996) is used so often, not only in the GIS field, but in other fields as well. It seems that the reason could lie in the number of citations that Chang's publication has—over 1200 in SCOPUS. While the work of Wang et al. (2008) that describes the inappropriateness of EAM is significantly less known—just over 200 citations in SCOPUS. The work of Krejčí et al. (2016) is very recent and so far has no citations. The number of citations might be the reason Chang's method is more commonly used than other methods as a solution for fuzzy AHP.

This case illustrates the current situation in the GIS field, in which outdated approaches and methods are sometimes used for significant periods of time with no reflection on new trends and developments in the fields from which the methods were acquired. However, this deficiency may negatively affect the outcomes, and in the case of decision-making it may cause problems. To avoid the mentioned issues, it is necessary to continuously update the methods used in GIS by acquiring new knowledge from other fields.

Acknowledgements The paper was supported by Internal Grant Agency of Palacký University Olomouc (project IGA_PrF_2016_008—Advanced monitoring, spatial analysis and visualization of urban landscape) and by the ERASMUS + project no. 2016-1-CZ01-KA203-024040.

References

Banai, R. (1993). Fuzziness in geographical information systems: Contributions from the analytic hierarchy process. *International Journal of Geographical Information Systems, 7*(4), 315–329.

Barzilai, J. (1997). Deriving weights from pairwise comparison matrices. *The Journal of the Operational Research Society, 48*(12), 1226–1232.

Burian, J., Brychtova, A., Vavra, A., & Hladisova, B. (2016). Analytical material for planning in Olomouc, Czech Republic. *Journal of Maps, 12*(4), 649–654.

Burian, J., Stastny, S., Brus, J., Pechanec, V., & Vozenilek, V. (2015). Urban planner: Model for optimal land use scenario modelling. *GEOGRAFIE, 120*(3), 330–353.

Caha, J., & Drážná, A. (2016). Examples of FuzzyAHP package application (ver. 0.8.0). Retrieved from https://cran.r-project.org/web/packages/FuzzyAHP/vignettes/examples.html [28. 11. 2016].

Chandio, I. A., Matori, A. N. B., WanYusof, K. B., Talpur, M. A. H., Balogun, A. L., & Lawal, D. U. (2013). GIS-based analytic hierarchy process as a multicriteria decision analysis instrument: A review. *Arabian Journal of Geosciences, 6*(8), 3059–3066.

Chang, D.-Y. (1996). Applications of the extent analysis method on fuzzy AHP. *European Journal of Operational Research, 95*(3), 649–655.

Du, X., Zhou, K., Cui, Y., Wang, J., Zhang, N., & Sun, W. (2016). Application of fuzzy analytical hierarchy process (AHP) and prediction-area (P-A) plot for mineral prospectivity mapping: A case study from the Dananhu metallogenic belt, Xinjiang, NW China. *Arabian Journal of Geosciences, 9*(4).

Elaalem, M., Comber, A., & Fisher, P. (2011). A comparison of fuzzy AHP and ideal point methods for evaluating land suitability. *Transactions in GIS, 15*(3), 329–346.

Feizizadeh, B., & Blaschke, T. (2013). GIS-multicriteria decision analysis for landslide susceptibility mapping: Comparing three methods for the Urmia lake basin, Iran. *Natural Hazards, 65*(3), 2105–2128.

Feizizadeh, B., Shadman Roodposhti, M., Jankowski, P., & Blaschke, T. (2014). A GIS-based extended fuzzy multi-criteria evaluation for landslide susceptibility mapping. *Computers & Geosciences, 73,* 208–221.

Hanss, M. (2005). *Applied fuzzy arithmetic: An introduction with engineering applications*. Berlin, New York: Springer.

Hopkins, L. D. (1977). Methods for generating land suitability maps: A comparative evaluation. *Journal of the American Institute of Planners, 43*(4), 386–400.

Ishizaka, A., & Lusti, M. (2006). How to derive priorities in AHP: A comparative study. *Central European Journal of Operations Research, 14*(4), 387–400.

Jankowski, P. (1995). Integrating geographical information systems and multiple criteria decision-making methods. *International Journal of Geographical Information Systems, 9*(3), 251–273.

Klir, G. J., & Pan, Y. (1998). Constrained fuzzy arithmetic: Basic questions and some answers. *Soft Computing—A Fusion of Foundations, Methodologies and Applications, 2*(2), 100–108.

Krejčí, J., Pavlačka, O., & Talašová, J. (2016). A fuzzy extension of analytic hierarchy process based on the constrained fuzzy arithmetic. *Fuzzy Optimization and Decision Making, 16*(1), 89–110.

Nazari, A., Salarirad, M. M., & Bazzazi, A. A. (2012). Landfill site selection by decision-making tools based on fuzzy multi-attribute decision-making method. *Environmental Earth Sciences, 65*(6), 1631–1642.

Pazand, K., Hezarkhani, A., & Ghanbari, Y. (2014). Fuzzy analytical hierarchy process and GIS for predictive Cu porphyry potential mapping: A case study in Ahar-Arasbaran Zone (NW, Iran). *Arabian Journal of Geosciences, 7*(1), 241–251.

Saaty, T. L., & Tran, L. T. (2007). On the invalidity of fuzzifying numerical judgments in the analytic hierarchy process. *Mathematical and Computer Modelling, 46*(7–8), 962–975.

Tesfamariam, S., & Sadiq, R. (2006). Risk-based environmental decision-making using fuzzy analytic hierarchy process (F-AHP). *Stochastic Environmental Research and Risk Assessment, 21*(1), 35–50.

van Laarhoven, P. J. M., & Pedrycz, W. (1983). A fuzzy extension of Saaty's priority theory. *Fuzzy Sets and Systems, 11*(1), 229–241.

Wang, Y. M., Luo, Y., & Hua, Z. (2008). On the extent analysis method for fuzzy AHP and its applications. *European Journal of Operational Research, 186*(2), 735–747.

Project Catastrum Grenzsteine—State of the Art in Czechia

Václav Čada and Ondřej Dudáček

Abstract This paper summarizes information on project Catastrum Grenzsteine and its state of the art in Czechia. Project Catastrum Grenzsteine aims at submitting selected historical boundary marks and related infrastructure for the UNESCO World Heritage title. Reasons for this proposal—example of continuity of administrative units, example of technical knowledge, etc.—are given briefly while the rest of the paper presents several researches that have already been accomplished in this scope—reconstruction of boundaries of former administrative units is based on written documentation of former cadastres. Classification of boundary lines expressing probability of the presence of historical boundary marks is based on analyses of landscape and coincidence of former boundaries. Finally, the web application for crowdsourcing of historical boundary marks data is described.

Keywords Boundary · Boundary mark · Cadastre · UNESCO · Cultural heritage

Introduction

Since ancient history, administrative unit (e.g. municipality, dominion) and real property boundaries have been marked in a landscape. Former administrative units were often bordered by natural landmarks such as gullies, ravines or chines. On the other hand, boundaries were frequently marked with artificial boundary marks. Ditches, walls, heaps and boundary stones (either hewn or unhewn) were used as artificial boundary marks. Nowadays, when such a boundary mark is found, it is most probable that the mark was fitted in place from 16th to 19th century (Fig. 1).

V. Čada (✉) · O. Dudáček
Department of Geomatics, Faculty of Applied Sciences,
University of West Bohemia, Technická 8, Pilsen, Czech Republic
e-mail: cada@kgm.zcu.cz

O. Dudáček
e-mail: odudacek@kgm.zcu.cz

I. Ivan et al. (eds.), *Dynamics in GIscience*, Lecture Notes in Geoinformation and Cartography, DOI 10.1007/978-3-319-61297-3_4

Fig. 1 Example of boundary mark (year 1821)

Historical boundaries and boundary marks are unique evidence of ownership, relations among neighbouring landowners and ownership rights. Historical boundary marks and related documentation present also worthy evidence of the level of technical knowledge (especially of land survey) achieved by our ancestors. Design of some boundary marks illustrates the fortune of neighbouring owners and might be an artwork by itself.

Moreover, in many cases ancient boundary marks illustrate continuity of administrative units through history up to present. In the Czech Republic, cadastre maps of the majority of cadastre units are digitized from analogue maps with fathom scale. Therefore historical boundary marks might be used for making up the transformation key.

Project Catastrum Grenzsteine

The Austrian Society for Surveying and Geoinformation (ASG) initiated the project which goal is to submit "Boundaries and Boundary Marks" for the UNESCO World Heritage title. Boundary marks significant for their shape, history or location, important monuments of triangulation network and even domiciles of the most important historical institutions responsible for land survey and registry (e.g. Austrian Military Geographic Institute) should be selected and proposed for the UNESCO World Heritage Title (Waldhauesl et al. 2015).

UNESCO specifies several criterions for submitting for World Heritage Title. It is assumed that the project "Boundaries and Boundary marks" will aim at following criterions (UNESCO 2016).

- Criterion II: "To exhibit an important interchange of human values, over a span of time or within a cultural area of the world, on developments in architecture or technology, monumental arts, town-planning or landscape design."

- Criterion IV: "To be an outstanding example of a type of building, architectural or technological ensemble or landscape which illustrates (a) significant stage(s) in human history."
- Criterion VI: "To be directly or tangibly associated with events or living traditions, with ideas, or with beliefs, with artistic and literary works of outstanding universal significance. (The Committee considers that this criterion should preferably be used in conjunction with other criteria)."

This project was internationally presented to other states, especially those that were united in Austro-Hungarian Empire, and a possibility of joining this project was offered. Namely in Czechia, the project was presented by professor Waldhaeusl (ASG) at the ISPRS 2016—XXIII ISPRS Congress in Prague. Czech Office for Surveying, Mapping and Cadastre being informed about the project and expressed its endorsement. So did the Czech Union of Surveyors and Cartographers.

Czech partners can contribute to the project because the idea of protection of historical boundary marks as a cultural heritage is not new in Czechia. Several boundary marks are already protected by the National Heritage Institute. Boundaries of former administrative units were reconstructed and the presence of historical boundary marks were analysed in a sample area. Results of these analyses were taken into account when designing the information system of former administrative units and web application for collecting historical boundary marks data.

Reconstruction of Boundaries of Former Administrative Units in a Sample Area

As a sample area a part of Bohemia where boundary changes of administrative units occurred was selected. Administrative units in this area have been reconstructed since the period of Berní rula (fax rule—from 1654). The sample area in this period consisted of Plzeňský region, Podbrdský region and Vltavský region.

History of Administrative Units in Bohemia Since the Middle of the Seventeenth Century

For better understanding of this section, administrative units have been stated with its equivalents according to the NUTS classification (Fig. 2). The content of this section briefly comprises the history of administrative units only in the extent needed for understanding following sections.

In the period of Berní rula (from 1654) the kingdom had four-level system of administrative units: kingdom (NUTS 0), region (NUTS 3), dominion (NUTS 4) and municipality (cadastre unit). The number of regions in the whole kingdom was

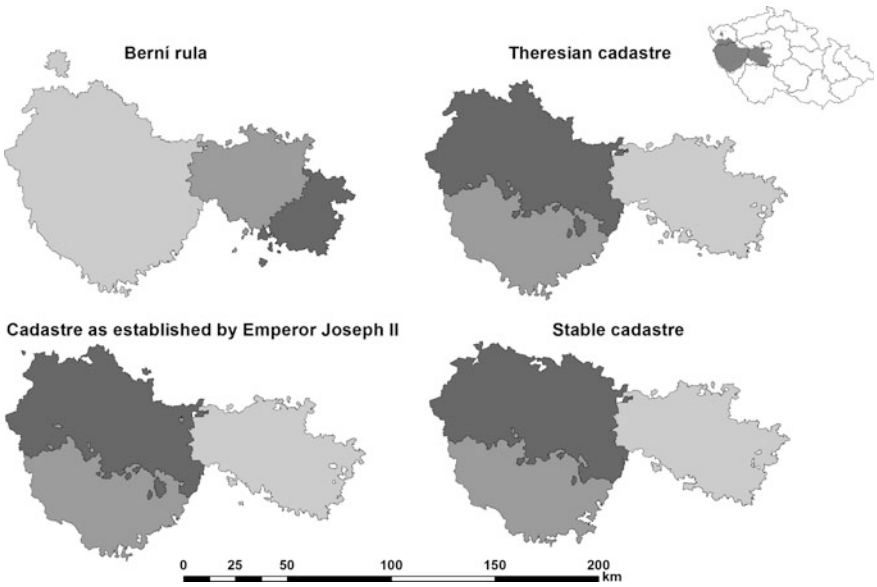

Fig. 2 Sample area

fifteen. A dominion was a basic administrative units composed from municipalities owned by the same owner. They often covered various areas among dominions and in some cases caused a discontinuity of dominion. It is clear that boundaries were often changed during this period according to changes of ownership.

In 1748 the Berní rula was replaced with the theresian cadastre. The four-level system of administrative units was preserved whereas boundaries changed. Bohemia was divided into sixteen regions in this period.

In 1789 the cadastre as established by Emperor Joseph II. came in force but after one year it was replaced by theresian cadastre and finaly in 1792 by theresian-joseph cadastre. It combined areas measured for cadastre as established by Emperor Joseph II. and fiscal preference of nobility of the theresian cadastre. Cadastral municipality was established as a new basic administrative unit being ranked between municipality and region.

Stable cadastre was established in the year 1817 according to the patent of Emperor Francis I. Former system od administrative units was replaced by another one in 1849 which is not an object of this analysis.

Reconstruction of Boundaries

Geometry of reconstructed boundaries is based on those registered in the real estate cadastre of the Czech Republic in vector form and also in written documentation of

former land registries mentioned in previous section. The content of both types of documentation was digitized and stored in a database.

The content of Berní rula written documentation was published in 1950s in publications (Doskočil 1953a, b). Dominions were ordered by regions and a list of theirs municipalities was stated for each dominion. These publications were digitized via OCR text recognition.

The content of theresian cadastre was taken inventory in 1989. Dominions were sorted by regions and ordered alphabetically. List of its municipalities was stated for each dominion. Analogous inventory was made for cadastre as established by Emperor Joseph II. These inventories were digitized manually because of their quality is not suitable for scanning and OCR text recognition. Information on administrative units of stable cadastre are noted as marginal information in maps of stable cadastre.

Once the data are stored in database it is possible to find matching municipalities through all periods, connect them through relations and reconstruct approximate boundaries using boundaries of the real estate cadastre of the Czech Republic or, if available in vector format, on boundaries of stable cadastre or cadastre of lands. When using relations in the database it is possible to derive information on all administrative units limited by given boundary line (Nováková 2006).

The most notable disadvantage of presented reconstruction is the presumption that former boundary lines were coincident with boundary lines of the real estate cadastre of Czech Republic. Even that this presumption is mostly valid it is still necessary to notify that such a boundary line might be an exception.

Analysis of the Presence of Historical Boundary Marks

Analysis of the presence of historical boundary marks described below offered some important results. Input data for this analysis is boundary layer with information on coincident boundaries of former administrative units (see previous section) and selected landscape layers—forest land, water streams, water bodies and marsh.

The main idea of the analysis is to split boundary lines into segments with similar probability of the presence of historical boundary marks. This probability depends on various factors, first of all on the land use in the area of interest. It is assumed that historical boundary marks in areas with high exploitation (such as fields) are not preserved whereas boundary marks in areas in relatively stable areas (such as forests) are preserved. It is also known that banks of water streams and bodies were often used as a natural boundaries. Therefor there is a low probability of the presence of artificial boundary marks. Another factor is the importance of examined boundary, e.g. it is more probable that a boundary of dominium that occurred through all periods was marked with artificial boundary marks than boundary of municipality that occurred only in one period (Nováková 2008).

Classification of Boundary Lines

Boundary lines of the cadastre units registered in the real estate cadastre of the Czech Republic are splitted into segments—each segment begins and ends at an intersection of three (alternatively four and more) neighbouring cadastre units. Each segment stores information on coincidence with other boundaries (Berní rula dominion, Berní rula region, theresian cadastre dominion, etc.) as an attribute.

An intersection with forest land layer is computed and this information is stored as an attribute. The intersection with water streams and bodies is also computed and stored as an attribute.

For each segment of boundaries coefficient of presence is counted according to following equation:

$$\begin{aligned} \text{coeff} = ((&2[\text{BR\_domi}] - [\text{BR\_do\_part}]) + (2[\text{TK\_domi}] - [\text{TK\_do\_part}]) \\ &+ (2[\text{JK\_domi}] - [\text{JK\_do\_part}]) + (2[\text{JK\_muni}] - [\text{JK\_mu\_part}]) \\ &+ (2[\text{SK\_domi}] - [\text{SK\_do\_part}]) + [\text{SK\_muni}] + [\text{Marsh}] \\ &+ 3([\text{Forest}]))([\text{Water\_stream}])([\text{Water\_body}]) \end{aligned} \tag{1}$$

Phenomena which correspond to the square brackets are explained in Table 1. Value of a square bracket is 0 if the given phenomenon doesn't occur or 1 if the given phenomenon occurs for boundaries and forest. Similarly 0 if given phenomenon occur or 1 if given phenomenon doesn't occurs for water stream, body and marsh.

Value of calculated coefficient lies between 0 and 15 (Fig. 3). The higher value, the higher probability of presence of boundary marks. When coefficients counted for boundary lines segments in sample area are analysed and confronted with actually found boundary marks, then can be noticed that 32% of boundary marks are in range 15–9, 85% in range 15–4 and 15% in range 4–0. Therefor it can be assumed that coefficient equation is well specified (Urbancová 2009).

Table 1 Explanation of equation (1)

Text in brackets	Phenomenon
BR	Berní rula
TK	Theresian cadastre
JK	Cadastre as established by Emperor Joseph II.
SK	Stable cadastre
_domi	Dominion boundary
_do_part	Uncertain dominion boundary
_muni	Cadastral municipality boundary
_mu_part	Uncertain cadastral municipality boundary
Forest	Forest
Water_stream	Water stream
Water_body	Water body
Marsh	Marsh

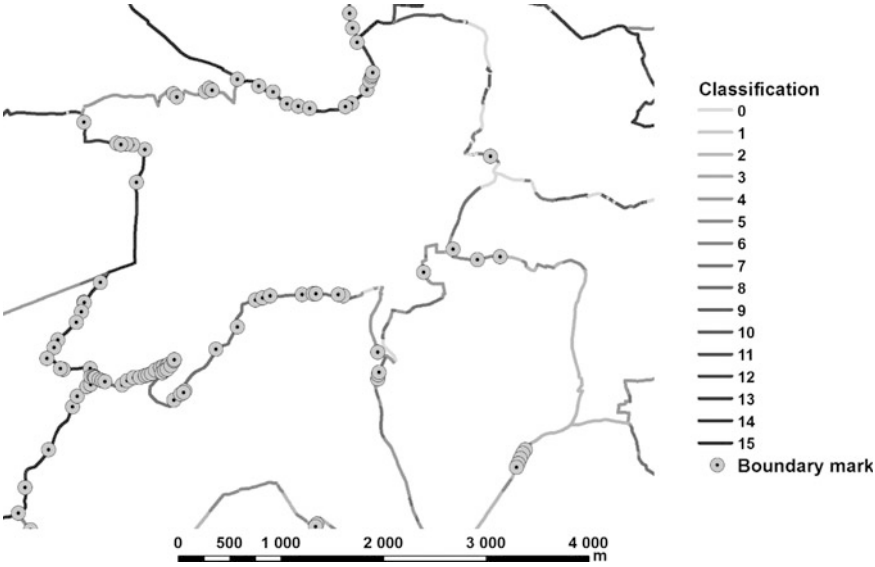

Fig. 3 Example of classification of boundary lines and boundary marks found

Created layer of classified boundary segments, especially when published as WMS or similar service, allowing creation of various map meshups, can be useful for users when searching for historical boundary marks on boundaries of cadastre units.

Web Application for Collecting Historical Boundary Marks Data

Application for collecting historical boundary marks data includes web interface implemented in PHP and JavaScript and a database that communicates with the web interface. Information required for uploading boundary mark via web interface are codes of neighbouring cadastre units, coordinates in S-JTSK coordinate system, type of the boundary mark, date of the day when the boundary mark was found and of the day when it was surveyed. Last required information is the name of uploader.

Some facultative information can be added to this required information: height of the boundary mark (in Baltic Vertical Datum—After Adjustment), quality code of the mark, identification number of the mark, assumed year/period when the mark was fitted in place, description of the mark, photography and contact to uploader. Upload from file is also supported. In such a case the marks can differ only in coordinates and identification numbers.

Other functionalities are searching for boundary marks in dependence on cadastre unit, coordinates or type, printout of all boundary marks stored in database and visualization of the boundary marks in a map (Urbancová 2009).

The main purpose of this application was collecting data about boundary marks along boundaries of cadastre units during the process of digitizing of analogue cadastral maps. Presently, the application is not accessible for the public because it is obvious that it has to be optimized for its new purpose—crowdsourcing of data about boundary marks with unique historical and cultural importance. Several ways how to optimize this application for new purpose are mentioned in following list. New application should:

- be international while the current version is Czech only,
- support an international coordinate system (possibly WGS-84) or more national systems with possibility of transformation into selected system,
- store accuracy information on the coordinates (when crowdsourced a lot of boundary marks probably won´t be measured with geodetic equipment),
- support editing of existing data record,
- support more complex database queries such as searching boundary marks on given proximity from selected location,
- attract more attention through the attractive interface and additional content such is related law explanation, 3D visualisation etc.

Conclusion

Project Catastrum Grenzsteine presents the unique opportunity with international significance that can protect the most important monuments of land survey in former Austro-Hungarian Empire. Moreover this project can popularise land survey on its own, its importance and its contribution to the society (peaceful and legally guaranteed real estate ownership and others).

State of the art of the evidence of historical boundary marks in Czechia takes advantage of experiences that was gathered in forepassed years. Common characteristic of presented works is that their primary purpose was utilisation during the digitizing analogue cadastral maps which does not mean that they cannot be used for newly arisen purpose. Presented analyse of the presence of historical boundary marks provides valuable concept of workflow that allows to optimize field works and search for historical boundary marks more effectively. Classified boundary lines can be easily used to highline important historical boundaries where the probability of presence of unique historical boundary marks is relatively higher. The database of already found boundary marks can be examined and extraordinary boundary marks can be selected for project Catastrum Grenzsteine. Gathered knowledge and expertise should be valuable contributions to this project.

References

Doskočil, K. (1953a). Berní Rula 2—Popis Čech r. 1654. Souhrnný index obcí, osad a samot k berní rule. 1.díl. Státní pedagogické nakladatelství, Prague, (in Czech).

Doskočil, K. (1953b). Berní Rula 2—Popis Čech r. 1654. Souhrnný index obcí, osad a samot k berní rule. 2.díl. Státní pedagogické nakladatelství, Prague, (in Czech).

Nováková, M. (2006). Vývoj územně správního členění a dominií od pol. 17. stol. na vybraném území ČR. Bachelor thesis. University of West Bohemia. Faculty of Applied Sciences. Thesis supervisor Libuše Poustková, (in Czech).

Nováková, M. (2008). Analýza hraničních znaků při obnově katastrálního operátu). Diploma thesis. University of West Bohemia. Faculty of Applied Sciences. Thesis supervisor Václav Čada, (in Czech).

UNESCO World Heritage Centre. UNESCO World Heritage Centre—The criteria for selection <http://whc.unesco.org/en/criteria/>, 25. 11. 2016.

Urbancová, L. (2009). Informační system pro evidenci hraničních znaků. Diploma thesis. University of West Bohemia. Faculty of Applied Sciences. Thesis supervisor Václav Čada, (in Czech).

Waldhauesl, P., Koenig, H., & Mansberger, R. (2015). Boundary and Boundary Marks Substantive Cultural Heritage of Extensive Importance. ISPRS Ann. Photogramm. Remote Sens. Spatial Inf. Sci., II-5-W3, 329–334.

Dynamics of Legal Changes in Polish Cadastre

Agnieszka Dawidowicz, Anna Klimach and Ryszard Źróbek

Abstract In more developed countries, contemporary cadastral system design is premised on the need for credibility, accuracy, timeliness, flexibility, completeness, and availability. Cadastral Systems as the official land information systems for the entire country operate on the basis of clearly defined principles contained in the legislation. Any need to modernize the system require changes in legislation. This paper focuses specifically on cadastral system flexibility, which stems directly from the dynamics of law. The method used to develop the approach is based upon dynamics of legal changes in the context of the international development concepts. The approach is then applied to the Polish cadastral system. It is found that a measure of real estate cadastre legal flexibility is it's ability to react to dynamic, changing rules and situation. Globally, this means that the proposed approach can be adopted to determine cadastral flexibility in terms of its legal framework.

Keywords Cadastre · Land administration system · System flexibility · Legal flexibility · Legal dynamic

Introduction

A range of factors have led to the development of new land administration concepts over the last two decades. Works by Enemark et al. (2005, 2014), Enemark (2010a, b), Williamson et al. (2010), Mitchell and Zevenbergen (2011), Dawidowicz and Źróbek (2012a, b) justify the need for concepts including Cadastre 2014, LADM, Cadastre 2034, and Cadastre 2.0. These concepts offer new functional solutions for land information systems. Accompanying these new functions are a range of system characteristics including credibility (guarantee 100% security of transactions without

A. Dawidowicz (✉) · A. Klimach · R. Źróbek
Department of Real Estate Resources, Faculty of Geodesy,
Geospatial and Civil Engineering, University of Warmia and Mazury
in Olsztyn, Prawochenskiego Street 15, 10-720 Olsztyn, Poland
e-mail: dawidowiczagnieszka@wp.pl

I. Ivan et al. (eds.), *Dynamics in GIscience*, Lecture Notes in Geoinformation and Cartography, DOI 10.1007/978-3-319-61297-3_5

the need for additional verification), accuracy (precision), timeliness, flexibility (suitability of the system to the needs of beneficiaries in terms of information content and form of organization and new functional concepts), the completeness (in terms of area and scope of the content) and availability (easy form of access to information for all users).

It is worth to emphasize the publication of Enemark et al. (2014) under the title Fit-For-Purpose Land Administration, where in the first place is mentioned on flexibility in the context of spatial data capture approaches to provide for varying use and occupation. According to the authors (Enemark et al. 2014) the approach used for building land administration systems in less developed countries should be flexible and focused on citizens' needs, such as providing security of tenure and control of land use, rather than focusing on top-end technical solutions and high accuracy surveys. The system flexibility turns out to be a strategic feature of the cadastral systems development.

Therefore, this paper focuses on flexibility. In this context, flexibility means the system must be capable of adapting to changing organizational needs and more importantly, broader societal needs. These goals can be complied not only by the technological modernization of the system, but most of all by identifying specific determinants in the legislation. We argue that flexibility of a system is conditioned by social and political support. The success of any project is therefore dependent not only of the essence of the underlying concept, technology or financial resources, but also the fundamental provisions in national law. Taken together, these factors are responsible for the flexibility of the system that is in full readiness for adaptation to a new functionality.

The more specific focus of the paper is on the need to determine a universal measure of flexibility. We propose a model for measuring flexibility in cadastral systems, especially legal flexibility within the meaning of legal changes dynamic.

The study shows the Polish legal activity, as a gauge of system flexibility will shows the Polish cadastral system's capacity for adaptation.

Materials and Methods

Formulating a methodology for testing the flexibility of the cadastre, the following assumptions and preconditions were adopted:

- 'flexibility' is defined as "easily adaptable to new conditions" in alignment with Polish Scientific Publisher dictionary (PWN http://sjp.pwn.pl/sjp/elastyczny;2556392 access 22.09.2016),
- 'legal flexibility' is defined as per Sobota (1991), Mills (2008), Wolff (2011) as 'continuous (current) adaptation of existing law or formulation of a new law to the new needs',
- 'legal dynamic' is defined as per Governatori and Rotolo (2015) as dynamic changes of the law,

– 'cadastre' is defined in alignment with Gaździcki (1995) spatial information systems definition as "interrelated elements or components, where each element represents the various aspects of the system." Hence, we propose a following algorithm:

Cadastral system = {C_1, C_2, C_3, C_4, C_5, C_6, C_7, C_8, C_9, C_{10}, C_{11}, C_{12}},
where: $\mathbf{C_1}$ Legal Framework, $\mathbf{C_2}$ Organizational framework, $\mathbf{C_3}$ Economy, $\mathbf{C_4}$ Model of reality, $\mathbf{C_5}$ Geodetic and cartographic works, $\mathbf{C_6}$ Data, $\mathbf{C_7}$ Functionality, $\mathbf{C_8}$ Procedures, $\mathbf{C_9}$ Technology, $\mathbf{C_{10}}$ Standards, $\mathbf{C_{11}}$ Staff, $\mathbf{C_{12}}$ System surroundings. These elements are shown in Fig. 1.

The adopted definition is compatible with the cadastre definitions formulated e.g. by Hensen (1995), UN/FIG (1996), FIG (1995, 1998) or Dale and McLaughlin (1999), where cadastre is defined by distinguishing characteristics of the system. Gaździcki's definition emphasizes the systemic factors: any associated study of the cadastral system's complex nature should be "comprehensive, taking into account

Fig. 1 Cadastre elements. *Source* Own study on the basis of Gaździcki (1995)

various aspects of the cadastral system and leading to the determination of the dominant factors in a given situation and the most important relationships between them" (Gaździcki 1995).

To examine the legal flexibility of Polish real estate cadastre focused the literature for determination of the global trends of cadastral systems development. Successively identified the current real estate cadastre legislation in Poland. Finally localized changes in Polish legislation relating to the real estate cadastre at the turn of the last twenty years and analyzed the legal flexibility in the context of development concepts.

Results and Discussion

Global Concepts of Cadastral Systems Development

Analysis of events and concepts of cadastral systems development have allowed to identify the key concepts in the field of cadastre development which were presented on the following timeline (Fig. 2):

Above concepts were developed among others in the following studies: (Molen, 2003; Lemmen et al. 2003; Lemmen and Oosterom van 2006, 2013; Kaufmann and Kaul 2004; Stoter et al. 2004; Steudler 2004; Laarakker 2008; Krelle and Rajabifard 2010; Kalantari et al. 2010; Williamson et al. 2010; Land 2011; Kaufmann 2012) (Enemark et al. 2014; FIG 1998, 1999, 2002, 2010, 2014; UN 2015; UN-ECE 1996, 2005a, 2005b; De Vries 2016; Shrestha et al. 2016).

Identified concepts presented in the above timeline were determined by several factors. They are grouped into three key areas: key organizations, key technology, civilization trends (Fig. 3).

The direction of cadastre development indicates to achieve in the first place benchmarks of "Cadastre 2014" and then "Cadastre 2.0" (Dawidowicz and Źrobek 2014) and assumes ultimately achieve the following benchmarks especially in the aspects of cadastral system technology:

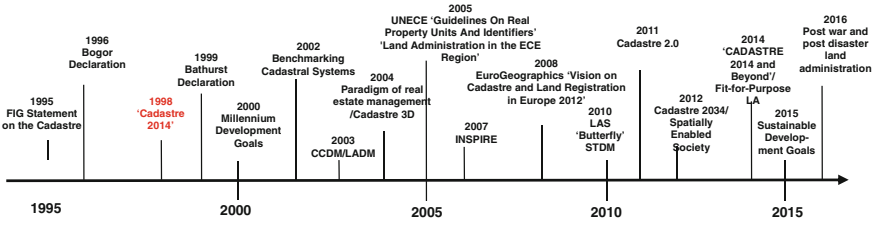

Fig. 2 A Global concepts on cadastre development. *Source* Own study

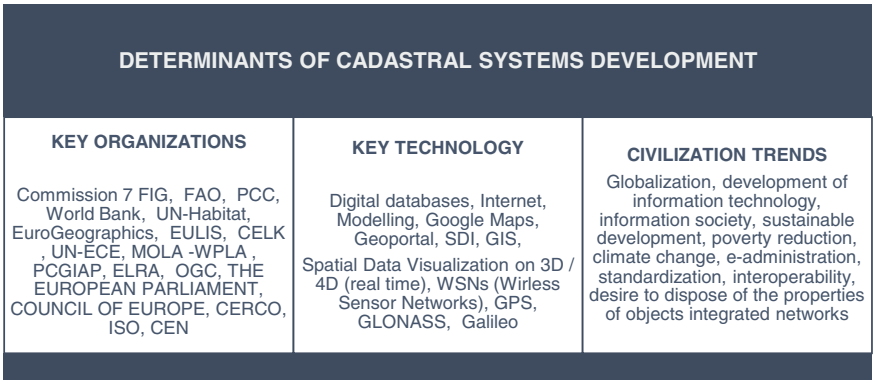

Fig. 3 Factors affecting the new concepts of cadastral systems development. *Source* Own study

- digital technology supply data (electronic data transmission), storing, updating and sharing;
- processes automation of data collection and updating;
- the software should allow integration of graphic and descriptive data, and imaging any content in any format (2D, 3D, 4D);
- inclusion of GIS technology to share cadastral data in spatial information infrastructure (SDI) and for open spatial analysis;
- mobile cadastre through mobile devices and desktop (such as mobile phones, tablets, notebooks and other);
- cadastre in Cloud Computing.

Current Real Estate Cadastre Legislation in Poland

This section synthesizes the results from the analysis of the current real estate cadastral legislation in Poland, along with the changes that have occurred since 1995. The legal basis for Polish real estate cadastre is set out in article 2 point 8 of Act of Geodesy and Cartography (1998).

Meanwhile, the basic legal provisions concerning the cadastre are included in the three major laws and two regulations:

- Act of 17 May 1989. Geodetic and Cartographic Law, (**number of changes: 47**),
- Act of 6 July 1982 on Land and Mortgage Register (**number of changes: 28**)
- Act of 4 March 2010 on Spatial Information Infrastructure (number of changes: 2), making the transposition of the INSPIRE Directive 2007/2/EC of the European Parliament and of the Council of 14 March 2007 establishing an Infrastructure for Spatial Information in the European Community (INSPIRE), (OJ. EU L 108, 25.04.2007, p. 1, as amended).

- Regulation of Regional Development and Construction Minister—29 March 2001 on the real estate cadastre (**number of changes: 2**),
- Regulation of the Minister of Administration and Digitization of 29 November 2013. Amending the regulation on the real estate cadastre.

In addition, the most important implementing rules in this area resulting from the Acts are:

1. Regulation of Council of Ministers of 17 July 2001 on the show in the real estate cadastre data relating to land, buildings and premises, located in enclosed areas,
2. Regulation of the Justice Minister of 21 November 2013 on the establishment and operation of land registers in a computer system (**number of changes: 4**, act repealed),
3. Regulation of the Minister of Administration and Digitization of 5 September 2013 on the organization and the mode of conducting the state geodetic and cartographic stock (act replaced the previous one),
4. Regulation of the Minister of Internal Affairs and Administration of 20 October 2010 on the register of databases and spatial data services covered by the infrastructures for spatial information,
5. Regulation of Council of Ministers of 17 January 2013 on the Integrated Real Estate Information System,
6. Regulation of the Minister of Administration and Digitization of 9 July 2014 concerning the making available materials of state geodetic and cartographic stock, licensing and the model of Document Fees Calculations,
7. Regulation of the Minister of Administration and Digitization of 8 July 2014 on the forms for notification surveying and cartographic works, notice of the execution of this works and transferring their results to the national geodetic and cartographic stock.

Further to the legislation and regulation, in 2003 the Surveyor General of Poland introduced the technical guidelines—Instructions G-5 "Real Estate Cadastre", recommended for use, but since 2013 the harmonization of data sets have occurred in accordance with the standard ISO 19152.

As part of the real estate cadastre convergence, tasks resulting from about 20 acts are included, the most significant of them are:

- on public road—Act of 21 March 1985 on public roads (**number of changes: 70**): the General Director for National Roads and Motorways, a central government body competent in matters of national roads has to cooperate with the authorities competent in the field of real estate cadastre in the range of exchange data on roads and transport culverts.
- water law—Act of 18 July 2001 Water Law (**number of changes: 51**): establishes the creation of a water cadastre with particular data of flowing and standing waters within the territory of the State harmonized with real estate cadastre.

- geological and mining law—Act of 9 June 2011 Geological and Mining Law (**number of changes: 22**): The areas covered by the extraction of minerals shall clearly indicate, regulate the legal status and record in the real estate cadastre.
- construction law—Act of 7 July 1994 Construction Law (**number of changes: 80**): In the real estate cadastre are recorded the data from documentation of building construction like: building design, construction log, protocols of partial and final acceptances, drawings and descriptions for implementing object, surveying logs, cadastral lists of changes in ground, book of measurements.
- on forests, Act of 28 September 1991 on forests (**number of changes: 59**): in the real estate cadastre are recorded the arrangements of forest management plans and simplified forest management plans relating to borders and areas of the forest.
- on Spatial Planning, Act of 27 March 2003 on Spatial Planning (**number of changes: 41**): Land use plans drawn up on the copy of the basic or cadastral map.
- on real estate management, Act of 21 August 1997 on land management (**number of changes: 86**) as part of the public real estate management, the minister competent in these matters leads, according to the real estate cadastre, suitable records designed for the needs of public entities.
- on the protection of agricultural and forest land, Act of 3 February 1995 on the protection of agricultural and forest land (number of changes: 30): For the purposes of this Act "agricultural land" is meaning as land defined in the real estate cadastre as farmland and on the non-agricultural and non-forest purposes can allocate land primarily indicated in the real estate cadastre as a wastelands, and in their absence - other land with the lowest production suitability.
- on public statistics, Act of 29 June 1995 on public statistics (**number of changes: 27**): in the real estate cadastre must be recorded the statistical identifiers of territorial division.

As it can be seen after analysis of Journal of Laws, most of the above acts and regulations have had their amendments or first notice in 2012–2014. This means that it is constantly updated law. Proof of this are especially subscriptions in the regulations of other public records related to the real estate cadastre in terms of their adjustment update. In this case, it can be concluded that the analysis of the current regulations in terms of their timing of announcements gives a first picture of the legal flexibility.

Results of Polish Cadastral System Legal Flexibility Analysis

All changes to the current Polish cadastre legislation presented in the previous chapter are relatively fresh and related to data harmonization and cooperation of national public information systems with the reference real estate cadastre system (Buśko and Meusz 2014) as well as interoperable work in spatial information infrastructure.

In response to the concept of Cadastre 2014 and the related studies significant changes were observed in the Polish law from 1999 to 2013. Especially since 1999 until 2007 observed changes in the law in order to achieve assumptions of Cadastre 2014. After 2007 INSPIRE Directive had a strong influence on the Polish law and the concept of Land Administration Domain Model (Bydłosz 2015).

Context of amendments to the provisions in the analyzed period was mainly:

- Digitization of real estate cadastral database and land and mortgage register,
- Adjusting the national legislation to the existing EU legislation, including the interoperability sets and spatial data services,
- Harmonization of the real estate cadastre sets with other data sets contained in the databases, including geodetic records of public utilities,
- Standardize the data sets contained in the local cadastral databases and creating through the sharing of these data on the principles specified in the Act of spatial information infrastructure.
- Refine and standardize the information collected in the Registry on prices and real estate values,
- Introduction of GML format as the format for exchange and sharing of cadastral data and data from registry on prices and real estate values,
- Development of rules for classifying land for specific types of arable land,
- Adaptation of owners groups and subgroups scheme to the Act on land management,
- Extension of the cadastral data summaries scope on soil science classes data.

After a careful examination the time to introduce these changes and the adoption of the new rules was dynamic and relatively short. Adaptation of a number of legal acts to technical and organizational changes in the real estate cadastre in two years seems to be smooth and flexible, taking into account the procedures for enacting legislation in Poland, which is presented on the diagram (Fig. 4).

There isn't established minimum or maximum period of legislation in Polish Constitution and Work regulations of the Seym and the Senate. For example, in 2012 in the procedure of introducing changes in the law or the adopting a new law lasted an average of 145 days (http://www.academia.edu/8168668/Analiza_dzia%C5%82alno%C5%9Bci_ustawodawczej_Sejmu_VI_kadeccji access 06.12.2014). It is period from first reading to third reading and for example the last change of Act of Geodesy and Cartography (the most important act for real estate cadastre) was made in 27 days (from first reading to third reading) (Fig. 5).

The above law draft was received on 6 May 2014, first reading was on 9 May 2014 and third reading was on 5 June. There were 57 days from receiving the bill to final signed it by President of Republic of Poland.

Dynamic reactions of Polish law as a response to the cadastral system modernization needs resulting from the global concept and development trends showed that the Polish legislation was and still is steady and in full readiness. In the past 27 years was introduced 77 new laws directly or indirectly on the Polish cadastral system development. At the same time introduced 47 amendments in the Geodesy

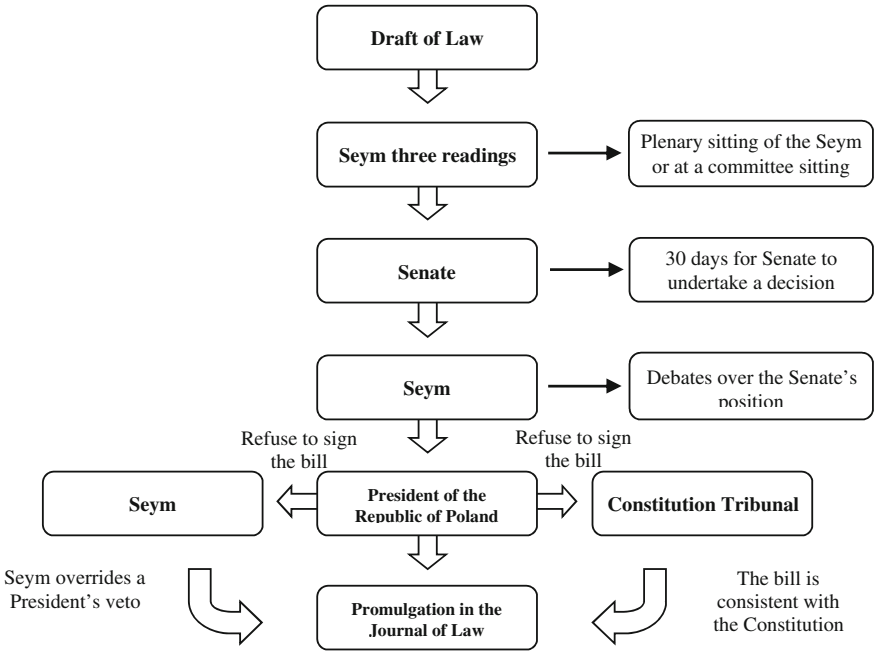

Fig. 4 Procedure for making changes in the law and the enacting the new law in Poland. *Source* Own study by the Polish Constitution of 2 April 1997 *and* Work regulations of the Seym and the Senate

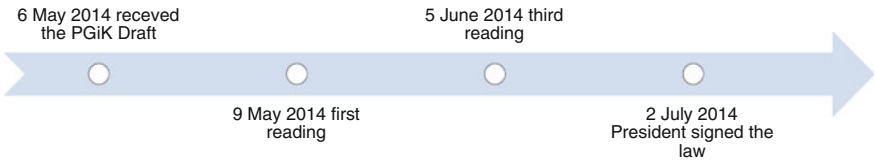

Fig. 5 Chronology of the procedure for adopting the last change in the Act of Geodesy and Cartography. *Source* Own study

and Cartography Act (Fig. 6). To examine the continuity of changes relating directly to cadastre in the Act of Geodesy and Cartography summarized and visualized the changes in this most important law for cadastre.

According to the definition of legal flexibility, where the determinant is the continuity of changes (the current regulation of the law as a response to the development activities), rather than jumping, can be observed unique legal flexibility for real estate cadastre. The graph (Fig. 6) shows the almost every year activity of the law. This activity visualization is a needed form of legal flexibility monitoring to improve the real estate cadastre.

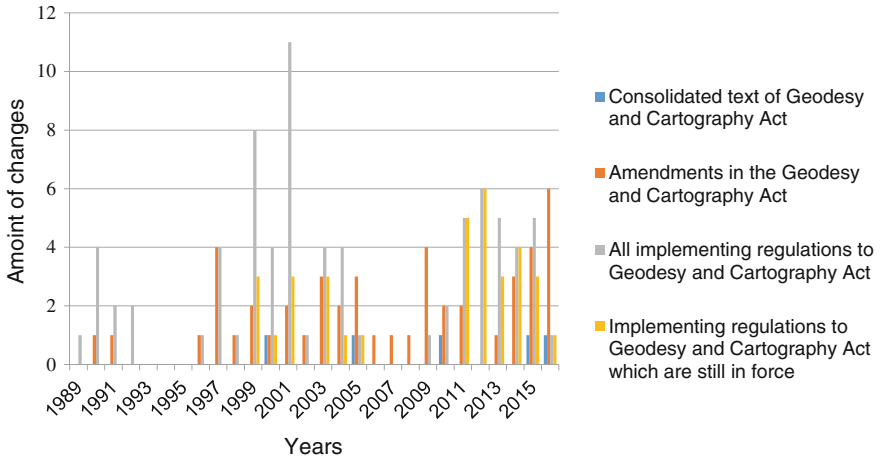

Fig. 6 Visualization of polish cadastre legal changes situation. *Source* Own study

There is a question after this analysis: "Is it possible to end the evolution of cadastral systems?"

Conclusions

In the context of the analyses can draw many relevant conclusions. First of all this analysis shows the potential of legal flexibility within the cadastral system in Poland. The provisions of law relating to real estate cadastre are regularly, dynamic updated and adapted to emerging needs and development trends. Changes in the law were the reaction to the emerging development concepts and guidelines of the European Union. The number and frequency of legislative amendments indicate the significant potential for cadastral system development in Poland. This means that the cadastral system is characterized by high flexibility. Polish cadastral system seeks to achieve determinants of "Cadastre 2014" and related concepts. The proposed approach can be adopted to determine the cadastre flexibility in terms of the legal framework and new concepts activity.

Systematic study of the legal flexibility of individual cadastral systems can give a picture of country development and help to quickly respond to political stalemate (economic) in terms of the system.

References

Buśko M, & Meusz A. (2014). *Current status of real estate cadastre in Poland with reference to historical conditions of different regions of the country*. 9th International Conference on Environmental Engineering (ICEE), Vilnius, Lithuania, 22–23 May 2014. doi:10.3846/enviro.2014.196, eISSN 2029-7092, eISBN 978-609-457-640-9. http://leidykla.vgtu.lt/conferences/ENVIRO_2014/Abstracts/5/196.html

Bydłosz, J. (2015). The application of the land administration domain model in building a country profile for the Polish cadastre. *Land Use Policy, 49,* 598–605.

Dale, P., & McLaughlin, J. (1999). *Land administration*. New York: Oxford University Press Inc.

Dawidowicz A., & Źrobek R. (2014). Analysis of concepts of cadastral system technological development. *Procedia Engineering*. eISSN2029-7092, eISBN978-609-457-640-9. doi:10.3846/enviro.2014.201, http://leidykla.vgtu.lt/conferences/ENVIRO_2014/Articles/5/201_Dawidowicz.pdf

Dawidowicz, A., & Źrobek, R. (2012a). Determination of the reference cadastral system benchmarks in the light of current research. *Journal of the Polish Real Estate Scientific Society, 20*(4), 5–17. http://www.tnn.org.pl/tnn/publik/20/TNN_tom_XX_4.pdf

Dawidowicz, A., & Źrobek, R. (2012b). *The evolving role of the cadastre in the land administration system in Poland,* FIG/FAO International Seminar State Land Management in Transitional Countries: Issues and Ways Forward, Budapest, Hungary, Ministry of Rural Development, 20–21 September 2012 pp. 1-13, Free access 30.06.2015 http://www.fig.net/resources/proceedings/2012/Hungary_2012_comm7/3.3_paper_dawidowcz_et_al.pdf

De Vries, W. T. (2016). *Post disaster consolidation of land, memory and identity*. International Federation of Surveyors, Article of the Month, May 2016, pp. 1–12, http://fig.net/resources/monthly_articles/2016/may_2016/de_vries_may_2016.pdf

Enemark, S., Williamson, I., & Wallace, J. (2005). Building modern land administration systems developed economies, pending publication. *Journal of Spatial Science, 50*(2), 51–68.

Enemark, S. (2010a). *From cadastre to land governance: The role of land professionals and FIG,* Annual World Bank Conference on Land Policy and Administration, April 26–27, 2010, Washington D.C.

Enemark, S. (2010b). *The evolving role of cadastral systems in support of good land governance, open symposium FIG 7 commission, September 2010*. Karlovy Vary: Czech Republic.

Enemark, S., Bell, K. C., Lemmen, Ch., & McLaren, R. (2014). *Fit-for-purpose land administration. International Federation of Surveyors (FIG)* (pp. 44). Frederiksberg, Denmark: Jensen Print.

FIG. (1995). *FIG statement on the cadastre,* FIG publication No. 11, FIG Office, Copenhagen. http://www.fig.net/commission7/reports/cadastre/statement_on_cadastre.html (5.12.2010).

FIG. (1998). Cadastre 2014. A vision for a future cadastral system. FIG publication No 15, http://www.fig.net/cadastre2014/translation/c2014-english.pdf (22.02.2013).

FIG. (1999). *Bathurst declaration*. http://www.fig.net/pub/figpub/pub21/figpub21.htm (5.12.2010).

FIG. (2002). *Reforming the cadastre*. In Kaufmann J., Steudler D. 2002. *Benchmarking Cadastral Systems.*

FIG. (2010). *The social tenure domain model. A pro-poor land tool*. Edited by Lemmen Ch. 2010. FIG publication No. 52, p. 21, http://www.fig.net/pub/figpub/pub52/figpub52.pdf (30.01.2015).

FIG. (2014). Cadastre 2014 and beyond. FIG publication No 61, p. 84, http://www.fig.net/pub/figpub/pub61/Figpub61.pdf (16.06.2014).

Gaździcki, J. (1995). *Systemy katastralne* (p. 184). Warszawa: PPWK.

Governatori, G., & Rotolo, A. (2015). *Logics for legal dynamics. In logic in the theory and practice of lawmaking* (pp. 323–356). Switzerland: Springer International Publishing. doi:10.1007/978-3-319-19575-9_12

Henssen, J. (1995). *Basic principles of the main cadastral systems in the world*. In Proceedings of the One Day Seminar held during the Annual Meeting of Commission 7, Cadastre and Rural

Land Management, of the International Federation of Surveyors (FIG), May 16, Delft, The Netherlands.
INSPIRE Directive 2007/2/EC of the European Parliament and of the Council of 14 March 2007 establishing an Infrastructure for Spatial Information in the European Community (INSPIRE).
Kalantari, M., Rajabifard, A., & Bennett, R. (2010). Modern land administration; technical characteristics. FIG Congress 2010. Facing the Challenges—Building the Capacity. April 11–16, 2010, Sydney, Australia.
Kaufmann, J., & Kaul, Ch. (2004). Assessment of the Core Cadastral Domain Model from a Cadastre 2014 Point of View. In Proceedings of the workshop standardization in the cadastral domain, Bamberg, Germany, 9–10 December 2004, FIG, Denmark.
Kaufmann, J. (2012). *Towards cadastre 2034*. Proceedings International FIG Symposium & Commission 7 Annual Meeting, Innsbruck, Austria.
Krelle, A., & Rajabifard, A. (2010). *Cadastre 2014: New challenges and direction*. FIG Congress 2010. Facing the Challenges—Building the Capacity. April 11–16, 2010, Sydney, Australia.
Laarakker, P. (2008). EuroGeographics' vision on cadastre and land registration in Europe 2012, FIG working week 2008, Integrating Generations, Stockholm, Sweden, June 14–19, 2008.
Land, N. (2011). *Cadastre 2.0—Next generation of cadastre*. Presentation on 3rd Cadastral Congress. November 23–25, 2011, Warsaw, Poland.
Lemmen, CH., Oosterom van, P., Zevenbergen, J., Quak, W., & Molen van der, P. (2003). *Further progress in the development of the core cadastral domain model.* FIG Working Week, Paris, France, April 13–17, 2003.
Lemmen, CH., & Oosterom van P. (2006). *Version 1.0 of the FIG core cadastral domain model*. XXIII FIG Congress. Munich, Germany, October 8–13, 2006.
Lemmen, CH., & Oosterom van, P. (2013). *The land administration domain model standard*. 5th Land Administration Domain Model Workshop, September 24–25, 2013, Kuala Lumpur, Malaysia, p. 20, http://www.fig.net/news/news_2013/ladm2013/01.pdf (30.01.2015).
Mills, A. (2008). *The Dimension of Public Policy in Private International Law*. 4 J. Priv. Int'l L. 201–236, 336; Chapter 3.2.
Mitchell, D., & Zevenbergen, J. A. (2011). Toward land administration systems to support climate change mitigation payments. *Land Tenure Journal: Open Access, 2*, 57–79.
Molen van der, P. (2003). *The future cadastres—Cadastres after 2014*. Proceedings of FIG Working Week and 125th Anniversary of FIG, Paris, France, April 13–17, 2003.
PWN. (http://sjp.pwn.pl/sjp/elastyczny;2556392 access 22.09.2014).
Shrestha, R., Tuladhar, A., & Zevenbergen, J. (2016). *Exploring land governance in post-disaster: A case of informal settlement*. International Federation of Surveyors. Article of the month—January 2016. pp. 1–16. http://fig.net/resources/monthly_articles/2016/january_2016/shrestha_etal_january_2016.pdf
Sobota, K. (1991). *System and flexibility in law. Argumentation* (Vol. 5, pp. 275–282). Berlin: Kluwer Academic Publishers (Printed in the Netherlands).
Steudler, D., Williamson, I.P., Rajabifard, A., & Enemark, S. (2004). *The Cadastral Template Project. FIG Working Week "Good Practices in Land Administration and Cadastre"*, Athens, Greece, May 22–27, 2004.
Stoter, J., Oosterom, P., Ploeger, H., & Aalders, H. (2004). *Conceptual 3D Cadastral Model Applied in Several Countries. FIG Working Week 2004, Athens, Greece*. May 22–27, 2004, p. 27. http://fig.net/pub/athens/papers/ts25/TS25_1_Stoter_et_al.pdf (30.12.2015).
UN. (2015). *Transforming our world: The 2030 Agenda for Sustainable Development. UE Sustainable Development Agenda, Resolution A/RES/70/1*, pp. 35. http://www.un.org/ga/search/view_doc.asp?symbol=A/RES/70/1&Lang=E (1.07.2016).
UN-ECE. (1996). *Land administration guidelines, UNECE, Geneva*. http://www.unece.org/env/hs/wpla/docs/guidelines/lag.html (08.04.2014).
UN/FIG. (1996). *The bogor declaration*. United Nations Interregional Meeting of Experts on the Cadastre, Bogor Indonesia, March 1996.
UN-ECE. (2005a). *Guidelines on real property units and identifiers.* Geneva.

UN-ECE. (2005b). *Land administration in the UNECE Region. Development trends and main principles,* Geneva.

Williamson, I. P., Enemark, S., Wallace, J., & Rajabifard, A. (2010). *Land administration for sustainable development* (p. 497). Redlands, California: ESRI Press Academic. ISBN 978–1-58948-041-4.

Wolff, L. Ch. (2011). Law and flexibility—Rule of law limits of a rhetorical silver bullet. *The Journal Jurisprudence. J. Juris*, 549–567.

Automatic Detection and Monitoring of Cyanobacterial Blooms in the Context of the Marine Cadastre

Agnieszka Dawidowicz, Marcin Kulawiak, Krzysztof Bruniecki and Marek Ogryzek

Abstract In the wake of the European and global spatial data infrastructures (SDI) it is important to build information systems which use and serve thematic data in compliance with the INSPIRE Directive. In the context of hydrographic data, the Directive requires EU member states to collect and share information on maritime areas divided into regions and sub-regions, as well as coastal zone management areas. These data are part of recently developed marine cadastres. According to the INSPIRE Directive the marine cadastres should be supplemented with information on the physical condition of the seas as well as on the specific natural characteristics and phenomena occurring in the seas. The latter can include dynamic information on marine pollution such as cyanobacterial blooms. The paper presents the concept of dynamic satellite-based cyanobacteria bloom detection for the purpose of its analysis in the context of marine cadastre.

Keywords Marine cadastre · SDI · Cyanobacteria · AVHRR · Geovisual analytics

A. Dawidowicz (✉)
Department of Real Estate Resources, Faculty of Geodesy, Geospatial and Civil Engineering, University of Warmia and Mazury, Prawochenskiego Street 15, 10-720, Olsztyn, Poland
e-mail: dawidowiczagnieszka@wp.pl

M. Kulawiak · K. Bruniecki
Department of Geoinformatics, Faculty of Electronics, Telecommunication and Informatics, Gdansk University of Technology, Gabriela Narutowicza Street 11/12, 80-233 Gdansk, Poland

M. Ogryzek
Department of Planning and Spatial Engineering, Faculty of Geodesy, Geospatial and Civil Engineering, University of Warmia and Mazury, Prawochenskiego Street 15, 10-720 Olsztyn, Poland

I. Ivan et al. (eds.), *Dynamics in GIscience*, Lecture Notes in Geoinformation and Cartography, DOI 10.1007/978-3-319-61297-3_6

Introduction

In the wake of the European and global spatial data infrastructures (SDI) it is important to build information systems which use and serve thematic data in compliance with the INSPIRE Directive. In the context of hydrographic data, the Directive requires EU member states to collect and share information on maritime areas divided into regions and sub-regions, as well as coastal zone management areas. These data are part of recently developed marine cadastres. Since these type of spatial data are directly related to maritime activities, therefore they could be coordinated by appropriate national maritime administration and harmonized with their maritime SDIs. Such infrastructures are already in use, or under development in many European countries (Bruniecki et al. 2015). The maritime SDI include information on zones which are closed for boating and fishing, vessel traffic separation schemes, the boundaries of harbours, anchorages and many others.

Recent years have seen dynamic advancements in the field of marine cadastre development (Dawidowicz and Źróbek 2014; Srebro et al. 2010; Strain et al. 2006; Sutherland and Nichols 2004; Sutherland et al. 2004; Barry et al. 2003; Fowler and Treml 2001). Countries with access and shares in territorial marine waters tend to register those areas in their national cadastral systems. It is expected that the existing, and currently developed marine cadastres in individual countries will contain information regarding various stakeholders and activities in the marine environment such as inland development, coastal activities, agriculture, tourism related activities, indigenous issues, marine parks or protected areas, aquaculture, oil and gas exploration, shipping, waste management, cables, pipelines and shipwrecks as well as dynamic phenomena that appear periodically in the maritime areas. The latter data are particularly difficult to collect due to their dynamic nature which requires new tools for real-time monitoring and updating.

Moreover, according to the INSPIRE Directive the marine cadastres should be supplemented with information on the physical condition of the seas as well as on the specific natural characteristics and phenomena occurring in the seas. The latter can include dynamic information on marine pollution such as cyanobacterial blooms.

Cyanobacterial blooms are becoming an increasingly important problem for many water reservoirs across the globe. Given enough nutrition, they easily dominate the reservoir's natural phytoplankton and grow in numbers large enough to make the water dangerous to animals and humans alike (Stewart et al. 2006). The presence of cyanobacteria has many adverse effects on the affected basin. First of all, large colonies of cyanobacteria increase water turbidity, which makes it unusable for agricultural and industrial applications (Klapper 1991). Dense colonies of harmful algae may also cause problems for sailors and thus negatively affect the local industry (Pitois et al. 2000). Aside from affecting water clarity, harmful algae tend to generate unpleasant odour which drives away enthusiasts of boating and swimming (Dodds et al. 2009). More serious effects of cyanobacterial blooms include elevation of water pH and oxygen depletion, which have a devastating effect on indigenous flora and fauna of the water reservoir (Havens 2007). Finally, certain types of cyanobacteria

are highly toxic. For example, ingesting even relatively small amounts of Microcystis aeruginosa can damage the subject's liver, intestines, and nervous system (Hu et al. 2010). All of this makes cyanobacteria dangerous to the well-being of humans and animals which are in any way dependant on the affected water reservoir.

Because cyanobacterial blooms are a physical phenomena which occurs in a geographical context, and the marine cadastre is entirely composed of geographical data, both of these data types may be integrated, managed and analysed by means of a Geographic Information System (GIS). Historically, GIS has been proven to be a valuable tool for acquisition, processing, integration and visualization of data obtained from a variety of marine sensors (Kraak 2004).

Monitoring water reservoirs for signs of cyanobacterial blooms has been a subject of intense research for many years. Aside from in situ measurements, which are the most reliable but also the most expensive method of cyanobacteria detection, much attention has been paid to appropriate application of remote sensing. In 1997 Kahru demonstrated a method of detecting cyanobacterial blooms in the Baltic Sea by analysing a time series of Advanced Very High Resolution Radiometer (AVHRR) images. The detection algorithm focused on the high reflectance of the blooms in the visible AVHRR band (Kahru 1997). Although the method showed promise, ultimately the atmospheric correction characteristic of AVHRR prevented the author from obtaining automatic data classification (Kahru et al. 2007). Other detection methods involved computation of the Normalized Differential Vegetation Index (NDVI). Several researchers from around the world applied NDVI to detection of cyanobacterial blooms with varying degrees of success (Kahru et al. 1993; Chen and Dai 2008; Oyama et al. 2014), however the index has generally been found to be too sensitive to interference to produce a consistent time series (Hu et al. 2010). Later research turned to other data sources and techniques, such as Medium Resolution Imaging Spectroradiometer (MERIS) used by Gower et al. (2006) to present algal blooms in the Gulf of Mexico, or Moderate Resolution Imaging Spectroradiometer (MODIS) used by Hu to detect floating algae in the South Atlantic (Hu 2009). These new sensors deliver substantially more spectral bands which in turn enables instant verification of classification results, e.g. by comparison to composite true colour images (Hu et al. 2010). However, due to the seasonal differences in spectral reflectance, results obtained even with the more advanced sensors still needs to be verified manually.

This paper presents a concept Web-based Geographic Information System dedicated for automatic satellite-based detection of cyanobacterial blooms for the purpose of their analysis in the context of a marine cadastre.

Materials and Methods

Accurate detection and monitoring of cyanobacteria via remote sensing depends on the quality of analysed images. In particular, the source data must be free of interference such as clouds which obscure the analysed water basin. This means that

the source of data should provide as many images per day as possible, to have a better chance of obtaining a clean image. Out of the three satellite sensors described in the preceding section, only two are still available because MERIS has been phased out due to termination of the Envisat operation. This leaves AVHRR and MODIS, which is a successor of AVHRR and improves its performance by providing higher spatial resolution (up to 250 m in nadir vs. 1 km for AVHRR) and greater spectral resolution (36 bands vs. 5 bands). On the other hand, AVHRR still has an important advantage in temporal resolution. This is due to the higher number of AVHRR-equipped satellites (seven satellites) over the number of satellites using the MODIS sensor (two satellites). In addition, from each passing AVHRR satellite a local ground station will receive a minimum of two daytime scenes and two night time scenes (depending on the ground station's location). The Gdansk University of Technology Faculty of Electronics, Telecommunications and Informatics in Gdansk, Poland, operates a 1.5 m-wide HRPT/MetOp-A/B local satellite ground station, capable of obtaining data (via the High Resolution Picture Transmission—HRPT stream) from the NOAA-15, 16, 17, 18 and NOAA-19 as well as MetOp-A/B meteorological satellites. The station was selected as a primary source of data for the presented research.

In order to automate the process of cyanobacteria bloom detection, a dedicated Web-based Geographic Information System (GIS) was developed (Kulawiak 2016). The system provides automatic processing of satellite images obtained directly from the ground station, for the purpose of detection and visualization of cyanobacterial blooms in the Baltic Sea area. Although the system is self-contained, the use of open standards of data exchange enables it to be used as a source of data for various applications. For instance, with a minor modification of the client application, the system could enable the integration of data in the context of the marine cadastre (Fig. 1).

The images captured by the satellite ground station are automatically processed by the Satellite data integration module, which puts together lines of the HRPT stream to form images, masks out missing data and converts the obtained images into multiband GeoTIFF. The GeoTIFF files are then passed on to the Cyanobacteria detection module, which extracts AVHRR bands 1 (0.58–0.68 μm) and 2 (0.725–1.0 μm) from the file and uses them to compute NDVI for the entire image. This single-band raster is then used to perform land and cloud masking by removing all pixels with NDVI values larger than −0.2. Next, the module performs Cyanobacteria detection on the images. AVHRR-based Cyanobacteria detection is founded on the high reflectance in the visible (650 nm) band, which is clearly visible on water bodies. However, automatic identification of algae colonies using AVHRR has thus far been unsuccessful due to the sensor's high variability in recorded spectral reflectance between consecutive images (Hu et al. 2010; Kahrua and Elmgren 2014). Because this, instead of value thresholding, the module performs Cyanobacteria detection by comparing the values of band 1 reflectance to that of band 2 (Ahn et al. 1992; Hu and He 2008). If a pixel cluster with sufficiently high difference is not identified, the image is discarded from further processing. Otherwise, the module computes the range of value differences and applies

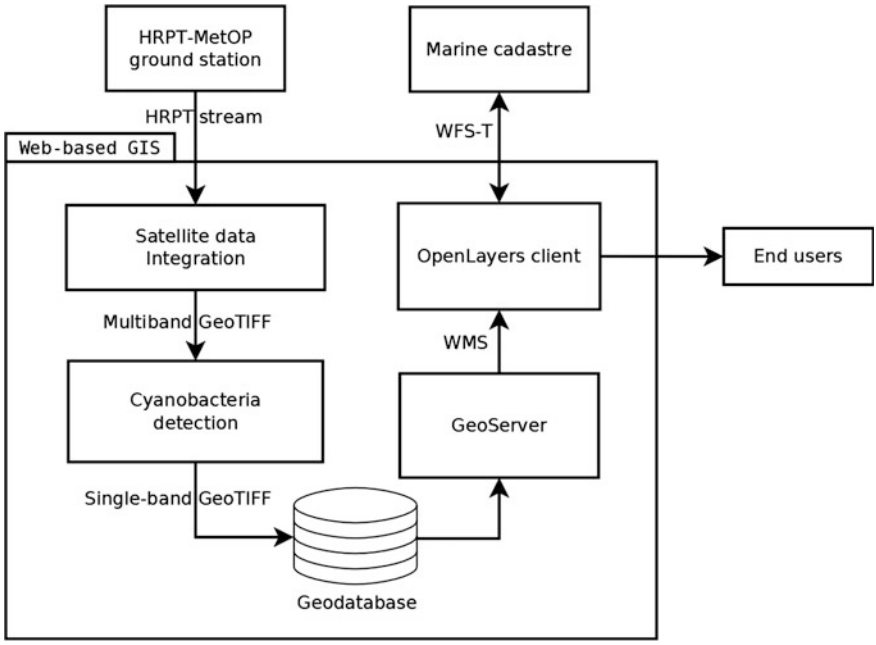

Fig. 1 Proposed architecture of the Web-GIS for Cyanobacteria detection and analysis in the context of a marine cadastre

paradigms of Geovisual Analytics to perform adaptive palette matching in order to graphically represent the changes in density of cyanobacterial accumulations. The resulting image and its colour palette are stored in the Geodatabase and registered in the GeoServer module. GeoServer is an Open Source Web Map server with excellent support for open standards of data exchange and dissemination such as OGC Web Map Service (WMS), Web Feature Service (WFS) or Web Feature Service Transactional (WFS-T). Once registered in GeoServer, the images are remotely accessible to clients through the WMS protocol. The presented system provides users with a Web client built in DHTML using the Open Source OpenLayers library. The client uses WMS and WFS to integrate data obtained from the GeoServer with information from a remote Marine Cadastre database. Because the marine cadastre infrastructure in Poland is still in development and has not been integrated with the Polish SDI, the Marine Cadastre database in the proposed system has been simulated using a separate GeoServer instance. The "Marine cadastre" module serves hydrographic maps of maritime areas to authorized clients via the WFS-T protocol. WFS-T is an open standard which enables authorized clients to perform transactional updates to data stored on the server. The client module displays the marine cadastre as a vector layer overlaid on the latest cyanobacteria accumulation analysis layer, which in turn is overlaid on a True-colour satellite image of the Southern Baltic region. The presented modified

system is meant to serve as a testing ground for new applications of marine cadastre during the ongoing discussion about the final shape of the dataset as well as its infrastructure in Poland.

Results and Discussion

The Web-based GIS for operational algae bloom detection in the Baltic Sea, which would serve as the basis for the proposed solution, has been applied to automatic cyanobacteria detection during the blooming seasons of 2013 and 2014. A sample comparison of the cyanobacteria detection results with quasi true colour visualization obtained from the MODIS Aqua sensor on 25.07.2014 is presented in Fig. 2. The detected cyanobacteria are presented in shades of green, where a darker shade corresponds to a lesser density of the bloom.

The presented algorithm has shown to produce a fairly accurate representation of cyanobacteria coverage, even in scenes contaminated by thin cirrus clouds (as is the case in Fig. 2) (Kulawiak 2016). The occurrence of cyanobacteria accumulations indicates several tiers of water pollution, cyanobacteria itself being a secondary-tier pollutant. This is because the primary source of nutrients (which cause an increase in organic productivity and thus boost cyanobacteria growth) is human activity such as farming and chemical industry production (Sivonen et al. 1989; Lehtimäki et al. 1997).

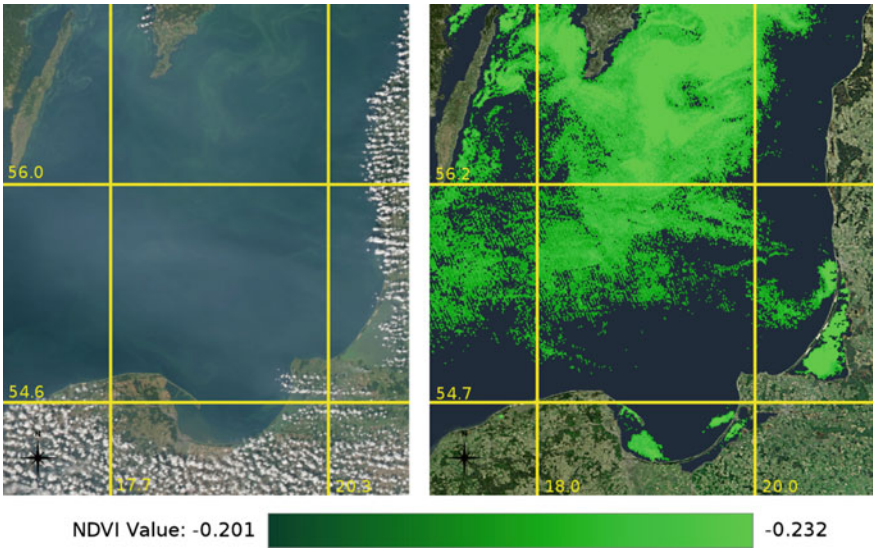

Fig. 2 Comparison of Quasi True Color visualization of the Southern Baltic Sea on 25.07.2014 obtained via MODIS (*left*) with results of Cyanobacteria detection performed on from AVHRR sensor data overlaid on a True Color MODIS image (*right*). Images were captured at 10:45 GMT (MODIS) and 11:27 GMT (AVHRR)

Thus, investigation of the detected cyanobacterial blooms in the context of a marine cadastre may provide information regarding the pollution levels of every researched region.

Assuming the cadastre contains information regarding the administrator of management areas (parcel), the system allows for its easy identification. A sample visualization of interactive identification of the administrator of a water management area polluted with cyanobacteria blooms via by means of marine cadastre is shown in Fig. 3.

Aside from administrator name and address, the marine cadastre should also contain their contact data such as phone and email, which would allow third parties to quickly deliver relevant information e.g. regarding detected cyanobacteria pollution.

Moreover, assuming the marine cadastre contains cyanobacteria pollution status fields (such as "low", "medium", "high") for every management area, the client module can modify them by means of WFS-T. This enables authorized parties to perform remote update services to the marine cadastre via its SDI, which means that the changes become immediately visible to all clients. However, data security would require the maintenance of a strict white list of institutions authorized to make such changes to the marine cadastre data set,

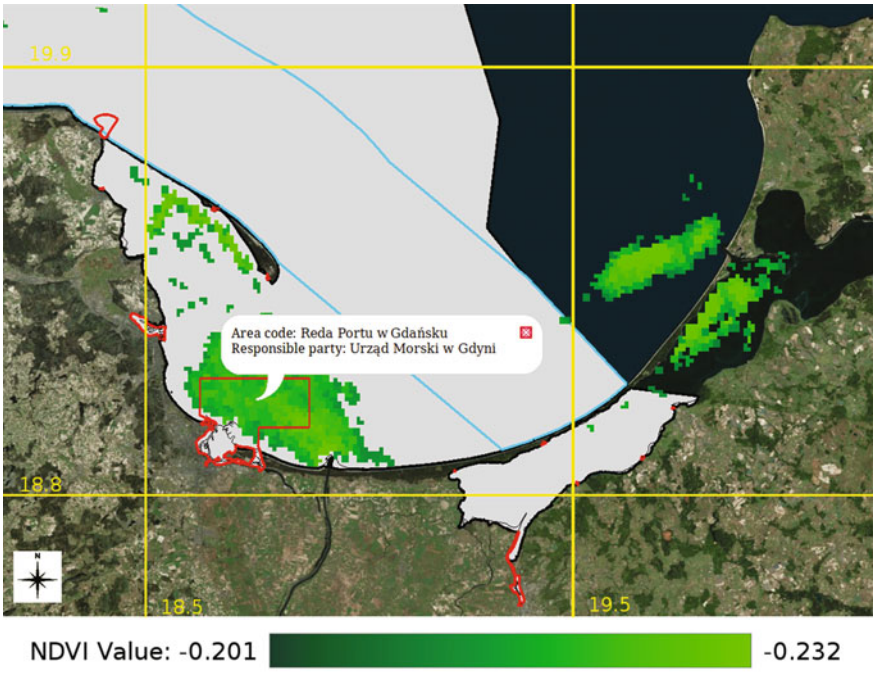

Fig. 3 Sample visualization of interactive identification of the administrator of a water management area polluted with cyanobacteria blooms by means of marine cadastre

which may be hard to realize in practice. This being said, it is clear that even a read-only access to marine cadastre data shows great potential. The experience gathered by testing the presented solution dictates that the presented process of identifying cyanobacteria-infested parcels and notifying their administrators is well suited for use in an automated early warning system. By expanding the presented solution with a server-side analytics module, it would be possible to automatically detect cases of the cyanobacteria data overlapping with regions of the marine cadastre. This in turn would allow for generating automatic reports involving information such as percentage of cyanobacteria coverage, or whether the accumulation is likely to reach shores. Such reports then could be automatically emailed to the responsible parties.

Conclusions

This paper presents a concept system integrating and processing data from a simulated marine cadastre. The system is meant to serve as a testing ground for ideas about the contents and application of marine cadastre during the ongoing discussion about the final shape of the dataset as well as its infrastructure in Poland and the European Union. The proposed system uses the simulated marine cadastre SDI for the purpose of data acquisition as well as modification and update. In this context, a read-only access to a marine cadastre containing management area administrator data enables the implementation of a dedicated monitoring system which enables third parties to provide warnings e.g. related to cyanobacteria infestation of selected areas. Should the cadastre contain detailed administrator contact information, there is a possibility to deliver automated warning messages on-the-fly via e-mail. This way an automated system could potentially generate a daily detailed pollution report, containing information such as management area pollution coverage percentage, or the likelihood of encountering algae accumulations near the shores of each management area. Timely delivery of such reports would enable quick implementation of countermeasures as well as damage assessment and cleanup operations. Moreover, assuming the marine cadastre contains cyanobacteria pollution information and its SDI allows for its remote modification by authorized parties, it is possible for the marine cadastre to be updated with latest information regarding cyanobacteria pollution on a daily basis. The integration of data from such third-party systems and sources will be a key milestone for the creation of a multi-purpose, complete marine cadastre, which in turn is an important prerequisite for successful trans-sectoral and cross-border co-operation.

Acknowledgements The MODIS image used in this paper has been obtained from the NASA OceanColor website.

References

Ahn, Y.-H., Bricaud, A., & Morel, A. (1992). Light backscattering efficiency and related properties of some phytoplankters. *Deep-Sea Research, 39,* 1835–1855.

Barry, M., Elema, I., & van der Molen, P. (2003). Ocean governance and the marine cadastre: The Netherlands North Sea. *Geomatica, 57*(3), 313–325.

Bruniecki K., Chybicki A., Dadić V., Grzetić Z., Ivanković D., Kulawiak M., et al. (2015) *The concept of INSPIRE directive implementation for marine administration in Poland*. In: GIS and Water Resources. Croatian Information Technology Society, GIS Forum.

Chen, Y., & Dai, J. (2008). Extraction methods of cyanobacteria bloom in Lake Taihu based on RS data (in Chinese with English abstract). *Journal of Lake Science, 20,* 179–183.

Dawidowicz, A., & Źróbek, R. (2014) Multipurpose water-marine cadastre in Poland—The directions of development. *Acta Adriatica, 55*(2), 127–144 (December 2014), ISSN 0001–5113. http://jadran.izor.hr/acta/pdf/55_2_pdf/55_2_4.pdf

Directive 2007/2/WE of the European Parliament and Council, of March 14th 2007, establishing the Infrastructure of Spatial Information in the European Community (INSPIRE) (OJ L 108, 25.4.2007, pp. 1–14),

Dodds, W. K., Bouska, W. W., Eitzmann, J. L., Pilger, T. J., Pitts, K. L., Riley, A. J., et al. (2009). Eutrophication of U.S. freshwaters: Analysis of potential economic damages. *Environmental Science and Technology, 43*(1), 12–19.

Fowler, C., & Treml, E. (2001). Building a marine cadastral information system for the United States—A case study. *Computers, Environment and Urban Systems, 25*(4), 493–507.

Gower, J., Hu, C., Borstad, G., & King, S. (2006). Ocean color satellites show extensive lines of floating Sargassum in the Gulf of Mexico. *IEEE Transactions on Geoscience and Remote Sensing, 44*(12), 3619–3625.

Havens, K. E. (2007). Cyanobacteria blooms: Effects on aquatic ecosystems. In H. K. Hudnell (Ed.), *Proceedings of the Interagency, International Symposium on Cyanobacterial Harmful Algal Blooms (ISOC-HAB): State of the Science and Research Needs* (pp. 733–747). New York: Springer.

Hu, C. (2009). A novel ocean color index to detect floating algae in the global oceans. *Remote Sensing of Environment, 113*(10), 2118–2129.

Hu, C., & He, M. X. (2008). Origin and offshore extent of floating algae in Olympic sailing area. *Eos, Transactions American Geophysical Union, 89*(33), 302–303.

Hu, C., Lee, Z., Ma, R., Yu, K., Li, D., & Shang, S. (2010) Moderate resolution imaging spectroradiometer (MODIS) observations of cyanobacteria blooms in Taihu Lake, China. *Journal of Geophysical Research: Oceans (1978–2012), 115*(C4).

Kahru, M., Leppänen, J. M., & Rud, O. (1993). Cyanobacterial blooms cause heating of the sea surface. *Marine Ecology Progress Series, 101,* 1–7.

Kahru, M. (1997). *Using satellites to monitor large-scale environmental changes: a case study of cyanobacterial blooms in the Baltic Sea. Monitoring algal blooms: new techniques for detecting large-scale environmental changes* (pp. 43–61). Heidelberg Berlin: Springer.

Kahru, M., Savchuk, O. P., & Elmgren, R. (2007). Satellite measurements of cyanobacterial bloom frequency in the Baltic Sea: interannual and spatial variability. *Marine Ecology Progress Series, 343,* 15–23.

Kahru, M., & Elmgren, R. (2014). Multidecadal time series of satellite-detected accumulations of cyanobacteria in the Baltic Sea. *Biogeosciences, 11*(13), 3619–3633.

Klapper, H. (1991). *Control of eutrophication in inland waters*. Chichester, UK: Ellis Horwood Ltd.

Kraak, M.-J. (2004). The role of the map in a Web-GIS environment. *Journal of Geographical Systems, 6,* 83–93.

Kulawiak, M. (2016). Operational algae bloom detection in the Baltic Sea using GIS and AVHRR data. *Baltica, 29*(1), 3–18. doi:10.5200/baltica.2016.29.02.

Lehtimäki, J., Moisander, P., Sivonen, K., & Kononen, K. (1997). Growth, nitrogen fixation, and nodularin production by two Baltic Sea cyanobacteria. *Applied Environmental Microbiology, 63*(5), 1647–1656.

Oyama, Y., Matsushita, B., & Fukushima, T. (2014). Distinguishing surface cyanobacterial blooms and aquatic macrophytes using Landsat/TM and ETM+ shortwave infrared bands. *Remote Sensing of Environment, 157*, 35–57.

Pitois, S., Jackson, M. H., & Wood, B. J. B. (2000). Problems associated with the presence of cyanobacteria in recreational and drinking waters. *International Journal of Environmental Health Research, 10*(3), 203–218.

Sivonen, K., Kononen, K., Carmichael, W. W., Dahlem, A. M., Rinehart, K. L., Kiviranta, J., et al. (1989). Occurrence of the hepatotoxic cyanobacterium Nodularia spumigena in the Baltic Sea and structure of the toxin. *Applied Environmental Microbiology, 55*(8), 1990–1995.

Srebro, H., Fabrikant, I., & Marom, O. (2010, April). *Towards a Marine Cadastre in Israel*. In FIG Congress (p. 17).

Stewart, I., Webb, P. M., Schluter, P. J., Fleming, L. E., Burns, J. W., Gantar, M., et al. (2006). Epidemiology of recreational exposure to freshwater cyanobacteria—An international prospective cohort study. *BMC Public Health, 6*(1), 93.

Strain, L., Rajabifard, A., & Williamson, I. (2006). Marine administration and spatial data infrastructure. *Marine Policy, 30*(4), 431–441.

Sutherland, M., Cockburn, S., & Nichols, S. (2004). Toward a 3D marine cadastre in support of good ocean governance: A review of the technical framework requirements. *Computers, Environment and Urban Systems, 28*(5), 443–470.

Sutherland, M., & Nichols, S. (2004). The evolving role of hydrography in ocean governance and the concept of a Marine Cadastre. *Hydrographic Journal*, 13–17.

Fuzzy Spatio-Temporal Querying the PostgreSQL/PostGIS Database for Multiple Criteria Decision Making

Renata Ďuračiová and Jana Faixová Chalachanová

Abstract Multiple criteria decision making usually means selection of the best objects or their parameters which best meet conditions or criteria. Human decision making often involves also uncertain and vague criteria. The terms as a short distance, a high building or long time are commonly used in human speech. Nevertheless, it is not necessary to describe them exactly. In case of decision making based on lot of data and multiple criteria, data are usually stored in databases and a query language is used for handling and querying them. In this case, the criteria should be defined in a formal computer language. The standard for querying data in relational databases is the Structured Query Language (SQL). All objects and phenomena, and everything people do, is experience in space and time. Space and time, therefore, should be used as a framework for querying and reasoning about information stored in database systems. Databases, in which spatial and temporal data types are included and functions for their handling are supported, are called the spatio-temporal databases. To spatio-temporal query a database, an extension of standard SQL to support spatial and temporal data is needed. Uncertain spatio-temporal queries are not yet standardized and they are a current topic of research. For uncertain queries creation and expression of uncertain decision criteria, development of new methods and techniques is required. One of the most widely used approach to model, analyse and process uncertain and vague data is fuzzy set theory. Therefore, in this paper, we propose a new way of application fuzzy set theory to spatio-temporal querying. For the case study realisation, the open source PostgreSQL database system extended by the PostGIS we have used. The implementation of the proposed principles of fuzzy set theory to spatio-temporal querying databases can bring an opportunity for the efficient decision making based on multiple uncertain criteria.

R. Ďuračiová (✉) · J. Faixová Chalachanová
Faculty of Civil Engineering, Slovak University of Technology in Bratislava,
Radlinského 11, 810 05 Bratislava, Slovakia
e-mail: renata.duraciova@stuba.sk

J. Faixová Chalachanová
e-mail: jana.chalachanova@stuba.sk

I. Ivan et al. (eds.), *Dynamics in GIscience*, Lecture Notes in Geoinformation and Cartography, DOI 10.1007/978-3-319-61297-3_7

Keywords Spatio-temporal database · Fuzzy querying · Multiple criteria decision making · PostgreSQL

Introduction

Modelling of uncertainty of spatio-temporal data is not a new topic of research, but approaches and tools for creation of uncertain spatio-temporal queries to databases are still not sufficiently supported. For data querying and manipulation in relational and object-relational databases, the Structured Query Language (SQL) is standard (International Organization for Standardization (ISO) standard ISO 9075-1:2011 Information technology—Database languages - SQL also known as ISO SQL:2011 Standard). ISO SQL:2011 Standard includes, inter alia, support for temporal data types. The spatial data types and standard functions for spatial data analysis are included in both the Open Geospatial Consortium (OGC) specification Simple Feature Access (SFA) and standard ISO 19125 (ISO 19125-1:2004 Geographic information—Simple feature access—Part 1: Common architecture) and ISO 19125-2:2004 Geographic information—Simple feature access—Part 2: SQL option). The handling of uncertain data in relational and object-relational databases is not yet standardized, and is presented only as the subject of research in several papers. The some concepts and first results of uncertain data modelling and querying are presented, for instance, in papers (Buckles and Petry 1982; Kacprzcyk et al. 2010; Hudec 2009; Caha et al. 2014b; Ďuračiová 2014; Carniel et al. 2016). Those papers introduce possibilities to extend SQL for the processing of uncertain data and vague queries in databases, but they mostly do not include spatio-temporal data. Therefore, the aim of this paper is to introduce a simple way for uncertain spatio-temporal data querying to object-relational database, which can be useful in multiple criteria decision making (MCDM) based on uncertain thematic, spatial or temporal criteria.

For uncertainty modelling, fuzzy set theory (Zadeh 1965) we use. Much work has been focused on an application of the fuzzy set approaches to modelling of spatial or temporal data uncertainty (Burrough and Frank 1996; Bosc et al. 2005). Fuzzy sets have been used, for example, for the definition of fuzzy spatial data types (Schneider 1999; Jiang and Eastman 2000; Schneider 2008; Carniel et al. 2016); fuzzy spatial topology (Tang et al. 2006); and also fuzzy spatial decision making (Malczewski 1999; Morris and Jankowski 2005; Petry et al. 2005; Changa et al. 2008; Caha et al. 2014a). In spatio-temporal data processing, fuzzy techniques have been used to measure uncertainties about geographical data and decision rules (Robinson 1988), or to represent imprecise concepts (Malczewski 1999). Soft temporal data have been described, for example, in Christakos et al. (2001), Deng et al. (2008). Fuzzy classes, domains for imprecise vague data, and fuzzy equality operators are defined in Cuevas et al. (2008), semantic interpretation of fuzzy spatial queries is described in Wang (1994, 2000), Cuevas et al. (2008), and some theoretical aspects of flexible querying spatio-temporal data are presented in De Caluwe

et al. (2004a, b), Sözer et al. (2008), Emrich et al. (2012). Furthermore, several approaches dedicated to modelling and handling spatio-temporal data uncertainty have been developed (De Caluwe et al. 2004a), but their practical applications are still not sufficient.

Therefore, in this paper, we introduce a new approach to data querying to object-relational database, based on uncertain spatial and temporal criteria. For data storing and handling, we use the most widely used open source database system PostgreSQL extended with the PostGIS spatial data support. The result is a simple way for formulation of uncertain spatio-temporal queries without having to install special programs and other software tools to the PostgreSQL/PostGIS database system.

Materials and Methods

Everything people do, is experience in space and time. Space and time, therefore, constitute conditions for the existence of all objects and phenomena. As such they are used as a framework for querying and reasoning about information kept in databases (De Caluwe et al. 2004b), which can be used as the basis for MCDM. State of each object in space and time is given by its thematic attribute values, which can be represented as the third dimension of decision making (Fig. 1 left). All these dimensions may be inherently affected by uncertainty (Fig. 1 right).

Therefore, for fuzzy spatio-temporal querying to a database, we need to define multiple criteria SQL queries to relational databases, but also extend common possibilities of SQL to support handling of temporal data, spatial data, and also modelling of uncertain decision criteria.

Multiple Criteria Queries to Relational Databases

Spatio-temporal MCDM usually means selection of the best location, appropriate objects or their parameters with the best fulfilment of conditions for a future action.

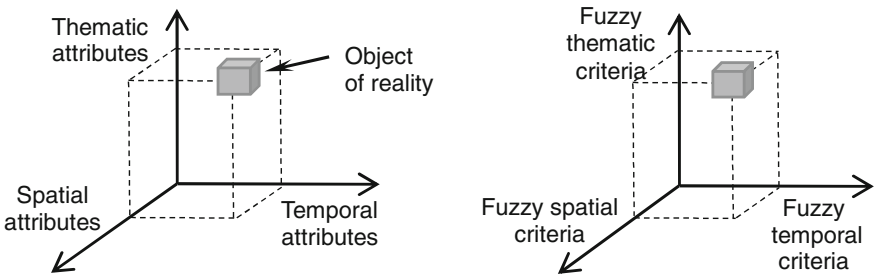

Fig. 1 Object of reality in the space time (*left*) and spatio-temporal decision criteria (*right*)

For MCDM based on data that are stored in relational or object-relational databases, SQL is commonly used.

The basic syntax of command SELECT, which is used for data selection from a database, is as follows:

```
SELECT List_of_attributes
FROM List_of_tables
WHERE Conditions;
```

If the criteria for decision making are given, SQL query contains usually their aggregation realised by logical operator AND (Fig. 2).

The SQL query is then defined as follows:

```
SELECT List_of_attributes
FROM List_of_tables
WHERE c_1 AND c_2 AND … AND c_n;
```

where **c_1**, **c_2**, … **c_n** are criteria defined for MCDM.

Storing and Querying Data in Spatio-Temporal Databases

A temporal database is a database that includes querying and handling data involving time and supports a temporal data model and a temporal version of SQL (ISO 9075:2011). Temporal table have usually two fields added, *valid_from* and *valid_to* (Fig. 3). There are three basic temporal data types implemented in object-relational databases: DATE, TIME, and TIMESTAMP. The duration of a period of time can be represented by a value of an interval type (ISO 9075-1:2011). There are also two classes of intervals defined in ISO SQL:2011 Standard: year-month intervals, and day-time intervals. Basic syntax of temporal query in accordance with ISO SQL:2011 Standard is:

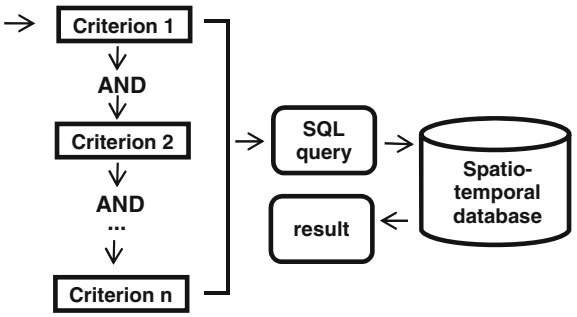

Fig. 2 Aggregation of criteria in multiple criteria decision making

```
SELECT List_of_attributes
FROM List_of_tables
AS OF SYSTEM TIME Datetime
WHERE Conditions
```

A spatial database is a database that is optimized to store and query spatial data in spatial tables. The spatial table is a table with spatial (geometry or geography) column (the_geom). This column can be added to conventional tables stored in object-relational databases. Basic spatial data types and spatial functions for querying and analysis of spatial data stored in object-relational databases are included in standard ISO 19125 or OGC specification SFA. One of the basic spatial function for MCDM is ST_Distance, which is very useful for decision making based on spatial properties of objects. Simple spatial SQL query using function ST_Distance can be created, for example, as follows:

```
SELECT List_of_attributes
FROM Table 1 T1, Table 2 T2
WHERE ST_Distance(T1.the_geom,T2.the_geom)[< |<= |=| >=| >]k;
```

where the_geom is spatial attribute (e.g. data type POINT or POLYGON) and k is a constant.

Then the basic structure of conventional spatio-temporal table can include some conventional thematic attributes, two temporal attributes and the spatial attribute (Fig. 3).

Modelling of Uncertain Queries Using Fuzzy Set Theory

Two people can use a different vocabulary or use the same words in different ways. That means that also definitions of criteria or query in common language is very

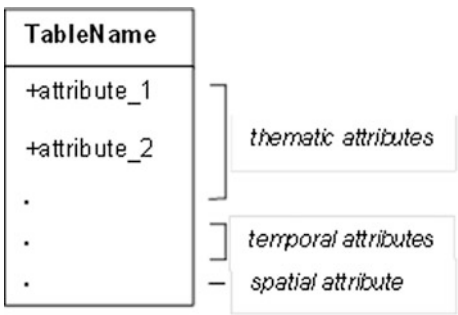

Fig. 3 The basic structure of spatio-temporal table

often affected by uncertainty. This type of semantic uncertainty can be very well treated by fuzzy set theory (Zadeh 1965; Shekhar and Xiong 2008). It is also important to note that fuzzy set theory does not work with the concepts of randomness and probability, but expresses uncertainty in terms of fuzziness or vagueness (Kosko 1990).

Fuzzy set theory was first introduced by Zadeh (1965): "Let X be a space of points (objects), with a generic element of X denoted by x. Thus, $X = \{x\}$. A fuzzy set (class) A in X is characterized by a membership (characteristic) function $\mu_A(x)$ which associates with each point in X a real number in the interval [0,1], with the value of $\mu_A(x)$ at x representing the "grade of membership" of x in A."

Because of simple implementation, the linear membership functions are the most widely used. For example, the most known trapezoidal membership function $\mu_{A'}(x)$ of the fuzzy set $A' = \{(x, \mu_A(x)); x \in X\}$ is defined as follows:

$$\mu_{A'}(x) = \begin{cases} 0 & \text{if } x < a, \\ \frac{x-a}{b-a} & \text{if } a \le x < b, \\ 1 & \text{if } b \le x \le c, \\ \frac{d-x}{d-c} & \text{if } c < x \le d, \\ 0 & x > d \end{cases} \tag{1}$$

The trapezoidal membership function $\mu_{A'}(x)$ is shown in Fig. 4, where $\chi_A(x)$ represents the characteristic function of the crisp set A:

$$\chi_A(x) = \begin{cases} 1, & \text{if } x \in A, \\ 0, & \text{if } x \notin A. \end{cases} \tag{2}$$

In general, the characteristic function takes a value of either 1 or 0 (Fig. 4), while a range of values of fuzzy membership function is interval [0,1] (higher values of fuzzy membership function indicates higher degrees of set membership) (Klir and Yuan 1995).

Other commonly used membership functions include the triangular membership function, which is the special case of the trapezoidal function for $c = d$, the S-shaped membership function, L-shaped membership function, etc. (Ross 2010). Especially for a more reliable description of uncertainty in measurement of spatial objects (Kreinovich et al. 1992), the Gaussian membership function

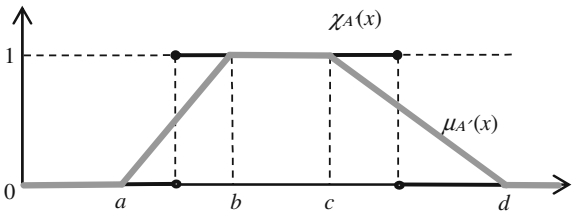

Fig. 4 The crisp set (A) versus the trapezoidal fuzzy set (A')

$$\mu_A(x) = e^{\frac{-(x-c)^2}{2\sigma^2}} \tag{3}$$

can be used (σ^2 is the variance and c the expected value).

The logics used to build the expressions, which make up the core of the queries, can be the traditional binary (Boolean) logic, a ternary logic (Kleene's logic), a four value logic (Belnap's logic), multivalue logic, or general one (fuzzy logic) (De Caluwe et al. 2004b). There are many ways of extending the basic crisp set operations to fuzzy sets (Schneider 1999) and Boolean logic to fuzzy logic. In general, the operations of fuzzy conjunction (AND), fuzzy disjunction (OR), and fuzzy complement (NOT) are, in accordance with basic concept of fuzzy set theory, represented as generalizations of crisp ones.

If we comply with the definitions presented in Zadeh (1965) and *A'* and *B'* are fuzzy sets, then

$$A' \cap B' = \{(x, \mu_{A' \cap B'}(x)) | x \in X \wedge \mu_{A' \cap B'}(x) = \min(\mu_{A'}(x), \mu_{B'}(x))\} \tag{4}$$

$$A' \cup B' = \{(x, \mu_{A' \cup B'}(x)) | x \in X \wedge \mu_{A' \cup B'}(x) = \max(\mu_{A'}(x), \mu_{B'}(x))\} \tag{5}$$

$$\neg A' = \{(x, \mu_{\neg A'}(x)) | x \in X \wedge \mu_{\neg A'}(x) = 1 - (\mu_{A'}(x))\} \tag{6}$$

In fuzzy set theory and fuzzy logic, intersection (conjunction) and union (disjunction) are generally expressed by triangular norms (t-norms) and triangular conorms (t-conorms), respectively (Grabisch 2009).

Creation of Multiple Criteria Fuzzy Spatio-Temporal SQL Queries

Based on the syntax of the SELECT command in SQL and basic principles of fuzzy set theory, the fuzzy SQL query for MCDM could be defined in the following way:

```
SELECT List_of_attributes
FROM List_of_tables
WHERE fuzzy_c_1 Fuzzy_AND fuzzy_c_2 Fuzzy_AND … Fuzzy_AND fuzzy_c_n;
```

where ***fuzzy_c_1***, ***fuzzy_c_2***,… ***fuzzy_c_n*** are uncertain criteria and Fuzzy_AND is fuzzy conjuction.

To express the fulfilment of i-th fuzzy_c_i criterion, for example, by the trapezoidal membership function (1), we can use SQL command CASE (conditional expression):

```
(CASE
  WHEN x>=a AND x<b THEN (x-a)/b-a)
  WHEN x>=b AND x<=c THEN 1
  WHEN x>=c AND x<d THEN (d-x)/d-c)
  ELSE 0 END) AS mi_i
```

where x is variable value of the fuzzy set A', a, b, c, d are parameters of the trapezoidal membership function, and mi_i is a degree of membership of a feature in the fuzzy set A'.

As an effective alternative, the degree of membership in the fuzzy set A' can be expressed using the functions LEAST (returns the least value in a list of expressions) and GREATEST (returns the greatest value in a list of expressions), if they are implemented in the used database management system (DBMS) (Ďuračiová 2014):

```
(LEAST(GREATEST(LEAST(((x-a)/(b-a)),((d-x)/(d-c))),0),1)) AS mi_i
```

This function can be also used for both spatial and temporal criteria modelling.

As a fuzzy logical operator AND, standard conjunction (also known as the minimum t-norm) (3) we use:

```
(LEAST(mi_1,mi_2,... mi_n))
```

Implementation of the Basic Principles of Multiple Criteria Fuzzy Spatio-Temporal SQL Queries into the PostgreSQL/PostGIS Database System

In this paper, we propose a simple way of implementation of fuzzy set theory into SQL querying by defining several new fuzzy functions. For implementation of the fuzzy spatial functions and fuzzy spatial queries realisation, we use the open source PostgreSQL/PostGIS database system. First, we suggest to define the following basic fuzzy membership functions, which can be used for universal processing of fuzzy thematic, spatial, and temporal criteria:

```
Fuzzy_Tpz(a,b,c,d,x) – the trapezoidal fuzzy membership function,
Fuzzy_Trg(a,b,d,x) – the triangular fuzzy membership function,
Fuzzy_S(a,b,x) – the S-shape fuzzy membership function,
Fuzzy_L(c,d,x) – the L-shape fuzzy membership function,
Fuzzy_Gs(c,sig,x) – the Gaussian fuzzy membership function.
```

Using procedural language PL/pgSQL in the PostgreSQL DBMS, the `Fuzzy_Tpz` function can be written in the following way:

```
CREATE OR REPLACE FUNCTION public."Fuzzy_Tpz"(
 a real,
 b real,
 c real,
 d real,
 x real)
 RETURNS real AS
$BODY$BEGIN
    RETURN (MIN(MAX(MIN(((x-a)/(b-a)),((d-x)/(d-c))),0),1));
END;$BODY$
 LANGUAGE plpgsql VOLATILE
 COST 100;
ALTER FUNCTION public."Fuzzy_Tpz"(real, real, real, real, real)
 OWNER TO postgres;
```

function `Fuzzy_Gs is` can be created as follows:

```
CREATE OR REPLACE FUNCTION public."Fuzzy_Gs"(
    c real,
    sig real,
    x real)
 RETURNS real AS
 $BODY$BEGIN
    RETURN (exp((-(x - c)^2)/(2 * sig^2)));
END;$BODY$
 LANGUAGE plpgsql VOLATILE
 COST 100;
ALTER FUNCTION public."Fuzzy_Gs"(real, real, real)
 OWNER TO postgres;
COMMENT ON FUNCTION public."Fuzzy_Gs"
(real, real, real) IS 'Gaussian fuzzy
membership function';
```

where `sig` is the variance and `c` the expected value.

All other types of fuzzy membership functions (L-shaped, S-shaped, and triangular) can be represented in a similar manner.

The above functions can be used directly in MCDM, but also in the definition of the more specific spatial and temporal fuzzy functions. For expression of fuzzy spatial criteria in multiple criteria queries, for instance, the following basic fuzzy spatial function can be created and subsequently used (Fig. 5):

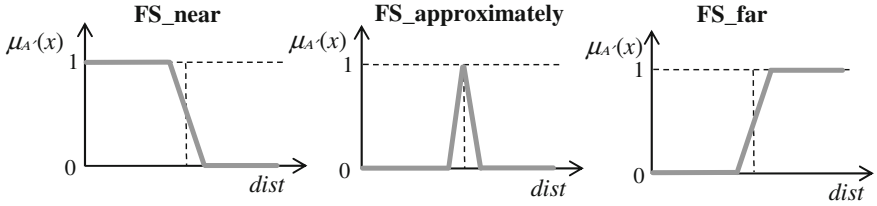

Fig. 5 Fuzzy spatial database functions: fuzzy spatial near (*left*), fuzzy spatial approximately (*middle*), fuzzy spatial far (*right*)

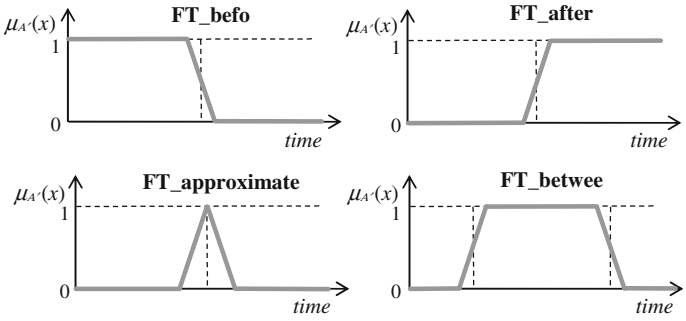

Fig. 6 Fuzzy temporal database functions: fuzzy temporal before (*top left*), fuzzy temporal after (*top right*), fuzzy temporal approximately (*bottom left*), fuzzy temporal between (*bottom right*)

- `FS_near(c,d,dist)`—fuzzy spatial near,
- `FS_approximately(a,b,d,dist)`—fuzzy spatial approximately,
- `FS_far(a,b,dist)`—fuzzy spatial far,

where `a`, `b`, `c`, `d` are parameters of the piecewise linear fuzzy membership function and `dist` is a distance of the selected spatial object from the spatial object given by decision criteria. To compute the distance in the fuzzy spatial criteria, we apply the spatial function ST_Distance().

To create the SQL queries with uncertain temporal criteria, we propose to implement and use the special fuzzy temporal functions such as (Fig. 6):

- `FT_before(c,d,time)`—fuzzy temporal before,
- `FT_after(a,b,time)`—fuzzy temporal after,
- `FT_approximately(a,b,d,time)`—fuzzy temporal approximately,
- `FT_between(a,b,c,d,time)`—fuzzy temporal between,

where time is a temporal information expressed as number.

For processing fuzzy temporal criteria, we use, for example, the temporal attribute `valid_from` with DATETIME data type and the temporal function `age (TIMESTAMP)` implemented in the PostgreSQL DBMS or the computed attribute `today - valid_from`. For extraction subfield count of years from interval,

we can use the extract function: `EXTRACT(field FROM source)`. The extract function returns values of type double precision, which can be used as argument in the fuzzy temporal functions.

All the above functions can be implemented in the database system in the above mentioned form and consequently used to determine the degree of membership to the corresponding fuzzy set. In this way, we can express, for example, uncertain temporal or spatial criteria such as: "*far from the city centre*", "*about 500 m from the bus station*", "*about a year ago*", "*approximately in June*", etc.

It is important to note, that all thematic, spatial and temporal criteria could be expressed by the basic fuzzy function such as `Fuzzy_Tpz`, `Fuzzy_Trg`, `Fuzzy_L`, `Fuzzy_S`, and `Fuzzy_Gs`, which are defined above. For example, the `Fuzzy_L` function, which is designed for modelling the L-membership function, can be used for expression the `FS_near` and the `FT_before` functions; the `Fuzzy_S` function can be applied in definition of the functions `FS_far` and `FT_after`; the triangular `Fuzzy_Trg` function can be used as the `FS_approximately` function for spatial criteria or `FT_approximately` function for temporal criteria; and the `Fuzzy_Tpz` function, which is designed for modelling the fuzzy trapezoidal membership function, can be used for the modelling of the `FT_between` function.

Due to the completeness of the solution, it is also necessary to create functions for fuzzy aggregation operators. For example, the standard fuzzy logical operator AND, which is the most important operator in the process of MCDM, can be implemented as follows:

```
CREATE OR REPLACE FUNCTION public."Fuzzy_AND_Min" (
  m1 real,
  m2 real)
 RETURNS real AS
$BODY$BEGIN
   RETURN least(m1,m2);
END;$BODY$
  LANGUAGE plpgsql VOLATILE
 COST 100;
ALTER FUNCTION "Fuzzy_AND_Min"(real, real)
 OWNER TO postgres;
```

To implement other t-norms and t-conorms, the function body can be created, for example, according to Ďuračiová (2014). Another way is to use the procedural language PL/pgSQL to define the function body. For example, the function body of the drastic t-norm `Fuzzy_AND_Drs` can be written as follows:

```
BEGIN
  IF m1 = 1 THEN RETURN m2;
  ELSIF m2 = 1 THEN RETURN m1;
  ELSE RETURN 0;
  END IF;
END;
```

If the above described functions are implemented in a database system, they can help to formulate most of the fuzzy spatio-temporal queries much more efficiently. If needed, the function body of any other less known operation, such as the nilpotent minimum:

$$T_{nM}(a,b) = \begin{cases} \min(a,b) & \text{if} \quad a+b>1. \\ 0 & \text{otherwise} \end{cases} \tag{7}$$

can be whenever created. For example, based on the above formula, the new `Fuzzy_AND_MNi` function can be written in PL/pgSQL as follows:

```
BEGIN
  IF m1 + m2 > 1 THEN RETURN least(m1,m2);
  ELSE RETURN 0;
  END IF;
END;
```

Case Study

As a case study, spatio-temporal MCDM based on the ZB*GIS*® (the fundamental database for GIS in Slovakia) data we present. The database schema of the ZB*GIS*® is defined in accordance to the FACC DIGEST (Digital Geographic Information Exchange Standard) and the task is to find all large parking areas that are close to the sports field and were actualized approximately two years ago. Then the following fuzzy spatio-temporal query to object-relational database based on the ZB*GIS*® can be used as an example:

Q: Select all large parking areas (from table Parking_areas) that are close to sports field (stored in the table Sports_field) and were actualized approximately two years ago.

This spatio-temporal query includes three fuzzy terms: *large parking area*, *close to sport field* and *approximately two years ago*, which can be modelled using fuzzy sets. It is important to note that each fuzzy term can be expressed by the specific

fuzzy membership functions dependent on the context of its use. For example, the above fuzzy terms can be modelled by the following fuzzy sets:

The fuzzy set A ("*Large parking areas*"):

$$\mu_A(x) = \begin{cases} 0 & \text{if } x < 600, \\ \frac{x-600}{400} & \text{if } 600 \leq x \leq 1000, \\ 1 & \text{if } x > 1000. \end{cases} \tag{8}$$

The fuzzy set D ("*Parking areas close to the sports field*"):

$$\mu_D(x) = \begin{cases} 1 & \text{if } x < 150, \\ \frac{500-x}{350} & \text{if } 150 \leq x \leq 500, \\ 0 & \text{if } x > 500. \end{cases} \tag{9}$$

The fuzzy set T ("*Parking areas actualised approximately two years ago*"):

$$\mu_T(x) = \begin{cases} 0 & \text{if } x < 18, \\ \frac{x-18}{4} & \text{if } 18 \leq x < 22, \\ 1 & \text{if } 22 \leq x \leq 26, \\ \frac{30-x}{4} & \text{if } 26 < x \leq 30, \\ 0 & x > 30 \end{cases} \tag{10}$$

Parameters of the fuzzy membership functions A, D, and T are in square meters, meters, and in months, respectively. In solution that we suggest in this paper, the fuzzy membership function A can be represented by the `Fuzzy_S` function using the spatial `ST_area` implemented in the PostgreSQL/PostGIS database system. The fuzzy membership functions D and T can be simply expressed by the `FS_near` function and the `FT_approximately` function, respectively.

Therefore, if we have two tables `Parking_areas(id, type, valid_from, valid_to, the_geom)` and `Sports_field(id, use, valid_from, valid_to, the_geom)`, the SQL command for the spatio-temporal query using fuzzy functions can be written as follows:

```
SELECT
 id,
 ST_Area(the_geom) AS a, "Fuzzy_S"(600,1000,a) AS mi_a,
 ST_Distance(P.the_geom,S.the_geom) AS d, "FS_near"(150,500,
d) AS mi_d,
 time AS t, "FT_approximately"(18,22,26,30,t) AS mi_t,
 "Fuzzy_AND_Min"(mi_a,mi_d,mi_t) AS mi
FROM Parking_Areas AS P, Sports_field AS S
WHERE mi > 0;
```

The result of the fuzzy spatio-temporal query can be created as a spatial table and can then be visualized in GIS software environment (e.g. QGIS or ArcGIS). The visualization of the result of the above query is presented in Fig. 7.

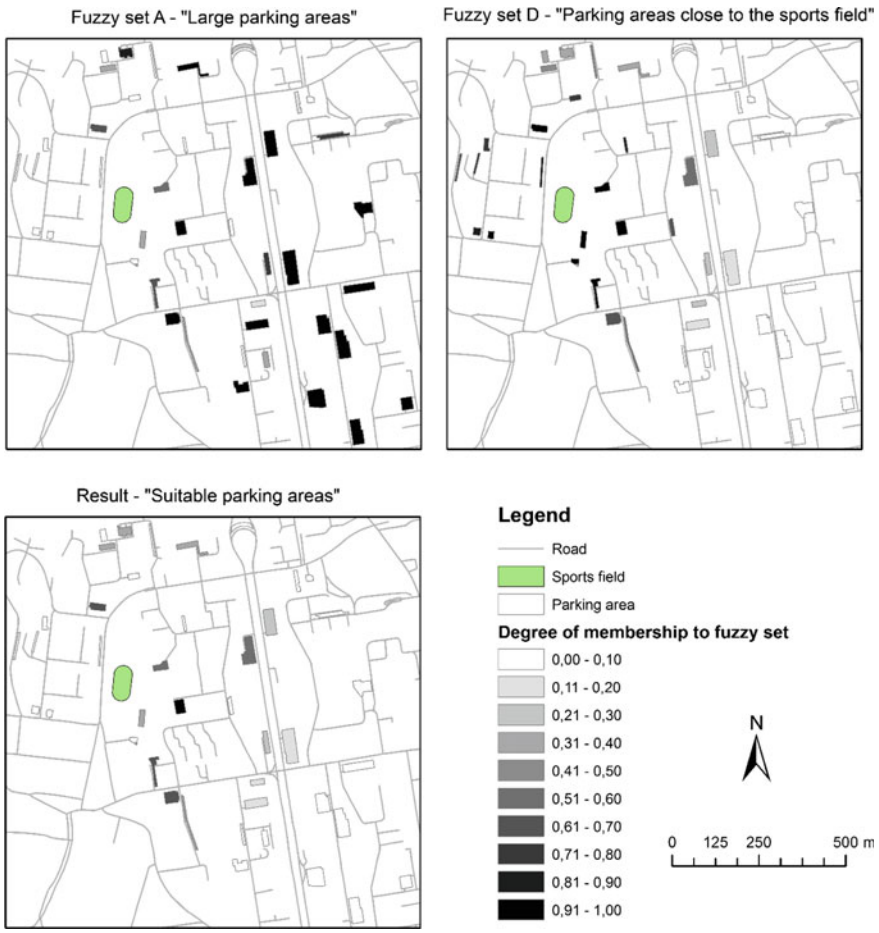

Fig. 7 The visualization of the result of the fuzzy spatio-temporal query: degree of membership to the fuzzy set A (*top left*), degree of membership to the fuzzy set D (*top right*), degree of membership to the result fuzzy set "suitable parking areas" (*bottom left*)

Conclusions and Discussion

The result of this paper is a proposal for implementation of the basic principles of fuzzy set theory into spatio-temporal querying object-relational databases. Fuzzy spatio-temporal querying enables both natural and effective data querying in the process of MCDM. The approach proposed in this paper brings an appropriate solution for spatial decision making based on the data stored in a database system. We have introduced the implementation of the fuzzy membership functions and the fuzzy logical operators AND into the PostgreSQL database system with the PostGIS extension. All implemented fuzzy spatial and fuzzy temporal functions can be used in common form of the SQL queries using the SELECT command. The main advantages of our proposal includes:

- spatial and temporal data handling,
- fast and simple implementation in open source software environment,
- independence from other software tools (it does not require installation and use of other special tools),
- applicability in solving various types of tasks, which use the process of MCDM based on uncertain thematic, spatial and temporal criteria.

The further improvement and the development of the proposed approach to uncertain spatio-temporal querying can focus on an additional development and implementation of other principles of fuzzy set theory into database systems. Then can be created a complex set of tools for fuzzy spatio-temporal data querying and analysis based on uncertain criteria.

Acknowledgements This work was supported by the Grants No. 1/0682/16 and No. 1/0954/15 of the Grant Agency of Slovak Republic VEGA.

References

Bosc, P., Kraft, D., & Petry, F. (2005). Fuzzy sets in database and information systems: Status and opportunities. *Fuzzy Sets and Systems, 156*(3), 418–426.

Buckles, B., & Petry, F. (1982). A fuzzy model for relational databases. *International Journal of Fuzzy Sets and Systems, 6*(3), 213–226.

Burrough, P., & Frank, A. (Eds.). (1996). *Geographic object with indeterminate boundaries* (Vol. 2). GISDATA Series. London: Taylor and Francis.

Caha, J., Nevtípilová, V., & Dvorský, J. (2014a). Constraint and preference modelling for spatial decision making with use of possibility theory. In M. Polycarpou, A. C. P. L. F. De Carvalho, J.-S. Pan, M. Woźniak, H. Quintian, & E. Corchado (Eds.), *Hybrid artificial intelligence systems SE—13* (Vol. 8480, pp. 145–155). Berlin: Springer International Publishing.

Caha, J., Vondráková, A., & Dvorský, J. (2014b). Comparison of crisp, fuzzy and possibilistic threshold in spatial queries. In A. Abraham, P. Krömer, & V. Snášel (Eds.), *Innovations in bio-inspired computing and applications SE—22* (pp. 239–248). Berlin: Springer International Publishing.

Carniel, A Ch., Ciferri, R. R., & Ciferri, C. D. A. (2016). Handling fuzzy points and fuzzy lines using the fuzzy geometry abstract data type. *Journal of Information and Data Management, 7,* 37–51.

Changa, N. B., Parvathinathanb, G., Jeff, B., & Breedenc, J. B. (2008). Combining GIS with fuzzy multicriteria decision-making for landfill siting in a fast-growing urban region. *Journal of Environmental Management, 87,* 139–153.

Christakos, G., Bogaert, P., & Serre, M. C. (2001). *Temporal GIS: Advanced functions for field-based applications*. Berlin, Heidelberg, New York: Springer.

Cuevas, L., Marín, N., Pons, O., & Vila, M. A. (2008). pg4DB: A fuzzy object-relational system. *Fuzzy Sets and Systems*, *159*, 1500–1514.

De Caluwe, R., Guy De Tre, G., & Bordogna, G. (Eds.). (2004a). *Spatio-temporai databases: Flexible querying and reasoning*. Berlin, Heidelberg, New York: Springer.

De Caluwe, R., Guy De Tre, G., & Bordogna, G. (2004b). Basic notations and rationale of the handling of imperfect information in spatio-temporal databases. In R. De Caluwe, G. Guy De Tre, & G. Bordogna (Eds.), *Spatio-temporal databases: Flexible querying and reasoning*. Berlin, Heidelberg, New York: Springer.

Deng, L., Liang, Z., & Zhang, I. (2008). A fuzzy temporal model and query language for FTER databases. In *Eighth International Conference on Intelligent Systems Design and Applications (ISDA 2008)* (pp. 77–82), Kaohsiung, Taiwan, November 26–28.

Ďuračiová, R. (2014). Implementation of the selected principles of the fuzzy set theory into spatial database system and GIS. In: *SGEM 2014, 14th GeoConference on Informatics, Geoinformatics and Remote Sensing*, *Conference Proceedings* (Vol. I, pp. 627–634), Albena, Bulgaria, June 17–26, STEF92 Technology Ltd., Sofia.

Emrich, T., Kriegel, H. P., Mamoulis, N., Renz, M., & Zuefle, A. (2012). Querying uncertain spatio-temporal data. In *The 28th IEEE International Conference on Data Engineering (ICDE 2012)* (pp. 354–365), Washington, DC., April 1–5, 2012.

Grabisch, M., Marichal, J.-L., Mesiar, R., & Pap, E. (2009). *Aggregation functions*. *Encyclopedia of mathematics and its applications* (Vol. 127). Cambridge: Cambridge University Press.

Hudec, M. (2009). An approach to fuzzy database querying analysis and realisation. *ComSIS, 6*(2), 127–140.

Jiang, H., & Eastman, J. R. (2000). Application of fuzzy measures in multi-criteria evaluation in GIS. *International Journal of Geographical Information Science, 14*, 172–184.

Kacprzcyk, J., Petry, F.-E., & Yazici, A. (2010). *Uncertainty approaches for spatial data modeling and processing: A decision Support perspective*. New York: Springer Science and Business Media LLC.

Klir, G. J., & Yuan, B. (1995). *Fuzzy sets and fuzzy logic: Theory and application*. New Jersay: Prentice-Hall PTR.

Kosko, B. (1990). Fuzziness vs. probability. *International Journal of General Systems*, *17*, 211–240.

Kreinovich, V., Quintana, C., & Reznik, L. (1992). Gaussian membership functions are most adequate in representing uncertainty in measurements. In: *Proceeding NAFIPS: North America Fuzzy Information Processing Society Conference, NAFIPS* (pp. 618–624), Puerto Vallarta, Mexico, December 15–17, NASA Johnson Space Center, Houston.

Malczewski, J. (1999). *GIS and multicriteria decision analysis*. New York: Willey.

Morris, A., & Jankowski, P. (2005). Spatial decision making using fuzzy GIS. In F. E. Petry, V. B. Robinson, & M. A. Cobb (Eds.), *Fuzzy modeling with spatial information for geographic problems* (pp. 275–298). Berlin, Heidelberg: Springer.

Petry, F. E., Robinson, V. B., & Cobb, M. A. (2005). *Fuzzy modeling with spatial information for geographic problems*. Berlin, Heidelberg: Springer.

Robinson, V. B. (1988). Some implications of fuzzy set theory applied to geographical databases. *Computers & Geosciences, 16*(7), 857–872.

Ross, T. J. (2010). *Fuzzy logic with engineering applications* (3rd ed.). Chichester: Wiley.

Shekhar, S., & Xiong, H. (2008). *Encyclopedia of GIS*. New York: Springer Science and Business Media LLC.

Schneider, M. (1999). *Uncertainty management for spatial data in databases: Fuzzy spatial data types*. In: *International Symposium on Advances in Spatial Databases* (pp. 330–351), Springer.

Schneider, M. (2008). Fuzzy spatial data types for spatial uncertainty management in databases. In J. Galindo (Eds.), *Handbook of research on fuzzy information processing in databases* (pp. 490–515). Information Science Reference.

Sözer, A., Yazıcı, A., Oğuztüzün, H., & Osman, T. (2008). Modeling and querying fuzzy spatiotemporal databases. *Information Sciences, 178,* 3665–3682.

Tang, X., Fang, Y., & Kainz, W. (2006). Fuzzy topological relations between fuzzy spatial objects. In L. Wang et al. (Eds.), *FSKD 2006 LNAI 4223* (pp. 324–333). Berlin, Heidelberg: Springer.

Wang, F. (1994). Towards a natural language user interface: An approach of fuzzy query. *International Journal of Geographical Information Systems, 8*(2), 143–162.

Wang, F. (2000). A fuzzy grammar and possibility theory-based natural language user interface for spatial queries. *Fuzzy Sets and Systems*, *113*(1), 147–159.

Zadeh, L. (1965). Fuzzy Sets. *Information and Control, 8,* 338–353.

Dynamic Visualization of Transit Information Using Genetic Algorithms for Path Schematization

Marcelo Galvao, Francisco Ramos, Marcus Lamar and Pastor Taco

Abstract In this paper, we present a genetic algorithm for path octilinear simplification. The octilinear layout, recognized worldwide in metro maps, has the special property that edge orientations are restricted to eight angles. The proposed search technique combines possible solutions to find a solution with a desired balance between faithfulness to the original shape and reduction of bends along the path. We also aim the genetic algorithm to real-time response for dynamic web visualizations so we can experiment on how algorithms for the visualization of schematic maps can be availed in a context of mobile web devices in order to empower efficiency in transmitting transit and navigation information. A prototype of a web application and real transit data of the city of Castellón in Spain were used to test the methodology. The results have shown that real-time schematizations open possibilities concerning usability that add extra value to schematic transit maps. Additionally, performance tests show that the proposed genetic algorithms, if combined with topological data and scale variation transformation, are adequate to sketch bus transit maps automatically in terms of efficiency.

Keywords Transit map · Schematic generalization · Octilinear graph · Genetic algorithm · Digital map · Web visualization · Public transportation

M. Galvao (✉)
Institute for Geoinformatics, University of Münster, Münster, Germany
e-mail: galvao.marcelo@uni-muenster.de

F. Ramos
Institute of New Imaging Technologies, Jaume I University, Castellón, Spain
e-mail: francisco.ramos@uji.es

M. Lamar
Departamento de Ciência da Computação, University of Brasília, Brasília, Brazil
e-mail: lamar@unb.br

P. Taco
Programa de Pós-Graduação em Transportes, University of Brasília, Brasília, Brazil
e-mail: pwgtaco@gmail.com

I. Ivan et al. (eds.), *Dynamics in GIscience*, Lecture Notes in Geoinformation and Cartography, DOI 10.1007/978-3-319-61297-3_8

Introduction

Schematic map differs from cartographic maps by being more diagrammatic. Unnecessary information can be omitted to point users' attention to a specific purpose. Usually, to achieve a schematic configuration, paths and polygons are submitted to simplification processes, and dense areas are enlarged to increase readability.

In the past 15 years, many researchers have published work addressing the automatic schematization of transit maps, and the metro map layout is the most common design found in those publications. The angle restriction of the edges and reduction of bends along the transit lines, among other characteristics, makes the metro map layout an efficient information tool for transit purposes (Allard 2009). It is easier for the passengers to follow a path with their eyes and to identify connections in decision points.

With the help of growing computer power, the results achieved by automatic drawing algorithms ever more closely resemble to results of professional handmade maps (Nollenburg and Wolff 2011). This context, together with the emerging mobile communication technology, opens new possibilities for the usage of schematic maps. They will be able to turn from a static piece of information to an informative tool that reflects the changes in time and the specific needs of a traveler. Moreover, by being created on demand, interactivity could be explored so the user can go from a network overview into desired details depending on the context of usage.

Static transit maps, usually handmade by professional designers, are costly and so aimed for the general public. They need to be complete in order to serve the public but they are often overloaded with unnecessary information if only individual needs are considered. Alternatively to static maps, wayfinding transit route applications, like the service powered by Google™, mainly give step-by-step instructions for a specific chosen route. Although efficient in wayfinding, this method requires a new consult on every route the passenger wants to take and by not providing familiar and alternative lines for a general view of the route it is not meant to support passenger to build their own mental map.

In this paper, we present a genetic algorithm (GA) for path schematization. We aim this solution to a real-time application and build it as a restful web service in order to explore schematization on demand for mobile applications. We assume that the web platform, in addition to allowing independent universal access to the information, allows applications to connect to external services that can empower dynamic information to visual information tools. In our prototype, instead of origin and destination, we use points of interest (POI) of the traveler to select for schematization only the part of the transit lines that connect those POIs. Also, we use the location awareness of mobile devices to provide real-time information to facilitate the use of the schematic maps in a navigation context. We show that, by interaction, a passenger can zoom to stations to view them in a cartographic map what would be useful during walking navigation.

The proposed GA for path schematization, which a preliminary version was presented in Portuguese at XXVI ANPET Congress (Galvao et al. 2014), uses a fitness function that measures the proportion of bends in the path and its faithfulness to the original shape and by changing the value of a parameter in the fitness function it is possible to set if the final solution should care more about bend reduction and less to faithfulness or vice versa. Although the presented technique is a simple path schematization, we use topological network data to make a strategical division of the graph that allows us to establish a sequence of schematization respecting straightness along transit lines and reducing topological faults in the final design.

We aimed our methodology to bus networks because (i) it is the most common mode of public transportation (PT); (ii) schematic maps are more scarce for this modality in comparison to subway services; (iii) because bus networks are usually more complex in their morphology and size, in a way that a solution meant for bus should work for metro or others PT means. Real transit data of Castellón de la Plana (Spain), a typical medium size European city, has been used to produce the final sketches.

Related Work

"The metro layout problem" (Hong et al. 2004) has been addressed by dozens of publications since the end of the 1990s. In surveys such as those presented by Wolff (Drawing subway maps: A survey, 2007) or Nöllenburg (A Survey on Automated Metro Map Layout Methods, 2014) it is possible to find descriptions and evaluations of many of them. Each research addresses the problem in a specific way for a specific purpose and the techniques developed are as diverse as possible.

Avelar (2002) presented in her doctoral thesis one of the first complete studies about computing octilinear maps for public transportation. The relevance of this work extends the algorithm itself. Even being a computational research, important design aspects like definitions of schematic maps, map styles classification, symbology conventions and design considerations for aesthetically pleasant maps are covered. Moreover, Avelar handles data modeling aspects essential to the topological characteristics of transport maps and objects of interest.

Regarding the algorithm, the presented method (Anand et al. 2007) first simplify the lines using Douglas-Peucker, then simulated annealing is used to iteratively move the vertices to conform with octilinear positions without violating the network topology. The algorithm aims to create octilinear schematization of road networks. The presented results showed success in preserving the topology of Zurich's road network and having most of the edges in octilinear position (some edges could not be octilinearly placed). However, in terms or performance, they were not adequate for real-time solutions.

Nöllenburg and Wollf (2011) identify design rules presented in real metro maps around the world, so they aimed their method for high-quality results. Nöllenburg

(2005) also proved that the metro layout problem is part of the NP-Complete class of decision problems. It means that the time to solve this problem grows exponentially proportional to the size of the instance. These results drive computer scientist who deals with the problem to use heuristics searches, treat instances differently, change the definition of the problem, or to use optimizations.

Given this knowledge, Nöllenburg (2005) models the problem in mixed-Integer programming (MIP), a mathematical programming that uses linear and integer constraints. That way, and using a commercial MIP solver design for efficiency (CPLEX), Nöllenburg obtained results of visual quality similar to ones made manually by a professional designer. Additionally, his solution was able to create space to label all stations properly. However, even using CPLEX, the execution time cannot be guaranteed to be short, varying from a few minutes to hours depending on the complexity of the network. More recently, increments on the of the MIP solution, as those presented by Oke and Siddiqui (2015), succeed in reducing the time of execution.

Wang and Chi (2011), as the best of our knowledge, are the first to aim the research of automatic schematic maps into personalized solution for mobile devices. They assume that for better readability in small displays, the route of interest of the user should be more prominent in the resulting schematic maps. They use energy function to give priority to a specific route and then they use a least square method to find the final layout. Although tested only in a desktop application (not in a mobile environment), their results show that a real-time solution for the problem is able to add extra value to schematic maps, opening a new door of possibilities to be explored in schematic maps.

Genetic Algorithms for Path Schematization

Although path schematization approaches to the metro layout problem does not guarantee the topological correctness in the resulting layout, this constraint was sacrificed for performance purposes, since the combination of preserving the topology, octilinear layout, and bend reduction is responsible for the NP-Hardness of the problem (Nöllenburg 2014).

Path schematization requires first that the transit graph must be disjoint into non-overlapping paths that cover the whole graph. To obtain a reduced set of paths, a depth-first search algorithm is performed in the network. The resulting set of paths is then sent to be schematized by the GA and a new schematic position for each station is calculated.

We start describing the encoding of a chromosome. Second, we show how the mutation and cross-over process are performed. After, we show how the populations are generated. Finally, we explain the fitness function and the selection process.

Encoding the Chromosome

An important step in developing a genetic algorithm is to define how to encode the chromosome of an individual. Individuals from a given population are the fundamental units of a genetic algorithm. They identify possible solutions to a given problem and, at this present study, an octilinear path is considered an individual.

Due to the geometric nature of the problem, the most intuitive way of encoding a chromosome is using the Cartesian coordinates of stations. However, in order to facilitate other operations involved in a genetic algorithm, instead of using the Cartesian coordinate system, it was used a sort of relative polar coordinate system.

The relative polar coordinate system represents one path with n points by selecting as origin point p_0 one of the extremes of the line. The p_0 is represented by its Cartesian coordinate, i.e., its (x, y) values The only point adjacent to p_0, p_1 is represented by the polar coordinate relative to p_0, i.e., a value (r_1, θ_1) where r represents the distance between p_0 and p_1, and θ the angle formed by the segment that unites the points p_0 and p_1 and the axis x. The other point adjacent to p_1, p_2, is represented by relative polar coordinate to p_1, i.e., a value (r_2, θ_2). This representation made by relative polar coordinates goes until point p_n, forming the chromosome of the path. Figure 1 illustrates an example of a path with its chromosome value. The first gene, i.e., (15.0, 36.) represents the Cartesian coordinate of the first station. The other genes, such as (21.55, 315) indicates that this station is 21.55 units away from the previous station with azimuth direction of 315°.

Mutation and Cross-Over

After encoding the chromosome, the next step is to define the other basic operations of a genetic algorithm. Crossover and mutation help guarantee diversity for further generations.

The mutation operation consists in randomly changing one of the chromosome genes. The mutation process helps prevent a permanent fixation on a local

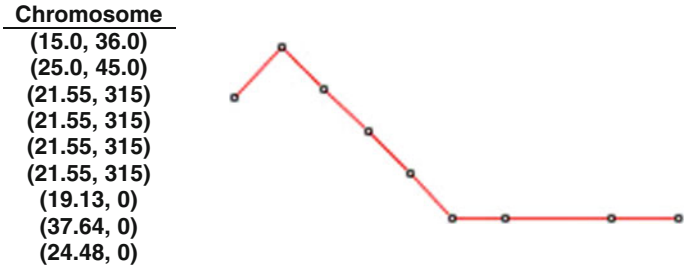

Fig. 1 Example of octilinear path and its respective chromosome genes

minimum in the solution space. Since a gene is represented by the values (r, θ), the mutation of a chromosome corresponds to alter the r and θ values of a gene. In order to avoid disproportional distortions in the process, the mutation process randomly alters the value r inside a margin of 50%, and θ mutation is done by adding or reducing 45° to its original value, thus keeping octilinearity of a chromosome.

The crossover operation consists in randomly combining two chromosomes to generate a new one. The crossover process chosen for this project is the crossover between two points. Having as input two chromosomes, the crossover process select two random points of the path as cutting points, then two parts of the first chromosome are joined together with the complementary missing part of the second chromosome. Table 1 exemplifies a crossover between chromosomes having points 3 and 6 as cutting points. Note that the resulting chromosome "Chrom. 1 × Chrom. 2" is a combination of the genes in bold of "Chrom. 1" and "Chrom. 2".

It is worth mentioning that for both, the crossover and the mutation, if the input chromosomes represent octilinear paths, the resulting chromosome will be octilinear, since the mutation and crossover are the only way to generate new individuals. If the initial population is composed only by octilinear members, all the individuals produced by the GA will be octilinear.

Generating the Populations

The input of the GA process is a path, in other words, a sequence of stations Cartesian coordinates. From this input, the GA generates n valid chromosomes. Those n chromosomes represent the elementary chromosome group and are used as individuals on the first population as well. The number of individuals per population remains constant in the evolutionary process and the population size n for the experiments in this project was ten.

To create the elementary group of chromosomes the path is submitted to n Douglas-Peucker line simplification and for each simplification a different distance

Table 1 GA for octilinear path schematization crossover

Chrom. 1	Chrom. 2	Chrom. 1 × Chrom. 2
(31.00, 97.00)	(31.00, 97.00)	**(31.00, 97,00)**
(16.15, 90)	(16.15, 90)	**(16.15, 90)**
(26.51, 0)	(26.51, 0)	**(26.51, 0)**
(24.36, 0)	**(26.51, 45)**	**(26.51, 45)**
(24.36, 0)	**(18.26, 45)**	**(18.26, 45)**
(24.36, 0)	**(32.97, 0)**	**(32.97, 0)**
(19,00, 315)	(34.24, 315)	**(19.00, 315)**
(41,5, 270)	(34.25, 225)	**(41.50, 270)**
(30,87, 0)	(30.87, 0)	**(30.87, 0)**
(16,88, 0)	(16.88, 0)	**(16.88, 0)**

dimension is set as a parameter. As a result, n different paths with a possible different number of bends are created. From each of those paths, an octilinear version from them is created in a way that all curves that connect two bends is restricted to the octilinear orientation, and the stations between two bends are distributed in an equidistant way through the curve.

To generate an offspring from a population, the individuals from this population are selected to mutate and cross between themselves to form new individuals. In order to guarantee diversity and avoid local minimum fixation, an individual of the elementary group is randomly selected to be added in the offspring as an intruder.

Fitness Function and Selection Process

Individuals with favorable genotypes must be more selectable to reproduce so that their genes are in greater numbers in next generation. The goal of the fitness function is to evaluate a chromosome according to its degree of adaptation as a solution to a problem, thus, the fitness function returns an index that represents a level of how good this chromosome is as a solution.

To facilitate to be followed with the eyes, the paths in a schematic map should avoid as possible bends on its way. However, reducing bends from a path causes displacements from its original layout and a disproportional distortion must be avoided as well. In order to find a balance between those two aesthetics factors, the fitness function calculates the distance from the individual to its original shape and a weighted arithmetic mean of the number of bends in the individual to form a single resulting index.

The distance factor is the mean of the distances between the respective points from chromosome path and its original path. Let $L = (a_0, a_1, a_2, \ldots, a_n)$ be the original path, and $L' = (b_0, b_1, b_2, \ldots, b_n)$ the octilinear path to be evaluated, and let $d(a, b)$ be the Euclidean distance between point a and b, the distance factor $\overline{d}$ can be calculated as:

$$\overline{d} = \frac{\sum_{i=1}^{n} d(a_i, b_i)}{n}$$

The bend factor is a weighted mean of the number of bends in the schematic path in a way that obtuse bend have more weight than oblique ones. Let $|x^\circ|$ be the number of bends with x degree in a schematic path, the bend factor Z can be calculated as:

$$Z = \frac{1 * |45^\circ| + 3 * |90^\circ| + 5 * |135^\circ|}{n}$$

Using the distance factor and the bend factor the fitness function return the final index η as a function of $\overline{d}$ and Z.

$$\eta = f(\overline{d}, Z)$$

With the fitness function, the GA evaluates each chromosome of a population and then it orders them according to their indexes. Individuals evaluated with lower index have more chances to be chosen than the ones worse evaluated. This kind of selection is called ranking selection. In order not to lose the best solution of a generation, the selection process is also elitist. It means that the best solution of a population is copied to its offspring.

Evolutionary Process

Due to the evolutionary process, it is expected that the best individual of a determined generation has a better or equal index values than the best individual of its previous generation. In order to understand the evolutionary effect in schematization of the path, we create an experiment that graphically shows a sequence of the best different solutions over successive generations (Galvao et al. 2014). In Fig. 2 is possible to note this morphological evolutionary process and how the algorithm tends to reduce the number of bends without disproportional distortions to its original shape.

Network Practical Results

This section presents the results of the genetic algorithm for path schematization as a solution for a real transit network map. We used real transit data of Castellón de la Plana (Spain) which is composed of 19 transit lines and 173 stations (nodes). Since our *path*-solution schematization does not concern about scale variation, i.e., regions with more density of stations getting a larger share of the available space than others, we use a single focal fish-eye transformation (Sarkar and Brown 1994) having the center of Castellón (most congested area) as focal point. Analogous to Ti and Li (2014) method, we execute the fish-eye transformation as pre-step before the genetic algorithm. Figure 3 show the visual effect of the fish-eye in the spatial transit data from Castellón.

To obtain a minimal set of paths, a depth-first search algorithm is performed through the topological transit data. The resulting set of paths is then sent to be schematized by the GA, and a new schematic position for each station is calculated. Figure 4 illustrate the network using the calculated schematic position of the vertices. For this graph, the browser waited for 1.34 s (from request to response), in which, the GA was responsible for 0.39 s of the whole process. Table 2 details, for each key operation, the total execution time spent.

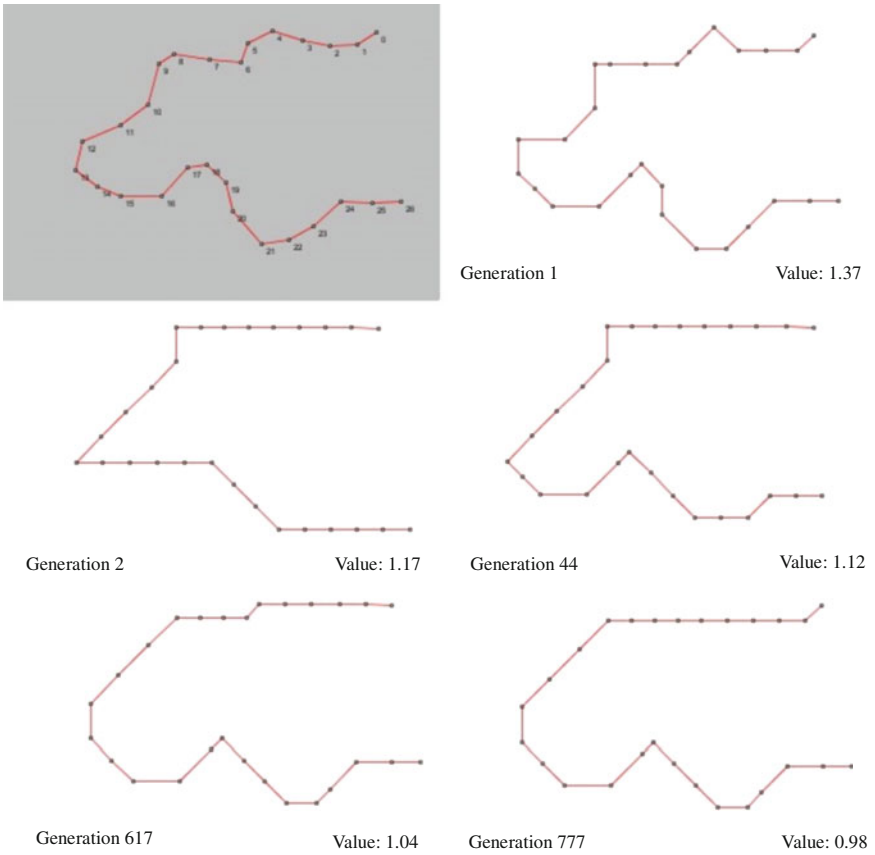

Fig. 2 Illustration of octilinear path evolutionary adaptation

Fig. 3 Fish-eye effect in the network of Castellón

Fig. 4 Final result after applying the GA for octilinear path schematization in Castellón bus network

Table 2 Distribution of independent operations execution time over the total

Operation	Execution time (s)
6 × Query database plus creation of data structures	0.89
Depth-first-search	0.01
Fish-eye transformations (all features)	0.01
GA for all paths (octilinear schematization)	0.39
GeoJSON composition	0.02
Others	0.02
Total	1.34

Using Automatic Schematization for Dynamic Transit Information

The larger the city the more complex the public transportation system tends to be. An extreme example is Sao Paulo, Brazilian largest city. Every day, 8 million passengers make use of the system in at least one of its 1387 operatives transit lines (São Paulo Transporte 2016). Even for the most skilled cartographer, the creation of an easy-to-read transit schematic map with all 1387 lines is a challenging task. In a computational perspective, such a big instance represents a too long execution time for real-time applications and, moreover, a layout with good usability cannot be

guaranteed. In this context, we built an application prototype to test the usage of schematic maps on a new perspective that takes advantage of efficient automatic drawing algorithms and the hypermedia of web applications.

Usually, a routine of a person in a city is limited to a few spots. For example, a student goes from home to the campus, from the campus to the sport club, a from the sport club back to home. A tourist goes from the airport to the hotel, from the hotel to a monument, from a monument back to the hotel. Why it makes necessary the whole set of 1387 lines to be presented, e.g., to a tourist in Sao Paulo? Digital schematic maps allow us to construct maps with a limited set of information that will attend the needs of an individual. This is more or less the concept of the handmade sketch maps as an alternative to the all-in-one paper maps.

In order to produce personalized schematic maps we assume that the process of producing schematic data must be made in real-time. This efficiency in the process is crucial. First, it helps information in the map to be updated to the last changes in the operations of the service. Second and more important is that for different areas and a different set of lines it is required a different schematic layout. Changes in the area result in changes in scale and in the dimension of the map. Variation in the set of lines implies density variation in the elements on the map. Since an adequate transit schematization depends on dimension, scale, and density, a new schematization is required for every personalized map produced.

To identify the set of lines that are valuable to a user, first, it makes necessary to identify the points of interest (POI) of this user. The POIs are usually locations in the city where the user often goes or intends to go. This data can be obtained from mobile devices from favorite places stored or current locations of the user for example. The prototype made for this project allows the users to manually add markers to a map indicating their POIs. Then we make use of the *Direction Service* powered by the Google Maps JavaScript API to identify the lines useful to travel between those points. Figure 5 exemplify this process. In Fig. 5a the markers indicates the POIs of the user. In Fig. 5b, those POIs are visualized in the schematic map with all network lines. In Fig. 5c only the lines useful for connecting the POIs are drawn.

The spatial transit data is schematized in the server in response from a GET method and sent to a web client in JavaScript Object Notation (JSON), that way we can represent the schematic data in Scalable Vector Graphics (SVG). Vector-based graphics allow programmers to explore interaction and to add dynamic information to each spatial feature independently. Figure 6 shows examples of implementations in our prototype that illustrates how a digital vector-based map can be more useful as an information seeker tool than static maps. Figure 6a, b the user zoom into a station by clicking on it and the cartographic details of the region are shown. In Fig. 6c a line(path) is enhanced on demand to avoid users to lose the focus while following it with the eyes. Figure 6d exemplifies how dynamic data can be explored in vector-based schematic maps. The prototype uses the location awareness of browsers to facilitate passengers to locate themselves during a trip. The current and the next station are indicated with intermittent rings. The given implementations are just examples on how the usability of schematic maps can be improved if they can be produced on demand for web applications.

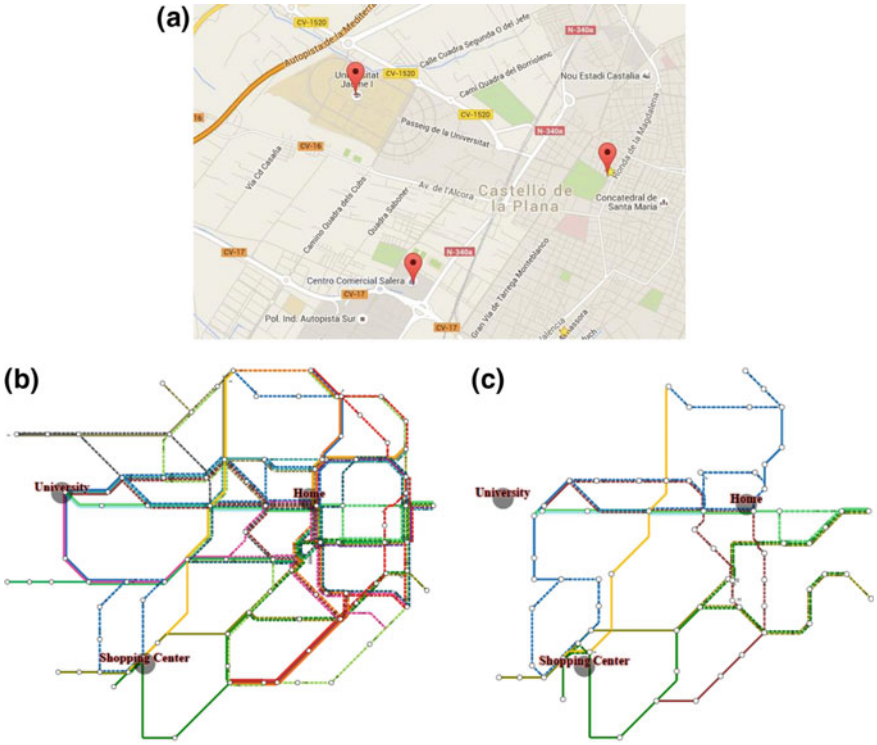

Fig. 5 "Less is more". Schematic map information reduction by traveler's relevant lines selection. **a** Points of interest. **b** Map with all lines. **c** Map with relevant lines only

Discussion

The octilinear layout proved to be a useful configuration for schematic transit maps and the success of Beck's first map (London tube map) confirm this (Allard 2009). However, the evaluation of specific octilinear graph layout solution for a given transit network representation is trickier and, in many aspects, are subjective requiring it to be surveyed for a more precise analysis.

Nöllenburg (2014) has been trying to systemize design principles that help in the evaluation of octilinear maps. The evaluation here made is based on those rules and the comments are referred to Fig. 4. The topological correctness is not guaranteed by the GA path schematization. However, our method tends to keep the stations close to their original position, so the resulting configuration tends to keep the original topology. To avoid topological inconsistencies in path schematizations, Li and Dong (2010) adopted a strategy that detects and resolves spatial inconsistencies on every insertion of a schematized path. Although more studies regarding impact in the execution time are necessary, the same strategy could be adopted for our method. In opposite to extras edge crossing, our resulting maps presents significant

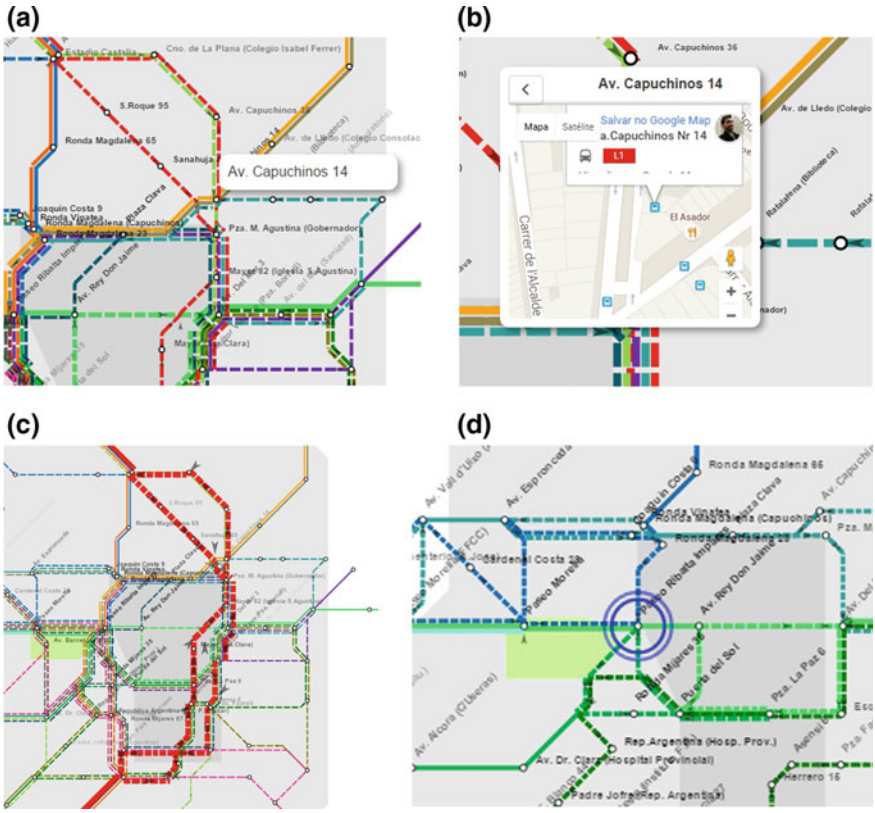

Fig. 6 Examples of interaction and dynamic information in schematic maps on demand. **a** Vector-based schematic map. **b** Metric map layer is shown after a click. **c** Line is highlighted after a click. **d** Blue rings indicate passenger's location

quantities of edges overlaying, which means when two edges lay over the same axis. Most of those violations have been programmatically identified and a solution and future work suggestion can include the overlapping edges in the same edge structure to be drawn in parallel.

The edge orientation restriction is not violated. All edges have been drawn in one of the octilinear orientation. Minimization of bends is an aesthetics principle and it is impossible to draw all lines in a straight line. Pursuing this aesthetic is even more challenging for bus networks that are at the street level and have more complex morphology than metro networks. The GA fitness function helps to keep the number of bends small and avoids sharp turns, additionally, it is possible to set the depth-first search to give straightening preference to a specific path or line over others as illustrated in Fig. 4, where we set the Tram line, that crosses the city in the east-west direction, to have preference to be rectified over the others.

The geometric distortion is minimized by the GA as well, but it plays a conflicting role with the bends minimization. Changing the parameter in the fitness function it is

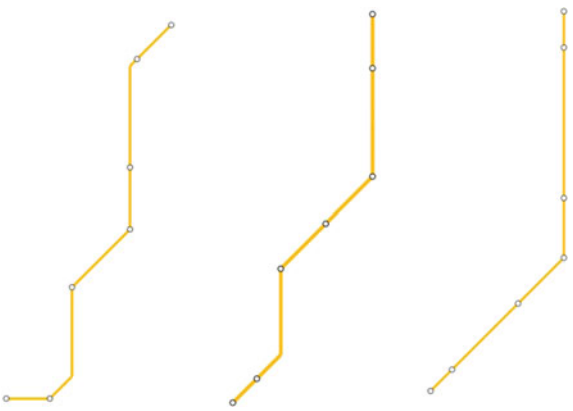

Fig. 7 GA octilinear schematization with different weights for bends reduction

possible to drive the results to less distortion or to fewer bends. Figure 7 illustrates the effect of this parameter in the fitness function. The figure on the left gives more priority to less distortion, while the one in the right to fewer bends.

Conclusion

The proposed genetic algorithm for octilinear path schematization combined with topological transit data and the fish-eye transformation was able to sketch within a predictable time octilinear schematic maps for bus networks. As a consequence of the evolutionary process, the resulting maps tend to have a reduced number of bends while keeping the final shape close to the original. The fish-eye transformation ran as a pre-step and makes the distribution of the spatial features more uniform along the available space. Using depth-first search in the network data, we are able to establish lines or paths to have straightness priority over others, an effect found in many classical metro map designs.

Our proposed method was able to generate the right data structures and compose the schematic transit information to full visualization and interactivity in the web environment. Using real transit data from Castellón, a web application was developed to a practical test of the methodology. Several functionalities were included allowing the user to specify his/her needs and interact with the schematic data in order to increase the power of schematic maps as a transit information source. We show that real-time computed schematization allows a transit map to be personalized and more dynamic, adequate to the visual information-seeking "mantra" proposed by Shneiderman (1996), "overview first, zoom and filter, then details on demand".

We were not always able to guaranty topological correctness. However, topological inconsistencies like extra edge crossing tend to be small because of the way depth-first search divided the graph and because the algorithm tends to avoid

distortions (distance) in the resulting layout, meaning that the topology of the original input is used as information for some topology correctness in the output. We understand that, to make the technique viable as an automatic drawing solution, the topological inconsistencies need to be iteratively solved. Nevertheless, the proposed genetic algorithm can be used for computer-assisted generation of schematic transit maps.

Acknowledgements Paper produced as a result of the dissertation submitted for the Degree of MSc in Geospatial Technology. Work supported by grant H2020-EU.1.1.—EXCELLENT SCIENCE—European Research Council (ERC).

References

Allard, J. (2009). The design of public transport maps. *Doctor thesis*. Politecnico di Milano.

Anand, S., Avelar, S., Ware, J. M., & Jackson, M. (2007). Automated schematic map production using simulated annealing and gradient descent approaches. *GISRUK* (pp. 414–419). Citeseer.

Avelar, S. (2002). Schematic maps on demand: Design, modeling and visualization. *PHD Thesis*. Technische Wissenschaften ETH Zürich.

Galvao, M. D., Lamar, M. V., & Taco, P. W. (2014). Desenho automático de mapas octalineares de rede de transporte pú}blico utilizando algoritmo genético. *TRANSPORTES*, 21–30.

Hong, S.-H., Merrick, D., & Do Nascimento, H. (2004). The metro map layout problem. *International Symposium on Graph Drawing* (pp. 482–491). Berlin: Springer.

Li, Z., & Dong, W. (2010). A stroke-based method for automated generation of schematic network maps. *International Journal of Geographical Information Science, 24*(11), 1631–1647.

Nöllenburg, M. (2005). Automated drawing of metro maps. *Technical Report 2005–25*. Universität Karlsruhe, Fakultät für Informatik.

Nöllenburg, M. (2014). *A survey on automated metro map layout methods.* ITI Wagner, Department of Informatics, Karlsruhe Institute of Technology (KIT), Tech. Rep.

Nollenburg, M., & Wolff, A. (2011). Drawing and labeling high-quality metro maps by mixed-integer programming. *IEEE Transactions on Visualization and Computer Graphics, 7*(5), 626–641.

Oke, O., & Siddiqui, S. (2015). Efficient automated schematic map drawing using multiobjective mixed integer programming. *Computers & Operations Research, 61*, 1–17.

São Paulo Transporte. (2016, January 25). *Indicadores*. Retrieved from SPTrans: http://www.sptrans.com.br/indicadores/

Sarkar, M., & Brown, M. H. (1994). Graphical fisheye views. *Communications of the ACM, 37*(12), 73–83.

Shneiderman, B. (1996). The eyes have it: A task by data type taxonomy for information visualizations. In *Proceedings, IEEE Symposium on Visual Languages* (pp. 336–343). IEEE.

Ti, P., & Li, Z. (2014). Generation of schematic network maps with automated detection and enlargement of congested areas. *International Journal of Geographical Information Science, 28*(3), 521–540.

Wang, Y.-S., & Chi, M.-T. (2011). Focus + context metro maps. *Transactions on Visualization and Computer Graphics, 17*(12), 2528–2535.

Wolff, A. (2007). Drawing subway maps: A survey. *Informatik-Forschung und Entwicklung, 22*, 23–44.

Configuration of Wireless Sensor Network in Olomouc

Vendula Hejlová and Tomáš Pohanka

Abstract Wireless sensor network is a new fast evolving technology used in both environmental and socioeconomic applications. The usage of this technology in a city environment is influenced by many factors dealing with technical parameters of the nodes, parameters of terrain and other disturbing factors in a city such as signal interruptions, etc. The biggest advantage of this technology is the real-time monitoring. Every wireless sensor network has technical parameters that are tested in a real terrain deployment. Distribution of nodes under the real conditions is adjusted to the results of the technical tests. These parameters include determination of the least loaded communication channel, computation of data delivery ratio (DDR), testing of battery consumption under defined conditions and determination of received signal strength indicator (RSSI). Experimental wireless sensor network was established in Olomouc in 2015. Wireless nodes Waspmote Plug and Sense produced by Spanish company Libelium are used. Olomouc wireless sensor network is oriented on meteorological monitoring. The attention is aimed at air pollutants related to traffic. The nodes are situated to two clusters—the first cluster is located to the uptown part of Olomouc, the second one is located to the centre of Olomouc. The communication between nodes and gateway is carried out using IEEE 802.15.4 protocol. The goal of this paper is to evaluate technical data from the real deployment of the nodes and to use it for the design of optimal wireless sensor network using Libelium devices equipped with 802.15.4 radio.

Keywords Wireless sensor network · Parameters of nodes · Libelium · Meteorological monitoring

V. Hejlová (✉) · T. Pohanka
Department of Geoinformatics, Palacký University in Olomouc,
17. listopadu 50, Olomouc, Czech Republic
e-mail: venda.hejlova@gmail.com

T. Pohanka
e-mail: tomas.pohanka@upol.cz

I. Ivan et al. (eds.), *Dynamics in GIscience*, Lecture Notes in Geoinformation and Cartography, DOI 10.1007/978-3-319-61297-3_9

Introduction

The variety of sensors connected to a wireless device is huge. Many applications can use this technology. Communication possibilities of wireless sensor network components are extensive. The usage of communication technology depends on a lot of factors including application, operating environment, needed communication distance, etc.

The aim of this paper is to verify the communication possibilities of wireless nodes Waspmote Plug and Sense, models Smart Environment (SE) and Smart Agriculture (SA), produced by Spanish company Libelium. These nodes are used for monitoring in two clusters in Olomouc. The purpose of this wireless sensor network is meteorological monitoring including observation of air pollutants related to traffic. The communication is based on the radio interfaces and protocols primarily developed for communication in wireless sensor network. The four technical parameters including identification of the least loaded communication channel, data delivery ratio (DDR), battery consumption, received signal strength indication (RSSI) were tested during the real wireless sensor network real operation. These parameters were evaluated and the efficient values of them were suggested.

The first part of this paper is aimed at wireless sensor network functionality, the second one shows the possibilities of wireless sensor network usage and the third one introduces the technology and regions of interest in Olomouc. The four technical parameters of the nodes are evaluated. The optimal values of technical parameters for this network are suggested. Finally, the possibility of thematic data usage is proposed.

Wireless Sensor Network

Wireless sensor network consists of three major hardware components: wireless nodes, gateway and server part (Murthy and Manoj 2004). Every wireless node consists of following parts: microprocessor, battery, communication unit, memory, built-in sensors and interface for connecting sensor boards/sensors (Jabeen and Nawaz 2015; Sinha and Chandrakasan 2001). Data can be saved in the node memory, sent from the node to one of routers or directly to a gateway. Routers are wireless nodes gathering data from other nodes. They send data either to another router or directly to a gateway. Every node has identificator (ID) and unique address (MAC). This information enables to set the configuration of nodes within the wireless sensor network. Gateway is a controlling point of the whole wireless sensor network. Gateway is a central gathering part of values obtained by nodes. Data can be either stored in the database integrated to the gateway or they can be routed to a database server for a long time storage (Murthy and Manoj 2004). The communication among nodes and between nodes and gateway is carried out on the basis of protocols primarily developed for wireless sensor networks.

The communication in a wireless sensor network can be carried out on long or short distances depending on the used communication technology. IEEE 802.15.4 and Zigbee are the protocols designed for communication in wireless sensor networks. Arrangement of nodes and design of communication paths determine the wireless sensor network topology. Star, tree and mesh are the most frequently used topologies. Three radio bands are delimited for free communication −868 MHz in Europe, 915 MHz in America. Band 2.4 GHz is free for worldwide use. The 2.4 GHz band is divided into 14 channels (Akyildiz and Vuran 2010; Murthy and Manoj 2004).

State of Art

The purpose of the wireless sensor network construction has to be specified at the beginning of the wireless sensor network installation. Wireless sensor network is usually used on environmental and socioeconomic field nowadays (El-Bendary et al. 2013). Yick et al. (2008) divided the applications of wireless sensor networks into two categories—tracking and monitoring. Wireless sensor networks are not limited to these applications and they can be used for monitoring of selected phenomenon. Wireless sensor networks have a huge potential in crisis management Kaur et al. (2012), Řezník (2012), Benkhelifa et al. (2014). Marin-Perez et al. (2012) and Neal et al. (2012) describe flood system using protocols primarily developed for wireless sensor networks observing the values of water state. The crisis management is also associated with the development of the fire monitoring system Yu et al. (2005), Bayo et al. (2010). Applications of wireless sensor networks for monitoring of air pollutants are described in the survey presented by Yi et al. (2015). Roseline et al. (2013) points out the need for air pollutants monitoring in Asia, especially in China and India. These countries are developing air pollutants monitoring system using IEEE 802.15.4 and Zigbee protocols for communication between nodes, MySQL database servers for data storage and visualization tools in the form of graph or maps (Google Maps, LabView) to display measured values in the real time Hu et al. (2011), Prasad et al. (2011), Liu et al. (2012), Khemnar et al. (2013).

The term most commonly associated with wireless sensor network is “Smart” (Townsend 2013). A lot of cities in the Czech Republic have adopted concept for building “Smart City”. “Smart City” is a development vision to integrate information, communication technology and Internet of Things to manage cities’ assets —these assets include waste management, lighting control, mobility, parking management, water supply and air quality control. The goal of this concept is to improve the quality of life, to increase the energy consumption and to improve the efficiency of services (Townsend 2013). Písek is marked as the first Czech “Smart City”. First applications of wireless sensor networks are aimed at street lights control, energy management and detection of free parking spots (Polanský 2016). Other “Smart” projects in Kolín, Pardubice or Valašské Meziříčí are aimed at waste

management (Černý 2016; Česká televize 2016). This technology can be used to improve the efficiency of functionality indoor so that term "Smart House" became very popular. Fernández et al. (2016) describes integration of information about weather, ships and cargoes in the port and depicts this integration as "Smart Port". "Smart Dust" is a term for very small and cheap wireless devices communicating with the receiver. These wireless devices are spread in the landscape and they are most frequently used during military actions (Pister, n.d.). Other example using term "Smart" is associated to sensors integrated to a bicycle to control the air quality in the direction of bicycles' movement (Cho and Yoo 2014). The expansion of this technology is expected in the future.

Outdoor distribution (3D distribution) of wireless nodes needs verification of wireless devices technical parameters to suggest the optimal parameters for the wireless sensor network. Emary and Ramakrishnan (2013) aimed their research at distribution algorithms in 3D environment. They studied technical parameters of wireless devices—the most important technical parameters in distribution process of nodes including data delivery ratio (DDR), battery consumption and received signal strength indication (RSSI). Determination of the least frequently used channel within the 2.4 GHz band is demanded at the beginning.

Wireless Sensor Network Components Used for Meteorological Monitoring

Technical parameters of Waspmote Plug and Sense nodes, models Smart Agriculture and Smart Environment, were investigated. The hardware of these nodes is encapsulated into a plastic box (Fig. 1). The technical platform inside the encapsulation consists of motherboard and sensor board. Motherboard is the most important part including microprocessor, battery, communication unit, pins for connecting sensor board and input/output pins. Sensors are connected to the sensor board, maximum of six sensors in the configuration prescribed by the producer can be connected to the sensor board (Libelium 2016a). IEEE 802.15.4 is the used communication protocol. This protocol is the elementary one for wireless sensor network devices communication. Six sensors monitoring temperature, relative humidity, NO_2, CO_2, VOC and air pollutants were connected to the model Smart Environment. Two sensor connectors for monitoring temperature/relative humidity, wind speed/direction were used in the model Smart Agriculture. Lithium rechargeable battery is integrated, the capacity of this battery is 6600 mAh, the voltage ranges from 3.3 to 4.2 V. The battery is waterproof and its operation temperature is between −10 and 50 °C. The external 5 dBi antenna with SubMiniature version A (SMA) connector is integrated to the node. The nodes are situated at the height of 2 m above the ground with minimum distance of 5 m from buildings and trees. The recording interval was set either to one or five minutes during all the measurements. Five positions for nodes have been distributed

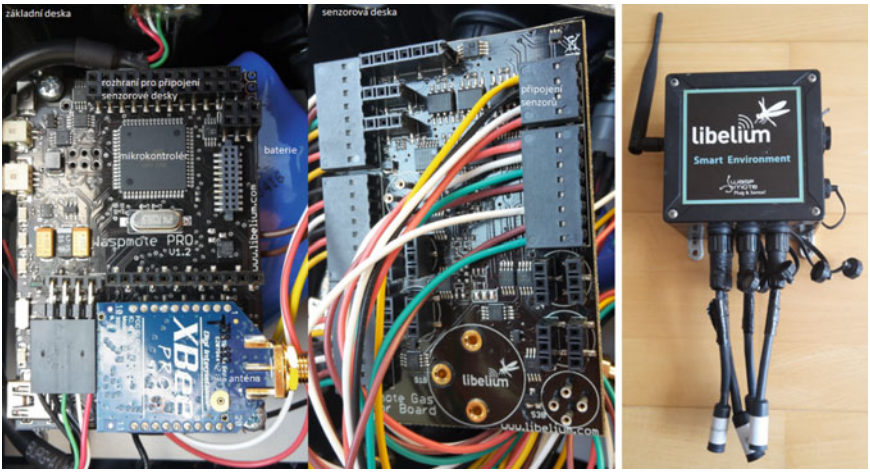

Fig. 1 Motherboard and sensor board (*on the left*), wireless node encapsulation with connected sensors and antenna (*on the right*)

outdoor and two nodes' positions were situated indoor in the first cluster. Two nodes positions were outdoor in the second cluster. The nodes do not have to be situated at all the positions all the time because the limited number of nodes owned by the Department of Geoinformatics.

The measured values are gathered in a gateway called Meshlium. It is a Linux router receiving data from the nodes with IEEE 802.15.4 wireless communication interface. The wired interface is used for connection the gateway to ethernet. This step enables distant connection to this device. This device has integrated MySQL database where the measured data from nodes are stored. Meshlium has more communication interfaces such as WiFi (primarily for wireless communication with computers), GSM/GPRS (primarily for communication with remote server). The gateways are situated indoor behind the windows in the both clusters.

Region of Interest and Parameters of Olomouc Wireless Sensor Network

The first cluster is situated in the uptown part—Olomouc–Holice, in the Scientific Park of Palacký University. The second cluster is located in the centre of Olomouc, in the campus of the Faculty of Science. The first cluster is smaller one because it serves as a testing cluster. The conditions are more stable at this uptown part, lower number of factors influencing the communication between nodes and the gateway occurs here. The elementary parameters of the wireless sensor network are

Table 1 Elementary information about Olomouc wireless sensor network configuration

Wireless sensor network configuration	Wireless sensor network parameters
Application (purpose) of the wireless sensor network	Meteorological monitoring
Architecture of the wireless sensor network	Clustered
Number of clusters	2
Localization of the first region of interest	Olomouc–Holice
Localization of the second region of interest	Olomouc center
Size of the first region of the interest	0.082 km^2
Size of the second region of the interest	0.2 km^2
Number of positions for nodes in the first region of interest	2
Number of positions for nodes in the second region of interest	7
Localization of nodes at the defined height above the ground	2 m

summarized in the table (Table 1). The nodes in the first cluster have been operating since 1st May 2015. The nodes in the second cluster operated in two short periods (25th September–9th October 2014, 9th December–16th December 2014), followed by continuous monitoring from 1st July 2016.

The clusters are situated 2.4 km far from each other. Every cluster has defined number of positions for wireless nodes and for gateway (cluster head). MySQL database is integrated in the both gateways (cluster heads). Primary data are stored in these two integrated databases. Data from these two databases are transmitted to another server database. Gross errors are filtered before the data is inserted to the server database. Elementary data operations take place in the server database (Fig. 2).

Results of Technical Parameters Tests

The tests of technical parameters including data delivery ratio and battery consumption were described in Emary and Ramakrishnan (2013). The technical results from the measurements used in Olomouc are summarized in this chapter. First, the search for the least loaded communication channel is realized in the both clusters. Secondly, data delivery ratio was evaluated. The battery consumption was also computed. Finally, the quality of RSSI using two different omnidirectional antennas was tested.

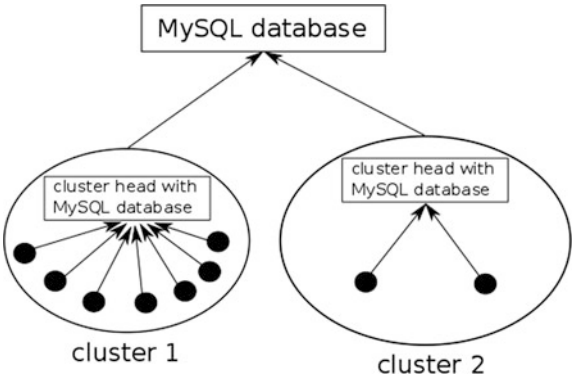

Fig. 2 Communication scheme and data storage

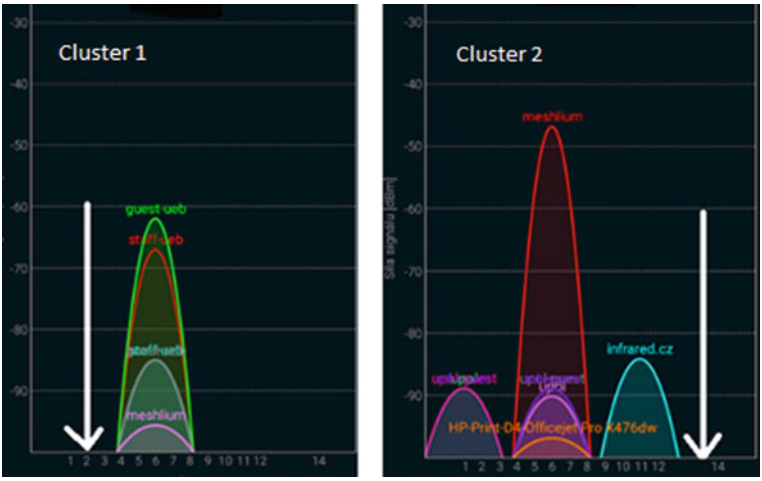

Fig. 3 The usage of communication channels in the first cluster on 2nd August, 1:02 pm (*on the left*) and in the second cluster on 1st August 2016, 3:13 pm (*on the right*)

Identification of the Least Loaded Communication Channel

The least loaded communication channel was identified in the both clusters. The band 2.4 GHz is the most frequently used one by WiFi. The loading of this band by WiFi was investigated in WiFi Analyser programme. This is the open source programme for Android, so that the investigation is performed from a smartphone (Fig. 3). Overall, the first cluster is less loaded by the communication, all the devices communicate in the middle sixth channel. The channel two was selected as the one for communication in the wireless sensor network for the first cluster. More devices communicating in different channels are situated in the second cluster. The most loaded channel in the second cluster is also the sixth one. The channel selected for communication in this cluster is the last but one—0 × 17. It was assumed that

WiFi is the major communication protocol using this radio band. It is important to do more tests at the beginning of the measurements because the situation is changing in time so that the tests were repeated in the both clusters. The communication channel tests have to be performed when the data delivery ratio is decreasing because the selected channels could be newly used for communication.

The communication in the selected channels and in the most loaded ones in both clusters was tested. The difference was significant. Data from nodes operating in the most loaded channels were not delivered to the gateway for distance longer than 5 m, so that it was confirmed that this configuration is unusable in the real application and searching for the least loaded communication channel is an important step.

Data Delivery Ratio (DDR)

Data delivery ratio indicates the percentage of successfully delivered data from a node to the gateway. Data delivery ratio is decreasing with longer distance, lower battery state, situation of obstacles in the communication path, presence of disturbing signals or technical problems with antenna. Data delivery ratio is computed as the ratio of the count of the real sent data and the count of data that should be delivered at the selected time period. This ratio was computed for different periods of time. It was computed for 31 days after situation of the node to the given position (Fig. 4). This experiment took part in the first cluster. The lowest data delivery ratio was at the position B—the node situated at this position was located out of the line of sight so that even when it is situated at the short distance from gateway the number of transmitted data was low. The obstacle in the form of the building situated in the communication path was a huge problem. The node situated at the C position had technical problems. This position was cancelled because this place was used as a new field for an agriculture experiment so that the measurements could not be repeated. Position E and F had different data delivery ratio because they were situated near to each other and the signal from one node disturbed the signal from the other node. Surprisingly, high data delivery ration was computed for position A.

Battery Consumption

Battery consumption depends on many factors so that battery consumption was tested in different configurations in indoor and outdoor conditions. The tested batteries were one year old but the nodes with these batteries were not used before this experiment. The tests in indoor conditions were aimed at investigation of battery consumption in different recording intervals and consumption of different sensors connected to a node. The indoor tests were performed through wired connection of nodes to the computer using PuTTy suit v0.65 programme

Fig. 4 Data delivery ratio in the first cluster. *Source* ČÚZK, Orthophoto from Department of Geoinformatics drone

cooperating with the IDE (Integrated Development Environment), programme native for Waspmote Plug and Sense programming. The outdoor tests were performed in the both clusters. The observed schemes were aimed at investigation of nodes´ distance from the gateway, influence of obstacles and meteorological conditions. The batteries of nodes were fully charged at the beginning of all the experiments. The charging process of the nodes was time consuming and took approximately 142 h (144 h from computer, 140 from electricity). According to the capacity of the batteries the process should be shorter but the reality was different.

Graph (Fig. 5) shows the battery discharging trend during four different recording periods. The shorter interval of recording the higher battery consumption was determined. The hypothesis in the trend was confirmed but the differences between the shortest and the longest recording interval were not as high as expected. The recording interval depended on the purpose of the wireless sensor network and the needed recorded values of measured phenomenon. All sensors were connected to the node during this experiment.

Every sensor had different energy consumption. This data was written in the Technical Guide (Libelium 2016b). Sensor recording NO_2 values was the one with the lowest energy consumption from the air pollutants sensors. Air Pollutants 2

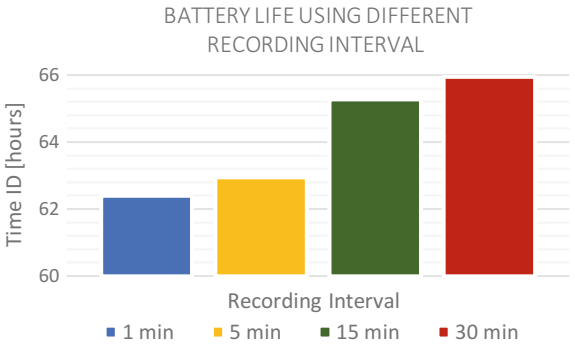

Fig. 5 Battery life in different recording intervals

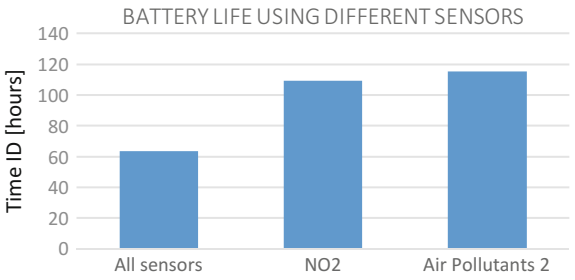

Fig. 6 Battery life using different sensors

sensor was the one with the second highest energy consumption. The indoor tests did not confirm this information described in the Technical Guide as shown in the graph (Fig. 6). If all sensors were connected to the node the battery consumption was the highest as expected. The recording interval for this experiment was set to one minute.

The average daily battery consumption was computed for two nodes operating for the longest time in the terrain. The node (ID 437, SE) was situated indoor, it had connected all the sensors and sent data to the gateway in the real time. The second node (ID 362, SE) was situated outdoor 61 m from the gateway. This node sent data every five minutes. The graph (Fig. 7) demonstrates that the battery values were very similar at the beginning of the experiment. The battery levels of node situated outdoor were higher in the middle part of battery life. It meant that shorter recording interval had higher influence on battery level than longer distance from the gateway. These differences were lower after nine months of operation and with the changing meteorological conditions (Lower temperatures caused faster battery discharging). If the temperature decreased under 10 °C, the battery was faster depleted.

The outdoor battery tests were aimed at definition of the reliable communication distance in the wireless sensor network using the components with the above defined configuration (Fig. 8). All the sensors (but the one indoor (ID 437, SE)) sent data at the same five minute recording interval. The indoor node had one

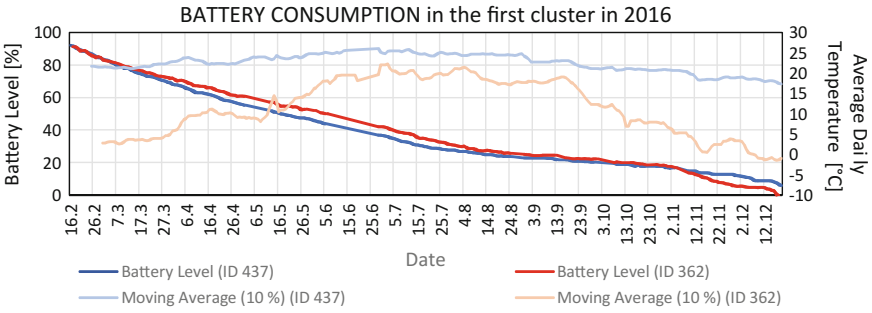

Fig. 7 Battery consumption and average daily temperatures obtained by two nodes operating in the first cluster

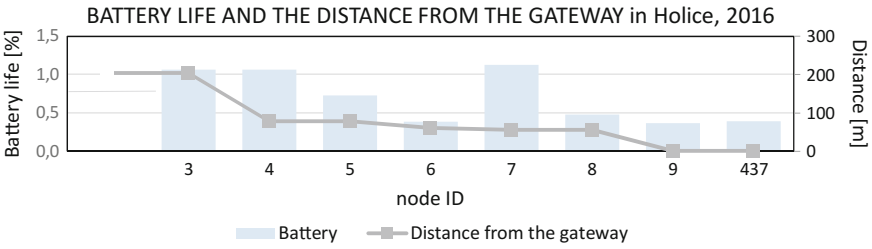

Fig. 8 Battery life at different distances from the gateway

minute recording interval. Nodes with IDs 4, 7, 8, 9 were models Smart Agriculture, the rest of nodes were Smart Environment models. All the sensors were always connected to the node, batteries were fully charged, their state after the situation to the terrain and state at the end of their operation cycle was identified, this number was divided by the number of operating days ((battery life at the beginning—battery life at the end)/number of days in the terrain). The lower number of battery life the lower battery consumption was detected. The trend is obvious—the longer distance from the gateway the shorter battery life. Node ID 7 was the exception—this state was caused by the bad battery state.

The obstacles had no influence on the battery consumption. Data delivery ratio was strongly influenced by the obstacles.

Meteorological conditions influenced the battery life. Higher temperatures warm the battery placed under the black encapsulation and the battery was faster depleted. Figure 7 shows that the battery was faster depleted when the temperatures were under zero. It was necessary to observe the battery level in these days to replace the nodes in time.

Received Signal Strength Indication (RSSI)

The received signal strength was measured in dBi. The values of this variable typically ranges from −30 to −100 dBi in data transmission experiments, the higher value of the variable the higher quality of the signal. The typical RSSI values for reliable communication of Waspmote Plug and Sense devices is −37 dBi (Libelium Networking 2016). The lower RSSI value, the lower data delivery ratio is indicated. This variable is logarithmic (Bardwell 2002). The values of this variable depend on communication technology, distance between communicating devices, obstacles, their structure and number of signal disturbing influences (Deak et al. 2012). This experiment was realized from 28th June to 30th June 2016 in the second cluster. One node was situated outdoor (sender) and sent data to the second one (receiver) situated indoor. Receiver was situated at the distance of 98 m from the sender. Receiver sent data to the gateway database where the RSSI values of the sender were indicated (Fig. 9). First, the high-performance antennas were tested. Secondly, the low-performance antennas were used for the test at the same configuration as the previous ones. The battery of sending node was fully charged at the beginning of the tests. Battery in the sender decreased five times faster than the battery in the receiver in the both cases. The communication interval between the nodes was set to one minute. Using high-performance antennas surprisingly showed worse RSSI values, the average value was set to −72.42 dBi (Fig. 10). Using low-performance antennas showed better RSSI values, the average value was 61.45 dBi. Data delivery ratio was low in the both cases. It was set to 42% using low-performance antennas. High-performance antennas showed over one per cent better values of data delivery ratio than low-performance ones.

The experiment with nodes equipped with two low-performance antennas situated at the distance of 150 m was realized. The RSSI values were bad, the average

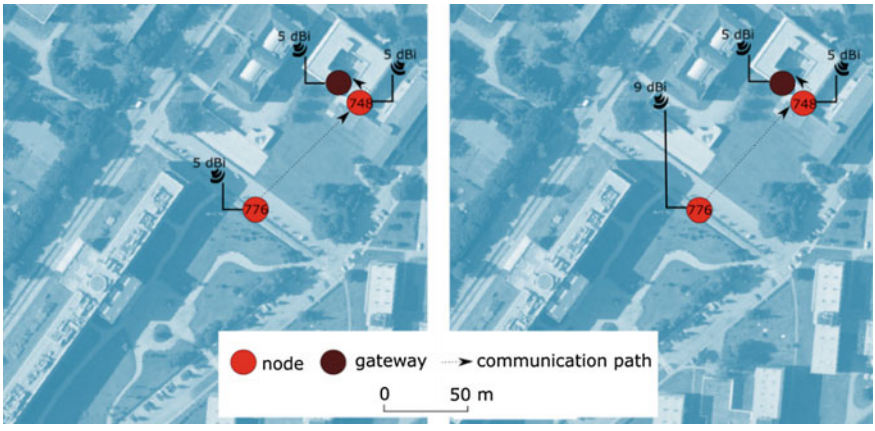

Fig. 9 Configuration of nodes sending RSSI values

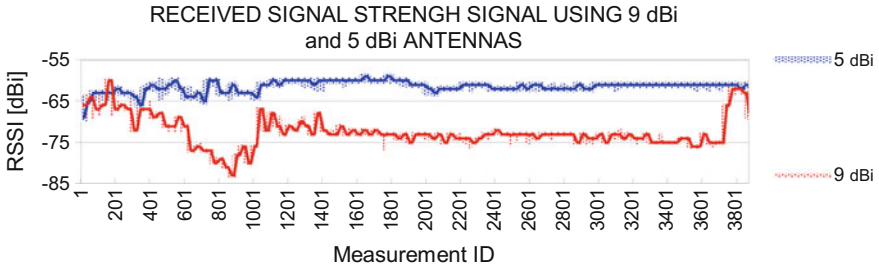

Fig. 10 RSSI values during the experiment

value was set to −80 dBi. This confirmed the fact that RSSI values depend on distance. The communication at the distance longer than 100 m could be problematic in city conditions.

Evaluation of the Results

The results showed that it is necessary to detect the least communication loaded channel. If the communication in the wireless sensor network was set in one of more loaded channels the reliability of data delivery ratio was decreasing. The distance longer than 100 m between sender and receiver was problematic because battery was faster depleted, RSSI values were too low and the reliability of communication was low either. Battery consumption was influenced by many factors. The factors influencing the battery life at most were recording interval and meteorological conditions. Five minute recording interval was set to meteorological monitoring because the values of measured meteorological phenomena did not change so quickly. The obstacle in the form of buildings or terrain breaks in the communication path decreased data delivery ratio. The indoor temperatures were optimal for nodes operation because high data delivery ratio and low battery consumption were identified.

Data from correctly configured wireless sensor network are the basis for meteorological analysis. The analysis of average temperatures values obtained by sensors in the terrain were realized in Olomouc. The temperature sensors were situated in the sun shields at the height of 2 m above the ground in the both clusters. Temperature measurement precision was set to 0.2 or 2 °C, depending on the used model of the node. Model Smart Environment had lower measurement precision than mode model Smart Agriculture. One more precise model of node was situated in every cluster during all the measurements. The average value 21.1 °C in the first cluster and 21.2 °C in the second cluster were the average values obtained by more precise nodes. Figure 11 shows the average temperatures computed from data obtained in climatological terms in July. Average values were higher in the centre of the city. This indicated that the urban heat island could be presented. The nodes with data

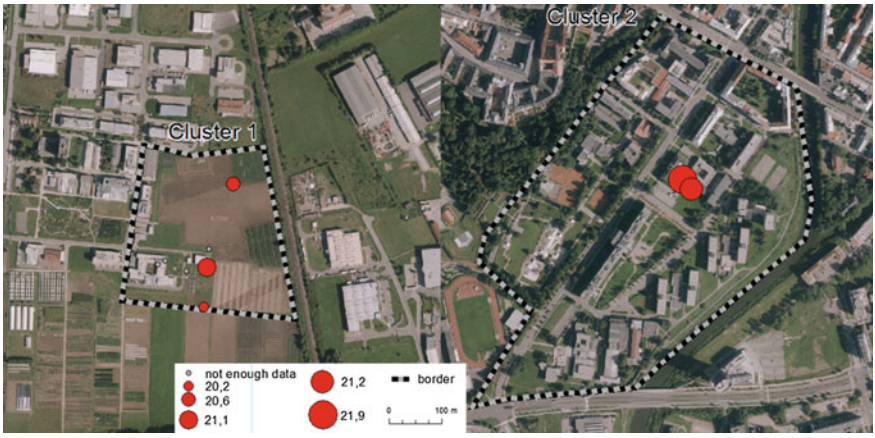

Fig. 11 Average temperature values [°C] obtained by nodes in July

delivery ratio lower than 50% were not considered, that is why item "not enough data" appears in the legend. The measured values were used for evaluation of daily and monthly courses of meteorological and chemical phenomena in Olomouc.

Conclusion

The construction of wireless sensor network is a process that needs a verification. The verification is done on the basis of nodes technical parameters tests in the terrain. The most commonly used technical parameters for verification including selection of not so loaded communication channel, definition of the data delivery ratio, determination of battery life in different configurations and determination of signal strength.

These parameters were tested in the real deployed wireless sensor network in Olomouc. Waspmote Plug and Sense nodes produced by Libelium using IEEE 802.15.4 protocol were deployed in two clusters in Olomouc. First, the communication least loaded channels in the both clusters were determined. This step increased the data delivery ratio from nodes to the gateway. The results showed that the highest influence on the distribution of nodes had obstacles situated in the communication path. Distance between communicating nodes had the second highest influence on data success delivery and battery consumption. The reliable communication distance for Olomouc wireless sensor network was set to 100 m. Other parameters such as recording interval, number of sensors have to be considered during the technical parameters tests. These tests should be done at the beginning of wireless sensor network configuration because the positions with high reliability of data delivery are identified. The nodes are used for long term monitoring in the terrain, analysis and predictions are computed from the data.

Acknowledgements This paper was created within the project TA 04020888 Contactless monitoring and spatio-temporally modeling variability of selected soil differing characteristics, with financial support from the Technology Agency of the Czech Republic.

References

Akyildiz, I. F., Vuran, M. C. (2010). *Wireless sensor networks*. Wiley, Hoboken.

Bardwell, J. (2002). *Converting signal strength percentage to dBm values*. Wildpackets, Canada.

Bayo, A., Antolín, D., Medrano, N., Calvo, B., Celma, S. (2010). Early detection and monitoring of forest fire with a wireless sensor network system. *Procedia Eng., Eurosensor XXIV Conference Eurosensor XXIV Conference, 5*, 248–251. doi:10.1016/j.proeng.2010.09.094

Benkhelifa, I., Nouali-Taboudjemat, N., Moussaoui, S. (2014). Disaster Management projects using wireless sensor networks: An overview. *2014 28th International Conference on Advanced Information Networking and Applications Workshop,* Waina, pp. 605–610. doi:10.1109/WAINA.2014.99

Černý, A. (2016). *O2 IT services [WWW Document]. O2 IT Serv*. URL http://www.o2its.cz/chytre-mesto-kolin/ (accessed October 30, 16).

Česká televize. (2016). *Ve Valašském Meziříčí začali používat chytré popelnice. Samy ohlásí, že jsou plné [WWW Document]. ČT24*. URL http://www.ceskatelevize.cz/ct24/regiony/1956904-ve-valasskem-mezirici-zacali-pouzivat-chytre-popelnice-samy-ohlasi-ze-jsou-plne (accessed November 26, 16).

Cho, J., & Yoo, J. (2014). Implementation of distributed health-aware bicycle system for making real-time air-pollution map. *IEMEK Journal of Embedded Systems and Applications, 9,* 229–235. doi:10.14372/IEMEK.2014.9.4.229

Deak, G., Curran, K., & Condell, J. (2012). A survey of active and passive indoor localisation systems. *Computer Communications, 35,* 1939–1954. doi:10.1016/j.comcom.2012.06.004

El-Bendary, N., Fouad, M. M. M., Ramadan, R. A., Banerjee, S., & Hassanien, A. E. (2013). Smart environmental monitoring using wireless sensor networks. In *Wireless sensor networks: From theory to applications*. CRC Press: Boca Raton.

Emary, I. M. M. E., & Ramakrishnan, S. (2013). *Wireless sensor networks: From theory to applications*. London: CRC Press.

Fernández, P., Santana, J. M., Ortega, S., Trujillo, A., Suárez, J. P., Domínguez, C., et al. (2016). SmartPort: A platform for sensor data monitoring in a seaport based on FIWARE. *Sensors, 16,* 417. doi:10.3390/s16030417

Hu, S.-C., Wang, Y.-C., Huang, C.-Y., & Tseng, Y.-C. (2011). Measuring air quality in city areas by vehicular wireless sensor networks. *Journal of Systems and Software, 84,* 2005–2012. doi:10.1016/j.jss.2011.06.043

Jabeen, F., & Nawaz, S. (2015). In-network wireless sensor network query processors: State of the art, challenges and future directions. *Information Fusion, 25,* 1–15. doi:10.1016/j.inffus.2015.01.007

Kaur, H., Sawhney, R. S., & Komal, N. (2012). Wireless sensor networks for disaster management. *International Journal of Advanced Research in Computer Engineering and Technology, 1,* 129–134.

Khemnar, D., Kasar, A. R., & Tembhurnikar, N. P. (2013). GRIN—WSN based air pollution monitoring system.

Libelium. (2016a). Waspmote Plug&Sense Technical Guide.

Libelium. (2016b). Waspmote Plug&Sense Sensor Guide.

Libelium Networking. (2016). Wapmote 802.15.4 Networking Guide.

Liu, J.-H., Chen, Y.-F., Lin, T.-S., Chen, C.-P., Chen, P.-T., Wen, T.-H., et al. (2012). An air quality monitoring system for urban areas based on the technology of wireless sensor networks. *International Journal on Smart Sensing and Intelligent System, 5,* 191–214.

Marin-Perez, R., García-Pintado, J., & Gómez, A. S. (2012). A real-time measurement system for long-life flood monitoring and warning applications. *Sensors, 12,* 4213–4236. doi:10.3390/s120404213

Murthy, C. S. R., & Manoj, B. S. (2004). *Ad Hoc wireless networks: Architectures and protocols*. Upper Saddle River, NJ, USA: Prentice Hall PTR.

Neal, J. C., Atkinson, P. M., & Hutton, C. W. (2012). Adaptive space–time sampling with wireless sensor nodes for flood forecasting. *Journal of Hydrology, 414–415,* 136–147. doi:10.1016/j.jhydrol.2011.10.021

Pister, K. S. J., n.d. Smart Dust.

Polanský, R. (2016). Smart City Písek. Czech Smart City Clust.

Prasad, R. V., Baig, M. Z., Mishra, R. K., Rajalakshmi, P., Desai, U. B., & Merchant, S. N. (2011). Real time wireless air pollution monitoring system. ICTACT Journal on Communication Technology, *2*, 370–375.

Řezník, T. (2012). *Emergency support system management of geographic information for command and control systems*. Brno: Univerzita obrany.

Roseline, R., Devapriya, M., & Sumathi, P. (2013). Pollution monitoring using sensors and wireless sensor networks: A survey. *International Journal of Application or Innovation in Engineering & Management, 2*.

Sinha, A., & Chandrakasan, A. (2001). Dynamic power management in wireless sensor networks. *IEEE Design and Test of Computers, 18,* 62–74. doi:10.1109/54.914626

Townsend, A. M. (2013). *Smart cities: Big data, civic hackers, and the quest for a New Utopia*. New York: W. W Norton & Company.

Yi, W. Y., Lo, K. M., Mak, T., Leung, K. S., Leung, Y., & Meng, M. L. (2015). A survey of wireless sensor network based air pollution monitoring systems. *Sensors, 15,* 31392–31427. doi:10.3390/s151229859

Yick, J., Mukherjee, B., & Ghosal, D. (2008). Wireless sensor network survey. *Computer Networks, 52,* 2292–2330. doi:10.1016/j.comnet.2008.04.002

Yu, L., Wang, N., & Meng, X. (2005). Real-time forest fire detection with wireless sensor networks. In *Proceedings of the 2005 International Conference on Wireless Communications, Networking and Mobile Computing*, IEEE, pp. 1214–1217.

Risk Management as a Stimulus for a Settlement and Landscape Transformation? Soil Erosion Threat Assessment in the Fields of Four Deserted Villages Based on LiDAR-Derived DEMs and 'USLE'

Lukáš Holata, Jiří Kapička, Radek Světlík and Daniel Žížala

Abstract This paper draws attention to the dynamics beyond the shaping of historical landscape and deals with the settlement abandonment and landscape transformation during the Later Middle Ages. Despite long-lasting debate about the reasons of this process, explicit explanation is still missing. Among others, ecological issues, including soil erosion, have been frequently mentioned, although not always supported by data. We examine four deserted villages in the Czech Republic —Bzík and Kamenice in Pilsner region (Bohemia) and Bouchenec and Novošice in the Drahany Uplands (Moravia). Their remains have been preserved in woodlands and, therefore, the extent of medieval ploughlands could be reconstructed. LiDAR-derived DEMs and Universal Soil Loss Equation (USLE) have been applied to assess the soil erosion threat of the village fields. The results of the modelling indicate a high erosion threat for the majority of fields. This factor, together with resulting soil degradation, can be considered as a reason for the abandonment and subsequent landscape transformation.

L. Holata (✉)
Department of Archaeology, University of Exeter, Laver Building, North Park Road, Streatham Campus, Exeter EX4 4QE, United Kingdom
e-mail: l.holata@exeter.ac.uk

J. Kapička · D. Žížala
Research Institute for Soil and Water Conservation, Žabovřeská 250, 156 27 Praha 5 - Zbraslav, Czech Republic
e-mail: kapicka.jiri@vumop.cz

D. Žížala
e-mail: zizala.daniel@vumop.cz

R. Světlík
Gulag.cz z.s., Na Dolinách 524/40, 147 00 Praha 4, Czech Republic
e-mail: radek.svetlik@gulag.cz

I. Ivan et al. (eds.), *Dynamics in GIscience*, Lecture Notes in Geoinformation and Cartography, DOI 10.1007/978-3-319-61297-3_10

Keywords Landscape archaeology · Settlement abandonment · Landscape transformation · Water erosion · Middle Ages

Introduction

The current landscape is a record of various transformations and human activities in the past. In several parts of Europe, it also contains prehistoric elements (cf. Rippon 2004, 6–14). The main character of the Central European landscape had been formed during the 13th century as a result of a stabilisation of a settlement pattern and a nucleation of villages (cf. Klápště 2005). Nevertheless, since then, the landscape has undergone further dynamic development (especially due to the intensification of agriculture and the industrialisation) and most of the medieval elements have therefore been overlaid. Well visible remains of the medieval landscape (e.g. hedgerows) are to a large extent spatially restricted (cf. Houfková et al. 2015). The first large-scale map sources (e.g. the 18th and 19th century military maps of the Czech lands) do not fully reflect the 'archaic form of the landscape' and it is not possible to use them (directly, without additional data) for the reconstruction of older, medieval situation (Štěpánek 1967, 727). Also, woodland areas may not be 'ancient'; many of them had not existed in the Middle Ages and appeared later, during the (early) modern period. Nevertheless, due to this afforestation, many remains of past human activities have been preserved (cf. Kuna and Tomášek 2004), among other deserted medieval villages (DMVs).

The current settlement pattern can be considered as the remnant of a high medieval lay-out. A rough estimate indicates more than 5000 settlements that had been abandoned in the area of the Czech Republic in the period between the 13th and the 17th century (cf. Nekuda 1961, 176; Smetánka 1988, 9). The phenomenon of settlement abandonment during the late medieval and/or postmedieval period is documented in most European countries (e.g. Pohlendt 1950; Beresford 1954; Beresford and Hurst 1971; Gissel et al. 1981; Chapelot and Fossier 1985; Smetánka 1988; Dyer and Jones 2010). Many reasons for it have been suggested, both environmental and cultural. However, this disappearance has not been explicitly answered. In addition to more general statements (as 'Retreat from Margins', agricultural crisis or '*Fehlsiedlung*': cf. Abel 1966; Postan 1973) or a number of crisis events (wars, epidemics and famines have been frequently stated), the disruption of the ecosystem and ecological issues (cf. Klápště 2005, 269), including soil erosion, has been mentioned (cf. below).

Remains of numerous deserted villages, including their hinterlands, have been documented during large-scale field surveys (cf. Černý 1979, 1992; Klápště 1978; Smetánka and Klápště 1981; Vařeka et al. 2006). On their basis, we are able to distinguish specific types of earthworks, among others also those associated with ploughlands. The economy of medieval villages that depended mostly on arable agriculture is expected in highly elevated/exposed/agriculturally marginal areas as well (cf. Žemlička 1980; Boháč 1983; Měřínský 1987; Klír 2008) and it is

supported by artifactual evidence (cf. iron agricultural tools from DMV Spindlebach in Ore Mountains situated 800–880 m a.s.l. : Hylmová et al. 2013) and the palynology (Rybníčková and Rybníček 1975; Nekuda and Jankovská 2005; Jankovská 2006, 2011; Petr 2008).

Currently, the identification of the remains of past human activities, especially line features such as field boundaries, is facilitated by LiDAR data, despite the fact that these objects are hardly discernible by the surface survey (cf. Malina 2015, 516). Using DTM 5G (Digital Terrain Model of the Czech Republic of the 5th generation) and subsequent ground-truthing, more complete image of past settlement areas (abandoned villages and their hinterlands) have been obtained, even the total extent of original ploughlands (cf. Vařeka et al. 2011, 335; Čapek 2013; in print; Čapek et al. 2013; Holata and Světlík 2015; Malina 2015). This allows us, together with the analytical potential of LiDAR-derived DEMs, to assess the process of the settlement abandonment as well as the dynamics in the land use during the historical period from a different perspective.

The Evidence for the Erosion During the Medieval Period

The evidence of the large-scale soil erosion during the medieval period comes from many European areas and beyond. An exceptional erosion (and other land degradation) is documented in the area of North Atlantic (e.g. Jakobsen 1991; Dugmore and Buckland 1991; Amorosi et al. 1998; Dugmore et al. 2000, 2005; Hannon et al. 2001; Greipsson 2012; Silva-Sánchez et al. 2015) as the impact of the *landnám* (colonization and settlement of new areas, destruction of vegetation cover, inappropriate land management) and the Little Ice Age. In England, substantial alluviation and influxes of sediments into river valley floodplains occurred during the Late-Saxon to the high Middle Ages and the cessation of alluviation in the late Medieval period corresponds with the contraction/desertion of settlements, abandonment of the ridge-and-furrow cultivation, enclosure of the open fields and the shift to grassland in general (Robinson 1992, 206; Lambrick 1992, 217–223; Rippon 2012, 232–240). The evidence also comes from southern Europe (e.g. van Andel 1990; Boone and Worman 2007).

In the case of Central Europe, high hillslope erosion during the Middle Ages is demonstrated mainly in Germany based on many case studies (e.g. Rösner and Töpfer 1999; Dotterweich 2005, 2008; Enters et al. 2008; Dreibrodt et al. 2010; Larsen et al. 2016). It is associated with deforestation and farming activities at a high altitude, on steeper slopes, introducing the three-field crop rotation system, synchronous with the highest intensity of the land use. The end of medieval period is considered as a one of the peaks of increased soil erosion in the Czech Republic (Beneš 1995, 143).

Concurrently, soil erosion has been mentioned in connection with deserted settlements as a reason for their abandonment (e.g. Iceland: Sveinbjarnardóttir 1991; Dugmore et al. 2006; the Lower Alentejo of southern Portugal: Boone and

Worman 2007; Germany—the Harz mountains: Linke 1983; abandoned Oberwürzbach in the Black Forest: Schreg 2009, 327–328; or Horb in western Schwanberg: Hildebrandt 2004). In the context of the Czech medieval settlement, it has been supposed as one of the ecological effects of the extensive deforestation and extensive agricultural land use (Boháč 1982, 46; Černý 1982, 104–105; 1983, 430; Vermouzek 1985, 70). Thick sediments have been documented in the deserted village of Bystřec in the Drahany Uplands together with erosion control elements (Hrádek 2006). However, statements addressing the erosion threat are only a presumption for many cases, not approved by empirical research.

Aims of the Paper in a Broader Perspective

The main aim of this paper is to (1) assess erosion threat in the fields of four deserted villages using LiDAR-derived DEMs and the USLE equation. The subject of our interest is water erosion which has the greatest importance in the region of Central Europe. More specifically, we intend to (2) determine whether the soil erosion threat and its consequences could be included among the reasons for abandonment of these villages and their management as a stimulus for subsequent landscape transformations.

Our intention corresponds with the current settlement transformations study approach which are now perceived in the context of wider transformations of land-use; the role of the natural environment in shaping cultural landscapes has been recently pointed out (especially Williamson 2004) and this issue is currently assessed, among others, in terms of human-environmental interactions as well. The hazards, sustainability, cultural responses to risk and environmental stress, and the resilience of human communities and societies in the past have been reflected in recent studies (e.g. Gerrard and Petley 2013; Curtis 2014), also in the context of medieval rural settlement and its economy (Schreg 2011, 2014).

Materials and Methods

Sites Selection, Their Characteristics and History

Due to previous surface surveys (cf. Černý 1992; Vařeka et al. 2008), all sites have been very well charted. Their selection also reflects different natural environments, topographies and diverse field system types. It allows us to assess the soil erosion threat under different conditions, type of field system, and thus different effect of field boundaries on the soil protection (cf. Janeček 2002, 118; Šarapatka 2012, 226).

The remains of the deserted village of *Kamenice* (residential area 440–470 m a.s.l., Pilsner region) are situated on the slopes under the hilltop. It had a radial field pattern around the residential area in the centre, most of field boundaries run along fall lines or in the angle of ca. 45° to the slope gradient, especially in the steepest parts (slope = 8°–12°, mean of the all ploughland = 4.67°). *Bzík* (Pilsner region, 535–560 m a.s.l.) is also situated under a hilltop, in the area of very steep slopes which in several parts reach to over 15° (mean = 8.18°). Field boundaries run along contours; furthermore, a large part of the field system is arranged in terraces. *Bouchenec* used to be the highest settlement in the Drahany Uplands (679–693 m a.s.l.), situated in a slight hillock near the highest point of the whole area. Its fields were placed on mild continual slopes (up to ca. 7°, mean = 4.63°). The field plots are arranged diagonally to the slope gradient, this is however documented in older plans only, not in LiDAR data. The hinterland of the deserted village of *Novošice* (Drahany Uplands, 553–574 m a.s.l.) was situated in the undulated terrain with very variable gradient of slopes (from flat areas to very steep slopes around ca. 20°, mean = 5.57°). In general, slight field boundaries preserved in the relief indicate a variable arrangement of field plots both along and perpendicular to contours (Fig. 1).

Based on the written evidence and a collected pottery, the existence of sites in the Pilsner region is dated from the 12th/13th to the 15th century (cf. Vařeka et al. 2008). The villages in the Drahany Uplands had been occupied from the 13th century. Bouchenec was deserted in the first half of the 15th century, Novošice in the first half of the 16th century (cf. Černý 1992).

Fig. 1 Location of deserted medieval villages

Identification of the Past Land-Use (Based on LiDAR Data and Surface Surveys)

For this analysis, georeferenced plans of sites in the Drahany Uplands were used (Černý 1992; Holata 2013). Additional relief formations, especially in the villages' hinterlands, have been identified in the LiDAR data (DTM 5G; applied visualisation cf. Zakšek et al. 2012; Doneus 2013). Their interpretation has been verified by recent surface surveys. The categorisation and vectorisation of all the identified remains have enabled the reconstruction of land-use for all deserted villages in the GIS. Field plots as well as residential, communication and mining areas have been delimitated. Potential meadows, pastures and forests have been located based on negative evidence and in accordance with the statements of historiography (especially Míka 1960; Lom 1973; Beranová 1975; Petráň and Petráňová 2000; Fig. 2). Having used these sources, intensely used parts of fields around residential areas have been delimitated as well, albeit only arbitrarily because of the missing field evidence.

Preprocessing of LiDAR-Derived DEMs for the Purpose of Soil Erosion Modeling

Still visible remains of field boundaries signify that original medieval relief has been preserved under woodland canopies up to the present. Nevertheless, it contains also later and recent objects (especially charcoal wooden platforms, tree windfalls or roads and forest ways) which had to be eliminated for the calculation of erosion threat models. More extensive objects documented by LiDAR data have been removed from the original point cloud and slight terrain anomalies have been smoothed with the resampling of DEMs to 3 m and by using the Low-pass filter.

Soil Erosion Modeling

Water erosion is quantified using average annual soil loss (A) (t ha^{-1} year^{-1}) which is calculated on the basis of *USLE* (Universal Soil Loss Equation; Wischmeier and Smith 1965; 1978) in order to assess the soil erosion threat:

$$A = R * K * L * S * C * P$$

where R is the rainfall erosivity factor (20 MJ ha^{-1} cm h^{-1} was proposed as an average value for the Czech Republic until 2012—it is considered as an optimal solution, because past climate reconstructions testify for dry as well as rainy periods during village existence—cf. Kotyza et al. 1990; Kotyza 1992; Brázdil and Kotyza 1997). K is the soil erodibility factor, expressing soil susceptibility in terms of

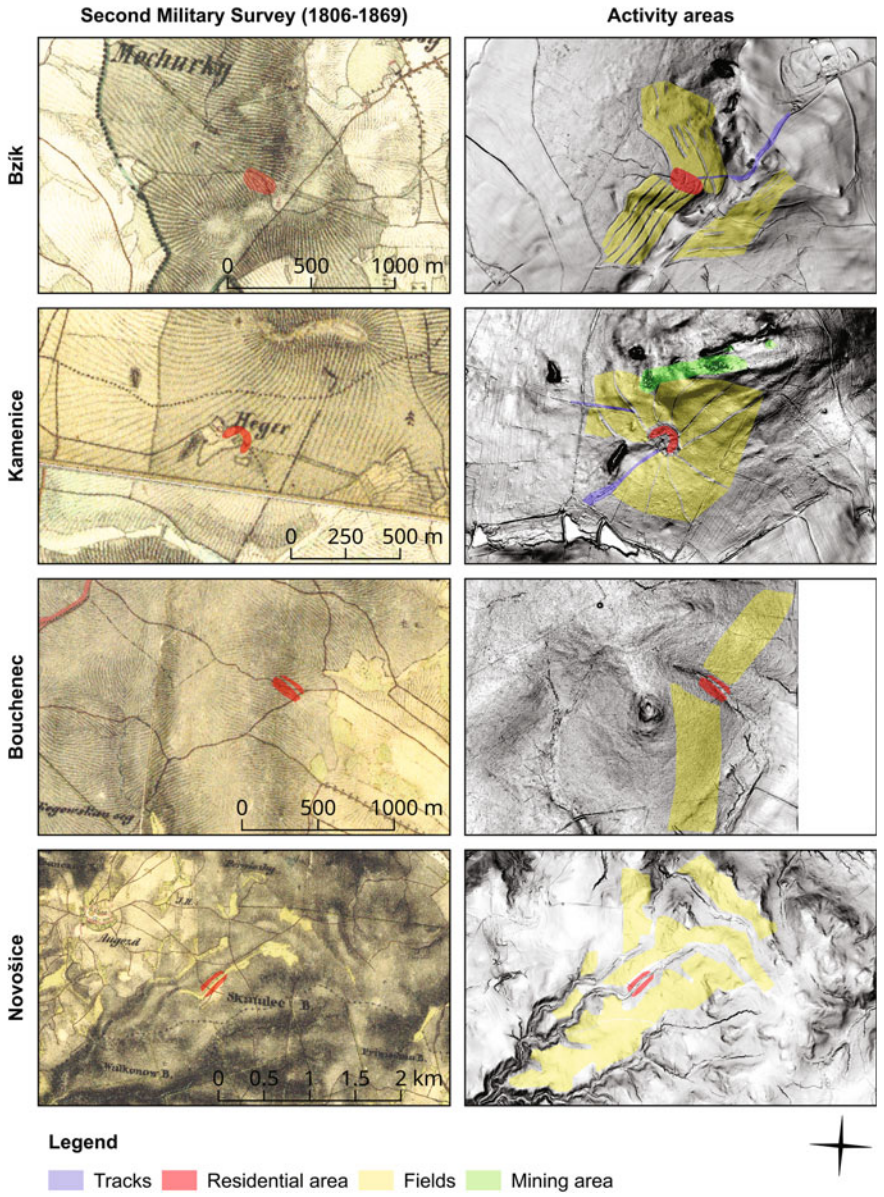

Fig. 2 Historical mapping with the range of woodlands and the reconstruction of medieval activity areas against the DTMs (visualised by anisotropic sky-view factor)

erosion depending on soil texture and structure. It was derived from forestry typology of soil types (SLT, ÚHUL 2013). *LS* is a 'topographic factor' combining the influence of the slope length and gradient (derived from modified LiDAR-based

DEMs). *C* is the cover-management factor, expressing the influence of sowing methods and agro-technology. Three-field crop rotation system has been considered together with the cultivation of flux, vegetable and legumes in the fields around residential areas (in accordance with Míka 1960; Lom 1973; Beranová 1975; Petráň and Petráňová 2000; for the settings of the factors in the Czech Republic cf. Novotný et al. 2016).

Data Evaluation

Resulting models have been divided into 6 categories of erosion threat (after Novotný et al. 2016; Fig. 3). On this basis, two thresholds have been determined (below 1.0 t ha^{-1} $year^{-1}$ without threat or very slightly threatened, below 4.0 t ha^{-1} $year^{-1}$ as max. tolerable limit of soil loss, higher values means heavy erosion threat). Sites are compared with each other (using the boxplots with both thresholds; Fig. 4) and also with the long-term annual soil loss in current agricultural land in the Czech Republic (Table 1). In addition, flowlines have been also generated and displayed against field boundaries to assess their role in soil protection (Fig. 3).

Results

Kamenice: Almost the entire ploughland is threatened by erosion. Only restricted and fragmentary areas (3.5% of the total extent of fields) are threatened very slightly, but they occur in the most distant parts of the ploughland, in the hilltop position. The largest part of the whole extent of fields (51.3%) is threatened only slightly. Higher level of threat can be found around the residential area (mostly medium, but locally also heavily). Considerable is the extent the areas that are very heavily or even extremely threatened (28.4%). These areas are scattered especially in the north-east–north-west parts of the ploughland with the steepest slopes. In addition to this, field boundaries run here in the direction of water run-off and their impact on the erosion reduction is minimal. Overall, with the exception of three southern fieldplots, high erosion threat occurs across all the ploughland.

Bzík: Very high erosion threat is registered here, despite the fact that all field boundaries break the water run-off and a large part of the ploughland is arranged into terraces (heavily—extremely threatened areas cover 40.6% of which extreme is 25.6%). Affected were particularly upper parts of fieldplots and the terraced transect south from the residential area. Nevertheless, the extent of very slightly threatened areas is larger (17.8%) than in the case of Kamenice, but identically as in the previous case, these areas are situated in the fringe of ploughland in the southern and south-eastern–eastern part.

Bouchenec: Erosion threat is low in the ploughland (37.6% of the area is very slightly threatened, 33.8% then slightly). These areas cover both parts of the fields

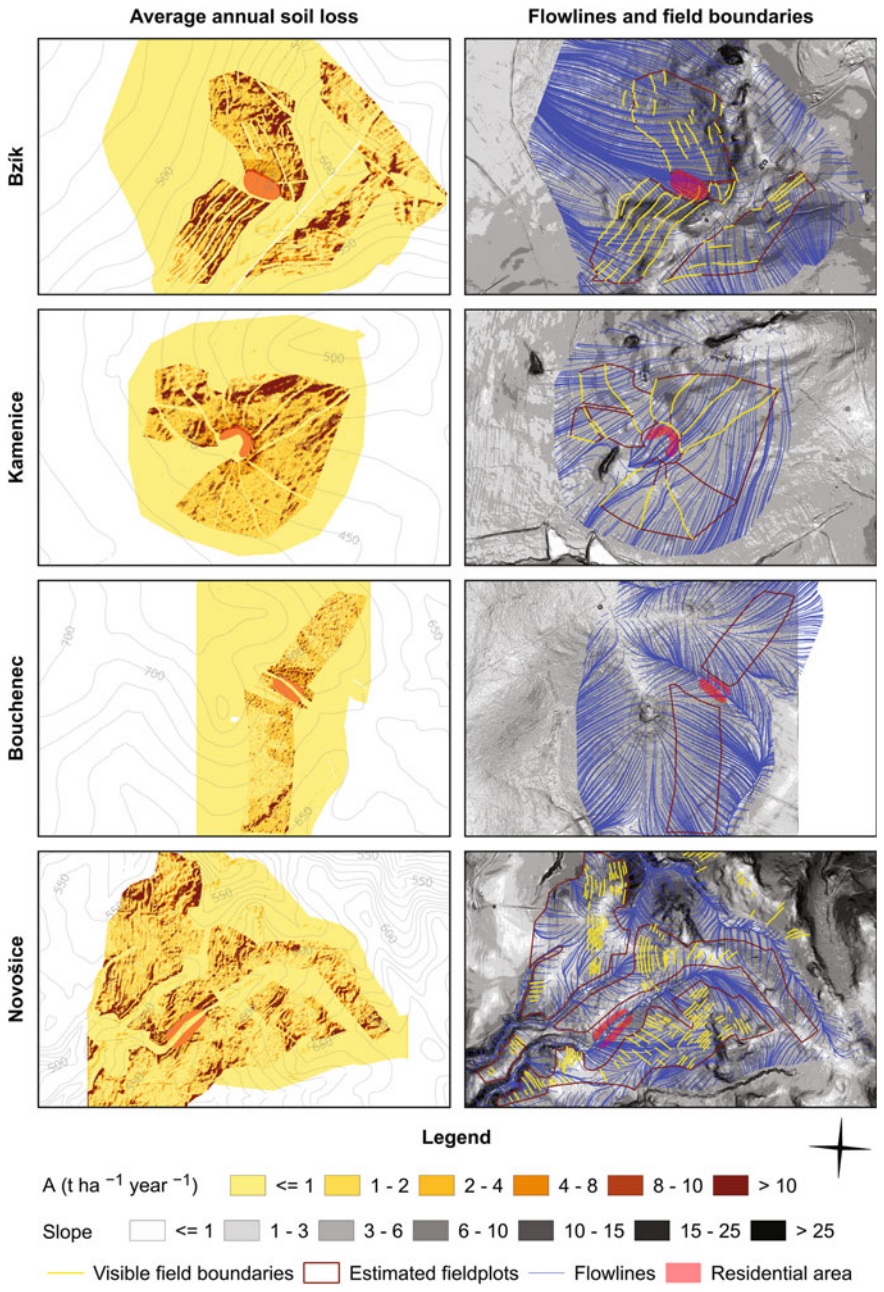

Fig. 3 Soil loss in the ploughlands (*left*) and flowlines against field boundaries and slope (*right*). The scale is the same as in the Fig. 2

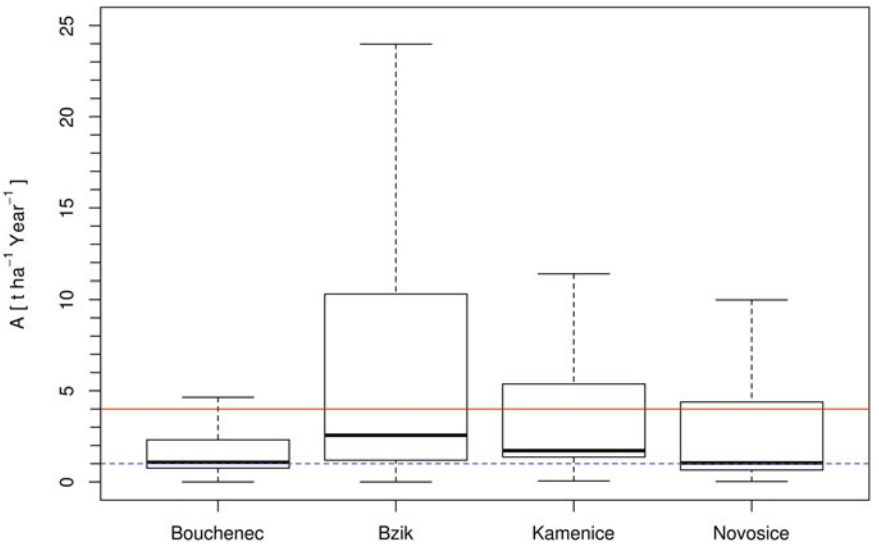

Fig. 4 Boxplots of erosion threat for all sites

Table 1 The erosion threat of the sites and compared with the current Czech agricultural land

Average annual soil loss (A)	A [t ha^{-1} Year^{-1}]	Distribution (%)				
		Bouchenec	Bzík	Kamenice	Novošice	Czech R.
Very slightly threatened	Below 1.0	37.6	17.8	3.5	45.2	49.6
Slightly threatened	1.1–2.0	33.8	26.5	51.3	18.0	18.3
Medium threatened	2.1–4.0	12.0	15.1	16.8	10.0	15.6
Heavily threatened	4.1–8.0	9.5	10.8	9.7	13.7	10.4
Very heavily threatened	8.1–10.0	2.4	4.2	3.2	3.7	2.0
Extremely threatened	Above 10.1	4.6	25.6	15.5	9.5	4.2
Total		100	100	100	100	100

(lowest values are recorded in the central area of the southern field). Heavily—extremely threatened areas are restricted to local anomalies and scattered around the whole ploughland. Only in the southern part they are concentrated into the continuous strip (also because of the absence of field boundaries). Another area with higher erosion threat adjoins the edge of the village in the northern field.

Novošice: Undulating relief of the village hinterland also implies very variable threat of the soil erosion. Almost half of the ploughland is very slightly threatened (45.2%), especially in the central part of the southern and eastern fields. However, heavily—extremely threatened parts spread to over 26.9% of the ploughland (9.5% is extreme threat). These are documented across the whole extent of ploughland,

mostly in the northern fringe, but also in the broader residential area surroundings. As most of the field boundaries are slight only, their influence on soil protection is low (in addition to this, most of them are not situated transversally, especially in the area adjacent to the village from the south-east).

Only in case of Novošice, the extent of a very slightly threatened area corresponds with the current agricultural land in the Czech Republic. Together with Bouchenec percentages show similar trend in the range of categories (but the extent of heavily—extremely threatened areas is higher). On the contrary, there is an opposite trend in the case of Kamenice and especially in Bzík with large areas of heavily—extremely threatened areas and limited range of very slightly threatened areas. A high erosion threat occurred despite the fact that field plots are divided into small sections (in contrast to the current fields). However, the placing of meadows around streams is considered to be a positive factor in terms of erosion threat, which protects the streams against soil accumulation.

Discussion

The results are mostly determined by the characteristics of LiDAR-derived DEMs, especially their resolution and vertical accuracy of the relief under woodland canopies (local depressions are most problematic). The quality of the DEM should be verified by a surface survey and selected testing areas compared with a detailed measurement using a total station. Other factors in USLE (especially *R* and *C*) could be only expertly estimated based on the current knowledge of historiography. In contrast with the modelling of erosion threat in current agricultural land, percentages of areas with erosion threat cannot be considered absolutely, but only as an expression of the main trend.

From today's perspective, all occupied areas are not suitable for agriculture in terms of soil erosion threat. Although threat in Bouchenec is low and restricted to small areas, it was the higher settlement in the whole region and a very low agricultural potential is assumed (only slight erosion threat could have a serious impact). High erosion threat is documented despite the fact that the ploughlands are divided into small fieldplots (compared to the current agricultural practice). Most of the fields occupied slopes, often with very steep gradient and for that reason heavy erosion threat occurred also in areas where field boundaries interrupt the surface run-off, or in terraced fields in Bzík—even this arrangement did not protect the high soil loss there. In this respect, the issue of accumulated material on field boundaries has emerged. Written sources for post-medieval period indicate the effort to carry soil from various places back to the fields (cf. Černý 1930; Cílek 2012, 95). This work activity is deemed as a necessary workload during the year as a coping and mitigation of erosion threat. Nevertheless, many field boundaries are parallel with flowlines as well and erosion threat is heightened by the lay-out of the field system. In the cases of Kamenice and Novošice, sedimentation of the soil deposits could have occurred in the residential areas as a consequence of their position below the

fieldplots, missing soil protection elements and also supposed intensely used parts around them.

As a consequence of high erosion threat together with growing crops with high nutritional requirements (grain) and the three-field crop rotation system (inclusive of winter months without vegetation cover), overall soil depletion and degradation is taken into account: higher erosion > higher nutrient run-off > reduction of organic matter in soil > reduction the quality of the soil structure > higher predisposition to desiccation > lack of soil moisture for plants > poor germination. Economy of these villages, if it depended only upon arable agricultural, is considered vulnerable because of low yields. Currently, we are still far away from the understanding why or for what reasons these parts of the landscape were occupied and used for arable agriculture, whether their location was mistaken based on the perception of past communities and what were the particular causes for their final abandonment. Nevertheless, following our results, we argue that arable agriculture of such areas was a risk management, which can be considered as one of the reasons for their abandonment and a stimulus for landscape transformation. Contrasted to other documented cases, the vast majority of these ploughlands were not incorporated into the surrounding territories and used for arable agriculture by their communities (cf. Štěpánek 1969, 663–679; Smetánka 1988, 47). It resulted in the transformation of the landscape and afforestation of original settlement areas.

Considering risk management of past communities also implies remarkable dynamics beyond the settlement abandonment and landscape transformations: choice of the position for occupation and perception of the landscape > village economy, intense arable agriculture and the role of subsistence strategies > soil degradation caused by long-term using of unsuitable areas for agriculture > response of communities to the stress (coping with the high erosion threat and mitigation of implications) > the role of possible transformation of the village ecosystem as an adaptation to changing conditions > sustainability of village economy > decision to abandon the settlement > leaving the areas without agricultural use > change of land-use.

All sites indicate different problems than we have in current agriculture. On the one hand high erosion threat occurred also in small and discontinuous fieldplots. On the other hand, a high proportion of grassland (although it should be confirmed by additional evidence) protected the watercourses. It evokes a comprehensive approach of agricultural land use concerning ‘inputs’ and ‘outputs’: soil without any degradation = good yields = necessary adequate care.

Conclusion

We assessed, based on the LiDAR-derived DEMs and USLE, the soil erosion threat in the fields of four deserted villages. Our outputs indicate that the only a minor extent of ploughlands is without erosion threat or threatened very slightly. On the

contrary, the range of heavy—extremely threatened areas is considerable. The lowest erosion threat is documented in Bouchenec (the highest settlement in the whole region), the high erosion threat occurs in the both sites in the Pilsner region, especially Bzík. From this point of view, none of the settlement areas are suitable for agricultural use, which is considered as risk management in these environments. Soil erosion threat and subsequent soil degradation can be included among the reasons for abandonment these villages and their management as a stimulus of subsequent landscape transformations. Our outcomes imply remarkable dynamics in the process of settlement abandonment and beyond the shaping of historical landscape in general. Although this is the first support of such statement for the Czech deserted villages based on data, other procedures (especially empirical research) are necessary for the validation.

Software

LiDAR data were interpolated in Surfer 12 using Natural Neighbor algorithm. Elimination of later and recent objects and filtering of LiDAR data were realised in QGIS. Relief Visualisation Toolbox (RVT) was used for LiDAR data visualisation. USLE2D and Esri ArcGIS 10.3 (with Spatial Analyst and 3D Analyst extensions) were used for calculations of erosion threat models. Graph was prepared using Rstudion (R version 3.3.2). An Internet application, the Erosion Control Calculator (http://kalkulacka.vumop.cz) was used for C factor.

Sources of Support

This work was supported by the Ministry of Agriculture of the Czech Republic [grant number NAZV QJ1230056 - The Impact of the expected Climate Changes on Soils of the Czech Republic and the Evaluation of Their Productive Functions] and by the H2020-MSCA-IF-2014 ‘ABANDONMENT—People under Pressure: Settlement Abandonment and Human Responses to Environmental and Socio-Economic Stress during the Medieval and Postmedieval Periods’.

References

Abel, W. (1966). *Agrarkrisen und Agrarkonjunktur in Mitteleuropa vom 13.–19. Jahrhundert*. Hamburk/Berlin: Parey.

Amorosi, T., Buckland, P. C., Edwards, K. J., Mainland, I., McGovern, T. H., Sadler, J. P., et al. (1998). They did not live by grass alone: The politics and palaeoecology of animal fodder in the North Atlantic region. *Environmental Archaeology, 1,* 41–54.

Beneš, J. (1995). Erosion and accumulation processes in the late holocéne of Bohemia, in relation to prehistoric and medieval landscape occupation. In M. Kuna & N. Venclová (Eds.), *Whither archaeology? Papers in honour of Evžen Neustupný*. Praha: ARÚ.

Beranová, M. (1975). *Zemědělská výroba v 11./14. století na území Československa*. Praha: Academia.

Beresford, M. W. (1954). *The lost villages of England*. London: Royal Geographical Society.

Beresford, M. W., & Hurst, J. G. (Eds.). (1971). *Deserted medieval village*. London: Lutterworth Press.

Boháč, Z. (1982). Katastry – málo využitý pramen k dějinám osídlení. *Historická geografie, 20,* 15–87.

Boháč, Z. (1983). Vesnice v sídelní struktuře předhusitských Čech. *Historická geografie, 21,* 37–116.

Boone, J. L., & Worman, F. S. (2007). Rural settlement and soil erosion from the Late Roman Period through the Medieval Islamic Period in the Lower Alentejo of Portugal. *Journal of Field Archaeology, 32,* 115–132.

Brázdil, R., & Kotyza, O. (1997). Kolísání klimatu v Českých zemích v první polovině našeho tisíciletí. *Archeologické rozhledy, 49,* 663–699.

Čapek, L. (2013). Využití dat leteckého laserového skenování ke studio středověké a novověké krajiny Velechvínského polesí, okr. České Budějovice. In: M. Gojda & J. John et al., *Archeologie a letecké laserové skenování krajiny*. Plzeň: Západočeská univerzita v Plzni.

Čapek, L. (in print). Lotniczy skaning laserowy i opuszczone średniowieczne wsie południowych Czech, In. M. Gojda (ed), *Lux Ex Caelo*. Warsaw: Archaeologica Hereditas – Prace Institutu Archeologii UKSW.

Čapek, L., John, J., & Stolz, D. (2013). Příspěvek leteckého laserového skenování k poznání dvou zaniklých středověkých vesnic mezi Líšnou a Točníkem. In: M. Gojda & J. John. et al., *Archeologie a letecké laserové skenování krajiny*. Plzeň: Západočeská univerzita v Plzni.

Černý, V. (1930). *Hospodářské instrukce. Přehled zemědělských dějin v době patrimonijního velkostatku v XV. – XIX. století*. Praha: Československá Akademie Zemědělská.

Černý, E. (1979). *Zaniklé středověké osady a jejich plužiny: metodika historicko-geografického výzkumu v oblasti Drahanské vrchoviny*. Praha: Academia.

Černý, E. (1982). Dosavadní výsledky a závěry historickogeografického výzkumu zaniklých středověkých osad a jejich plužin na Drahanské vrchovině. *Historická geografie, 20,* 89–112.

Černý, E. (1983). Vztah zaniklých plužin k rozloze lesů na Drahanské vrchovině v období vrcholného feudalismu. *Archaeologia Historica, 8,* 423–431.

Černý, E. (1992). *Výsledky výzkumu zaniklých středověkých osad a jejich plužin: Historicko-geografická studie v regionu Drahanské vrchoviny*. Brno: Muzejní a vlastivědná společnost.

Chapelot, J., & Fossier, R. (1985). *The village and house in the middle ages*. London: B. T. Batsford Ltd.

Cílek, V. (2012). Geodiverzita a paměť krajiny. In: I. Machar & L. Drobilová et al., *Ochrana přírody a krajiny v České republice. Vybrané aktuální problémy a možnosti jejich řešení*. 1. díl. Olomouc: Univerzita Palackého v Olomouci.

Curtis, D. (2014). *Coping with crisis: The resilience and vulnerability of pre-industrial settlements*. Farnham: Ashgate.

Doneus, M. (2013). Openness as visualization technique for interpretative mapping of airborne lidar derived digital terrain models. *Remote Sensing, 5,* 6427–6442.

Dotterweich, M. (2005). High-resolution reconstruction of a 1300 year old gully system in northern Bavaria, Germany: A basis for modelling long-term human-induced landscape evolution. *The Holocene, 15,* 994–1005.

Dotterweich, M. (2008). The history of soil erosion and fluvial deposits in small catchments of central Europe: Deciphering the long-term interaction between humans and the environment—A review. *Geomorphology, 101,* 192–208.

Dreibrodt, S., Lubos, C., Terhorst, B., Damm, B., & Bork, H.-R. (2010). Historical soil erosion by water in Germany: Scales and archives, chronology, research perspectives. *Quaternary International, 222,* 80–95.

Dugmore, A., & Buckland, P. (1991). Tephrochronology and late holocene soil erosion in south Iceland. In J. K. Maizels & C. Caseldine (Eds.), *Environmental change in Iceland: Past and present*. Dordrecht/Boston/London: Kluwer academic Publishers.

Dugmore, A. J., Church, M. J., Buckland, P. C., Edwards, K. J., Lawson, I. T., Mcgovern, T. H., et al. (2005). The norse landnám on the north atlantic islands: An environmental impact assessment. *Polar Record, 41,* 21–37.

Dugmore, A. J., Church, M. J., Mairs, K.-A., McGovern, T. H., Newton, A. J., & Sveinbjarnardóttir, G. (2006). An over-optimistic pioneer fringe? Environmental perspectives on medieval settlement abandonment in Þórsmörk, South Iceland. *Dynamics of Northern Societies: Proceedings of the SILA/NABO Conference on Arctic and North Atlantic Archaeology* (pp. 335–345), Copenhagen, May 10–14, 2004, Copenhagen: Aarhus University Press.

Dugmore, A., Newton, A., Larsen, G., & Cook, G. T. (2000). Tephrochronology, environmental change and the norse settlement of Iceland. *Environmental Archaeology, 5,* 21–34.

Dyer, C., & Jones, R. (Eds.). (2010). *Deserted villages revisited*. Hatfield: University of Hertfordshire Press.

Enters, D., Dörfler, W., & Zolitschka, B. (2008). Historical soil erosion and land-use change during the last two millenia recorded in lake sediments of Frickenhauser See, northern Bavaria, central Germany. *The Holocene, 18,* 243–254.

Gerrard, C., & Petley, D. (2013). A risk society? Environmental hazards, risk and resilience in the later Middle Ages in Europe. *Natural Hazards, 69,* 1051–1079.

Gissel, S., Jutikkala, E., Österberg, E., Sandnes, J., & Teitsson, B. (1981). *Desertion and land colonization in the Nordic Countries c. 1300–1600*. Stockholm: Almqvist & Wiksell.

Greipsson, S. (2012). Catastrophic soil erosion in Iceland: Impact of long-term climate change, compounded natural disturbances and human driven land-use changes. *CATENA, 98,* 41–54.

Hannon, G. E., Wastegård, S., Bradshaw, E., & Bradshaw, R. H. W. (2001). Human impact and landscape degradation on the Faroe Islands. *Biology and Environment: Proceedings of the Royal Irish Academy, 101,* 129–139.

Hildebrandt, H. (2004). Die spätmittelalterliche Wüstungsperiode aus der Sicht der Bodenerosionstheorie, betrachtet vornehmlich am Beispiel der Wüstung Horb im westlichen Steigerwald. *Bamberger Geographische Schriften Sonderfolge, 7,* 121–137.

Holata, L. (2013). Settlement patterns in Drahany Uplands (Czech Republic): GIS and quantitative methods based approach. In G. Earl et al. (eds.), *Archaeology in the Digital Era, vol. II. e-Papers from the 40th Conference on Computer Applications and Quantitative Methods in Archaeology* (pp. 636–644), Southampton, March 26–30, 2012, Amsterdam: Amsterdam University Press.

Holata, L., & Světlík, R. (2015). Detailed digital terrain models in the research of deserted settlements: Hydrological modelling and environment of settlement areas. In K. Růžičková & T. Inspektor (Eds.), *Surface models for geosciences*. Lecture notes in geoinformation and cartography, Amsterdam: Springer.

Houfková, P., Burnerl, J., Pospíšil, L., Karlík, P., Beneš, J., Bernardová, A., et al. (2015). Origin and development of long-strip field patterns: A case study o an abandoned medieval village in the Czech Republic. *CATENA, 135,* 83–91.

Hrádek, M. (2006). Odezva přírodního prostředí v okolí Bystřece na odlesnění krajiny. In L. Belcredi, *Bystřec. O založení, životě a zániku vsi*. Brno: Muzejní a vlastivědná společnost.

Hylmarová, L., Klír, T., & Černá, E. (2013). Kovové předměty ze zaniklého Spindelbachu v Krušných horách. K výpovědi detektorového průzkumu. *Archaeologia Historica, 38,* 569–609.

Jakobsen, B. H. (1991). Soil erosion in the Norse settlement area of Østerbygden in southern Greenland. *Acta Borealia, 8,* 56–68.

Janeček, M. (2002). *Ochrana zemědělské půdy před erozí*. Praha: Powerprint.

Jankovská, V. (2006). Pyloanalytický výzkum. In: Belcredi, L., *Bystřec. O založení, životě a zániku středověké vsi*. Brno: Muzejní a vlastivědná společnost.

Jankovská, V. (2011). The Middle Ages in pollen-analytical research on the territory of the Czech Republic. *Bulletin of Geography Physical Geography Series*, *4*, 47–70.

Klápště, J. (1978). Středověké osídlení Černokostelecka. *Památky archeologické, 69,* 423–475.
Klápště, J. (2005). *Proměna Českých zemí ve středověku*. Praha: Lidové noviny.
Klír, T. (2008). *Osídlení zemědělsky marginálních půd v mladším středověku a raném novověku*. Praha: Univerzita Karlova, Filozofická fakulta.
Kotyza, O. (1992). Archeologické a přírodovědné prameny jako prameny historické klimatologie. *Archaeologia Historica, 17,* 449–459.
Kotyza, O., Pejml, K., & Sládková, J. (1990). Několik poznámek ke kolísání klimatu v Čechách 14. – 15. století. *Archaeologia Historica, 15,* 511–516.
Kuna, M., & Tomášek, M. (2004). Povrchový výzkum reliéfních tvarů. In M. Kuna et al., *Nedestruktivní archeologie*. Praha: Academia.
Lambrick, G. (1992). Alluvial archaeology of the Holocene in the Upper Thames Basin 1971–1991: A review. In S. Needham & M. G. Macklin (Eds.), *Alluvial archaeology in Britain*. Oxford: Oxbow Books.
Larsen, A., Robin, V., Heckmann, T., Fuelling, A., Larsen, J. R., & Bork, H.-R. (2016). The influence of historic land-use changes on hillslope erosion and sediment redistribution. *Holocene, 26,* 1248–1261.
Linke, M. (1983). Medieval deserted fields and deserted villages in the Lower Harz Mountains—An interim report. In B. K. Roberts & R. E. Glasscock (Eds.), *Villages, fields and frontiers*. *Studies in European Rural Settlement in the Medieval and Early Modern Periods.* Oxford: B.A.R.
Lom, F. (1973). Vývoj osevních postupů a soustav hospodaření v Českých zemích – Metodologická studie. *Vědecké práce zemědělského muzea, 13,* 215–263.
Malina, O. (2015). Hledání neviditelného. Relitky plužiny zaniklých středověkých vsí a možnosti jejich detekce a interpretace na datech LLS. *Zprávy památkové péče, 75,* 513–520.
Měřínský, Z. (1987). Příspěvek k možnostem rekonstrukce středověké krajiny, území zaniklých vesnic a typů sídlišť. *Archaeologia Historica, 12,* 111–128.
Míka, A. (1960). *Nástin vývoje zemědělské výroby v Českých zemích v epoše feudalismu*. Praha: SPN.
Nekuda, V. (1961). *Zaniklé osady na Moravě v období feudalismu*. Brno: Krajské nakladatelství.
Nekuda, R., & Jankovská, V. (2005) Mstěnice – zaniklá středověká ves, pyloanalytické zhodnocení přírodního prostředí v okolí středověkého vodního mlýna. In V. Hašek, et al. (Ed.), *Ve službách archeologie*. Brno: Muzejní a vlastivědná společnost.
Novotný, I., Žížala, D., Kapička, D., Beitlerová, H., Mistr, M., Kristenová, H., et al. (2016). Adjusting the CPmax factor in the Universal Soil Loss Equation (USLE): Areas in need of soil erosion protection in the Czech Republic. *Journal of Maps, 12,* 58–62.
Petr, L. (2008). Pylový rozbor zaniklých rybníčků a vývoj prostředí po zániku vesnic, In V. Dudková, et al. (Ed.), *Hledání zmizelého. Archeologie zaniklých vesnic na Plzeňsku*. Plzeň: Západočeské muzeum.
Petráň, J., & Petráňová, L. (2000). *Rolník v tradiční evropské kultuře*. Praha: Set Out.
Pohlendt, H. (1950). *Die Verbreitung der mittelalterlichen Wüstungen in Deutschland*. Göttingen: Geographisches Institut der Universität.
Postan, M. M. (1973). The economic foundations of medieval society. In M. M. Postan (Ed.), *Essays on medieval agriculture and general problems of the medieval economy*. London: Cambridge University Press.
Rippon, S. (2004). *Historic landscape analysis*. York: Council for British Archaeology.
Rippon, S. (2012). *Making sense of an historic landscape*. Oxford: Oxford University Press.
Robinson, M. (1992). Environment, archaeology and alluvium on the river gravels of the South Midlands. In S. Needham & M. G. Macklin (Eds.), *Alluvial archaeology in Britain*. Oxford: Oxbow Books.
Rösner, U., & Töpfer, C. (1999). Historische Bodenerosion *auf* Flurwüstungen im westlichen Steigerwald. *Mitteilungen der Fränkischen Geographischen Gesellschaft, 46,* 27–74.
Rybníčková, E., & Rybníček, K. (1975). Ergebnisse einer Paläogeobotanischen Erforschung. In V. Nekuda, et al. (Ed.), *Pfaffenschlag – Zaniklá středověká ves u Slavonic. Příspěvěk k dějinám středověké vesnice*. Brno: Blok.

Šarapatka, B. (2012). Zemědělská krajina a biodiverzita. In I. Machar & L. Drobilová, et al. (Eds.), *Ochrana přírody a krajiny v České republice*. *Vybrané aktuální problémy a možnosti jejich řešení. 1. díl.* Olomouc: Univerzita Palackého v Olomouci.

Schreg, R. (2009). Development and abandonment of a cultural landscape—Archaeology and environmental history of medieval settlements in the northern Black Forest. In J. Klapste & P. Sommer (Eds.), *Medieval rural settlement in marginal landscapes*. Ruralia VII. Turnhout: Brepols.

Schreg, R. (2011). Feeding the village—Reflections on the ecology and resilience of the medieval rural economy. In J. Klapste & P. Sommer (Eds.), *Processing, storage, distribution of food. Food in the medieval rural environment*. Ruralia VIII. Turnhout: Brepols.

Schreg, R. (2014). Ecological approaches in medieval rural archaeology. *European Journal of Archaeology, 17,* 83–119.

Silva-Sánchez, N., Schofield, J. E., Mighall, T. M., Martínez Cortizas, A., Edwards, K. J., & Foster, I. D. L. (2015). Climate changes, lead pollution and soil erosion in south Greenland over the past 700 years. *Quaternary Research, 84,* 159–173.

Smetánka, Z. (1988). *Život středověké vesnice*. *Zaniklá Svídna.* Praha: Academia.

Smetánka, Z., & Klápště, J. (1981). Geodeticko - topografický průzkum zaniklých středověkých vsí na Černokostelecku. *Památky archeologické, 72,* 416–458.

Štěpánek, M. (1967). Plužina jako pramen dějin osídlení (Příspěvky k dějinám osídlení 1). *Československý časopis historický, 15,* 725–746.

Štěpánek, M. (1969). Strukturální změny středověkého osídlení II. *Československý časopis historický, 17,* 649–679.

Sveinbjarnardóttir, G. (1991). A study of farm abandonment in two regions of Iceland. In J. K. Maizels & C. Caseldine (Eds.), *Environmental change in Iceland: Past and present*. Dordrecht/Boston/London: Kluwer Academic Publishers.

ÚHUL. (2013). *Přehled lesních typů a souborů lesních typů v ČR*. Brandýs nad Labem: Ústav pro hospodářskou úpravu lesů.

van Andel, T. H., Zangger, E., & Demitrack, A. (1990). Land use and soil erosion in prehistoric and historical Greece. *Journal of Field Archaeology, 17,* 379–396.

Vařeka, P., Aubrechtová, A., Hnízdilová, P., Novák, R., Rožmberský, P., & Veselá, R. (2006). *Archeologie zaniklých středověkých vesnic na Rokycansku I.* Plzeň: Ing. Petr Mikota.

Vařeka, P., Holata, L., Přerostová, H., & Švejnoha, J. (2008). Zaniklé středověké vesnice na Blovicku (Plzeňský kraj). *Archaeologia Historica, 33,* 85–100.

Vařeka, P., Holata, L., Rožmberský, P., & Schejbalová, Z. (2011). Středověké osídlení Rokycanska a problematika zaniklých vsí. *Archaeologia Historica, 36,* 319–342.

Vermouzek, R. (1985). Vyplavené vesnice na Tišnovsku a jižní Moravě. *Vlastivědný věstník moravský, 1,* 68–75.

Williamson, T. (2004). *Shaping medieval landscapes: Settlement, society, environment.* Macclesfield: Windgather Press.

Wischmeier, W. H., & Smith, D. D. (1965). *Rainfall-erosion losses from cropland east of the rocky mountains: Guide for selection of practices for soil and water conservation (Agricultur.)*. Washington: U.S.Governmental Printing Office.

Wischmeier, W. H., & Smith, D. D. (1978). *Predicting rainfall erosion losses: A guide to conservation planning*. U.S. Department of Agriculture Handbook No. 537 (Agricultur.). Washington: U.S. Governmental Printing Office.

Zakšek, K., Oštir, K., Pehani, P., Kokalj, Ž., & Polert, E. (2012). Hill-shading based on anisotropic diffuse illumination. *GIS Ostrava 2012—Surface models for geosciences* (pp. 283–297), Ostrava, January 23–25, Ostrava: VŠB—Technical University of Ostrava.

Žemlička, J. (1980). *Vývoj osídlení dolního Poohří a Českého Středohoří do 14. století*. Praha: Academia.

Multidimensional Evaluation of Public Transport Accessibility

Jiří Horák, Igor Ivan, Vít Voženílek and Jan Tesla

Abstract Public transport conditions are analysed using simulated commuting to important employers and recording data about significant features of all simulated trips. Two forms of overall public transport accessibility evaluation are compared—rule based and multivariate based classifications. Rule based classification was developed in several variants integrating two or four indicators, average and non-aggregated values. More valuable results were obtained using extended set of indicators for non-aggregated trips. The multivariate classification utilizes a novel approach to K-means cluster analysis using decile values. The comparison of both classifications shows a primary role of expert based classification. K-means cluster analysis based on deciles or median values are suitable for establishing more common typology but not for a local accessibility evaluation.

Keywords Accessibility · Public transport · Multidimensional evaluation · K-means · Multicriteria evaluation · Spatial simulation

J. Horák (✉) · I. Ivan · J. Tesla
Institute of Geoinformatics, Faculty of Mining and Geology,
VŠB-Technical University of Ostrava, 17. listopadu 15/2172,
708 33 Ostrava-Poruba, Czech Republic
e-mail: jiri.horak@vsb.cz

I. Ivan
e-mail: igor.ivan@vsb.cz

J. Tesla
e-mail: jan.tesla@vsb.cz

V. Voženílek
Department of Geoinformatics, Faculty of Science, Palacky University,
17. listopadu 50, 771 46 Olomouc, Czech Republic
e-mail: vit.vozenilek@upol.cz

I. Ivan et al. (eds.), *Dynamics in GIscience*, Lecture Notes in Geoinformation and Cartography, DOI 10.1007/978-3-319-61297-3_11

Introduction

The dynamics in the context of personal activities include many aspects where a part of physical activities is conditioned by a physical personal mobility determined by (for the certain scale ranges) personal features, a spatial distribution of places (where a person operates), geographical features of the territory and a transportation system (facilitating a personal mobility). The main factor how to improve a personal dynamics is a support of its mobility through improvements of the transportation system. The mobility evaluation of geographical locations and the whole territory can be based on transport accessibility.

The transport accessibility evaluates a relative "nearness" of one place to other places using transport means. It is a complex concept that is not easy to define and certainly not easy to measure. Some authors provide recommendations what criteria should be included in its evaluation (Vanderbulcke et al. 2009). Geurs and van Wee (2004) identified four basic types of accessibility measures:

1. Infrastructure-based measures used for evaluation of the performance or service level of transport infrastructure.
2. Location-based measures applied for analysing accessibility at locations.
3. Person-based measures evaluate accessibility at the individual level which may measure limitations of individual's freedom of action in the environment in the context of space-time geography (Hägerstrand 1970).
4. Utility-based measures focused on evaluation of economic benefits that people collect by utilisation of the spatially distributed activities.

More factors influence a perception of public transport (PT) suitability than those shaping the individual automobile transport. Quite often the evaluation of public transport accessibility is based only on connectivity measurements like frequencies of transit connections or vehicles (i.e. Křižan 2007; Cebollada 2009; Marada et al. 2010; Currie 2010; Tesla et al. 2015). Another approach to evaluate the connectivity is to measure road distances, travel time, travel costs or number of changes (metric, time, cost, topological accessibility according i.e. Horák 2006; or weighted travel time Jánošíková and Kubáni 2000). The combined evaluation of transit distances and a transit frequency measures was provided i.e. Curtis and Scheurer (2010). Service Area Ratio (SAR) and Access Area Ratio (AAR) proposed by Benenson et al. (2010) compare a relative local performance of public transport against individual automobile transport; nevertheless these indicators evaluate and compare only travel time. The importance of person characteristics is stressed by White and Dolan (2009) or Zajíčková et al. (2016) incorporating richness of activities and potential quality of life of the individual.

The evaluation of potential for personal dynamics requires to prefer person-based measurements of accessibility in terms of an individual's ability to exploit opportunities considering person's daily activity program and spatio-temporal constraints (Kwan 1998; Geurs and Ritsema van Eck 2001). The setting of measurements may include person's preferences of transport modes

(Zajíčková et al. 2014) or other personal transport related parameters (i.e. Pochobradsky et al. 2016), utilize knowledge of important commuting flows by given sector of industry (Horák et al. 2014), urban differentiation of accessibility zones within cities (Voženílek et al. 2016) or different attractiveness of various targets (Burian et al. 2016).

Current accessibility measures address only part of the critical features of public transport system. Criteria like the number of changes are fully omitted or they are included only in parameter setting for searching public transport connections (as a hard threshold to limit only "acceptable" connections).

More complex evaluation requires to have a suitable system to record all important characteristics of public transport utilization (to record travel time, price, distance, number of changes, waiting time, but also vehicle occupancy, amenities etc.), their adequate quantification and appropriate way of integration. Integrated accessibility evaluation can utilize:

1. Rule based classification
2. Multi-criteria evaluation
3. Multivariate analysis
4. Methods of artificial intelligence (machine learning, neural networks etc.)

The goal of the paper is to demonstrate possibilities of rule based and multivariate based evaluation of public transport accessibility, and compare them. Both classifications will apply multidimensional approach where dimensions are represented by selected significant factors influencing commuting.

Data Sources and Settings

To demonstrate the multidimensional evaluation we have focused on the accessibility of employers, because they constitute for economically active people the most important reason for mobility. Also in terms of social engagement the options and conditions for commuting to work represent the most watched issue. Only important employers with more than 100 employees located in all working premises within the pilot area plus 20 km buffer have been selected as potential destinations (194 in total). The pilot area is the Ostrava public transport zone XXL which covers Ostrava and surrounding municipalities served by the Ostrava city public transport system (Fig. 1). The accessibility has been evaluated for median centres of each inhabited Basic Statistical Units BSU (delimitation of BSU according to the Czech Statistical Office, 2016, 280 BSU in total).

The scenario of personal daily activities includes the commute to randomly selected important employer to 6:45 (7:00 is the most frequent begin of working time according to the survey (Horák et al. 2017), 15 min is usual preparatory time) while the travel cannot start before 4:15, eight hours work and return home (limiting time is 22:00). The maximal walking distance to a public transport stop is 5 km

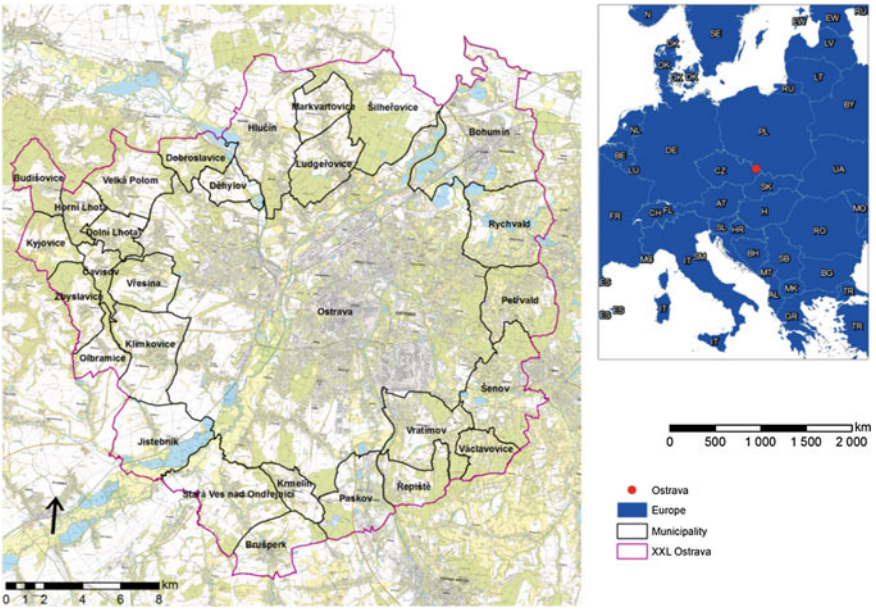

Fig. 1 Ostrava in Europe and its public transport zone XXL

(to not strictly limit accessibility in peripheral villages) and the transport is tested between 3 stops closest to the origin and the destination (9 combination) according to Ivan (2010, 2016) and also commuting on foot is evaluated (to reach very close employers where using of public transport is useless). The testing day was 11.6.2014 and the shortest connection has been preferred when more than one connection has been found. The total number of evaluated connections is 1,086,400. Following variables from each trip have been recorded: starting time, finish time, duration, distance, number of changes, price, walking distance to/from stop, transport mode (public transport/walking). The evaluation is based on the daily aggregation of trips and combination with other known parameters like requested beginning of working time etc. Finally we used following indicators of travel conditions per day (evaluated in each location):

- DURATION FULL—total travel time (including travel time by public transport and walking to/from the stop as well as waiting for a connection), in minutes (walking speed was 4 km/h),
- DURATION—travel time by public transport, in minutes,
- WALKDIST—the walking distance between the used transport stop and the origin or destination), in metres,
- CHANGES—the number of changes during the transport,
- DISTANCE—transport distances (they should have a direct impact on the cost of transportation), in metres,

- WAITING TIME—sum of waiting time before and after the working time (between the arrival and the begin of work, between the work finish and the departure), in minutes,
- SHARE OF DESTINATIONS—share of accessible destinations from all destinations, in %.

These partial indicators are to be utilised for overall accessibility evaluation. Nevertheless, the final selection of indicators for each evaluation method depends on its formal requirements.

Rule Based Classification

The most straightforward way to combine all indicators is to apply a rule based classification where each indicator is separately classified into general levels of suitability for commuting. Such general classification scheme may contain following 6 classes ranging from excellent conditions (A) to poor quality (E) and unusable travel connections (X) (Table 1).

The easiest way is to classify the local accessibility conditions according to average values of indicators. Such way we have evaluated the accessibility of the Ostrava territory in Horák et al. (2017) using average of DURATION FULL and average of CHANGES for 100 randomly selected important employers (see previous chapter for settings) and the classification in Table 1. The accessibility evaluation shows overall dominating sufficient (D) and poor (E) conditions in Ostrava XXL (Fig. 2). According to this evaluation almost all municipalities in the suburb of Ostrava except of Petřvald, Šenov, Ludgeřovice and part of Hlučín has a quite bad situation.

Nevertheless, using only average values may hide substantial differences in conditions, especially large variability of commuting conditions in one place. Figure 3 provides histograms of DURATION FULL for two BSUs with similar variability but strongly different value distributions as well as mean values.

Table 1 Classification of commuting conditions in the city (Horák et al. 2017)

Changes per day	Duration full (in minutes per day)					
	0–29	30–59	60–89	90–119	120–149	Over 150
0	A	B	C	D	D	E
1	B	C	C	D	D	E
2	C	C	D	D	E	E
3	D	D	D	E	E	X
4	D	D	D	E	X	X
5	E	E	E	X	X	X
6	E	E	E	X	X	X
More	X	X	X	X	X	X

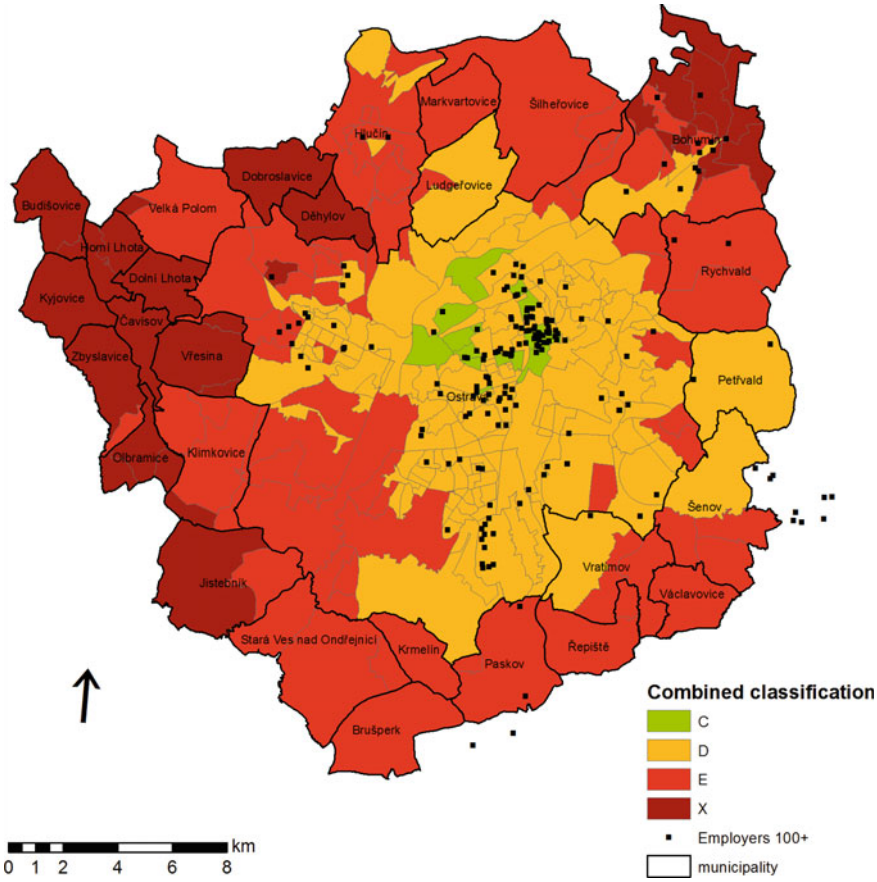

Fig. 2 Rule based classification of employers' accessibility (DURATION FULL, CHANGES)

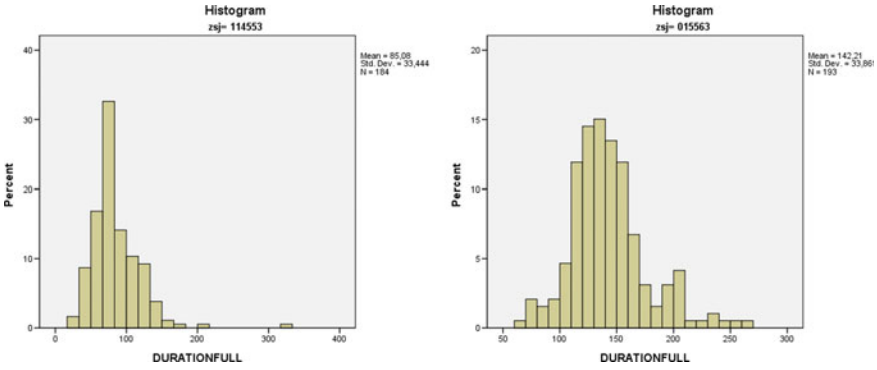

Fig. 3 Different distribution of DURATION FULL for two BSUs with similar variability

The extended solution applies the classification scheme to each commuting case (both-way trips from each location to every employer and return). This way we obtain in each place frequencies of commuting possibilities classified into A to X categories, plus no connection. It represents the number of important employers accessible on quality conditions A to X from each location.

To display and interpret results it was necessary to select one category or a suitable combination. We have explored histograms and variability of various combinations. Finally the sum of first 4 categories (A–D) as an indicator of "suitable commuting" to important employers (Fig. 4 left) was selected. The best conditions are indicated in BSUs where more than 60% of important employers are "suitable" accessible and the worst one possess this share below 20%. Due to higher concentration of employers in slightly NE position from the coordinate centre of Ostrava it is anticipated to have more advantages in NE parts of the territory. The best conditions occur in the main populated BSUs of the Ostrava municipality (except of several peripheral BSUs mainly in the western part like Krásné Pole or Globus), but also in eastern municipalities Petřvald, part of Šenov, and part of Vratimov. About 50% of important employers are accessible in several weaker evaluated BSUs of Ostrava, but also in all quite distant southern municipalities as well as in several northern municipalities (Ludgeřovice, Markvartovice, parts of Hlučín, Bohumín, Rychvald). To the opposite very bad conditions (bellow 20%) can be found in almost all western and south-western municipalities (except of Velká Polom situated on the I/11 road) and in the most of BSUs in Bohumín.

The evaluation based on more than two indicators requires appropriate setting of classification for combinations.

The next indicators were integrated to the classification scheme using a method where every additional indicator is treated independently and may only worsen the situation. Good conditions of the additional indicator do not change the classification in Table 1, weak conditions decrease the classification by one level and not

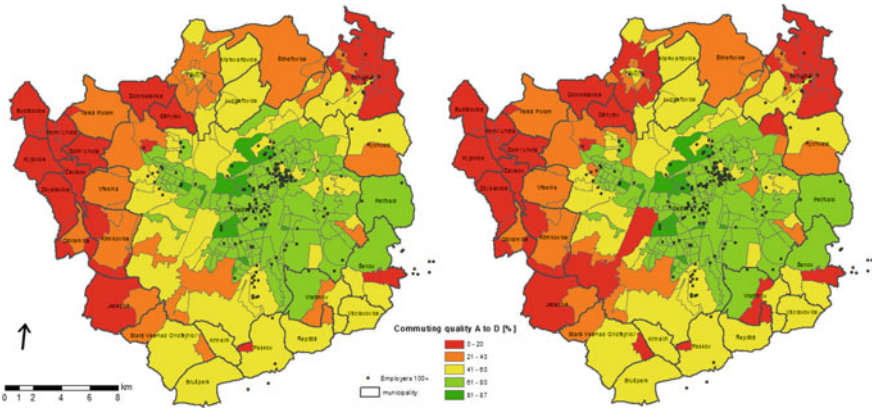

Fig. 4 Share of important employers accessible by commuting quality A to D based on two (*left*) and four (*right*) indicators

acceptable conditions rewrite the previous classification. We set good conditions for WALKDIST below 2 km per day, weak conditions between 2 and 4 km, and not acceptable over 4 km. The WAITING TIME uses limits of 45 and 120 min, respectively. Due to these limits 1196 daily trips (from 51,229, 2.3%) obtained worse classification.

The final evaluation using extended set of 4 indicators (Fig. 4 right) shows where the situation is more serious and almost unacceptable for public transport usage. Most changes are caused by long walking distances to and from active transport stops (usually between 2 and 4 km) like in Hlučín, Stará Ves, Vratimov which seems to have very limited conditions to use PT. Also in weakly serviced BSUs in Ostrava prevail this reason and only in 6% of trips the WAITING TIME crosses the limits which is interpreted as a bad frequency of PT.

Multi-criteria Evaluation

The rule based classification can be improved using a multi-criteria approach. Weighted linear combination WLC introduced by Eastman and Jiang (1996) summarizes in each locality the multiplication of factor score (standardized evaluation of local suitability of the given factor) and the factor weight. To set factors' weights the Saaty hierarchical process can be applied (Saaty 2001). Ordered Weighted Average extends the solution using an additional set of weights controlling the order of weight (which means to control the level of compromising solution).

The main advantage is in different weights applied for each partial indicator of accessibility which enable to reflect different impacts of these factors to real commuting (compare with equal weights in multivariate methods). Also there is no need to establish borders of several classes as in the expert's combined classification, only the minimal and maximal values are necessary to be set up.

Multivariate Analysis

The expert's combined classification is subjective due to setting of class limits, the multi-criteria evaluation due to factors weights and setting of min-max limits.

Multivariate analysis enable to analyse relationships among number of variables, number of cases, to identify important factors influencing one independent variable and to reduce dimensionality of the tasks (Rencher and Christensen 2012). In our case following types of analysis should contribute best to understand commuting conditions and to distinguish groups of similar locations: K-means analysis to identify and describe clusters of similar conditions, Correspondence Analysis to

identify groups of similar features (behaviour) and MultiDimensional Scaling to reduce number of variables and to interpret relative proximity of objects by all transformed variables.

Exploratory spatial data analysis has been provided for all variables to understand their statistical behaviour and mutual relationships (incl. scatter plots and correlation analysis). To reduce multicollinearity and to preserve important features influencing personal commuting behaviour following variables have been selected —total travel time per day (DURATION FULL), daily walking distance to/from stop (WALKDIST), number of changes per day (CHANGES) and waiting time to the start of next activity (WAITING TIME).

For each location we have a set of evaluated both-way trips (to each accessible employer, number of trips usually 150–180 from maximal 194). Two main questions were raised—how to select employers (targets) and how to represent values of each variable. Targets may be selected fully randomly (i.e. 100 randomly selected employers for each origin), rule based (i.e. within one hour of travel time) or gravity based (i.e. select locally prospected employers according to combination of travel time and attractiveness of employer measured by i.e. number of employees), some combination of above options or we can apply no selection (thus to evaluate travel conditions to all employers). To represent value of variables in origins usually some local mean value (usually average or median) is applied. Nevertheless such evaluation may be insufficient due to the evaluation of only central value which may hide internal variability and mask predominant bad evaluated trips by several exceptionally well evaluated trips.

To obtain more balanced evaluation of the trip distribution the quantiles of the variables were employed. In our case deciles has been applied. Thus instead of one central value a set of 9 values describes the distribution of each variable.

First, the hierarchical cluster analysis (HCA) to reveal natural groupings among 280 locations (BSU) has been conducted. The setting includes the Ward's cluster method for cluster formation, the squared Euclidean distance as a dissimilarity measure and standardization of all variables. The final part of the agglomeration schedule is in Table 2.

The coefficients (distances between two joined clusters) show a continual increase without any important break (Fig. 5). The recommended range of the number of clusters is 4–7. That is why the K-means has been applied for different number of clusters (7, 6, 5, 4) to understand behaviour and differences of resulted classification in maps. Finally, it was decided to use 5 clusters.

ANOVA has confirmed the significance of all variables ($p < 0.001$). The majority of BSUs was classified into cluster No. 1 (131), followed by the cluster No. 3 (84), while 5th, 2nd and 4th cluster has only 28, 22 and 15 members, respectively. The last three clusters contain approximately ¼ of BSU with some serious issues in public transport commuting conditions.

Distances between 5 final clusters (Table 3) show high differences between clusters No. 2 and 4, 1 and 4, 1 and 5, 1 and 2. It confirms the relative closeness of 1st and 3nd clusters, 4th and 5th clusters and a separate position of 2nd cluster.

Table 2 Final part of agglomeration schedule for HCA

Stage	Cluster combined		Coefficients	Stage cluster first appears		Next stage
	Cluster 1	Cluster 2		Cluster 1	Cluster 2	
….	….	….	….	….	….	….
268	5	7	1,989.262	252	251	270
269	6	13	2,105.989	263	266	278
270	5	30	2,284.096	268	250	272
271	2	16	2,462.287	259	257	275
272	4	5	2,664.878	265	270	276
273	63	65	2,883.698	264	255	277
274	1	17	3,168.260	258	261	276
275	2	23	3,608.584	271	267	277
276	1	4	4,103.210	274	272	278
277	2	63	4,972.281	275	273	279
278	1	6	6,586.049	276	269	279
279	1	2	10,044.000	278	277	0

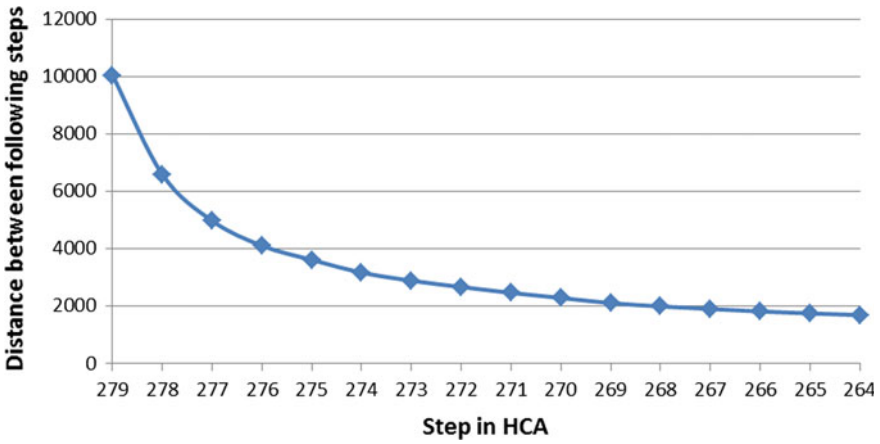

Fig. 5 Distances between two clusters joined in the given step (X axis, 279 = 1) during HCA

Table 3 Distances between cluster centres

Cluster	1	2	3	4	5
1		10,231	4,750	13,180	11,160
2	10,231		9,038	14,218	9,281
3	4,750	9,038		9,881	6,672
4	13,180	14,218	9,881		7,440
5	11,160	9,281	6,672	7,440	

The next step was to describe members of each cluster and to interpret the meaning of each cluster.

Deciles represent only 9 points in the distribution. To discover real outputs of clustering we classified all trips according to the identifier of cluster assigned to BSU by decile based K-means. Thus it is possible to use appropriate statistical exploratory tools (i.e. box plot) not only for 9 values of each original variable in each location but to analyse all recorded trip from the same origin (51,229 in total) (Fig. 6). Even more, we can analyse distribution of other variables (Fig. 7) not yet included in the cluster analysis to see all differences between clusters.

Finally, each cluster can be evaluated following way:

- No. 1—very low total travel time (about 70 min per day in average) and number of changes (2.5 in average), slightly below average walking distance (1156 m in average), very low waiting time to activity (7 min in average) and the highest share of accessible employers (98.5% in average).
- No. 2—very high walking distance to stops (2188 m in average), above average total travel time (115 min in average) and number of changes (3.4 in average) and below average waiting time to activity (10 min in average), above average share of accessible employers (97% in average). This situation shows a bad walking accessibility of used travel stops but these stops are well served by PT.

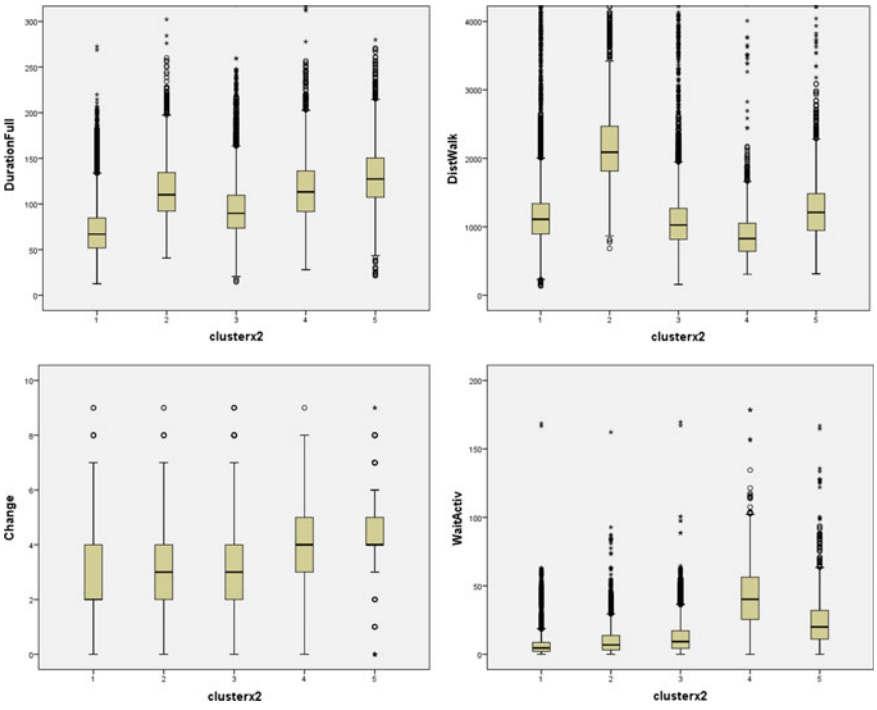

Fig. 6 Distribution of all trip values in each cluster for 4 main variables (duration full, walking distance, number of changes, waiting time to next activity)

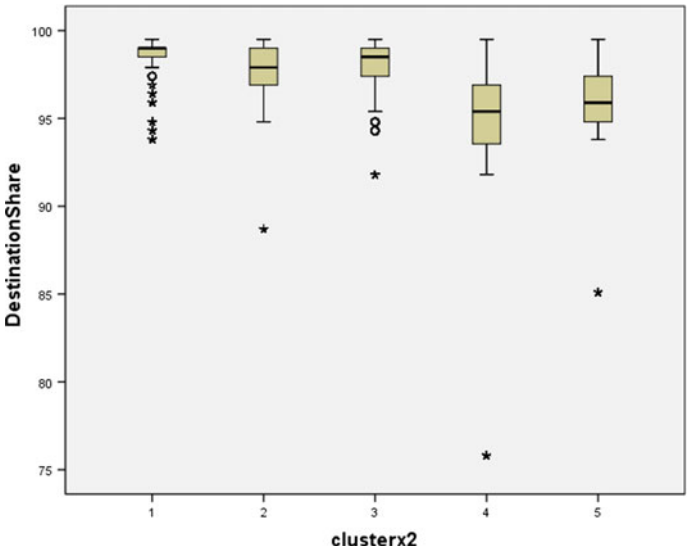

Fig. 7 Share of accessible important employers in each origin according to clusters

- No. 3—slightly above average total travel time (94 min in average) and number of changes (3.5 in average), slightly below average walking distance (1079 m in average) and average waiting time to activity (12 min in average), the high share of accessible employers (97.9% in average). Conditions are similar to 1st cluster, but differ by worse duration and slightly worse waiting time.
- No. 4—very high waiting time to activity (43 min in average), above average total travel time (117 min in average) and number of changes (3.7 in average), low walking distance (900 m in average) and the lowest share of accessible employers (94.5% in average). Problems rest with a bad transport service (frequency as well as connectivity), more changes and fewer targets.
- No. 5—very high total travel time (130 min in average) and number of changes (4.4 in average), slightly above average walking distance (1249 m in average), high waiting time to activity (23 min in average) and below average share of accessible employers (95.3% in average). The group is typical by long travel time, more changes and long walking to stops, offering fewer targets.

The spatial distribution of cluster members is obviously heterogeneous (Fig. 8 left). The first cluster covers the centre of Ostrava and Petřvald, accompanied by several BSUs extending well accessible area mainly towards south. Members of the 2nd cluster typical by long walking to a preferred stop surround a centre of Hlučín where central stops are much more suitable for commuting than less operated stops around. Similarly this type of commuting problems are indicated in several BSUs inside Ostrava and peripheral BSUs in some other municipalities like Vratimov, Stará Ves, Klimkovice etc., rarely whole municipalities are classified such way (Čavisov or Dobroslavice). BSUs of the 3rd cluster naturally surround the best

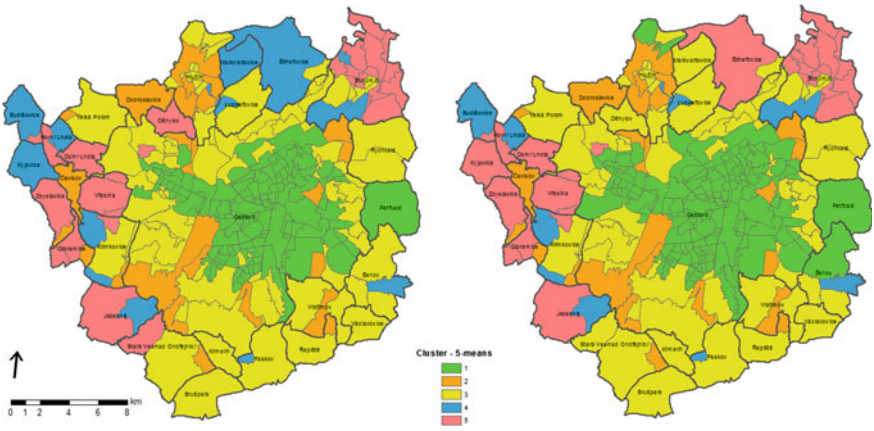

Fig. 8 Commuting conditions based on 5-means cluster analysis in Ostrava XXL using deciles (*left*) and median (*right*)

classified BSUs (1st cluster) and extends suitable accessible area from Ostrava towards south, east and NW. Members of 4th cluster (typical by long waiting times) are less populated municipalities on mainly the northern and western border of the pilot area or isolated parts of several other municipalities. The 5th cluster can be found in majority of Bohumín and in a set of municipalities in the western part where the commuting is complicated by both topography conditions (a hilly region) and specifically developed transport system (a local tram combined with buses, limited direct connections to the centre).

To evaluate a contribution of clustering based on deciles, a control K-means cluster analysis for only median values was performed (for the same number of clusters). Reclassification of the cluster identifiers for the median-based K-means was performed to enable comparison of results and to quantify changes. The result is displayed in Fig. 7 right. Differences are mapped in the contingency Table 4. More than 91% of BSUs share the same classification. The 2nd class is fully equal—it means the cluster is really different from others and it contains specific BSUs. 17 BSUs (6%) was changed from class 3 to 1. There are 3 changes from 4 to 5 (Kyjovice, Bohumín, Šilheřovice) and comparing both results, clustering on deciles seems to provide better classification. Other value changes show BSUs in transition (atypical values) where both classifications are possible.

Table 4 Differences between k-means for all deciles and median

ID cluster based on all deciles	ID cluster based on median (after reclassification)	Change the class by				
		−2	−1	0	1	2
1	1			130		
1	3					1
2	2			22		
3	1	17				
3	3			67		
4	3		1			
4	4			11		
4	5				3	
5	3	2				
5	5			26		
	Sum	19	1	256	3	1
	Share (%)	6.79	0.36	91.43	1.07	0.36

Conclusion

A new system of simulated commuting trips enables to record a set of variables describing various impedance measures of the public transport connections. We call them dimensions to emphasize the different role of connected issues. The complex evaluation can jointly integrate the set of indicators. The rule based evaluation was developed in several variants which differ by the number of indicators and their aggregation. Best results were obtained using extended set of indicators (total travel time, number of changes, walking distance, waiting time) and non-aggregated results (thus to evaluate each trip separately). Further, a multivariate cluster analysis of indicators was provided. A novel approach to make a cluster analyse based on deciles has been tested. The comparison shows a little difference between K-means clustering based on deciles and median in our case. This indicates median based K-means clustering will be usually sufficient for automated (unsupervised) classification.

K-means clustering is efficient to distinguish special conditions in commuting—i.e. long walking distances in case of cluster No. 2 or partly also enable to detect places with longer waiting time to an activity. K-means clustering enable also to distinguish the level of accessibility but the separation of classes is not perfect what is not surprising. The conditions usually do not change so sharply and the usage of more indicators strengthens a smoothing effect where a significant change of one indicator may be balanced by small changes of other indicators.

Also the equal weights of all indicators and the equal interval classification of each variable are not welcome. Obviously differences between very low and low transport time are perceived less significantly than differences between high and very high transport time. Similarly non-linear behaviour can be found for other

variables. Another issue is that the optimisation (clusterization) is based on local conditions (here for one city) which limits the comparison between cities or regions.

To summarize, the rule based classification utilizing evaluation of all trips and all indicators is still irreplaceable in the accessibility evaluation even though its dependency to the subjective setting of limits (or class borders). K-means clustering is useful mainly to distinguish different conditions in commuting, to create a regional typology and to understand variability of conditions not bounded by expert's rules.

Acknowledgements The research is supported by the Czech Science Foundation, project Spatial simulation modelling of accessibility, No. 14-26831S. Data is provided by the courtesy of the Czech Statistical Office.

References

Benenson, I., Martens, K., Rofé, Y., & Kwartler, A. (2010). Public transport versus private car GIS-based estimation of accessibility applied to the Tel Aviv metropolitan area. *The Annals of Regional Science, 47*(3), 499–515.

Burian, J., Zajíčková, L., Popelka, S., & Rypka, M. (2016). Spatial aspects of movement of Olomouc and Ostrava citizens. In 16th International Multidisciplinary Scientific GeoConference SGEM 2016, www.sgem.org, SGEM2016 Conference Proceedings, Book 2, Vol. III, pp. 439–446. doi: 10.5593/sgem2016B23.

Cebollada, A. (2009). Mobility and labour market exclusion in the Barcelona Metropolitan Region. *Journal of Transport Geography, 17*(3), 226–233.

Currie, G. (2010). Quantifying spatial gaps in public transport supply based on social needs. *Journal of Transport Geography, 18,* 31–41.

Curtis, C., & Scheurer, J. (2010). Planning for sustainable accessibility: developing tools to aid discussion and decision-making. *Progress in Planning, 74,* 53–106.

Eastman, J. R., & Jiang, H. (1996). Fuzzy measures in multi-criteria evaluation. In *Proceedings, Second International Symposium on Spatial Accuracy Assessment in Natural Resources and Environmental Studies*. Fort Collins, GIS World Inc., pp. 527–534.

Geurs, K., & van Wee, B. (2004). Accessibility evaluation of land-use and transport strategies: Review and research directions. *Journal of Transport Geography, 12*(2), 127–140.

Geurs, K. T., & Ritsema van Eck, J. R. (2001). *Accessibility measures: Review and applications*. RIVM Report 408505 006. National Institute of Public Health and the Environment.

Hägerstrand, T. (1970). What about people in Regional Science? Papers of the Regional Science Association 24(1), 6-21.

Horák, J. (2006). Transport accessibility evaluation. *Geografie, 111*(1), 115–132.

Horák, J., Burian, J., Ivan, I., Zajíčková, L., Tesla, J., Voženílek, V., et al. (2017, under review). Prostorové simulační modelování dopravní dostupnosti s empirickou studií Olomoucka a Ostravska. 350 pp. ČGS, edition Geographica.

Horák, J., Ivan, I., & Tesla, J. (2014). Improved gravity models of commuting conditions: A Czech case study. In *International Conference on Traffic and Transport Engineering*, ICTTE 2014 Beograd, November 27–28, 2014, pp. 171–179. ISBN: 978-86-916153-2-1.

Ivan, I. (2010). Docházka na zastávku a její vliv na dojížďku do zaměstnání. *Geografie*, *115*(4), 393–412. ISSN 1212-0014.

Ivan, I. (2016). Interchange nodes between suburban and urban public transport: Case study for the Czech Republic. *Acta Geographica Slovenica, 56*(2), 221–233. doi: 10.3986/AGS.754, http://ojs.zrc-sazu.si/ags/issue/view/144.

Jánošíková, Ľ., & Kubáni, A. (2000). *Dopravná dostupnosť obcí. Komunikácie*. Vydavatelství Žilinské univerzity. Vol. 2, No. 4, pp. 9–15. ISSN 1335-4205.

Križan, F. (2007). Regionálna typológia územia Bratislavy na základe dostupnosti supermarketov a hypermarketov. *Geografický časopis, 59*(4), 373–385.

Kwan, M. P. (1998). Space-time and integral measures of individual accessibility: A comparative analysis using a point-based framework. *Geographical Analysis, 30*(3), 191–216.

Marada, M., Květoň, V., & Vondráčková, P. (2010). *Doprava a geografická organizace společnosti v Česku. Geographica*. Praha: Česká geografická společnost.

Pochobradsky, T., Kozel, T., & Krejcar, O. (2016). Design and implementation of mobile travel assistant. *Recent developments in intelligent information and database systems,* 423–432. Berlin: Springer.

Rencher, A. C., & Christensen, W. F. (2012). *Methods of multivariate analysis*. New York: Wiley. ISBN: 978-0-470-17896-6.

Saaty, T. L. (2001). *Fundamentals of decision making and priority theory*. Pittsburgh, Pennsylvania: RWS Publications. ISBN 0-9620317-6-3.

Tesla, J., Horák, J., & Ivan, I. (2015). Frequency analysis of public transport between Czech municipalities. In *Proceedings of 15th International Multidisciplinary Scientific GeoConference SGEM 2015*, www.sgem.org. ISBN: 978-619-7105-34-6/ISSN 1314-2704, June 18–24, 2015, Book 2, Vol. 1, 593–600.

Vanderbulcke, G., Steenberghen, T., & Thomas, I. (2009). Mapping accessibility in Belgium: A tool for land-use and transport planning? *Journal of Transport Geography, 17*(1), 39–53.

Voženílek, V., & Burian, J. (2016). Accessibility zones of the university according to students' transportation preferences. In *16th International Multidisciplinary Scientific GeoConference SGEM 2016*, www.sgem.org, SGEM2016 Conference Proceedings, Book 2, Vol. III, 19–26.

White, M. P., & Dolan, P. (2009). Accounting for the richness of daily activities. *Psychological Science, 20*(8), 1000–1008.

Zajickova, L., Vozenilek, V., Burian, J., & Tucek, P. (2014). Demand specifications for geodata within a public transport system. In *Conference Proceedings SGEM 2014, 14th International Multidisciplinary Scientific GeoConference*. STEF92 Technology Ltd., June 19–25, 2014, Vol. 1, 555–562. ISBN: 978-619-7105-10-0/ISSN 1314-2704.

Zajíčková, L., Voženílek, V., & Rypka, M. (2016). The choice of means of transport and daily movements in urban environment. In *16th International Multidisciplinary Scientific GeoConference SGEM 2016*, www.sgem.org, SGEM2016 Conference Proceedings, Book 2, Vol. III, 487–494.

Zhang, X., Huang, H., & Zhang, H. M. (2008). Integrated daily commuting patterns and optimal road tolls and parking fees in a linear city. *Transportation Research Part B: Methodological*, *42*(1), s. 561–582.

Verification of the Movement Speed on Communication Network and the Vehicle Movement Modelling Possibilities for Defence and Crisis Management

Martin Hubáček, Martin Bureš, Kateřina Šimková and Vlastimil Kratochvíl

Abstract The road transport is one of the basic types of moving people and material during situations of crisis. As far as it can be said the movement of vehicles is connected to the existing road network. Vehicles of military units and rescue teams must be able to move also outside communications. Knowledge of speed restrictions doe to the influence of individual landscape objects is therefore important for proper transport planning. That is the reason why part of the research is focused on monitoring of the vehicle movements on communications and on field and forest roads. To monitor the vehicles there are used GNSS receivers. Position and velocity records are then analysed according to characteristics of the communications and their surroundings. Based on previously conducted and processed measurements it is possible to demonstrate the influence of road type and curvature on the vehicle speed. Indeterminate results occurred in cases of the slope and obstacles around communications. The results and conclusions after completion of the research will help with more realistic planning of vehicle movements in situations of crisis.

Keywords Transport · Vehicle movements · GIS · Route planning

M. Hubáček (✉) · M. Bureš · K. Šimková · V. Kratochvíl
Department of Military Geography and Meteorology, Faculty of Military Technologies, University of Defence, Kounicova 65, 662 10 Brno, Czech Republic
e-mail: martin.hubacek@unob.cz

M. Bureš
e-mail: martin.bures@unob.cz

K. Šimková
e-mail: katerina.simkova@unob.cz

V. Kratochvíl
e-mail: vlastimil.kratochvil@unob.cz

I. Ivan et al. (eds.), *Dynamics in GIscience*, Lecture Notes in Geoinformation and Cartography, DOI 10.1007/978-3-319-61297-3_12

Introduction

Movement is one of the primary natures of the civilization. Every second ten thousands of people are moving from one place to another and the same can be said about million tons of material. Our civilization is dependent on transport. Transport paralysis causes serious problems. Those can be caused by natural phenomenon (weather, landslides, earthquakes, floods …) but also by the impact of human activity (traffic accidences, industrial incidents, big demonstrations, blockades of communications, war conflicts …). During situations of crisis traffic can be considerably limited, but it is still necessary to transport rescue teams, military units, humanitarian help and materials in time to requested locations. If possibilities of air transport, which are influenced by weather conditions (Ohshige et al. 2006; Dejmal et al. 2015), capacity and landing capability in chosen destination (Kricke and Schaefer 1997), are excluded, the most fundamental way of transport on the ground is road transport. By railway it is possible to transfer a big amount of material and many people at once for a long distance (Landex 2009; Xia and Zhang 2016), however there is an infrastructure limitation and it is quite difficult to repair potential route damages. Even thou there is a possibility to use railway, it is still necessary most of the time to make a final part of transport to selected destination on a road or through terrain. So communication network and road transport is essential not just for daily life but especially in situations of crisis.

Road network can be characterized by many parameters. Between the most important ones that are examined primarily by military geography (Collins 1998; Laurman and Rybansky 2002) belong:

- density of a road network;
- structure of a road network;
- quality and technical state of communications;
- technical parameters of communications and objects on them.

Various parts of the world therefore have a different quality of communications. Technical state and density of the road network is influenced mainly by population density, economic and geographic conditions (Murray-Tuite 2006; Ivan et al. 2013; Ivan 2016). Characteristics of a communication network then influence planning of transports. Today are for this purpose used GIS tools that allow road analysis. Algorithms used to find optimal route (Cheng and Chang 2001; Rybansky 2014) are common part of most web mapping services. These services allow anybody, with internet connection but without owning any data or technology, to search and plan transportation. Some more sophisticated systems are using information about traffic limitations, density, accidents and other complications (Kanoh and Hara 2008; Niaraki and Kim 2009). Yet not all results of planed arrival times fully agree with real times that are necessary for a transport. Example of comparison of different planning routes is shown in Table 1.

Table 1 Times and lengths of routes computed by on-line route planners

Tachov–	Tabor km (h:min)	Jesenik km (h:min)	Svitavy km (h:min)	Vsetin km (h:min)	Novy Bor km (h:min)	Chomutov km (h:min)
mapy.cz	172 (2:18)	415 (4:52)	345 (3:49)	485 (4:47)	255 (2:56)	139 (1:50)
dopravniinfo.cz	173 (2:01)	397 (4:25)	351 (3:20)	484 (4:05)	254 (2:32)	127 (1:35)
google.com	182 (2:23)	396 (4:44)	339 (3:36)	484 (4:53)	275 (2:56)	126 (1:37)
Skoda	182 (2:27)	396 (4:56)	339 (3:45)	484 (4:59)	275 (3:05)	126 (1:41)
ViaMichalin	191 (3:13)	399 (6:01)	344 (4:22)	482 (5:15)	260 (3:41)	134 (2:11)
TomTom	188 (2:40)	401 (4:59)	344 (3:45)	486 (4:47)	277 (3:03)	127 (1:47)

Another limitation of planning in these systems is that they are focused only on the communication network. Rescue teams and military units very often move outside transport network and use field and forest roads for many types of vehicles. That can be planned but also not planned. That is why planning of transport in situations of crisis must be more complex and has to allow include movements on every kind of road, also on unpaved roads and off-road terrain. The main goal of this article is to show ways how to verify speed coefficient of a vehicle movement on different types of communications and also in terrain. The analysis is based on movement mapping of real machines and it tests influence of geographical conditions on communications and in their proximity on real speed of the vehicle.

Initial Conditions and Data Collecting for Model Verification

The speed of a vehicle moving on a road is limited by two factors. The first one is legislation (Law No. 361/2000 2000) which determines maximal allowed speed on a particular road. The second one is technical parameters of a vehicle (Cibulova et al. 2015; Rybansky et al. 2015), these determine maximal speed which is the vehicle able to produce considering geographical conditions. Most cases are influenced by the first factor. However, if communication leis in difficult terrain (steep slope, curving of roads, unclear environment, weather conditions …) the speed of a vehicle is mostly influenced by technical parameters of a vehicle and additionally by experiences of a driver. The research is focused on geographical conditions that influence final speed of a vehicle and ways of solving this problem are focused on this main goal. Conducted research was developed as a respond to the requirements of ACR (Army of Czech Republic) commanders which during transport planning demand more accurate results of movement calculations.

If the legislation, that most of the times must be followed, is neglected, the speed of a vehicle is influenced by the technical parameters. Speed calculations can be determined by laboratory-measured characteristics of a vehicle. One of the ways how to solve this is identifying a traction curve (Rybansky et al. 2015) of the vehicle. This curve determines dependence of engine power on gear. This diagram can be used to define influence of terrain slope on theoretical maximal speed of vehicle. Different way how to determine this speed is based on questionnaire survey of drivers that for a longer period of time drive particular type of vehicle. This kind of survey cannot be focused on determining influence of terrain slope because estimating slope can be quite subjective. But it is usually focused on determining type of the surface or categorising communications. An example can be Table 2 (Rybansky 2009) that is based on a questionnaire survey. It defines coefficient of vehicle deceleration for different types of communications considering technical parameters of a road and traffic density.

Verifying data obtained this way is possible, but only by realizing real transport that allows to receive sufficiently large set of data about position and speed of a vehicle. Data collecting for verifying initial assumptions takes places in two different periods of time.

The first period was mainly focusing on vehicle movement on unpaved roads and in terrain. Data were collected in 2015 in military training area Libavá. It is located 15 km northeast from Olomouc in the Oderské vrchy. The area is characterized by rugged terrain which is mostly covered by forests. The actual movements of vehicles were made in an open field with ways partly covered by vegetation (grass, scrublands, sparse growing self-seeded trees) and along paved and unpaved roads. Vehicles were not during these tests moving on communications. There was used majority of the military vehicles belonging to ACR:

- Personal off-road vehicles LR 110 and UAZ 469, IVECO M65
- Tatra trucks T815 8x8 and T810 6x6
- Combat vehicle PANDUR II, BVP 2 and T-72M4 CZ

Table 2 Overview of the types of communications and their attributes

Category of communications	Classes according to the national importance	TUC (transportation use category) (KTO 25 2007)	Coefficient of deceleration (Rybansky 2009)
Highways	Highways	002	0.872
Main roads	1st class roads	206	0.834
Secondary roads	2nd class roads	207	0.733
Other state roads	3rd class roads	210	0.533
Paved roads	Paved roads	205	0.533
Routes (field, forest)	Routes (field, forest)	208	0.435

Data collecting for speed and vehicle location evaluation was made by GNSS receiver Trimble GEOEXPLORER 3000 and 6000 with TerraSync software. To every receiver was added external antenna so the signal receiving would be without problems. During transfer tests were these antennas placed on top of a vehicle right in the middle. Recordings were made every second and received data were later categorized in Pathfinder Office system by post processing method. For correcting were used data from network of permanent stations CZEPOS (Land Survey Office CZEPOS). Throughout the tests every type of vehicle drove more than 100 km, which gets more than 20,000 records for every vehicle.

Received values of vehicle speeds were compared to theoretical speeds. Those were calculated based on technical parameters of a vehicle and influence of geographical features. Those were described as deceleration coefficient for various types of landscape (Rybansky and Vala 2009; Rybansky et al. 2015; Hofmann et al. 2015) (terrain, vegetation, soils, waters, communications …). Discovered results show considerable variability of differences between theoretical and real speed (Talhofer et al. 2015, 2016). This can be explained by two assumptions that were made based on the results:

- theoretical coefficients that describe particular types of landscape take shape differently than the real influence;
- the way particular coefficients are combined does not describe the real conditions.

The real reason for these differences is probably combination of both of these influences. That is why an easier approach was considered. That way should be eliminated most of the influences and a vehicle movement should be evaluated with landscape types in consideration. So the first step is communications and terrain. After these aspects will be more precise and verified, models will be extended.

With this in mind started in summer 2016 second part of the process focused on vehicle movement on communications. Until now were data collected only by passenger cars and microbuses. Next year is planed data collecting by trucks and buses. Date collecting will be made the same way as before. Last processed records were made in October. Measured data received on communications make less than 1000 km and were made throughout all categories of communications. That makes about 55,000 records.

Data Filter and Records Enrichment

Considering large amount of data that were received, it is necessary to categorize them before they can be processed. The categorization is made according to surface of terrain or type of communication a vehicle drove on. There was also made elimination of incorrect and unsuitable records. During this process generally valid principles were sustained so that sample data stay as objective as possible (Böhm

et al. 1990; Barry and Morris 1991). Filtration of measured records is made by error elimination and selection of records that are considered unsuitable according to examined phenomena. Following points are the ones that were filtered:

- Records with insufficiently accurate position—records which position shifted outside of the defined rout;
- Records with error in speed—records with speed more than was technically possible for a vehicle (e.g. 1340 km/h), these records are usually connected to the ones with error in position;
- Records around the inaccurate ones—assuming lower accuracy of GNSS receiver position and speed determination;
- Record around settlements—processed by using topographic databases;
- Records with purely assigned attributes of communication and its vicinity—done after addition of attributes.

After elimination of incorrect records, next step was to enrich records of information necessary for filtration, data analysis and examining influence of surroundings on speed of a vehicle. For records enrichment and selection are used vector geodatabase DMU25 (Digital landscape model 1:25,000) (KTO 25 2007) and digital elevation models DMR4 and DMR5 (Land Survey Office. DMR4G; Land Survey Office. DMR5G). At first there must be done elimination of points that were located in settlements. It is necessary because of law regulations that significantly limit speed of vehicles (Law No. 361/2000 2000). If settlements layer is not part of DMU25 than build-up area layer is used for this purpose. This layer represents blocks of buildings in urban areas. Build-up area layer does not represent settlements and communication lines go through its polygons only rarely. This shortcoming was solved by using the buffer polygons around buildings. When setting its size there were assessed speed records inside and outside of the resulting "settlements". As suitable value for minimum interference in the recorded data was chosen buffer size 50 m. Although the optimal distance was selected, there is possibility that some of the eliminated records from communications in vicinity of settlements without a speed limit could have been suitable for processing. Considering the total number of position records the quantity of these suitable yet eliminated records is insignificant and does not affect final results.

For analysing how is driving speed dependent on the type of communication, there are added attributes of traffic usage to the records. This information comes from DMU25 and is implemented by using function "Spatial Join" with method "Closets". The results obtained this way must be visually verified at the intersection of two different communication categories and at places where two different roads are parallel. In these cases, in particular when one of those parallel communications is a highway. When driving in the right lane of a highway it can cause assignment of records to the parallel communication (usually path). This is due to the fact that the record is for example 10 m from the line that should represent the highway but only 8 m from the parallel path. Visual check then proves that the record of speed 130 km/h does not belong to category path (Fig. 1). For further processing of files

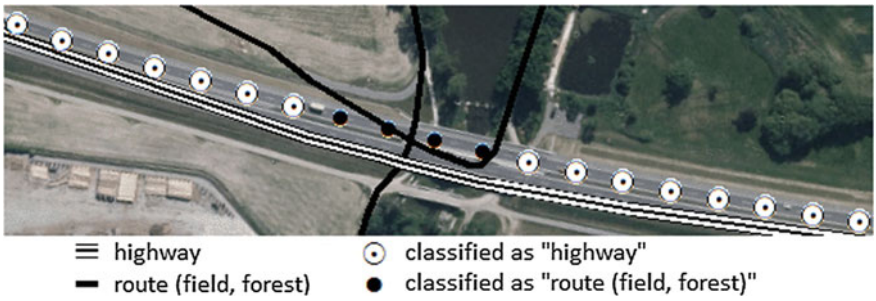

Fig. 1 Example of wrong classification of category path

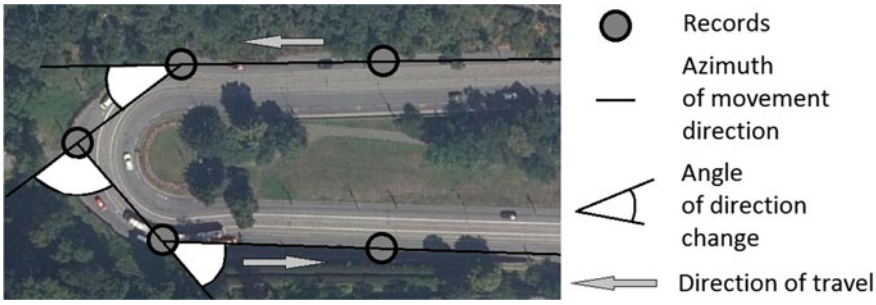

Fig. 2 Illustration of computing of direction change

with received records there is assumed to be automated control of these errors. Beside the attribute of traffic usage there are to all records added attributes of width of the road, this information was also received from DMU25.

Considering surroundings influence on speed of movement there is, in addition to information about the character of traffic use and the width of the communication, added information if the road goes through forest. It is assumed that grown vegetation around the road influences speed of movement. Mainly on lower class communications. To add this information it is again used function buffer, this time with value 20 m, on layer vegetation from DMU25. If the points are inside of this buffer zone they are assigned as a "forest" if they are not then as "outside forest".

Another added attribute is information about a change of direction. Considering that the communications layer does not contain information about the radius of turns is this information replaced by calculated value of drive direction changes. Based on the timestamp and position of vehicle there is made of azimuth of movement direction from previous point to next the one calculation for every record. From these azimuths can then be determined the angle which provides information about direction change (turning) of vehicle (Fig. 2). Thus it is used to assess how much is the road tortoise.

The last step for this type of enrichment of point records is adding information about terrain slope in the recorded point. To obtain information about slope there are used two different models of relief. When moving on roads where there is no presumption of micro-relief shapes and where thus can be assumed continues slope change, the information is extracted from DMR4. When moving along the roads and in open terrain, the information about slope is extracted from more accurate DMR5.

Data, that are added this way and also cleansed of errors and unsuitable records, are now ready for assessment of individual hypotheses about the influence of landscape components on the speed of movement.

Data Analysis and Assessment of the Influence of Landscape Components on the Speed of Movement

Just as previous analysis (Talhofer et al. 2016) showed, the actual speed of vehicles in motion is significantly different than the theoretical speed. These differences are the most apparent when the vehicle moves in terrain and on communications with worse quality. Comparing measured data obtained during cross-country movement tests in Libavá focused primarily on two factors, namely, terrain slope and type of surface on which the vehicle moves. When excluding the influences of landscape, the vehicle speed is mainly effected by slope of relief and recorded speed should therefore correspond to the values obtained from the speed traction curves. In reality the courses of speed changes considerably varies. An example of the slope influence on the speed is demonstrated on Fig. 3. Performed testing shows that lower slope values have less impact than assumed. Slope over 15° is represented by small amount of measurements, and therefore can't be currently used for data analysis.

Another possible method is to compare the measured results with results of a survey. As an input data for compering are used the coefficients of vehicle deceleration received by questionnaire survey. In this survey, researching the impacts of

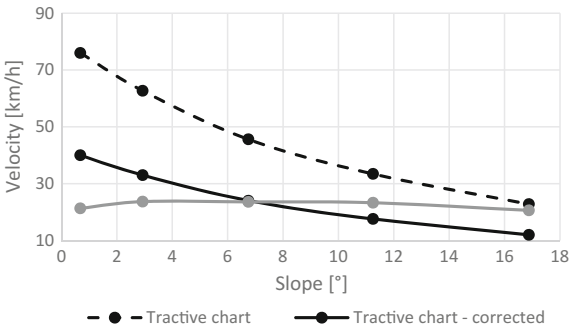

Fig. 3 Comparison of tractive chart and measured speed

object on the ground on vehicle movement, about 100 experts were asked (Rybanský). Among other things, respondents commented on the impact of the quality of communication and traffic density on a total throughput of a given typo of communication. Based on their responses were by method of weighted averages determined coefficient of deceleration on various types of roads, Table 2. The average speed of vehicles moving on various types of roads, is given by the product of the design speed and deceleration coefficient. As will be showed below in the text, even this method is not optimal and measured values do not correspond to the calculated results. The results, especially for lower quality roads, are overvalued compare to reality.

Considering these facts and based on the experience of testing were formulated the following hypotheses about the influence of terrain on vehicle movement:

- A vehicle is moving faster on higher category road, due to expected higher quality of communication.
- Vehicle speed is affected by the slope of terrain and higher the slope, lower the speed.
- A vehicle is moving faster on wider roads than on narrow roads.
- On more tortuous roads and in sharp turns is the vehicle movement slower than in straight parts of roads.
- Vehicle movement is affected by view conditions around the communication and in presence of obstacles is speed of a vehicle reduced.

Verification of these hypotheses is based on measurements. The authors are aware that part of the data collecting on roads is not complete, but current results already provide enough information for preliminary confirmation or disproof of the hypotheses.

Influence of Quality of Communication

Categorization of communication type impact is based on how catalogue DMU25 is sorted. DMU25 is derived from the standardized catalogue FACC (Feature and Attribute Coding Catalogue) (DIGEST 2.1 2000) with regard to certain national

Table 3 Basic speed statistics of different types of communications

TUC	206	207	210	205	208
Average speed	80.9	78.3	67.4	29.5	13.1
Standard difference	14.8	14.8	12.0	5.7	3.2
Minimal speed	6.8	5.9	8.1	7.4	5.3
Maximal speed	110.0	109.7	99.8	44.5	22.7
Number of records	8138	4837	1443	172	950
Average speed	80.9	78.3	67.4	29.5	13.1

specifications (KTO 25 2007). Sorting of the communications is done according to the category (quality) and usually represents sorting into classes according to the national importance (Table 2).

From the analysis were excluded highway sections, where significant effects on the examined speed parameters were not expected. Overall summary of the impact of types of roads according to traffic usage on the speed is processed in Table 3.

From the values in the table is visible decrease in the average speed of vehicle depending on category of communication. These results were expected and to be expected for other vehicle categories. Even though there are not available the same data, it is possible to do a partial analysis for data obtained from testing in Libavá. From tested vehicles were chosen LR110 to represent category of passenger cars and T815 8x8 to represent trucks. Tests were realized only on paved roads, field and forest roads and in open terrain. Therefore results will be analysed only for these three categories of roads (surface). Figure 4 show graphs of speeds these vehicles reached sorted according to the type of communication. In addition to the type of communication the graphs also show influence of the slope on the speed.

Compared to passengers cars is averaged achieved speed 10 km/h higher. This is mainly due to higher ground clearance of vehicle and overall different type of chassis. An interesting finding is minimal effect of the slope on vehicle speed when moving on this type of communication. This can be because of the low vehicle speed and using lower gear which allows to overcome higher slope without deceleration. During next tests will be this aspect monitored more. Right now there is search for suitable area both on roads and in open terrain. The goal is to find testing areas with slope more than 20°.

The average speeds for both vehicles are very similar (Table 4) and so deceleration caused by the road type (surface) is most probably not dependent on design maximal speed and also not on the vehicle type. It is most probably dependent just on the type of surface. So far this argument applies only to the road categories with lower quality. How will look the effect of the difference in technical parameters on other types of roads, can't be yet responsibly predicted.

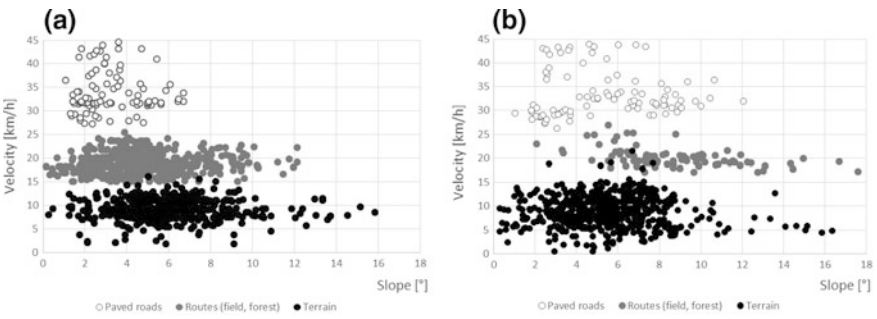

Fig. 4 Examples of records of off-road vehicles (**a** Tatra T815 8x8, **b** Land Rover 110)

Table 4 Average speed of off-road vehicles on different surfaces

	Paved roads	Field routes	Terrain
LR 110	33.5	20.1	8.9
T 815	33.9	18.8	9.2

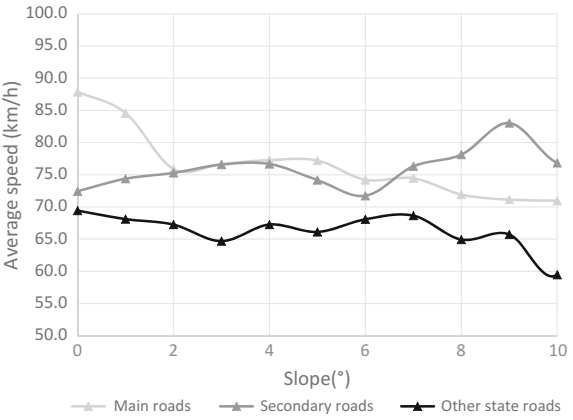

Fig. 5 Average speed through road slope range

Influence of Terrain Slope

The second monitored influence is terrain slope. Its insignificant impact on speed when LR110 and T815 8x8 moves slower have already been mentioned in the previous paragraphs. When driving passengers cars and microbuses on already travelled roads, were mostly received slopes from 0° to 10°, higher values were recorded only exceptionally. From measured data it can be concluded that the expected downward tendency is fulfilled only in first-class roads. The other two types of analysed roads have not shown this tendency (Fig. 5). By closer examination of the measured data it can be observed a trend of deceleration due to the slope even on third-class roads. The decrease is due to the overall lower speed starting to show up with slope approaching 10°. Expectations are at this moment not clearly proven or disproven. It may be due to the relatively short length of travelled slopes. Categories such as paved roads and field/forest roads were not in the analysis included for a small amount of records with higher slope. Verifying that the slope actually influences the vehicle deceleration will be subject of further research.

Influence of Width of the Road

In addition to the slope of communications it is possible from DMU25 also learn about a width of a lane (paved part of rad). Figure 6 shows how impact of this

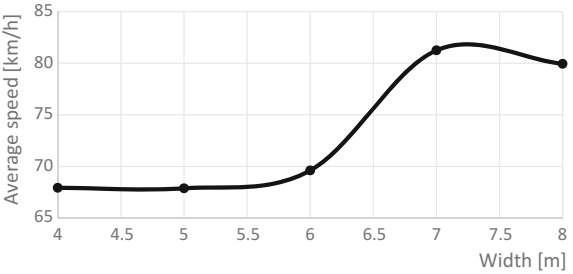

Fig. 6 Influence of width of the road

characteristic can look like. Roads that were rode on and later processed has a minimum width 4 m and a maximum width exceeds 10 m. These cases were due to a low number for purpose of processing merged to 8+ m category. Records with width 8+ m or more have a lower frequency. That is why for this parameter right now can't be made any definite conclusions. Trend for individual communications is ambiguous and makes fluctuating impression. When analysing all records, regardless of the type of communication and merging values into category 8, it is possible to observe dependence. But it can't be considered generally proven.

Influence of Turning Radius of the Road

Besides its own lane widths, are driving characteristics, maximum speed of vehicle included, influenced by turning radius of roads. That is why for some types of communications are already in phase of their construction defined minimum allowed turning radius (CSN 73 6101 2000). This information is not listed in available databases so it was replaced by the value of angle that express direction change of vehicle from its previous direction (Fig. 2) The way it was calculated is described in the previous chapter. Unlike the previous two examined attributes (slope and width of communication, the influence of direction changes on the speed can be seen very clearly. It is described on Fig. 7.

For easier interpretation were direction changes divided into intervals after five degrees. Values above 15° occurred only in few cases in the field/forest road category and due to small data amount were excluded. The measured data clearly demonstrate that on common roads direction change forced by tortuousness of communications slows the vehicle down. Currently can be said that deceleration value for direction change within interval 5°–10° is 16% and within interval 10°–15° it is 41%. On paved roads and on field/forest roads it was not possible to confirm this effect. In the case of paved roads it can be due to a lower amount of data. But more possible reason is the low speed of vehicle on this type of communication, same in case of field/forest roads. On this type of communication despite the large amount of measured data and wide range of direction change

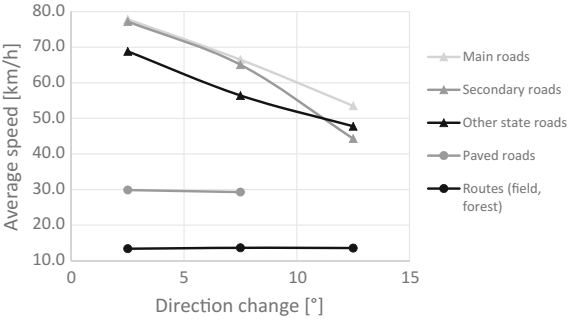

Fig. 7 Average speed at intervals of direction change

Table 5 Deceleration caused by forest

	1st class road (206)		2nd class road (207)		3rd class road (210)	
Slope (°)	Deceleration	Difference	Deceleration	Difference	Deceleration	Difference
0–5	YES	−1.3	NO	3.2	NO	2.0
5–10	NO	1.9	YES	−5.3	YES	−6.0
10–15	YES	−10.4	YES	−1.1	NO	5.7

values (even more than 15°) is this effect insignificant. In this case significant deceleration is caused mainly by the type of communication. Testing this phenomenon for other vehicle categories will be part of the following tests.

Influence of Obstacles Around Communication

The last hypothesis is connected to assumption that the presence of obstacles around communication reduces view conditions, thereby slows down the vehicle. In this phase of testing was observed only effect of forest. Calculated differences between the speeds of a vehicle driving on one type of communication in the forest and outside the forest range from 1 to 3 km depending on the type of road. Therefore the impact of forest around communication can be considered insignificant. For this reason, an analysis was made of simultaneous influence of forest around communication and change of direction. Results can be fined in Table 5. The calculated results are significantly irregular. In some of the cases deceleration is greater in turns and tortuous sections of roads surrounded by forest than in open space (in table labelled as YES). In other cases it is the opposite and lower average speed is in open country (in table labelled as NO). The table also contains differences of average speed in monitored part of roads. Based only on calculations made so far it is not possible to confirm or disprove this hypothesis so it will be subjected to further examination.

Discussion and Conclusion

Analysis of the influence of selected geographic elements on the speed of vehicle movement on communications has confirmed some of the assumed hypotheses. Especially effect of the overall quality of communication and influence of road tortuousness on change of vehicle direction. The remaining hypotheses failed to be clearly proven or disproven.

Several new findings can be made from obtained results. The first of them is directed to the amount of data. Despite almost 1000 km driven on roads, in some cases is the amount of data due to their sorting insufficient. Data collecting will have to be supplemented by a specifically planed routes to ensure that all the observed areas will have at least few hundred records. Especially it will be needed to find areas with greater slope. These experiences will be mainly used for other types of equipment, both driving on roads and during tests in Libavá.

The second observation is connected to methods of evaluating the impact of obstacles around roads on speed of movement. There will be tried another way in the future which is based on not confirming the effect of forests around roads. There will be no more monitoring closeness of objects around communications. Instead the tests will be focused on view conditions of a driver inside the vehicle. Using data from digital surface model it is scheduled to analyse how large sections of roads are visible from a vehicle. It is assumed that already proven influence of direction change of vehicle movement is to some extant connected to view conditions. And beside vegetation, relief and micro-relief shapes around the communication can also have negative impact.

The results are not final and proposed methods of analysis of the impact of selected geographic elements on the vehicle speed do not represent a complex solution. The authors are aware of the fact that during the analysis were not considered other two very important factors, such as weather conditions and experience of the driver. Tests show that especially the second factor is very important, mainly during off-road drives. However, currently there are not sufficient preconditions for it to be properly analysed. Meteorological conditions are already partially addressed in the ongoing data collecting which is happening also during winter. Some of the rides were made during foggy weather, drizzle, rain or snow. However, these result must be yet processed.

The main conclusions can enrich and refine transport planning of military units and rescue teams. The first is to determine the maximal speed of transport on lower-quality types of communications. Then demonstrating the impact of the chassis of wheeled vehicle adapted for diving in difficult conditions is insignificant. Another is finding possibility to parametrize road section depending on the turning radius for determining the maximal speed of movement in these sections. The conclusions are not definitive and especially the mathematical expressing is still in planning. However obtained results still contribute to a complex modelling of movement possibilities in situations of crisis where the movement is bound to both communications and off-road areas.

Acknowledgements This paper is a particular result of the defence research project DZRO K-210 NATURENVIR managed by the University of Defence in Brno.

References

Barry, B. A., & Morris, M. D. (1991). *Errors in practical measurement in surveying, engineering, and technology*. Rancho Cordova, CA: Landmark Enterprises.

Böhm, J., Radouch, V., & Hampacher, M. (1990). *Theory of errors and adjustment calculation*. Praha: Geodeticky a kartograficky podnik. (in Czech).

Cibulova, K., Hejmal, Z., & Vala, M. (2015). The influence of the tires on the trafficability. In *Proceedings of ICMT 2015—International Conference on Military Technologies 2015*, Brno, May 19–21, IEEE, Brno, pp. 219–222.

Cheng, M. Y., & Chang, G. L. (2001). Automating utility route design and planning through GIS. *Automation in Construction, 10*(4), 507–516.

Collins, J. M. (1998). *Military geography for professionals and the public*. Sterling: Potomac Books Inc.

CSN 73 6101. (2000). *Design of roads and highways*. Cesky normalizacni institute, Praha, Czech Republic (in Czech).

Dejmal, K., Novotny, J., & Hudec, F. (2015). Assessment optimization of weather forecast: Terminal aerodrome forecast (TAF)—for 24 hours. In *Proceedings of ICMT 2015—International Conference on Military Technologies 2015*, Brno, 19–21 May, IEEE, Brno, pp. 325–328.

DIGEST 2.1. (2000). *Part 4 Feature and attribute coding catalogue*. DGIWG.

Hofmann, A., et al. (2015). Creation of models for calculation of coefficients of terrain passability. *Quality & Quantity, 49*(4), 1679–1691.

Ivan, I, et al. (2013). Evaluation of public transport accessibility at municipality level in the Czech Republic. In *Proceedings of 13th International Multidisciplinary Scientific Geoconference*, Albene, 16–22 June, SGEM, Albene, pp. 527–534.

Ivan, I. (2016). Interchange nodes between suburban and urban public transport: Case study for the Czech Republic. *Acta Geographica Slovenica, 56*(2), 221–233.

Kanoh, H., & Hara, K. (2008). Hybrid genetic algorithm for dynamic multi-objective route planning with predicted traffic in a real-world road network. In *Proceedings of the 10th Annual Conference on Genetic and Evolutionary Computation*, Atlanta, GA, July 12–16, ACM, New York, pp. 657–664.

Kricke, K. D., & Schaefer, D. (1997). Low-level flight capability of a future military transport aircraft based on commercial avionics. In *Proceedings of AIAA/IEEE Digital Avionics Systems Conference*, Irvine, October 26–30, IEEE, Irvine, pp. 24–32.

KTO 25. (2007). *Katalog topografickych objektu*. MoD, Dobruska, Czech Republic (in Czech).

Land Survey Office. *CZEPOS,* http://czepos.cuzk.cz (December 04, 2016) (in Czech).

Land Survey Office. *DMR4G, Digital Terrain Model of the Czech Republic of the 4th generation*. http://geoportal.cuzk.cz (December 04, 2016).

Land Survey Office. *DMR5G, Digital Terrain Model of the Czech Republic of the 4th generation*. http://geoportal.cuzk.cz (December 04, 2016).

Landex, A. (2009). Evaluation of railway networks with single track operation using the UIC 406 capacity method. *Networks and Spatial Economics, 9*(1), 7–23.

Laurman, L., & Rybansky, M. (2002). *Military geography*. MoD, Praha. (in Czech).

Law No 361/2000. (2000). Zakon o provozu na pozemnich komunikacich, Chamber of Deputies of the Parliament of the Czech Republic, Praha, Czech Republic (in Czech).

Murray-Tuite, P. M. (2006). A comparison of transportation network resilience under simulated system optimum and user equilibrium conditions. In *Proceedings of 2006 Winter Simulation Conference*. Monterey, CA, December 3–6, IEEE, Monterey, pp. 1398–1405.

Niaraki, A. S., & Kim, K. (2009). Ontology based personalized route planning system using a multi-criteria decision making approach. *Expert Systems with Applications, 36*(2), 2250–2259.

Ohshige, K., et al. (2006). Influence of weather on emergency transport events coded as stroke: Population-based study in Japan. *International Journal of Biometeorology, 50*(5), 305–311.

Rybansky, M. (2009). *The cross-country movement—The impact and evaluation of geographic factors*. Brno: CERM.

Rybansky, M. (2014). Modelling of the optimal vehicle route in terrain in emergency situations using GIS data. In *Proceedings of 8th International Symposium of the Digital Earth*, Kuching, August 26–29, IOP Publishing, Kuching, pp. 21–31.

Rybansky, M., & Vala, M. (2009). Geographic conditions of military transport using roads and terrain. In *Proceedings of International Conference on Military Technologies ICMT*, Brno, May 5–6, University of Defence, Brno, pp. 560–568.

Rybansky, M., et al. (2015). Modelling of cross-country transport in raster format. *Environmental Earth Sciences, 74*(10), 7049–7058.

Talhofer, V., et al. (2015). Verification of digital analytical models: Case study of the cross-country movement. In *Proceedings of ICMT 2015—International Conference on Military Technologies* 2015, Brno, May 19–21, IEEE, Brno, pp. 203–209.

Talhofer, V., Hoskova-Mayerova, S., & Hofmann, A. (2016). Towards efficient use of resources in military: Methods for evaluation routes in open terrain. *Journal of Security Sustainability., 6*(1), 53–70.

Xia, W., & Zhang, A. (2016). High-speed rail and air transport competition and cooperation: A vertical differentiation approach. *Transportation Research Part B: Methodological, 94,* 456–481.

Retrieving of GNSS Tropospheric Delays from RTKLIB in Real-Time and Post-processing Mode

Michal Kačmařík

Abstract Global Navigation Satellite Systems (GNSS) allow a precise estimation of atmospheric water vapour what is successfully used in weather forecasting, namely in Numerical Weather Prediction (NWP) models. In this study the quality of real-time and post-processed zenith total delay (ZTD) values from GPS (Global Positioning System) Precise Point Positioning (PPP) technique processing is investigated. GPS observations from a month-long period and eight European stations were processed in RTKLIB program package. Two versions of real-time processing solutions using different real-time IGS (International Global Navigation Satellite Systems Service) products (IGS01, IGS03) and two versions of post-processed solutions using different strategies were evaluated. Obtained ZTDs were compared with the final IGS ZTD product. The mean RMSE (root-mean-square error) was 10.3 mm for real-time solution based on the IGS03 real-time product and 12.2 mm for the other solution based on the IGS01 product. Both post-processed solutions reached a mean RMSE of about 5 mm. The better real-time ZTD solution from RTKLIB using IGS03 product was therefore close to the 10 mm value defined as a target ZTD accuracy necessary for their usage in NWP models and nowcasting applications in meteorology.

Keywords GNSS meteorology · Real-time · Precise Point Positioning · Zenith total delay · RTKLIB

Introduction

Global Navigation Satellite Systems are globally used for user position estimation in a still increasing number of applications. Nevertheless, their ability to sense water vapour in the troposphere is known to a much lesser extent. The concept of a

M. Kačmařík (✉)
Institute of Geoinformatics, VŠB-Technical University of Ostrava,
17. listopadu 15, 70833 Ostrava-Poruba, Czech Republic
e-mail: michal.kacmarik@vsb.cz

I. Ivan et al. (eds.), *Dynamics in GIscience*, Lecture Notes in Geoinformation and Cartography, DOI 10.1007/978-3-319-61297-3_13

method called GPS meteorology was successfully introduced by Bevis et al. (1992) and since then a lot of investigations were made in this field. For years, only the U. S. GPS system was used for GPS meteorology. In most recent times the term transformed from GPS meteorology to GNSS meteorology since other GNSS systems like GLONASS, BeiDou or Galieo have been started to be used as well (Douša 2010; Li et al. 2014). However, in the presented study only signals from GPS satellites were processed so the term GNSS refers only to GPS unless otherwise is stated.

Microwave signal travelling from GNSS satellite to ground-based receiver enters two parts of Earth's atmosphere, the ionosphere and the troposphere. Since the ionosphere is a dispersive medium for GNSS signal frequencies of 1–2 GHz, its influence can be eliminated by the appropriate combination of two signals at two different frequencies. On the contrary, the troposphere represents a non-dispersive medium for described signals and its effect therefore cannot be eliminated directly from observations. However, it can be precisely calculated by determining the signal delay due to the troposphere. The typical total signal delay due to the troposphere is about 2.3 m in the zenith direction for a receiver placed at mean sea level. This parameter is called Zenith Total Delay (ZTD) and is the main outcome of GNSS meteorology processing. The total signal delay can be separated into hydrostatic part (Zenith Hydrostatic Delay, ZHD), caused by the atmospheric constituents, and wet part caused specifically by water vapour (Zenith Wet Delay, ZWD). The hydrostatic part accounts for 80–90% of the total delay and is much less variable in space and time than the wet part. ZHD can be precisely computed using Saastamoinen model (Saastamoinen 1972) which relies on atmospheric pressure values in the place of GNSS receiver antenna. After quantifying ZTD and separating ZHD, it is possible to convert ZWD into the Integrated Water Vapour (IWV). This parameter represents a total amount of water vapour in the zenith direction above the GNSS receiver in millimetres.

Both ZTD and IWV values can be assimilated into NWP models. However in reality usually ZTD values are assimilated since they represent original GNSS meteorology output not distorted by ZWD to IWV conversion shortcomings. The operational usage of GNSS meteorology products for NWP assimilation started approximately a decade ago. In Europe, this activity is coordinated mainly in the framework of the EUMETNET EIG GNSS Water Vapour Programme (E-GVAP, 2005–2017, Phase I-III, http://egvap.dmi.dk). Many studies demonstrated a positive impact of the GNSS meteorology products assimilation on weather forecasts of precipitation, especially of the short-time ones (Vedel and Huang 2004; Guerova et al. 2006; Shoji et al. 2009; Bennitt and Jupp 2012; Mahfouf et al. 2015). GNSS data processing for those purposes are currently still running in a near real-time mode with the delivery of results usually between 90 and 120 min after the observations. However, with the development of high update-rate NWP models and growing need for using ZTD fields for nowcasting and monitoring of short-term extreme weather events the demand for ZTD products with much shorter latency and still high quality is growing. Therefore, GNSS ZTD data processing running in

real-time is inevitable. For a more detailed information about the GNSS meteorology and its state of the art the reader is referred to Guerova et al. (2016).

A significant step in a development of real-time ZTD solutions was an official start of the IGS real-time service (RTS, http://www.igs.org/rts) in the December 2012. Within this service a set of products with corrections of broadcasted ephemeris and satellite clock errors are provided in real-time using RTCM formats and NTRIP protocol for their network dissemination. Several research institutions presented their first results of GNSS ZTD real-time processing soon after the IGS RTS started. Douša and Václavovic (2014) realized a nine-month long campaign for 36 global GNSS reference stations using their own G-Nut/Tefnut software. When their real-time ZTDs were compared to official post-processed ZTD products a mean standard deviation (SDEV) of about 6–10 mm was acquired and significant biases up to 20 mm occurred at some stations. Results from one-month long period including 20 global stations processed in BKG NTRIP Client were presented by Yuan et al. (2014) where the RMSE of real-time ZTDs were below 13 mm. A comprehensive validation of atmospheric parameters (ZTD, IWV, horizontal gradients, STD) retrieved from GNSS multi-constellation real-time processing was presented by Li et al. (2015). It showed that combined solution based on a multi-constellation performed with higher accuracy and robustness than solutions based only on a single GNSS (e.g. GPS, GLONASS, BeiDou, Galileo). A positive impact of GPS + GLONASS real-time ZTD processing against a single GPS or GLONASS processing was also reported by Lu et al. (2016). Ahmed et al. (2016) presented an extensive comparison of real-time ZTD solutions based on three different software (G-Nut/Tefnut, PPP-Wizard and BKG NTRIP Client) using a month-long period, 22 global stations and three different RTS products. In terms of standard deviation solutions from the G-Nut/Tefnut performed the best followed with BKG NTRIP Client. PPP-Wizard without implementation of precise antenna models reached much worse results especially in terms of bias.

In the April of 2015 the Real-time Demonstration campaign (RT-Demo) has started within the COST ES1206 Action (GNSS4SWEC, "Advanced Global Navigation Satellite Systems tropospheric products for monitoring severe weather events and climate"). So far seven institutions joined this activity and are delivering their ZTD solutions for all or a set of 32 GNSS reference stations. One of them is based on NWP model forecasts, the rest on GNSS observation processing. The first validation results (Douša et al. 2016) are very promising for some of the solutions reaching SDEV values around 6-10 mm while confronted with official post-processed ZTD products (IGS and EUREF final solutions). However, most of the solutions showed rather large biases up to 20 mm at some stations. An online monitoring tool for this campaign is freely available at http://www.pecny.cz/cost/rt-tropo/. GNSS real-time ZTD solution called RT03 presented in this study is the solution called TUOG within the RT-Demo campaign.

The aim of this study was to evaluate a potential of RTKLIB software library for GNSS meteorology purposes both in real-time and post-processing mode since it has not been investigated yet.

GNSS Data Processing in RTKLIB

RTKLIB is an open source program package allowing standard and precise positioning with GNSS observations. It offers a very broad functionality in terms of supported positioning modes (single, DGNSS, PPP, RTK), input data formats and protocols, tools for GNSS data editing and visualizing, etc. It comprises of individual executable application programs (AP) when most of them are available both in GUI (Graphical User Interface) and CUI (Command Line User Interface) versions. For this study RTKLIB version 2.4.2 with applied p11 patch was used. For presented real-time ZTD solutions application program RTKNAVI was used and for post-processed solutions RTKPOST in its CUI version called RNX2RTKP.

Description of real-time positioning in RTKLIB and available troposphere modelling options are provided in the following sub-chapters. For more information about RTKLIB, the reader is referred to Takasu (2009), Takasu (2010) and the official website at http://www.rtklib.com/rtklib.htm.

Real-Time GNSS Positioning

Application program RTKNAVI (in CUI form called RTKRCV) allows a real-time positioning in all abovementioned positioning modes. Nevertheless, for real-time ZTD processing the Precise Point Positioning method is the most suitable one. The technique was introduced by Zumberge et al. (1997) and independently processes observations from a single receiver (zero-differenced observations). Due to that data processing from many receivers can be easily distributed on individual hardware devices unlike the typical network solution based on double-differenced observations. PPP relies on precise products of satellite ephemeris and corrections of satellite clock errors. Its well-known disadvantage is a long convergence time interval of about thirty minutes which the solution needs to reach high quality (positioning) results. Also, ambiguities can be resolved to their integer values if only uncalibrated phase delays corrections from external source are provided and applied.

PPP in RTKLIB is supported in three different versions—PPP kinematic (receiver is moving during the measurement), PPP static (receiver position is static during the measurement) and PPP fixed (coordinates of the receiver are fixed to a known position and only other unknown parameters are estimated from observations). In this study the second option was used. Raw input observation data and precise products can come from Real-Time streams in RTCM format or from a set of (proprietary) file formats. Observations from GPS, GLONASS, Galileo and BeiDou satellites can be processed. As abovementioned in this study only GPS was used while a GPS + GLONASS constellation testing for real-time ZTD solution is planned to be done in a near future. Whole estimation process of PPP solution is based on an extended Kalman filter (Gelb 1974). Available models in the RTKLIB

include receiver and satellite antenna phase center offsets and variations, solid earth tides, ocean tide loading (cannot be applied in real-time mode), phase wind-up effect or detection of eclipsing satellites. Information about applied settings for presented PPP ZTD solutions can be found in Table 2.

Troposphere Modelling

RTKLIB supports three different ways of troposphere modelling. The first simple option is based on a Saastamoinen model and standard atmosphere parameters. The second option relies on tropospheric corrections of MOPS model from Satellite-based Augmentation System (SBAS) signals. The last possibility represents a precise troposphere model and it was used in this study. The precise model is based on a typical approach of ZTD computation during precise GNSS data processing. ZHD value is modelled by Saastamoinen model and standard atmosphere parameters and then ZWD is estimated as an unknown parameter during the processing. For mapping the observations from their original elevations to zenith direction the Niell mapping function (Niell 1996) is applied. Since RTKLIB version 2.4.2 the Global Mapping Function (GMF, see Böhm et al. 2006) representing a more current approach is supported however only after recompiling of application programs what was not done for the purposes of presented study.

Linear horizontal gradient parameters representing the first-order spatial asymmetry of the delay around the station can be optionally estimated together with ZTD values as unknown parameters in RTKLIB. This step is generally meant to have a positive impact on troposphere modelling for post-processed GNSS ZTD solutions. Usually a model presented in MacMillan (1995) is used for horizontal gradients computation however the official user manual of RTKLIB version 2.4.2 does not describe the form of implementation of this functionality. In case of presented real-time ZTD solutions horizontal gradients were not estimated in order not to further increase the number of unknown parameters in the processing system. However, it is planned to test this step and evaluate the real influence of horizontal gradients on real-time ZTD estimation and their own quality.

Selected GNSS Reference Stations and Period

Originally data from nine European GNSS reference stations and thirty-two days long period from November 9 to December 10 2016 were processed. Since IGS final ZTD solution was used as the reference one in this study and station MALL is not a part of the IGS station network, this station had to be excluded from the evaluation. From this reason, all the comparisons presented in this paper are based on eight stations and basic information about them are presented in Table 1.

Table 1 Information about selected GNSS reference stations

Station name	Country	LAT [°]	LON [°]	El. height [m]	Receiver	Antenna and radome	
BRST	France	48.3804	−4.4966	65.8	TRIMBLE NETR9	TRM57971.00	NONE
HERT	United Kingdom	50.8674	0.3344	83.3	LEICA GRX1200GGPRO	LEIAT504GG	NONE
HOFN	Iceland	64.2672	−15.1868	82.5	LEICA GR25	LEIAR25.R4	LEIT
MATE	Italy	40.6491	16.7045	535.6	LEICA GRX1200GGPRO	LEIAT504GG	NONE
NICO	Greece	35.1409	33.3964	155.0	LEICA GR25	LEIAR25.R4	LEIT
ONSA	Sweden	57.3952	11.9255	45.5	JAVAD TRE_G3TH DELTA	AOAD/M_B	OSOD
WTZR	Germany	49.1441	12.8789	666.0	LEICA GR25	LEIAR25.R3	LEIT
ZIM2	Switzerland	46.8770	7.4650	956.4	TRIMBLE NETR9	TRM59800.00	NONE

ZTD Solutions Description

As already mentioned four individual ZTD solutions were realized in RTKLIB. Two of them were running in a real-time mode (RT01 and RT03) and the other two in a post-processing mode (PPFR and PPBS). Basic information about all solutions are given in Table 2.

The only difference between both real-time ZTD solutions was the used IGS real-time stream with satellite ephemerides and clock error corrections. RT01 solution used the IGS01 product and RT03 the IGS03 product. IGS01 represents a single epoch product available for GPS satellites when both ephemerides and satellite clock corrections are provided in 5 s interval. IGS03 product is based on a Kalman filtering approach and is available for GPS and GLONASS satellites. It provides corrections for broadcasted ephemerides in 60 s interval and corrections for satellite clock errors in 10 s interval.

As is apparent from Table 2 the only difference in settings of two post-processed ZTD solutions PPFR and PPBS was the applied strategy of PPP solution. In case of PPFR (Post-processed Forward) only a forward running Kalman filter was used so the solution is similar to the real-time processing in this regard. For PPBS (Post-processed Backward Smoothing) a backward smoothing in time is added after forward Kalman filter run. This step should improve the quality of tropospheric parameters and avoid problems of PPP convergence or re-convergence period previously mentioned in the paper. RTKLIB manual unfortunately does not provide a description of implemented backward smoothing algorithm. Both post-processed

Table 2 Information about GNSS ZTD solutions realized in RTKLIB

	RT01 (RT03)	PPFR (PPBS)
GNSS	GPS	
Products	IGS01 (IGS03) RTS	IGS Rapid
Observation sampling rate	1 s	30 s
Elevation cut-off angle	10°	7°
Strategy applied	Forward Kalman Filter	Forward Kalman Filter (Forward Kalman Filter + Backward smoothing)
Antenna model	igs08_1918.atx	igs08_1926.atx
Troposphere	A priori ZHD Saastamoinen model, estimated ZTD corrections	
Mapping function	Niell	
ZWD estimation interval	1 s	30 s
Horizontal gradients estimated	No	Yes, every epoch
Ionosphere	Eliminated using ionosphere linear combination	
Ocean tidal loading	Not applied	Applied (FES2004)

solutions were processing observations from RINEX files with 30 s sampling rate and used a full set of IGS Rapid products (precise ephemerides, satellite clock errors corrections and earth rotation parameters files).

RTKLIB runs a separate instance of RTKNAVI application program to process data from one station. Each instance must have it owns access both to observation data stream and stream with ephemeris and clock corrections (correction stream). On top of that if a broadcasted navigation message is not a part of an observation stream, one more stream must be used which provides these information (e.g. RTCM3EPH stream from IGS RTS). During the presented study one extra instance of RTKNAVI was running to only receive correction stream (or broadcasted navigation message stream) and store it into a text file to reduce the computer network load. Then all other instances of RTKNAVI performing the ZTD solution for a selected station were reading the IGS RTS stream or RTCM3EPH stream from this file.

For validation purposes the IGS final tropospheric product (Byram et al. 2011) containing ZTD and horizontal gradient values were used as a reference ZTD solution. The stated ZTD accuracy of this solution is 4 mm and values are available in 5 min interval. The processing itself is based on the PPP technique realized in Bernese GPS Software 5.0 with the use of IGS final precise products.

Results

Results for realized comparisons between the reference IGS final ZTD product and all RTKLIB ZTD solutions are presented in this chapter. Firstly, general information about the validation methodology are given followed by evaluation of ZTD availability and finally ZTD quality.

ZTDs in IGS final solution are provided in five minutes' interval therefore this was the interval selected for presented comparisons. Since post-processed solutions were based on individual processing of daily RINEX files (it means one PPP run per one day and one GNSS reference station) ZTDs from the first and the last hour of the day were excluded from the comparisons to eliminate the influence of PPP convergence period and day boundary problem.

Availability of Produced ZTDs

Percentage of available ZTD epochs for individual solutions is presented in Table 3. For both RTKLIB post-processed solutions and the IGS final solution the average availability was around 99% and except one case (IGS final solution at station ONSA) always stayed above 96%. The real-time ZTD solution RT01 based on IGS01 product reached only a little bit lower average availability of 97%. However, the second real-time ZTD solution RT03 based on the combined IGS03

product was worse with 89% of available ZTD epochs on average. The difference was mainly due to visibly lower availability of ZTDs in RT03 solutions at stations BRST, MATE, NICO and ONSA while the other four stations performed very similarly to RT01. The lower availability for RT03 solution can be due to data gaps both in observation data streams and correction product streams related to computer network load.

Quality of Produced ZTDs

For the computation of comparison statistics only the epochs where ZTD values from all five solutions were available had to be selected. Therefore, if a ZTD value from a single solution was missing for a specific epoch, the epoch did not enter the comparison at all. For the comparison results presented below in Figs. 1 and 2 and Table 4 an outlier detection and their exclusion was applied. Firstly, standard deviation values were computed for comparisons between the IGS final solution and all evaluated RTLIB solutions from all available epochs of ZTDs. Secondly, all epochs where the difference between ZTD value from IGS final product and ZTD value from a selected RTKLIB solution exceeded 3× the computed SDEV, were excluded from the final statistics computation. Numbers of epochs excluded from individual RTKLIB solutions are shown in Table 4.

Figure 1 presents results of comparisons between the IGS final ZTD product and all RTKLIB ZTD solutions at individual GNSS reference stations and Table 4 summary results for individual solutions over all stations. RKTLIB showed a reasonable performance in both versions of post-processed ZTD solutions. The standard deviation representing the stability of solutions oscillated around 4.5 mm at all stations except BRST where it reached almost 7 mm. PPFR solution based only on a forward Kalman filter delivered better bias values than PPBS solution. PPBS also had nearly three times more outlier ZTD values than PPFR solution which were excluded from the statistics computation as is apparent from Table 4.

Table 3 Percentage of available ZTD epochs for individual solutions (all = 100%)

Station name	RT01	RT03	PPFR	PPBS	IGS
BRST	94.4	76.6	99.9	99.9	100.0
HERT	98.5	94.9	100.0	100.0	96.9
HOFN	99.0	97.7	99.9	99.9	100.0
MATE	97.5	78.1	99.9	96.8	100.0
NICO	95.5	87.3	99.9	99.9	100.0
ONSA	95.4	87.8	96.9	96.9	93.8
WTZR	97.9	95.5	99.8	99.8	100.0
ZIM2	94.1	94.2	100.0	100.0	100.0
Mean	96.5	89.0	99.5	99.2	98.8

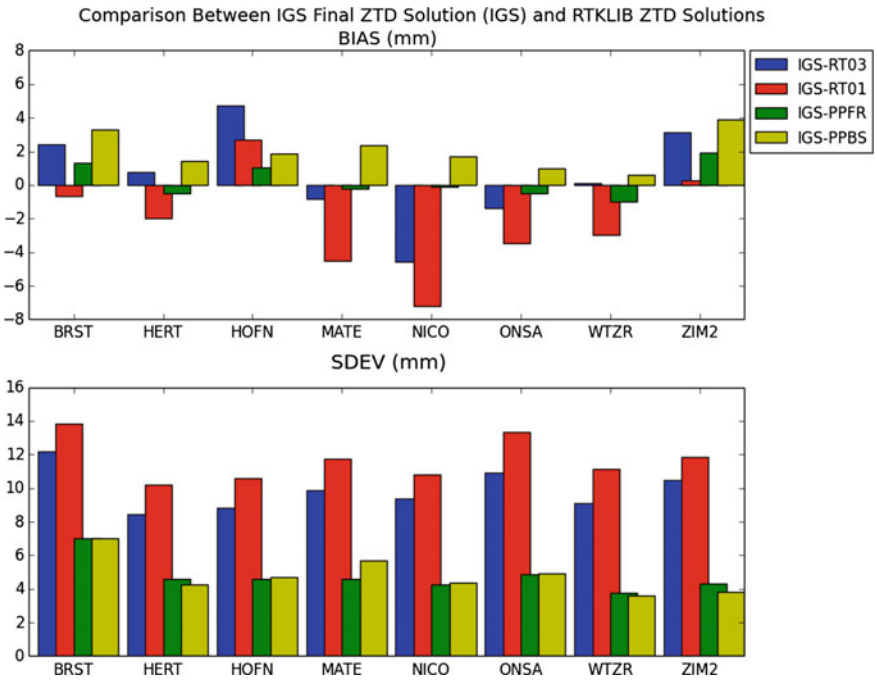

Fig. 1 Comparison between ZTDs from IGS final solution and RTKLIB real-time (RT01, RT03) and post-processed (PPFR, PPBS) solutions—bias (*top*) and standard deviation (*bottom*)

The applied backward-smoothing (PPBS solution) therefore surprisingly did not bring any positive income to the post-processed ZTD solution.

The degradation of quality of real-time ZTD solutions compared to post-processed ones can be seen in approximately doubled SDEV values ranging from 10.2 to 13.8 mm in case of RT01 and from 8.4 to 12.2 mm in case of RT03. The RT03 solution based on IGS03 combined product showed better quality of ZTDs than RT01 not only in terms of SDEV but also in bias and number of excluded outlier values. The RT03 overall RMSE values ranged between 8.4 and 11.0 mm at individual stations with an exception of 12.4 mm for station BRST and biases never exceeded ±5 mm. Within the E-GVAP project various user requirements for GNSS meteorology were defined including requirements on accuracy of ZTD and IWV values for their use in NWP models and meteorological nowcasting (Offiler 2010). The threshold value for ZTD accuracy was set to 15 mm, target value to 10 mm and optimal value to 5 mm. If we consider the IGS final ZTD product as true reference the presented real-time RT03 ZTD solution from RTKLIB meets the threshold value in case of all stations and oscillates around the target value in case of all except the BRST station.

Besides the results based on a whole time period also a daily stability of real-time RTKLIB ZTD solutions was evaluated. Figure 2 shows daily mean biases

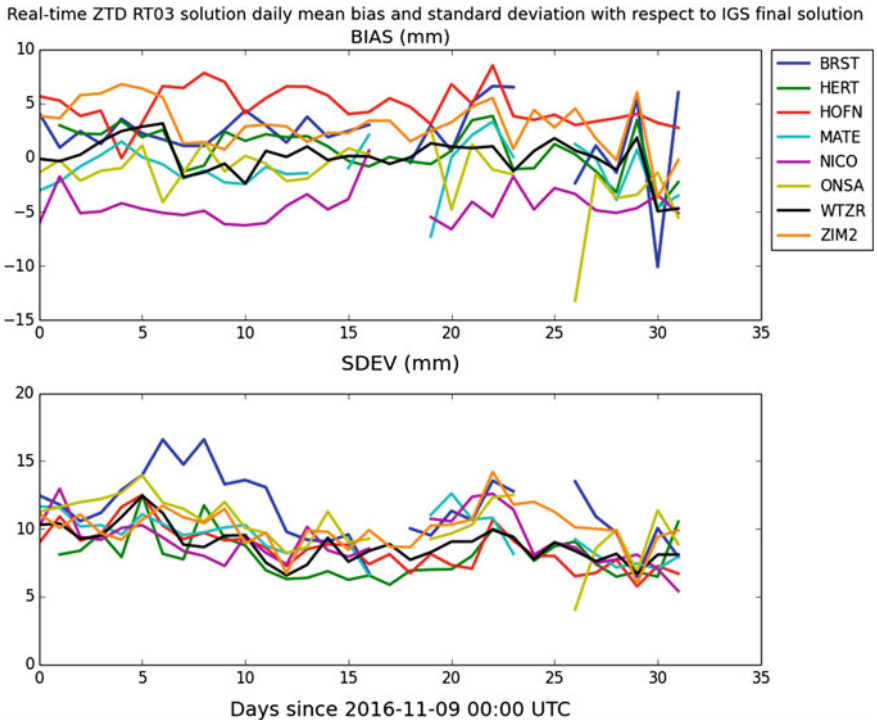

Fig. 2 Real-time ZTD RT03 solution daily mean bias (*top*) and standard deviation (*bottom*) with respect to IGS final ZTD solution

Table 4 Comparison of ZTD from IGS final ZTD solution and solutions realized in RTKLIB

Solution	Bias (mm)	SDEV (mm)	RMSE (mm)	Number of pairs	Pairs excluded
RT01	−2.2	11.7	12.2	58,416	825
RT03	0.5	9.9	10.3	58,416	338
PPFR	0.3	4.7	4.8	58,416	314
PPBS	2.0	4.8	5.3	58,416	893

Mean values computed over all stations are presented

and standard deviation values for RT03 solution at all reference stations. The daily mean biases stayed rather stable within the range of ± 6 mm at all stations with a few occasional exceptions at some of stations. Similar situation was present also for standard deviation. Poorer overall results of station BRST when compared to other stations were partly caused by a period between day 5 and 12 of the processed period. During these days SDEV values of BRST reached up to 16.6 mm and were visibly higher than those of all other stations. Daily stability of RT01 real-time solution showed similar patterns as presented RT03 solution in terms of bias.

However daily SDEV values evinced higher day-to-day variation with a typical range of about ±8 mm.

Conclusion

The main focus of this paper was to initially evaluate quality of GNSS ZTD processing in the freely available RTKLIB program package. Observations from eight GNSS reference stations and month long period were processed in two versions of real-time solutions based on different IGS RTS products and two versions of post-processed solutions. All four ZTD solutions from RTKLIB were then compared with the IGS final ZTD product.

Post-processed ZTD solution PPFR based on a forward Kalman filter reached on average virtually no bias and SDEV of 4.7 mm. The second post-processed solution PPBS adding a backward smoothing in time to the forward Kalman filter had an average bias of +2 mm over all stations and showed problems with outlying ZTD values. The step of applying backward smoothing for PPP ZTD solution in RTKLIB therefore cannot be recommended upon obtained results. Daily stability of both post-processed solutions was at the level of a few millimetres both in bias and SDEV.

Real-time solution RT03 based on a combined IGS03 IGS RTS product reached an average standard deviation of 9.9 mm with biases ranging at individual stations between −4.6 and +4.7 mm. With its overall mean RMSE value the RT03 solution was close to the 10 mm value defined as a target ZTD accuracy needed for meteorology applications. The other real-time solution RT01 based on a single epoch IGS01 IGS RTS product was systematically shifted against the IGS final solution of about −2.2 mm on average with individual station biases ranging from −7.2 to 0.2 mm. It also provided slightly higher mean SDEV value of 11.7 mm and much more outlying ZTD values than RT03. On the other hand RT03 solution had availability problems at half of the processed stations where RT01 solution performed flawlessly.

The relatively low number of processed GNSS reference stations together with not extensive time period could distort the absolute values of statistical parameters obtained in the comparison however should still provide a reasonable information about RTKLIB usability for ZTD PPP processing both in real-time and post-processed mode what was the main motivation of this study. A much more comprehensive evaluation of real-time ZTD solutions including the RT03 solution from presented study are planned within the abovementioned RT-Demo campaign of GNSS4SWEC COST Action. To conclude it seems that at least on the basis of presented results the RTKLIB program package is able to provide good quality ZTD estimates from its PPP processing run both in post-processing and real-time mode.

Acknowledgements The author acknowledges the support from the Czech Ministry of Education, Youth and Sports (project no. LD14102). The study has been organized within the E.U. COST Action ES1206 (GNSS4SWEC) project.

References

Ahmed, F., Václavovic, P., Teferle, F. N., Douša, J., Bingley, R., & Laurichesse, D. (2016). Comparative analysis of real-time precise point positioning zenith total delay estimates. *GPS Solutions, 20,* 187. doi:10.1007/s10291-014-0427-z

Bennitt, E., & Jupp, A. (2012). Operational assimilation of GPS zenith total delay observations into the met office numerical weather prediction models. *Monthly Weather Review, 140*(8), 2706–2719. doi:10.1175/MWR-D-11-00156.1

Bevis, M., Businger, S., Herring, T. A., Rocken, C., Anthes, R. A., & Ware, R. H. (1992). GPS meteorology: Remote sensing of atmospheric water vapour using the global positioning system. *Journal Geophysical Research, 97,* 15787–15801.

Böhm, J., Niell, A., Tregoning, P., & Schuh, H. (2006). Global MappingFunction (GMF): A new empirical mapping function based on numerical weather model data. *Geophysical Research Letters, 33,* L07304. doi:10.1029/2005GL025546

Byram, S., Hackmann, C., & Tracey, J. (2011). Computation of a highprecision GPS-based troposphere product by the USNO. In *Proceedings of the 24th International Technical Meeting of The Satellite Division of the Institute of Navigation (ION GNSS 2011)*, Portland, USA, September 19–23, 2011.

Douša, J. (2010). Precise near real-time GNSS analyses at Geodetic Observatory Pecny—Precise orbit determination and water vapour monitoring. *Acta Geodynamica et Geromaterialia, 7,* 7–18.

Douša, J., & Václavovic, P. (2014). Real-time zenith tropospheric delays in support of numerical weather prediction applications. *Advances in Space Research, 53,* 1347–1358. doi:10.1016/j.asr.2014.02.021

Douša, J., et al. (2016). Real-time demonstration and benchmark campaigns for developing advanced troposphere products. In *IGS Workshop 2016*, Sydney, Australia, February 8–12, 2016.

Gelb, A. (Ed.). (1974). *Applied optimal estimation*. USA: The M. I. T Press.

Guerova, G., Bettems, J. M., Brockmann, E., & Matzler, C. (2006). Assimilation of COST 716 near-real time GPS data in the nonhydrostatic limited area model used at MeteoSwiss. *Meteorology and Atmospheric Physics, 91*(1–4), 149–164. doi:10.1007/s00703-005-0110-6

Guerova, G., Jones, J., Douša, J., Dick, G., de Haan, S., Pottiaux, E., et al. (2016). Review of the state of the art and future prospects of the ground-based GNSS meteorology in Europe. *Atmospheric Measurement Techniques, 9,* 5385–5406. doi:10.5194/amt-9-5385-2016

Li, M., Li,W., Shi, C., Zhao, Q., Su, X., Qu, L., et al. (2014). Assessment of Precipitable water vapor derived from ground-based beidou observations with precise point positioning approach. *Advances in Space Research,* doi:10.1016/j.asr.2014.10.010

Li, X., F. Zus, C. Lu, G. Dick, T. Ning, M. Ge, et al. (2015). Retrieving of atmospheric parameters from multi-GNSS in real time: Validation with water vapor radiometer and numerical weather model. *Journal of Geophysical Research: Atmospheres, 120*. doi:10.1002/2015JD023454

Lu, C., Li, X., Ge, M., Heinkelmann, R., Nilsson, T., Soja, B., et al. (2016). Estimation and evaluation of real-time precipitable water vapor from GLONASS and GPS. *GPS Solutions, 20,* 703–713. doi:10.1007/s10291-015-0479-8

MacMillan, D. S. (1995). Atmospheric gradients from very long baseline interferometry observations. *Geophysical Reseach Letters, 22,* 1041–1044. doi:10.1029/95GL00887

Mahfouf, J.-F., Ahmed, F., Moll, P., & Teferle, F. N. (2015). Assimilation of zenith total delays in the AROME France convective scale model: A recent assessment. *Tellus A, 67,* 26106. doi:10.3402/tellusa.v67.26106

Niell, A. E. (1996). Global mapping functions for the atmospheric delay at radio wavelengths. *Journal of Geophysical Research, 101,* 3227–3246.

Offiler, D. (2010). Product requirements document version 1.0–21 December 2010. EIG EUMETNET GNSS Water Vapour Programme (E-GVAP-II), Met Office.

Saastamoinen, J. (1972). Atmospheric correction for the troposphere and stratosphere in radio ranging of satellites. *Geophysical Monograph Series, 15,* 247–251. doi:10.1029/gm015p0247

Shoji, Y., Kunii, M., & Saito, K. (2009). Assimilation of nationwide and global GPS PWV data for a heavy rain event on 28 July 2008 in Hokuriku and Kinki, Japan. *Scientific Online Letters on the Atmosphere, 5,* 45–48. doi:10.2151/sola.2009-012

Takasu, T. (2009) RTKLIB: Open source program package for RTK-GPS. In *FOSS4G 2009*, Tokyo, Japan, November 2, 2009.

Takasu, T. (2010). Real-time PPP with RTKLIB and IGS real-time satellite orbit and clock. In *IGS Workshop 2010*, Newcastle upon Tyne, England, June 28–July 2, 2010.

Vedel, H., & Huang, X. (2004). Impact of ground based GPS data on numerical weather prediction. *Journal of the Meteorological Society of Japan, 82*(1B), 459–472. doi:10.2151/jmsj.2004.459

Yuan, Y., Zhang, K., Rohm, W., Choy, S., Norman, R., & Wang, C. S. (2014). Real-time retrieval of precipitable water vapor from GPS precise point positioning. *Journal of Geophysical Research: Atmospheres, 119*(16), 10044–10057.

Zumberge, J. F., Heflin, M. B., Jefferson, D. C., Watkins, M. M., & Webb, F. H. (1997). Precise point positioning for the efficient and robust analysis of GPS data from large networks. *Journal Geophysical Research, 102*(B3), 5005–5017. doi:10.1029/96JB03860

Geo-Dynamic Decision Support System for Urban Traffic Management

Jan Kazak, Mieczysław Chalfen, Joanna Kamińska, Szymon Szewrański and Małgorzata Świąder

Abstract The paper presents the geo-dynamic decision support system (DSS) for urban traffic management issues. For this purpose, ArcGIS and Tableau softwares were used. Additionally, a self-defined transportation model based on Dijkstra's algorithm was created. The use of our own calculation model allowed for the full accessibility to all parameters of the analysed scenarios which was one of the key assumptions of the research. Functionality of the proposed DSS was tested on three scenarios. Each scenario presents congestion on the road network after the conclusion of events in main landmarks in Wrocław (Poland): the city stadium, the National Forum of Music and the Centennial Hall. The proposed DSS allows for dynamic analysis of urban traffic, including recalculation processes according to the changing congestion on a road network. Moreover, cumulative urban traffic assessment allows you to define hot spots on a network, which should be especially monitored by public services. An interactive dashboard reduces technical details of an analysis which helps to avoid the cognitive problems of the decision making process for a layman. The results prove the feasibility of the integration of the ArcGIS, self-defined transportation model and Tableau. The proposed solution enables full access to the transportation analysis' assumptions, as well as the use of a simple and intuitive interactive dashboard for the decision making process.

Keywords Urban traffic modelling · Dijkstra's algorithm · Tableau · Decision support system · Visual data analysis

J. Kazak (✉) · S. Szewrański · M. Świąder
Department of Spatial Economy, Wrocław University of Environmental and Life Sciences, ul. Grunwaldzka 55, 50-357 Wrocław, Poland
e-mail: jan.kazak@upwr.edu.pl

M. Chalfen · J. Kamińska
Department of Mathematics, Wrocław University of Environmental and Life Sciences, ul. Grunwaldzka 53, 50-357 Wrocław, Poland

I. Ivan et al. (eds.), *Dynamics in GIscience*, Lecture Notes in Geoinformation and Cartography, DOI 10.1007/978-3-319-61297-3_14

Introduction

Contemporary urban space management forces local governments to search for new tools and solutions for their problems. The implementation of the smart city concept is strongly connected with the use of new technologies and capabilities that bring sustainable development goals within reach at the local scale (Ahvenniemi et al. 2017). Parallel to increasing the amount of available spatial data (An et al. 2016) there is a need to discover our ability to harness and analyse this data. In such a reality, cities are gaining greater control over their development. However, it is worth taking this challenge because those cities which are well instrumented and are connected by core systems are able to use this data and become the most successful (Zhuhadar et al. 2017). Technical support in the city management process allows for the ability to find optimized solutions which fit to each analysed case study. It increases the efficiency of public policies implementation and plays a key role from the point of view of quality of life (Przybyła et al. 2014).

One of the most crucial problems in modern cities is the issue connected with traffic management. The constantly increasing mobility of users requires a better understanding of these processes, as well as an impact of public policies into that phenomenon (Maggi and Vallino 2016). Some aspects of urban traffic issues are the matter of scientific research and are already aided by decision support models, e.g. road traffic control coordination (Dahal et al. 2013), road incidents (Hashemi and Abdelghany 2016), environmental impact mitigation (Ruiz-Padillo et al. 2016), risks assessment of hazardous materials transportation (Torretta et al. 2017) or even tsunami risk mitigation (Ai et al. 2016). The results of all of the mentioned models are very precise and well described from the scientific point of view. However, as it was highlighted by the initiative for cleaner and better transport in cities—CIVITAS, the first step in transport management should be based on policy context (CIVITAS 2015). Thus, there is a need to create systems which are simple to understand and would avoid cognitive problems (Tremblay et al. 2017). To avoid the negative impact of the implementation of improper actions, the system should be able to analyse alternative scenarios. According to the business intelligence pyramid, what links data mining and the final decision making are simulation models which are based on What-if? analysis (Golfarelli and Rizzi 2009). Therefore, the system should provide feedback to decision-makers about the possible effects of their decisions and as a result allow them to make better decisions based on knowledge.

From the technical point of view it is important to use common and well established mathematical models of calculations. One of the well known methods in transportation issues is Dijkstra's algorithm (Dijkstra 1959), which helps solve time-dependent problems (Ayed et al. 2011) and can react automatically according to changing circumstances (Szücs 2015). Because of the fact that the algorithm responds to new situations and reanalyses the optimal solution in each case, it could

be the right mathematical model for a dynamic system. As a result, it not only gives the optimal path but the list of possible solutions (Caha and Dvorský 2015). Dijkstra's algorithm is commonly used together with GIS to include spatial data (Ortega et al. 2014; Siljander et al. 2015; Pamučar et al. 2016) and finally to support users with a spatial presentation to enable visual analytics on the modelled results. Therefore, the aim of the research was to create a user-friendly decision support system (DSS) for urban traffic management which would include dynamic and spatial parameters in the simulation process.

Materials and Methods

The main goal of the research was to create a DSS which includes geographical and time attributes to support urban traffic management. The study presents the possibilities of the results that could be obtained according to traffic modelling, as well as a visual presentation of these results. The case study is Wrocław (Poland). The city struggles with urban traffic problems and according to the mobile data analysis, in the group of the seven biggest Polish cities, the amount of delay caused by traffic jams during peak hours increased the most—from 7:05 in 2011 to 8:52 in 2015 (Deloitte and Targeo 2016). Wrocław was one of the European Capitals of Culture in 2016 and because of that everyday traffic wa was additionally influenced by the congestion caused by people who attended big cultural events in different parts of the city. For that purpose, three What-if? scenarios were created. All of the scenarios present possible variants of car departures after cultural events that can be organized in the city. The first scenario assumes the departure of 9000 cars from the city stadium (capacity approx. 43,000 people) which is located close to the highway. The second scenario assumes the departure of 900 cars from the National Forum of Music (capacity approx. 2600 people) and the Opera (capacity approx. 1600 people) which are located close to the city centre. The third scenario assumes the departure of 900 cars from the Centennial Hall (capacity approx. 8000 people) which is located on the island connected to the city centre by two bridges.

All the scenarios were tested in the proposed geo-dynamic decision support system which combine ArcGIS, the self-created mathematical model based on Dijkstra's algorithm, with Tableau, which is one of the business intelligence systems (Fig. 1). The model is able to analyze any theoretical scenario depending on the needs of the local government. The results are presented on an interactive dashboard which enables the layman to process them and assess the potential impact of all predefined variants.

The data source for the road network was OpenStreetMap (OSM). Traffic congestion was assumed as in the scenarios presented above. As the proposed model constitutes the important part of the research itself, more detailed descriptions of all the stages are presented in the following parts.

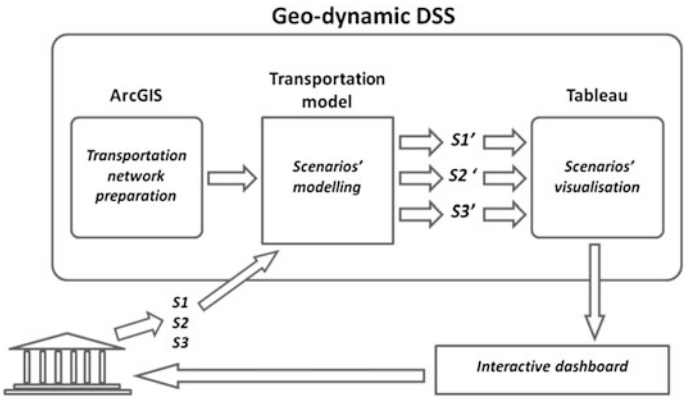

Fig. 1 Research conceptual framework

Geo-Dynamic DSS Components

Database Preparation for Linear Network Flow

The accuracy of transport network analysis depends directly on input data preparation. It plays a significant role on the effectiveness of linear network flow. The input data represents the linear layer of roads from the OSM source. As OSM data are open source and any user has the ability to update the data, there is a need for data verification in compliance with their plausibility and accuracy.

The first stage of the linear network preparation is the verification of data plausibility, which is connected with the linear objects updating. This stage involves creating the missing sections of the existing roads or removing objects that physically do not exist yet. At this stage, an important element is self-knowledge or the ability to use additional sources (i.e. WFS, other maps or database) by an analyst preparing the data.

The next stage of preparing the linear network is the verification of the data accuracy. This step is intended to ensure the completeness of the model, which should guarantee the complete database. The completeness of the database is tantamount to comprising all attributes describing each object. This database has to primarily contain information about road determinants i.e. one-way or maximum speed limits.

Subsequently, the verified and updated linear network has to be split into smaller lengths sections (i.e. 100 m). There is a need to create a set of points based on the specified distance along a linear network, then split the linear network with a generated set of points. This step allows the fragmentation of linear objects, which make the modelling flow of a linear network possible.

The final stage of data preparation for transport network analysis is to calculate the geometry (length) of linear objects from split analysis and calculate the coordinates of objects. It is crucial to calculate the start coordinates of the linear n-object (X and Y coordinates) and the end coordinates of the nearest linear object to the

linear n-object. These two pairs of coordinates allow to indicate the common point between two segments (which could be a node between them). The operation is necessary to determine the sequence of network segments.

Dijkstra's Algorithm for Traffic Modelling

For modelling purposes, the original, self-defined, macroscopic, continuous and random-deterministic model of urban traffic was created. The model enables to simulate traffic in an optional time step. In contrast to cellular automata models, the position of vehicles is described in a continuous movement. Random elements are the starting points and destinations. In a graph in a deterministic manner, the streets and trajectories of moving vehicles are defined. The model consists of three basic parts: a network of streets, characteristic of the behaviour of the vehicle in traffic and the algorithm selecting the routes for vehicles.

A network of streets is represented as a directed graph. The nodes of the graph correspond to crossroads and additionally are also located in the characteristic points of the street (turns, changing the parameters of the street, etc.). Each node has a specific name, location in the local coordinate system and in the geographical coordinates system, as well as a list of nodes with which it is directly connected. The edges of the graph correspond to the sections of the streets. Each section has a defined capacity based on a number of lanes in each direction and the maximum permissible speed limit.

Each vehicle in the model has a predetermined maximum speed limit, which can not be exceeded even if the parameters of the road allow that. However, in current research it was assumed that each vehicle travels on a road section with a maximum speed limit on each section of the network. No distinction between types of drivers was made (aggressive, average, insurance or other type of driving style).

The algorithm of traffic modelling comprises the following components:

- selection/determination of the starting and target nodes—can be given as a node_ID or randomized with a defined two-dimensional density function,
- determination of the trajectory of motion of each vehicle from the starting point to the destination point according to the established criteria by using Dijkstra's algorithm (Dijkstra 1959) to find the shortest path in the graph,
- modelling variable speed of traffic during the simulation.

The movement of vehicles in the model is based on the following elements:

- t_i—distance between the *i*-th vehicle and the previous one, measured in time unit [s],
- l_i—length of the *i*-th vehicle [m],
- k—density of vehicles on the analysed road section [vehicle km^{-1}],
- v_i—velocity of the *i*-th vehicle on the analysed road section [km h^{-1}].

By t_i distance, it is meant the time that the i-th vehicle (specifically, the farthest point in the direction of movement) needs to overcome the distance to the previous vehicle (specifically, it is the most extended point in the direction opposite to the direction of movement) in the direction of movement. Considering the movement of the vehicles in a microscopic scale on the road with a length of S (assuming no possibility of exit or entry on this road during the trip on each road section) the length occupied by one i-th vehicle was determined, where the distance between the vehicles can be described by the formula:

$$s_i = v_i\left[\mathrm{km\,h^{-1}}\right] \cdot t_i[\mathrm{s}] = v_i t_i \frac{1}{3600}[\mathrm{km}] \tag{1}$$

Taking into account the length of the vehicle and the distance between the vehicles described above (1), we can set inequality:

$$\sum_{i=1}^{n}\left(\frac{l_i}{1000} + v_i\frac{t_i}{3600}\right) \le S \tag{2}$$

The road section with a length S in the inequality (2) is presented as the sum of lengths of all n vehicles on the road, taking into account both the length of the vehicles and the distances between vehicles. Knowing that the speed of vehicles on the road section depends on the current traffic density k, it is assumed that the speed of each vehicle is equal to the maximum which is able to be achieved with the current density.

$$v_i = v(k) \text{ for each } i = 1, 2, \ldots, n \tag{3}$$

The formula (2) then takes the form:

$$\sum_{i=1}^{n}\frac{l_i}{1000} + v\sum_{i=1}^{n}\frac{t_i}{3600} \le S \tag{4}$$

By setting the average length of a moving vehicle in meters:

$$\bar{l} = \frac{1}{n}\sum_{i=1}^{n} l_i \tag{5}$$

we get:

$$n\frac{\bar{l}}{1000} + \frac{v \cdot n}{3600}\sum_{i=1}^{n}\frac{t_i}{n} \le S \tag{6}$$

Appearing in formula (6) the sum of t_i/n represents the mean arithmetic value of the distance (measured in time units) between vehicles, which is an estimator of the

expected value of the probability distribution of distances between all vehicles on the road section.

In natural traffic, the ability for a safe distance between all vehicles can be maintained only in a few conditions, e.g. calm and steady traffic on a highway. In other cases, especially in urban traffic, the distance between vehicles depends on many factors. In this study it is assumed that the distance between vehicles is a random variable based on a priori distribution and well-known parameters. Assuming that the probability distribution of distances between vehicles is known (T) and its finite expected value $E(T)$, the formula (6) is presented as follows:

$$n\frac{\bar{l}}{1000} + \frac{v \cdot n}{3600}E(T) \leq S \tag{7}$$

Hence:

$$v(k) \leq \frac{1}{k} \cdot \frac{3600}{E(T)} - \frac{3.6\bar{l}}{E(T)} \tag{8}$$

Based on other studies $E(T)$ was set as 2 s and l was set as 5 m (Kamińska and Chalfen 2016). The proposed model was verified by the case study of urban freeway traffic in Atlanta (Wang et al. 2011). In the same traffic conditions the vast majority of the distances between vehicles was in the range between 1.2 and 2.2 s (Fig. 2).

Theoretical speed calculated according to the formula is limited by the maximum permissible speed limit on the network section and for each car. At the start each vehicle trajectory to the destination point is determined. Trajectory for each vehicle is determined by the current density at the network at the moment of entering the roads. As a result the speed of movement throughout the city at each section is calculated.

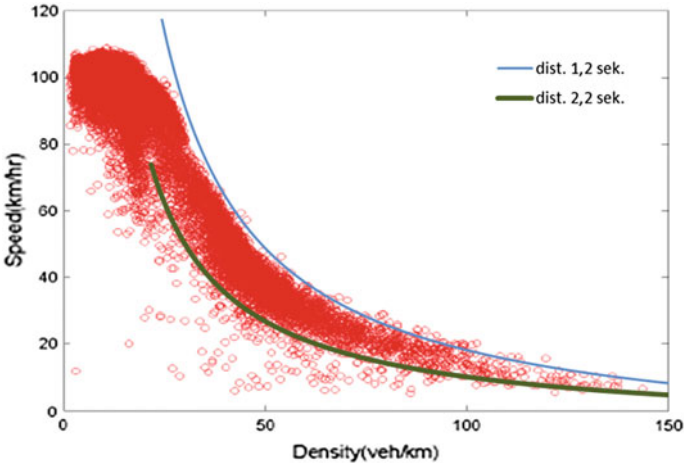

Fig. 2 Figure of empirical data of Wang et al. (2011) and designated $v(k)$

However, when the vehicle actually comes to each section of the street, the speed on this section is recalculated taking into account new traffic density (based on the new allocation of all vehicles on the model). The vehicle moves along a predetermined trajectory by uniform motion, i.e. place where the vehicle reaches in a fixed period of time Δt is calculated. The Δt time step in the simulation is optional, usually used Δt = 1–10 s. It is allowed to change the predefined trajectory in the model (at the start of each journey) so that the time-varying traffic density in a city is taken into account. Such a possibility of trajectory change is allowed only when the vehicle passes through the node having more than two neighbours. As a result of the simulation the model calculates the location of all vehicles in motion and the load on the network (e.g. the number of vehicles within the various edges of the graph or the average moving speed).

Data Visualization

Simulation data was visualised in Tableau Desktop. Raw data files contain id, path sequence, nodes coordinates as well as the number of cars per 5 min, and cumulative number of cars. The street names were coded. There were from 13,936 to 62,712 records in each simulation. Tableau provides a live connector to many data sources so it is possible to work directly with the data online. However, in predefined scenarios there is no need to work on online databases, as the only information that could be updated is a road network (where changes are not that dynamic). After connecting to the data source, the raw data was recognized as an attribute table and could be opened and processed in Tableau. All data were divided into measures and dimensions. Dimensions are used for categorisation, breaking down and grouping. Measures enable to sum, count and calculate the average value of objects. Both measures and dimensions can be discrete or continuous.

The raw data interpreter was used to set up geographical roles: latitude and longitude. Path sequence was applied to describe the directed edges between the nodes. Time data had been used as a parameter for time series mapping. Originally, a fully animated dashboard was built. To avoid misinterpretation problems, the filters for the minimum car number which should be mapped were used. Dynamic mapping of the car traffic simulation was built with the use of the original WMS Tableau basemap. All analyses, as well as data exploration, have been carried out with the use of VizQL—formal language for describing tables, charts, graphs, maps, time series, tables and visualizations.

Scenarios' Analysis

The use of DSS allowed for a spatio-dynamic model for each predefined scenario. Due to time steps in the procedure it was possible to create animations for a better visualization of urban traffic flows. However, in the paper, the following twelve

time steps are presented in a small multiple picture (Fig. 3). Such a method of visualization shows the rhythm of urban metabolism. The results of scenarios modelling potentially highlighted the most common problems in the organization of events in the analysed localizations in Wrocław.

As it was mentioned in Section "Dijkstra's algorithm for traffic modelling", the destination points in the simulations are chosen randomly. However, the structure of the road network on a case study is characterised by a higher density of nodes in the core of the city than on the outskirts of the city (Fig. 4). Therefore, the result of the random allocation of destination points will also influence a higher density in the city centre.

The first scenario shows that even the location close to the highway does not solve most of the traffic problems. As the route of the highway is rather a bypass of Wrocław for transit traffic, destination points outside of the city are served by this road. In hardly any case did it seem useful for urban traffic needs. However, a significant share of vehicles used one of the urban streets (Legnicka Street). Many cars (additional to regular traffic) entering one section of the street in one moment may impact a higher risk of accidents. That is why in the first scenario, a possibility of redefining the optimal trajectory to the destination point according to changing conditions was extorted. An accident was located on one of the most congested roads due to check the mechanism of the recalculation of trip trajectories for each vehicle.

The second scenario shows that the location in the city centre with a high density of road network with comparable parameters influence a rather regular distribution of vehicles. In that case it is especially important to remember that the results of the simulations present additional value to regular traffic congestion which is quite a problematic issue at certain moments of a day. Identification of regular peak hours and traffic flows at each part of the city is possible from the data collected by intelligent transportation system (ITS) which was applied in the city between 2008 and 2015. Knowing the cycles of traffic flows enables, for instance, to cooperate between municipal services responsible for cultural events and traffic management units to avoid an accumulation of vehicle congestion.

The third location is the Centennial Hall which is placed on an island. There are two bridges connecting the island to the city centre, however, one of them is close to the object. Therefore, the third scenario shows the so-called bottleneck issues in the network. In a short term management it might be rational to analyse a temporal reorganization of traffic in that neighbourhood to decrease the congestion. Such actions are already implemented in many cases and they are the elements of Active Traffic Management, e.g. closing street lanes, changing direction of lanes, changing traffic light priorities, etc. (Karoń 2016). Taking into account that in the same neighbourhood the ZOO and open exhibition area are also located, which influences traffic problems regularly, in long term management it might be necessary to analyse an option for the construction of a new bridge to divert directions.

All of the above case study conclusions were possible to identify because of the use of an interactive dashboard (Fig. 5). The final dashboard was composed with a standard bar and line charts, interactive filters and highlights. The data was broken down by the street name, so the operator is able to indicate which roads have the

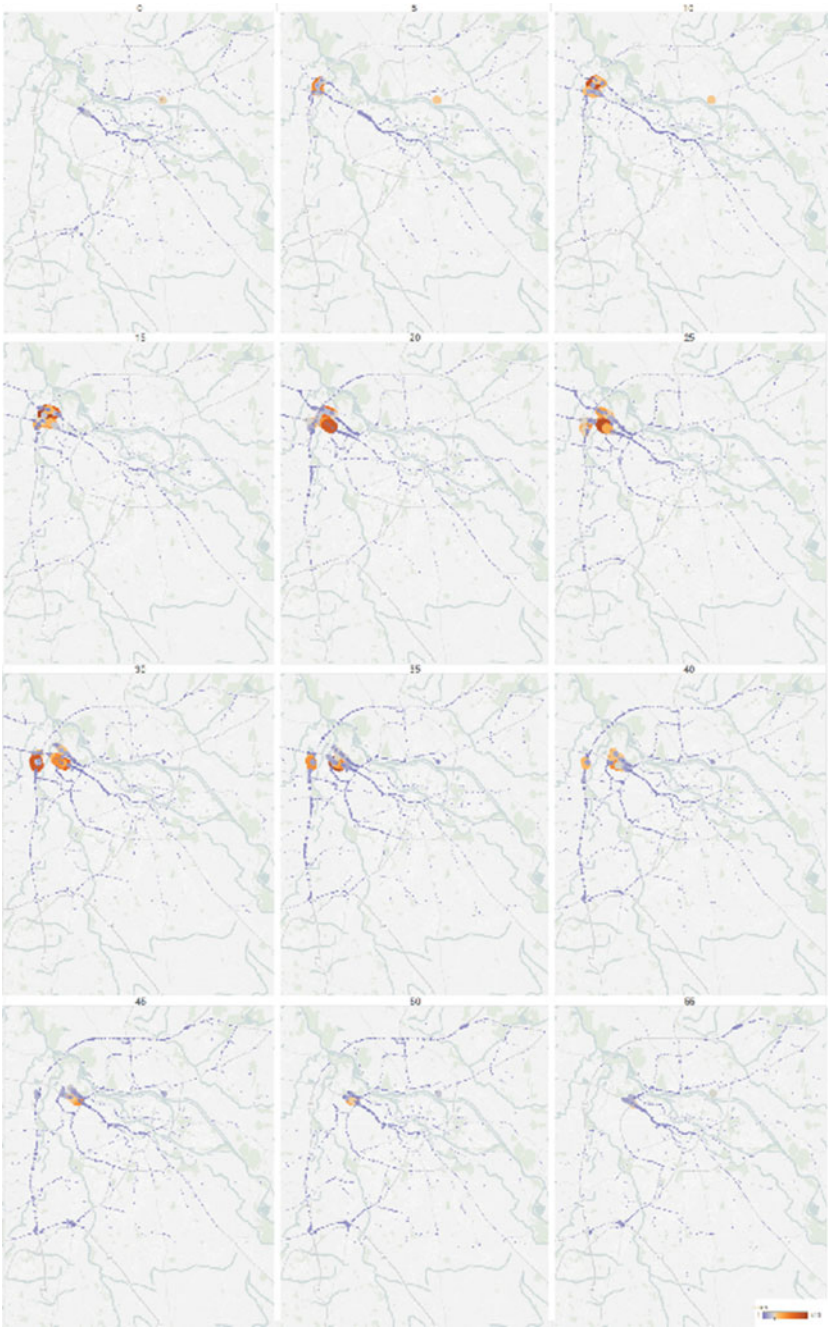

Fig. 3 Dynamic changes of network congestion in scenario no. 1

Fig. 4 Density distribution of road network nodes

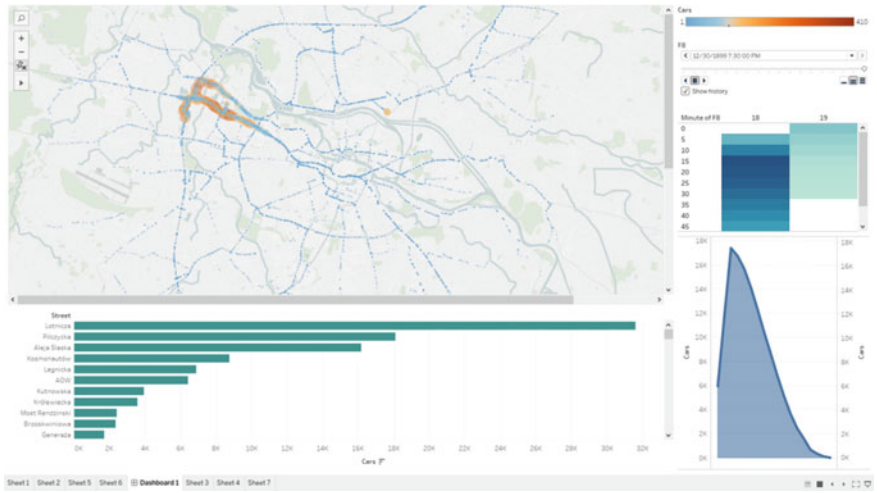

Fig. 5 Interactive dashboard

highest car congestion during each simulation. Moreover, to visualize the dynamic character of the data, a time series line chart was applied. The dashboard is fully interactive, so one can select any number of nodes on a map and indicative charts will show summaries for only the selected items. As the date and time filter is

active, it is possible to follow the data within the time frame. The dashboard can be published in a cloud service and accessed by anyone who is interested. Such a way of publishing results enables a layman who has no experience with spatial or transportation modelling, as all available functions give him access to time slider, charts and the ability to select a specific area on the map.

Conclusions

The presented DSS aims to provide geo-dynamic analysis of urban traffic congestion on a road network. The applied solution enables to recalculate transportation trajectories according to time-varying traffic density on each section of a network. The use of Dijkstra's algorithm allowed to store the information about the spatial distribution of all the modeled vehicles and to optimize trips to destination points. The knowledge of possible traffic flows is crucial for the effective management of those processes. It could be used, for example, to support intelligent transportation systems which have become more and more popular. The proposed solution also gives information about cumulative congestion assessment. Such information might support not only traffic lights management but also temporary changes in traffic organization (e.g. closing street lanes, changing direction of lanes, changing traffic light priorities, etc.).

Besides transportation model for traffic calculations, the DSS presents the results in an interactive dashboard which limits variables to those which could be easily changed by users by intuitive functions. It is possible to get such outputs like cumulative load of vehicles, traffic congestion in each simulation time step, summary or average value of cars at each node or road section depending on a selection, etc. The time necessary for reporting the outcomes is reduced to a minimum (real-time reporting) which allows for better decision making based on knowledge. The Interactive dashboard enables to visualize the dynamic attributes as animation which helps to better understand traffic flows. The proposed solution reduces the cognitive problems with the use of DSS which is possible due to the limited accessibility to modeling results. Besides the transportation model, the elements used for DSS already exist. Therefore, the proposed concept fulfills the idea of diffusion of innovation which is based on defining new connections between existing solutions to improve the analysed issue.

References

Ahvenniemi, H., Huovila, A., Pinto-Seppä, I., & Airaksinen, M. (2017). What are the differences between sustainable and smart cities? *Cities*, *60*(Part A), 234–245. https://doi.org/10.1016/j.cities.2016.09.009.

Ai, F., Comfort, L. K., Dong, Y., & Znati, T. (2016). A dynamic decision support system based on geographical information and mobile social networks: A model for tsunami risk mitigation in Padang, Indonesia. *Safety Science, 90,* 62–74.

An, S., Yang, H., Wang, J., Cui, N., & Cui, J. (2016). Mining urban recurrent congestion evolution patterns from GPS-equipped vehicle mobility data. *Information Sciences, 373,* 515–526.

Ayed H., Galvez-Fernandez C., Habbas Z., & Khadraoui D. (2011). Solving time-dependent multimodal transport problems using a transfer graph model. *Computers & Industrial Engineering, 61*(20), 391–401.

Caha, J., & Dvorský, J. (2015). Optimal path problem with possibilistic weights. In I. Ivan, I. Benenson, B. Jiang, J. Horák, J. Haworth, & T. Inspektor (Eds.), *Geoinformatics for intelligent transportation* (pp. 39–50)., Lecture Notes in Geoinformation and Cartography Cham: Springer International Publishing.

CIVITAS. (2015). *Policy note: Intelligent transport systems and traffic management in urban areas*. CIVITAS WIKI consortium.

Dahal, K., Almejalli, K., & Hossain, M.A. (2013). Decision support for coordinated road traffic control actions. *Decision Support Systems, 54*(2), 962–975.

Deloitte and Targeo (2016) *Raport o korkach w 7 największych miastach Polski*. Warszawa: Deloitte Polska.

Dijkstra E. W. (1959). A note on two problems in connection with graphs. *Numerische Mathematik, 1*, 269–271.

Golfarelli, M., & Rizzi, S. (2009). What-if simulation modeling in business intelligence. *International Journal of Data Warehousing and Mining, 5*(4), 24–43.

Hashemi, H., & Abdelghany, K. F. (2016). Real-time traffic network state estimation and prediction with decision support capabilities: Application to integrated corridor management. *Transportation Research Part C, 73,* 128–146.

Kamińska, J., & Chalfen, M. (2016). An influence of safe distance between vehicles on traffic speed and density. *Autobusy: technika, eksploatacja, systemy transportowe, 17*(6), 578–582.

Karoń, G. (2016). Strategies of Active transportation and demand management. *Komunikacja publiczna, 3*(64), 39–46.

Maggi, E., & Vallino, E. (2016). Understanding urban mobility and the impact of public policies: The role of the agent-based models. *Research in Transportation Economics, 55,* 50–59.

Ortega, E., Otero, I., Mancebo, S. (2014). TITIM GIS-tool: A GIS-based decision support system for measuring the territorial impact of transport infrastructures. *Expert Systems with Applications, 41*(16), 7641–7652.

Pamučar, D., Gigović, L., Ćirović, G., & Regodić, M. (2016). Transport spatial model for the definition of green routes for city logistics centers. *Environmental Impact Assessment Review, 56,* 72–87.

Przybyła, K., Kulczyk-Dynowska, A., & Kachniarz, M. (2014). Quality of life in the regional capitals of Poland. *Journal of Economic Issues, 48*(1), 181–196.

Ruiz-Padillo, A., Ruiz, D. P., Torija, A. J., & Ramos-Ridao, Á. (2016). Selection of suitable alternatives to reduce the environmental impact of road traffic noise using a fuzzy multi-criteria decision model. *Environmental Impact Assessment Review, 61,* 8–18.

Siljander, M., Venäläinen, E., Goerlandt, F., & Pellikka, P. (2015). GIS-based cost distance modelling to support strategic maritime search and rescue planning: A feasibility study. *Applied Geography, 57,* 54–70.

Szücs, G. (2015). Decision support for route search and optimum finding in transport networks under uncertainty. *Journal of Applied Research and Technology, 13*(1), 125–134.

Torretta, V., Rada, E. C., Schiavon, M., & Viotti, P. (2017). Decision support systems for assessing risks involved in transporting hazardous materials: A review. *Safety Science, 92,* 1–9.

Tremblay, S., Gagnon, J.-F., Lafond, D., Hodgetts, H. M., Doiron, M., & Jeuniaux, P. P. J. M. H. (2017). A cognitive prosthesis for complex decision-making. *Applied Ergonomics, 58,* 349–360.

Wang, H., Li, J., Chen, Q.-Y., & Ni, D. (2011). Logistic modeling of the equilibrium speed–density relationship. *Transportation Research Part A: Policy and Practice, 45*(6), 554–566.

Zhuhadar, L., Thrasher, E., Marklin, S., & Ordóñez de Pablos, P. (2017). The next wave of innovation—Review of smart cities intelligent operation systems. *Computers in Human Behavior, 66,* 273–281.

Probabilistic Map-Matching for Low-Frequency GPS Trajectories

Kira Kempinska, Toby Davies, John Shawe-Taylor and Paul Longley

Abstract The ability to infer routes taken by vehicles from sparse and noisy GPS data is of crucial importance in many traffic applications. The task, known as map-matching, can be accurately approached by a popular technique known as ST-Matching. The algorithm is computationally efficient and has been shown to outperform more traditional map-matching approaches, especially on low-frequency GPS data. The major drawback of the algorithm is a lack of confidence scores associated with its outputs, which are particularly useful when GPS data quality is low. In this paper, we propose a probabilistic adaptation of ST-Matching that equips it with the ability to express map-matching certainty using probabilities. The adaptation, called probabilistic ST-Matching (PST-Matching) is inspired by similarities between ST-Matching and probabilistic approaches to map-matching based on a Hidden Markov Model. We validate the proposed algorithm on GPS trajectories of varied quality and show that it is similar to ST-Matching in terms of accuracy and computational efficiency, yet with the added benefit of having a measure of confidence associated with its outputs.

Keywords Map-matching · Gps data · Hidden markov model · Dynamic programming

K. Kempinska (✉) · T. Davies
Department of Security and Crime Science, University College London,
Gower Street, London, UK
e-mail: kira.kowalska.13@ucl.ac.uk

T. Davies
e-mail: toby.davies@ucl.ac.uk

J. Shawe-Taylor
Department of Computer Science, University College London,
Gower Street, London, UK
e-mail: j.shawe-taylor@ucl.ac.uk

P. Longley
Department of Geography, University College London,
Gower Street, London, UK
e-mail: p.longley@ucl.ac.uk

I. Ivan et al. (eds.), *Dynamics in GIscience*, Lecture Notes in Geoinformation and Cartography, DOI 10.1007/978-3-319-61297-3_15

Introduction

Over the last years we have witnessed a rapid increase in the availability of GPS-receiving devices, such as smart phones or car navigation systems. The devices generate vast amounts of temporal positioning data that have been proven invaluable in various applications, from traffic management (Kühne et al. 2003) and route planning (Gonzalez et al. 2007; Kowalska et al. 2015; Li et al. 2011) to inferring personal movement signatures (Liao et al. 2006).

Critical to the utility of GPS data is their accuracy. The data suffer from measurement errors caused by technical limitations of GPS receivers and sampling errors caused by their receiving rates. The accuracy of the data can be improved by averaging multiple trajectories (Brundson 2007; Demšar et al. 2015). Alternatively, when digital maps are available, it is common practice to improve the accuracy of the data by aligning GPS points with the road network. The process is known as map-matching.

Most map-matching algorithms align GPS trajectories with the road network by considering *positions* of each GPS point, either in isolation or in relation to other GPS points in the same trajectory. The techniques, although often computationally efficient, are not very accurate in cases when the sampling rate is low or the street network complexity is high.

More advanced map-matching techniques utilise both *timestamps* and *positions* of GPS points in order to achieve a higher degree of accuracy. A highly popular example of a spatio-temporal algorithm is ST-Matching (Lou et al. 2009). It uses spatial information to find candidate roads for each GPS point and then seeks a sequence of candidate roads that best matches the temporal profile of the GPS trajectory. The algorithm is easy to implement, computationally efficient and has been shown to outperform purely spatial map-matching approaches, especially when the sampling rate is low. The major limitation of technique, and the before-mentioned spatial approaches, is its deterministic nature. It would always snap a GPS trajectory to a road network, regardless if it even came from the road network in the first place. The lack of confidence scores associated with its outputs might lead to very misleading results, especially when the data quality is low.

In isolation from the deterministic developments, *probabilistic* approaches to map-matching have been designed that address the issue of confidence using probabilities. They also belong to the class of spatio-temporal techniques as they use both spatial and temporal information when calculating probabilities of specific map-matching outputs. They typically represent the map-matching problem using a hidden Markov Model (HMM) where hidden states are true positions that are learnt from noisy GPS trajectories (Goh et al. 2012; Jagadeesh and Srikanthan 2014; Newson and Krumm 2009). The most likely map-matching output can then be efficiently learnt by applying a dynamic programming algorithm, such as the Viterbi algorithm, to the HMM lattice. Probabilistic approaches calculate the most likely or a few most likely road paths and output them together with their likelihoods.

They are methodologically powerful, but largely isolated from the rest of the map-matching community, often limiting their uptake by researchers and practitioners from other fields.

In this paper, we present a map-matching algorithm that bridges the gap between the deterministic and probabilistic classes of spatio-temporal algorithms. It is an adaptation of the well-established ST-Matching that turns it from being deterministic to fully probabilistic. The adaptation brings the best of the deterministic and probabilistic worlds into a highly accurate and computationally efficient map-matching algorithm that is capable of expressing levels of map-matching confidence. The proposal is inspired by apparent similarities between ST-Matching and HMM-based approaches to map-matching.

The paper is outlined as follows. It begins by introducing ST-Matching and a general HMM-based framework as its probabilistic counterpart. It analyses similarities and differences between the two approaches in order to propose a probabilistic adaptation of ST-Matching, called probabilistic ST-Matching or PST-Matching in short. It evaluates the robustness of PST-Matching on a range of GPS trajectories of varied frequencies and levels of noise. Similarly to ST-Matching, the proposed algorithm shows high accuracy on datasets with low GPS frequency, yet with the added benefit of confidence scores associated with its outputs.

Problem Statement

In this section, we define the problem of probabilistic map-matching.

Definition 1 (*GPS trajectory*): A sequence of GPS points, where each GPS point contains latitude, longitude and timestamp.

Definition 2 (*Road network*): A directed graph with vertices representing road intersections and edges representing road segments. Bidirectional road segments are represented by two edges, each corresponding to a single direction of flow. Roads and intersections can be uniquely identified using their IDs.

Definition 3 (*Path*): A connected sequence of street segments in the road network.

Given a road network and a GPS trajectory, the goal of probabilistic map-matching is (*1*) *to find the most likely path that the GPS trajectory was generated from and* (*2*) *to quantify the confidence that the path is indeed the true path taken* (Fig. 1).

Methodology

In this section, we describe our probabilistic ST-Matching algorithm in detail. We begin by introducing its components: the ST-Matching algorithm (deterministic) and a general HMM-based approach (probabilistic). We then outline modifications

Fig. 1 Exemplary road network with a GPS trajectory to be map-matched

required to make the ST-Matching algorithm fit the general HMM-based framework, thus turning it into a probabilistic technique.

ST-Matching Algorithm

ST-Matching is a deterministic map-matching approach that combines spatial and temporal information to effectively align low-sampling-rate GPS trajectories with the road network. It is easy to implement and has been shown to outperform more traditional map-matching approaches in terms of accuracy and running time. Its architecture consists of two basic steps: candidate graph preparation and best path computation.

(1) *Candidate graph*:

Candidate graph stores all possible true paths given a GPS trajectory. Nodes of the graph are candidate position for each GPS observation, edges are shortest road paths between neighbouring candidate positions. The preparation of the graph involves the following steps.

Firstly, candidate positions are computed by retrieving road segments within radius r of each GPS observation and then finding a position on each segment at the shortest distance to the relevant observation. The procedure is exemplified in Fig. 2. The obtained candidate positions are represented as nodes in the candidate graph. The number of candidate positions can differ among GPS observations, depending on the number of street segments within the search radius. In the paper, we use $c_{i,j}$ to denote the jth candidate position of GPS observation p_i.

Secondly, shortest paths between pairs of candidate positions at adjacent time steps are evaluated based the road topology. They are represented as edges in the candidate graph, as shown in Fig. 2b.

Finally, the nodes and edges of the candidate graph are weighted based on the spatio-temporal profile of the GPS trajectory and the topology of the underlying

(a) candidate positions **(b)** candidate graph

Fig. 2 Exemplary road network with a GPS trajectory to be map-matched

road network. Their weights reflect their *observation* and *transmission probabilities*, respectively.

Definition 4 (*Observation probability*): Given a GPS observation p_i at time step i and a corresponding candidate position $c_{i,j}$, it defines the probability that the GPS observation p_i is emitted from the candidate position $c_{i,j}$.

The observation probability is specified as a Gaussian distribution of the distance between p_i and $c_{i,j}$:

$$\mathrm{N}(\mathrm{c}_{i,j}) = \frac{1}{\sqrt{2\pi}\sigma} e^{\frac{(\mathrm{x}_{i,j}-\mu)^2}{2\sigma^2}} \tag{1}$$

where $x_{i,j}$ is the distance between p_i and $c_{i,j}$. The mean μ of the distribution is set to zero, the standard deviation σ is empirically estimated.

Definition 5 (*Transmission probability*): Given two candidate positions $c_{i-1,j}$ and $c_{i,k}$ for two neighbouring GPS observations p_{i-1} and p_i, it defines the probability that the "true" path from p_{i-1} to p_i follows the shortest path from $c_{i-1,j}$ to $c_{i,k}$.

The transmission probability is defined as follows:

$$\mathrm{V}(\mathrm{c}_{\mathrm{i-1,j}} \rightarrow \mathrm{c}_{\mathrm{i,k}}) = \frac{d_{i-1\rightarrow i}}{s_{(i-1,j)\rightarrow(i,k)}} \tag{2}$$

where $d_{i-1\rightarrow i}$ is the Euclidean distance from p_{i-1} to p_i and $s_{(i-1,j)\rightarrow(i,k)}$ is the length of the shortest path from $c_{i-1,j}$ to $c_{i,k}$.

The above definition only considers spatial information when calculating the likelihood of transmission. A spatio-temporal version of the transmission probability is also considered in the original paper (Lou et al. 2009) and could be easily incorporated into the methodology presented in this paper in the future.

(2) *Best path search*:

Once the candidate graph is defined and its nodes and edges are weighted according to the observation and transmission probabilities, respectively, a dynamic

programming method is applied in order to find a path through the graph with the maximum weight. The path represents the most likely "true" path that the GPS trajectory was generated from.

The method proposed in (Lou et al. 2009) calculates the most likely path by recursively evaluating the following equation:

$$f(t,k) = N\left(c_{t,k}\right) + \max_{j}\left[f(t-1,j) \cdot V\left(c_{t-1},j \rightarrow c_{t,k}\right)\right] \tag{3}$$

with $f(1,k)$ initialised to $f(1,k) = N(c_1,k)$. In the above equation, $f(t,k)$ represents the total weight of the most likely sequence of positions ending at position $c_{t,k}$, based on GPS observations at time steps $1:t$. Once the recursion reaches $t = T$, the obtained sequence of positions and the shortest paths between them form the most likely path given the GPS trajectory.

General HMM-Based Approach

Hidden Markov Model (HMM) is an established framework for probabilistic time-series modelling. It provides a principled way of representing uncertainty in measurements taken over time and as such is suitable for modelling uncertainty inherent to noisy GPS trajectories.

There have been numerous probabilistic approaches to map-matching based on HMMs (Goh et al. 2012; Jagadeesh and Srikanthan 2014; Newson and Krumm 2009). They typically use a HMM to represent possible "true" paths and their probabilities and then search for one or more paths with the highest probabilities as the map-matching output.

Drawing similarities to the ST-Matching algorithm, a HMM can be understood as a candidate graph from which the most likely path can be retrieved via a dynamic programming routine known as the Viterbi algorithm.

(1) *Candidate graph*:

HMM provides a graph structure for storing possible paths in a probabilistic manner. Nodes of the graph are hidden states that can represent candidate positions at each time step. Edges are transitions between the hidden states and can represent possible paths taken between candidate positions at adjacent time steps. The structure of the graph in the context of map-matching is, in fact, equivalent to that of the candidate graph in ST-Matching (see Fig. 2b for an example).

Nodes are assigned emission probabilities that quantify the likelihood of the observations given the hidden states at each time step. The emission probability is defined as the conditional probability $p(p_i|c_{i,j})$ of observing p_i given that the true state at time step i is $c_{i,j}$. In the map-matching context, it is equivalent to the observation probability given in Definition 4.

Edges are given so-called transition probabilities. The transition probability is a discrete conditional distribution $p(c_{i,k}|c_{i-1,j})$ that defines the probability of transitioning from hidden state $c_{i-1,j}$ at time step $i-1$ to another hidden state $c_{i,k}$ at time step i. In our context, it is the probability of following the shortest path between candidate positions corresponding to these hidden states. The transition probability can be any discrete distribution, such as the ST-Matching transmission probability in Definition 5, but more rigorously defined to ensure that basic rules of probability are satisfied. In particular, the following statement must hold:

$$\sum_k p(c_{i,k}|c_{i-1,j}) = 1 \tag{4}$$

(2) *Best path search*:

The most likely path is inferred as the most likely sequence of hidden states using a dynamic programming technique known as the Viterbi algorithm (Bishop 2006). The algorithm finds the state sequence with the highest joint probability over the states and the GPS observations, which is the product of the emission and transition probabilities along the sequence. It efficiently searches the space of all possible sequences by recursively evaluating the maximum joint probability for each state at each time step as follows:

$$w_{t,k} = p(p_t|c_{t,k}) \cdot \max_j [w_{t-1,j} \cdot p(c_{t,k}|c_{t-1,j})] \tag{5}$$

with $w_{t,k}$ initialised to $w_{t,k} = p(p_1|c_{1,\mathrm{k}})$. In the above equation, $w_{t,k}$ represents the joint probability of the most likely sequence of hidden states until time step t. Once the recursion reaches time step $t = T$, the most likely path is formed by the most likely sequence of hidden states and the shortest paths between them.

Notice that the Viterbi algorithm is almost equivalent to the ST-Matching algorithm in (3). If one replaced the observation and transmission probabilities in (3) with the more general emission and transition probabilities of the Viterbi algorithm, respectively, the ST-Matching algorithm would only differ in the way it applies the most recent emission probability to the result of the *max* operation (addition instead of multiplication). However, it lacks the probabilistic treatment of the Viterbi approach which not only finds the most likely path but also quantifies the likelihood that it is indeed the true path taken using its joint probability.

Probabilistic ST-Matching Algorithm

Having introduced the ST-Matching algorithm and a general HMM-based approach, it has become apparent that the two approaches share a lot of similarities. In this section, we formalise the observation and outline modifications required

to make the ST-Matching algorithm fit the probabilistic framework, thus giving it the ability to express map-matching confidence in a probabilistic manner. We term the proposed modification the probabilistic ST-Matching (PST-Matching) algorithm.

(1) *Candidate graph*:

Candidate graph of PST-Matching is very similar to the original ST-Matching graph. It shares the same graphical structure and defines the observation probability according to the same formula in (1). It requires a modified transmission probability, however, as the original definition in (2) does not satisfy basic rules of conditional probabilities, such as the summation rule in (4). We satisfy the requirement by proposing a normalised transmission probability:

$$V_{pst}\left(c_{i-1,j} \rightarrow c_{i,k}\right) = \frac{V\left(c_{i-1,j} \rightarrow c_{i,k}\right)}{\sum_k V\left(c_{i-1,j} \rightarrow c_{i,k}\right)} \tag{6}$$

(2) *Best Path Search*:

The dynamic programming routine of PST-Matching is a modification of that of ST-Matching (3) that turns it into a Viterbi algorithm. The modification simply requires replacing the addition operation in (3) with multiplication. When applied to the candidate graph outlined above, the proposed algorithm takes the following recursive form:

$$f_{pst}(t,k) = N\left(c_{t,k}\right) \cdot \max_j \left[f_{pst}(t-1,j) \cdot V_{pst}\left(c_{t-1},j \rightarrow c_{t,k}\right)\right] \tag{7}$$

with $f_{pst}(1,k)$ initialised to $f_{pst}(1,k) = N(c_1,k)$. As in any Viterbi algorithm, the quantity stored in $f_{pst}(t,k)$ at the final time step is the joint probability of the most likely path. It serves as a measure of map-matching confidence that the original ST-Matching algorithm is lacking.

Method Validation

Data

The dataset used for validating the proposed algorithm is a complete GPS trajectory of a police patrol vehicle during its night shift (9 pm to 7am) in the London Borough of Camden on February 9th 2015. The dataset contains 4800 GPS points that were emitted roughly every second when moving.

Further datasets of degraded quality are artificially created from the acquired data in order to test the robustness of the proposed algorithm on a range of GPS trajectories of varied sampling rates and levels of noise. Their sampling rate is

manipulated by removing GPS points at chosen intervals. Their level of noise is controlled by perturbing GPS point by Gaussian noise with zero mean and a chosen standard deviation. There is already some random Gaussian noise inherent to the data. However, since Gaussian distributions are additive, i.e. adding two Gaussian random variables results in another Gaussian random variable with mean and variance equal to the sum of the added means and variances, any additional amount of noise can be simulated once the standard deviation of the original noise distribution is empirically found.

Accuracy Testing

Since there is no ground truth available, we propose a validation framework based on the well-established technique of cross-validation (Barber 2012). We split available GPS observations into training and test sets according to the split ratio of 9:1, i.e. 90% training and 10% testing. In practice, this equates to us removing every 10th GPS point from each GPS trajectory for training (see Fig. 3). We proceed by aligning the trajectory of training GPS points with the road network using our proposed PST-Matching algorithm. We then record how far off the predicted path each test point is. The more off, the more erroneous our map-matching proposal. We use the average distance across all test points as the measure of map-matching error made.

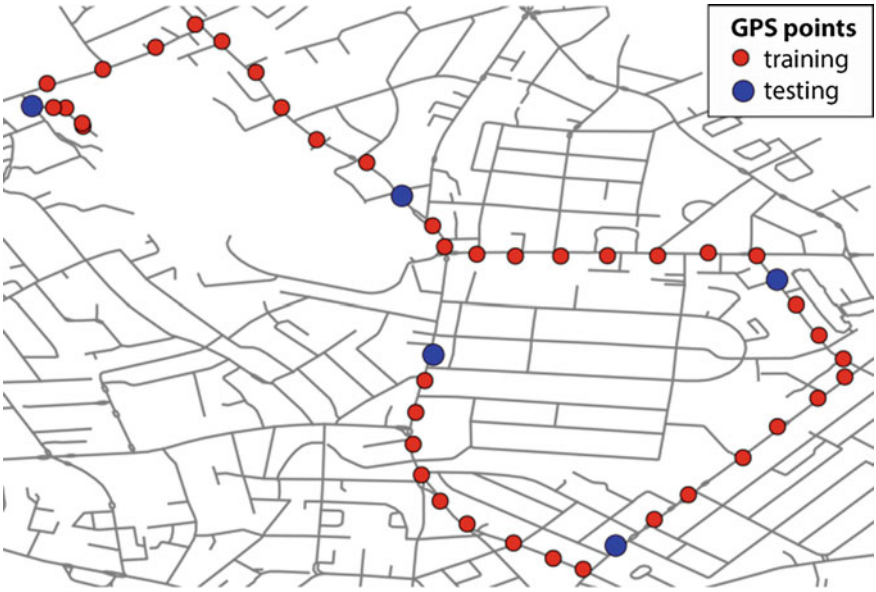

Fig. 3 Exemplary GPS trajectory with points split into training and test sets

Results

We tested the proposed PST-Matching algorithm on datasets of varied quality and compared its accuracy against that of the original ST-Matching algorithm. See Fig. 4 for exemplary map-matching outputs and Fig. 5 for a summary of the algorithm's performance across all datasets. Similarly to ST-Matching, the algorithm shows high accuracy on datasets with noise as high as 30 meters standard deviation and sampling rates of up to 90 s. Such extreme conditions are rarely found in real datasets; hence the algorithm should be successful on real GPS trajectories without the need for any prior adjustments or parameter fitting.

We noticed a slight drop in performance at very low sampling rates of 1–2 s (see Fig. 5a). This is likely caused by the fact that frequent, noisy observations tend to pull rather violently towards different path proposals. The algorithm also gradually deteriorates at higher levels of measurement noise, unlike the original ST-Matching algorithm (see Fig. 5b). This is due to the normalisation of the transmission probability according to (6), which fails to penalise candidate points that are clearly off the "true" path. As a result, as the measurement noise increases, there are more points off the path that PST-Matching accidentally includes in the most likely path.

We investigated how confidence of PST-matching solutions, expressed as joint probabilities, changes with the sampling rate and the level of noise of GPS data.

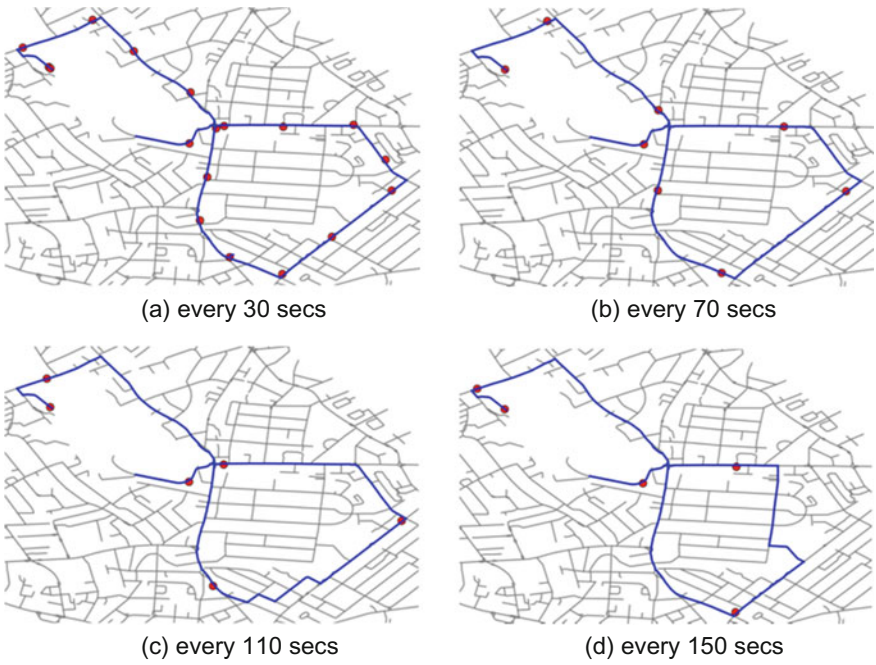

Fig. 4 Exemplary PST-matching solutions at different sampling rates

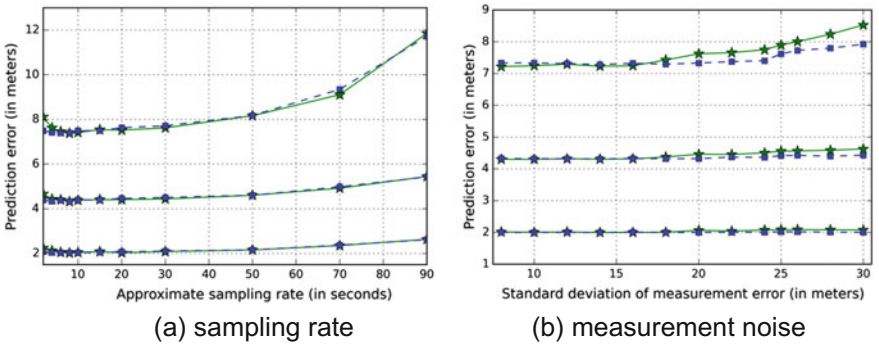

Fig. 5 Accuracy of PST-matching (*green*) and ST-matching (*blue*) on datasets with varied GPS sampling rates and noise represented as 25th, 50th and 75th percentiles of map- matching errors

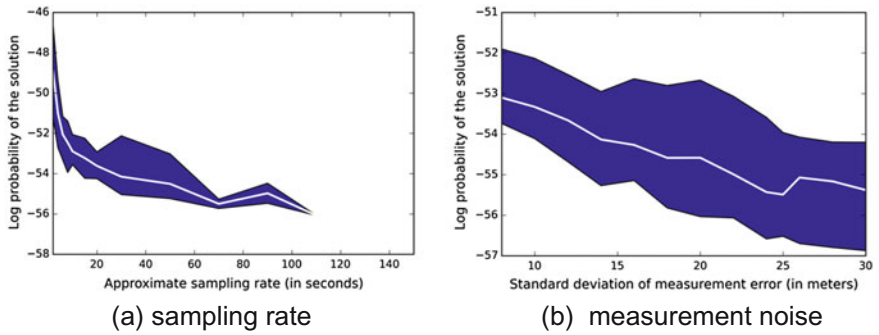

Fig. 6 Map-matching confidence on datasets with varied GPS sampling rates and noise represented as 25th, 50th and 75th percentiles of log probabilities of map-matching outcomes

Since the joint probability of a solution is the product of observation and transmission probabilities along the most likely sequence (see 7), its value depends on the length of the input GPS sequence. We ensured that the dependence did not skew our analysis by applying PST-Matching to a sliding window (of length ten) over input GPS trajectories. The idea guaranteed that confidence scores were comparable and gave the algorithm the ability to process GPS trajectories in an online manner. The obtained confidence scores are shown in Fig. 6. On average, the scores decline as data become noisy and sparse. This trend is exemplified in Fig. 7, where after adding noise to the data, the quality and confidence of the map-matching output gradually drops. These intuitive results show that the confidence scores are closely aligned with the quality of map-matching results and, as such, could prove indispensable when dealing with GPS data of unknown quality.

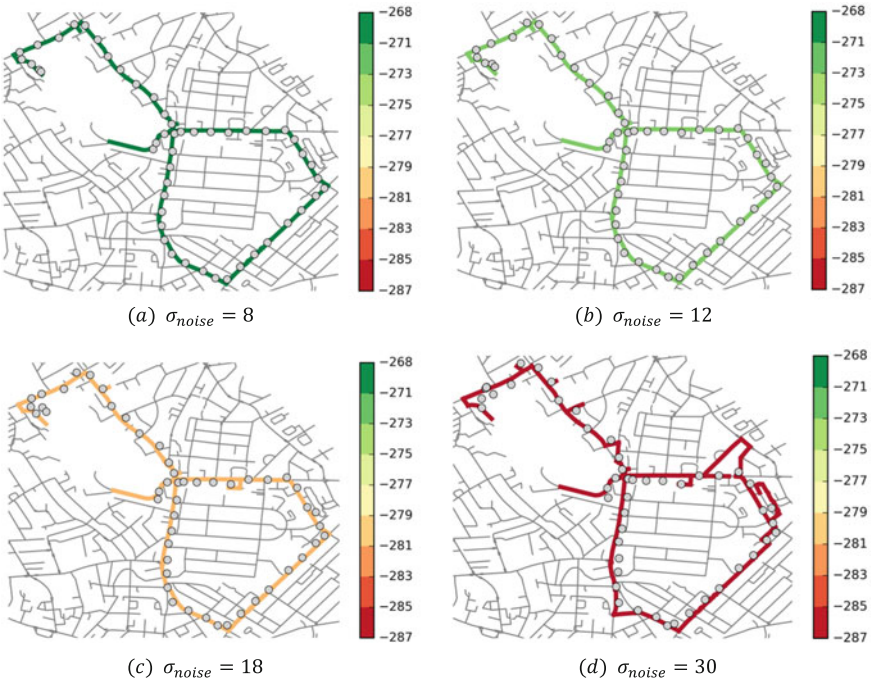

Fig. 7 Exemplary PST-Matching outcome with confidence (expressed as log probability) on a GPS trajectory with varied noise standard deviation (in meters)

Conclusions

In this paper, we propose a new probabilistic map-matching algorithm called PST-Matching for aligning sparse and noisy GPS trajectories with a road network. The algorithm is a probabilistic extension of a popular deterministic algorithm called ST-Matching that has been shown to outperform more traditional map-matching algorithms on datasets of low sampling rates. The proposal brings high computational efficiency and accuracy of ST-Matching into the probabilistic world, hence giving it the ability to express confidence about its outputs. The measure of confidence is particularly important when dealing with traffic datasets of low accuracy. We validate the proposed algorithm on a range of GPS trajectories of varied quality to show that it has as high accuracy on low-frequency and noisy datasets as the original ST-Matching algorithm, yet with the added benefit of expressing beliefs about the quality of its output using probabilities.

Acknowledgements This work is part of the project - Crime, Policing and Citizenship (CPC): Space-Time Interactions of Dynamic Networks (www.ucl.ac.uk/cpc), supported by the UK Engineering and Physical Sciences Research Council (EP/J004197/1). The data provided by Metropolitan Police Service (London) are greatly appreciated.

References

Barber, D. (2012). *Bayesian reasoning and machine learning*. Cambridge: Cambridge University Press.

Bishop, C. M. (2006). *Pattern recognition and machine learning*. Berlin: Springer.

Brundson, C. (2007). Path estimation from GPS tracks. In *Proceedings of the 9th International Conference on GeoComputation*, National Centre for Geocomputation, Maynooth University.

Demšar, U., Buchin, K., Cagnacci, F., Safi, K., Speckmann, B., Van de Weghe, N., et al. (2015). Analysis and visualisation of movement: an interdisciplinary review. *Movement Ecology*, *3*(1), 5.

Goh, C. Y., Dauwels, J., Mitrovic, N., Asif, M. T., Oran, A., & Jaillet, P. (2012). Online map-matching based on Hidden Markov model for real-time traffic sensing applications. In *2012 15th International IEEE Conference on Intelligent Transportation Systems* (pp. 776–781). IEEE.

Gonzalez, H., Han, J., Li, X., Myslinska, M., & Sondag, J. P. (2007). Adaptive fastest path computation on a road network: a traffic mining approach. In *Proceedings of the 33rd International Conference on Very Large Data Bases* (pp. 794–805).

Jagadeesh, G. R., & Srikanthan, T. (2014). Robust real-time route inference from sparse vehicle position data. In *17th International IEEE Conference on Intelligent Transportation Systems (ITSC)* (pp. 296–301). IEEE.

Kowalska, K., Shawe-Taylor, J., & Longley, P. (2015). Data-driven modelling of police route choice. In *Proceedings of the 23rd GIS Research UK conference*.

Kühne, R., Schäfer, R.-P., Mikat, J., & Lorkowski, S. (2003). New approaches for traffic management in metropolitan areas. In *Proceedings of the 10th Symposium on Control in Transportation Systems*, Tokyo.

Li, Q., Zeng, Z., Zhang, T., Li, J., & Wu, Z. (2011). Path-finding through flexible hierarchical road networks: An experiential approach using taxi trajectory data. *International Journal of Applied Earth Observation and Geoinformation, 13*(1), 110–119.

Liao, L., Patterson, D. J., Fox, D., & Kautz, H. (2006). Building personal maps from GPS data. *Annals of the New York Academy of Sciences, 1093,* 249–265.

Lou, Y., Zhang, C., Zheng, Y., Xie, X., Wang, W., & Huang, Y. (2009). Map-matching for low-sampling-rate GPS trajectories. In *Proceedings of the 17th ACM SIGSPATIAL International Conference on Advances in Geographic Information Systems—GIS '09* (p. 352). New York, USA: ACM Press.

Newson, P., & Krumm, J. (2009). Hidden Markov map matching through noise and sparseness. In *Proceedings of the 17th ACM SIGSPATIAL International Conference on Advances in Geographic Information Systems—GIS '09* (p. 336). New York, USA: ACM Press.

Multilingual Sentiment Mapping Using Twitter, Open Source Tools, and Dictionary Based Machine Translation Approach

David Kocich

Abstract Online social networks are a popular communication tool for internet users. Millions of users share opinions on different aspects of everyday life. Therefore, microblogging websites are rich sources of data for opinion mining and sentiment analysis. Our current research based on the analysis of migration using various social networks required to implement a tool for automated multilingual analysis of sentiment from as many languages as possible. Usually, all available tools handle to work only with English written texts which are the most common on the social media. Few open source tools which can process French, German and Spanish texts exist too, but it is not optimal to reimplement and join different approaches together. Another requirement is the ability to process dynamic data streams and static historical datasets with high efficiency. Lesser accuracy and completeness of evaluated messages is acceptable as a counterweight for these general requirements. The paper presents sample data collection from Twitter for the opinion mining purposes. We perform multilingual sentiment analysis of the collected data and briefly explain experimental results. The analysis is made with the use of custom built solution utilising the AFINN-165 which is manually evaluated dictionary of English words. This dictionary was translated into other languages using Google Translate API that was tested during the process. It is then possible to determine positive, negative and neutral sentiment. Results of the research bring new insights, offer a possibility for wider use and allow optimisation of the wordlists/tool resulting in the better results of future research. Geospatial analysis of first experimental results undercovers interesting relation between time, location and a sentiment which enables readers to think of various use cases.

Keywords Sentiment analysis · Opinion mining · AFINN-165 · Twitter · Open source

D. Kocich (✉)
Institute of Geoinformatics, Faculty of Mining and Geology, VŠB-Technical University of Ostrava, 17. listopadu 15, 708 33 Ostrava-Poruba, Czech Republic
e-mail: David.Kocich@vsb.cz

I. Ivan et al. (eds.), *Dynamics in GIscience*, Lecture Notes in Geoinformation and Cartography, DOI 10.1007/978-3-319-61297-3_16

Introduction

Online social networks and internet media have become not only a new source of information for many people but also a new source of information about many people. Earlier it was common to share some private content (feelings, emotions, opinions) only personally, by phone or an email. Earlier it was common to use direct communication (talks, SMS, calls), but nowadays we share our personal life and opinions more over tweets, Facebook posts, Instagram photos, and through many other social networks. Users share stories, feelings, experience, things from everyday life and also various personal data. People often find these ways more useful for some reasons. In the case of Twitter, people do not realise that their content can is public and many aspects possibly analysed in different ways. Twitter offers free access to its data which are a subject of analysis in this research paper too. In some countries, tweets with mentions or Facebook posts also substitute the standard SMS because of expensive tariffs provided mobile operator. In Turkey, people are able and do not fear to overcome connectivity problems even if the network is banned (Letsch 2014), and they are willing to find a way to keep sharing actual content.

For the researchers and analytic teams, social networks are a rich source of information not only about our opinions and current mood. Users often share content together with a timestamp, current precise position and other metadata. Many people chat, discuss the latest news, post what are they doing and share everyday life and feelings over the social networks. This content is often public, sensitive and privacy can be an issue which should not be forgotten. The online social media sentiment analysis is not a new topic.

Bollen et al. (2011) describes that users could be divided into the two content camps—first group share information about themselves, the other one share mainly news and both groups express the mood state. Authors employ Profile and Mood States (POMS), which are usually used in psychology, and examine the six mental states (tension, depression, anger, vigour, fatigue and confusion). Biever (2010) describes a similar approach to predict stock markets. Another usual approach is classification into the two or three more general categories—positive, neutral, and negative (Mislove et al. 2010).

Usually, topics cover areas such as data processing and a creation of text corpus generally (Pak and Paroubek 2010) or corpus analysis with the aim to specific topics like flu and epidemic detection (Lampos et al. 2010) and detection of vulgar and offensive messages (Xiang et al. 2012). The majority of research papers utilise English as the only language of analysis with the result that multilingual analyses are often rare. In order to provide the best possible results, it is required to perfect wide spectrum of tasks. The description of problems, thoughtful analysis, and improvement of each one problematic language (Chinese, Japanese, Arabic) is required to enable performant sentiment analysis (Refaee and Rieser 2014). Errors caused by using automated approaches are often an issue. Optimisation of applied approaches or process of reducing errors for semantic analysis is advised to obtain

better results—e.g. by normalisation of words (Nguyen et al. 2015); completeness and precision improvements by utilising the multilingual sentiment mining with the graph-based pattern extraction from emotions (Saravia et al. 2016). At the end, there are issues such as irony in messages which is hard to recognise without any wider context. Sun et al. (2017) describes a complete review of techniques, use cases and tools for opinion mining and the optimisation of all related processes.

In our future research, which deals with the analysis, knowledge learning, prediction of global human mobility and migration patterns through different online social networks, we found it necessary to utilise an approach or a tool which can derive additional information from written content and enrich our analyses. For our solution, the tool should process data from different sources (database storage and dynamic online data streams), and offer good performance to be used with high volumes of data. It is required to use not computationally intensive approaches, so the vulnerable data streams are processed and stored without issues. Data stream processing has limitations in the number of data processing steps (usually only one or two) and in the process response time which needs to be low enough. In a case of delay, the number of incoming messages in memory will be raising, eventually fall over and cause errors.

The most straightforward approach is to adapt one of available (open-source) tools and implement a custom extension to handle required multilingual analysis. There are few libraries for sentiment analysis—the most favourite tool called simply Sentiment implements dictionary based approach (AFINN). This evaluated keyword list is originally a tab separated file distributed under Open Database License (ODbL) v1.0. The sentiment tool is customizable, and other available dictionaries are e.g. NRC Emotion Lexicon (non-commercial) and SentiWordNet (commercial). The adjustment of a sentiment library with the translation of AFINN dictionary enables to create a custom version of a solution and effectively perform multilingual sentiment analysis.

Several translating APIs and approaches to implement the sentiment analysis tool were reviewed. It is required to address the discussion about the impact of mismatch using the automated machine translation approaches (Google, Bing, and other translation APIs). Duh et al. (2011) presented the result of an experiment which confirms that both instance and labelling mismatch occur, but labelling mismatch is not a factor in performance degradation. Authors estimated the translation error rate to 24%, and after the manual validation, only 4% of English-Japanese translations were classified as sentimentally incorrect (with negated value). Remaining words usually have no sentiment difference (person vs. human). Authors of the study performed manual verification test of the translations meaning on one of the most complicated language pairs still with satisfactory results. First versions of the Google Translate API utilised the machine translation system using the rule-based translation approach. This practically means that it was necessary to store relations between each pair of translations for every available different language which was inefficient. Later on, translations were processed with the statistical approaches and phrase-based system (Koehn et al. 2003). During the September 2016, Google implemented the translate API with neural networks to

improve text translations to perfection. The GNMT (Google Neural Machine Translation system) achieves by an average 60% fewer errors compared to the previously used phrase-based production system (Wu et al. 2016), which thus allows wider use and provides better translations. We choose to use Google Translate API because it offers the most advanced solution nowadays and a satisfactory error rate presented (Duh et al. 2011) is acceptable for our solution. Latest improvement of the Google Translate API together with the availability of many languages helped with the decision to implement the multilingual sentiment analysis tool using machine translation approach.

For the preview of a method and tool in this research paper, we analyse one-day sample Twitter dataset containing localised tweets from the whole world. With all the available texts posted online by the users, the raising amount of localised information available on various social networks, an advance of computational technology, it is further possible to examine relations between sentiment, emotions, time, location and other properties. Pánek and Benediktsson (2017) proves that emotional maps are demanded and useful for further analysis and usability on municipal offices, strategic and city planning, police departments, tourism, and real estate market. Results can be used in various ways but still, this topic is most popular within academia (Hauthal and Burghardt 2016). Nowadays, the cities are being instrumented with the infrastructure that enables real-time analysis of city life (Kitchin 2014) and it can be expected that the described automated techniques of extraction from user generated content are going to be more interconnected with data collected by questioners and web platforms in the future. This trend will provide better results of analyses and thereby more informed and quality life to the citizens.

Contributions and Organisation

The main contributions of this research paper are:

- Description of common characteristics and problems of the sample Twitter dataset which can be found in chapter “Sample Twitter dataset”.
- Preview of an effective tool for automatic multilingual evaluation of the sentiment from input texts and an approach to the online/offline large scale geospatial sentiment/emotional mapping—more in section “The sentiment analysis tool and keywords dictionary”.
- Description of an approach to automatic wordlist translation to other world’s languages is available in chapter “Google translate API”.
- Experimental results of the text analysis, description of connected problems, and visualisation using the sentiment data aggregated to the country level.
- Results of the research (tools and translated dictionaries) were published as open source and are further optimised and developed.

Data Manipulation and Processing

Sample Twitter Dataset

Social networks and other high-volume sources of data are often problematic because of their uncertainty. With our custom developed open-source tool named *Twitter-smart-geo-stream* it was able to collect the sample of data from the Twitter Streaming API. The tool offers customization of whole Twitter Stream download process together with many possibilities of automated data stream processing. It is possible to easily handle tasks such as setup of the connection, storage databases, filtering parameters to collect only relevant data (by source devices, check for spam by the amount of content and variance of localisation), data validity control, improvement of irregularities, data compression and direct creation of derived datasets.

This collection is one day sample of approximately 5.5 million of tweets localised worldwide. Acquisition date of the collection is 29.2.2016, and all tweets contain UTC timestamp together with metadata about the user. Around 85% of the data on Twitter is geolocated at least to the municipal level, and the remaining 15% to the precision of GPS device. Localisation contains metadata about POI or administrative area (Kocich and Horák 2016). The common problem is that the users do not have to write about the location of which they published a tweet. Often, they share content about a different place, and we usually can't easily detect and distinct between these two cases. However, for part of the messages, the geoparsing of the input text can be used to detect more about geolocation of the emotions. This text encoded localisation can be direct (providing a unique name of the place) or indirect (500 m west from the town square) (Horák et al. 2011).

Messages send by the users all over the world are automatically tagged by the used language, and this information is sent with the other tweet metadata. However, this information does not have to be correct every time and can cause an inaccuracy in the estimation of sentiment value. Tweets usually contain text together with hashtags (#topic), mentions (@name), retweets, URL links, media (images, videos), emoticons, punctuations and repeating characters which all have to be processed properly to evaluate the sentiment value. There are over several hundred source applications (desktop, mobile, IoT devices, connected accounts on other social networks) posting to Twitter. It is possible to analyse further part of tweets based on the written content and enrich the context of the published message for better interpretation of the user's mood deviation.

The Sentiment Analysis Tool and Keywords Dictionary

American MIT MediaLab develops open source library called Sentiment which enables to evaluate sentiment value in various English written texts. The tool

depends on the NodeJS JavaScript V8 engine which has an architecture that allows asynchronous processing. This library is primarily designed for performance and depending on the used hardware. It handles to evaluate up to around 550,000 short texts (per one computing instance) in a second which is double the amount compared to the second most popular NodeJS sentiment analysis library. The evaluation process counts token words and their preassigned weight. This tool utilised AFINN-111 (created in 2011) as a keyword dictionary recently. During the year 2016 it changed, and now the source data for sentiment analysis are from the AFINN-165 dictionary. This improved version of the wordlist contains 3382 words which are manually evaluated and ranked on the scale from −5 to +5 (Nielsen 2011).

The result of a text analysis is an overall sum of each word's value (described as a "score") or score divided by the number of words in the message (described as "comparative"). The result can be neutral if both words labelled as positive and negative are in the text. This can be shown on the result of an example analysis of a text "Traffic jam is stupid", which looks like following:

$$\left(\{\textbf{tokens}:[\text{'traffic'},\text{'jam'},\text{'is'},\text{'stupid'}],\text{words}:[\text{'stupid'}],\text{score}:-2,\text{comparative}:-0.5,\right.$$
$$\left.\text{positive}:[],\text{negative}:[\text{'stupid'}]\}\right).$$

The major advantage of the tool is performance and that there is no need to store and configure any external database. The build/update process of custom keyword lists is an adequately easy task. Users have the ability to append and overwrite word-value pairs from the AFINN dictionary which offers higher modularity of the tool. It is possible to validate further, rebuild and improve the multilingual wordlists.

A new latest version of the sentiment tool enables to use also the sentiment analysis of the emoticons in the text and possibility to invert the sentiment value when negatives are used (evaluates "pretty" as positive and "not pretty" as negative). Other dictionaries can, of course, provide different results.

Google Translate API

Google offered the Google Translate API for free to the year 2011, but because of high usage, Google decided to make it available only for paying customers. The access keys restrict access to the API, and the translation or language detection of 1 million characters cost 20 dollars nowadays. Regular customers have limited translation 2 million characters each day and 100,000 characters per each 100 s. Advanced customers can buy elevated limits. Google does not apply any copyrights to the translated text, although it bans the usage of a service to the creation of similar translating solutions and its optimisation. The Google Translate API enables to translate English to 104 other different languages (Google 2016). Full and up to

date list is available in the API documentation. The translate API responds on two types of requests which are:

- the information about currently available languages to translate from required source language set as a request parameter (mainly used for automation of translating processes)
- Translation of a word/phrase (or list of separate phrases) from source language to another.

Results

By the analysis of our sample one day data collection, it was possible to detect messages in totally of 62 different languages sent from all over the world. There were two additional categories which were described by the attribute UND (abbreviation of "undefined") and second by the empty string value of the language identifier. Altogether there were approximately around 15% of unidentified tweet messages in our collection, and it is unknown why these two categories are not as labelled as one. There were also several language codes which were not available to process using the Google Translate API. These language codes are CKB (Sorani Kurdish), BO (Tibetan) and few other unidentified codes which are probably errors because they are not available in any version of the ISO-639 standard which defines language representation. Part of the unidentified and unlabelled tweet messages contain only URL addresses, emoticons and media files (photos, videos) without any text comment which makes it impossible to categorise.

As can be seen from the figure showing a distribution of tweets per language (Fig. 1), the occurrence of languages in published tweets has an exponential function and approx. 80% of messages are written in 20% of languages (Pareto principle). Fifteen languages with less than 100 occurrences were hidden. The only extraordinary case is the Chinese language (with 0.1% of use in a total), but that we explain by the restriction of access to Twitter and availability of alternative Chinese social networks (WeChat, RenRen, Weibo). Similar nationwide blocking of access to Twitter (and other social networks) did take place in Turkey also where, on the other hand, the social network experienced, even more, users connected through VPN (Letsch 2014). The availability of almost the same size or popular alternatives can be the main factor why people do not use Twitter.

A recent version of freely published and used AFFIN-165 dictionary was translated to 102 languages available by the Google Translate API at the time of conducting the research. For completeness, totally 153 world languages are listed in the ISO-639-1. For an unknown reason, it was not repeatedly possible to translate into the Icelandic (IS) and Taiwanese Mandarin (ZH-TW) languages. The API possibly experienced a temporal error, and it returned only empty or error response messages for these languages. The translation process was vulnerable to several

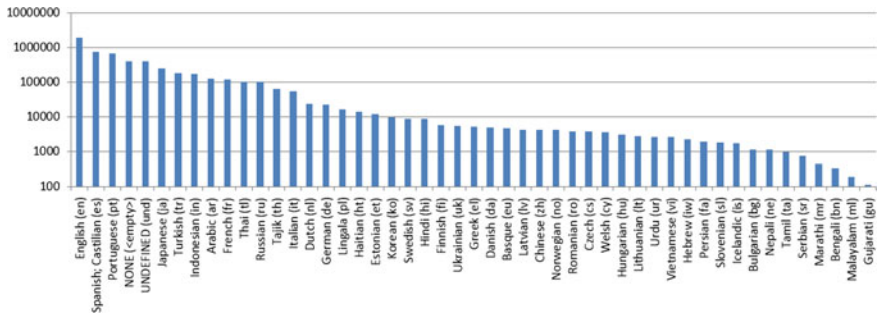

Fig. 1 Frequency of used languages in the sample Twitter dataset

problems which impacted overall quality and completeness of translated dictionaries:

- Occasionally, some of the translations were returned from the API as undefined—there are no translations for words that look correct in English. This problem is subject to manual control and corrections by translators.
- Sometimes the translations of the word are exactly same also in different languages—it is often a case of not frequently used, artificial words and abbreviations of the common, well-known English phrases (e.g. OMG, LOL). In the case of words, it is an API mistake, and in the case of abbreviations, it is discussable which equivalent abbreviation is used in the language for the phrase representing the same meaning. These abbreviations can be both the same in other language or completely different (by the words of the foreign language).
- API returns only one option for each translation which should be the most optimal one which results that some words (nice, pretty, beautiful, good looking) are all translated to a single word (schön in German) which leads to the reduction of unique words contained in other dictionaries. These words usually have the slightly different meaning and associated sentiment score than the one currently paired with the translated word.

The original English AFINN contains 3382 unique words and the other languages from 2166 to 3229. From a view to the language variety, the richest languages are Uzbek, Indonesian, Maori and the poorest are Corsican, Zulu, and Yiddish. The higher number of translated words may have a positive impact on a ratio of evaluated messages and the precision of the estimated sentiment value. Any further improvement of the translated results will be utilised using the crowdsourced approaches (using e.g. Amazon Mechanical Turk, Transifex, Pootle). Future improvement requires establishing the set of evaluated sentences (Kotzias et al. 2015) to validate the accuracy of current translations and to prioritise the translations improvement for languages with the lowest credibility.

The next step of the analysis was to analyse sentiment value from the sample dataset. For a first preliminary preview of tool functionality, the analysis results are

currently presented as aggregated to the country level. Country codes can be interpreted using the ISO 3166-1 alpha-2 international country code standard. Figure 2 shows the results of an analysis ordered by the percentage of tweets tagged as positive. The messages were written in any language within the boundaries of each country. Countries with less than 1000 tweets were removed from the chart for readability purposes. Cases with many tweet occurrences were mainly small island countries with high touristic activity. Due to the attractiveness of these places and low amount of published tweets, the positivity of messages was between 40 and 80%. A high percentage of neutrally evaluated tweets can be explained by the errors with parsing of special characters in the text (Arabic, Chinese). Languages with a high value of texts evaluated as neutral suggest that wordlist correction should be done for the main languages used in the given country. Overall higher prevalence of positive tweets (80%) can be possibly explained by the fact that the users usually share positive posts and only occasionally anything that is sad (Hauthal and Burghardt 2015).

By the estimation of a difference between positive and negative tweets, we can present total happiness around the world (Fig. 3). The countries that have the biggest positive/negative difference are India, Canada, Great Britain, Ireland, Zambia, Australia, and the Philippines. Some countries (Kenya, New Zealand, Ghana) have less than 10,000 tweets published and though results have smaller credibility.

Map visualisation presented in the Fig. 4 undercovers the sentiment in specific parts of the world which correlate with the major global events during the examined period (29 February 2016). Countries with less than 1000 evaluated tweets were excluded. In more countries, the social media users have more positive sentiment than negative, and according to the experimental analysis of aggregated country

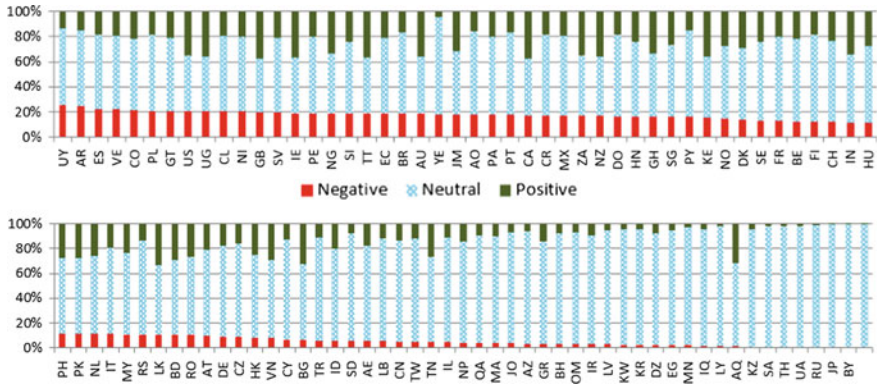

Fig. 2 Countries presented by the percentage of negative, neutral, and negative sentiment in tweets

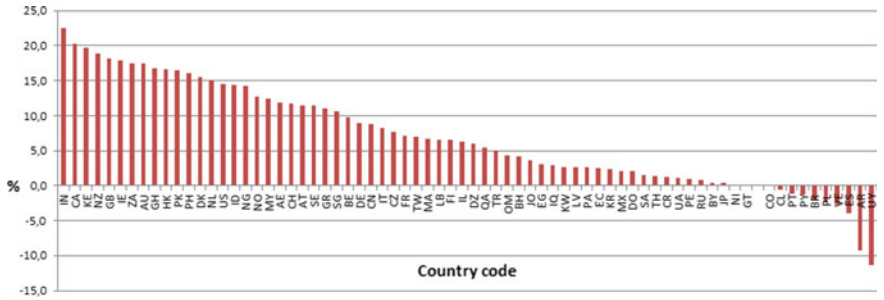

Fig. 3 Difference between Positive-negative messages in each country

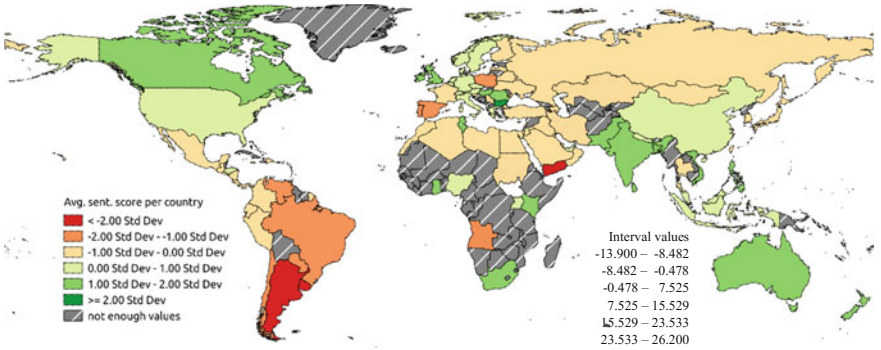

Fig. 4 Visualisation of the difference between positive and negative messages over the world

level data, there are more countries with happy inhabitants than the sad ones. There are some exceptions in the overall more positive sentiment over the world. Some of them can be explained by the global historical events influencing the activity on social networks, news and media. During February, the main topic in the South America was the outbreak of a Zika virus. In Yemen, the civil war started in 2015 and continued lasting at the time of data sample collection.

However, from a geographical perspective, local or regional aspects play a significant role too and it demands further analysis to explore and understand evolution and all causes of the current trend. The next and more detailed analysis concerns the two sample cities—London with 6500 analysed tweets (Fig. 7) and New York 5700 analysed tweets (Fig. 8) collected in one day. The dimensions of the hexagon cell in London are doubled compared to New York because of the larger area of London city. The cell size in the hexagonal grid was adjusted to cover the area continuously and to provide enough points which were used to count an

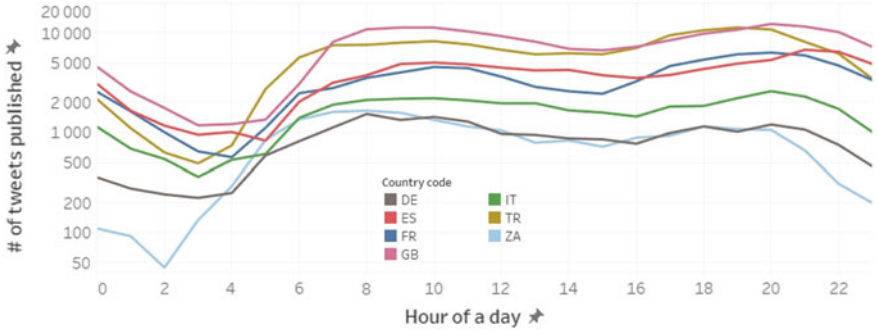

Fig. 5 Overall frequency of tweeting activity in selected countries per hour of a day

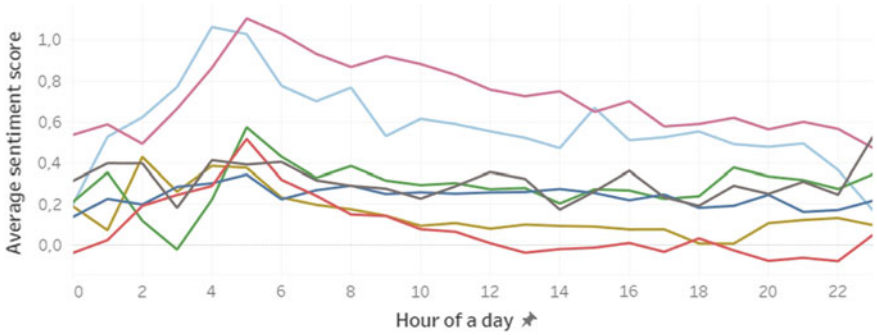

Fig. 6 The average sentiment score of all messages in selected countries per hour of a day

average sentiment score of a cell. After the visual evaluation of the analysis, in both cities, the sentimentally negative areas are concentrated on the city edges. In the case of Manhattan, there is a visible cluster of green (positive) hexagons around Columbia University and Central Park. On the other side, the Harlem neighbourhood with high poverty and crime is overlaid by the cluster of red (negative) messages.

There are no significant differences (Fig. 5) in the dynamics of the tweeting activity between different countries however there is a rapid improvement of the average sentiment score around morning hours (Fig. 6) which was caused mainly by the people being happy with the results of the Oscar awards that were held the previous evening (Figs. 7 and 8).

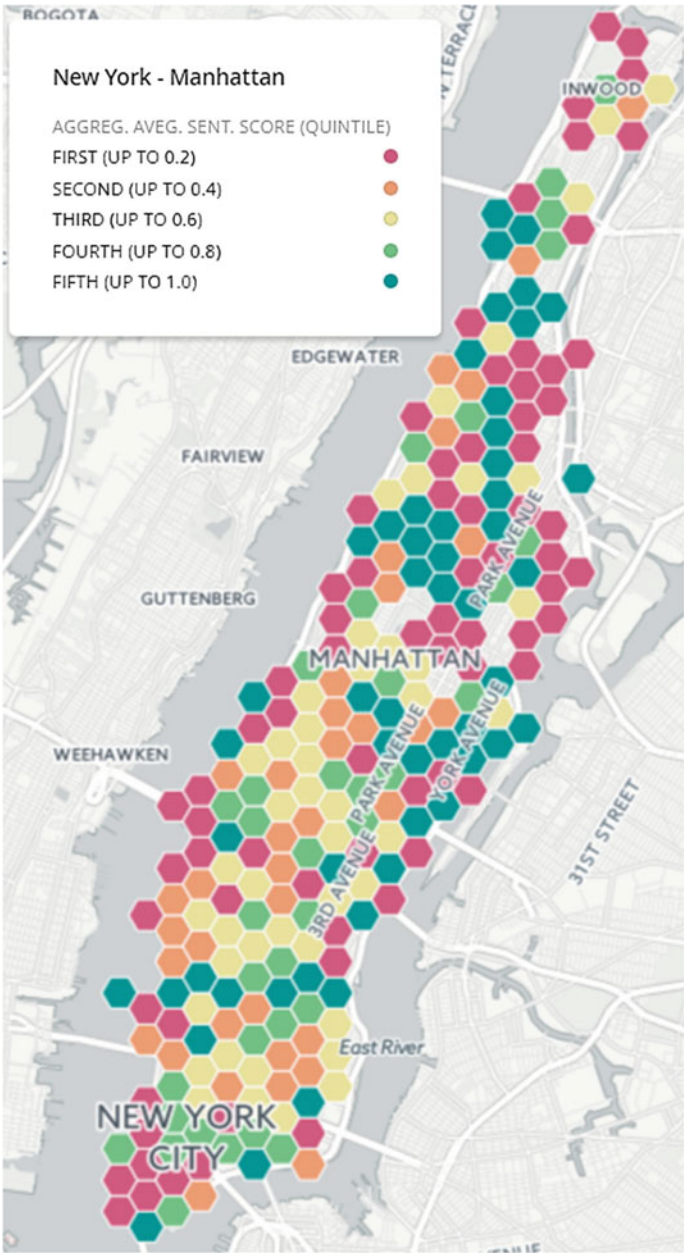

Fig. 7 New York—average sentiment score analysis using hexagonal grid method

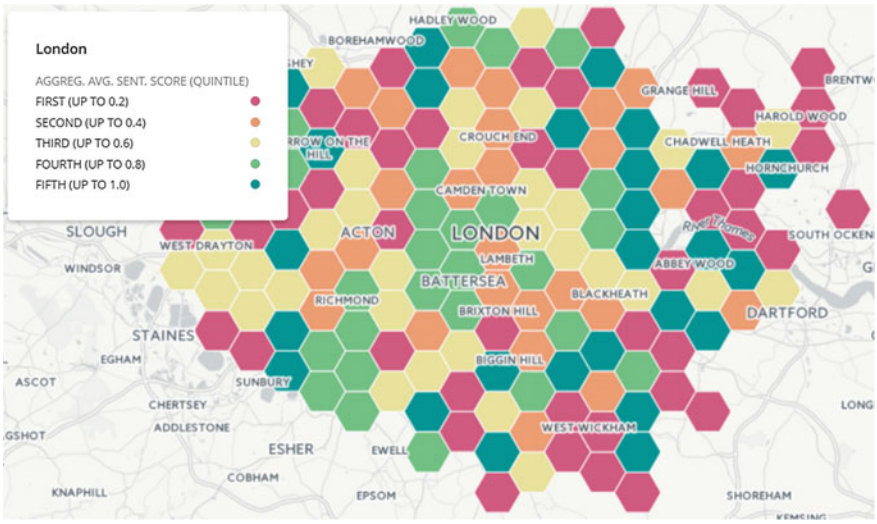

Fig. 8 London—average sentiment score analysis using Hexagonal grid method

Conclusion and Discussion

Microblogging on social networks nowadays became one of the major types of the communication. A huge amount of information contained in microblogging websites makes them an attractive source of data for opinion mining and sentiment analysis.

The main purpose of this article is to describe the process and implementation of automatic sentiment evaluation from more than 100 languages using the data from online social networks. Despite the revealed issues, the results are fulfilling our current needs which were described in the introduction and there was no need to reimplement and connect many different solutions. This research led to the contribution to the available open source tool sentiment which is an efficient and modular solution for sentiment analysis. First evaluations prove that proposed tool and techniques are efficient on both static data and dynamic data streams. The possible sources of data for the tool are online social media or any other written texts. The used experimental dataset is presented to show first experimental results (Google API performance; results of sentiment analysis; geospatial analysis with both data aggregated globally and on the municipal level for London and New York using aggregation to the hexagonal grid). The outcome of this research enables to further analyse localised emotions of the crowd on small, medium and large aerial scale levels. Research of the can ask questions such as if and how the worldwide and continental events (elections, Olympic Games, financial crisis, wars) impact on the emotions of people (or only certain minorities) in some region and specific period. Explanation of various phenomena can be done by incorporation a database

of events (e.g. GDELP project containing around 300 categories of localised events). Further analysis of correctly filtered long-term data collections can provide better insights, correlations, and understanding with e.g. crime or various socio-economic factors (Ivan et al. 2016). There is also space to examine the impact of natural events (weather changes, storms, tornadoes, drought, and floods) influence the mood. The research on a city or regional scale can be valuable mainly in multicultural cities and further used by the local decision makers.

We continue with long-term data collections from a data stream, periodical collections and historical data exports from various social networks. The outlook of the research topic can include optimisation of sentiment analysis process, possibly an interdisciplinary research, and geospatial analysis in the higher level of detail with the aim to certain phenomena and its spatiotemporal patterns. Currently, there is web platform under development which enables to visualise and examine aggregated sentiment of the social media users interactively.

Acknowledgements The research is supported by the VŠB-Technical University of Ostrava, the Faculty of Mining and Geology, grant project Crowdsourced geodata, No. SP2016/41. Access to computing and storage facilities owned by parties and projects contributing to the National Grid Infrastructure MetaCentrum provided under the programme "Projects of Projects of Large Research, Development, and Innovations Infrastructures" (CESNET LM2015042), is greatly appreciated.

Supplementary Materials

Translated AFINN165 dictionary and customized version of sentiment library are available online on Github (dkocich/afinn-165-multilingual, dkocich/sentiment) (Kocich 2017).

References

Biever, C. (2010). Twitter mood maps reveal emotional states of America. *New Scientist, 207,* 14. doi:10.1016/S0262-4079(10)61833-7

Bollen, J., Mao, H., & Pepe, A. (2011). Modeling public mood and emotion: Twitter sentiment and socio-economic phenomena. *ICWSM, 11,* 450–453.

Duh, K., Fujino, A., & Nagata, M. (2011). Is machine translation ripe for cross-lingual sentiment classification? In *Proceedings of the 49th Annual Meeting of the Association for Computational Linguistics: Human Language Technologies*, *HLT '11*, Short Papers (Vol. 2, pp. 429–433). Stroudsburg, PA, USA: Association for Computational Linguistics.

Google. (2016). *Google translate API—Fast dynamic localization | google cloud platform* [WWW Document]. Google Dev. URL:https://cloud.google.com/translate/. Accessed 6.20.16.

Hauthal, E., & Burghardt, D. (2015). *Temporal occurrence and time-dependency of georeferenced emotions extracted from user-generated content*. Presented at the 18th AGILE International Conference on Geographic Information Science, Lisbon.

Hauthal, E., & Burghardt, D. (2016). Mapping space-related emotions out of user-generated photo metadata considering grammatical issues. *The Cartographic Journal, 53,* 78–90. doi:10.1179/1743277414Y.0000000094

Horák, J., Belaj, P., Ivan, I., Nemec, P., Ardielli, J., & Růžička, J. (2011). Geoparsing of Czech RSS news and evaluation of its spatial distribution. In R. Katarzyniak, T.-F. Chiu, C.-F. Hong, & N. T. Nguyen (Eds.), *Semantic methods for knowledge management and communication, studies in computational intelligence* (pp. 353–367). Berlin, Heidelberg: Springer.

Ivan, I., Kocich, D., & Horák, J. (2016). Identification of crime environmental factors based on spatial human data integration. In: *SGEM Conference Proceedings*, *Presented at the SGEM 2016 : 16th International Multidisciplinary Scientific Geoconference* (Book2 Vol. 1, pp. 697–704), Albena, Bulgaria. doi:10.5593/SGEM2016/B21/S08.087

Kitchin, R. (2014). The real-time city? Big data and smart urbanism. *GeoJournal, 79,* 1–14. doi:10.1007/s10708-013-9516-8

Kocich, D. (2017). Afinn-165-multilingual [online]. Available from: https://github.com/dkocich/afinn-165-multilingual

Kocich, D., & Horák, J. (2016). Twitter as a source of big spatial data. In *SGEM Conference Proceedings, Presented at the SGEM 2016 : 16th international multidisciplinary scientific geoconference* (Book2 Vol. 1, pp. 921–928). Albena, Bulgaria. doi:10.5593/SGEM2016/B21/S08.116

Koehn, P., Och, F.J., & Marcu, D. (2003). Statistical phrase-based translation. In *Proceedings of the 2003 Conference of the North American Chapter of the Association for Computational Linguistics on Human Language Technology—Volume 1*, *NAACL '03* (pp. 48–54). Stroudsburg, PA, USA: Association for Computational Linguistics. doi:10.3115/1073445.1073462

Kotzias, D., Denil, M., de Freitas, N., & Smyth, P. (2015). From group to individual labels using deep features. In *Proceedings of the 21th ACM SIGKDD International Conference on Knowledge Discovery and Data Mining, KDD '15* (pp. 597–606). New York, NY, USA: ACM. doi:10.1145/2783258.2783380

Lampos, V., Bie, T. D., & Cristianini, N. (2010). Flu detector—Tracking epidemics on twitter. In J. L. Balcázar, F. Bonchi, A. Gionis, & M. Sebag (Eds.), *Machine learning and knowledge discovery in databases* (pp. 599–602)., Lecture Notes in Computer Science Berlin Heidelberg: Springer.

Letsch, C. (2014). Turkey twitter users flout Erdogan ban on micro-blogging site. *The Guardian*, *21*.

Mislove, A., Lehmann, S., Ahn, Y.-Y., Onnela, J.-P., & Rosenquist, J.N. (2010). *Pulse of the nation: U.S. mood throughout the day inferred from twitter* [WWW Document]. URL:http://www.ccs.neu.edu/home/amislove/twittermood/. Accessed 7.1.16.

Nguyen, V. H., Nguyen, H. T., & Snasel, V. (2015). Normalization of vietnamese tweets on twitter. In A. Abraham, X. H. Jiang, V. Snášel, & J.-S. Pan (Eds.), *Intelligent data analysis and applications, Advances in intelligent systems and computing* (pp. 179–189). Berlin: Springer International Publishing.

Nielsen, F.Å. (2011). A new ANEW: Evaluation of a word list for sentiment analysis in microblogs. ArXiv: 11032903 Cs.

Pak, A., & Paroubek, P. (2010). Twitter as a corpus for sentiment analysis and opinion mining. In *LREc* (pp. 1320–1326).

Pánek, J., & Benediktsson, K. (2017). Emotional mapping and its participatory potential: Opinions about cycling conditions in Reykjavík, Iceland. *Cities, 61,* 65–73. doi:10.1016/j.cities.2016.11.005

Refaee, E., & Rieser, V. (2014). An arabic twitter corpus for subjectivity and sentiment analysis. In *LREC* (pp. 2268–2273).

Saravia, E., Argueta, C., & Chen, Y.-S. (2016). Unsupervised graph-based pattern extraction for multilingual emotion classification. *Social Network Analysis and Mining, 6,* 92. doi:10.1007/s13278-016-0403-4

Sun, S., Luo, C., & Chen, J. (2017). A review of natural language processing techniques for opinion mining systems. *Information Fusion, 36,* 10–25. doi:10.1016/j.inffus.2016.10.004

Wu, Y., Schuster, M., Chen, Z., Le, Q.V., Norouzi, M., Macherey, W., et al. (2016). Google's neural machine translation system: bridging the gap between human and machine translation. ArXiv: 160908144 Cs.

Xiang, G., Fan, B., Wang, L., Hong, J., & Rose, C. (2012). Detecting offensive tweets via topical feature discovery over a large scale twitter corpus. In *Proceedings of the 21st ACM International Conference on Information and Knowledge Management, CIKM '12* (pp. 1980–1984). New York, NY, USA: ACM. doi:10.1145/2396761.2398556

Dynamic Zoning in the Course of GIS-Based Football Game Analysis

Gilbert Kotzbek and Wolfgang Kainz

Abstract This paper is one of a series of articles about GIS-based game analysis in association football and presents an approach to *dynamic zoning* of football pitches based upon the players' movements. For this purpose, tracking data are employed, which were kindly provided by *ProzoneSports*. Since football is highly dynamic, spaces are constantly changing over the entire game's period. Therefore, it is reasonable to capture these alterations in the team's use of space and to analyse them. In order to do so a *Python* script which automatically trisects the pitch vertically in a defenders', midfielders', and forwards' zone was developed. It can be executed as a custom tool in *ArcGIS* and determines the zones' height, width and area. Furthermore, its functionality can be considered the basis for manifold analysis opportunities. To provide an example, in the paper's second part another custom tool for *ArcGIS* is presented, which applies the conception of *dynamic zoning* for analysing the teams' offensive qualities based upon the defenders' zone's vertical height. This paper's overall objective is to highlight the benefits of *dynamic zoning* in the course of football game analyses. Moreover, the demonstration of the tools' functionality is intended to foster the discussion about the presented conception's methodological principles as well as its potential application areas. In addition to this, an expert survey was conducted interviewing professional game analysts from Austria and Germany. The results provide evidence that the conception of *dynamic zoning* is worth to refine, as it provides a novel approach of analysing the game.

Keywords GIS-based football game analysis · Geographical information systems (GIS) · Sports analytics · Dynamic zoning · ProzoneSports

G. Kotzbek (✉) · W. Kainz
Department of Geography and Regional Research,
Faculty of Earth Sciences, Geography and Astronomy,
University of Vienna, Universitätsstraße 7, 1010 Vienna, Austria
e-mail: gilbert.kotzbek@univie.ac.at

W. Kainz
e-mail: wolfgang.kainz@univie.ac.at

I. Ivan et al. (eds.), *Dynamics in GIscience*, Lecture Notes in Geoinformation and Cartography, DOI 10.1007/978-3-319-61297-3_17

Prologue and Introduction

This paper was written in the context of the author's doctoral thesis (Kotzbek 2017), which examined the practicability of GIS in the course of football game analyses. Besides a brief overview of the project's main issues and aims (Kotzbek and Kainz 2014, 2015a) the data provided by *ProzoneSports* was reviewed, classified (Kotzbek and Kainz 2015b), and an approach towards automated GIS-based analysis of scoring attempt patterns was presented so far (Kotzbek and Kainz 2016). In general, analysing football games demands the zoning of the pitch if the game's spatiotemporal components should be taken into account appropriately. For this purpose, static analysis zones such as the common pitch's vertical trisection are utilised. However, the pitch is also spatially segmented by default according to the FIFA's Law of the Game (Fédération Internationale de Football Association 2016). In addition to fictional analysis zones, the predefined pitch zones are marked and hence visible. Moreover, they can be also applied for a wide range of spatial analyses.

As space is crucial in football, knowledge about where something happened during the game is of great importance because only then the question why something happened can be answered. Furthermore, if the causes of certain circumstances are known one might be able to control or influence comparable situations in the future. Concerning this, the spatial classification of game relevant actions as well as the observation of the ever-changing teams' occupied areas is appropriate. In this context, the utilisation of the pitch's default segments might be decent for some purposes but is definitely limited. Therefore, analytical zonings are often applied and selected in dependence upon the particular issue.

A review of the literature addressing this topic is unsatisfactory. The vast majority of contributions focus on other aspects and cover the utilised zoning alternatives only marginally. Moreover, almost all of them are static and hence lack flexibility. In regard of this, Fig. 1 exemplarily illustrates six different zoning options, which have been applied in previous studies. In comparison to each other, option *b* is of particular interest as it is the only model that features zones that are based on tactical position roles (Di Salvo et al. 2007), whereas almost the rest is aligned along the predefined pitch lines except for option *c* (Lucey et al. 2012). Notwithstanding this the zonings' fields of application vary. For example, Clayton (2011) applied option *f* supplementary to option *d* for analysing attacks within the foremost attacking zone. A similar variation to *d* is option *a* which divides the central pitch area more consistently. This approach was utilised by Pollard and Reep (1997) to evaluate the effectiveness of the teams' strategy. Furthermore, option *e* was employed by Cotta et al. (2013) in order to analyse passing networks. In contrast to these zonings, Lucey et al. (2012) consistently segmented the pitch in equally large rectangles irrespective of its predefined marking lines in order to analyse passing sequences.

Whether a zoning alternative is practicable or not depends on the purpose of its application. Hence, an evaluation of different zoning alternatives is not intended in the course of this study. Instead of this, this article's main objective is to highlight

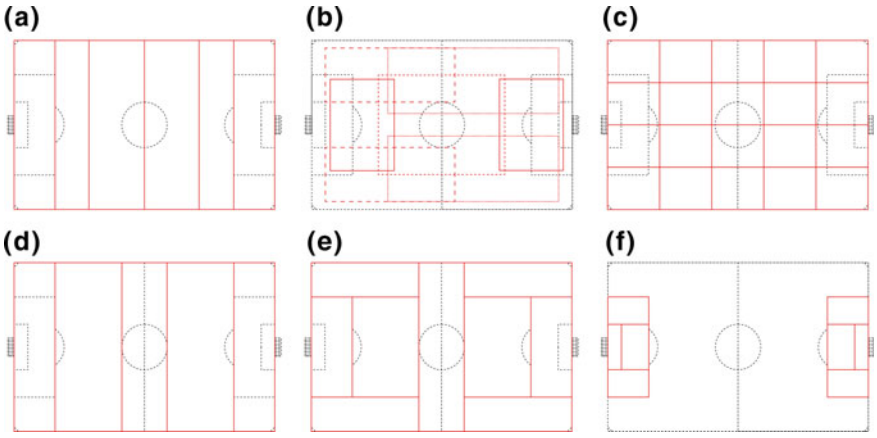

Fig. 1 Common zoning alternatives. *Source* Pollard and Reep (1997) (**a**), Di Salvo et al. (2007) (**b**), Lucey et al. (2012) (**c**), Clayton (2011) (**d**), Cotta et al. (2013) (**e**), Clayton (2011) (**f**)

the benefits of *dynamic zoning* in the course of football game analyses. Since football is not static, it is worthwhile to consider dynamic alternatives. In this context, evidence is provided by Vilar et al. (2013) who demonstrated an approach towards dynamic segmentation of the teams' occupied areas and defined it as convex hulls around the outfield players. Based on this, numerical dominance was analysed.

In contrast to this local zoning, a global approach encompassing the entire pitch is presented in this paper. In practical terms a custom tool for *ArcGIS for Desktop 10.x* named *Dynamic Zoning* was developed. It is based on *Python* and automatically trisects the pitch's area based upon the players' changing positions. The tool's outcome consists of three zones for each team, which together cover the whole pitch and represent the areas of the teams' defenders, midfielders and forwards at a given moment. Although this tool's functionality covers the basic conception of *dynamic zoning* only, it can be considered as the basis for manifold analysis opportunities. In order to provide an example of the conception's practical application, another *ArcGIS* custom tool for the determination of the teams' offensive qualities is also described. Moreover, the conception's practicability and the tools' applicability in the course of game analyses were evaluated by professional game analysts from Austria and Germany. Concerning this an expert survey was conducted, which was assessed conducting a multi-level content analysis.

The rest of this paper is organised as follows: First, the applied data is briefly outlined. Then the conception of *dynamic zoning* in general as well as the *Dynamic Zoning* tool in particular are described in the paper's first main part. In its second part, the *Analyse Offensive Qualities* tool is presented. Since the tools' code are too extensive to display, both tools are described in as much detail as possible, including their input parameters and their functionality. Afterwards, the expert

survey's design as well as the experts' feedback are concisely summarised. Finally, this paper is concluded in its last chapter, whereby not only the benefits of *dynamic zoning* but also suggestions for the tools' improvements are discussed.

A Brief Overview on the Data and the Systems Applied

Although football-specific geo data consists of event and tracking data, the application of the latter were necessary only in the course of this study. It represents the players' and the ball's movement, constantly gathered with 10 fps as consecutive point data (Kotzbek and Kainz 2015b). Owing to this recording rate far more than a million single tracking data points are provided for one game only. As each point is equipped with a *time stamp* and *frame* the process of *dynamic zoning* can be conducted for every tenth of a second.

The data was provided by *ProzoneSports*, the European market leader (Castellano et al. 2014) that recently joined forces with the US company *STATS* (STATS Sports Data Company 2016). The characteristics of tracking data are applicable to the data definition of both Mitchell (2009) as well as Zeiler and Murphy (2010) and hence can be described as point features whose appearance is time-dependent. Besides this, referring to Dodge et al. (2008) to classify the data as *Moving Point Objects* (MPO) is also appropriate.

Its spatial information is provided as X/Y-coordinates based on a local spatial reference system, and its origin is located at the pitch's centre. Although *ProzoneSports'* data spatially refers to the international standardised pitch size of 105 m × 68 m and hence minor inaccuracies due to scaling are possible, several studies indicate that the tracking data's spatial accuracy is sufficient for analysis purposes (Di Salvo et al. 2006, 2009; O'Donoghue and Robinson 2009).

Since the data is usually provided as xml files, it is necessary to prepare them in a GIS appropriate manner. For this purpose, the so called *Match Data Preparation* tool was developed. It automatically converts the raw data to point feature classes (FC), separated into tracking objects as well as half time and arranges them within feature datasets (FDS) located in a file geo database (GDB). Moreover, a pitch composed of point, line and polygon FCs can be created optionally. As this tool's functionality was already demonstrated (Kotzbek and Kainz 2015b), detailed information about it are omitted here. As the process of *dynamic zoning* requires team specific FCs which attributively contain the players' tactical positions, two additional tools have to be executed in advance in order to update the game's GDB. Whilst the *Add Formation Index* tool classifies the players as goalkeepers, defenders, midfielders and forwards based upon their tactical positions stored within the FCs' names, the *Team Merge* tool, merges the single tracking FC according to their *Team ID* (Kotzbek 2017).

ArcGIS for Desktop 10.4 for Desktop—Background Geoprocessing 64 Bit developed by *Esri* was applied for this study's purposes not only because it is a robust and well documented GIS, but also owing to the author's long-term practical experience with it. Notwithstanding this, it is assumed, that other GIS such as *QGIS*

for instance are also suitable for analysing football games in general. As *Python* is preferred by *Esri* (Zandbergen 2010) it was reasonable to apply it for the development of game analysis tools. However, the tools' target group composed of professional game analysts might not be familiar with executing *Python* scripts. Hence, the scripts are prepared as custom tools for *ArcGIS* providing the users with a graphical user interface (GUI) in form of tool dialog boxes (TDB) which are more accessible and intuitive. Furthermore, custom tools can be combined to geoprocessing packages, and their distribution can therefore be considered straightforward.

In the course of this study the utilised computer system was based on a Windows 7 64 Bit OS with 8 GB RAM and an Intel® Core™ i5-3470 CPU with 3.2 GHz. This information has to be taken into account when interpreting the tool's performance.

Part I: The Conception of Dynamic Zoning and Its Implementation

In general, this first approach towards *dynamic zoning* is based upon the defenders' and forwards' average X-coordinates, whose axes are parallel to the pitch's side lines. These thresholds can be determined for either period of time or a specific time stamp and divide the pitch vertically in a *defending*, *central* and *attacking zone*. Arithmetic averaging was applied as a compromise because it is considered more robust towards the tactical zones' random coalescence. For instance, employing the foremost position might be critical in corner situations as tall defenders tend to get the header within the opponent's penalty area. By contrast, utilising the backmost position fail to not mirror the course of the game accurately.

For this purpose, the *Dynamic Zoning* tool was developed which requires six input parameters as illustrated in Fig. 2. Besides the selection of an input GDB which corresponds to the *Match Data Preparation* tool's output GDB, the point of

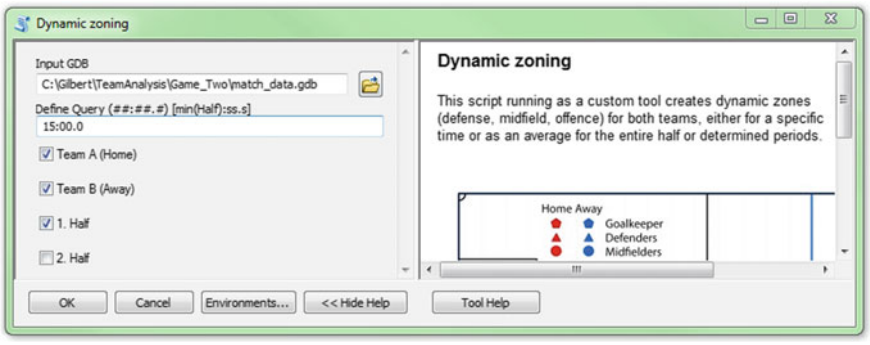

Fig. 2 Tool dialog box of the dynamic zoning tool. *Source* Kotzbek (2017)

time for which the *dynamic zoning* should be conducted has to be entered. As the tool mirrors a first draft of the basic conception, its functionality is limited to the zoning at certain points of time only. Besides these two mandatory parameters, it is up to the user to execute the tool for either both teams and half times respectively or just one of them. In regard of the default input parameters as shown in Fig. 2, the process lasts 21 s on average. In the following the tool script's main parts are described in as much detail as possible albeit code fragments cannot be provided as space is limited. However, the code is readily shared on request.

A number of preliminary measures such as the localisation of the FDS in which according to the input parameters the required merged team-specific tracking data are stored have to be conducted initially. Since the names of all FCs contain the data's *Half ID* and *Team ID*, its identification and localisation is straightforward. Although direct inputs of the required FCs would be an option, demanding a GDB as an input prevents incorrect selections by the users and is thus preferable.

After the creation of the output GDB which is composed of half time specific FDS, the given point of time is converted into a *Frame* value. For this purpose, the entered string is divided by the *colon* in order to cast the two single parts to float numbers, which are then multiplied by 600 and 10 for the *minute* and *second* value respectively. This procedure is feasible since the data's recording rate is constant and known. The addition of both values corresponds to the *Frame* value.

Subsequently the teams' game directions are determined by detecting the home team's goalkeeper's position at the game's very first frame. As the coordinate system's origin is located at the pitch's centre the algebraic sign of that position's X-coordinate can be applied for the assignment. Based upon this information the game directions of both teams and half times are derived.

As stated at this chapter's beginning, the players' X-coordinates are applied for the zoning process. In contrast to the determination of the game direction, the position values along the abscissa have to be normalised. In order to prevent incorrect calculations of the zones' thresholds this measure is necessary as the defenders' average X-positon can be composed of values left and right of the pitch's halfway line. Therefore, the outfield players' X-coordinates are translated to a new origin. Its ordinate runs along the team's own goal line. Then, the two calculated average positions of the defenders and forwards are denormalised so that the team's three zones can be generated on the pitch in relation to the original coordinate system in the pitch's centre. Again, the game direction has to be taken into account.

Once the separation lines have been placed correctly, the corner points of the zones' polygons are determined. Whilst the defending zone is spanned between the team's own goal line and the defenders' average position line, the attacking zone stretches from the forwards' average line to the opponent's goal line. In between the midfielders' area or central zone is located (see Fig. 3). Executing the *ArcGIS* system tools *CreateFeatureClass* and *InsertCursor* polygon FCs are created and finally united utilising the *ArcGIS* system tool *Union*. Conclusively, the zones' area, width and height are extracted while iterating through the output FC applying a *SearchCursor*.

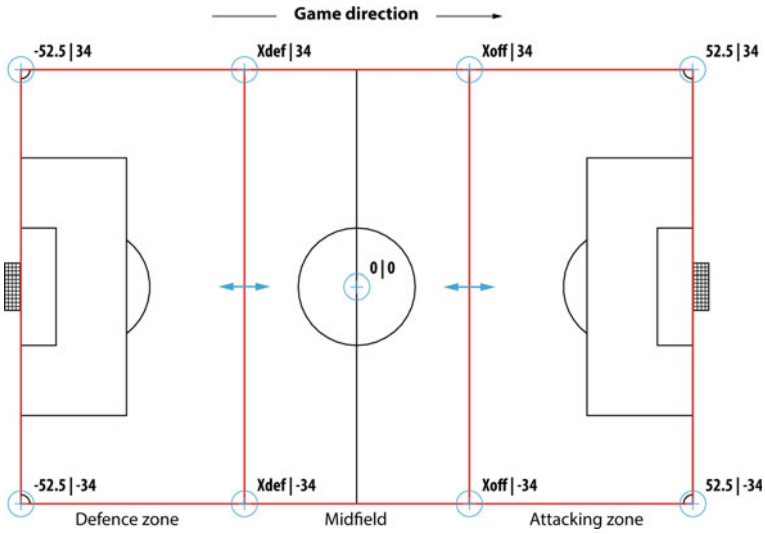

Fig. 3 Schematic depiction of the zone's corner points. *Source* Kotzbek (2017) modified

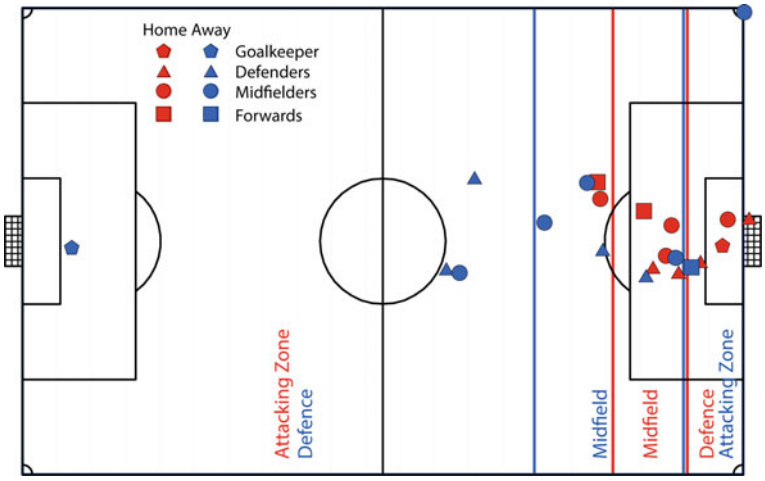

Fig. 4 Exemplarily outcome of the dynamic zoning tool at a certain point of time. *Source* Kotzbek (2017) modified, data ProzoneSports

After the *Dynamic Zoning* tool has successfully been executed for each selected team an output FC containing all three zones at the entered point of time is available. Figure 4 exemplarily illustrates the tool's graphical outcome immediately before the away team kicks a corner. Although this approved the basic conception's

feasibility, it does not provide information about its practicability in the course of football game analyses. Therefore, a potential case of application is demonstrated in the next chapter.

Part II: Determination of the Offensive Quality Based on Dynamic Zoning

Based on the conception of *dynamic zoning*, the teams' offensive quality can be determined assessing the defenders zone's vertical length. This is reasonable as it is assumed that the bigger the defending zone, the higher the team's vertical play is and hence the more offensive the team is. As a consequence, this information not only facilitates statements about pressing play but also spatially displays the interdependency of both teams' use of space. In order to categorise the teams' offensive quality a third of the international pitch's default length of 105 m was applied as a threshold. In dependence upon the game direction the vertical separation line is located 35 m in front of the team's own goal line and divides the pitch into areas of *low* and *strong* offensive quality. However, these are further narrowed by enlarging the linear threshold to an area of *middle* offensive quality between 30 and 40 m measured from the goal line. As this classification is arbitrarily defined, the outcome's significance has to be reviewed.

This conception was implemented as a custom tool for *ArcGIS* named *Analyse Offensive Qualities*. Its TDB is illustrated in Fig. 5 and consists of ten input parameters altogether. Besides the mandatory entry of the input GDB as well as the

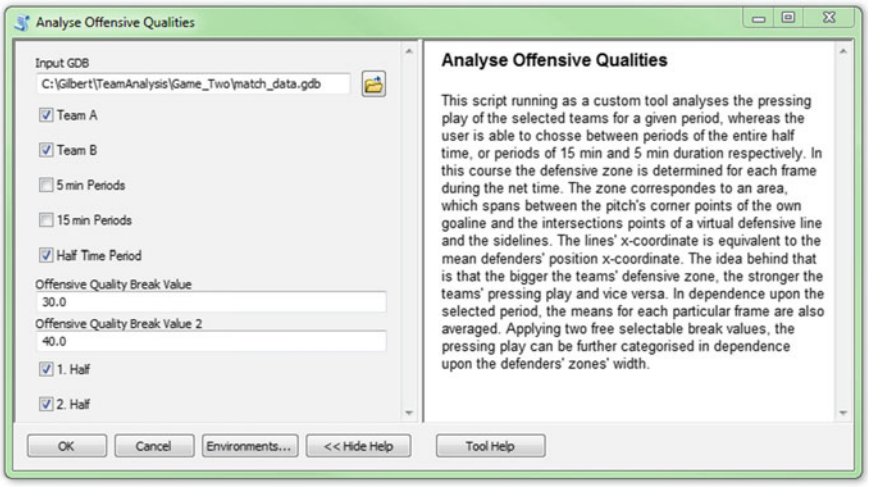

Fig. 5 Tool dialog box of the analyse offensive qualities tool. *Source* Kotzbek (2017)

selection of the teams and half times to be analysed, not only three analysis periods can be chosen but also the classification's two break values. In consideration of the previously described applied computer system the tool's length of execution varies in dependence upon the selected analysis period. Whilst on average the analysis process in regard of the entire half times takes 4 min, analysis periods of 5 and 15 min require 8 and 5 min respectively.

Since the tool's code is almost identical to the one of the *Dynamic Zoning* tool, main differences are only briefly described hereafter. First of all, the process is limited to the determination of the teams' defending zones. Furthermore, instead of the assessment's restriction to certain points of time, the teams' mean vertical defending height is calculated for predefined analysis periods. For this purpose, the *ArcGIS* system tool *Dissolve* is applied to the defensive line's position for each frame of the selected analysis period. Afterwards the determined mean values are read out utilising a *SearchCursor* and are summarised. The result is then divided by the number of frames. Conclusively, two new fields named *Length* and *Off_Quality* are added to the output polygon FC. The new attributes are updated based upon the extracted polygons length as well as according to the input parameters. The tool's outcome is exemplarily illustrated in Fig. 6 that shows the teams' defending areas for both half times.

Whilst the away team (Team B) was marginally higher positioned in the first half, the opposite case was true in the game's second period. Although additional information about the teams' play can be obtained, their significance is limited at least with regard to the analysis of entire half times. Therefore, applying shorter analysis periods such as 5 min each, leads to a more informative outcome as illustrated in Fig. 7. It displays that the teams' offensive qualities correlate which can be expected as the players' movements are ball-oriented in general. The defensive lines' mean heights are illustrated as vertical lines parallel to the goal lines and are colour-coded in dependence upon the *Team ID* (A = red, B = blue) from light to dark according to the game's chronology.

In this half time the home team (Team A) scored three goals, although the away team played more offensively on average as illustrated in Fig. 6. The first goal was

Fig. 6 Comparison between the overall offensive qualities of both teams for both half times. *Source* Kotzbek (2017) modified, data ProzoneSports

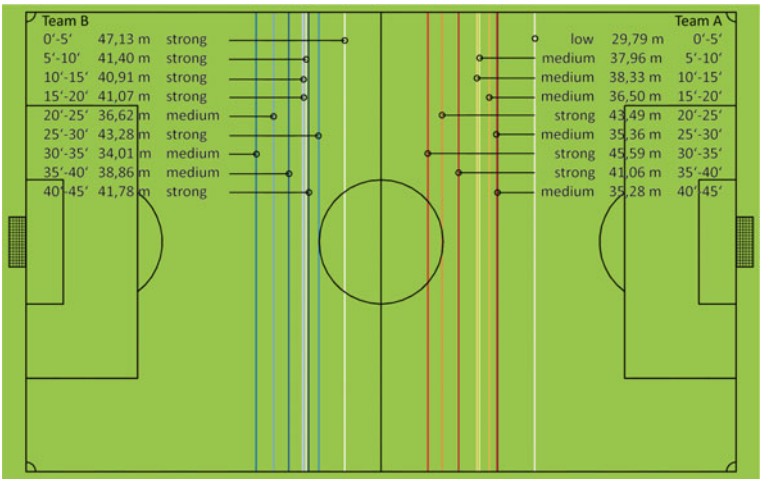

Fig. 7 Comparison between the offensive qualities of both teams for the first half, distinguished in periods of 5 min each. *Source* Kotzbek (2017), data ProzoneSports

scored in the 5th minute during a strong offensive period of the visiting team. As a consequence, their attacking play ceased but was still *strong* for the subsequent quarter of an hour, followed by a short strong offensive by the home team. As the away team gained back control over the game again between the 25th and the 30th minute, the hosts stroke back and scored twice in the 31st and 36th minute. Figure 7 suggests that after the 3:0 the home team did not risk their comfortable lead and primarily focussed on the defence until the half time break.

Since the tool covers one specific facet of the game only, it is important to relate its outcome to the results of other tools such as the developed *Analyse Scoring Attempts* custom tool for *ArcGIS*, which was already presented by the authors (Kotzbek and Kainz 2016). With this, further information to interpret the outcomes can be taken into account. For example, the obtained results indicate that the first goal was scored as a consequence of a ball possession oriented build up play, whereas a direct free-kick and a corner lead to the 2:0 and 3:0 respectively.

The tool's outcome is not only a quantification of the teams' collective offensive play, but also mirrors an aspect of the game's course. Furthermore, it is a source for suggestions about the teams' game style. However, in this particular context it is necessary to analyse a bigger data set comprising games of an entire season for example. With this, it would be conceivable to detect patterns within the teams' offensive play. For instance, it could be questioned whether a team tends to drop deep after scoring a goal. Apart from this particular purpose, it is reasonable to combine different game relevant information such as about ball possession, current score, minute of play or the competition in which the match was played.

Evaluation of the Tools by Professional Game Analayst

Both tools were presented separately to eight game analysts employed by Bundesliga clubs in Austria and Germany. Subsequent to each demonstration an expert survey was conducted in order to evaluate the conception of *dynamic zoning* as well as both tools' functionality. According to Bogner et al. (2014) the survey can be described as partly standardised and explorative. To ensure the feedbacks' completeness a guideline comprising questions about the tools' parameters, possibilities for further developments and its practicability in the course of football game analyses, was utilised. Since the survey's design is described in detail in the author's thesis (Kotzbek 2017), it is only briefly outlined hereafter.

In the thesis' scope the experts were already questioned about contemporary football game analysis' methods and techniques in late 2014. Therefore, the research project was not unknown to them when the second survey was conducted from 9 June 2016 to 4 July 2016. Whilst three interviews were conducted face-to-face, the other experts were questioned online via *Skype*. Irrespective of this, all dialogues were recorded acoustically in order to archive them and to produce interview protocols. These written recordings can be considered as content-related summaries and are appropriate for the assessment of collectively shared interpretative knowledge (Bogner et al. 2014). Furthermore, the protocols were analysed applying a multi-level qualitative content analysis according to Mayring (2010). Since this method cannot be standardised, adjustments in dependence upon certain analysis purposes are inevitable (Mayring 2010). However, in general this approach is intended for the systematical extraction of a text's key messages (Gläser and Laudel 2004). Based on this, the information is classified in terms of a textual structuring and was further assessed employing a frequency analysis in order to weigh the experts' feedback. Although the design's last part corresponds to a quantitative method, it is also suitable for multilevel qualitative content analysis as it facilitates the possibility to strengthen or weaken statements (Mayring 2010). As a result, several individual feedbacks are textually combined to collectively shared statements.

The evaluation of the conception of *dynamic zoning* concluded that it is *interesting* and *fine* but besides a pitch's vertical trisection, horizontal zones also have to be taken into account. Moreover, the majority of experts contradicted the author's assumption whereupon the players' mean X-coordinates are suitable as thresholds. Instead of this, they consider the utilisation of the teams' backmost and foremost positions as more appropriate in this context. Nevertheless, it was recommended to implement both approaches so that the demarcation criteria is freely selectable. According to two experts, *dynamic zoning* can also be applied for analysing a team's spatial compactness. Furthermore, the separation lines indicate spatial disparities within the teams' tactical lines.

Before the second tool was presented the majority of experts had difficulties to name certain fields of application for *dynamic zoning*. However, subsequently they

acknowledged its applicability for analysing a team's offensive qualities. The tool's methodology was predominantly described as *good*, *innovative* and *interesting*. In this sense, the approach is suitable not only for the pressing play's assessment, but also for the evaluation of the compliance with the coach's tactical guidelines. Moreover, drawing conclusions about the opponent's game style is considered possible. In addition to this, the tool provides further information about a team's compactness as well as insights into the game's course which is indicative of a team's dominance.

Besides these benefits, it is controversial whether a causality can be derived from the obvious correlation between the teams' offensive qualities illustrated in Fig. 7. Furthermore, despite the tool's functionality, the experts' opinions about the tool's practicability in the course of football game analyses differ. Whilst at least half of them saw potential cases of application, the other half was indecisive and suggested improvements. Among others, these comprised the implementation of freely selectable pressing play parameters, the additional consideration of the highest defending line for the determination of the offensive dominance, individual selectable analysis periods, the attacking play's horizontal distinction as well as contextual classifications in order to analyse the dynamic of the game's flow.

Discussion and Conclusions

The evaluation provides evidence that the conception of *dynamic zoning* as well as both demonstrated tools are worth to be developed further. For this purpose, the experts' recommendations about adaptation possibilities have to be imperatively taken into account as professional game analysts represent the tools' prime target group. It is particularly reasonable to not only additionally fragment the pitch into horizontal zones dynamically, but also to reconsider the demarcation criteria as mean values might convey false impressions of the game. Furthermore, the creation of animated and/or interactive tool outcomes are worth to consider as this measure would provide more detailed information about the dynamic game's flow. In this case the zones' determination is reasonable for every *frame*. Although valuable feedback was already obtained in this context, it is advisable to refine the concept and the tools in close cooperation with game analysts in order to configure the development process more systematically, efficiently and purposefully. Moreover, as the presented approach corresponds to a first draft an extensive study of movement analysis in other sports disciplines is certainly insightful in the course of the approach's revision.

According to the experts, *dynamic zoning* provides new interesting perspectives on the game which provides insights into a team's pressing play, dominance, spatial compactness and game style. Moreover, assessing the zones is considered as suitable to evaluate the compliance with the coach's tactical guidelines. Hence, it can be concluded that *dynamic zoning* facilitates manifold analysis opportunities.

However, caution should be exercised if it is attempted to derive causalities as verifications of the conception's as well as tools' functionality are outstanding yet.

Besides the recommendations quoted in the last chapter, the experts argue that the success of GIS in the scope of football game analyses is essentially connected to the establishment of an appropriate interface to the video analysis. "As both approaches have their shortcomings, a combination of both would alleviate these." (Kotzbek 2017) As it is common practise to time tag game relevant events within video footages of football games an attributive conjunction to the georeferenced data's time stamp already exists. Hence, the connection between both analysis approaches is feasible. However, among other details such as the interface's functionality and access are not contrived yet. This strengthens the demand for interdisciplinary team work.

In order to address a larger part of the target group it seems to be advisable to provide the tools for free and open source GIS since it is assumed that this would attract financially weaker clubs too. As *Python* scripts can also be applied for process automation in *QGIS* for instance, the effort to revise the tools would be negligible. Moreover, according to the experts the development of an independent graphical user interface, which not only provides access to video footages but also facilitates the possibility to call several analysis tools is worth considering, as it is expected to be more user friendly.

To sum up, this paper introduces a novel conception of a football pitch's *dynamic zoning* based upon the players' movements applying GIS. Although several aspects of the conception's first draft were judged favourably by professional game analysts, it cannot be considered sophisticated so far owing to outstanding issues. Hence, further developments are necessary. In this context, we encourage our colleagues to participate in the field of both, GIS-based football game analysis in particular as well as sports analytics in general.

References

Bogner, A., Littig, B., & Menz W. (2014) Interview mit Experten. Eine praxisorientierte Einführung. In R. Bohnsack, U. Flick, C. Lüders & J. Reichertz (Eds.), *Qualitative Sozialforschung*. Praktiken—Methodologien—Anwendungsfelder. Springer: Wiesbaden.

Castellano, J., Alvarez-Pastor, D., & Bradley, P. S. (2014). Evaluation of research using computerized tracking systems (Amisco® and Prozone®) to analyse physical performance in Elite Soccer: A systematic review. *International Journal of Sports Medicine, 44*(5), 701–712.

Clayton, R. B. (2011). Profiling the effectiveness of attacking play leading to a goal attempt in men's under 21 Elite Academy Level Soccer. *Journal of Loughbhorough College Research*, 1274–1282.

Cotta, C., Mora, A. M., Merelo, J. J., & Merelo-Molina, C. (2013). A network analysis of the 2010 FIFA world cup champion team play. *The Journal of Systems Science and Complexity, 26,* 21–42.

Di Salvo, V., Collins, A., McNeill, B., & Cardinale, M. (2006). Validation of Prozone®: A new video-based performance analysis systeme. *International Journal of Performance Analysis in Sport, 6,* 108–119.

Di Salvo, V., Baron, R., Tschan, H., Calderon Montero, F. J., Bachl, N., & Pigozzi, F. (2007). Performance characteristics according to playing position in Elite Soccer. *International Journal of Sports Medicine, 28,* 222–227.

Di Salvo, V., Gregson, W., Atkinson, G., Tordoff, P., & Drust, D. (2009). Analysis of high intensity activity in premier league soccer. *International Journal of Sports Medicine, 30*(3), 205–212.

Dodge, S., Weibel, R., & Lautenschütz, A. K. (2008). Towards a taxonomy of movement patterns. *Information Visualization, 7,* 240–252.

Fédération Internationale de Football Association. (2016). http://www.fifa.com/mm/Document/FootballDevelopment/Refereeing/02/36/01/11/LawsofthegamewebEN_Neutral.pdf. Accessed on November 21, 2016.

Gläser, J., & Laudel, G. (2004). *Experteninterviews und qualitative Inhaltsanalyse als Instrumente rekonstruierter Untersuchungen*. Wiesbaden: Verlag für Sozialwissenschaften.

Kotzbek, G., & Kainz, W. (2014) Football game analysis: A new application area for cartographers and GI-scientists? In *Proceedings of the 5th International Conference on Cartography and GIS* (vols. 1, 2, pp. 299–2014), Riviera, Bulgaria.

Kotzbek, G., & Kainz, W. (2015a). GIS-based football game analysis—A brief introduction to the applied data base and a guideline on how to utilise it. In *Proceedings of the 27th International Cartographic Conference*, Rio de Janeiro, Brazil, pp. 1–10.

Kotzbek, G., & Kainz, W. (2015b). Das Runde muss ins GIS—Neue Wege im Bereich der Fußball-Spielanalyse. GIS. *Science, 3,* 117–124.

Kotzbek, G., & Kainz, W. (2016). Towards automated GIS-based analysis of scoring attempt patterns in association football. In *Proceedings of the 19th AGILE Conference on Geographic Information Science*, Helsinki, Finland, pp. 1–6.

Kotzbek, G. (2017). GIS-gestützte Spielanalyse. Studie zur Zweckmäßigkeit geographischer Informationssysteme im Kontext raumzeitlicher Analysen des Fußballspiels am Beispiel von ArcGIS sowie auf Basis fußballspezifischer Geodaten von ProzoneSports. Doctoral thesis at the University of Vienna.

Lucey, P., Bialkowski, A., Carr, P., Foote, E., & Matthews, I. (2012). Characterizing multi-agent team behavior from partial team tracing: Evidence from the english premier league. In *Proceedings of the 26th AAAI Conference on Artificial Intelligence*, Toronto, Canada, pp. 1387–1393.

Mayring, P. (2010). *Qualitative Inhaltsanalyse*. Beltz, Basel: Grundlagen und Techniken.

Mitchell, A. (2009). *The Esri® guide to GIS analysis*. Redlands: Esri Press.

O'Donoghue, P. G., & Robinson, G. (2009). Validity of the ProZone® player tracking system: A preliminary report. *IJCSS, 8*(1), 38–52.

Pollard, R., & Reep, C. (1997). Measurinrg the effectiveness of playing strategies at soccer. *The Statistician, 46*(4), 541–550.

STATS Sports Data Company. (2016). http://www.stats.com. Accessed on November 21, 2016.

Vilar, L., Araújo, D., Davids, K., & Bar-Yam, Y. (2013). Science of winning soccer: Emergent pattern-forming dynamics in association football. *The Journal of Systems Science and Complexity, 23,* 73–84.

Zandbergen, P. A. (2010). *Python*. Redlands: Scripting for ArcGIS, Esri Press,

Zeiler, M., & Murphy, J. (2010). Modeling our world. In *The Esri® guide to geodatabase concepts*. Redlands: Esri Press.

Spatio-Temporal Traffic Flow Forecasting on a City-Wide Sensor Network

Felix Kunde, Alexander Hartenstein and Petra Sauer

Abstract Intelligent transportation systems (ITS) all around the world are collecting and processing huge amounts of data from numerous sensors to generate a ground truth of urban traffic. Such data has set the foundation of traffic theory, planning and simulation to create rule-based systems but it can also be very useful for time-series analysis to predict future traffic flow. Still, the acceptance for data-driven forecasting is quiet low in productive systems of the public sector. Without enough probe data from floating cars (FCD) ITS owners feel unable to reach an accuracy like private telecommunication or car manufacturing companies. On the other hand, investigating into FCD requires a thoughtful treatment of user privacy and a close look on data quality which can also be very time consuming. With this paper we prove that a modern deep learning framework is capable to operate on city-wide sensor data and produces very good results with even simple artificial neural networks (ANN). In order to forecast space-time traffic dynamics we are testing a Feed Forward Neural Network (FFNN) with different geotemporal constraints and can show where and when they have a positive but also a negative effect on the prediction accuracy.

Keywords Traffic forecasting · Time series analysis · Spatio-temporal data mining · Neural network · Deep learning

F. Kunde (✉) · A. Hartenstein · P. Sauer
Beuth University of Applied Sciences Berlin, Luxemburger Str. 10,
13353 Berlin, Germany
e-mail: fkunde@beuth-hochschule.de

A. Hartenstein
e-mail: s58380@beuth-hochschule.de

P. Sauer
e-mail: sauer@beuth-hochschule.de

I. Ivan et al. (eds.), *Dynamics in GIscience*, Lecture Notes in Geoinformation and Cartography, DOI 10.1007/978-3-319-61297-3_18

Introduction

Improvements in the machine learning domain are raising the question if an ITS can be a 100% driven by data from sensors—learning how traffic patterns evolve, which rules to apply for switching traffic lights and how to navigate traffic streams without causing more congestion. The idea is fascinating but also puts higher requirements on the quality of data. Static sensors can be unavailable or report shifted values for hours what urges the use of additional sources like floating car data (FCD) (Graser et al. 2012). On the other hand, it has to be considered if the throughput of FCD is really high enough on each trajectory at any given time to be a representative sample of the real traffic. While it is not expensive to extend fleets of GPS-equipped vehicles or to crowd source location data from smart phones (Apps, Social Media), data privacy remains a critical issue (Jeske 2015).

The ITS of Dresden (called VAMOS) uses data from around 1000 sensors installed along freeways and main roads (induction loops, infrared traffic eyes and cameras). In addition FCD from around 500 taxi cabs is map matched against a generalized routing graph and included in the calculation of travel times. Even though the system incorporates past travel times from every network segment it only generates an image of the current traffic situation. Tests have shown that messages displayed on traffic signs to inform drivers on upstream traffic congestion can get very inaccurate the more distant the sign is located from the incident (Pape and Körner 2016). Therefore, a solid traffic forecasting algorithm that can produces close predictions only on static sensor data would be a great win for the system.

In this paper we present a possible solution which is based on a Feed Forward Neural Network (FFNN). We are taking a subset of 135 double induction loops which are distributed across Dresden. To capture spatio-temporal dependencies of the sensor network we include a spatial weight matrix into our model. In next section we will provide an overview of related work that has been done in past years to improve data-driven traffic forecasting and point out some limitations. After an introduction to related work we will explain our experimental setup followed by the "Results" Section. We evaluate our findings in the Section "Discussion and Future Work" and conclude with an outlook on further research.

Related Work

Short-term traffic forecasting based on sensor data has seen many different approaches in the last decades, be it for freeways or arterial road networks, with univariate or multivariate inputs and for different time lags (Vlahogianni et al. 2014). Lippi et al. (2013) point out that it is often difficult to compare them because of their heterogeneous setup. The applied methods are ranging from classical parametric solutions like autoregressive statistics for time series (ARIMA) (Box, Jenkins 1976) (Williams and Hoel 2003), k-Nearest neighbors on historic data sets (Leonhardt and Steiner 2012), Bayesian networks (Sun et al. 2006) to

non-parametric predictions by support vector machines (SVM) (Lippi et al. 2013) or artificial neural networks (ANN) (Liu et al. 2006).

In recent years ANNs have become popular again due to the hype around the term "Deep Learning". Complex deeply nested architectures are now computable on most modern machines. Thus, a growing research activity in using these networks for traffic forecasting can be noted. Because of their underlying algorithms ANNs are very good in detecting non-linear patterns e.g. like irregular traffic congestion. This is why they are regarded as to be superior against model-driven approaches. Two popular types of ANNs are Convolutional Neural Networks (CNN) and Recurrent Neural Networks (RNN). CNNs are designed to extract features from the input data using kernel functions. They operate well on fuzzy data such as images. RNNs are able to learn sequences in data, which makes them interesting for prediction use cases.

RNNs seem like a good fit for traffic forecasting and have been used by Liu et al. (2006) and Zeng and Zhang (2013). Because RNNs can only operate on a rather small sequence Hochreiter and Schmidhuber (1997) created the Long Short Term Memory (LSTM) ANN which uses internal filters (called "gates") to reduce the learning overhead that occurs in "simple" RNNs. So far, not many efforts have been made to use LSTMs for traffic forecasting (Ma et al. 2015). In the work of Zhang et al. (2017) an LSTM has been coupled with a CNN. The CNN would extract patterns such as traffic congestion from heat maps and the LSTM would learn how the patterns evolve.

Many studies have also proven the relevance of a spatial dimension to improve the accuracy of the predictions. The idea is to not only look at the historic values of the target sensor but also to incorporate data from all other sensors filtered by a spatial weight matrix to strengthen the relation between neighbours (Kamarianakis and Prastacos 2005; Cheng et al. 2014). However, in ANN-driven research the spatio-temporal models are often fallen short in terms of complexity (e.g. freeway setting, low number of sensors) compared to ARIMA-based approaches. Therefore, we combine our experiments on FFNNs with ideas from Cheng et al. (2014).

Experimental Setup

Neural Network Architecture

For further description of the network architecture we are using the same naming convention as in Lipton et al. (2015). We have implemented a FFNN using Google's Tensor Flow framework (tensorflow.org). The network consists of one output layer o and one hidden layer h. The number of input nodes i and output nodes k is defined by the number of sensors we consider as a valid input source (98% availability of measurements in the training data set). The number of hidden nodes j is set to 60 in every training session. For each layer we are using a sigmoid

activation function l (1) to produce the value v of every neuron (2). The sigmoid function $\sigma(z)$ is a classical nonlinear function and a good choice if we want to detect nonlinear patterns in our data.

$$l = \sigma(z) = \frac{1}{1 + e^{-z}} \tag{1}$$

$$v_j = l_j\left(\sum_{j'} w_{jj'}.v_{j'}\right) \tag{2}$$

Here j' stands for nodes that are connected with the hidden neuron j and w is the weight of edges jj'. The root mean square error (RMSE) is our loss function $L(\hat{y}_k, y_k)$ which modifies the network on each iteration using backpropagation (Rumelhart et al. 1985). The weights between the neurons are adjusted by stochastic gradient descent (SGD) with a mini batch size of 20 and a learning rate of 0.01. The backpropagation algorithm subsequently calculates the derivatives of L from output nodes k (3) to hidden nodes j with respect to their corresponding activation function (4).

$$\delta_k = \frac{\partial L(\hat{y}_k, y_k)}{\partial \hat{y}_k} \cdot l'_k\left(\sum_j w_{kj} \cdot v_j\right) \tag{3}$$

$$\delta_j = l'\left(\sum_{j'} w_{jj'} \cdot v_{j'}\right) \sum_k \delta_k \cdot w_{kj} \tag{4}$$

Data Preparation

From the VAMOS data archive we have extracted three month of measurements from all double induction loops (July to September 2015). We choose this sensor group as it is most representative for the traffic in Dresden. The loops are installed only on main roads and with enough distance to traffic lights to avoid noise from waiting queues. They are detecting the speed, number of cars (occupancy), time on sensor, length of cars and gaps between cars. All variables are minutely aggregated and can be zero if there are no cars in one minute. Therefore, we are taking a 50 min moving average (MA) of the time series as input. As for now, we omit time steps where the input or output vectors contain missing values. In our test case we had to reduce the number of double induction loops to 59. Still, we got a good spatial distribution across the city (see Fig. 1).

For our test case we have started with using only the occupancy as input value which is later normalized to a range between 0 and 1. We generate an input matrix and a target matrix with the following structure, where each line represents an input vector to the neural network:

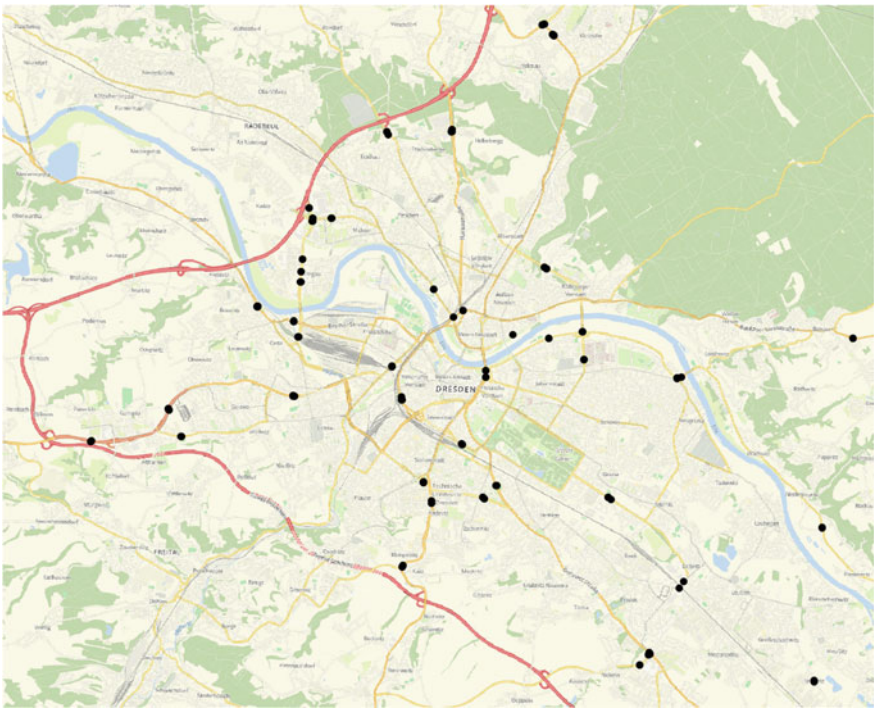

Fig. 1 Location of sensors selected for training

$$\begin{bmatrix} x_{s_1,t_0} & \cdots & x_{s_n,t_0} \\ \vdots & \ddots & \vdots \\ x_{s_1,t_n} & \cdots & x_{s_n,t_n} \end{bmatrix} \begin{bmatrix} x_{s_1,t_0+offset} & \cdots & x_{s_n,t_0+offset} \\ \vdots & \ddots & \vdots \\ x_{s_1,t_n+offset} & \cdots & x_{s_n,t_n+offset} \end{bmatrix} \tag{5}$$

Here x stands for the smoothened and normalized occupancy value detected at a sensor s at time step t where offset can be the occupancy value in the next 5, 10, 15, 30 and 45 min. Our strategy to define neighbours of each sensor is inspired by the work of Cheng et al. (2013). Only sensors from where traffic can get to the target within a given time lag are considered. We are using the Isochrone API of the Open Source routing engine Graphhopper (graphhopper.com/api/1/docs/isochrone/) which produces a reverse flow isochrone polygon for a given time lag for each sensor. The intersecting sensors are the neighbours. We do not apply any further weighting yet as our ANN should be able to learn by itself which neighbours are having a higher impact for a future state at the target sensor. We make an exception and take only isochrones for 5 min even for bigger prediction horizons because 10-minute isochrones can already cover great areas of Dresden and, thus, include many sensors. Moreover, our isochrones are fixed and not dynamic as in Cheng

et al. (2014). The resulting adjacency matrix has to be applied against the input matrix.

In the end, we came up with four different input settings to analyse the effect of including other sensors into our predictions:

- $\text{FFNN}_{\text{simple}}$: Only historic values of the target sensor to predict a future value
- FFNN_{NN}: Only historic values from nearest neighbours excluding the target sensor
- $\text{FFNN}_{\text{NN+}}$: Only historic values from nearest neighbours including the target sensor
- FFNN_{all}: Historic values from all sensors

We also want to measure possible improvements by including temporal sequences in the input matrix. Polson et al. (2016) have shown that sequential information can also be passed to a FFNN by appending the time lags to the matrix to mimic a RNN. We are also applying this strategy in four additional tests ($\text{mFFNN}_{\text{simple/NN/NN+/all}}$) using a sequence of m time steps. In our case we choose a sequence of 5 min, because it correlates with our isochrone radius.

$$\begin{bmatrix} x_{s_1,t_0} & \cdots & x_{s_n,t_0} & x_{s_1,t_1} & \cdots & x_{s_n,t_1} & \cdots & x_{s_n,t_m} \\ \vdots & \ddots & \vdots & \vdots & \ddots & \vdots & \ddots & \vdots \\ x_{s_1,t_n} & \cdots & x_{s_n,t_n} & x_{s_1,t_{n+1}} & \cdots & x_{s_n,t_{n+1}} & \cdots & x_{s_n,t_{n+m}} \end{bmatrix} \begin{bmatrix} x_{s_1,t_{m+offset}} & \cdots & x_{s_n,t_{m+offset}} \\ \vdots & \ddots & \vdots \\ x_{s_1,t_{n+m+offset}} & \cdots & x_{s_n,t_{m+offset}} \end{bmatrix} \tag{6}$$

Training

We train our FFNN with one month of data for July 2015 and test it against the data sets from August and September 2015. For all eight FFNN architectures we train each sensor with five different temporal offsets as described above. Theoretically, around 44,600 time steps (1440 min for 31 days minus the offset) can be fed in as input. The inputs are selected randomly from the time series.

Results

For evaluating our results, we are using the mean absolute error (MAE) as defined in (7), which is a common measure in research:

$$MAE = \frac{1}{N}\sum_{k=1}^{N}|\hat{y}_k - y_k| \tag{7}$$

$\hat{y}_k$ stands for the predicted value. Table 1 shows an exemplary result for one sensor. Many aspects seen here also apply to other sensors, e.g. lowest MAE when including all sensor and sequence information and highest MAE when filtering the input by the targets nearest neighbours incl. historic values of the target itself.

To fully understand the differences between given time lags, FFNN model and sensor location we feed our results into a spatial database and visualize them in a set of maps (see Fig. 2). In Dresden many double induction loops are installed in a group of four—a sensor on each lane for both sides of the road. Therefore, we style the layer with the Point Displacement feature of the open source geographic information system QGIS (qgis.org). In general, the results of all different FFNN setups are very good. But, we are colouring the sensor locations from green (low MAE) to red (slightly higher MAE) in order to better spot the differences of the trained models.

Temporal Dimension

Again, we can see that including nearest neighbours and the target produces the highest MAEs in our tests. Like the results from Table 1 adding sequence information to the input matrix does not have a great beneficial impact on the predictions. Especially for small time lags the result of simple FFNNs are comparable to the ones with sequences. On the other hand, temporally extended FFNNs are better for longer prediction horizons.

Spatial Dimension

In contrast to the results of many other papers in the field of spatio-temporal traffic forecasting, adding neighbourhood information decreased the accuracy in many cases. It's obvious that an ANN works best when it is fed with input values of the whole ground truth, but we did not expect it to be worse than taking only values of the target ($FFNN_{single}$). Nevertheless, the $FFNN_{NN}$ setup seems to be a superior choice for greater time lags (>15 min).

Table 1 MAE for different prediction horizons for one sensor

FFNN type	t5	t10	t15	t30	t45
$FFNN_{single}$	0.5042	0.5743	0.6679	0.9698	1.2970
$FFNN_{NN}$	0.6255	0.6660	0.7248	0.9831	1.0299
$FFNN_{NN+}$	1.7177	1.7157	1.7236	1.7813	1.8928
$FFNN_{all}$	0.4975	0.4933	0.5262	0.7474	1.0299
$mFFNN_{single}$	0.4324	0.5213	0.6137	0.9360	1.2771
$mFFNN_{NN}$	0.5616	0.6080	0.6667	0.9231	1.2519
$mFFNN_{NN+}$	1.6420	1.6543	1.6862	1.8126	1.9612
$mFFNN_{all}$	0.3998	0.4086	0.4521	0.6405	0.8684

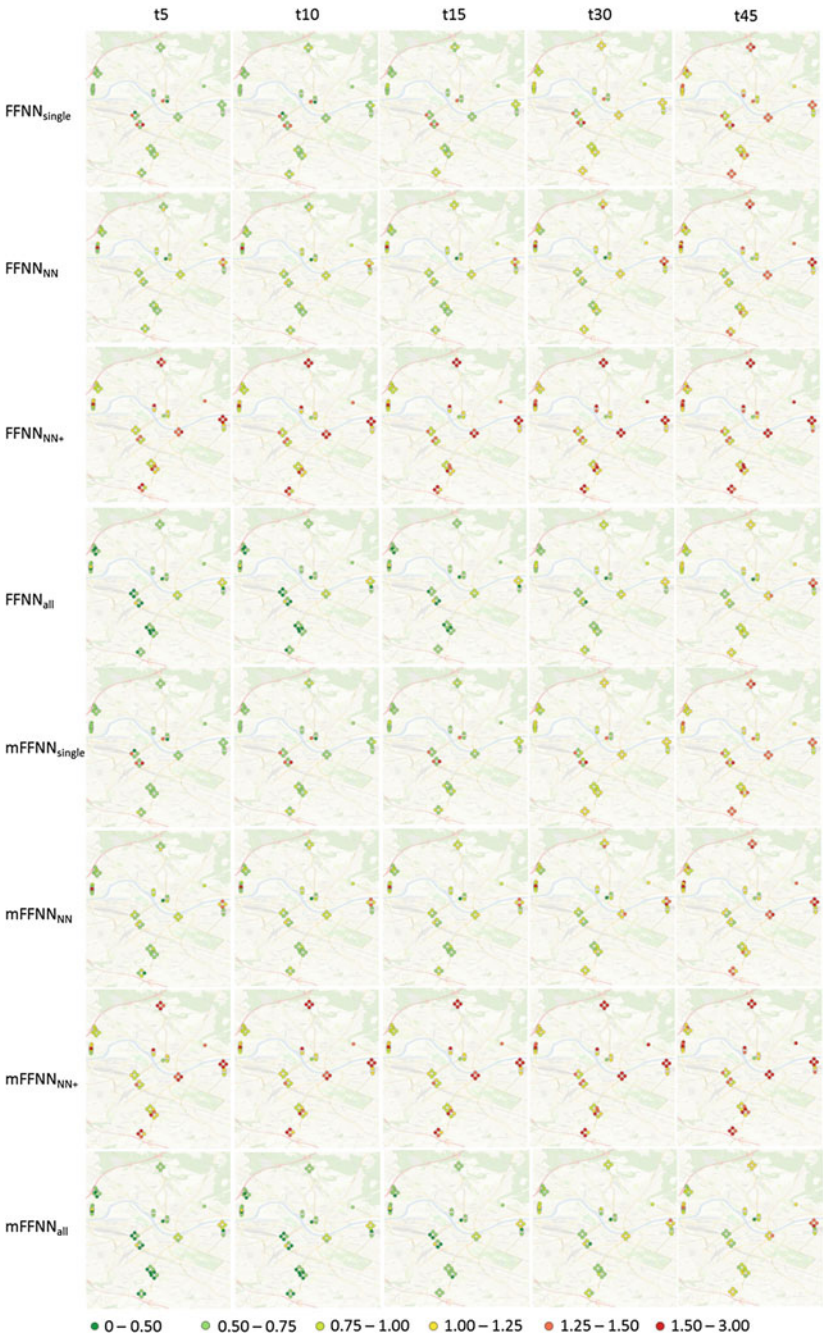

Fig. 2 MAEs of all tested sensors for different prediction horizons and different FFNN architectures

In the map series of the $FFNN_{single}$ tests we notice groups of sensors where two of them have a low MAE and the other two have a considerably higher error. As there is no styling rule about which point represents which lane we have to take a closer look. When zooming in, it can be seen that the predictions for sensors at the inner side of the road are less accurate (see Fig. 3). The pattern also occurs at other locations. It probably depends on the selected variable occupancy. The outer lane of a road has probably a higher and more regular occupancy throughout the day and night than the inner lane.

The MAE does not only vary for single groups but also across the city. For small time lags, predictions for loops on the in- and outgoing main roads of Dresden are more accurate than in the city centre. For longer time windows this pattern is turning to the opposite. In other words, traffic in the centre, which is probably more non-linear than on a main road leading to a freeway, is better predictable for FFNNs trained on bigger temporal offsets. But, these FFNNs work less accurate on linear traffic patterns compared to FFNNs trained on small time lags.

Discussion and Future Work

Our approach shows the best performance when we apply all available spatial and temporal information to the neural network. This strengthens the general assumption that neural networks are very good at learning spatio-temporal patterns from a huge amount of data. As for now, we have only used a rather simple measure—the MAE—to validate our results. In general, our MAE is very low in all our test runs. When looking at the average traffic distribution of one sensor over one year (see Fig. 4) we can see that it follows a quite regular trend (grey area is the standard deviation). In the morning hours between 5 and 8 o'clock there is a strong increase of traffic volume. Then the graph follows a valley of moderate traffic density during the day with a less steep curve. After the evening rush hour the traffic constantly decreases to a minimum at night. In this example, we can extract five different rather unique temporal traffic patterns which also occur at many other sensors of our sample with varying local maxima. Given a small temporal offset of just a few minutes and the great smoothing of 50 min moving average we produce many

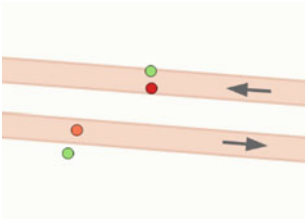

Fig. 3 MAEs of sensors on different street lanes (same colour scale as in Fig. 2)

examples that are very easy to predict. The figure also shows a curve of traffic at January 1st which is, of course, very different from the yearly average. In our future work we will focus on how the predictive power of the model will keep up especially in these situations.

Comparing the prediction with the actual observed value on a time line helps to understand which periods were easier to predict than others. This is done in Fig. 5 for one week of August 2015 (time 0 = Monday midnight). The solid line represents the target, the dotted lines are showing the prediction results of 3 different FFNNs. It can be seen that our predictions come very close to the real value, especially when the amount of traffic is increasing in the morning and decreasing in the evening. The FFNN has only problems to predict zero values during night time and sometimes it over- or underestimates the traffic during the peak periods. It seems that the FFNN can either not distinguish between the two rush hour periods or it relies on the patterns learned from the previous month. This can be solved by adding information about daytime to the input vector.

What is also really interesting to see in Fig. 5 is the ability of the network to learn the differences between weekends and weekdays. This can be a hint that filtering the input by a spatial weight matrix introduces a bias that—while being reasonable in traffic theory—might not be necessary. It would be interesting to see how other ANN architectures behave given the same input than in our experiments. Especially, when using RNNs the model complexity and training time will grow exponentially. Therefore, using a sparse matrix as input can be a mandatory compromise in order to have a scalable solution. Using FFNNs did not cause any performance problems. The training and testing of a given FFNN setup for one sensor only took a few minutes.

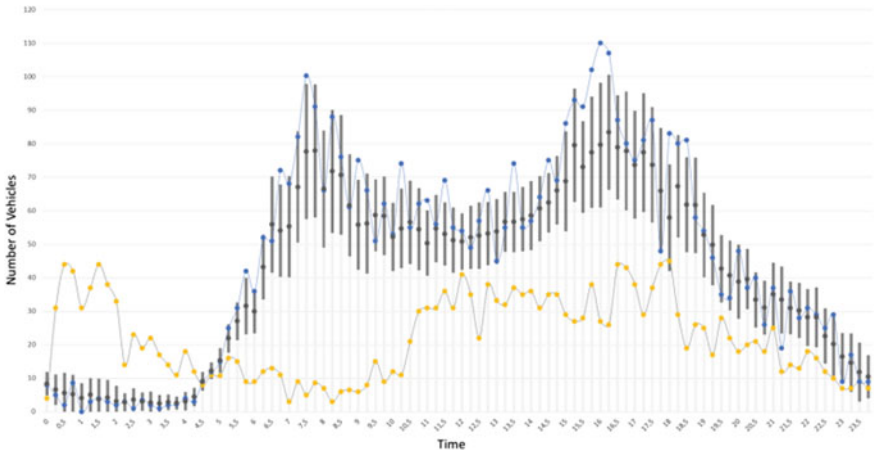

Fig. 4 Number of vehicles for one sensor on two wednesdays in 2014. The *yellow line* depicts January 1st of 2014 and the *blue line* shows a typical Wednesday (April 16th of 2014). Additionally, the *grey rectangles* visualize the standard deviation for number of vehicles in one year (occupancy)

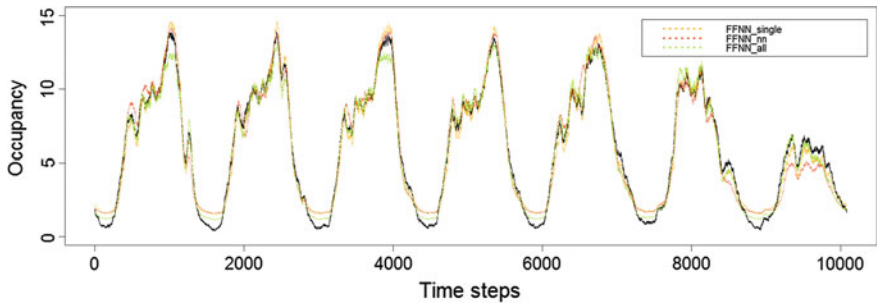

Fig. 5 Predicted occupancy (*dotted line*) versus observed values (*osolid line*)

This question would also be essential when installing a continuous learning where newly detected data is included in cyclic training sessions to adapt to recent changes in the urban traffic. It needs to be evaluated how long a trained model can be used for prediction and how often it needs to be updated. If an ITS would react on behalf of the predictions e.g. by displaying proper messages to drivers through signs or smartphone apps, it could generate new traffic patterns the ANN hasn't see before. This could lead to false predictions and thus frustrated drivers. A regular training from scratch could produce too much overhead when using complex ANNs. Srivastava et al. (2014) have suggested a so called Dropout mechanism, where an existing model is destroyed partly and rearranged in a new training session with updated inputs.

Conclusion

In this paper we have presented the potential of deep learning on traffic sensor data. While the usage of neural networks for short-term traffic forecasting had been used in many different studies most often the spatial dimension is not included or neglected because of a simplistic training scenario with a low number of sensors. We are working on a sensor network that is distributed across an entire city. Therefore, we can see that the accuracy of our predictions is varying by location, prediction horizon and model selection.

So far, we can make the following statements: (i) Filtering the input by nearest neighbours puts too much bias into the neural network. Still, such a filtering can be relevant when testing with more complex ANNs. (ii) Including sequence information in the FFNN input generally improves the accuracy, which is why we will work with RNNs (LSTMs) in the future. (iii) For short-term predictions with small offsets simple FFNNs already provide very good results. Bigger gaps between predicted and observed values can sometimes be found for morning peaks and during nights. (iv) FFNNs trained on short time lags produce a higher error for

non-linear traffic patterns than FFNNs trained on longer temporal offsets and vice versa.

It is planned that the developed algorithms (available under: https://github.com/MAGDa-BeuthHS/dlsd) will be tested against real-time data from the ITS of Dresden. We also plan to apply our algorithm on historic travel times of network links. By doing so we should be able to better capture spatio-temporal dynamics. This also raises the question if a proper traffic and travel time prediction really requires more FCD from individuals rather than extending the network of static sensors. We believe that for data privacy reasons it is important to improve algorithms for analysing time series data of anonymous sensor networks.

Acknowledgements The work was supported by the Federal Ministry for Economic Affairs and Energy (BMWi) under grant agreement 01MD15001B (Project: ExCELL).

References

Box, G. E., & Jenkins, G. M. (1976). *Time series analysis: Forecasting and control*. San Francisco: Holden-Day.

Cheng, T., Wang, J., Haworth, J., Heydecker, B., & Chow, A. (2014). A dynamic spatial weight matrix and localized space–time autoregressive integrated moving average for network modeling. *Geographical Analysis, 46*(1), 75–97.

Graser, A., Dragaschnig, M., Ponweiser, W., Koller, H., Marcinek, M., & Widhalm, P. (2012). FCD in the real world system capabilities and applications. In *Proceedings of the 19th ITS World Congress*, Vienna, Austria.

Hochreiter, S., & Schmidhuber, J. (1997). Long short-term memory. *Neural Computation, 9*(8), 1735–1780.

Jeske, T. (2015). Sicherheit und Datenschutz in nicht-interaktiven Crowdsourcing Szenarien. Dissertation. Technische Universität Hamburg-Harburg. Available at: https://tubdok.tub.tuhh.de/bitstream/11420/1249/1/Dissertation_Tobias_Jeske.pdf (in german).

Kamarianakis, Y., & Prastacos, P. (2005). Space–time modeling of traffic flow. *Computers & Geosciences, 31*(2), 119–133.

Leonhardt, A., & Steiner, A. (2012). Instance based learning for estimating and predicting traffic state variables using spatio-temporal traffic patterns. In *TRB 91th Annual Meeting*, Washington, D.C.

Lippi, M., Bertini, M., & Frasconi, P. (2013). Short-term traffic flow forecasting: An experimental comparison of time-series analysis and supervised learning. *IEEE Transactions on Intelligent Transportation Systems, 14*(2), 871–882.

Lipton, Z. C., Berkowitz, J., & Elkan, C. (2015). A critical review of recurrent neural networks for sequence learning. arXiv preprint arXiv:1506.00019

Liu, H., van Zuylen, H., van Lint, H., & Salomons, M. (2006). Predicting urban arterial travel time with state-space neural networks and Kalman filters. *Transportation Research Record: Journal of the Transportation Research Board*, 99–108.

Ma, X., Tao, Z., Wang, Y., Yu, H., & Wang, Y. (2015). Long short-term memory neural network for traffic speed prediction using remote microwave sensor data. *Transportation Research Part C: Emerging Technologies, 54,* 187–197.

Pape, S., & Körner M. (2016). Verkehrslageprognose unter Berücksichtigung der dynamischen Kapazitäten an LSA-abhängigen Knotenpunkten zur qualitativen Aufwertung der

Verkehrslageinformation im Verkehrsmanagementsystem VAMOS. *25. Verkehrswissenschaftliche Tage 16. und 17. März 2016 in Dresden*. (in german).

Polson, N., & Sokolov, V. (2016). Deep learning predictors for traffic flows. arXiv preprint arXiv:1604.04527

Rumelhart, D. E., Hinton, G. E. & Williams, R. J. (1985). Learning internal representations by error propagation (No. ICS-8506). California University San Diago La Jolla Institute for cognitive science.

Srivastava, N., Hinton, G., Krizhevsky, A., Sutskever, I., & Salakhutdinov, R. (2014). Dropout: A simple way to prevent neural networks from overfitting. *Journal of Machine Learning Research, 15,* 1929–1958.

Sun, S., Zhang, C., & Yu, G. (2006). A Bayesian network approach to traffic flow forecasting. *IEEE Transactions on Intelligent Transportation Systems, 7*(1), 124–132.

Vlahogianni, E. I., Karlaftis, M. G., & Golias, J. C. (2014). Short-term traffic forecasting: Where we are and where we're going. *Transportation Research Part C: Emerging Technologies, 43,* 3–19.

Williams, B. M., & Hoel, L. A. (2003). Modeling and forecasting vehicular traffic flow as a seasonal ARIMA process: Theoretical basis and empirical results. *Journal of Transportation Engineering, 129*(6), 664–672.

Zeng, X., & Zhang, Y. (2013). Development of recurrent neural network considering temporal-spatial input dynamics for freeway travel time modeling. *Computer-Aided Civil and Infrastructure Engineering, 28*(5), 359–371.

Zhang, J., Zheng, Y., Qi, D. (2017). Deep spatio-temporal residual networks for citywide crowd flows prediction. In *Thirty-First AAAI Conference on Artificial Intelligence*.

Applications of GIS in Analysis of Mars

Marta Kuźma, Łukasz Gładysz, Mateusz Gralewicz and Paweł Krawczyk

Abstract This article presents the results of the project that aims to demonstrate the possibility of using images from space probes and satellite images for the analysis and creation of databases of spatial information systems. The introduction contains basic information about the planet Mars. The scope of work involves a combination of satellite images mosaic. On the basis of these images a 3D model was created, showing the landing place for Mars rovers. It presents the largest craters, canyons and other characteristic objects. All the information is contained in the database. Places that may be suitable for settlement have been determined on the basis of analyses carried out on a 3D model. The analysis took into account the temperature, slope inclination, the distance from craters and volcanoes and the occurrence of dust and sandstorms, as well as other factors favouring the colonization of the surface of Mars. The project was prepared to constitute a future basis for determining potential areas of habitation on Mars.

Keywords GIS · Spatial analysis · Mars

Introduction

Mars is a celestial body that evoked numerous speculations and studies on the possible colonization of the planet by humans (Wall 2016). The climatic conditions on its surface and the availability of water make it the most hospitable planet in the solar system (excluding Earth).

Moon has been proposed as the first place to be colonized by human civilization, but unlike it, Mars has the potential to sustain the existence of life forms. Mars is being considered by many scientists as the ideal planet for future colonization and for creating conditions for the existence and development of life due to its

M. Kuźma (✉) · Ł. Gładysz · M. Gralewicz · P. Krawczyk
Faculty of Civil Engineering and Geodesy, Military University of Technology, Warsaw, Poland
e-mail: marta.kuzma@wat.edu.pl

I. Ivan et al. (eds.), *Dynamics in GIscience*, Lecture Notes in Geoinformation and Cartography, DOI 10.1007/978-3-319-61297-3_19

appropriate location for colonization purposes and its potential for the existence of a developed ecosystem in the distant future (Shiga 2008).

The colonization of Mars is an interesting topic that has stimulated not only the imagination of dreamers, but also of many people of science. The project of colonization of Mars may be a useful experiment that will influence the future of the human race (Wall 2016).

Mars (Fig. 1) is the fourth planet from the Sun. Named after the Roman god of war, it is often referred to as the "Red Planet" because the iron oxide prevalent on its surface gives it a reddish appearance (Zubrin and Wagner 1997). Mars is a terrestrial planet with a thin atmosphere, whose surface features resemble both the impact craters of the Moon and the valleys, deserts, and polar ice caps of Earth. There are also other types of terrain, similar to the ones on Earth: volcanoes, valleys, deserts and polar ice caps.

The period of rotation around its axis is slightly longer than that of the Earth and is 24.6229 h (24 h 37 min 22 s) long (NASA, Mars Exploration). The comparison of the most important parameters of the Earth and Mars is shown in Table 1.

The aim of the research work presented in this study was to investigate the possibility of colonizing Mars. For this purpose, pictures from space probes and

Fig. 1 Image of Mars (Viking 1)

Table 1 Comparison of the most important parameters of the Earth and Mars (NASA, Mars Exploration)

	Earth	Mars
Average distance from Sun (km)	149×10^6	228×10^6
Average speed in orbiting Sun (km/s)	30	23
Diameter (km)	6378	3397
Tilt of Axis	23.5°	25°
Length of year	365,25 Days	687 Earth Days
Length of day	23 h 56 min	24 h 37 min
Acceleration of gravity	approx. 9.8 * s^{-2}	3.7 m * s^{-2}
Temperature	−88 to 58 °C	−140 to 30 °C

satellite imagery have been used. They contain information about the terrain, the presence of minerals, temperature distribution, as well as other factors favouring the colonization of the surface of Mars. The scope of work included combining selected satellite images, mosaicking and developing a 3D model based on these images. After the model had been completed, the rover landing sites and their specifications were indicated. It presents the largest craters, canyons and other characteristic objects. All the information is gathered in the developed database. Potential places of residence were determined basing on spatial analysis.

Humans have been fascinated by outer space since the ancient era. For many centuries, we have asked ourselves new questions about the universe around us. Some of them still have not been answered the overriding question still is: "Are we alone in the universe?". Of course, many scientists spin their own theories about this, but no studies have confirmed nor ruled out the existence of other species in space yet. Gradually, we are trying to answer the questions posed by scientists. However, the ability to answer them is closely connected with the development of technology, which enables capturing new data. Just as the seventeenth century witnessed a rapid development of astronomical research related to the invention of the telescope, so in the twentieth and twenty-first centuries, this development was caused by the possibility to launch probes, spacecraft and satellites into space. This provided a new opportunity and allowed the acquisition of data that researchers had only dreamed of before. New opportunities also mean new challenges posed by the scientists themselves.

Currently, a lot of time is spent searching for places in the universe that could be alternative places for colonization. We decided to join the research and to attempt to find out how to present the possibilities of colonization of Mars—the planet that is considered the second (after the Earth) friendliest to humans in the Solar System.

The history of space missions to Mars dates back to 1960, but it was only in 1964. when the American space probe Mariner 4 obtained the first 21 images of the Red Planet. The first success followed by the rivalry between America and the Soviet Union resulted in a rapid development of infrastructure aimed at the development of space missions, which abounded in many missions to Mars, and there were a total of 41.

Methods

Man has always wanted to explore the stars and other wonders of the universe. Some do it; they even leave the orbit of our planet as astronauts. Others watch them and analyse in observatories using telescopes. Still others build remote-controlled devices that travel to places where no man has travelled before. Our work is based on the data collected by spacecraft.

To carry out the analyses we used satellite images and numerical terrain models obtained during the orbital missions:

- Mars Global Surveyor (MGS): Mars Orbiter Laser Alimeter (MOLA)—this experiment measured the height of Martian surface features like mountains and depths of valleys, MOC (Mars Orbiter Camera)—this camera produced a daily wide-angle image of Mars similar to weather photographs of the Earth, while it also took narrow-angle images, Thermal Emission Spectrometer (TES)—this instrument analysed the atmosphere and mapped the mineral composition of the surface by analysing infrared radiation, which scanned the heat emitted from the surface of Mars (NASA, Jet Propulsion Laboratory (JPL))
- Viking Mission to Mars—The primary mission objectives were to obtain high resolution images of the Martian surface, to characterize the structure and composition of the atmosphere and surface, and to search for evidence of life (NASA's Viking Mission to Mars)

The source data used in the project:

1. The image-resolution panchromatic radiometric 8 bits, one pixel corresponds to 460 × 460 m, source: Viking Mission to Mars,
2. Digital Terrain Model—a pixel corresponds to 460 meters, source: Mars Orbiter Laser Alimeter (MOLA),
3. Place of the occurrence of sandstorms—raster data, radiometric resolution of 8 bits, the pixel size corresponds to 3.6 × 3.6 km, source: Mars Orbiter Laser Alimeter (MOLA) (TES),
4. Temperature—raster data, radiometric resolution of 16 bits, the pixel size corresponds to 7.5 × 7.5 km, source: Mars Orbiter Laser Alimeter (MOLA) (TES).

All data were obtained from the websites of NASA and related websites cooperating with them: HiRISE and USGS.

In the studies undertaken the Authors have processed the data obtained by means of unmanned space missions (probes and satellites) with use of GIS (Geographic Information System) software. This software was used, because it allows linking and advanced processing of raster and vector database data. The main tools that were used were those for processing raster data and performing spatial analysis.

In order to find potential colonization sites, the climatic parameters that allow human survival were determined, followed by spatial analysis to find those areas that meet the specified criteria on Mars. The following factors were taken into account to find potential colonisation sites:

1. Temperature
2. The slope of the land
3. The distance from craters
4. The occurrence of sandstorms

During the analysis the following criteria related to the possibility of settling on Mars were identified:

1. Temperatures ranging from −30 to 30 [°C]
2. The terrain with a slope of land below 5/100 m
3. The distance from volcanic craters and, depending on their diameter +20 [km]
4. Dust/sand storms: the wavelength sensing lack of dust in the range of 0, 94–1, 00 [μm].

Results and Discussion

Raster data were calibrated using bilinear interpolation, because it is the most efficient method for the calibration of raster images and it does not overload the host processor as much as the Cubic Convolution (Butowtt and Kaczyński 2003), (Borowiec 2006). This data is calibrated to the MTM2000 (the Martian Transverse Mercator), based on the cylindrical transverse Mercator projection. This system was developed by NASA and it is dedicated to the works related to Mars.

The project required to use the digital terrain model created for the surface of the planet. However, it was not enough to merely know the position of specific altitudes in order to detect places suitable for colonization. Potential colony areas should be quite flat and characterized by low height differences of land. To find such areas, an analysis of DTM designating drops of land on the Martian surface was conducted. A further analysis of raster DTM was performed, with use of SLOPE (Fig. 2) to

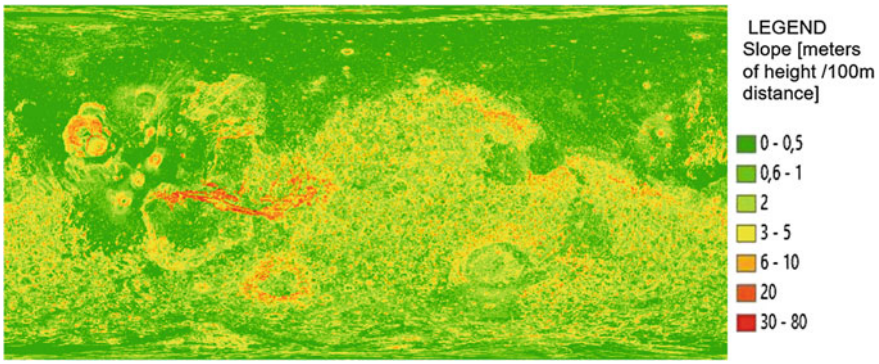

Fig. 2 Map of Mars slope, made on the basis of DTM. *Source* own study

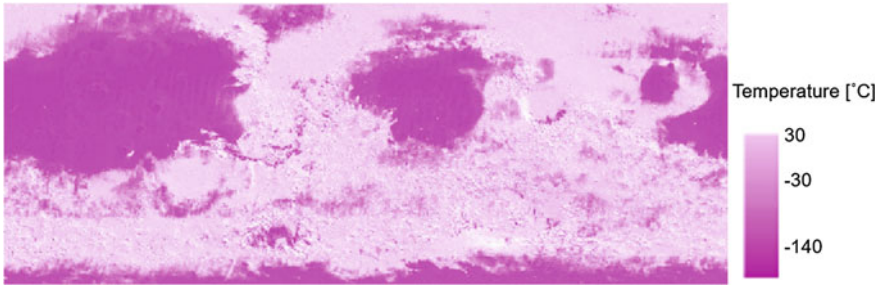

Fig. 3 Temperature on Mars. *Source* own study

determine the inclinations. This function is based on a pixel value, which in this case determines the height of the point on the ground. For each pixel the maximum decline in the area is specified—in reference to the values of adjacent pixels. Finally, after using this tool maps of inclinations were created, with pixel values reflecting the slope at each given point.

The results of this work are shown in Fig. 2. The ranges of data obtained as a result of this analysis are shown in the legend in units of m/100 m (Fig. 2 right). Areas with an inclination not exceeding 5/100 m were deemed as suitable for colonization.

Another analysis was conducted to select areas with the appropriate thermal conditions for settlement. In the analysis of the locations suitable for colonization and human life, those areas where the adjustment range of CH is between −30 and 30 °C were selected (Lucchittas 1999). The analysis (Fig. 3) demonstrated that terrain formation affects the differentiation of temperatures in the atmosphere, just as expected.

Based on the images and the available data a database of the structure was compiled, including objects such as craters, volcanoes, canyons, geographic regions and landing sites of Mars rovers. Each object in the database is characterized by the following data:

1. Number of object,
2. Object Code,
3. Longitude.
4. Latitude.
5. Name,
6. Description and date of discovery (for craters, volcanoes, canyons, geographical regions).
7. Date of landing on Mars (for rover landing sites).
8. The diameter (for craters, volcanoes).
9. Surface area (applies to canyons, geographical regions).

Meteor craters and volcanic cones are objects that can clearly be interpreted in satellite images as areas of a certain diameter. However, they are unstable geological

areas (the applies particularly volcanoes), which were excluded from the areas considered suitable for colonization. The European Space Agency's Mars Express orbiter photographed lava flows interpreted in 2004 to have occurred within the past two million years, suggesting a relatively recent geologic activity. According to an updated study of 2011, it was estimated that the youngest lava flows occurred in the last few tens of millions of years (Hauber et al. 2011). The authors consider this age makes it possible that Mars is not yet volcanically inactive. Due to weather conditions and other orbital factors it is not always possible to land on the designated coordinate. This is why a protective buffer zone was used around areas excluded from colonization such as craters to prevent the spacecraft from landing, e.g. on the edge of a volcanic crater (Fig. 3).

These analyses were performed with use of the BUFFER function, which enabled us to draw circles of a diameter equal to the diameter of the crater increased by 20 km around craters.

According to the definition: Buffer is a simple operation which consists in determining the area within a specified distance from the target object (Potapowicz 2014). Buffers can be created around the point objects, lines and polygons (Fig. 4). This tool is perfect for determining the zones of influence or availability, as well as protection zones around selected areas.

In this way, the resulting polygons were categorized according to their diameter. They were then combined into a single polygon. The resulting exclusion area has been visualized on the raster display digital terrain model of the planet made with use of the MOLA camera (Fig. 5).

In order to avoid situations such as that described in the film "The Martian", in which the protagonist is left alone on Mars after a sandstorm, the project has taken into account the intensity of dust storms and the volume of moving rock dust inside the Martian atmosphere. This was enabled by analysing the imaging of the entire planet created in the thermal infrared channel.

The project was based on the obtained final result of the analysis performed by NASA (Fig. 6), which however did not provide raw data related to the movement of rock particles in the atmosphere. The analysis excluded areas that were considered as having adverse conditions by the authors of the grid. These areas are marked in yellow, orange and red on the grid. On the other hand, areas free of the occurrence of this phenomenon were marked in blue.

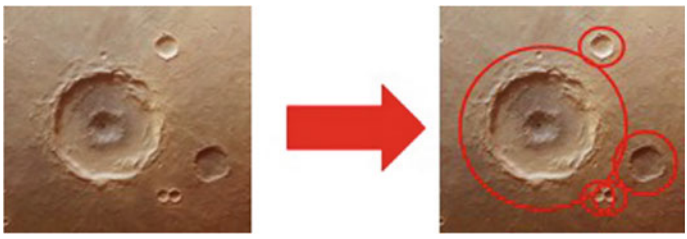

Fig. 4 Buffer of objects on Mars. *Source* own study

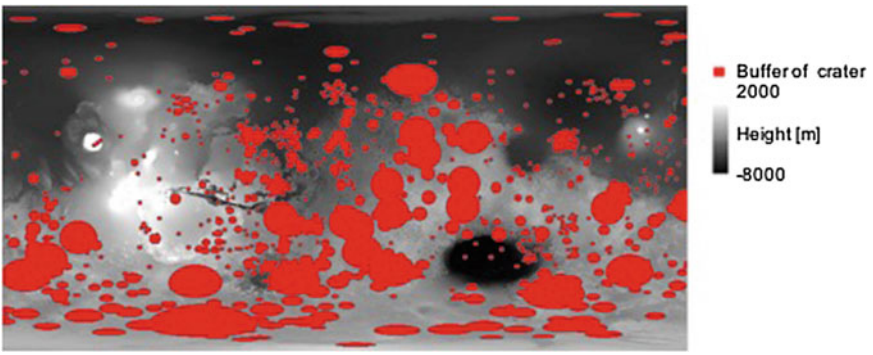

Fig. 5 Location of Martian craters and volcanoes, together with buffers. *Source* own study

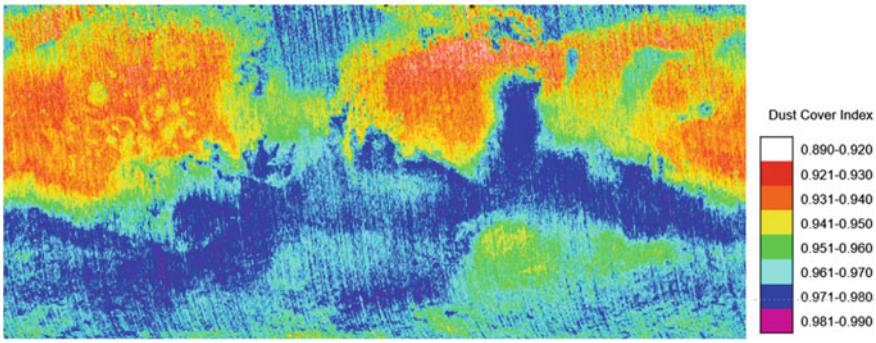

Fig. 6 Dust cover index (Ruff and Christensen 2002)

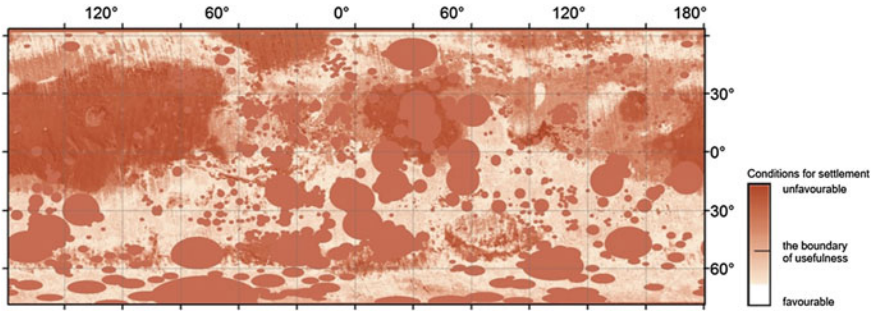

Fig. 7 The map of Mars colonization. *Source* own study

The obtained maps showing the various sub-factors were then combined to create overlays. In this way, the final result of the analysis, which is the location of land suitable for colonization, taking into account various factors was obtained (Fig. 7). The ultimate result was a map (Fig. 7) where sites of favourable conditions

for settlement are marked in lighter shade of brown. The result obtained after determining the adopted colonization limit and calculating the size of the area demonstrates that 43% of the surface of Mars could potentially be inhabited by humans. This is three times more than the surface area of the continent of South America.

Conclusion

The interest in Mars is increasing constantly, year by year. Data acquired as part of the space mission allow us to perform a series of analyses and to become motivated to further explore the Red Planet. Moreover, it gives us hope that the planet might become an alternative place to live.

The main objective of the project was to determine the most favourable places for the colonization of Mars. The factor that had the greatest impact on the final result was terrain analysis. As a result, many areas were not even taken into account. The temperature of the atmosphere on Mars is sufficiently close to that on the Earth's surface, which is why not many areas have been excluded due to air temperatures. Factors such as dust density and distance from craters and volcanoes were also of great importance in the analysis. A huge number of craters and volcanoes excluded certain areas, and the relatively high density of dust is a serious problem on the surface of Mars. The results of the analysis of potential places of residence demonstrate that the area which is the most convenient to live accounts for 43% of the surface of Mars. The created map of potential places of residence will constitute a basis for further studies and enable us to take into account new data and update it immediately.

References

Borowiec, N. (2006). *Geometric correction of high-resolution satellite imagery*. Poland: AGH Cracow.

Butowtt, J., & Kaczyński, R. (2003). *Photogrammetry*. Warsaw, Poland: Military University of Technology.

Hauber, E., Brož, P., Jagert, F., Jodłowski, P., & Platz, T. (2011, May 17). Very recent and wide-spread basaltic volcanism on Mars. *Geophysical Research Letters, 38*(10). Bibcode:2011GeoRL.3810201H. doi:10.1029/2011GL047310

Lucchittas, B. K. (1999) *Geologic map of Ophir and central Candor Chasmata (MTM–05072) of Mars: U.S. Geological Survey Geologic Investigations Series I–2568*. Available November 2, 2016, at http://pubs.usgs.gov/imap/i2568/

NASA, Mars Exploration. Available November 2, 2016, at http://mars.nasa.gov/allaboutmars/facts/#?c=inspace&s=distance

NASA's Viking Mission to Mars. Available November 2, 2016, at http://nssdc.gsfc.nasa.gov/planetary/viking.html

NASA, Jet Propulsion Laboratory (JPL). Available November 2, 2016, at http://mars.nasa.gov/mgs/

NASA. (2010). *Martian methane reveals the red planet is not a dead planet*. Available February 5, 2017, at https://www.nasa.gov/mission_pages/mars/news/marsmethane.html

Potapowicz, A. (2014) *Tutorial ArcGIS 10. Geoprocessing*. Available November 2, 2016, at http://urbnews.pl/tutorial-arcgis-10-geoprzetwarzanie-2/

Ruff, S. W., & Christensen, P. R. (2002). Bright and dark regions on Mars: Particle size and mineralogical characteristics based on Thermal Emission Spectrometer data. *Journal of Geophysical Research, 107*(e12), 5127. doi:10.1029/2001JE001580

Shiga, D. (2008). *Stephen Hawking calls for moon and mars colonies, daily news.* Available november 2, 2016, at https://www.newscientist.com/article/dn13748-stephen-hawking-calls-for-moon-and-marscolonies?feedId=online-news_rss20

Wall, M. (2016). *SpaceX's Elon Musk Unveils Interplanetary Spaceship to Colonize Mars*. Available November 2, 2016, at http://www.space.com/34210-elon-musk-unveils-spacex-mars-colony-ship.html

Zubrin, R., & Wagner, R. (1997). *The case for mars: The plan to settle the red planet and why we must*. Touchstone, New York. ISBN 978-0-684-83550-1. OCLC 489144963.

Czech System for Exploitation of Land Dynamics Using Copernicus Sentinel-1 Data

Milan Lazecký, Ivana Hlaváčová and David Kocich

Abstract The topic of this work covers current implementation of satellite radar (SAR) interferometry (InSAR) techniques for routine identification of dynamic land processes such as downhill creep and landslide activity, subsidence or displacements of various objects of infrastructure. With the emerge of European Copernicus programme, the need of effectivity in satellite Big Data processing increased. There are two Sentinel-1 satellites observing the Earth with 6 days revisit time, sending daily 100 TB of data to be archived. In case of the relatively small area of Czechia, the amount of data to be archived in a Czech national mirror is around 24 GB per day. Czech CESNET e-infrastructure has accepted the role of assessing Copernicus Ground Segment programme. A database mirroring Sentinel data over Czechia is established, however still in its early stage. A potential service based on an interferometric processing of Sentinel-1 data from this database has been prepared in Czech national supercomputing center IT4Innovations. As a basis of the system, several open-source projects were deployed, including MySQL-based burst metadatabase (TU Leeds), ISCE TOPS Processor (NASA/JPL), Doris coregistration algorithm (TU Delft) and StaMPS Small Baselines processor (Stanford University). Though more functionality can be rapidly developed, incorporating some of the own post-processing algorithms, even current early version of the system can yield interesting results by a fully automatic processing chain.

M. Lazecký (✉)
IT4Innovations, VŠB-Technical University of Ostrava, 17. listopadu 15, 70833 Ostrava-Poruba, Czech Republic
e-mail: milan.lazecky@vsb.cz

I. Hlaváčová
GISAT Corp, Prague, Czech Republic
e-mail: hlavacova@insar.cz

D. Kocich
Institute of Geoinformatics, Faculty of Mining and Geology, VŠB-Technical University of Ostrava, 17. listopadu 15, 708 33 Ostrava-Poruba, Czech Republic
e-mail: David.Kocich@vsb.cz

I. Ivan et al. (eds.), *Dynamics in GIscience*, Lecture Notes in Geoinformation and Cartography, DOI 10.1007/978-3-319-61297-3_20

Keywords SAR interferometry · Copernicus · Sentinel-1 · HPC · Displacements monitoring

Introduction

The role of geoinformatics is to give an information about our real world in a spatial model. By adopting temporal information, a four dimension model is created, describing dynamic changes of a specific parameter. Satellite remote sensing offers appropriate input data to prepare such model. Terrain dynamics can be observed by satellite radar (SAR) interferometry (InSAR). European programme Copernicus has developed and sent to orbit a European SAR satellite Sentinel-1A in April 2014 and its twin Sentinel-1B in April 2016. These two satellites fly in a synchronized orbit and acquire InSAR-ready images of any European area every six days. The ground resolution is moderate, around 20×5 m per pixel (in comparison with e.g. TerraSAR-X satellite that offers a resolution of even 25 cm/pixel). But the frequent revisits, global coverage and especially open access makes the data very demanded in the InSAR community. Using radio waves of 5.5 cm wavelength, it has a moderate sensitivity to vegetation and a potential to identify displacements of structures or terrain in a magnitude of down to few millimeters per year.

Various works have already shown the potential of Sentinel-1 interferometry and various groups prepare national InSAR-based maps and systems nowadays (Dehls 2016; Kalia 2016). With the confirmation of Czech e-infrastructure CESNET about active participation and preparation of a Czech Ground Segment to support Copernicus programme, a similar goal is achievable also in Czechia. Current experiments for InSAR-based identification of landslide hazard (Lazecky et al. 2016a), bridge displacements (Lazecky et al. 2016b) or subsidence of undermined zones (Lazecký et al. 2017) demonstrate a realistic potential for Sentinel-1 applications, as well as its limits in the Czech natural conditions. A semi-automatic Sentinel-1 InSAR processing system (Sentineloshka) is already functional and hosted in the Czech national supercomputing center, IT4Innovations. The aim of this system is to generate publicly available maps of terrain displacements, based on the satellite measurements. This will help to increase knowledge of public about the situation in their own neighbourhood and potentially to avoid risks of unknown hazardous situations.

Sentineloshka—The Processing System

The name of the system introduces information that it is specialized in processing of only Sentinel-1 images. Currently, the system involves steps drafted in Fig. 1. First, a system dedicated to pre-processing (running at CESNET infrastructure) identifies

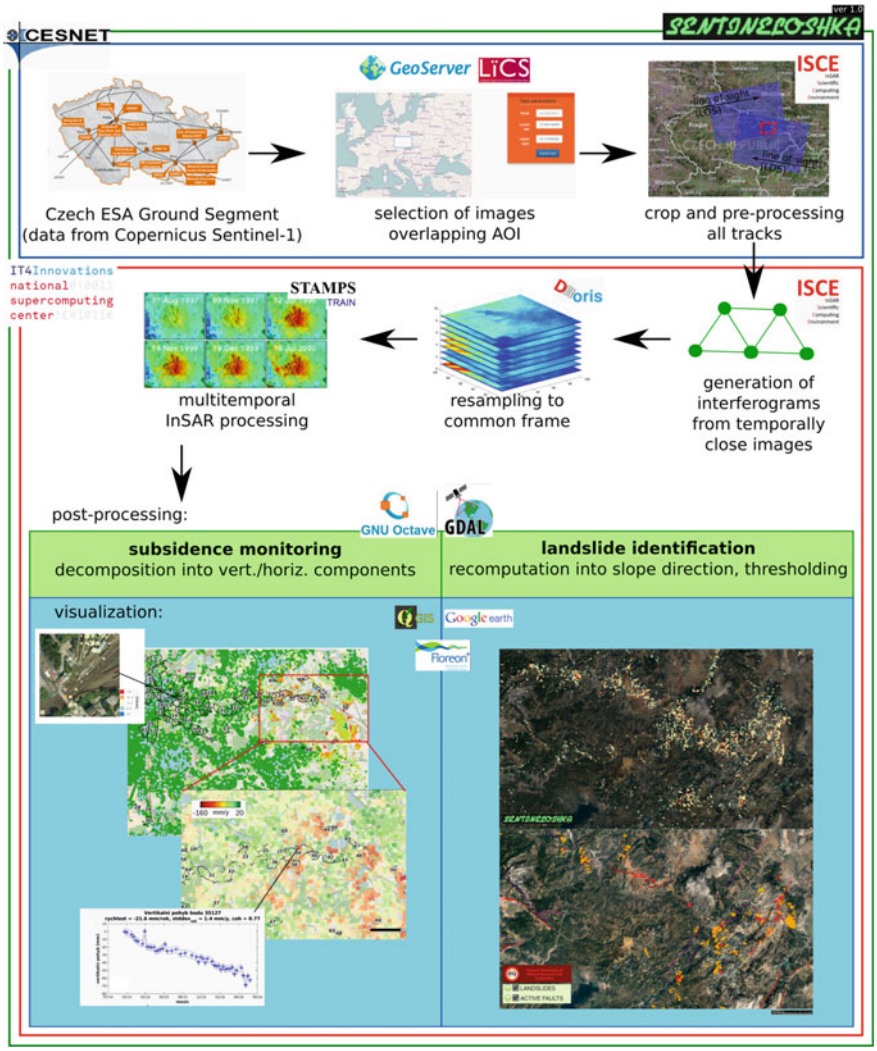

Fig. 1 Basic framework of Sentineloshka processing chain. Sentinel-1 data over selected area are cropped and pre-processed in CESNET environment (*upper figure*). Interferograms are generated, resampled into a common frame and used for SB processing in the IT4Innovations HPC environment (*middle figure*). Results from SB InSAR processing are visualized and post-processed, e.g. for subsidence monitoring or a landslide identification (*lower figure*)

Sentinel-1 images stored in a dedicated storage, based on the input of coordinates of the area of interest (AOI). These images are sorted based on their relative orbit identifier, ensuring interferometric consistence. Afterwards, the Sentinel-1 sub-images (called bursts) are exploited and pre-processed by including precise orbital data and calibrating the image intensity. Once pre-processed, the burst files

of each relative orbit stack are sent to the IT4Innovations High Performance Computing (HPC) facility for the main processing.

The HPC part of the Sentineloshka system performs series of operations for each relative orbit stack. In the first stage, differential interferograms are generated for the net of temporally short connections between all images. Two temporally successive images are used in combination with each image in the stack. The short temporal baselines of interferometric connections (of maximally 24 days) ensure overall high coherence, often with as minimal influence of vegetation in non-urban areas as possible. This strategy is generally named Small Baselines Interferometry (SB InSAR). After generation of interferograms, they are precisely co-registered to a common framework and optionally filtered by a selected spatial filter (e.g. Goldstein filter). Finally, they are sent to an SB InSAR processor in order to perform advanced estimation and removal of error sources and to achieve time series information about the progress of displacements of selected points. The whole processing chain is based on specific open-source codes, such as OpenSARkit (Vollrath et al. 2016), Doris (Kampes et al. 2003), ISCE (Zebker et al. 2010), STAMPS (Hooper 2008), TRAIN (Bekaert et al. 2015) and LiCS database (Li et al. 2016).

After the basic processing, several post-processing mechanisms were implemented. The main two algorithms allow: (a) landslide identification (Lazecky et al. 2016a) and (b) distinguishing between vertical and horizontal components of the displacement vector (Samieie-Esfahany et al. 2009). These algorithms are based on ways of a recomputation of displacements identified in the satellite line of sight (LOS) from all the input satellite tracks. In a case of landslide identification, the displacements are recomputed into the direction of slope, while decomposition algorithm assumes the existence of objects observed from at least two opposite orbital tracks that allow distinguishing between horizontal and vertical movement. Results of using both algorithms are under validation stage.

Deeper Insight into Processing Steps

CESNET Preprocessing Cloud: Once latitude and longitude coordinates of AOI corners are given, the script will send an SQL query to MySQL database based on LiCS solution (Li et al. 2016). This database links existing Sentinel-1 SLC zip files there were downloaded beforehand and recognizes bursts within these files. The SQL query returns set of Sentinel-1 zip files that include bursts covering the AOI and sorts it according to relative orbit track number. If the number of images is lower than the default value of 10, this relative orbit is dropped from further processing. Afterwards, for all the relative orbits tracks, its images are pre-processed, i.e. bursts overlapping AOI are extracted. For this purposes ISCE algorithms of topsApp.py script has been adapted to allow performing first two steps of its workflow (Agram et al. 2016) for a single image only. Additionally, the latest

SRTM in 1 arcsec resolution is automatically downloaded. All relative orbit folders are uploaded to the HPC server continuously with the processing.

HPC Processing: Once a relative orbit folder is uploaded, the images are combined in SB way—every image (except for first and last one) is connected with three other temporally close images. ISCE is called for each connection to perform all the steps to generate merged interferogram for all the uploaded bursts—only after successful interferogram generation, this interferogram is cropped to the AOI bounding box (including a 0.01° buffer zone around it). This processing is distributed to computing nodes by PBS scheduler since it is time and computationally extensive.

Once a generation of all interferograms is finished, a check is performed, dropping unsuccessfully generated combinations, in extreme case cutting the dataset into consistent chunks. Then a master image is selected in the middle of the dataset and all other interferograms are coregistered to it using Doris—the Doris processing has been parallelized for each interferogram per processing core. Only after the coregistration, the interferograms are cropped to the final bounding box, spatially filtered using Goldstein filter and exported to the STAMPS processing structure. Finally, the STAMPS processing is performed, based on universally selected parameters. Several own scripts related to noise filtering and points pre-selection as well as TRAIN atmosphere correction toolbox (Bekaert et al. 2015) are included in order to maximally increase the processing performance. The final result (including coherence quality parameter) is exported into a CSV file, ready to be loaded into a GIS software, e.g. Quantum GIS using giSAR toolbox (Guimaraes and Lazecky 2016).

Optionally, a script using GDAL library is prepared to convert the output format into an ESRI Shapefile format and to interpolate mean velocity values into a raster file. For landslide identification, only points at slopes are selected and their velocity model is recomputed towards slope direction, neglecting N-S direction and layover areas due to InSAR blind zones (Lazecky et al. 2015). Once all relative orbit directories are processed, the results are merged using the decomposition algorithm.

Example Case Study: Ostrava-Karvina Region

As the case study, Ostrava-Karvina region has been selected. This region is affected by a longterm black coal mining. While mines in Ostrava disappeared after their closures in 1990s, there are still mines active in Karvina region causing subsidence and other mining-induced problems in the region (e.g. increased presence of methane in the low atmosphere). Extents and dynamics of subsidence troughs are easily identifiable from classic InSAR processing, multitemporal interferometry allows an easy identification of continuous displacement of simple structures (especially houses) (Lazecky et al. 2016). Expected results were achieved also

using the Sentineloshka system, in the automatic way. Subsidence areas in the mine surroundings were detected and their rate estimated. Displacements of buildings in the edge of urbanized areas were identified.

In total, 140 Sentinel-1 images have been selected over Ostrava-Karvina region from four different orbital tracks, two from descending (N → S), two from ascending passes (S → N). The images were taken during the period of 10/2014–10/2016, the selected zone of interest contained area of around 35 × 35 km. Several images have been (automatically) dropped due to problems within the pre-processing stage. The SB InSAR processing has been performed separately for each data stack. Two of the data stacks showed large inconsistencies and their results were not taken into account. Applied software STAMPS is capable of fine-tuning the inter-steps of the processing. However since the experiment deals with the possibility of fully automatic processing chain, it was decided to drop the whole erroneous datasets from further consideration instead of manual attempts to correct them.

All tracks show similar results after SB processing—the estimated models are consistent, therefore the results can be considered reliable. In total, 257 interferograms were generated from the data stack. The processing took 13.5 h, however, part of the processing time was filled by waiting in the queue for processing tasks in the HPC querying system.

For visualization purposes, a specialized toolbox was prepared as a Python extension to Quantum GIS: giSAR (Guimaraes and Lazecky 2016). It allows importing processing results into the GIS environment able to perform post-processing functions, such as plotting time series of a selected point or interpolation etc. The giSAR is a basic open-source tool developed as a connector between heavy processing chain system of PS/SB InSAR and the world of GIS for an effective work with geospatial data. The currently existing version offers an import of InSAR-processed data in a comma-separated text file format (CSV) and a basic setting of a graphical representation of georeferenced PS/SB points in the environment of Quantum GIS open-source software (see Fig. 2). The future version should allow an easier access to selected processing tools already available in Quantum GIS or its other toolboxes. Graphical output of this tool is visible in Fig. 3, with OpenStreetMap and FreeGeodataCZ as the background layers. Non-expert users would prefer KML file plotting the results in widespread Google Earth framework. For a centralized solution, however, the optimal dissemination of results is to be provided by a web map environment, e.g. based on Geoserver.

The Fig. 3 shows the basic result—a map of a mean LOS velocity of displacements. Subsidence at undermined areas was properly identified and its rate was estimated (though the accuracy can be lower due to a less accurate SB InSAR method used here). An example of decomposition is provided in Fig. 4, based on small area processing of relative orbits 51 and 175.

Fig. 2 Basic window of Quantum GIS: giSAR toolbox offering preliminary functionality of importing InSAR-based CSV file as GIS layers

Discussion

Sentinel-1 is becoming very popular as the new generation of InSAR-capable satellites, especially thanks to high revisit rate, global archived coverage and the open access to the data. It still is limited due to physical constraints, known to every C-band SAR system. The SB InSAR tries to compensate the major problem that is the total loss of signal coherence in the case of presence of vegetation. Though 6 or 12 days is relatively short time, the signal is still decorrelated by the vegetation. It was found out that an exception exists during the seasons of diminished vegetation activity, such as early spring or late autumn. Winter period is covered by another source of decorrelation that is a snow. The current version of the system is based on SB InSAR that does not distinguish seasonal coherence. The algorithm uses spatial information between selected points; including unstable points (in vegetated areas) would cause errors that may propagate into originally stable points. These and other technical issues keep Sentinel-1 and InSAR generally from the state of a reliable technique for monitoring terrain displacements, though the theoretical accuracy of measurements using this technology is around 1 mm/year using persistent scatterers

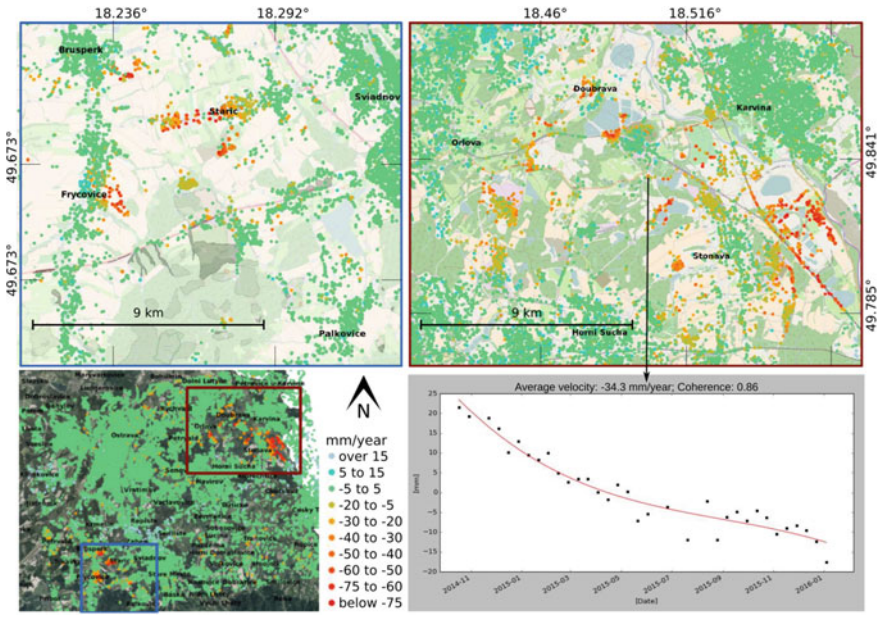

Fig. 3 Merged automatic SB InSAR result of descending relative orbits 51 and 124 showing subsidence in Karvina region (*red box*) and around Paskov mine (*blue box*); data from 10/2014–01/2016

(PS)-based techniques. The SB InSAR has been chosen here for the possibility of identification of movements in non-urban areas, though with lower precision, especially due to the merging of a short temporal information in order to compute a long temporal displacement value. There is a lot of further work needed into the development of a season-based InSAR processor that would indicate movements also in densely vegetation-covered areas. It is in the plan to use polarimetric footprints that would distinguish the vegetation cover (Donga et al. 2013) since Sentinel-1 is using both co-polarized and cross-polarized wave backscatter information, or at least some other public available data such as moderate-resolution land cover maps. Yet, the work demonstrates that the automatic system is currently able to evaluate displacements over solid structures (buildings, transportation structures etc.) and non-cultivated grass lands or sparsely vegetated areas.

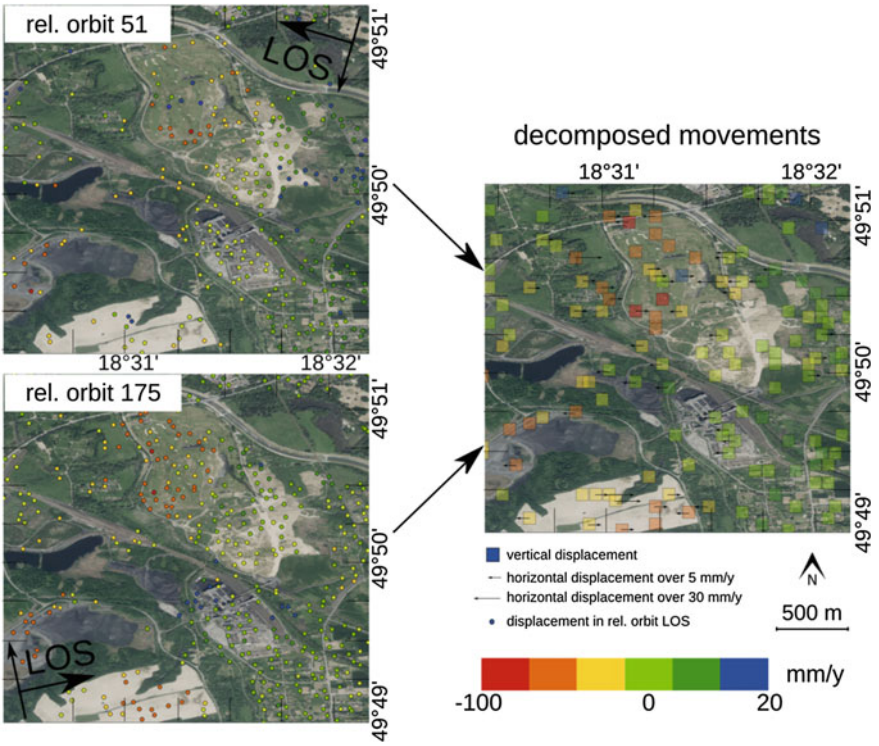

Fig. 4 Decomposition of displacement direction from data of descending and ascending tracks. Location is at the mining site of CSA Mine, Karvina

Conclusions

We demonstrate the potential of Sentinel-1 for monitoring of land dynamics in this and previous works. Areas sparsely covered by vegetation can be evaluated using a fully automatic chain, as prepared within Sentineloshka system (Lazecky 2016). The current preliminary version of the system allows to achieve only a static map describing temporal changes of a selected area. We consider it important to make such map publicly available, while it must be noted that the reliability of results is depending on local conditions and the interpretation of shown results is to be kept within the hands of an expert. However a public feedback is necessary in order to perform appropriate steps towards specific areas or structures.

Further steps of the system development include a special way to store Sentinel-1 data that would allow an effective automatic system for dynamic observations of up-to-date displacements of terrain or structures. In case of need, such dynamic implementation would allow fast assessment of deformations and could provide important information for risk identification. Based on the innovative data storage, we will be able to implement also more reliable processing techniques,

such as persistent scatterers (PS) or partially coherent PS technique. Such storage will be used also for non-interferometric SAR processing, using a radar backscattering coefficient of SAR images. This will allow automatized processing leading to e.g. current flood maps, time series useful for a change detection (forest loss, agriculture monitoring), soil moisture maps etc. The current state of described system is still in a preliminary stage with the development continuously ongoing. The main target is to generate reliable maps of active land displacements over the whole Czechia and share them publicly within an appropriate framework—the Czech Collaborative Ground Segment should provide such framework and public interactive maps are being kept as a topic under ongoing discussion.

Acknowledgements This work was supported by The Ministry of Education, Youth and Sports from the National Programme of Sustainability (NPU II) project "IT4Innovations excellence in science—LQ1602" and from the Large Infrastructures for Research, Experimental Development and Innovations project "IT4Innovations National Supercomputing Center—LM2015070". Access to computing and storage facilities owned by parties and projects contributing to the National Grid Infrastructure MetaCentrum, provided under the programme "Projects of Large Infrastructure for Research, Development, and Innovations" (LM2010005), is greatly appreciated. Authors are grateful to researchers sharing their development work, especially team of Leeds University led by Prof. Andrew Hooper that offered codes of the LiCS database and UNAVCO WInSAR for opening codes of ISCE software. The research is supported by the VŠB-Technical University of Ostrava, the Faculty of Mining and Geology, grant project Crowd sourced geodata, No. SP2016/41.

References

Agram, P., et al. (2016). *ISCE topsApp*. https://winsar.unavco.org/isce.html

Bekaert, D. P. S., Walters, R. J., Wright, T. J., Hooper, A. J., & Parker, D. J. (2015). Statistical comparison of InSAR tropospheric correction techniques. *Remote Sensing of Environment*. doi:10.1016/j.rse.2015.08.035

Dehls, J. (2016). The Norwegian national ground motion service—Experience from first year(s) of operation. Hannover: BGR, November 3–4, 2016.

Donga, J., Xiao, X., Chen, B., Torbick, N., Jin, C., Zhang, G., et al. (2013). Mapping deciduous rubber plantations through integration of PALSAR and multi-temporal Landsat imagery. *Remote Sensing of Environment, 134,* 392–402.

Guimaraes, P., & Lazecky, M. (2016). *giSAR (quantum GIS toolbox)*. https://github.com/espiritocz/giSAR

Hooper, A. (2008). A multi-temporal InSAR method incorporating both persistent scatterer and small baseline approaches. *Geophysical Research Letters 35*.

Kalia, A. (2016). *Ground motion service germany*. Hannover: BGR, November 3–4, 2016.

Kampes, B. M., Hanssen, R. F., & Perski, Z. (2003). Radar interferometry with public domain tools. In *Proceedings of FRINGE*, (Frascati), pp. 1–5.

Lazecky, M., Comut, F. C., Hlavacova, I., & Gurboga, S. (2015). Practical application of satellite-based SAR interferometry for the detection of landslide activity. *In WMESS, 2015,* 613–618.

Lazecky, M., Canaslan Comut, F., Nikolaeva, E., Bakon, M., Papco, J., Ruiz-Armenteros, A. M., Qin, Y., et al. (2016a). Potential of Sentinel-1A for nation-wide routine updates of active landslide maps. ISPRS 2016, *XLI-B7*, 775–781.

Lazecky, M., Hlavacova, I., Bakon, M., Sousa, J. J., Perissin, D., & Patricio, G. (2016b). Bridge displacements monitoring using space-borne X-band SAR Interferometry. *IEEE JSTARS PP, 99*, 6.

Lazecky, M. (2016). *Sentineloshka*. https://github.com/espiritocz/sentineloshka

Lazecký M., Jiránková E., & Kadlečík P. (2017). Multitemporal monitoring of Karvina subsidence trough using Sentinel-1 and TerraSar-X interferometry. *Acta Geodynamica et Geomaterialia, 14*(1, 185), 53–59. doi:10.13168/AGG.2016.0027

Li, Z., Wright, T., Hooper, A., Crippa, P., Gonzalez, P., Walters, R., et al. (2016). Towards InSAR everywhere, all the time, with Sentinel-1. In *International Archives of the Photogrammetry, Remote Sensing and Spatial Information Sciences—ISPRS Archives*, pp. 763–766.

Samieie-Esfahany, S., Hanssen, R., van Thienen-Visser, K., & Muntendam-Bos, A. (2009). On the effect of horizontal deformation on InSAR subsidence estimates. In *Proceedings of the Fringe 2009 Workshop*, ESA SP.

Vollrath, A., Lindquist, E., Jonckheere, I., & Pekkarinen, A. (2016). Open Foris SAR Toolkit—Free and open source command line utilities for automatized SAR data pre-processing. In *ESA LPS 2016*, Prague.

Zebker, H. A., Hensley, S., Shanker, P., & Wortham, C. (2010). Geodetically accurate InSAR data processor. *IEEE Transactions on Geoscience and Remote Sensing, 48,* 4309–4321.

Prediction Models for Landscape Development in GIS

Chukwudi Nwaogu, Antonín Benc and Vilem Pechanec

Abstract Ameliorating the impacts of global change on the physical and socioeconomic environment is essential for the restoration and sustainability of our ecosystems. Landscape modifications have been discovered as one of the primary causes of the environmental change and has therefore gained reasonable attention in the modeling techniques, because understanding the land use-land cover change (LULCC), the drivers and processes provides the solution to the environmental challenge. Sequel to this, several empirical methods and software for modeling LULCC have been developed and applied such as the spatial-statistical based (regressions, Artificial Neural Networks, GISCAME), Markov Chain, Cellular automata, the hybrid (CA-Markov), Agent-Based, CLUE, Land Change Modeler (LCM), Dinamica EGO, GEOMOD, and Scenarios for InVEST. This paper reviews the implementations, prospects, and the limits of these modeling software packages. Comparative assessment review of the models including their capabilities, applications and output were also highlighted. Finally, two of the models (LCM and CLUE) were used to predict the LULCC in a municipal area in south-east, Nigeria (a case study), and this helps to illustrate the afore-mentioned explanations and variations about the outputs of different models in assessing the LULCC of same location in time. Different models can behave differently when applied in same location at the same time as demonstrated by the applications of LCM and CLUE in our study. In addition to other LULC type dynamics in the models outputs, we have prediction map from CLUE showing higher built-up areas (42.7 km^2) compared with that of LCM result (35.2 km^2) while, the LCM projection revealed more areas for light vegetation cover (29.5 km^2) in comparison with the 16.5 km^2 from the CLUE model result.

C. Nwaogu (✉) · A. Benc · V. Pechanec
Department of Geoinformatics, Palacký University Olomouc,
771 46 Olomouc, Czech Republic
e-mail: cnwaogu@gmail.com

A. Benc
e-mail: antonin.benc@gmail.com

V. Pechanec
e-mail: vilem.pechanec@upol.cz

I. Ivan et al. (eds.), *Dynamics in GIscience*, Lecture Notes in Geoinformation and Cartography, DOI 10.1007/978-3-319-61297-3_21

Keywords Landscape change models · Land change modeler · CLUE · Markov chain · Cellular automata

Introduction

Land use is referred to the anthropogenic activities which have direct link to land, and utilizing its resources or creating an impact on it by interfering in the environmental processes that determine the functioning of land cover. Landscape (land use-land cover) changes are not only complex but also exert dynamic processes which are not only caused by the natural and anthropogenic systems but as well affect the human and biophysical components. Landscape variability has direct and indirect effects on all the planet spheres namely; lithosphere, hydrosphere, biosphere and atmosphere. The impacts of land use dynamics lead to most environmental issues which are of local, regional or global importance. The modifications in landscape especially by man Turner (1987) are critical issues of global concern, and changes in landscape cannot be comprehended without a good knowledge of the land use-land cover changes that drive the changes, vis-a-vis their interactions with human factors Ojima et al. (1991). Land use-land cover change models are spatially-explicit: they consider socio-economic and environmental causes and effects which make them most suitable applicable models to simulate landscape changes. These approaches can identify, assess, and predict the relationships between physical and socio-economic variables. Unlike the traditional models which are not able of simulating all these parameters, the combinations of existing geospatial data, geostatistical techniques, advanced GIS functionality and the Agent-Based approaches have produced good results in land use-land cover change prediction. The geospatial/geostatistical models can produce precisely accurate results that support land stakeholders including developers, managers, agriculturists, ecologists, environmentalist, economists and policy makers in achieving improved landscape administration and sustainable landscape management. *Aim/Objectives of this paper*: The choice of the most suitable model for assessing an area is very crucial and challenging. This is because every model produces a result but the question is, 'how reliable and applicable is this produced result' in relation to solving the targeted problem? As models have their individual strengths and limitations so they vary in their applications for achieving satisfactorily acceptable and sustainable results. For instance, a thoroughly tested model could have been used severally to produce good output for perfect decision in a temperate climate; there are possibilities that same model will give a poor result with wrong decision in either another location in temperate region or in a tropical environment. Therefore, achieving a good result today with a given landuse model is never a guarantee that same model will be perfect tomorrow when applied in the same area. It is in this context that this paper attempted to give the model users a first-hand glance information for model selections by briefly reviewing some of the landuse models, their capabilities and implementations, prospects and limitations, and applications and results. This study

reviewed some of the principal models and algorithms used for landscape change prediction such as regressions, Markov Chains (MC), Cellular Automata (CA), MC-CA hybrid, Neural network, Agent-Based, GEOMOD, LCM, CLUE, Dynamica EGO, Scenarios for InVEST, and GISCAME. Besides, the variations in the outputs of LCM and CLUE were also investigated and discussed with illustration from a study carried out in the South-East Nigeria where these two models were applied using same input data, at the same time and space yet, the results of the LULC change detected differed significantly.

Models and Algorithms Used for Landscape and Land Use Change Predictions

In this section of the paper, the review of the spatially explicit landscape and LULC models and their methodologies were briefly discussed. The use of geospatial-statistical methods has recently become popular in LULC studies including Linear regression, Logistic regression, Multinomial regression, Markov chain, Cellular automata, The Hybrid (MC-CA), Artificial Neural Network, Agent-based, and others. The brief overview of them have been summarized covering the geostatistical models (Table 1), their implementation and output (Table 2), their application software, development, capabilities and input (Table 3), and their strength and weakness in landscape/land use change projection (Table 4).

Regressions Models

Regression analysis is a vital statistical method used to investigate the association of a dependent variable with one or more independent variables. More complex methods of regression exist, which are intended for different types of dependent variables and data structures. Regression Analysis and its major types have been widely used in Land use- land cover change modeling (Table 1). *Linear regression* is a model that estimates the coefficients of a linear equation, involving one or more independent variables, that best predict the value of the dependent variable. Linear regression is a frequently used technique; however, in LUCC modelling, this regression is less popular because linear regression can only be applied for continuous dependent variables. Instead, logistic or multinomial regression is used, because land use is normally expressed as a discrete variable. An exception is NDVI data, which range between -1 and 1 and belong therefore to continuous data. Linear regression can also be used to derive input data, e.g. trends of population growth out of census data, or for validation. In linear regression analysis, it is possible to test whether two variables (or transformed variables) are linearly related and to calculate the strength of the linear

Table 1 Comparison of the regression/statistical models used for landscape change prediction

Regression models	Dependent variable type or data structure	Application land use class/type & examples
Linear regression	Continuous	Vegetation: Weiss et al. (2001); Settlement: Chen (2002); Urban growth: López et al. (2001), Agriculture: de Wolff et al. (2000)
Logistic regression	Discrete bivariate	General Land use: Verburg et al. (2004)
		Agriculture: Xie et al. (2014)
		Coastline assessment: Fasona et al. (2011)
		Ecosystem services: Serneels and Lambin (2001)
		Vegetation and deforestation: Schneider and Pontius (2001)
Multinomial regression	Discrete multivariate	Deforestation and agriculture: Mertens et al. (2002)
		Agriculture: Speybroeck et al. (2004)
Ordered logit/probit	Discrete ordered	Transport and deforestation: Chomitz and Gray (1996)
Tobit analysis	Censored continuous	Forestry and agriculture: Chomitz and Thomas (2002)
Simultaneous regression	Interdependent relations	Soil: Ben-Dor and Banin (1995)
Multilevel models	Hierarchically organized data sets	Agriculture and urbanization: Qian et al. (2010)

relationship if the relationship between the variables can be described by an equation of the form $Y = \alpha + \beta X$. *Logistic regression* deals with the estimated probability of the event Y (the dependent variable) based on independent variables (X), the occurrence of the phenomenon can affect Y. The variable Y takes only the values 0 and 1, where 0 indicates that the variable did not occur, while 1 indicates that the variable occurred (e.g. occurrence or non-existence of buildings). This denote a vector of independent variables as $x = (x1, x2, \ldots, xn)$ and a dependent variable as $y = g\ (x) = \beta 0 + \beta 1x1\ \ \beta 2x2 + \cdots + \beta nxn$ where βi are coefficients. Logistic regression model uses CLUE including CLUE-S or Dyna-CLUE respectively Pechanec (2014). *Multinomial logit models* are used for the case of a dependent variable with more than two categories. This type of regression is similar to logistic regression, but it is more general because the dependent variable is not restricted to two categories. Each category is compared to a reference category, e.g. all types of forest conversion are compared to the stable forest category.

Artificial Neural Networks (ANN) and *GISCAME* are also subcategories of empirical geospatial statistics. ANN models require formal statistical training to develop and can implicitly detect complex nonlinear relationships between different LULC types. ANN can be developed using multiple different training algorithms. A major limitation to ANN application in landscape change prediction is that it is prone to overfitting. GISCAME on the other hand was coined from GIS as geographic information system, CA for cellular automaton, ME representing

Table 2 Overview of LULC change detection and prediction models: implementation and output

Model and algorithm	Historical development continuation	Data driven	Land suitability	Expert knowledge combination	Neighborhood relationship result	Actor relationship result	Application examples
Statistical-based (e.g. regressions)	Feasible	Yes	Feasible	No	Feasible	Feasible	Vegetation Schneider and Pontius (2001); Agriculture (Xie et al. 2014); Coastline studies (Fasona et al. 2011)
Cellular automata (CA)	Consistent	Yes	Feasible	Yes/No[a]	Consistent	Unlikely	Landuse-cover Silva and Clarke (2002); wildfire propagation Clarke et al. (1995); Transport Benjamin et al. (1996)
Markov chain (MC)	Consistent	Yes[a]	Unlikely	Yes/No[a]	Unlikely	Unlikely	Urban planning (Weng, 2002); Landscape Turner (1987); Transport (Iacono et al. 2015); Agriculture & forest Opeyemi (2006)
CA—MC hybrid	Consistent	Yes[a]	Feasible	Yes/No[a]	Consistent	Feasible	Land use change Silva and Clarke (2002); Urban growth (Wang 2002)
Agent-based	Feasible	Yes	Feasible	No	Feasible	Consistent	Energy and climate change (Zhang et al. 2011; water management (van Oel et al. 2010)
Neural networks	Feasible	Yes[a]	Feasible	Yes/No[a]	Feasible	Feasible	Land transformation and model (Pijanowski et al. 2009; 2002)
CLUE	Consistent	Yes	Feasible	No	Feasible	Feasible	Agriculture and forestry (Veldkamp and Fresco 1996)
LCM	Consistent	Yes	Feasible	No	Consistent	Feasible	Nature Reserv Malach (2009); Settlement (Indrova and Kupkova 2015)
GEOMOD	Feasible	Yes	Feasible	No	Feasible	Unlikely	Watershed Benešová (2008)
DINAMICA	Feasible	Yes[a]	Feasible	Yes/No[a]	Feasible	Unlikely	Forestry and Agriculture Soares-Filho et al. (2002)
SCENARIOS for InVEST	Feasible	Yes[a]	Consistent	Yes/No[a]	Consistent	Consistent	Wetlands Harmáčková and Vačkář (2015)
GISCAME	Feasible	Yes[a]	Feasible	Yes/No[a]	Consistent	Consistent	Land use-landscape (Fürst et al. 2010); Soil and relief (Sponagel et al. 2005)

[a] Supports or requires expert knowledge or data driven based on the change potential creation procedure

Table 3 Characteristics of landscape change models: application software, development, capabilities and input

Evaluation parameter	CLUE	Land change modeler (LCM)	Geomod	Scenarios for InVEST	Markov chain (MC)	Cellula automata (CA)
Cost/price	Free	Commercial	Commercial	Free	Free	Free
Application type	Stand-alone	Component of IDRISI & Add-In ArcGIS	IDRISI component	InVEST component	Stand-alone/component of IDRISI	
Stability	High	Low	Medium	Very low	High	High
Support data format	ASCII	Raster-RST (Idrisi format)	Raster-RST (Idrisi format)	Raster-Esri GRID	ASCII	
Development	Long, custom development team	Long, custom development team	Long, custom development team	New: just beginning	Long, custom development team	Long, custom development team
LULC input	1 map	At least 2 maps	At least 2 maps	1 map	1–2 maps	1–2 maps
Defining potential transition	Numerical values	Automatic	Automatic	Nil	Automatic	Automatic
Works with area history	Very limited	Yes	Yes	Nil	Yes	No
Defining factors	Yes	Yes	Yes	Yes	Yes	Yes
Main purpose	Distribution of each LULC cells in relation to user-specified values based on the area's suitability	Identification of LULC changes and derived trends	Modeling category 1 changes in the future	Creating maps from LULC development scenarios	LULC change simulation	LULC change simulation

ASCII is the most common format for text files in computers and on the internet. In ASCII file, each alphabet, numeral or special character is represented with a 7-bit binary number (a string seven 0s or 1s). 128 possible characters are defined. Adapted and modified from Pechanec (2014)

Table 4 Summary of models/algorithms for landscape (LULC) change: strength and weakness

Model name/type	Variables needed	Strength	Weakness
Spatial-statistical	Land use data/map; geospatial attributes	Ease of computation; Future trends can be predicted based on historical data; Provides a statistical platform for more advanced modeling; Can deal with multivariate components; Allows for an evaluation of the "fit" of the model prediction and the data	Need data over long period of years to predict trends; Measurement errors in explanatory variables; Needs more methods to be performed before producing simulated maps; Not confined to single equation; Not all variables are linear/non-linear at same time as assumed during modeling; Difficult at times to define and integrate human parameters
Markov chain (MC)	Land use map	Ability to develop a prediction model with just two years of data; Ability to calculate performance even if data for some years is missing; Number of land classes is insignificant; Transition probability maps are developed	Lack of dependence on functional mechanisms; Devoid of simple assumptions of stationary makes analyses difficult; Depends on predictions of system behavior over time; Produces non-geospatial output
Cellular automaton (CA)	Built-up pixels/cells	Permits coding of several rules; modeling from the known to the unknown/developed cells; Good spatio-temporal and neighborhood interaction analysis	Negligence of human behavior influence on the spread of built-up areas; Exclusion of biophysical data; Allows for modeling of one land class
The hybrid: CA-MC	Land use map; no ancillary data	Best model for Spatial–Temporal Pattern stimulation; Gained from the advantage of both CA and MC models; Can produce a multi-class map	presence of non-real edges on the modeled maps contrast reality; No variables has utmost importance; Constraints from several factors such as slope, aspect, elevation and existing land-use proximity
Agent-based	Land use; socioeconomic; utilities data	Geospatial features; gives attention to very data; gives every variables individual attention; Includes socioeconomic data; combines the CA operation to detect changes in land use	Large data requirement; Agents' behavior requires coding
GEOMOD	Land use map	Operates at any spatial scale; can predict land use change in space, time and value; capable of using many kinds of spatial data	Large size of input databases required; High cost of implementation; Applicability only for unplanned land-use change

multi-criteria evaluation and was formerly called "Pimp Your Landscap". It considers the landscape as an integrative layer for interactions between different land use types, land users, and ecosystem processes, which contribute to the provision of ecosystem services (Fürst et al. 2010). GISCAME is based on three methodological approaches namely; cellular automaton (modified), geographic information system, and multi-criteria evaluation.

Markov Chain (MC)

Markov chain is a probabilistic state-transitional model with LULC at time (t + 1) and strictly a function of LULC at time (t). In this model, the transition rules for any given LULC class/type are dependent on the historical transition probabilities which are independent from status or dynamics of adjacent cells.

Cellular Automata (CA)

Though CA is a spatio-temporal extension of the Markov transitions models yet, can function as a state-transition model with neighborhood component. The transition rules of CA are defined by the current state of a cell, as well as by status of neighboring cells. Several general parallel CA-based land use simulation systems have been developed for users to implement parallel CA applications and in the operating background of CA. Examples include the *cellular automata environment for systems modeling (CAMEL)* and *cellular programming environment (CARPET)*; *SLUTH (slope, landuse, exclusion, urban extent, transportation and hillshade)* model, formerly called the Clarke Cellular Automaton Urban Growth Model; *LEAM "Land use Evaluation and Impact Assessment Model*"; *duo—Urban Evolution Dynamic Modelling* (Batty et al. 1999); *DINAMICA* model or model *METRONAMICA,* and *Dynamic Urban Evolution Model (DUEM)* (Heppenstall et al. 2012). The primary limitation of CA falls on the difficulty in the implementation of the transition rules especially where there are no existing standard techniques to define those rules. However, the development of *Multi-Criteria Evaluation*, and *fuzzy logic* has been used to resolve the challenge.

DINAMICA EGO (hereafter DINAMICA) uses transition probability maps that are based on the weight of evidence and genetic algorithm methods. These maps simulate landscape dynamics using both Markov chain matrices to determine the quantity of change and a cellular automata approach to reproduce spatial patterns. DINAMICA has been applied to a variety of studies, such as modeling urban growth, tropical deforestation from local to basin-wide scales, and fire regimes Soares-Filho et al. (2002).

The CA-MC models: The integration of CA-Markov promotes the transition probabilities of one pixel to be a function of neighboring pixels. The combinations

of CA-Markov tools have been used to resolve most of the challenges of integrating the natural and human variables in land use change forecasts. CA model is affected by neighborhood type, neighborhood size and cell size parameters, the hybrid has helped in resolving these problems.

Land Change Modeler (LCM) is an innovative land planning and decision support system that is fully integrated into the TerrSet software. LCM as typical tool for simulating and improving Ecological Sustainability promotes the modeling of land use changes. The LCM was first introduced to IDRISI 15.0 (Andes product) in 2006. Now LCM operates in IDRISI Selva 17.0 as one of many models for landscape and environmental modeling. Model LCM also works as an extension to ArcGIS software from ESRI. Extension is available for ArcGIS version 9.3 to the latest version of ArcGIS 10.3 Pechanec (2014). Land Change Modeler simplifies the complexities of change analysis with an automated, user-friendly workflow. Land Change Modeler allows you to rapidly analyze land cover change, empirically model relationships to explanatory variables, and simulate future land change scenarios. LCM like other models has unique features which make it important in landscape and land use change projection (Tables 2 and 4).

Agent-based modeling (ABM) also known as 'agent-based systems' (ABS) or 'agent-based modeling and simulation (ABMS)' is a natural method for describing and simulating a system composed of real-world entities especially when using object-orientated principles. Modeling with agents is more related to 'reality' than other modelling approaches. Agent-based simulations provide an opportunity to represent and test social theory which cannot easily be described using mathematical formulae. Modeling using agents has its roots in artificial intelligence and a new approach for modeling systems, working with so-called 'Agents' Pechanec (2014). Agent is real (living or inanimate) or abstract object capable of managing him/itself and his/its surroundings and able to communicate or interact with other agents (Verburg et al. 2004). Based on interactions with the environment and with others, agents are able to make decisions which in most cases consequently change their behavior. ABM recognizes and attempts to model the role of human policy-making in landscape change. ABM assumes that agent influences landscape and land use change in space and time. In ABM, landscape and land use trends emerge from interactions between human and natural processes. It is pertinent to note that in implementation, most studies used *genetic algorithms* which based on the 'survival of the fittest principles' to modeled Land use change while integrating ABM and GIS (Heppenstall et al. 2012). ABM has more advantages than weakness (Table 4) and has been widely applied in the predictions of landscape and land use change (Table 2).

The CLUE Model

The model CLUE (Conversion of Land Use and Its Effects) is a dynamic simulation model using empirically derived relations between landscape/land use change and driving forces from cross-sectional analysis at multiple scales (Verburg et al. 2004).

CLUE was developed in 1996 in the Netherlands followed by transformation to CLUE-S and dyna-CLUE. The model was designed for continental and national use. Because of the vastness of the studied area CLUE model worked on the principle of relative distribution of land cover in the pixel. The model produces better results at larger scales (e.g. continental) compared to smaller scales (e.g. local). CLUE was developed to simulate land use change using empirically quantified relations between land use and its driving factors in combination with dynamic modeling. The model differs from most other empirical models because it gives the possibility to simulate multiple land-use types simultaneously through the dynamic simulation of competition between land-use types (Verburg et al. 2004).

Scenarios for InVEST (Integrated Valuation of Environmental Services and Tradeoffs)

Scenarios for InVEST is a product of The Natural Capital Project's vision geared towards bringing together the people and institutions to incorporate the values of WWF, NCO organizations and ecosystem services into decision making for lasting sustainable development. It is out of these precepts that this Primer model "Scenarios for InVEST" was formed. The scenarios were developed using a combination of a spatially explicit land-use and cover change (LUCC) model and information on land-use plans and permits. The model aimed to combine information on historical trends in land-cover change with available spatial planning data. It is one of the newest Landscape change methods which creates maps from LULC using developed scenarios (Table 3).

Anambra South-East Municipal—A Case Study

Materials and Methods

Brief Description of the Case Study Area

South-east municipal area lies between 7° 32′N–7° 40′N and 5° 6′E–5° 24′E. and located at the confluence of River Niger within the severely gullied parts of Anambra State, Nigeria. It is one of the populous towns in Nigeria with 509,500 persons and 109 km^2 of land area. The vegetation of the study area is a sub-climax of the original rainforest, having been virtually cleared due to development. The area mean annual rainfall is between 1500 and 2500 mm and Mean annual temperature is between 22 and 27.5 °C.

Brief Description of Data Collection and Analysis

Ground control point data were acquired using handheld GPS, for the ground truth information. Landsat TM (1987), ETM+ (2002) and ETM+ (2015) with band 4, 3, 2 were used in this study. The IKONOS Image of year 2007 and ancillary data (base map) of Anambra, South-East, Nigeria at of scale 1:5000 showing the LULC were also used. All the spatial data layers were registered with Universal Transverse Mercator (UTM) coordinate system and sampled to pixel resolution of 30 m. The base maps were georeferenced, digitized and rectified for use in ArcGIS 10.1 domain. Data on land use-cover (LUC) was collected covering 1987, 2002 and 2015 including topo and aerial maps, satellite imageries while a reconnaissance survey data was collected in 2015 using GPS. The image processing procedures used for the study includes delineation of the study area, image pre-processing, design of classification scheme, image classification, accuracy assessment, analysis of the land use/land cover dynamics as well as the comparison of the changes between different years under consideration.

Based on the prior knowledge of the study area for over 23 years and a brief reconnaissance survey with additional information from previous research in the study area, the classification scheme was developed after FOA LULC Classification System with 5 classes/types namely; built-up area, bare soil, vegetation, waterbody, and riparian Vegetation (Table 5; Fig. 1). For change detection, the time-series of the imageries for 1987, 2002 and 2015 were used to obtain land use change information by using the post-classification comparison tools in ENVI 4.5 and ArcGIS 10.1 while, the prediction for 2035 was performed using LCM and CLUE models.

Results and Implication of the Study

The work will update land-use model users with the knowledge that; (i) most spatial statistics models are easy of computation but, needs long-term data range for valid change predictions; (ii) Markov chain has the potential to perform reasonably even

Table 5 Land use-land cover classification

S/N	Class	Description
1	Built-up area	Residential, Commercial, Industrial, Government facilities and settlement
2	Bare surface	Open land, non-vegetated land and erosion/sand depots
3	Vegetation	Evergreen forest (thick) with higher density of trees and light (shrubs and farmlands)
4	Water bodies	Open water such as river, ponds, Lagoons, dam and water logged area
5	Riparian vegetation	Type of vegetation found in water logged areas

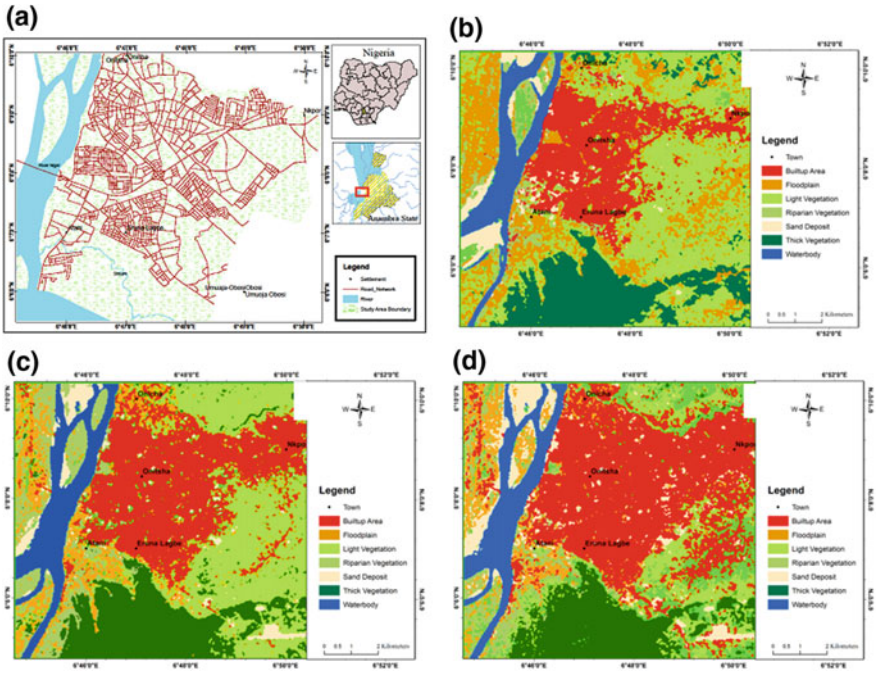

Fig. 1 Anambra South-East municipal area in Nigeria: **a** Topo-base/cadastral map; **b** Current LULC as at 2015; **c** LCM prediction output for 2035; **d** CLUE prediction output for 2035

if data for some study periods are omitted but, could also produce non geospatial results; (iii) Cellular automata is a good spatio-temporal and neighborhood relationships analytical model, though it tends to ignore the biophysical variables; (iv) CLUE is a stand-alone application software which is supported by ASCII data format, uses numerical values in defining potential transition, has limitations working with area history, and could promote user-specification values; (v) LCM is a component of Idrisi and add-In ArcGIS which is supported by raster data, and allows for input of more than two LULC maps, and behaves perfectly in LULC change detection.

Furthermore, the case study revealed that CLUE recorded higher built up areas (42.7 km^2) as compared which LCM result (35.2 km^2). On the other hand, LCM projection showed more areas for light vegetation (29.5 km^2) as compared with the 16.5 km^2 from the CLUE result. LCM projection for thick vegetation is about 4% higher than the CLUE projection for 2035. The area projected for the riparian vegetation between LCM and CLUE in 2035 differ by 1.3 km^2. In relation to the sand deposit and floodplains, CLUE projected percentage is higher than LCM by 2.9 and 5.2 respectively. After 20 years, LCM and CLUE forecast for built-up area were 12.6 and 19.5% respectively higher than the figure in 2015. Both models projected a decrease in areas for all the vegetation types in 2035 as compared with the 2015 values.

Discussion and Conclusion

The review of literature on landscape change models serves as the first step towards developing a good understanding of the applicability of the landscape and land use models and algorithms. A sufficient knowledge of the basic concepts and principles of a model serves as the modeler's user guide for better modelling with productive results. In addition, the decision makers rely on the applications and the results from the models hence, it is also pertinent for the policy makers to have reasonable knowledge of the models. However, there are several models and algorithms for landscape and land use change simulation but this paper focused on the selected few that are commonly used. The complexity prevalent in the application of some models for land use change assessment makes them difficult for either interoperability with other models or cumbersome to apply at another spatio-temporal domain. For example, computational complications and over-fitting problems hinder the effective use of ANN as a land use model. In sum, applying artificial neural networks or any other machine learning tools, the values ought not be considered as probabilities in reality yet, they are interpreted as such, thus representing values ranking the potential of change. On the other hand, CLUE and CA_MARKOV utilize maps that show the suitability of a location for each of the land use change types while, DINAMICA EGO and Land Change Modeler (LCM) calculate the probability and occurrence of each transition taking place Mas et al. (2014). It is based on this that the results of the two models from our case study differed. The prediction map from CLUE has higher built-up areas compared with that of LCM result while, LCM projected more light vegetation cover in comparison with the CLUE model result (Fig. 1; Table 6). The projected area for water never showed significant difference between LCM and CLUE results. This could be explained that both models have almost equal potential for detecting water bodies contrary to the obtained results on other LULC classes where wider differences existed. However, two to three other different models need be used to validate which model between LCM and CLUE was better predictor for the study.

Table 6 Comparison of land use class size for 2015 and 2035 projections with LCM and CLUE

	2015		2035 (LCM projection)				2035 (CLUE projection)			
Landuse-landcover	Area		Area		Diff.		Area		Diff.	
Class	(km^2)	(%)	(km^2)	(%)	(km^2)	(%)	(km^2)	(%)	(km^2)	(%)
Built-up area	21.5	19.7	35.2	32.3	13.7	12.6	42.7	39.2	21.2	19.5
Waterbody	10.1	9.3	8.4	7.7	−1.7	−1.6	8	7.3	−2.1	−2
Thick vegetation	21.6	19.8	16.3	14.9	−5.3	−4.9	12.1	11.1	−9.5	−8.7
Light vegetation	35.1	32.2	29.5	27.1	−5.6	−5.1	16.5	15.1	−18.6	−17.1
Sand deposits	3.4	3.1	4.6	4.2	1.2	1.1	7.7	7.1	4.3	4
Floodplain	8.9	8.2	9.7	8.9	0.8	0.7	15.4	14.1	6.5	5.9
Riparian vegetation	8.4	7.7	5.3	4.9	−3.1	−2.8	6.6	6.1	−1.8	1.6
Total	109	100	109	100			109	100		

In addition, it is erroneously misleading to justify a model based on its spatial results alone without considering the study goals and methodologies as well as the core focus of the model and the modeler's expertise. Model calibration, model simulation and model assessment are also important procedures which need to be given full attention before giving a final judgement about the performance of a model. More so, the selection of place, time, and format of the data must be taken into consideration when interpreting the model's performance, because these features can have profound influence on the modeling results. Conclusively, a given model can behave differently in different settings; similarly, different models can also behave differently when used in same location at the same time as demonstrated by the applications of LCM and CLUE in our study. However, the use of more simple models yields better performance compared to the complex models because the modeler finds it is easy to comprehend and explain the working processes: besides the results are easier to explain to the end-users, and the decision-makers.

Acknowledgements The support from the Department of Geoinformatics, Palacký University, Olomouc, Czech Republic, and Sambus Geospatial Limited, Nigeria are acknowledged. We also appreciate effort of the blind reviewers.

References

Batty, M., Xie, Y., & Sun, Z. (1999). Modeling urban dynamics through GIS-based cellularautomata. *Computers, Environ Urban Syst., 23,* 205–233.

Ben-Dor, E., & Banin, A. (1995). Near infrared analysis (NIRA) as a rapid method to simultaneously evaluate several spectral featureless constituents in soils. *Soil Science, 159,* 259–269.

Benešová, V. (2008). Modeling of landscape changes in the environment Idrisi. Bachelor thesis. Department of Geoinformatics, Faculty of Science, Palacky University in Olomouc.

Benjamin, S. C., Johnson, N. F., & Hui, P. M. (1996). Cellular automata models of Traffic flow along a highway containing a junction. *Journal of Physics A: General Physics, 29,* 3119–3127.

Chen K. (2002). An approach to linking remotely sensed data and areal census data. Intern. *Journal of the Indian Society of Remote Sensing, 23*(1), 37–48.

Chomitz, K. M., & Gray, D. A. (1996). Roads, land use and deforestation: A spatial model applied to Belize. *World Bank Economic Review, 103,* 487–512.

Chomitz, K.M., & Thomas, T.S. (2002). Determinants of land use in Amazonia: a fine-scale spatial analysis. *American Journal of Agricultural Economics 85,* 1016–1028.

Clarke, K. C., Riggan, P., & Brass, J. A. (1995). A cellular automaton model of wildfire propagation and extinction, Photogram. *Engineering & Remote Sensing, 60,* 1355–1367.

de Wolff T., Staal S., Kruska R., Ouma E., Thornton P., & Thorpe W. (2000). Improving GIS derived measures of farm market access: An application to milk markets in the East African highlands. In *Paper presented at the Fifth Seminar on GIS and Developing Countries (GISDECO 2000), 'GIS Tools for Rural Development'*, November 2–3, 2000, IRRI, Los Banos, Philippines.

Fasona, M., Tadross, M., Abiodun, B., & Omojola, A., (2011). Land systems response to water footprint in the wooded savannah of Nigeria. In: Salami, A.T., Orimoogunje, O.I (Eds.),

Environmental Research and Challenges of Sustainable Development in Nigeria. Obafemi Awolowo University Press, Ile-Ife, pp. 499–523.

Fürst, C., König, H., Pietzsch, K., Ende, H. P., Makeschin, F. (2010). Pimp your landscape—A generic approach for integrating regional stakeholder needs into land use scenario design and sustainable management support. *Ecology and Society, 15*(3), 34, 25.

Harmáčková, Z. V., & Vačkář, D. (2015). Modelling regulating ecosystem services trade-offs across landscape scenarios in Třeboňsko Wetlands Biosphere Reserve, Czech Republic. *Ecological Modeling, 295,* 207–215.

Heppenstall, A. J., Andrew, T., Crooks, L. M., & Batty, M. (2012). *Agent-based models of geographical systems*. Springer Science, Media B.V.

Iacono, M., Levinson, D., El-Geneidy, A., & Wasfi, R. (2015). A Markov chain model of land use change in the Twin Cities, 1958–2005. *Tema—Journal* of *Land Use*, *Mobility, 8*(6), 311–316.

Indrosová, M., & Kupková, L. (2015). Změny využití krajiny v suburbánní zóně Prahy v různých přístupech predikčního modelování. Geografie, 120, č. 3, s. 422–443. (English translate).

López, E., Bocco, G., Mendoza, M., & Duhau, E. (2001). Predicting land-cover and land-use change in the urban fringe: A case in Morelia city, Mexico. *Landscap Urban Plan., 55,* 271–285.

Malach, Š. (2009). Experience with land change modeler (LCM) in the analysis and prediction of changes in land use. In Misáková, L., & Klimánek, M. (eds.), *10. Seminar users Idrisi*, 1st edn. (pp. 36–48). Brno: Mendel University in Brno.

Mas, J.-F., Kolb, M., Paegelow, M., Olmedo, T. M. C., & Houet, T. (2014). Inductive pattern-based land use/cove r change models: A comparison of four software packages. *Environ Modelling Software, 51,* 94–111.

Mertens, B., Poccard-Chapuis, R., Piketty, M.-G., Lacques, A.-E., & Venturieri, A. (2002). "Crossing spatial analyses and livestock economics to understand defoestation processes in the Brazilian Amazon: the case of Sao Felix do Xingu in South Para." *Agricultural Economics, 27* (3), 269–294.

Ojima, D. S., Kittel, T. G., Rosswall, T., & Walker, B. H. (1991). Critical issues for understanding global change effects on terrestrial ecosystems. *Ecological Applications, 1,* 316–325.

Opeyemi, Z. A. (2006). *Change detection in land use and land cover using remote sensing data and GIS: a study of Ilorin its environs in Kwara state [MSc dissertation]*. Ibadan: University of Ibadan, Nigeria.

Pijanowski, B. C., Brown, D. G., Shellito, B. A., & Manik, G. A. (2002). Using neural networks and GIS to forecast land use changes: A land transformation model. *Computers, Environment and Urban Systems, 26,* 553–575.

Pijanowski, B.C., Tayyebi, A., Delavar, M.R., & Yazdanpanah, M.J., (2009). Urban expansion simulation using geographic information systems and artificial neural networks. *International Journal of Environmental Research, 3*(4), 493–502.

Pechanec, V. (2014). *Methods for creating scenerios of global change impacts on land use and modeling the functional relationship between changes in land use and the provision of ecosystem services: Analysis of options and tools for modeling future land use*. Study series 2, Olomouc, Czech Republic.

Qian, S. S., Cuffney, T. F., Alameddine, I., McMahon, G., & Reckhow, K. H. (2010). On the application of multilevel modeling in environmental and ecological studies. *Ecology, 91,* 355–361.

Schneider, L. C., & Pontius, R. G., Jr. (2001). Modeling land use change in the Ipswich watershed, Massachusetts, USA. *Agriculture, Ecosystems and Environment, 85,* 83–94.

Serneel, S., & Lambin, E. F. (2001). Proximate causes of land-use change in Narok District, Kenya: a spatial statistical model Suzanne. *Agriculture, Ecosystems & Environment, 85,* 65–81.

Silva, E. A., & Clarke, K. C. (2002). Calibration of the SLEUTH urban growth model for Lisbon and Porto, Portugal. *Computers, Environment and Urban Systems, 26*(6), 525–552.

Soares-Filho, B. S., Cerqueira, G. C., & Pennachin, C. L. (2002). Dinamica: A stochastic cellular automata model designed to simulate the landscape dynamics in an Amazonian colonization frontier. *Ecology Mod., 154*(3), 217–235.

Speybroeck, N., Berkvens, D., Mfoukou-Ntsakala, A., Aerts, M., Hens, N., van Huylenbroeck, G., et al. (2004). Classification trees versus multinomial models in the analysis of urban farming systems in Central Africa. *Agricultural Systems, 80*(2), 133–149.

Sponagel, H., Grottenthaler, W., Hartmann, K. J., Hatrtwich, R., Jaentzko, P., Joisten, H., et al. (2005). Bodenkundliche Kartieranleitung. Ad-hoc-AG Boden, Schwei-zerbart´sche Verlagsbuchhandlung, pp. 438 (English translate).

Turner, M. G. (1987). Spatial simulation of landscape changes in Georgia: A comparison of three transition models. *Landscap Ecology, 1,* 29–36.

van Oel, P. R., et al. (2010). Feedback mechanisms between water availability and water use in asemi-arid river basin: A spatially explicit multi-agent simulation approach. *Environment Modeling & Software, 25,* 433–443.

Veldkamp, A., & Fresco, L. O. (1996). CLUE-CR: An integrated multi-scale model to simulateland use change scenarios in Costa Rica. *Ecological Modeling, 91*(1/3), 231.

Verburg, P. H., Schot, P., Dijst, M., & Veldkamp, A. (2004). Land use change modelling: Current practice and research priorities. *GeoJournal, 61*(4), 309–324.

Weiss, E., Marsh, S. E., & Pfirman, E. S. (2001). Application of NOAA-AVHRR NDVI time-series data to assess changes in Saudi Arabia's rangelands. *International Journal of Remote Sensing, 22*(6), 1005–1027.

Weng, Q. (2002). Land use change analysis in the Zhujiang delta of China using satellite remote sensing, GIS and stochastic modeling. *Journal of Environmental Management, 64,* 273–284.

Xie, H., Wang, P., & Yao, G. (2014). Exploring the dynamic mechanisms of farmland abandonment based on a spatially explicit economic model for environmental sustainability: A case study in Jiangxi Province, China. *Sustainability, 6,* 1260–1282.

Zhang, B., Zhang, Y., & Bi, J. (2011). An adaptive agent-based modeling approach for analyzing the influence of transaction costs on emissions trading markets. *Environmental Modelling & Software, 26,* 482–491.

Land Use—Land Cover Change and Soil-Gully Erosion Relationships: A Study of Nanka, South-Eastern Nigeria Using Geoinformatics

Chukwudi Nwaogu, Onyedikachi Joshua Okeke, Simon Assuah Adu, Edeko Babine and Vilém Pechanec

Abstract This study aimed at identifying the land use-land cover (LULC) types and their changes by mapping the soil erodibility intensity, and estimating the LULC change caused by soil-gully erosion in Nanka region using geoinformatics tools. Data covering 1991, 2003 and 2015 were acquired from the Global Land Cover Facility (GLCF)-an Earth Science Data Interface, and from the National Space Research and Development Agency, Abuja (NASRDA). In addition, land use-land cover (LULC) data of Nanka and its environs were generated from the local government boundary map and Nigerian Administrative map at 1: 50,000 topographic scale. ENVI (version 4.7), ArcGIS 10.1, the RUSLE model and statistica software packages were used to process and analyse the data. The results revealed that areas with steep slopes have high and severe erosion levels except for Isuofia community which is on steep slope yet, has slight erosion because of the prevalence of dense forest vegetation cover. Integration of Remote Sensing, GIS and the RUSLE model has shown technical benefit, cost-effectiveness with reliable result and should be applied in the future assessment of erosion in Nigeria and other African countries.

Keywords Land use-land cover · Soil-gully erosion · GIS · RUSLE · Nigeria

C. Nwaogu (✉) · V. Pechanec
Department of Geoinformatics, Palacký University Olomouc,
771 46 Olomouc, Czech Republic
e-mail: cnwaogu@gmail.com

V. Pechanec
e-mail: vilem.pechanec@upol.cz

O.J. Okeke · S. Assuah Adu · E. Babine
Sambus Geospatial Limited, Ghana, Nigeria
e-mail: okaykaygeoinfo@gmail.com

I. Ivan et al. (eds.), *Dynamics in GIscience*, Lecture Notes in Geoinformation and Cartography, DOI 10.1007/978-3-319-61297-3_22

Introduction

Soil-gully erosion has been known as one of the major challenges to global environmental and socio-economic sustainability. Changes in climate and landscape have been held responsible for the devastating occurrence of soil erosion. Although the causes of soil-gully erosion could either be natural or human factors but the later has the tendencies of dominating especially in most developing countries (Noori et al. 2016). Poor water supply, low agricultural productivity and inadequate farmlands, loss of vegetation, contaminated underground water and freshwater ecosystems, as well as facilities destructions have been some of the primary effects of soil-gully erosion. However, the impacts of this environmental foe vary in space and time based on established management mechanisms, land use-land cover (LULC) types, climatic factors, topographic and lithological characteristics. The diversities and complexity in these contributing factors ranging from human activities to natural and biophysical variables have made the determination of soil-gully erosion difficult. Therefore, several erosion models including the physical (WEPP, ANSWERS, AGNPS, SHE), and the empirical models (USLE, RUSLE, MUSLE, FAO, Fournier, PSIAC, Modified PSIAC, EPM) have been developed and successfully applied in many soil-gully erosion assessments (Adediji et al. 2010; Pechanec et al. 2015; Seutloali et al. 2016). Recently, the introduction of Remote Sensing and GIS technologies and their combination with the empirical models have made the soil erosion monitoring more efficient, effective, reliable, faster and easier with sustainable results and low cost (Gelagaya and Minale 2016; Noori et al. 2016; Ali and Hagos 2016). For instance, the derived data from NDVI and DEM generated from the multi-temporal satellite imageries provides vital information on the vegetation cover, topography and management which boosts spatial estimation of soil erosion at various scales using C-factor, LS-factor and P-factor (Seutloali et al. 2016; Noori et al. 2016). These geospatial methods have made the potential effects of LULC and its changes on soil-gully erosion to be successfully achieved, and modelling and prediction of the relationships between LULC and soil-gully erosion has become easy and interesting.

This study aimed at (i) identifying the LULC types in Nanka region (ii) mapping the areas sensitive or vulnerable to the different erosion risk level (iii) appraise the LULC and its changes in 1991, 2003 and 2015 in relation to soil-gully erosion. We hypothesized that soil-gully erosion substantially affected the LULC as the LULC change influences the erodibility intensity in return. In this conceptual background, we addressed the following questions: (1) what are the major LULC class/type in Nanka? (2) which areas/communities have very high or low erosion risk? (3) how varied in size and type are the LULC change in the monitored years? (4) does the topography of the area play important role in the erosion risk?

Materials and Methods

Study Area

The study area is Nanka region which lies within the humid tropical rainforest belt of Nigeria (Fig. 1) with an annual rainfall of about 180–300 cm, average temperature range of about 25–27.5 °C, and mean annual sunshine hours of about 1750 h (Oguntoyinbo 1978). The geological setting in the study area is that of layered sequences in which a predominantly sandstone formation is underlain by a predominantly shale formation (Obiadi et al. 2011; Ezechi and Okagbue 1989). The soils of the study area are derived from the underlying Ameki Formation and Imo Shale and as such comprise mainly porous, red and brown sandy soils, and brown and pale clay soils (Obiadi et al. 2011).

The vegetation in the study area was influenced by hydrogeological factors including relief and lithology as well as other anthropogenic factors (Obiadi et al. 2011). The plant species cut across light rainforest to areas with scattered shrubs and trees forming southern-Guinea savanna. Furthermore, thick vegetation cover with emergent trees are dominant around waterbodies and the shaley lowlands while savannah vegetation and dispersed trees are notable on sandy highland (Obiadi et al. 2011). The study site is favourable for large semi-natural plantations such as mango, orange, cashew orchard and oilpalm trees. Socioeconomic activities involving slash-burn, grazing, firewood gathering, agriculture and construction

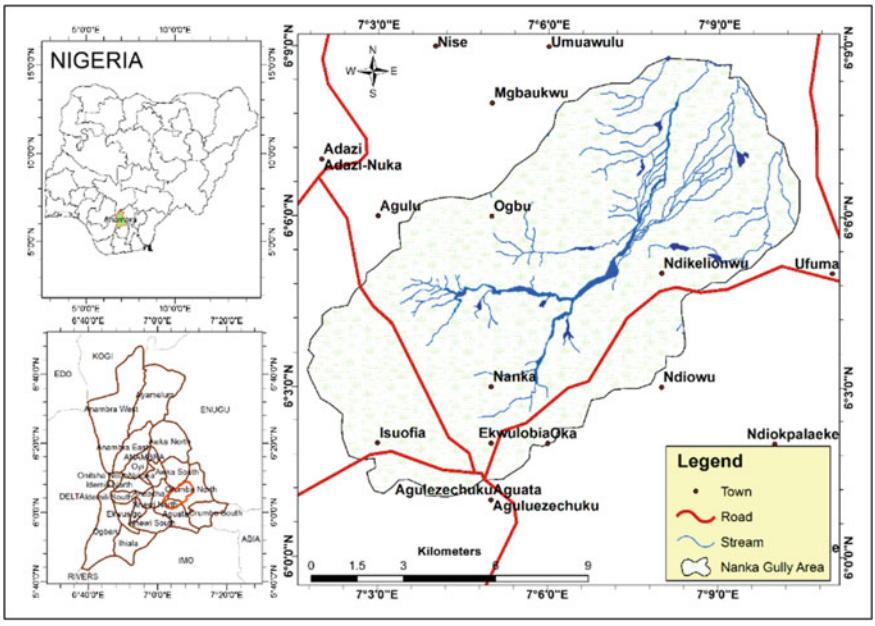

Fig. 1 *Study area* Nanka region in South-Eastern Nigeria

works have largely altered the natural vegetation. The rapid increase in these human activities has been a major cause of severe gully erosion and its associated challenges (Obiadi et al. 2011).

Brief Impacts of the Soil-Gully Erosion in the Study Area

The gully erosion has led to the loss of agricultural and residential lands estimated from the gully area which is more than 3442.2 ha of land (Fig. 2). Estimates of losses of lives in Agulu and Nanka which are pressed hardest were more than 200 persons in 1960s and 1970s. Findings revealed that there has been increase in the loss of farmlands; cash crops, pasture, soil fertility and the creation of wasted lands. In addition, the gully has forced migration: displacement of families and abandonment of properties. Communal facility and critical infrastructure are not left out as most roads linking communities are cut off while some areas remain without electricity, school, and hospital because either the available ones are being threatened by soil-gully encroachment or have been eroded into the gullies. Loss of human lives seems to have occurred rarely within the past decade, this may be due to the ability of affected population to move out of severely affected areas as environmental refugees to safer locations within and outside their communities. These measures further increase the population of the host communities and support severe demand of land.

Data Collection, Pre-processing, and Analyses

Landsat satellite images (30 m) including Nnaka region within longitude 7° 1′34″ E–7° 10′40″E and longitude 6° 8′58″N–6° 1′2″N covering 1991, 2003 and 2015 were acquired from the Global Land Cover Facility (GLCF) an Earth Science Data

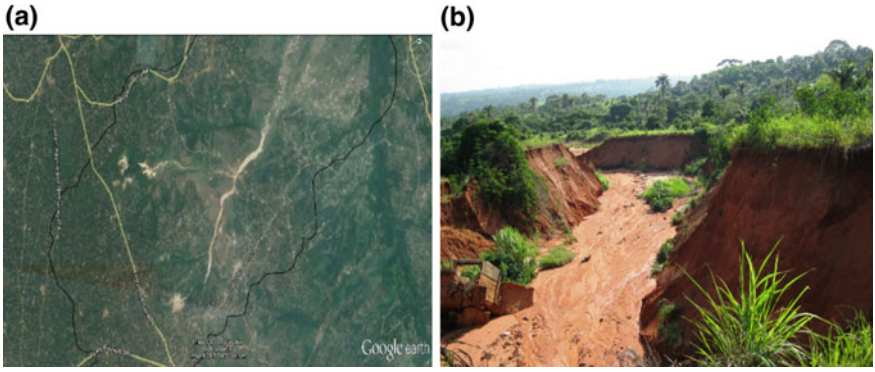

Fig. 2 **a** Satellite imagery from google earth **b** photograph of soil-gully erosion in the study area

Interface, and from National Space Research and Development Agency, Abuja (NASRDA). The land use-land cover (LULC) data of Nanka and its environs were carved out using the local government boundary map and Nigerian Administrative map at 1:50,000 topo scale.

Based on the priori knowledge of the study area for over 20 years and a brief reconnaissance survey with additional information from previous research in the study area, a classification. The classification scheme gives a rather broad classification where the LULC were identified by a single digit. The band 4, 3 & 2 images were imported into the ENVI (version 4.7) software to form colour composite of the study, using the vector frame in ArcGIS 10.1 software environment. The region of interest (ROI) was created from the map of the study area and saved as shape file. Based on the prior knowledge of the study area, a brief reconnaissance survey with additional information from previous researches in the study area, the classification scheme was developed which included built-up area, gully area, light vegetation, sand deposit, and thick vegetation (Table 1). The RUSLE model (A) which uses the same principles as USLE or MUSLE was integrated with ArcGIS by applying the erosion factors which were recently applied by several authors in the assessment of soil erosion and its risks (Adediji et al. 2010; Seutloali

Table 1 Major classified landuse-landcover (LULC) classes, categories, and description

LULC class	Categories	Description
Built-up area	Residential, commercial, industrial, recreation, and educational	Public, private, government, and commercial estates, Shopping malls, markets, stores, warehouses, trade-fair centers. Production sites, manufacturing factories for textiles, plastics, and leather products, Government facilities, and settlement
Gully area	Base level, Scarp, fracture, and incidental	Removal of soil on the surface or along drainage lines by surface water runoff caused by excessive removal of vegetation cover, inappropriate land use and compaction of the soil by grazing, farming, or other human activities. Gully erosion develop in susceptible areas
Sand deposit/bare surface	Open land and non-vegetated land	Sand deposits, rock outcrops, accumulation of sediments from river erosional and denudation processes. These often create floodplain in the area
Vegetation	Thick vegetation, light vegetation, savanna	Evergreen forest and mixed forests with higher density of trees, formed the thick vegetation. The light vegetation includes, arable or agricultural lands with crops, isolated short trees. Savanna here is mainly the guinea or derived savanna with scanty short trees, many shrubs, and grasses
Water bodies	Wetlands, ponds, rivers, streams, dams	Areas cover by open water such as river, ponds, Lagoons, dam, and water logged area

et al. 2016; Alkharabsheh et al. 2013; Mohammadi and Nikkami 2008; Gelagay and Minale 2016; Noori et al. 2016; Ali and Hagos 2016) were used for this study. The erosion factors included climate (rainfall) factor (R), surface geology-soil factor (K), topographic-slope factor, DEM (LS), land use-land cover factor (C), and other human management practices (P) which are either in support or against soil loss from erosion including farming practices, buildings, and deforestation/afforestation.

$$\text{The RUSLE model can be stated as } A = R \times K \times LS \times C \times P \tag{1}$$

where A = the calculated spatio-temporal mean soil loss per unit area expressed in tons km^2 $year^{-1}$; R = rainfall runoff erosivity factor which is computed as mean annual value using the rainfall data in Table 3 which covered the period of 24 years (1991–2015) and was collected from the Nigeria Metrological Agency (NIMET). K = soil erodibility factor which is the soil loss value per erosion index unit for a given soil as determined on as standard area. In this study, the K factor was derived using the methods of Wischmeier and Smith (1978) and Adediji et al. (2010) which based on soil organic matter, soil structure, soil texture, and soil permeability acquired from the soil and land use maps from Food and Agricultural Organization (FAO) survey in Nigeria through the attribute table information.

LS = slope length and steepness factor with L as the ratio of soil loss from the field slope length to soil loss from 5 m length under the same conditions while, S is the ratio of soil loss from field slope gradient to soil loss from a 10% slope under the same conditions. In this study, the LS was determined by developing the DEM (Fig. 6b) by using the topographic map and the 30 m satellite data of the study area.

$$LS = (As/22.13)^{m} \times (\text{Sin}\,\theta/0.09)^{n} \tag{2}$$

where As = upslope contributing areas per unit width of cell spacing; θ = slope angle (degrees), m and n are exponent of slope parameters for slope length and gradient.

C = cover factor which is the ratio of soil loss from given location with specified cover and management to soil loss from an identical area. In this study, the spatial evaluation of the C factor was reached by allocating values to land cover classes using classified remotely sensed data of the study sites. We developed several techniques for the determination of C factor using NDVI for soil loss assessment with RUSLE (van der Knijff et al. 2002; Alkharabsheh et al. 2013)

$$NDVI = [(NIR - RED)/(NIR + RED)] \tag{3}$$

where NIR is the amount of near-infrared light and RED is the amount of red light reflected by the land cover and absorbed by the satellite device.

In relation to the P factor, field data, satellite imageries, and land use-cover maps were employed in assigning the P-factor values (Table 2) by integrating Moore and Wilson (1992) and Wischmeier and Smith (1978) methods. P factor can be defined as the ratio of soil loss with prevention/support practices including agricultural

Table 2 Classified LULC, area, P factor, and C factor

Land use-land cover	Area (km^2)			C factor	P factor
	1991	2003	2015		
Built-up area	1.47	5.96	3.57	0.99	0.17
Gully area	12.70	7.29	4.20	0.98	0.11
Light vegetation	9.71	7.78	12.20	0.66	0.24
Sand deposit	31.46	49.53	39.42	0.86	0.08
Thick vegetation	69.95	54.89	66.21	0.78	0.36
Waterbody	0.81	0.64	0.48	0.00	0.01

techniques and other human activities such as crop rotation, conservation tillage, contour farming, terracing, plant residue application, strip cropping, agroforestry, and use of sandbag check dam, and others (Table 3).

Geographical and Statistical Analyses

ArcGIS 10.1 and the statistica software packages were used throughout the analyses because they provide all the functions required to determine the soil erosion using RUSLE model. To measure the areal extent of LULC classes in each erosion risk map, the zonal statistics (ArcGIS Spatial Analysis) was used. Furthermore, differences in the area of LULC classes were compared between 1991, 2003 and 2015 using the statistica.

Results and Discussion

Soil-Gully Erosion and LULC

The classified LULC and area for the study revealed that the thick vegetation recorded the highest LULC values of 69.95, 54.89 and 66.21 km^2 across the monitored years while water body has the lowest of 0.81, 0.64 and 0.48 km^2 respectively for 1991, 2003 and 2015 (Table 2; Figs. 3a–c, 4 and 5). The determined C factor was high in all the LULC classes except for the waterbody. The water body (0.01) also showed a low P factor compared with other LULC classes. The application of the ArcGIS, DEM, RUSLE, and field survey helped to classify the erosion intensity/level into five categories namely; none, low (slight), moderate, high, very high (severe) with their descriptions (Table 4). The areas with the slope gradient below 2.4^0 have high percentage of vegetation, no visible features of soil-gully erosion, though these areas have the lowest landmass compared with either the areas with moderate or severe gullies. The gullies cover more than

Table 3 Erosion and soil loss preventive/support measures

Key measures	Sub-categories	Descriptions
Bio-remediation	Conservation tillage	– When soil cover is up to 30% a tillage conservation system is defined
	Contour farming	– Method of growing crops "on the level" across or perpendicular to a slope rather than up and down the slope
	Vegetation planting	– The practice of afforestation whether of grasses or trees
	Litter-layer abandonment	– Leaving litter to decompose on the soil surface
	Sustainable cutting	– Cutting plants at a level that will promote their rapid regeneration without harming the soil
	Crop rotation	– Growing of different crops in succession on a piece of land to sustain soil fertility
	Use of plant residues	– Application of plant tissue and materials for mulching
	Terrace farming	– A type of farming that consists of different "steps" or terraces that are made in an arable land to curb erosion
	Strip cropping	– It involves planting row crops in strips across the slope, with alternate strips of grain and/or forage crops
Land management practices	Agroforestry	– Integration of trees, shrubs and crops on the same piece of land
	Stop grass/forest fires and indiscriminant deforestation	– Protecting the vegetation cover from being removed by fire or man
	Restricted grazing in open grassland	– Regulation of herbivores activities in open grassland areas
Local structural and mechanical	Use of sand bags	– Use of jute or polyethylene bags (50 kg) filled with sand to check the surface water flow

two-third of the entire study area, and were mainly found in Nanka, Ndikelionwu, Ogbu and Ekwulobia-oke communities (Table 5; Fig. 3a–c). It is also of important to note that rill erosion contributed to soil erosion with soil loss ranging from 13.8 to 22.2% and are commonly found in Isuofia, Ogbu and Ekwulobia-oke. The highest soil loss rate was recorded in Nanka (43.1%) with very high (severe) erosion level whereas, Isuofia community (5.3%) has the lowest percentage of soil loss with low (slight) erosion level. Severe erosion intensities and high soil losses have often been associated with higher slope gradients and heavy rainfall (Poesen et al. 2003; Adediji et al. 2010; Seutloali et al. 2016; Alkharabsheh et al. 2013; Mohammadi and Nikkami 2008; Gelagay and Minale 2016; Noori et al. 2016; Ali and Hagos 2016). Several studies have proved that soil-gully erosion increases with

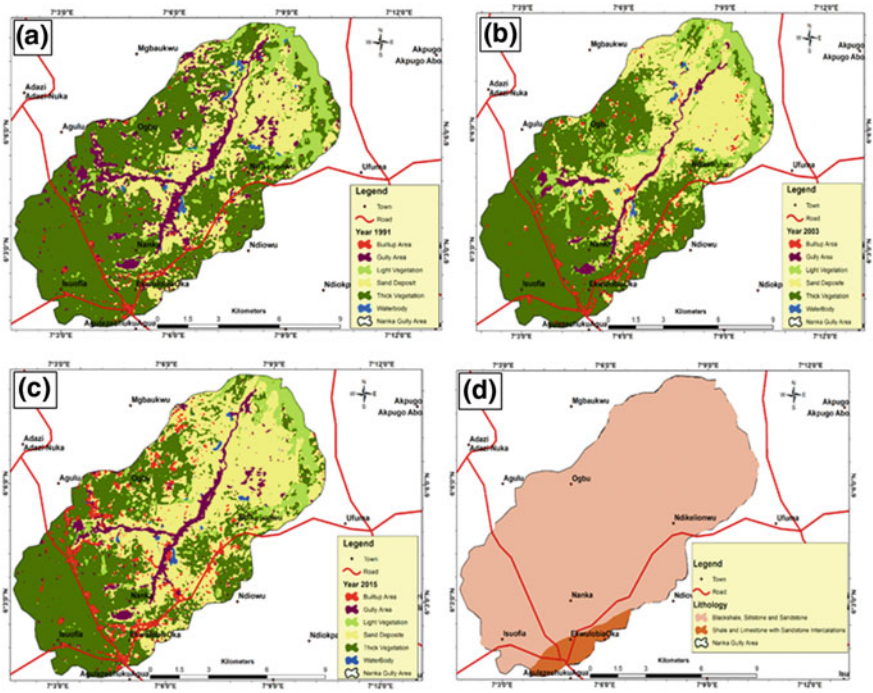

Fig. 3 Nanka region LULC and lithology **a** LULC 1991, **b** LULC 2003, **c** LULC 2015, **d** lithological characteristics

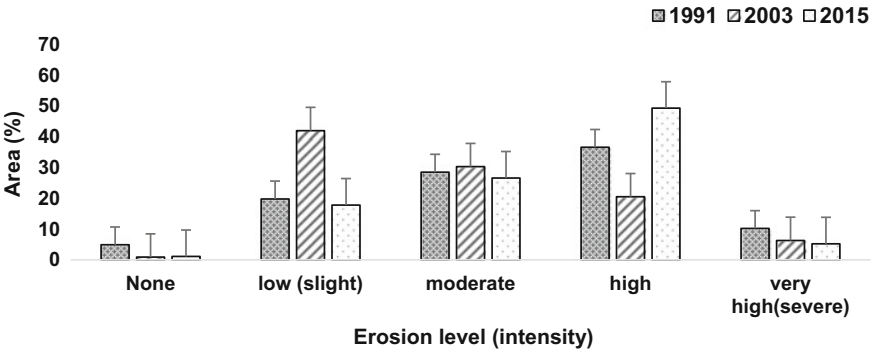

Fig. 4 Areas dominated by the different soil-gully erosion level in 1991, 2003, and 2015

increasing slope gradient (Cerda 2007; Seutloali and Beckedahl 2015) because as the slope gradient becomes steeper, soil infiltration declines which consequently increases the amount of surface run-off that promotes soil-gully erosion (Seutloali et al. 2015, 2016). Our study was consistent with these previous literatures except in

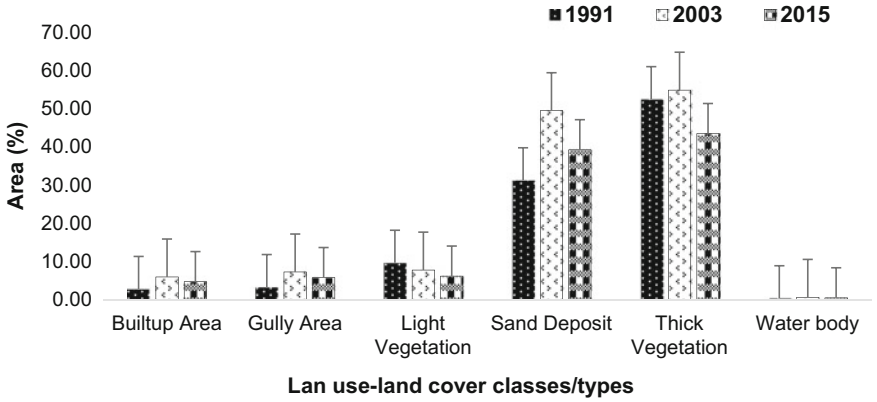

Fig. 5 The land use-land cover (LULC) change between 1991, 2003, and 2015

Table 4 Erosion intensity(level) classes, topographic variables, and area % for 1991, 2003 and 2015

Class	Erosion intensity	Erosion description	Slope (degree)	Vegetation (%)	1991 area (km^2)	(%)	2003 area (km^2)	(%)	2015 area (km^2)	(%)
1	None	No visible feature of erosion	2.3	Above 80	6.3	4.9	1.2	0.9	1.4	1.1
2	Low (slight)	Sheet to rill erosion	14.1	70–80	18.7	14.8	37.5	29	27.5	21.8
3	Moderate	Deep rill to medium gullies	22.6	50–70	35.9	28.5	42.1	33.3	46.2	36.6
4	High	Medium gullies to deep gullies formation	35.7	30–50	52.4	41.6	38.4	30.5	44.4	35.3
5	Very high (severe)	Fully developed deep gullies	49.4	Below 30	12.8	10.2	7.9	6.3	6.6	5.2

the case of Isuofia which revealed a contrasting scenario. Isuofia is located at the highest slope gradient (Table 5; Figs. 3, 6 and 7), and has the highest rainfall compared with other communities in our study, yet soil erosion and mean annual soil loss were relatively low. The influence of thick vegetation cover found in this area might be a good explanation for the low erosion and low soil loss in a high slope such as Isuofia (Adediji et al. 2010; Alkharabsheh et al. 2013), as the dense forest trees supported the soil against erosion (Zhao et al. 2016; Wang et al. 2016; Seutloali et al. 2016).

Table 5 Slope gradient, predominant erosion intensity (level), % soil loss, and rainfall under each community in Nanka region between 1991 and 2015

Community	Slope gradient	Dominant Erosion level	Mean % of soil loss	Rainfall (cm $year^{-1}$)
Ndikelionwu	35–40	High	22.20	200–300
Ogbu	20–30	Moderate	15.60	180–280
Nanka	35–40	Very high (severe)	43.10	250–310
Ekwulobia-Oke	20–30	Moderate	13.80	180–280
Isuofia[a]	>40	Low (slight)	5.30	280–320

[a]*Remarkably different* high slope gradient and heavy rainfall but with low erosion intensity and low soil loss due to cover

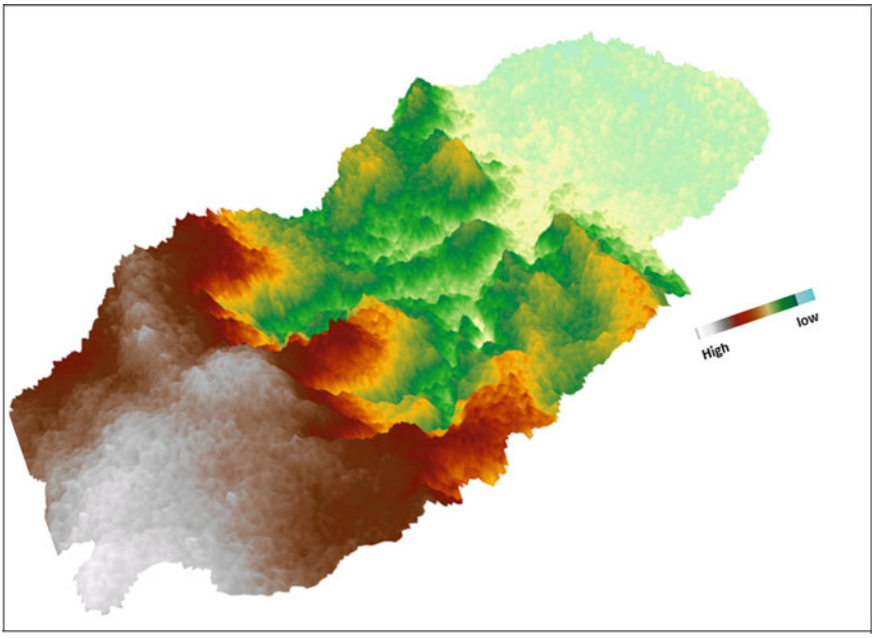

Fig. 6 3D model of the Gully area

Relationships Between Human Activities and Soil-Gully Erosion

Several authors have reported the roles of anthropogenic activities such as farming, grazing, logging, sand-querying, building and roads constructions on the LULC change which consequently create soil-gully erosion (Obiadi et al. 2011; Ezechi and Okagbue 1989; Tekwa et al. 2015; Onwuemesi et al. 1991; Ezechi and Okagbue 1989). In our study for example, the build-up areas increased from 1.47 km^2

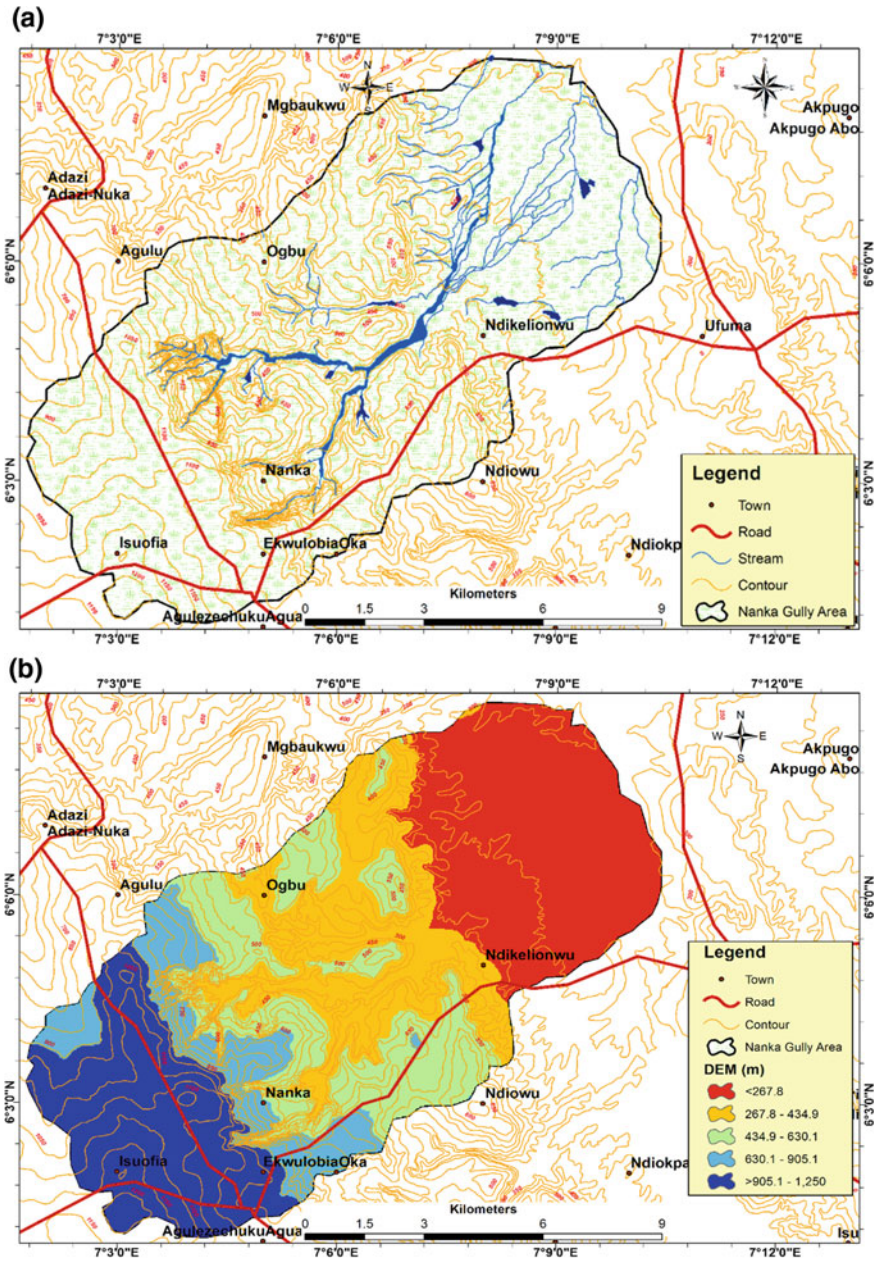

Fig. 7 Nanka region showing **a** relief, drainage, transport and settlement **b** DEM

(in 1991) to 5.96 km^2 (in 2003), and 3.57 km^2 (in 2015) (Fig. 5). This might also be an explanation for the increased soil-gully erosion and high soil loss in 2003 and 2015 as compared with 1991. The year, 1991 also recorded zero erosion intensity rate in comparison with the other years of this study (Fig. 4). The statistical analyses of the study revealed a significant increase of more than 20% in slight erosion between 1991 and 2003 which later declined in 2015. The moderate erosion level was almost same for all the monitored years. On the other hand, 2015 showed a significant increase of about 40% of moderate erosion intensity when compared with 2003. However, the percentage area coverage by very high (severe) erosion did not change significantly over the monitored years.

The decrease in the area percentage of the severe erosion in 2015 could be explained by the recently ecological management projects introduced by the government of Anambra state which included afforestation and decrease farming along the slopes.

Which is better to be said? 'LULC change causes soil-gully erosion or soil-gully erosion leads to change in LULC.' In our study for instance, more buildings tend to emerge at the areas with minimal erosion while the high and severe erosion areas have low housing structures as they are being destroyed by the erosion or abandoned by the residents in fear of the risks. The north-eastern part of the study area showed relatively high sand deposits because it lies within the lower slope of the entire area and the sediments from the top slopes accumulate down the slope. The high volume of sand deposits has covered some water bodies thus, reducing the number of the visible ground water bodies. In these cases, one could say that the soil-gully erosion has caused changes in LULC. On the other hand, the recent population growth has led to establishment of more built-up areas, clearing of more vegetative cover for agriculture and domestic fuel which have hitherto aggravated soil-gully erosion (Adediji et al. 2010, 2013).

Biophysical Variables and Soil-Gully Erosion

There are many studies which demonstrated the crucial roles of biophysical factors such as rainfall geology, and soil types in having substantial influence on the erosion (Egboka and Nwankwor 1985; Tekwa et al. 2015; Onwuemesi et al. 1991; Wang et al. 2016). In our study, however, the roles of geology and rainfall seemed to be minimal because more than 95% of the study area have same bedrock composition (Fig. 3d), and almost same amount of annual rainfall ranging between 180 and 320 cm (Table 5) which ought not to have shown any variations in the erosion intensity. Therefore, it could be concluded that topography and vegetation cover have domineering influence of the erosion level compared with other biophysical factors.

Conclusion

The main objective of this study was to identify the LULC types and the occurred changes by mapping the erosion vulnerability level, and appraise the LULC change caused by soil-gully erosion in Nanka region using geoinformatics tools. The findings of this study have revealed the effectiveness of Remote sensing, GIS and RUSLE methods in spatio-temporal assessment of soil-gully erosion. It could also be concluded that areas with steep slopes accounted for high and severe erosion intensities except for Isuofia community which is on steep slope yet, has slight erosion because of the prevalence of dense forest vegetation cover. This study has therefore opened more opportunities for ecologists and environmentalists in Nigeria and other countries in Sub-Saharan Africa to widely use the geoinformatics techniques in monitoring and managing soil and gully erosions.

Acknowledgements We acknowledge the support from the Department of Geoinformatics, Palacký University, Olomouc, Czech Republic, and Sambus Geospatial Limited, Nigeria are appreciated. The good effort of the blind reviewers, their kind corrections, and remarks were also acknowledged.

References

Adediji, A., Jeje, L. K., & Ibitoye, M. O. (2013). Urban development and informal drainage patterns: Gully dynamics in Southwestern Nigeria. *Applied Geography, 40,* 90–102.

Adediji, A., Tukur, A. M., & Adepoju, K. A. (2010). State of Nigeria using remote sensing (RS) and geographic information system (GIS). *Iranica Journal of Energy & Environment, 1*(3), 255–264.

Ali, S. A., & Hagos, H. (2016). Estimation of soil erosion using USLE and GIS in Awassa Catchment, Rift valley, Central Ethiopia. *Geoderma Regional, 7*(2), 159–166.

Alkharabsheh, M. M., Alexandrisis, G. B., Bilasb, G., & Misopolinos, N. (2013). Impact of land cover change on soilerosion hazard in northern Jordan using remote sensing and GIS. *Procedia Environmental Sciences, 19*(3), 912–921.

Cerdà, A. (2007). Soil water erosion on road embankments in eastern Spain. *Science of the Total Environment, 378,* 151–155.

Egboka, B. C. E., & Nwankwor, G. I. (1985). The hydrogeological and geotechnical parameters as agents for gully-type erosion in the Rain-Forest Belt of Nigeria. *Journal of African Earth Sciences, 3*(4), 417–425.

Ezechi, J. I., & Okagbue, C. O. (1989). A genetic classification of gullies in eastern Nigeria and its implications on control measures. *Journal of African Earth Sciences, 9,* 711–718.

Gelagaya, H. S. & Minale, S.A. (2016). Soil loss estimation using GIS and Remote sensing techniques: A case of Koga watershed, Northwestern Ethiopia. *International Soil and Water Conservation Research, 4*(2), 126–136.

Mohammadi, T. A., & Nikkami, D. (2008). Methodologies of preparing erosion features map by using RS and GIS. *International Journal of Sediment Research, 23,* 130–137.

Moore, D., & Wilson, J. P. (1992). Length–slope factors for the revised universal soil loss equation: Simplified method of estimation. *Journal of Soil and Water Conservation, 47*(5), 423–428.

Noori, H., Siadatmousavi, M., & Mojaradi, B. (2016). Assessment of sediment yield using RS and GIS at two subbasinsof Dez Watershed, Iran. *International Soil and Water Conservation Research, 4*, 199–206.

Obiadi, I. I., Nwosu C. M., Ajaegwu N. E., Anakwuba E. K., Onuigbo N. E., Akpunonu E. O., Ezim O. E. (2011). Gully Erosion in Anambra State, South East Nigeria: Issues and solution. *International Journal of Environmental Sciences*, *2*(2), 796–804.

Oguntoyinbo, J. S. (1978). *Climate and geography of Nigerian development*. Heinemann Education Books (Nig) Ltd., pp. 45–70.

Onwuemesi, A. G., Egboka, B. C. E., Orajaka, I. P., & Emenike, E. A. (1991). Implications of hydrogeophysical investigations of the Agulu-Nanka gullies area of Anambra state of Nigeria. *Journal of African Earth Sciences (and the Middle East), 13*(3–4), 519–526.

Pechanec, V., Brus, J., Kilianova, H., & Machar, I. (2015). Decision support tool for the evaluation of landscapes. *Ecological Informatics, 30,* 305–308.

Poesen, J., Nachtergaele J. Verstraeten, G., & Valentin, C. (2003). Gully erosion and environmental change: Importance and research needs. *Catena, 50*, 91–133.

Seutloali, K. E., Dube, T., Mutanga. O. (2016). Assessing and mapping the severity of soil erosion using the 30-m Landsat multispectral satellite data in the former South African homelands of Transkei. *Physics and Chemistry of the Earth, Parts A/B/C*, 1–9.

Seutloali, K. E., Beckedahl, H. R., Dube, T., Sibanda, M. (2015). An assessment of gully erosion along major armoured-roads in south-eastern region of South Africa: a remote sensing and GIS approach. *Geocarto International*, 1–24.

Tekwa, I. J., Laflen, J. M., & Kundiri, A. M. (2015). Efficiency test of adapted EGEM model in predicting ephemeral gully erosion around Mubi, Northeast Nigeria. International Soil and Water Conservation Research, 3(1), 15–27.

van der Knijff, J., Jones, R. J. A., Montanarella, L. (2002). Soil Erosion Risk Assessment in Italy. In: J. L. Rubio, R. P. C Morgan, S. Asins & V. Andreu (Eds.), *Proceedings of the third International Congress Man and Soil at the Third Millennium*. Geoforma Ediciones, Logrono. pp. 1903–1913.

Wang, Z., Jiao, J. Y., Rayburg, S., Wang, Q. L., & Su, Y. (2016). Soil erosion resistance of "grain for green" vegetation types under extreme rainfall conditions on the Loess Plateau, China. *CATENA, 141,* 109–116.

Wischmeier, W. H, & Smith, D. D. (1978). *Predicting rainfall erosion losses—A guide to conservation planning*. Series: Agriculture Handbook, USDA, Washington, D.C., pp. 3–4.

Zhao, J., Vanmaercke, M., Chen, L., & Govers, G. (2016). Vegetation cover and topography rather than human disturbance control gully density and sediment production on the Chinese Loess Plateau. *Geomorphology, 274,* 92–105.

Conditional Stochastic Simulation of Carbon Dioxide Concentrations

Lucie Orlíková

Abstract This paper deals with conditional stochastic simulation. Old, abandoned coal mines contain the vestiges of coal mine gas. Coal mine gas usually consists of methane, nitrogen and carbon dioxide. But despite that they no longer produce coal, these sites are still contributing to climate change by leaking carbon dioxide into the atmosphere. The concentrations of carbon dioxide were studied and used as input parameters for stochastic simulation. Kriged surface underestimates the high values and overestimates the low values. The simulation model is conditioned to reproduce the data at known sample points to minimize the variability between the simulated data and the true field data. The main aim of this investigation is to compare selected interpolation methods that are currently used in practice with stochastic simulation, based on the development of the values. The advantages and disadvantages of each approach are discussed. The study shall provide users with recommendations for selecting the optimal interpolation method and its application to real data.

Keywords Carbon dioxide · Stochastic simulation · Spatial analysis · GIS Ostrava 2017

Introduction

Old mines are still working, and mine shafts provide lateral and vertical conducts for gas to travel along. Old mine workings usually contain methane and carbon dioxide gases and these can often be misleading when surface monitoring is being carried out for landfill gas.

L. Orlíková (✉)
Institute of Geoinformatics, VŠB-Technical University of Ostrava,
17. listopadu 15, 70833 Ostrava-Poruba, Czech Republic
e-mail: lucie.orlikova@vsb.cz

I. Ivan et al. (eds.), *Dynamics in GIscience*, Lecture Notes in Geoinformation and Cartography, DOI 10.1007/978-3-319-61297-3_23

Gas migration is influenced by several climatic factors, namely atmospheric pressure, groundwater levels or even the temporary effects of a snow-fall, which can act like a blanket over the landfill site and surrounding land, preventing the gas from venting at the surface (Atkinson 1993).

With housing developments, the main problems to contend with are found on those developments that are in close proximity to active landfill sites. The biggest risk for people are abandoned mines which are not ventilated. Pockets of methane, carbon dioxide, and other deadly gases can form or simply displace oxygen with no visible sign. When people breath these gases, their muscles stop responding normally and their thinking becomes clouded. This is followed by unconsciousness and death.

When housing is to be constructed within 250 m of known active landfill sites, it is necessary to periodically conduct gas monitoring. The site should be monitored regularly over a long period, while recording any changes in barometric pressure.

Simulation produces a set of alternative maps, providing sampled information of an investigated attribute reproducing its true spatial variability. Geostatistical stochastic simulation allows better visualization of heterogenity and brings better assessment of the attribute uncertainty at non-sampled locations.

Simulation tries to reproduce the essential statistical characteristics of data distribution, such as histogram and spatial continuity, computing a set of alternative stochastic images of the random process and then carrying out an uncertainty analysis. Every kriging algorithm produces a unique and smooth map (Goovaerts 1997; Webster and Oliver 2007; Prusova and Orlikova 2012).

Knowledge of carbon dioxide distribution can provide valuable insight for gas monitoring and could be very useful for local planning authorities. The main objective of this work is to compare geostatistical methods, which are now used for the spatial distribution of carbon dioxide (kriging) with stochastic simulation.

There are many studies dealing with spatial distribution of carbon dioxide (Kissel 2006; Krasilnikov et al. 2008; Gentzis 2013; Karacan et al. 2011; Karacan and Diamond 2006; Kedzior et al. 2013; Pebesma 2014; Tercan and Sohrabian 2013). Based on a review of literature, it can be concluded that conditional stochastic simulation provides many advantages against kriging, which is used for estimating the spatial distribution of carbon dioxide at this moment.

Methodology

Conventional methods, such as inverse distance weighting, global polynomial interpolation and natural neighbour, combine data on the position of the sample with an intuitive notion of area of influence to produce usable results with no objective way to measure the reliability of these results. Statistical and probabilistic techniques have also been used to produce estimators for which confidence limits might be derived. Unfortunately, these techniques are suitable for random observations of samples without regard for spatial position (Royle et al. 1980;

Oliver 1990; Frimpong and Achireko 1998). Matheron (1971) developed the theory of regionalized variables in geostatistics specifically to solve the problems. The kriging technique is used to obtain the best linear, unbiased estimate of random field values, given a set of observed values. Kriging tends to underestimate values that are larger than average and to overestimate those that are smaller.

Hughes and Davey (1979) have also noted that:

- variograms do not accurately represent the mineralized zone because of inadequate data;
- theoretical models do not accurately fit the variogram data;
- kriging is insensitive to variogram coefficients; and
- the matrix involved in finding the coefficients sometimes tends to be illconditioned for certain geometrical bodies.

In geostatistics, the term "simulation" means the creation of values of one or more variables that emulate the general characteristics of those being observed in the real world. A simulated realization tries to mimic the true variability described by the second order functions such as covariance or the variogram. Unconditional simulation is simply an application of the general Monte Carlo technique, whereby values are created with a particular covariance function or variogram (Deutsch and Journel 1998).

A more realistic visualization of reality is achieved by the use of conditional geostatistical simulations, where the sample points are taken as known, but the interpolated points reproduce the variogram model including the local noise introduced by a nugget effect (Hengl 2009).

The simulation is conditioned on the sampled data, $z(x_i)$; $i = 1, 2, \ldots, N$, denoting the conditionally simulated values by $zC^*(x_j)$, $j = 1, 2, \ldots, T$. Where the data exist, the simulated values should be the same:

$$zC^*(x_i) = z(x_i) \quad \text{for all } i = 1, 2, \ldots, N \tag{1}$$

Elsewhere, $zC^*(x)$ may depart from true but unknown values in accordance with the model of spatial dependence adopted (Webster and Oliver 2007). Considering what happens when Z is kriged at x_0, where there is no measurement, the true value, $z(x_0)$, is estimated by $\hat{Z}(x_0)$ with an error $z(x_0) - \hat{Z}(x_0)$, which is unknown:

$$z(x_0) = \hat{Z}(x_0) + \{z(x_0) - \hat{Z}(x_0)\} \tag{2}$$

A characteristic of kriging is that the error is independent of the estimate, that is

$$E\left[\hat{Z}(y)z(x) - \hat{Z}(x)\right] = 0 \quad \text{for all } x, y \tag{3}$$

This feature is used to condition the simulation. A simulated field is created from the same covariance function or variogram as that of the conditioning data to give values $zS^*(x_j)$, $j = 1, 2, \ldots, T$, that include the sampling points, x_i, $i = 1, 2, \ldots, N$. Kriging at x_0 from the simulated values at the sampling points give an estimate

$\hat{Z}S^*(x_0)$. Its error, $Zs^*(x_0) - \hat{Z}S^*(x_0)$, comes from the same distribution as kriging error in Eq. 2. It can be used to replace the kriging error to give our conditionally simulated value as

$$zC^*(x_0) = \hat{Z}(x_0) + \left\{zS^*(x_0) - \hat{Z}S^*(x_0)\right\} \quad (4)$$

Conditional simulation is more appropriate than kriging where the interest is in the local variability of the property and too much information would be lost by the smoothing effect of kriging.

Pilot Area and Measurement Methodology

The Czech part of the Upper Silesian Coal Basin with a segment used for coal mining and known as the Ostrava-Karviná Coal Mining District (OKR) belongs in the Podbeskydská pahorkatina Hilly Land and Ostrava Basin.

Many mining activities in the underground coal mines ceased in the Ostravsko-Karvinsky region approx. 25 years ago. In 2014 Ostrava–Karvina mines extracted coal in four active mines in the areas of Karviná and Frýdek-Místek (Důl ČSM, Důl Karviná, Důl Darkov and Důl Paskov). The average depth of excavated coal deposits in the mining district is approx. 930 m under the surface and the yearly production is nine to ten million tons of coal. The disturbed rock mass continuously releases underground gases that cumulated in empty spaces, remnants of old mine works and cavings. They have the tendency to ascend to the surface. With respect to very dense settlements on the surface (Ostrava City and its vicinity), this uncontrolled gas escape can be very dangerous. Safety measures implemented as the prevention of dangerous states imply building of passive and active degassing systems, which necessitates the drilling of surface boreholes. The central part of the town of Orlova serves as the example of long-term implementation of safety measures including the possibilities of mine gas treatment.

The occurrence of methane in coal mines was given attention after the first severe accident in the Trojice Coal Mine in 1884 when the monitoring of methane occurrence in OKR coal mines was prescribed by law. Large minefields in the entire coal mining district were ventilated, which were gradually linked due to the extension of mining spaces, not only by means of mine works but also by means of irregular communication through worked-out areas and cave fields and through the Carboniferous massif with alterations of red-beds type.

The mining activities in the Ostrava coal mines (from 1776 to the end of coal mining in 1992) gave rise to an underground space of several hundred million cubic metres in volume, which has been reduced to approx. 50 milllion m^3 due to gradual flooding and caving consolidation (Takla and Král 1999). The space is now filled with a blend of mine and coal bed gases rich in methane which, leaks to the ground surface through pits and wells, Carboniferous windows, and disturbed massif at places of lower crust thickness (Marinec et al. 2005).

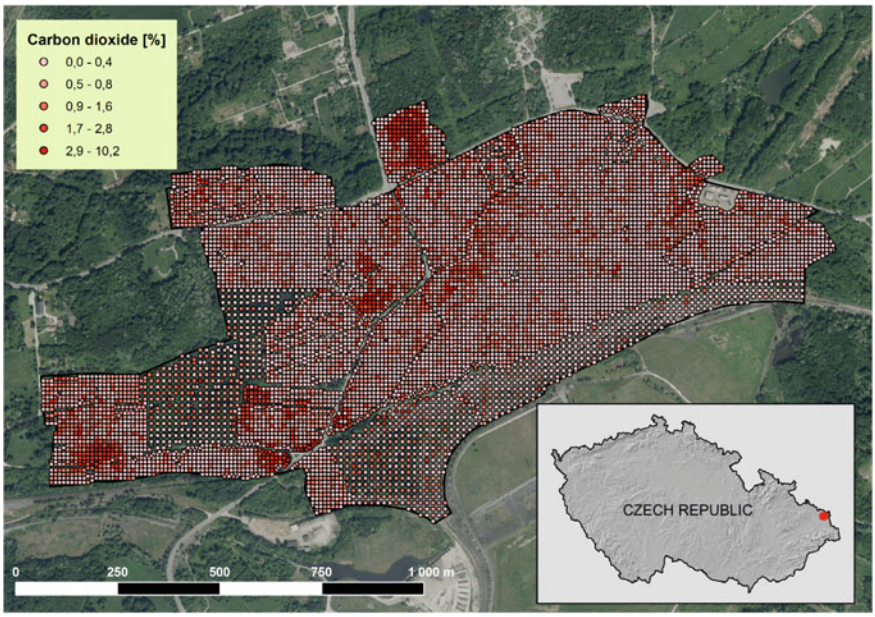

Fig. 1 Location map showing carbon dioxide measurement sites in Orlova

The concentrations of carbon dioxide were studied in Orlova, situated in the Moravian-Silesian region in the Czech Republic. Concentrations of carbon dioxide in soil air were measured on November 2, 2010, November 8–12, 2010, November 15 and November 18, 2010. The measurements could be performed only when the weather conditions are within the limits established for the safe use of all equipment and the value of barometric pressure at sea level is 1017 hPa or less.

The concentration of carbon dioxide in built-up areas were measured in 10-m steps, and in unbuilt areas the steps were 15 m (Hemza et al. 2006) (Figs. 1 and 2).

The result of the exploratory analysis is the statistical analysis of carbon dioxide concentrations.

The EDA (Exploratory Data Analysis) also investigates the normality of data. Most interpolation methods are based on linear estimates and require a normal distribution of sample data. If data fails in normality testing, it is necessary to conduct an appropriate data transformation to reach the normal distribution (Table 1).

The mean and median are quite dissimilar. In the ideal Normal, mean, median and mode are identical. The range is around 15.34 times the standard deviation—that is, 7.2 either side of the mean. As a general rule, the range should be somewhere between 4 and 6 standard deviations, depending on how many samples we had. The interquartile range for this data is around 0.43%. An ideal normal distribution has a skewness of zero and a standardized kurtosis of 3. Many researchers indicated that data normality (Wu et al. 2006) and coefficient of

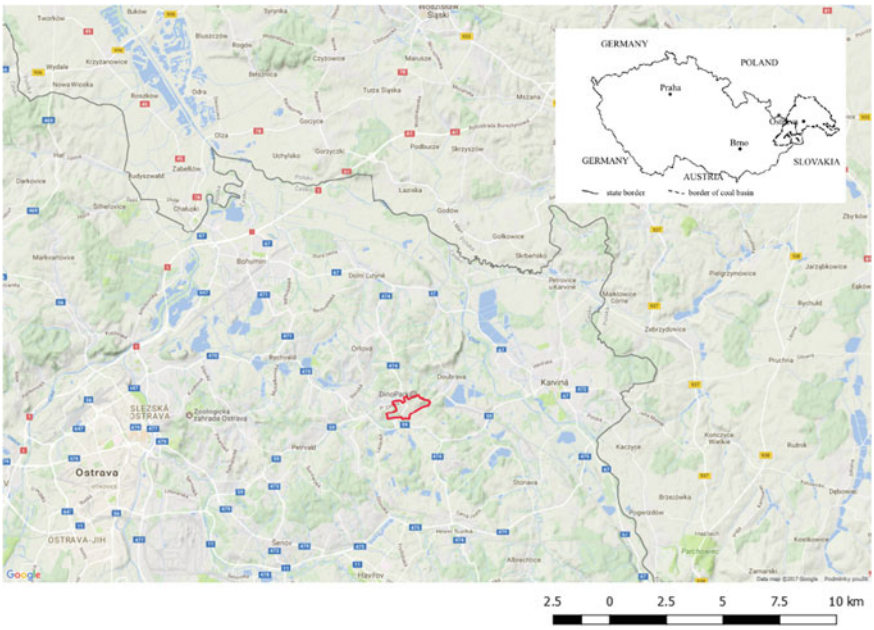

Fig. 2 Situation of the Upper Bituminous Coal Basin and pilot area in relation to the Czech Territory

Table 1 Carbon dioxide concentration's descriptive statistics (in %)

Mean	0.53
Std. deviation	0.66
Median	0.31
Sample variance	0.43
Kurtosis	20.3
Skewness	3.39
Range	10.15
N total	9230
Minimum	0
Maximum	10.15

variation (Heap et al. 2011) might affect the performance of spatial interpolation methods. The following methods of transformation were tested: the natural logarithm transformation, the transformation of the square and power transformation using a linear interpolation coefficient of skewness, which approximates the optimal value of the constant transformation estimate based on linear interpolation (Kanok 1996). The natural logarithm transformation was selected as the best transformation (Fig. 3).

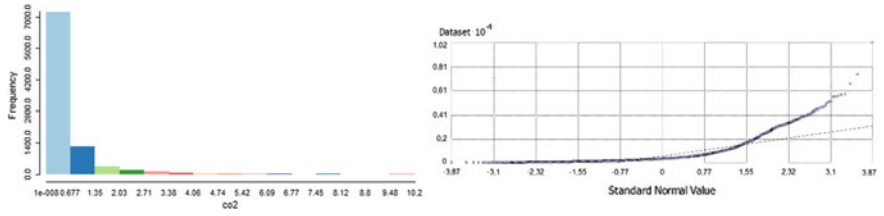

Fig. 3 Histogram and *q-q* plot of carbon dioxide concentrations

Table 2 Parameters for variogram (simple and ordinary kriging)

Parameter	Value
Nugget	0.1
Lag size	5
Number of lags	10
Search radius	40 m
Range	20
Partial sill	0.55

Stochastic Simulation and Other Interpolation Methods

The following methods were compared: simple kriging, ordinary kriging and conditional stochastic simulation. The simple kriging method was chosen for comparison because it is used for estimation by a company making carbon dioxide measurements. Ordinary kriging is the most widely used kriging method. The development of the shapes of contour lines and their credibility was examined.

The question whether it is necessary to involve all samples in the estimation procedure was also considered. Isaaks and Srivastava (1989) suggest only 12 samples for optimal results, but according to Wackernagel (1998) the optimal number of samples is 20. We used 24 samples in this case.

The variogram parameters, listed in Table 2, were configured for all methods. Simple kriging in ArcGIS Geostatistical Analyst is a necessary condition for simulation. Geostatistical layers resulting from other types of kriging cannot be used with this tool. The aim was to set the optimal parameters, so that the input to the simulation data is distorted as little as possible. This method is a mandatory input parameter in this software.

To generate conditional realizations, the conditioning data should be the same as the data that was used to construct the Simple Kriging model from which the simulation will be based; however, other datasets can be used to condition the realizations.

The setting parameters were prepared, as follows:

- Simple kriging
- Number of realization: 1000
- Conditional field: concentrations of carbon dioxide
- Cell size: 1 m

The higher number of realizations, the more accurate simulation results and the better reflection of the trend in the area. In general, the number of necessary simulations depends on the complexity of the spatial pattern and the relationships between typical scales. Usually smaller patterns need fewer realizations (Kanevski et al. 2009). The example simulations were compared with the number of implementations (300, 500 and 1000). The simulation with the highest number of implementations (1000 number of realization) seemed to repeat the initial smoothing interpolation, but in comparison with the kriging methods it is a negligible problem. Stochastic simulation generally gives better results than the conventional interpolation method.

Once the realizations have been produced, they are usually post-processed to obtain summaries of the results. The entire raster extent was post-processing—raster included the mean of all the cells in all the realizations that fell within the polygon. The results of the simulations were compared with the ordinary and simple kriging models (see Fig. 4). A detailed view of the estimation surface by a simple kriging method is in Fig. 5 (Table 3).

In this study, three surface estimation methods were explored and compared. Cross validation is usually used to compare accuracy of interpolation methods. It removes each data location one at a time and predicts the associated data value. Each of the kriging methods gives the estimated prediction of kriging standard

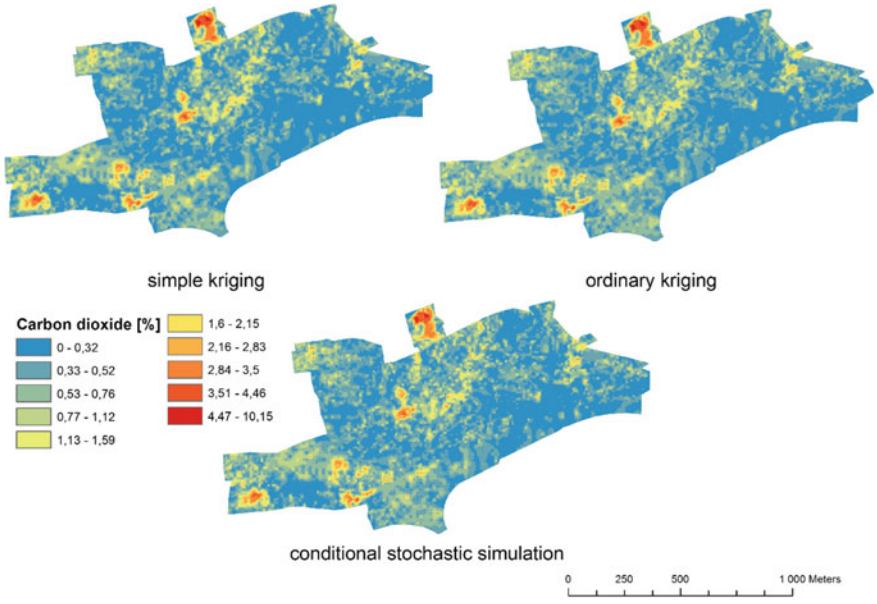

Fig. 4 Estimation surface by using—simple kriging, ordinary kriging and conditional stochastic simulation

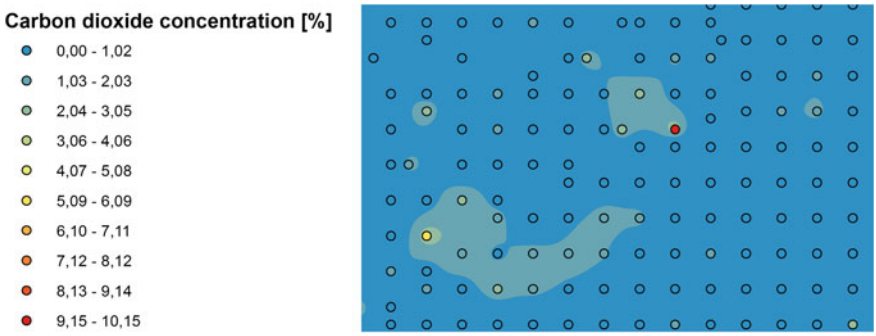

Fig. 5 Detail view of estimation surface by simple kriging

Table 3 Prediction errors for all methods

Parameter	Simple kriging	Ordinary kriging	Simulation
RMSE	0.515	0.513	0.108
Mean standardized	−0.002	−0.016	
Root mean square standardized	1.467	1.229	
Average standard error	0.600	0.662	

error. If the average standard errors are greater than the root mean squared prediction errors, you are overestimating the variability of your predictions. If the average standard errors are less than the root mean squared prediction errors, you are underestimating the variability in your predictions. Another way to look at this is to divide each prediction error by its estimated prediction standard error. They should be similar, on average, so the root mean squared standardized errors should be close to 1 if the prediction standard errors are valid. If the root mean squared standardized errors are greater than 1, you are underestimating the variability in your predictions; if the root mean squared standardized errors are less than 1, you are overestimating the variability in your predictions (Krivoruchko et al. 2003). The simple kriging method underestimates the variability in this case (the minimum value is 0%, the maximum value 7.8%, but the maximum measured value is 10.15%). The same problem is caused by ordinary kriging method (the minimum value is 0%, the maximum value 9.6%). The conditional stochastic simulation has the lowest root mean square error.

Conclusion and Future Work

In this study, we would like to show that there are other methods that can provide better results than conventional interpolation methods such as kriging. It was confirmed that conditional stochastic simulation gives good results in comparison

with other interpolation methods, especially in areas with the highest values. In these areas, simple and ordinary kriging methods underestimate the values. Gaussian models are widely used as reference models because they are theoretically consistent models.

Skewed, non-Gaussian and non-stationary data are common in geostatistical and environmental applications. Conventional geostatistical methods do not take into account these facts. Future work will investigate a method to deal with this sort of data. The suggested algorithm is Bayesian trans-Gaussian kriging where uncertainties could be specified on the trend, the co-variance function and the parameter of the transformation function. The Bayesian trans-Gaussian kriging avoids Markov chain Monte Carlo by using a bootstrapping procedure. For future work it will be better to split data into training and testing and to use testing data to compare the results.

Also, Artificial Neural Network approaches for the analysis and mapping of spatially distributed data will be taken into account.

References

Atkinson, M. (1993). *Structural foundations manual for low-rise building*. New york: CRC Press, Taylor&Francis Group.

Deutsch, C. V., & Journel, A. G. (1998). *GSLIB: geostatistical software library and user's guide* (2nd ed.). New York: Oxford University Press.

Frimpong, S., & Achireko, P. (1998). Conditional LAS stochastic simulation of regionalized variables in random fields. *Computational Geosciences, 2,* 37–45.

Gentzis, T. (2013). Coalbed methane potential of the Paleocene Fort Union coals in south-central Wyoming, USA. *Int. J. Coal Geol., 108,* 27–34.

Goovaerts, P. (1997). *Geostatistics for natural resources evaluation*. New York: Oxford University Press.

Heap, A. D., & Li, J. (2011). A review of comparative studies of spatial interpolation methods in environmental sciences: Performance and impact factors. *Ecological Informatics, 6*, 228–241.

Hemza, P., Kunz, A., & Vavrušák, Z. (2006). *Metodický postup 35/A1 - „Metanscreening – měření koncentrace důlních plynů v půdním vzduchu"*. Ostrava: DPB OKD.

Hengl, T. (2009). A practical guide to geostatistical mapping. University of Amsterdam (p. 291).

Hughes, W. E., & Davey, R. K. (1979). *Drill hole interpolation: Mineralized interpolation techniques in open pit mine planning and design* (pp. 51–64). Littletone: SME.

Isaaks, H. E., & Srivastava, R. M. (1989). *Introduction to applied geostatistics*. Oxford: Oxford University Press.

Kanok, M. (1996). *Statistical methods in management*. Czech Technical University in Prague.

Kanevski, M., Pozdnoukhov, A., & Timonin, V. (2009). *Machine learning for spatial environmental data—Theory, applications and software* (p. 377). New York: EPFL Press, Taylor and Francis Group.

Karacan, C. Ö., & Diamond, W. P. (2006). Forecasting gas emission for coal mine safety applications. In *Handbook for methane control in mining*. Information Circular No. 9486. Pittsburgh, PA: NIOSH.

Karacan, C. Ö., Olea, R. A., & Goodman, G. (2011). Geostatistical modeling of gas emission zone and its in-place gas content for Pittsburg-seam mines using sequential Gaussian simulation. *International Journal of Coal Geology, 90–91,* 50–71.

Kedzior, S., Kotarba, M. J., & Pekała, Z. (2013). Geology, spatial distribution of methane content and origin of coalbed gases in Upper Carboniferous (Upper Mississippian and Pennsylvanian) strata in the south-eastern part of the Upper Silesian Coal Basin, Poland. *International Journal of Coal Geology, 105*, 24–35.

Kissel, F. (2006). *Handbook for methane control in mining*. Pittsburg: Department of Health and Human Services, National Institute for Occupational Safety and Health.

Krasilnikov, P., Carré, F., & Montanarella, L. (2008). *Soil geography and geostatistics. Concepts and applications*. JRC European Commission: Germany.

Krivoruchko, K., Johnston, K., Ver Hoef, J. M., & Lucas, N. (2003). Using ArcGIS geostatistical analyst. ESRI, print in United States of America.

Martinec, P., Schejbalová, B., Hortvík. K., & Maníček, J. (2005). The effect of coal mining on the landscapes of the Ostrava region. *Moravian Geographical Reports, 2*(5). ISNN 12010-8812.

Matheron, G. (1971). Theory of regionalized variables and applications. Booklet No. 5, Les Cahiers du Centre de Morph. Math. CMM: Ecole Nat. Sup. Des Mines, Paris (p. 222).

Oliver, M. A. (1990). Kriging: A method of interpolation for geographical information systems. *International Journal of Geographic Information Systems, 4,* 313–332.

Pebesma, E. J. (2014). GSTAT user's manual. Department of Physical Geography, Utrecht University (p. 108).

Prusova, M., & Orlikova, L. (2012). Comparison of geostatistical approaches dealing with the distribution of snow. *Central European Journal of Geoscience, 4*(4), 603–613.

Royle, A. G., et al. (1980). *Geostatistics* (p. 168). New York: McGraw-Hill.

Takla, G., & Král. V. (1999). Průzkum a zajištění staveb na území s výstupy metanu. Stavby na poddolovaném území v současných podmínkách (Sborník konference). Dům techniky Ostrava s.r.o., Fakulta stavební VŠB-TU, Ostrava (pp. 91–99).

Tercan, A. E., & Sohrabian, B. (2013). Multivariate geostatistical simulation of coal quality data by independent components. *International Journal of Coal Geology, 112,* 53–66.

Wackernagel, H. (1998). *Multivariate geostatistics*. Berlin: Springer.

Webster, R., & Oliver, M. A. (2007). *Geostatistics for environmental scientists*. England: Wiley.

Wu, J., Norvell, W. A., & Welch, R. M. (2006). Kriging on highly skewed data for DTPA-extractable soil Zn with auxiliary information for pH and organic carbon. *Geoderma, 134,* 187–199.

Spatial and Temporal Comparison of Safety Perception in Urban Spaces. Case Study of Olomouc, Opava and Jihlava

Jiří Pánek, Vít Pászto and Petr Šimáček

Abstract Subjective and participatory mapping has become an important tool for urban planners and city administrations. Perceptions of safety can affect the quality of life and property prices. The presented paper describes participatory mapping exercises in three Czech cities, where questions were asked concerning people's subjective perceptions of safety during the day and at night. Respondents in Olomouc (n = 661), Opava (n = 901) and Jihlava (n = 106) respectively indicated 1516 (Olomouc); 3491 (Opava) and 894 (Jihlava) places as unsafe. The data was gathered over a period of two years; in Olomouc data was collected between 1st October and 2nd December 2015, in Opava the survey took place between 19th October 2016 and 30th December 2016, and in Jihlava in the period from 30th November 2015 until 4th March 2016. The data collected included information about the gender of the respondents and the day-time/night-time division of perceived safety, so it was possible to analyse gender differences as well as time specifics from the collected data. The results suggest that there are certain areas in all three cities that have similar patterns (train stations, city parks, dark and narrow streets, excluded communities).

Keywords Emotional mapping · Subjective data · Public participation · Geovisualisation

J. Pánek (✉)
Department of Development Studies, Faculty of Science, Palacký University Olomouc, 17. listopadu 12, 77146 Olomouc, Czech Republic
e-mail: Jiri.Panek@upol.cz

V. Pászto
Department of Geoinformatics, Faculty of Science, Palacký University Olomouc, 17. listopadu 50, 77146 Olomouc, Czech Republic
e-mail: vit.paszto@gmail.com

V. Pászto
Department of Computer Science and Applied Mathematics, Moravian University College, tř. Kosmonautů 1288/1, 779 00 Olomouc, Czech Republic

P. Šimáček
Department of Geography, Faculty of Science, Palacký University Olomouc, 17. listopadu 12, 77146 Olomouc, Czech Republic
e-mail: Petr.Simacek@upol.cz

I. Ivan et al. (eds.), *Dynamics in GIscience*, Lecture Notes in Geoinformation and Cartography, DOI 10.1007/978-3-319-61297-3_24

Introduction

Criminality is an integral part of our lives. It is not necessary to have our own personal experience of criminal acts because the high number of media reports about crime means that citizens are becoming passive actors in this phenomenon. Not only the actual incidence of crime, but the perception of crime, significantly affects our overall satisfaction and people's quality of life (Stasíková 2011). The need for security is generally considered to be one of the basic human needs (Maslow 1943) and crime is among the leading factors that undermine people's perceptions of safety. Due to a perceived reduction in safety, based on the fear of crime, there are changes in decision-making and in the behaviour of people in space and time (Koskela 1999; Pain 2001; Curtis 2012; Jíchová and Temelová 2012). Concerns about crime are subjective and dependent on many aspects of human life, so each individual in a given environment perceives different intensities of danger. Fear of crime is currently also seen as a serious social problem that has to be solved, because even a significant decrease in crime numbers may not ensure an increased perception of safety among the population (Kosová 2016). Fear of crime has become an important topic for research in many disciplines. Many authors favour the view that fear of crime is as serious as, or perhaps an even greater problem than, the crime itself (Clemente 1977; Brown and Polk 1996; Doran and Burgess 2012; Oc and Tiesdell 1997). Fear of crime—unlike the crime itself – is not limited by space and time; thus it has a greater potential to be spread among the population (Smith 1987; Perkins and Taylor 1996). Tracking the phenomena in space and time can help other activities aimed at reducing the fear of crime, e.g. when creating policy documents aimed at crime prevention or aimed at the development of a locality.

The concept of fear of crime has its roots in the 1960s, when riots occurred in the USA, and therefore opinion polls were organised with the aim of finding out more information about citizens. Questions regarding crime were among the surveyed topics, and the concept of "fear of crime" was seen for the first time (Jackson 2006; Wynne 2008). Geographical research plays a significant role in the concept of fear of crime since time, space and fear of crime are in a state of mutual interaction. A set of multiple aspects of "fear of crime" were analysed in studies by Canadian scientists Brantingham and Brantingham (1995) and Scottish authors Bannister and Fyfe (2001).

According to Jíchová (2013), the environment, the demographic characteristics of citizens, the amount of daylight, and even the current weather, play an important role in the perception of safety. One of the most important reasons for the fear of crime is the environment in which the individual is located. According to several studies (e.g. Newman 1972; Matthews 1992; Koskela 1999; Schmeidler 2000; Stasíková 2013; Hýža 2016; Kosová 2016; Pánek et al. 2017), the design and modification of the physical environment affects residents' perceptions of safety. Block and Block (1995) and Sherman (1995) stated that there are two basic types of localities with higher rates of criminality. The first type is called

"Crime Generators" and it is represented by places where there are a large number of people (e.g. shopping malls, entertainment centres, and sports stadiums), as this offers many opportunities to commit a crime. The second type is called "Crime Attractors," which are typical locations with suitable conditions for committing a crime (e.g. so-called "red-light districts"; Brantingham & Brantingham 1995). Apart from the above mentioned areas, it is possible to define other areas referred to as risky, because of their image as a place where safety is perceived to be insufficient (e.g. parks, underpasses, tunnels and train stations; Jíchová 2013).

Most people feel more concerned about their safety at night and this is justified by the fact that most crimes are committed at night; numerous studies have highlighted the issue of the difference between the perception of day-time and night-time (Samuels and Judd 2002; Hýža 2016; Kosová 2016). Typical places that change their character from day to night include; closed spaces such as pedestrian underpasses, subways, underground and multi-storey parking lots and train wagons. On the other hand, open spaces such as parks, sites along waterways and far-flung places, which can be can be dangerous if people have to leave the area quickly are often also considered unsafe (Valentine 2001; Tonkiss 2005). In the case of public transportation, whether it is day or night has a major impact on the perception of fear. Zítková (2013) points out that most people feel more concerned when using public transport after sunset and it is considered even more risky to walk to or from the train/bus/tram stops. The time of day is directly connected to the structure of the users of public space. While the day-time population is comprised of children, women and the elderly, during the night the population is particularly made up of men (Worpole 1992).

Most studies with a similarly focus (e.g. Valentine 1989; Smith and Torstensson 1997; Koskela and Pain 2000; Brownlow 2005) have claimed that gender is another important factor in the perception of fear by individuals, and of course there are many more factors which influence the fear of crime. This paper deals with mapping places which are perceived as dangerous by the inhabitants of three cities in Czechia. The main research question is: Are there locations that people are afraid of which have the same urban function across the cities studied? If so, what are typical urban functions of such places?

Background

The selected locations were Jihlava, Opava and Olomouc; the first two are middle-sized cities and Olomouc is the largest of the three and large in the Czech context.

Olomouc is a historical city in Czechia with a population of 100,154 (Czech Statistical Office 2016), and it is also the seat of The Regional Authority of the Olomouc Region and the sixth largest city in the country. The city is sometimes called the "city of parks" as several parks surround the historical city-centre. The parks, although perceived as a source of pride for the city, are often a source of

danger and criminality, mainly in the evenings and nights. The Olomouc Region stated, in its Strategy of Criminality Prevention 2013–2016 (Olomouc Region 2015) that one of its four visions is to increase the sense of safety in the region. Based on this document the authors believe that, emotional mapping and citizens perception of safety are in alignment with the long-term strategy of the region.

Opava is also a historical town, with a population of 57,676 (Czech Statistical Office 2016) and lies on the border between Czechia and Poland. In Opava, the safety perception mapping was organised in collaboration with the Statutory City of Opava and the local technical high school. According to the regional concept of prevention of criminality for the years 2012–2016, Opava is the region with the lowest amount of criminal acts per 10,000 inhabitants in Moravian-Silesian Region (202,3 criminal acts per 10,000 inhabitants).

The city of Jihlava, with 50,714 inhabitants (Czech Statistical Office 2016), is the seat of the Regional Authority of the Vysočina Region and lies in the central part of the region. The mapping of inhabitants' safety perceptions within the city was organised in collaboration with the city government and the local police forces. The city itself has no specific document concerning prevention of criminality. Thus, the city council uses the common document for the whole Vysočina Region in the field of criminality prevention. One of the main goals of the document is to increase inhabitants' perceptions of safety and increase the information about the defence possibilities against criminals.

Methods and Data

The data regarding the perception of safety were collected in all three cities via the participatory online web application called *PocitoveMapy.cz,* and paper-based questionnaires, which were then digitised via the above-mentioned application. Technically, the application is designed as a single-page web application using two main open-source JavaScript libraries; jQuery for basic user interactions and app control and Leaflet, the library for map interactions. The source code of the frontend part is divided into small modules (e.g. PM.init, PM.logic, PM.save.js, PM.storage). For production, the modules are concatenated with other libraries by Grunt Task Runner. The application can be configured with a JSON file containing basic map views, app steps and popup form content. The configuration file can be hard-coded or generated from a database at backend. The results from frontend are sent asynchronously to backend where it uses the authors' own simple MVC frame-work written in PHP script language. The MySQL database is used for storing metadata from users and geodata are stored in the GeoJSON format. The administration of the application is created with the help of the CSS framework Bootstrap and administrators are allowed to download the full metadata from MySQL, concatenated with GeoJSONs. Similar to other web-based tools for crowdsourced mapping, it allows users to collect spatial data on a slippery map background. Unlike Ushahidi, Umap, ArcGIS Online and many others, it does not

require the registration or installation of any specific software, plug-in or virtual server. The simplicity of the tool helps when engaging various target groups, yet it is still rich in information gathered. The tool has been used previously to map cyclists' safety in Reykjavík (Pánek and Benediktsson 2017); to map links between environment and public health in Czechia (Pánek et al. 2017); and for neighbourhood development activities in a small town in Bohemia (Pánek and Pászto 2017). There have also been attempts to map safety perception with the application (Pánek et al. 2017), nevertheless this paper presents a first time comparison of safety perception data across multiple cities in various temporal settings (day-time vs. night-time).

The collection of data was managed in several ways in order to include various groups of citizens. The research included: an analogue, paper-based questionnaire, a crowdsourcing web-based application, and in situ questionnaires with portable devices (tablets and laptops).

In Jihlava and Olomouc offline questionnaires were also used in order to diversify the respondents' structure and gather more answers. In these two cases, the web application *PocitoveMapy.cz* was then used to digitise the data from the analogue form and to merge all the collected information into one spatial file (GeoJSON).

The data was gathered (see Table 1) over a period of two years; in Olomouc the data was collected between 1st October and 2nd December 2015, in Opava the survey took place between 19th October 2016 and 30th December 2016, and in Jihlava in the period from 30th November 2015 to 4th March 2016.

The structure of the surveys was similar in all three case studies. Both the analogue and the digital collection procedure had two main questions for the respondents:

(a) mark places where you feel unsafe during the night-time (alternatively when it is dark),
(b) mark places where you feel unsafe during the day-time (alternatively there is light).

Table 1 Numbers of participating respondents and marked locations

	Olomouc	Opava	Jihlava
Total number of respondents	661	901	160
Male/female/NA	N/A	457/444/0	51/83/16
Percentage of total population (%)	0.6	1.5	0.3
Respondents from online sources	144	901	135
Respondents from offline sources	517	N/A	25
Number of collected locations	1516	3491	894
Male/female/NA	474/589/453		
Number of locations for day-time	407	1428	320
Number of locations for night-time	1109	2063	574

Source Kosová (2016; own survey)

For the analogue collection of data, trained interviewers (often students from Palacký University Olomouc) approached each respondent at random with the main task being to establish contact with him/her and to convince them to participate in the case study. Furthermore, the basic characteristics of the participants were collected, such as age, gender, whether they live in the city where the survey took place, and so forth.

From the geospatial point of view, the collected data was acquired as point layers (in the case of Olomouc and Opava) and as a polygon layer (in the case of Jihlava). To each point or polygon in both version respondents had the chance to add comments in writing. These comments are briefly described in the Results section. The polygon layer needed to be converted into points since the next step was to apply a hexagonal grid. Polygons were transformed into hexagonal grids via the polygons´ centroids (*spatial join*), which were assigned a value from the polygon. The authors are aware that the simplification of polygons to centroids is not optimal and may be affected by information loss, nevertheless, when whole polygons were used, the city was covered by large areas of similar values which made it difficult to identify hot-spots, which was the main aim of the research. As demonstrated and described in (Pánek and Pászto 2017), a hexagonal grid provides more comprehensive information than displaying a mesh of points. Furthermore, hexagonal grids proved to be an interesting alternative to classical grids (Burian et al. 2014).

Results

Olomouc

More detailed results from Olomouc were already published by Pánek et al. (2017), hence the description of results from Olomouc will be shortened. Places perceived as the most unsafe are located around the main train station (eastern part of the city), around the city centre (mainly in the surrounding parks and small streets), at localities in suburban residential areas (southern and south-eastern parts of the city) and at places with underpasses. Unlike the other two cities (Jihlava and Opava), in Olomouc there are significant differences in safety perceptions between day-time and night-time (Fig. 3). In Olomouc, respondents tended to mark places connected with fearful emotions during the night (or darkness; 1109 records) approximately three times more than during the day (407 records).

Places that were marked as unsafe during the day-time (see Fig. 1) were mainly the main train station, parks (especially Bezručovy Sady), pedestrian underpasses and residential areas which are partly treated as socially excluded localities (Nový Svět, Černá cesta). In optional commentaries respondents argued that these are places with “weird people, homeless people, pickpockets, drunk people, heavy traffic, underpasses and the Roma minority”, among other comments.

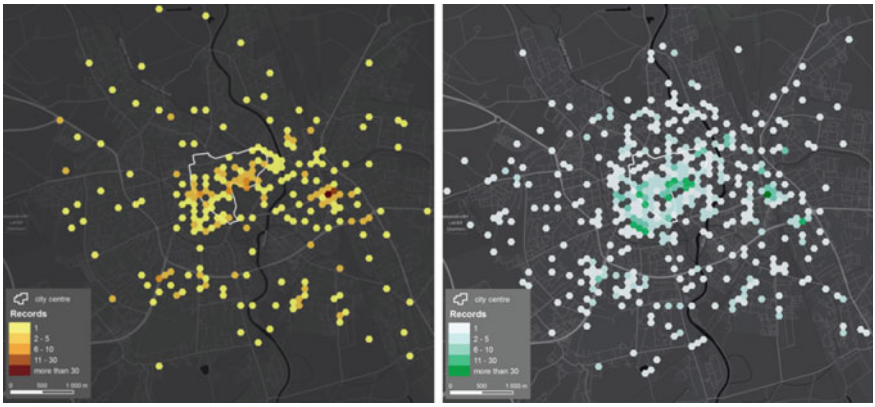

Fig. 1 Distribution of unsafe places in Olomouc by time of day (day on *left*, night on *right*)

Fig. 2 Distribution of unsafe places in Olomouc by gender (women on *left*, men on *right*)

Additionally, unsafe places (marked at least once) cover almost all the city centre during the night, and also localities with large blocks of flats in suburban residential areas are highlighted as unsafe. The main reasons respondents feel unsafe are "not enough street lights, dark streets, the homeless, drunk people, bad feelings, drug users, underpass, weird people".

Having compared the places perceived unsafe by men and women (Fig. 3), the authors found that male respondents are not as afraid in the city centre as women (Fig. 2). Also parks and underpasses are localities in which men feel less frightened. On the other hand, women did not mark the above-mentioned socially excluded localities as unsafe very often (maybe because they rarely visit those localities—according to the questionnaires), whereas men visited them more often. Nevertheless, there were also comments about positive aspects of the city, stating that Olomouc is perceived as much safer than other cities of a comparable size in

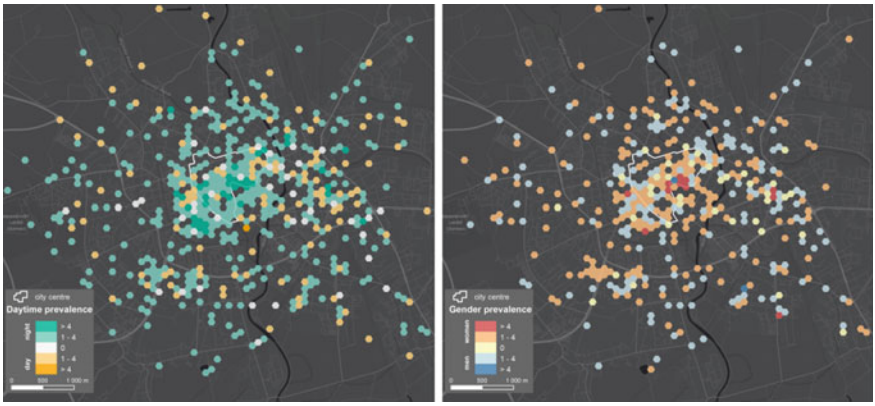

Fig. 3 Difference in safety perception in day-time and night-time (*left*), difference in safety perception by gender (*right*)

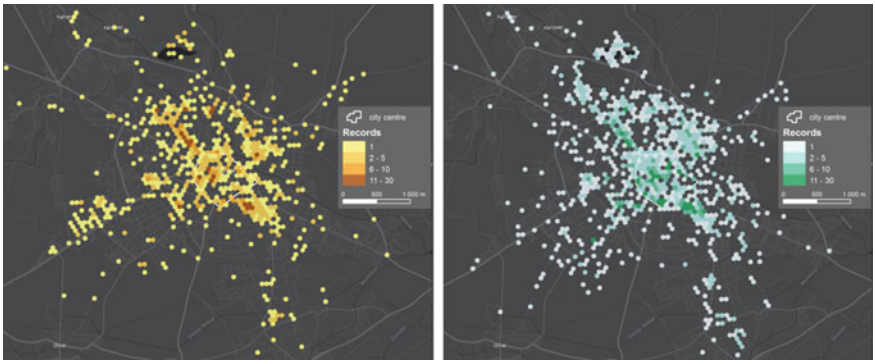

Fig. 4 Distribution of unsafe places in Opava by time of day (day on *left*, night on *right*)

Czechia. This fact is indirectly supported by the responses from Opava, which has half the population of Olomouc, but with a comparable amount of respondents there is almost double the amount of marked points.

Opava

As with Olomouc, respondents in Opava marked more places as unsafe during the night than during the day (Fig. 4), nevertheless the difference in the number of points is not as overwhelming as it was in the case of Olomouc. In Opava 1428 points and 2063 points were collected for day-time and night-time respectively. If compared (Fig. 6), several locations are marked as unsafe during the day as well as

Fig. 5 Distribution of unsafe places in Opava by gender (women on *left*, men on *right*)

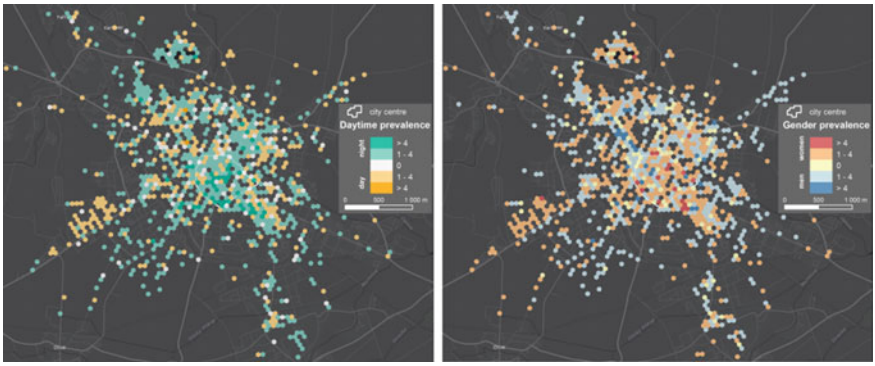

Fig. 6 Difference in safety perception in day-time and night-time (*left*), difference in safety perception by gender (*right*)

at night. These locations are mainly between the main train station (located southeast of the city centre) and the city centre. Furthermore, parks on the southern tip of the city centre are perceived as unsafe, mainly due to the groups of "homeless people" and "weird people", as often mentioned in comments attached to the marked points. Locations associated with the Roma minority in Opava are often perceived as unsafe in both time periods. Nevertheless, the intensity of personal unsafety is higher in these locations during the night. Other locations that are more often marked during the night are pedestrian underpasses and narrow dark streets in the city centre.

In the case study of Opava there were no significant differences (Fig. 6) among places perceived unsafe by men and women (Fig. 5), both of these groups often mentioned the area surrounding the main train station, including the building itself and street behind the train station towards the city parks. These streets were also associated with comments regarding such unsafe aspects as "homeless people",

Fig. 7 Distribution of unsafe places in Jihlava by time of day (day on *left*, night on *right*)

Fig. 8 Distribution of unsafe places in Jihlava by gender (women on *left*, men on *right*)

"drunk people" and "drug users". Other hot-spots perceived to be unsafe are the parks between the main train station and the city centre. Another hot-spot was the city centre itself, especially the two main squares. Excluded locations in the neighbourhood of Kateřinky, northeast from the centre or Rybářská street heading northwest from the centre were also hot spots.

Jihlava

From the spatial point of view, there are several localities which are significantly perceived by the residents of Jihlava as unsafe. The main square (Masarykovo náměstí), which lies in the central part of Jihlava, stands out as being a hot spot more than all the other localities. Other problematic localities are the housing estate called Horní Kosov in the northwestern periphery of the city and the area around the train station Jihlava-město, which lies north of the central part of the city.

The difference (Fig. 9) between a number of localities perceived as dangerous during the day and during the night is considerable (see Fig. 7). Respondents

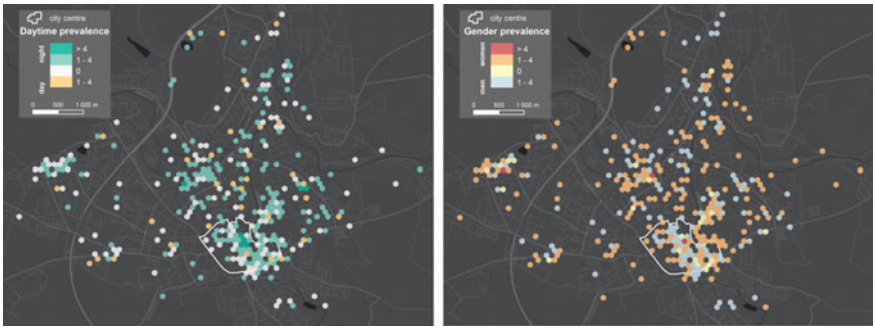

Fig. 9 Difference in safety perception in day-time and night-time (*left*), difference in safety perception by gender (*right*)

marked nearly twice as many localities for night-time than for day-time, which is in consensus with the two other cities. On the other hand, all localities showed up significantly during the night compared to the day.

If we focus on the gender factor (see Fig. 8), it is possible to observe a slightly differentiated perception of unsafety (Fig. 9). Besides the localities already mentioned as being commonly perceived as dangerous, women perceive relatively more fear in the park called Heulos (east of the main square). In comparison, men marked the area in front of the southern entrance to the shopping mall called City Park (south of the main square) fractionally more.

Discussion and Conclusions

Participatory mapping of safety perception has become popular in the last few years among various research groups across disciplines, varying from Computer and GIS Science (Gomez et al. 2016; Li et al. 2015; Melas et al. 2015; Traunmueller et al. 2015), criminology (Kounadi et al. 2015; Solymosi et al. 2015), neocartography and urban planning (Pődör et al. 2016; Salesses et al. 2013). Most authors agree that perceptions of safety are affected by whether it is night or day, whether people are in a built-up area or in the natural environment, and by previous experiences with the places and people occupying the places.

The presented study compared subjective safety perceptions, including both spatial information and commentaries in three Czech cities, and identified certain patterns in all three cities. Regardless of the time of day, the main train stations were considered as unsafe places in all three cities. Other negative locations common for all cities are city parks, excluded localities often inhabited by the Roma minority, and small, dark streets close to the city centres. Where there is a larger Roma minority living in a Czech city, the Roma minority neighbourhood is often

considered to be unsafe by the majority of the population (Government of the Czech Republic 2016; Pánek 2017).

The areas marked as unsafe within all three case-studies tended to be larger for females and at night-time. From the comments associated with the collected data, the most influential aspects that affected perceived safety were homeless people, drunk people, and drug addicts. Furthermore, some areas were considered unsafe due to a lack of street lighting or gloomy pedestrian underpasses.

Participatory mapping offers an easy-to-use and user-friendly tool, yet it is robust enough and provides outcomes (spatial data) familiar to city planners and local police representatives. A potential follow-up study could include real data about the crimes occurring in all three cities. The data would allow a comparison between perceived safety and the real level of criminality. Unfortunately, it is currently highly unlikely that the local police departments will share the data needed with the authors. If the data is acquired, quantitative and qualitative analyses could be performed and would shed light upon the reasons for the subjective perceptions.

Despite being unable to compare collected data with real datasets, the authors are confident that the conclusions drawn from the three case-studies may include some valuable insights for the growing field of safety perception research. For a future agenda, the authors plan to analyse the datasets in more detail by searching for inter-attribute relations (e.g. spatial correlations between gender, age, day-time, place of living, etc.), as well as relations with other socio-economic data (e.g. Points of Interest, official statistical data, demographic and economic data, etc.). In addition, the authors intend to apply rigorous spatial statistics, especially cluster analysis, in order to capture spatial relationships and patterns of the data.

Acknowledgement This paper is supported by the project no. 2016-1-CZ01-KA203-024040 Spatial exploration of economic data: methods of interdisciplinary analytics (Spationomy) funded by the European Union within the Erasmus+ programme.

References

Bannister, J., & Fyfe, N. (2001). Introduction: Fear and the city. *Urban Studies, 38*(5–6), 807–813.

Block, R. L., & Block, C. R. (1995). *Space, place and crime: Hot spots areas and hot places of liquor-related crime* [online]. Retrieved November 22, 2016, from http://www.popcenter.org/library/CrimePrevention/Volume_04/07-BlockBlock.pdf

Brantingham, P., & Brantingham, P. (1995). Criminality of place: Crime generators and crime attractors. *European Journal on Criminal Policy and Research, 3*(3), 1–26.

Brown, M., & Polk, K. (1996). Taking fear of crime seriously: The Tasmanian approach to community crime prevention. *Crime & Delinquency, 42*(3), 398–420.

Brownlow, A. (2005). A geography of men´s fear. *Geoforum, 36*(5), 581–592.

Burian, J., Pászto, V., & Langrová, B. (2014). Possibilities of the definition of city boundaries in GIS—The case study of a medium-sized city. In *14th SGEM GeoConference on Informatics, Geoinformatics and Remote Sensing* (Vol. 3, pp. 777–784). doi:10.5593/SGEM2014/B23/S11.099

Clemente, F., & Kleiman, M. B. (1977). Fear of crime in the United States: A multivariate analysis. *Social Forces, 56*(2), 519–531.

Curtis, J. W. (2012). Integrating sketch maps with GIS to explore fear of crime in the Urban Environment: A review of the past and prospects for the future. *Cartography and Geographic Information Science, 39*(4), 175–186.

Czech Statistical Office. (2016). Population of municipalities in the Czech Republic, 1 January 2016 [online]. Retrieved December 1, 2016, from https://www.czso.cz/documents/10180/32853387/1300721603.pdf/cba78096-1cf5-4fde-b20a-3074b2f135f9?version=1.0

Doran, B. J., & Burgess, M. B. (2012). *Putting fear of crime on the map: Investigating perceptions of crime using geographic information systems*. Berlin: Springer Science & Business Media.

Gomez, F., Torres, A., Galvis, J., Camargo, J., & Martinez, O. (2016). Hotspot mapping for perception of security. In *IEEE 2nd International Smart Cities Conference: Improving the Citizens Quality of Life, ISC2 2016 - Proceedings* (pp. 1–6). IEEE. doi:10.1109/ISC2.2016.7580815

Government of the Czech Republic. (2016). Report about the Roma minority in the Czech Republic in 2015. Retrieved from http://www.vlada.cz/cz/ppov/zalezitosti-romske-komunity/dokumenty/zprava-o-stavu-romske-mensiny-za-rok-2015-146576/

Hýža, M. (2016). Kriminalita v Olomouci a její vnímání obyvatelstvem města: připadove studie městských časti Olomouc-město, Hodolany, Novy Svět. Diploma thesis. Palacký University Olomouc – Faculty of Science. Supervisor: Petr ŠIMÁČEK.

Jackson, J. (2006). Introducing fear of crime to risk research. *Risk Analysis, 26*(1), 253–264 [online]. Retrieved November 22, 2016, from http://eprints.lse.ac.uk/archive/00000805

Jíchová, J. (2013). Kriminalita a její percepce v městském prostředí. Dissertation thesis. Charles University, Faculty of Science. Supervisor: Jana TEMELOVÁ.

Jíchová, J., & Temelová, J. (2012). Kriminalita a její percepce ve vnitřním městě: případová studie pražského Žižkova a Jarova. *Geografie, 3*(117), 329–348.

Koskela, H. (1999). Gendered exclusions: Women's fear of violence and changing relations to space. *Geografiska Annaler, 81B*(2), 111–124.

Koskela, H., & Pain, R. (2000). Revisiting fear and place: Women's fear of attack and the built environment. *Geoforum, 31*(2), 269–280.

Kosová, D. (2016). Lokality strachu z kriminality na území města Jihlavy. Diploma thesis. Palacký University Olomouc, Faculty of Science. Supervisor: Petr Šimáček.

Kounadi, O., Bowers, K., & Leitner, M. (2015). Crime mapping on-line: Public perception of privacy issues. *European Journal on Criminal Policy and Research, 21*(1), 167–190. doi:10.1007/s10610-014-9248-4

Li, X., Zhang, C., & Li, W. (2015). Does the visibility of greenery increase perceived safety in urban areas? Evidence from the place pulse 1.0 dataset. *ISPRS International Journal of Geo-Information*, *4*(3), 1166–1183. doi:10.3390/ijgi4031166

Maslow, A. H. (1943). A theory of human motivation. *Psychological Review*, *50*, 370–396 [online]. Retrieved November 19, 2016, from http://psychclassics.yorku.ca/Maslow/motivation.htm

Matthews, R. (1992). Replacing „Broken Windows": Crime, incivilities and urban change [online]. Retrieved November 22, 2016, from http://rogermatthews.net/images/papers/replacing_broken_windows.pdf

Melas, P., Correndo, G., Middleton, L., & Sabeur, Z. A. (2015). Advanced data analytics and visualisation for the management of human perception of safety and security in urban spaces. In *Environmental software systems. Infrastructures, services and applications* (pp. 445–454). Berlin: Springer International Publishing. doi:10.1007/978-3-319-15994-2_45

Newman, O. (1972). *Defensible space: Crime prevention through urban design*. New York: Macmillan.

Oc, T., & Tiesdell, S. (1997). *Safer city centres: Reviving the public realm*. London: SAGE.

Pain, R. (2001). Gender, race, age and fear in the city. *Urban Studies, 38*(5–6), 899–913.

Pánek, J. (2017). Emotional and subjective volunteered geographical information. In C. Campelo, M. Bertolotto, & P. Corcoran (Eds.), *Volunteered geographic information and the future of geospatial data, pp. 97–112*. IGI Global.

Pánek, J., & Benediktsson, K. (2017). Emotional mapping and its participatory potential: Opinions about cycling conditions in Reykjavík. *Iceland. Cities, 61*(1), 65–73. doi:10.1016/j.cities.2016.11.005

Pánek, J., Mařincová, L., Putalová, L., Hájek, J., & Marek, L. (2017). Crowdsourcing of environmental health quality perceptions: A pilot study of Kroměříž, Czech Republic. In M. Leitner & J. J. Arsanjani (Eds.), *Citizen empowered mapping* (Geotechnologies and the environment 18, pp. 261–280). Berlin: Springer. doi:10.1007/978-3-319-51629-5_12

Pánek, J., & Pászto, V. (2017). Emotional mapping in local neighbourhood planning: Case Study of Příbram, Czech Republic. *International Journal of E-Planning Research, 6*(1), 1–22. doi:10.4018/IJEPR.2017010101

Pánek, J., Pászto, V., & Marek, L. (2017). Mapping emotions: spatial distribution of safety perception in the city of Olomouc. In I. Ivan, A. Singleton, J. Horák, & T. Inspektor (Eds.), *Lecture notes in geoinformation and cartography: The rise of big spatial data* (pp. 211–224). Ostrava, Czech Republic: Springer International Publishing. doi:10.1007/978-3-319-45123-7

Perkins, D., D., & Taylor, R., B. (1996). Ecological assessments of community disorder: Their relationship to fear of crime and theoretical implications. *American Journal of Community Psychology, 24*(1), 63–107.

Pődör, A., Révész, A., Rácskai, P., & Sasvár, Z. (2016). Measuring citizens fear of crime of using a web application—A case study. *GI_Forum*, *2*, 123–133. doi:10.1553/giscience2016_02_s123

Salesses, P., Schechtner, K., & Hidalgo, C. A. (2013). The collaborative image of the city: Mapping the inequality of urban perception. *PLoS ONE, 8*(7), e68400. doi:10.1371/journal.pone.0068400

Samuels, R., & Judd, B. (2002). Public housing estate renewal—Interventions and the epidemiology of victimisation [online]. Retrieved November 22, 2016, from http://www.aic.gov.au/media_library/conferences/housing/samuels.pdf

Schmeidler, K. (2000). Prostředí města, urbanistická tvorba a sociální patologie. *Kriminalistika, 33* (4), 316–325.

Sherman, L. W. (1995). Hot spots of crime and criminal careers of places [online]. Retrieved November 22, 2016, from http://www.popcenter.org/library/crimeprevention/volume_04/02-Sherman.pdf

Smith, S. J. (1987). Fear of crime: Beyond a geography of deviance. *Progress in Human Geography, 11*(1), 1–23.

Smith, W. R., & Torstensson, M. (1997). Gender differences in risk perception and neutralizing fear of crime. *The British Journal of Criminology, 37*(4), 608–634.

Solymosi, R., Bowers, K., & Fujiyama, T. (2015). Mapping fear of crime as a context-dependent everyday experience that varies in space and time. *Legal and Criminological Psychology, 20* (2), 193–211. doi:10.1111/lcrp.12076

Stasíková, L. (2011). Relevantnost výskumu strachu z kriminality v urbánnej geografii. *Geografický Časopis, 63*(4), 325–343.

Stasíková, L. (2013). Genius loci vo vzťahu k strachu zo zločinnosti na príkladě postsocialistického sídliska. *Geografický časopis, 65*(1), 83–101.

Tonkiss, F. (2005). *Space, the city and social theory*. Cambridge: Polity Press.

Traunmueller, M., Marshall, P., & Capra, L. (2015). Crowdsourcing safety perceptions of people: opportunities and limitations. In T.-Y. Liu, C. N. Scollon, & W. Zhu (Eds.), *Social informatics* (Lecture No., pp. 120–135). Berlin: Springer International Publishing. doi:10.1007/978-3-319-27433-1_9

Valentine, G. (1989). The geography of woman's fear. *Area, 21*(4), 385–390.

Valentine, G. (2001). *Social geographies: Space & society*. Harlow: Pearson Education.

Worpole, K. (1992). *Towns for people: Tranforming Urban Life*. Buckingham: Open University Press.

Wynne, T. (2008). An investigation into the fear of crime: Is there a Link between the fear of crime and the likelihood of victimisation? *Internet Journal of Criminology* [online]. Retrieved November 19, 2016, from http://www.internetjournalofcriminology.com/wynne%20-%20fear%20of%20crime.pdf

Zítková, V. (2013). Kriminalita a místa strachu: časoprostorový pohled na příkladě velkého města. Diploma thesis. Palacký University Olomouc, Faculty of Science. Supervisor: Vladimír IRA.

Prediction of Land-Use Development Under Influence of Climate Change

Vilém Pechanec, Alexander Mráz, Antonín Benc, Karel Macků and Pavel Cudlín

Abstract Land-use change is considered one of the most critical processes when attempting to understand and model the global change. Land-use change has an interdependent relationship with the climate change. Climate change in the Czech Republic incurs a substantial pressure on human society and natural ecosystems through the increase of temperature and higher occurrence of droughts and floods. The principal purpose of the study was to model and assess the future land-use distribution in the Czech Republic based on historical land-use data and climate change information. For assessment of future ecosystem services, the current rate of ecosystem service fulfillment is set and compared in time and space with modeled situations. TerrSet's Land Change Modeller was used to create land-use projection models based on principles of historical trends and business as usual projection scenario. The land-use prediction was performed for the entire Czech Republic using HadGEM2-ES climate model with RCP 4.5 and RCP 8.5 emission scenarios. The output of the modeling was a set of raster maps which presented the future land coverage for each category and location. A spatio-temporal analysis was then performed to determine the difference in representation of each land cover category for a period 2012–2050. The results show that most severe change in the land cover appears in loss of agricultural sites mainly caused by increase in urban areas and

V. Pechanec (✉) · A. Mráz · A. Benc · K. Macků
Department of Geoinformatics, Faculty of Science, Palacký University in Olomouc, 17. listopadu 50, 77146 Olomouc, Czech Republic
e-mail: vilem.pechanec@upol.cz

A. Mráz
e-mail: alexander.mraz@upol.cz

A. Benc
e-mail: antonin.benc01@upol.cz

K. Macků
e-mail: karel.macku01@upol.cz

P. Cudlín
Centre for Research of Global Change at Academy of Sciences of the Czech Republic, Lipová 9, 37005 České Budějovice, Czech Republic
e-mail: cudlinp@czechglobe.cz

I. Ivan et al. (eds.), *Dynamics in GIscience*, Lecture Notes in Geoinformation and Cartography, DOI 10.1007/978-3-319-61297-3_25

forests. Planners and policymakers can use the results of this study to incorporate adaptation measures including the change of land use to more natural habitats and implementation of more ecological management to mitigate the adverse effect of urbanization and climate change. The contribution of the study is in presenting selected tools for modeling expected future land use and development of maps displaying future spatial distribution and quantification of land use categories for the Czech Republic.

Keywords Land use development · Climate change · CORINE land cover · Land change modeler

Introduction

Land-use change is considered one of the most critical processes when attempting to understand and model the global change. It is a result of complex interactions between human and environmental driving factors (Schaldach & Priess 2008) and it may impact soil, water, and atmosphere. Changes in land use may affect the climate while climate change will also influence opportunities for future land use (Dale 1997). Last decades of research have revealed the environmental impact of land use and land cover change on the release of carbon dioxide from the biosphere (Achard et al. 2004), decrease of biological diversity (Sala et al. 2000), change in atmospheric composition, and extensive modification of Earth's ecosystems (Foley et al. 2005). The research was also conducted to report the effect of land-use processes on human society (Lambin and Geist 2006). Planners and policymakers worldwide seek to understand land-use change due to long-term modification in climatic conditions and to direct land-use developments through a wide range of intervention and management strategies that would mitigate the adverse effect of climate change. To accomplish these tasks, they regularly employ models that simulate possible spatial land-use developments.

Modeling and analysis of the land cover changes would not be possible without a significant increase in quality of remote sensing data which are one of the most common data sources used in GIS (Zwoliński 2012). Description of land cover evolution can be obtained from a historical series of CORINE Land Cover (CLC) data. The CLC is a European program which was initiated in 1985 with updates produced in 2000, 2006, and 2012. For the recent CLC 2012 mapping campaign, there were 39 participating countries, including 32 European Environment Agency member states and seven collaborating countries (Büttner et al. 2012). The resulting computerized inventory consists of a land cover of the European Union member states and other European countries using 44 classes that are grouped into five main (level-one) categories including (1) artificial surfaces, (2) agricultural areas, (3) forests and semi-natural areas, (4) wetlands, and (5) water bodies (Heymann et al. 1994). The CLC uses a Minimum Mapping Unit (MMU) of 25 ha and a minimum width of 100 m for areal and linear phenomena, respectively.

The time series are complemented by change layers, which highlight changes in land cover with an MMU of 5 ha (EEA 2007).

In the Czech Republic, there is an apparent trend of gradual rise in average annual temperature amounting to approximately 0.3 °C over ten years regardless of considerable year-to-year fluctuations. The records of extreme weather conditions also show an increase in the number of days with high temperatures and reduction in the number of days with low temperature. The number of summer days during the year increased on average by 12 days, hot days by 6, and the number of freezing days dropped by 6. However, no clear trends have been observed in precipitation development and during last two decades, there has been an indistinctive rise in annual precipitation amount (Czech Republic 2013). Climatic change in the Czech Republic incurs a substantial pressure on human society and natural ecosystems through the increase of temperature and higher occurrence of droughts and floods. Since the ecosystems provide people with vital ecosystem services, such as food provision, water resource, climate regulation, it is important to assess the potential vulnerability of the ecosystem services in the Czech Republic.

Related Work

The primary drivers of land-use changes are climate change, human population, affluence, technology, political economics, political structure, attitudes, and values (Turner et al. 1993). Understanding how the current land cover will respond to transient patterns of global temperature, precipitation, or solar radiation requires reliance on computer models that can deal with some of the complexities of vegetation and climate systems (Dale 1997). Dale and Rauscher (1994) reviewed 14 categories of climate-change models and found that only three types considered the land-use change. They included global, regional, and landscape-transition models. Michetti (2012) presents a classification of models used for modeling the land use, land-use change, and forestry. The article also recognized that only small portion of presented models could correctly capture long-term nature of some land-use processes. Briassoulis (2000) offers an extensive discussion of the most commonly used land-use change models and their theoretical backgrounds. The models are divided into five main categories including statistical and econometric models, spatial interaction models, optimization models, integrated models, and models for which classification is not straightforward as they reflect a variety of modeling traditions. Koomen et al. (2007) provide a cross-sectional overview of current progress on the analysis of land-use change processes, the exploration of new methods and theories, and the application of land-use simulation models. In this book, modeling methods are divided based on seven theoretical and methodological backgrounds including economic principles, spatial interactions, cellular automata, statistical analysis, optimization, rule-based simulations, multi-agent models, and microsimulations.

Lawler et al. (2014) studied land-use change using an econometric model to predict spatially specific changes in land use across the continuous United States

from 2001 to 2051. The model estimated the probability of conversion among major land-use categories based on observations of past land-use change, land parcels characteristics, and economic return. The developed model showed rapid urban growth and loss of rangelands and pastures. The results demonstrated that the adoption of specific policies could influence land-use change and increase expected provision of some ecosystem services but at the expense of others. Gardner et al. (1994) developed a cellular automata model that explored the spatial distribution of two competing species with a severe perturbation in the abundance of the species, such as the one that might be caused by a severe drought. Huang et al. (2015) used Markov-based cellular automata model for simulating and forecasting urban land change in Wuhan City, China, using satellite images captured between 1999 and 2005. The change in land use and land cover in Hermanshah City, Iran, was accomplished by utilizing Markov Chain model, Landsat satellite images, and site information (Razavi 2014). Mishra et al. (2014) have employed IDRISI Land Change Modeller and Landsat satellite images to update the prediction and forecast map for years 2025 and 2035. Korateng et al. (2015) have utilized Cellular Automata and Markov Chain (Cellular Automata-Markov) to predict a land-use cover change for 2020 and 2030 for forest modeling of Ashanti Region, Ghana.

Objective

The objective of the presented study is to model future land-use distribution in the Czech Republic based on historical land-use data and climate change information. A secondary goal was to assess the change in land cover under the influence of the climate change.

Applied Methodology and Implementation

Historical land cover data describing the evolution of land cover in the Czech Republic comes from CORINE Land Cover (CLC) database inventory mapped in 1990, 2000, 2006, and 2012. Evolution of CORINE Land Cover is shown in Table 1. The CLC data were provided by Česká informační agentura životního prostředí (CENIA) in a vector format (polygons) at scale 1:100000 and supplemented with topography information including road and rail networks. The source of topographical data is Data200 geodatabase which represents a digital geographic model of the Czech Republic with accuracy and degree of generalization to map scale of 1:200,000 (ČÚZK 2016). The updated CLC vector layers were transformed to ETRS-89-LAEA coordinate system (INSPIRE 2010) and then converted to raster format with a cell size of 500 × 500 m using dominant share rule. Dominant share rule assigns a pixel value of the feature that occupies the largest proportion of that pixel (Liu et al. 2016).

Table 1 CORINE land cover evolution (Büttner 2012 and EEA 2007)

	CLC1990	CLC2000	CLC2006	CLC2012
Satellite data	Landsat-5 MSS/TM	Landsat-7 ETM	SPOT-4/5 and IRS P6 LISS III	IRS P6 LISS III and RapidEye
Time consistency	1986-1998	2000 ± 1 year	2006 ± 1 year	2011–2012
Geometric accuracy, satellite data (m)	≤ 50	≤ 25	≤ 25	≤ 25
Min. mapping unit/width	25 ha/100 m	25 ha/100 m	25 ha/100 m	25 ha/100 m
Geometric accuracy, CLC	100 m	better than 100 m	better than 100 m	better than 100 m
Thematic accuracy, CLC	≥ 85% (probably not achieved)	≥ 85% (achieved)	≥ 85% (not checked)	≥ 85%
Change mapping (CLCC)	Not implemented	Boundary displacement min. 100 m; change area for existing polygons ≥ 5 ha; for isolated changes ≥ 25 ha	Boundary displacement min. 100 m; all changes ≥ 5 ha are to be mapped	Boundary displacement min. 100 m; all changes ≥ 5 ha are to be mapped
Production time (years)	10	4	3	2
Documentation	Incomplete metadata	Standard metadata	Standard metadata	Standard metadata

TerrSet's Land Change Modeller (LCM) software was selected by authors for its ability to analyze land cover change, empirically model relationship between land cover and its explanatory variables, and project future changes. In particular, it provided tools to perform spatio-temporal analysis of spatial CLC data to determine the difference in representation of each land cover category and subsequent evaluation of trends in land coverage for each category and location for the period 2012–2050. First, LCM was used to assess dominant land use changes between time 1 (T1) and time 2 (T2) of two CLC maps (Fig. 1). The land-use changes identified between the two maps represent transitions from one land cover state to another and are used to evaluate losses and gains for each land-use class (Eastman 2016). Then, transition potential model was created using multi-layer perceptron (MLP) neural network based on a set of explanatory variables, also called drivers. The model combined eight drivers and one barrier for selected periods. The drivers used in the development of the model included altitude, slope, distance to the urban area, distance to water streams, distance to roads, population density, average daily temperature and average daily precipitation sum. The last two drivers were the only features that changed with time and were calculated using HadGEM2_ES climate

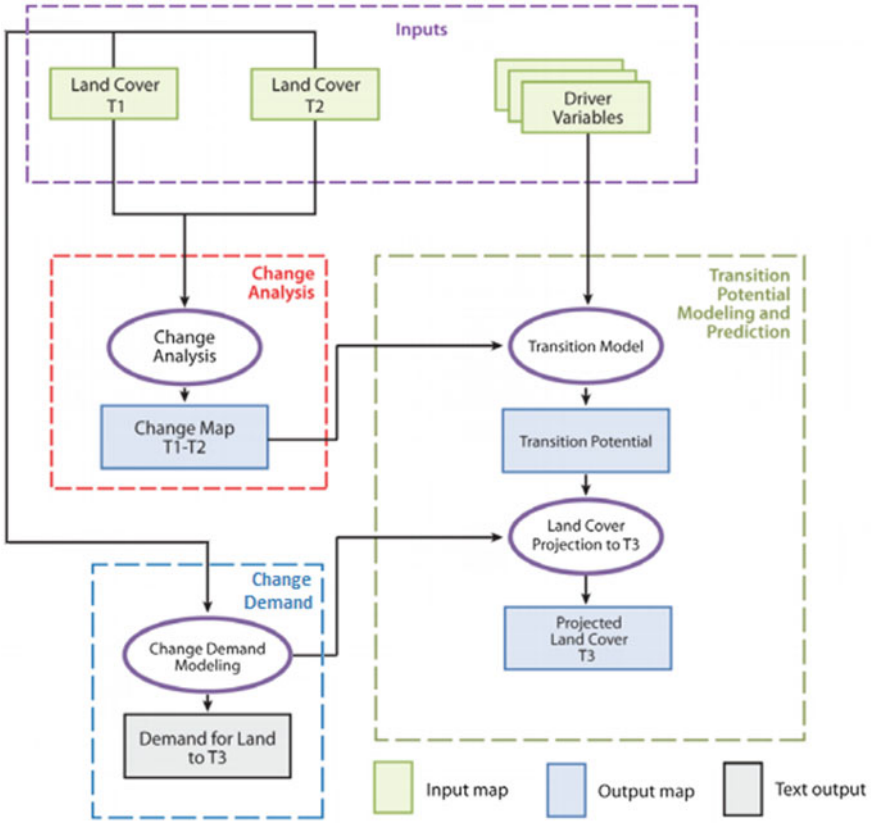

Fig. 1 Simplified flowchart for methodology used in this study

model (Collins et al. 2011) with Representative Concentration Pathway (RCP) 4.5 and RCP 8.5 emission scenarios (Meinshausen et al. 2011). RPCs are greenhouse gas concentration trajectories that describe possible climate futures, all of which are considered possible depending on how much greenhouse gases are emitted in the years to come (Weyant 2009). The climate models were developed as a part of the CzechAdapt project (CzechAdapt 2016). The other six drivers were set constant. The model also considered one barrier which defines the presence of large specially protected areas such as national parks and protected landscapes. The transition potential model was based on a given climatic model and emission scenario and interpolated for each land cover category. It expressed time-specific potential for land cover change. In the final step, a future scenario for a detailed data was predicted using the historical rates of change and the transition potential model (Eastman 2016). The simplified flowchart of used methodology is presented in Fig. 1. Model outputs and displays a spatial distribution and quantification of particular forms of land-use change that is result of prediction relations.

Results and Discussion

The output of the prediction analysis is a set of raster maps showing the future distribution of individual land cover categories in the Czech Republic based on predictive relationships derived from differences in the representation of land cover categories since 1990. The output from climate model HadGEM2-ES using two emission scenarios (RCP 4.5 and RCP 8.5) represents expected scenarios and their impact on landscape development in period 2012–2050. When interpreting the results, it is necessary to take into account the fact that the land cover development is a result of many factors, so the final maps do not reflect only dependence on climatic factors but also on other six drivers that have been included in the model. In scenarios where the response to climatic factors was small, the influence of other drivers, such as the proximity to the urban area, has prevailed. The output maps represent landscape segments at a resolution of 500 × 500 m and, therefore, some generalization of smaller segments has occurred. The sample outputs for Olomouc Region with 28 CLC classes grouped into five main land-use categories are presented in Fig. 2.

The developed models present a change in spatial distribution of all individual land cover classes in the predicted future. The total land cover area which changed its classification when compared to CLC 2012 inventory for two different

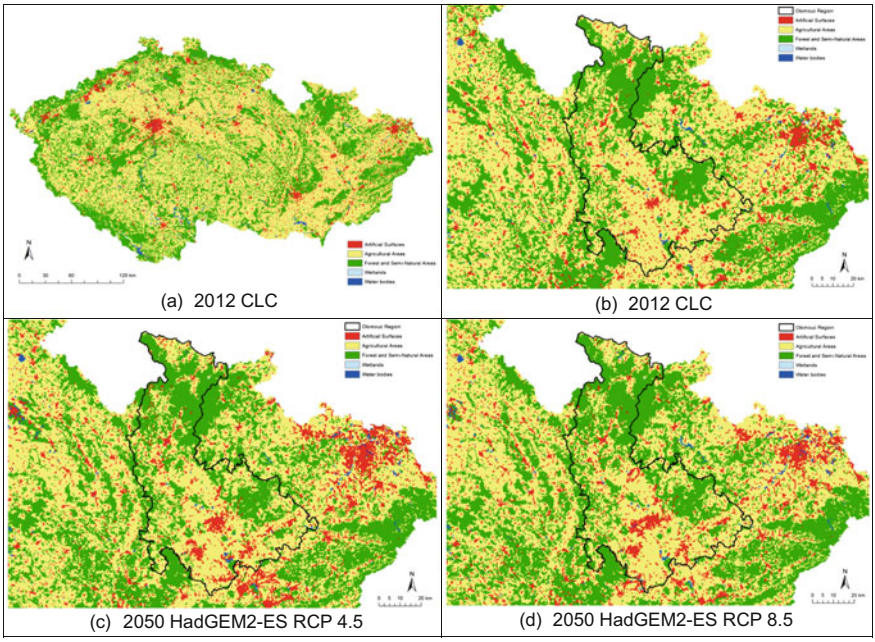

Fig. 2 Sample outputs of land-use change between 2012 and 2050 for Olomouc region. **a** 2012 CLC, **b** 2012 CLC, **c** 2050 HadGEM2-ES RCP 4.5, **d** 2050 HadGEM2-ES RCP 8.5

HadGEM2-ES emission scenarios is presented in Table 2. The results show that the 17.4 and 17.2% of the area changed its classification based on RPC 4.5 and RPC 8.5 emission scenarios, respectively. The 28 CLC classes were also grouped into five main land-use categories based on CORINE Land Cover Nomenclature for Level 1 classification (Copernicus Land Monitoring Service, 2010). The relative extent of each main land-use category for CLC 2012 and RPC 4.5 and RPC 8.5 emission scenarios is presented in Fig. 3. Based on the data presented in Fig. 3, the substantial change in the land cover appears in 2.5% loss of agricultural areas with approximately 1.0% going to the forests and 1.5% going to the urban areas. The increase in forest areas is due to last decade of reforestation efforts supported by the Czech government. The results also demonstrate that predicting the effect of climate change on local environmental conditions will be critical, especially for agricultural and forestry land. Both emission scenarios show a significant loss, close to 2000 km^2, in agricultural areas and relatively large gain in artificial surfaces. The models also show some increase in forest and semi-natural areas. The results indicate that both emission scenarios gave fairly similar results when data grouped in five main land-use (Level 1) CLC categories. By analyzing the results, important adaptation measures were devised and included the land-use change to more natural habitats and more ecological management of agricultural and forest soils. Also, mitigating solutions including restoration of near-natural tree species composition, restoration of natural water reservoirs in the form of natural wetlands in the upper catchment area, and reinstatement of natural functions of floodplains along the rivers were identified to significantly help with climate change adaptation.

Table 2 Difference in the area of territory for which the land-use class has changed for two emission scenarios

	Difference from 2012 to 2050	
HadGEM2-ES model	Area	
Emission scenarios	(km^2)	(%)
RCP 4.5	13,713	17.4
RCP 8.5	13,573	17.2

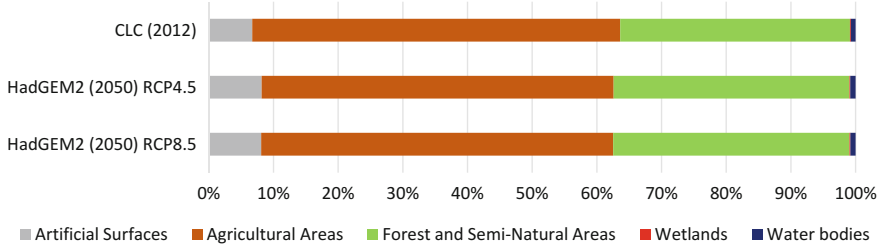

Fig. 3 Extent of CLC main land-use categories in Czech Republic (relative values in %)

Conclusions

Climate change in the Czech Republic incurs a substantial pressure on human society and natural ecosystems through the increase of temperature and higher occurrence of extreme weather conditions including droughts and floods. The increasing vulnerability of ecosystem services can, therefore, affect the future well-being of Czech residents. The land cover model was developed based on historical land-use data provided by CORINE Land Cover inventory geodatabase and climate change information to assess the future land-use distribution. The output maps show the distribution of various categories of land cover in the Czech Republic based on the predictive modeling derived from differences in the representation of land cover categories since 1990. The results of the prediction using HadGEM2-ES show that about 17.2% of the land cover area changed its classification when compared to CLC 2012 inventory. Results also suggest that the most severe and substantial change in the land cover appears to be a loss of agricultural land mainly due to increase in urban areas and forests. By analyzing the land-use prediction models, important adaptation measures to mitigate the effect of climate change were devised and included the land-use change to more natural habitats and more ecological management of agricultural and forest soils. The results of this work may also contribute to the planned sustainable development strategy "Strategy Czech Republic 2030" (Lánský et al. 2016).

References

Achard, F., Eva, H. D., Mayaux, P., Stibig, H.-J., & Belward, A. (2004). Improved estimates of net carbon emissions from land cover change in the tropics for the 1990s, *Global Biogeochemical Cycles, 18*, GB2008.

Briassoulis, H. (2000). Analysis of land use change: Theoretical and modeling approaches. *The Web Book of Regional Science* (http://www.rri.wvu.edu/webbook/briassoulis/contents.htm). Regional Research Institute, West Virginia University, USA, November 23, 2016.

Büttner, G., & Kosztra, B. (2012) CLC2012 addendum to CLC2006 technical guidelines—Final draft. Spain: European Topic Centre for Spatial information and Analysis.

Collins, W. J., et al. (2011). *Development and evaluation of an earth-system model—HadGEM2. Geoscientific model development* (Vol. 4, pp. 1051–1075). Göttingen: Copernicus Publications.

Copernicus Land Monitoring Service. (2010). CORINE land cover nomenclature conversion to land cover classification system. http://land.copernicus.eu/eagle/files/eagle-related-projects/pt_clc-conversion-to-fao-lccs3_dec2010, November 23, 2017.

CzechAdapt. (2016). CzechAdapt – Systém pro výměnu informací o dopadech změny klimatu, zranitelnosti a adaptačních opatřeních na území ČR (EHP-CZ02-OV-1-014-2014). http://www.klimatickazmena.cz/cs/o-nas/o-projektu/. November 29, 2016.

Czech Republic. (2013). Sixth National Communication of the Czech Republic Under the United Nations Framework Convention on Climate Change Including Supplementary Information Pursuant to Article 7.2 of the Kyoto Protocol. Ministry of the Environment, Prague.

ČÚZK. (2016). Data200: Introduction. http://geoportal.cuzk.cz/(S(hxpxxtfgkrbqyim1b2zrx5or))/Default.aspx?menu=229&mode=TextMeta&side=mapy_data200&text=dSady_mapyData200&. November, 2, 2016.

INSPIRE. (2010). D2.8.1.2 INSPIRE Specification on geographical grid systems—Guidelines. Italy: European Commission Joint Research Centre, Institute for Environment and Sustainability.

Dale, V. H., & Rauscher, H. M. (1994). Assessing impacts of climate change on forests: The state of biological modeling. *Climatic Change, 28,* 65–90.

Dale, V. H. (1997). The relationship between land-use change and climate change. *Ecological Applications, 7*(3), 753–769.

Eastman, R. (2016). *TerrSet manual*. Worcester, MA, USA: Clark University.

EEA Technical Report No. 17. (2007). CLC2006 technical guidelines. Luxembourg: European Environment Agency.

Foley, J., et al. (2005). Global consequences of land use. *Science, 309*(5734), 570–574.

Gardner, R. H., King, A. W., & Dale, V. H. (1994). *Interactions between forest harvesting, landscape heterogeneity, and species persistence. Modelling sustainable forest ecosystems* (pp. 65–75). Lafayette, Indiana, USA: Purdue University Press.

Huang, J., Wu, Y., Gao, T., Zhan, Y., & Cui, W. (2015). An integrated approach based on Markov Chain and cellular automata to simulation of urban land use changes. *Applied Mathematics and Information Sciences, 9*(2), 769–775.

Heymann, Y., Steenmans, Ch., Croissille, G., & Bossard, M. (1994). Corine land cover. Technical Guide. EUR12585 Luxembourg, Office for Official Publications of the European Communities.

Koomen, E., Stillwell, J., Bakema, A., & Scholten, H. J. (2007). Modelling land-use change; progress and applications. *Geojournal Library, 90*.

Korateng, A., & Zawilla-Niedzwiecki, T. (2015). Modelling forest loss and other land use change dynamics in Ashanti Region of Ghana. *Folia FOrestalia Polonica, Series A, 57*(2), 96–111.

Lambin, E. F., & Geist, H. (Eds.). (2006). *Land-use and land-cover change: Local processes, global impacts, global change—The IGBP series*. Berlin: Springer.

Lánský, O., Mottlová, M., Švihlíková, I., Tkáč, P., Vojtíšková, K., Vondrouš, D., et al. (2016). Czech Republic—Implementing the 2030 agenda on sustainable development. Spotlight on Sustainable Development 2016. New York, USA: Global Policy Forum.

Lawler, J. J., Lewis, D. J., Nelson, E., Plantinga, A. J., Polasky, S., Withey, J. C., et al. (2014). Projected land-use change impacts on eservices in the United States. *Proceedings of the National Academy of Sciences of the United States of America, 111*(20), 7492–7497.

Liu, J., & Mason, P. (2016). Techniques and applications. In J. G. Liu & P. J. Mason (Eds.), *Image processing and gis for remote sensing: Techniques and applications* (2nd Ed.). West Sussex, UK: Wiley-Blackwell.

Meinshausen, M. (2011). The RPC greenhouse gas concentrations and their extension from 1765 to 2500. *Climate Change, 109* (Special Issue), 213–241.

Michetti, M. (2012). Modelling land use, land-use change, and forestry in climate change: A review of major approaches. CMCC Research Paper, Issue RP0133, pp. 1–53.

Mishra, V. N., Rai, P. K., & Mohan, K. (2014). Prediction of land use changes based on land change modeller (LCM) using remote sensing: A case study of Muzaffarpur (Bihar), India. *Journal of the Geographical Institute Jovan Cvijic, SASA, 64*(1), 111–127.

Razavi, B. S. (2014). Predicting the trend of land use changes using artificial neural network and Markov Chain Model (Case Study: Kermanshah City). *Research Journal of Environmental and Earth Sciences, 6*(4), 215–226.

Sala, O. E., et al. (2000). Global biodiversity scenarios for the year 2100. *Science, 287*(5499), 1770–1774.

Schaldach, R., & Priess, J. A. (2008). Integrated models of the land system: A review of modelling approaches on the regional to global scale. *Living Reviews in Landscape Research, 2,* 1–34.

Turner, B. L., Moss, R. H., & Skole, D. L. (1993). Relating land use and global land-cover change: A proposal for an IGBP-HDP core project. HDP Report Number 5. Stockholm, Sweden: International Geosphere-Biosphere Programme.

Weyant, J., Azar, Ch., Kainuma, M., Kejun, J., Nakicenovic, N., Shukla, P. R., et al. (2009). Report of 2.6 Versus 2.9 Watts/m2 RCPP Evaluation Panel (PDF). Geneva, Switzerland: IPCC Secretariat.

Zwoliński, Z. (Ed.). (2012). *GIS—Teledetekcja Środowiska (GIS—Remote sensing of the environment)*. Naukowe, Poznań: Bogucki Wyd.

Methods of Using Self-organising Maps for Terrain Classification, Using an Example of Developing a Military Passability Map

Krzysztof Pokonieczny

Abstract The classification of terrain by its passability plays a significant role in the process of Intelligence Preparation of the Battlefield (IPB). In the process of developing passability maps, the classification of terrain to a specific class (GO, SLOW-GO, NO-GO). In this paper the problem of terrain classification to the respective category of passability was solved by the application of Self Organizing Maps by generating a continuous Index of Passability (IOP), which characterizes the terrain in a range from 0 (the impassable area) to 1 (the area of high manoeuvrability). The article describes the methodology of using this type of network to develop a terrain passability map. As a "case of use", three voivodeships located in the north-eastern part of Poland were selected. To prepare a training set, topographic vector data from VMap L2 and SRTM (Shuttle Radar Topography Mission) digital terrain model were used. Research was conducted on a primary grid field with dimensions 1 km × 1 km. As a result of the research conducted, normalised parameters associated with terrain cover were introduce into the neural network. As a result of the network learning, the analysed area was divided into classes, to which the index of passability (IOP) was arbitrarily subordinated. In the research results, the influence of the method of organisation of the input data on the generated maps of passability was defined. The tests were conducted on two sizes of a Kohonen map: 10 × 10 and 5 × 5 neurons. The described experiments proved that a properly taught artificial neural network is very well suited to the analysis of an area in terms of passability. The presented methodology is universal in nature and after the modification of parameters may be used to solve tasks of terrain classification associated with various subjects (division of soils, marking out areas for development, etc.).

Keywords Self organizing maps · Terrain classification · Index of passability · Geocomputation

K. Pokonieczny (✉)
Faculty of Civil Engineering and Geodesy,
Military University of Technology, Warsaw, Poland
e-mail: krzysztof.pokonieczny@wat.edu.pl

I. Ivan et al. (eds.), *Dynamics in GIscience*, Lecture Notes in Geoinformation and Cartography, DOI 10.1007/978-3-319-61297-3_26

Introduction

The essence of terrain classification is the search for and identification within the area of research of some characteristic fragments (patterns, also known as formations), which have similar characteristics. Issues associated with this have been discussed in many articles. In the paper by Han et al. (2016), the authors made an attempt to select mountain ridges, which should be protected. The selection was made on the basis of a specially constructed terrain model, by way of parameterisation and handling of many terrain factors. In an article by Irvin et al. (1997), image data was used in the process of classification, grouped with the use of continuous classification (fuzzy set) methods and unsupervised (ISODATA) classification techniques. Another method used in the classification of terrain is a cluster analysis. As an example, the method of k-means could be mentioned, which was described in the paper by Bielecka et al. (2014). The authors created a classification of geodetic districts in terms of the elements of land cover and the number of geodetic control points. Area classification performed in these terms, but in relation to the primary field that is a grid of squares of different sizes (100 and 200 m) was conducted in the work by Pokonieczny et al. 2014. An interesting solution to the problem of terrain classification is the use of artificial neural networks, which are one of the computational intelligence elements. In works by Bagheri et al. (2015) and Lee et al. (2012), multilayer perceptron neural networks were used. They were used for classification of soil types and predicting the production of surface water. Apart from multi-layer perceptron in data classification, other structures of artificial neural networks could also be applied. Grebby et al. (2011) presented an example of Kohonen artificial neural network usage to integrate satellite images with LIDAR data in order to identify the elements of land cover.

The justification for their use is that they are applicable in solving problems in which we have to deal with a large amount of input data and in which the algorithm to solve the problem is unknown or difficult to implement (Suzuki et al. 2013). This situation occurs in the discussed terrain classification—there are multiple parameters entered into the analysis, related to topography or land cover, and universal algorithm of operation is extremely difficult to implement. Taking this into account, the primary aim of the article is to present the terrain classification methodology developed by the author on the example of developing a terrain passability map. Artificial neural networks were used for this goal—specifically one type, that is SOM (Self Organizing Map), also known as Kohonen networks (Kohonen 1982).

Military Terrain Passability Map

The developed methodology will be presented on the basis of the development of a terrain passability map; thus another aim of the study is to determine to what extent and with what effect Kohonen neural networks can be used for this purpose.

Associated with the passability map is the concept of terrain assessment, which in military terms is the continuous process of collecting, analysing, processing and interpreting geographical information about both natural and anthropogenic terrain objects. The main aim of this activity is to predict the impact of land cover on carrying out military operations and missions and among the others, the terrain classification due to passability as one of the most important component has to be mentioned. It is based on the division of terrain into three classes (STANAG 3992, ed. 2):

- GO TERRAIN—does not require any additional measures for ensuring manoeuvres of forces operating in it,
- SLOW-GO TERRAIN—reduces possibility of troop manoeuvre movements, but to a lesser degree than NO-GO TERRAIN,
- NO-GO TERRAIN—hinders the movement of troops to a very large extent in all directions, drastically reducing the speed of movement.

The detailed parameters, which the above three-class terrain division is based on, are described both in the national (NO-06-A015 2012) as well as NATO (STANAG 2259, ed. 4 and STANAG 3992, ed. 2) standardization agreements. This information is also included in Field manual 5-33. Taken into account within the classification are such elements of land cover as: forests, road and hydrographic networks, built-up areas and landform (topography of terrain, including slope).

Artificial neural networks implement the requirements of fuzzy logic, and that is why we will be able to determine the passability in a continuous range, e.g. 0 and 1 (we are not limited to the classification into only three classes of passability). Therefore, it is possible to generate a continuous Index of Passability (IOP), which characterises the terrain in a range from 0 (the impassable area) to 1 (the area of high manoeuvrability). In order to facilitate the interpretation of the IOP, a division into 3 classes was made, identifying the following:

- from 0 to 0.33—NO GO terrain;
- from 0.34 to 0.66—SLOW GO terrain;
- from 0.67 to 1—GO terrain.

Research in this scope is described in the work Hofmann et al. (2014), which describes the determination of the passability factor using geographic spatial data and the *ArcGIS* software.

An attempt to use artificial intelligence in simulations of military operations was previously discussed in the paper by Campbell et al. (1997). In this publication, an automatic target recognition system was presented, taking into account both the topography and land cover. Among the others, Miller et al. (2013) proposed an automated system of military terrain analysis, allowing the selection of both parameters of analysis and output data such as optimal landing zone, the deployment of artillery positions etc. This system is intended for military planners. A similar approach was presented by Glinton et al. (2004), who compared a set of algorithms and tools to automate analysis of terrain, with results obtained by

experienced intelligence analysts. In the papers by Richbourg et al. (1996) and Lee et al. (2014) we can find the proposal of system that offers automatic and semi-automatic analysis performance of the terrain, concerning respectively: passability through forest and analyses of visibility. However, in the previously described solutions, the authors did not use artificial neural networks, but only an algorithmic approach (GIS analysis). Therefore, the aim of this research is to present a different approach to military analyses, based on the application of the ANN and SOM for automation of military terrain classification.

Methods

Passability is directly influenced by elements of land cover; therefore, to designate in this work, the Vector Map Level 2 topographic data base (in NATO countries, in line with NATO Geospatial Policy, military topographic databases such as Vector Maps are used) and SRTM (Shuttle Radar Topography Mission) digital terrain model was used. VMap L2 is a spatial, topographic database, equivalent to (in terms of detail) topographic map in scale 1:50,000. This publication is widely used by the Polish Armed Forces and other NATO countries. The objects are coded in accordance with NATO standard called DIGEST (Digital Geographic Information Exchange Standard defined in STANAG 7074 ed. 2). VMap L2 covers the entire area of Poland. The information in the database are grouped into 11 thematic categories, like hydrography, vegetation, cultural and others. In total, VMap L2 contains 253 feature classes of different spatial objects.

The research described in the work was conducted in the area of 3 voivodeships located in the north-eastern part of Poland. This is an area of over 81,000 km^2. What is important in the context of the research conducted, the area is characterised by varied land cover. In the analysed area are bodies of water (approx. 2% of the total area) and large, dense forest areas (27%). In the Mazowieckie Voivodeship there are expansive plains (the Łowicz-Błonie Plain) and the largest built-up area in Poland (the capital city of Warsaw). Other elements that influence passability are marshes (nearly 1% of the area) and highlands, where large land elevation differences occur (Fig. 1).

In the presented methodology, passability is determined in relation to the primary field measuring 1 km by 1 km. This is consistent with the requirements of normative documents (NO-06-A015). In the research area, a grid of 1 km × 1 km squares was generated (81,032 squares). For each one of them data was obtained on the elements of land cover located within each square. The VMap L2 database, discussed earlier, was used for this purpose. Depending on the geometric representation of object classes, the following data was gathered for each kilometre mesh of the primary field:

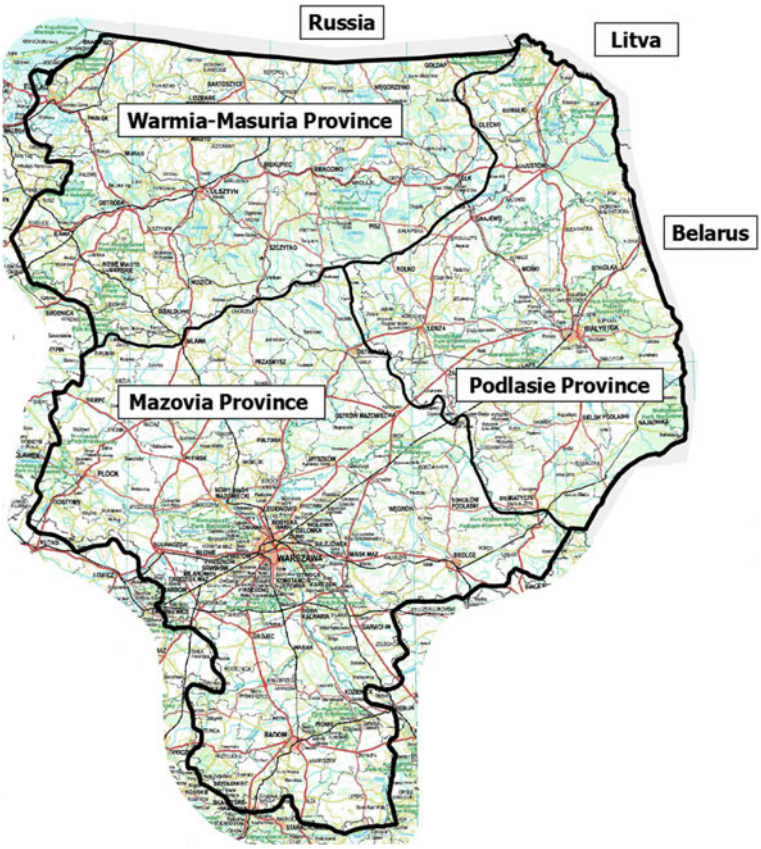

Fig. 1 The study area; *Source* Own elaboration and www.geoportal.gov.pl

- for surface (area) objects (e.g. forests, lakes, built-up areas)—the surface of the area located in a given mesh square;
- for linear (line) objects (rivers, roads, railways)—the length of the linear object located in a given mesh square;
- for singular point objects (buildings, farms)—the number of objects located in a given mesh square;
- for slope—the average value of the slope determined on the basis of all measurement points in a given mesh square.

Input data was prepared in two variants:

- In the first variant, 61 feature classes (out of a total of 253 classes) were selected from VMap L2. Through elimination, those classes unrelated to the land cover elements were excluded (administrative borders, contours, etc.) as well as those objects that, due to their small number in the analysed area, have a minor impact

on passability (mainly point objects, such as railway turning loops, roadside crosses, huts, etc.).

- In the second variant, the objects were grouped into categories according to Fig. 2. In total, 16 categories were established. Depending on the geometric representation of the object (area, line, point), this was the total area, length or number of objects that formed a given category. This procedure allowed for the reduction of the number of parameters entered into the neural network. Formula 1 shows this for the surface water class (A—area):

$$A_{hydrography} = A_{canal} + A_{fish\ farm} + A_{lake} + A_{river} \quad (1)$$

The ultimate result of this operation was the assigning to each 1 km × 1 km mesh square respectively 61 (for variant I) or 16 (for variant II) descriptive attributes, characterising the land cover in a given square. The presented method of modelling spatial data is a kind of conversion of the discrete (vector) model into a continuous model, in many respects similar to the raster model. In this way, some of the data stored in the topographical data base is lost. The advantage of this approach is the fact that the model built facilitates statistical operations (analyses) (Fig. 3).

All of the above operations were performed with the use of original, proprietary software. It carries out spatial queries with the use of the *PostgreSQL 9.5* software

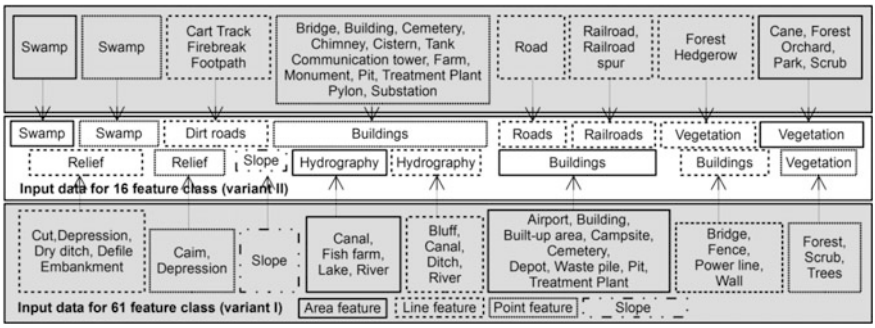

Fig. 2 The selection and grouping source data in two variants; *Source* Own elaboration

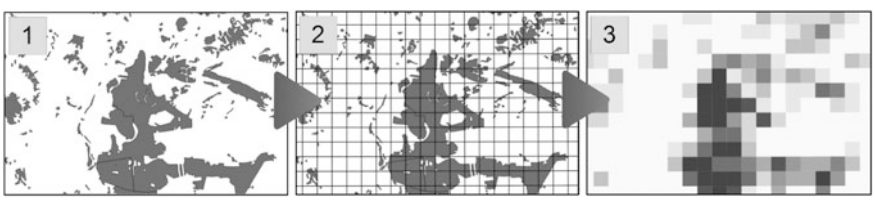

Fig. 3 Example of vector model conversion to grid for forest feature class; *Source* Own elaboration

with the *PostGIS 2.2* add-on. Using parallel processing algorithms (separation of 10 threads simultaneously querying the data base), gathering 253 parameters for each mesh square takes approx. 3.4 s (for a computer equipped with an *AMD Athlon II X4 640* processor).

In the presented methodology for the classification of an area by its passability, a Self-Organising Kohonen Map was used. These are two-layer networks (Kohonen 1996), in which the neurons located on the first layer are used only to enter the input data into the network. Essential data processing takes place in the neurons of the second (output) layer of the network, organised into a two-dimensional grid (a so-called map). Each neuron of this network is connected with all output elements (Fig. 3).

Before being entered into the input network neurons, all data was normalized to the interval $\langle 0, 1 \rangle$ according to the feature scaling method (Dodge et al. 2003):

$$V' = \frac{V - V_{\min}}{V_{\max} - V_{\min}} \cdot (new\_\max - new\_\min) + new\_\min \tag{2}$$

with V being an input value and the V′—normalized value of input. Consequently, [V_{min}, V_{max}] is the interval of input data and [new_max, new_min] is a new data range.

Operations related to the processing and SOM-type neural network learning were carried out using the Statistica 12.5 software (StatSoft 2016). In the process of learning, neurons cooperate with their neighbours and compete with neurons from other areas of the Kohonen map. As a result, the process orders the map in such a way that patterns similar to each other in the feature space are represented by neighbouring neurons of the output layer (objects close to each other are represented by adjacent neurons). The operation of the network is considerably influenced by the appropriate selection of the structure of the neural network (the number of input neurons, the size of the resulting Kohonen map, the number of learning periods). In the studies, network learning was carried out in 4 configurations. It was assumed that the network would be composed of respectively 61 and 16 input neurons (spatial data categories, for both variants). At the same time, studies were carried out for two dimensions of the output map of the neural network. Experiments were conducted for dimensions of 10 × 10 and 5 × 5 neurons. The networks were taught in 1000 leaning iterations, with the learning coefficient measuring 0.1 at the beginning and 0.02 at the end of the learning.

As a result of learning, certain map neurons (often with their neighbours) represent the related clusters (i.e. classes) of standards. This means that the taught neural network generates the strongest signals for the neuron that "represents" the input data most similar to it. In this way, the neural network classifies the terrain in terms of input date into as many classes as the size of the output, which is respectively 25 and 100 classes (Fig. 4). This classification is in no way connected to passability, because it was carried out solely for data regarding elements of land cover. In order to assign the grid squares to a specific passability index, a set of reference data was developed. Its creation included selecting a representative

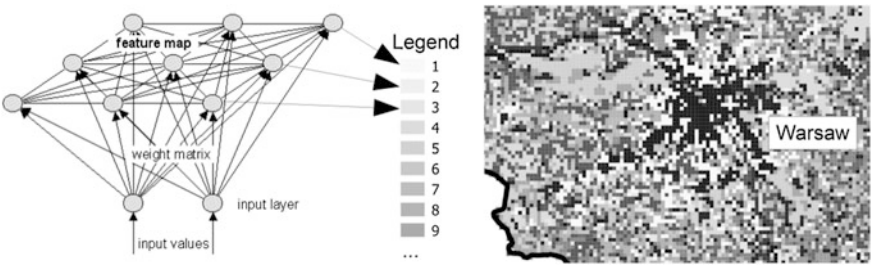

Fig. 4 Self-organizing maps in process of terrain classification; *Source* http://www.nnwj.de/kohonen-feature-map.html and own elaboration

Table 1 Sample values of index of passability assigned manually by the operator

		
IOP = 0.3	IOP = 0.5	IOP = 0.6

sample of, in the described example, 1000 randomly selected kilometre grid squares (making up 0.012% of all squares) from the training set (consisting of 81,032 squares). For all objects of this sample, an experienced operator appointed, on the basis of a topographic map, an Index of Passability (IOP) of terrain in ranges from 0 to 1. The results for the three sample grid squares are shown in Table 1.

Next, the land cover data for 1000 randomly selected grid squares (for the tests carried out, respectively 61 and 16 parameters) was introduced into the neural network. For each of them, the winning neuron (characterised by the highest values of stimulation for the input data) was indicated. Individual winning neurons were assigned a passability index, selected earlier by an operator. The final value of passability for each input neuron of the network was defined as the average value of individual indices of passability. In this way, each object class, represented by one output Kohonen network neuron was assigned an Index of Passability (IOP). The final stage of the work was determining the winning neuron for each of the 81,032 squares of the kilometre mesh, and thus the index of passability. Choropleth map and cartographic compilation, a method described by Medynska-Gulij (2010), were used for visualizing the results.

Results

As a result of the studies conducted, four neural networks were obtained in the course of an unsupervised learning process. Each of them was visualised as a Kohonen map (Fig. 5). Additionally, the number of kilometre mesh squares whose input data caused the highest stimulation was separately noted in the illustration for each output neuron. Analysing the spatial distribution of the object categories separated by the neural net, it is possible to indicate squares covered with dominant, similar elements of land cover. This relationship is shown in Fig. 5, where the dominant element of land cover represented by a neuron was assigned to that neuron by comparing the shape and spatial extent of the areas selected by the Kohonen network with a topographic map.

Introduction into the neural network of 1000 randomly selected squares of the kilometre mesh for which the index of passability was determined, allowed for assigning an IOP to each output neuron (Fig. 6). As can be seen, the size distribution of these indices allows for the identification of certain clusters (groups) of neurons, for which its value is similar. At the same time, in the case of a map

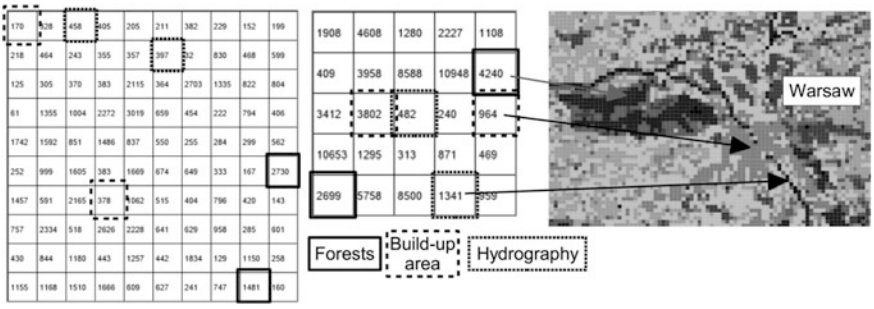

Fig. 5 Visualisation of SOM (10 × 10 and 5 × 5 neurons with 16 inputs) with quantity of represented grid squares. Selected neurons represent 3 elements of land cover indicated on the map; *Source* Own eleboration

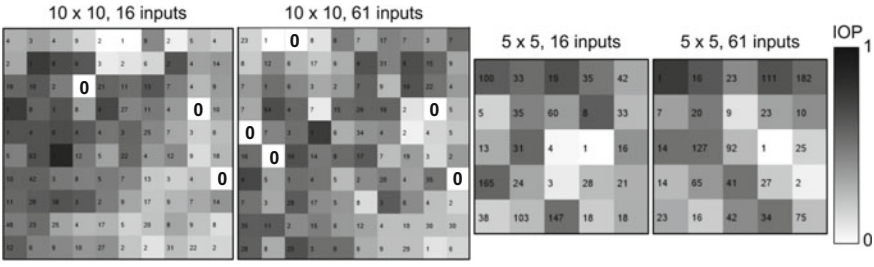

Fig. 6 Visualisation of generated SOM with quantity of winning grid squares from training set and IOP; *Source* Own elaboration

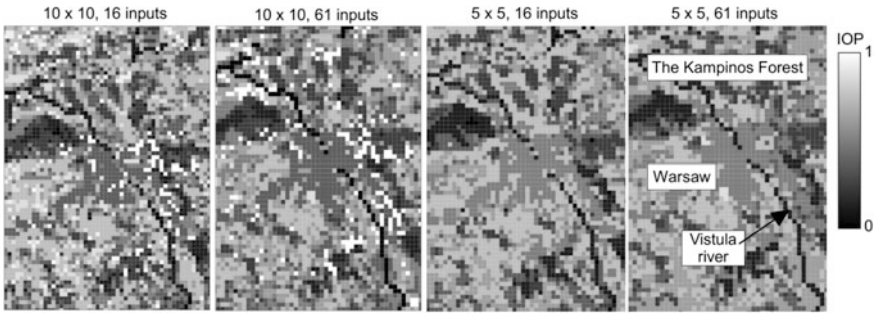

Fig. 7 Visualisation of fragments generated maps of passability; *Source* Own elaboration

Table 2 Results of statistical analysis for IOP generated by 4 SOM

SOM	Average	Std. dev	Pearson's correlation matrix			
			5 × 5—16 inputs	5 × 5—61 inputs	10 × 10—16 inputs	10 × 10—61 inputs
5 × 5—16 inputs	0.46	0.15	1	0.84	0.86	0.85
5 × 5—61 inputs	0.45	0.14	0.85	1	0.81	0.86
10 × 10—16 inputs	0.47	0.18	0.86	0.81	1	0.83
10 × 10—61 inputs	0.47	0.17	0.85	0.86	0.83	1

measuring 10 by 10 neurons, there are neurons which do not have any assigned mesh squares. In such cases, assigning an index of passability was not possible.

Input data on land cover for all (81,032) squares of the kilometre grid was introduced into the neural networks. Each square was assigned an index of passability. Four passability maps were obtained, covering the north-eastern area of Poland (Fig. 7). Additionally, basic statistical analyses were performed on the results obtained, and their results are visualised in Table 2.

Discussion

The presented methodology is largely automatic. Reference of analyses to the primary field means that the process of preparing the input data is lengthy and complicated. This is due to the large number of land cover parameters collected and the huge area of the analyses. Preparation of input data for 81,032 mesh squares takes approx. 24 h. Also automatically implemented is the neural network learning process and generation of classification maps. The only process the operator must

perform manually is to build a knowledge base, which in the illustrated example involved preparing 1000 squares of the kilometre grid to which an index of passability had to be arbitrarily assigned. Analysis of the results in the form of maps shows that all four neural networks assigned the IOP correctly. Impassable areas were indicated, covering areas of forests, rivers, or built-up areas. In turn, open areas in which a dense network of roads was present were assigned a higher index of passability, which coincides with the factual state.

The results illustrate that there is no significant difference between passability maps developed using 16 or 61 input parameters. This is confirmed by a high correlation coefficient (0.81–0.85), indicating a high similarity of data obtained from all SOMs. Detailed interpretation of passability maps and comparison with topographic maps showed, however, that the results obtained for 16 grouped input parameters give better results. The reason for this is a lower signal-to-noise ratio of input data to a higher number of parameters. Of considerable importance is also the shorter network learning period for 16 input parameters. The time required for this process is 30% of the learning period for a network with 61 parameters.

The size of the Kohonen map has a significant impact on the developed passability map, because it defines the number of categories the terrain is divided into. Although the value of the average index of passability was similar for all neural networks (0.46), analysis of the obtained maps indicates that in the case of a smaller Kohonen map output layer matrix (in the example of 5 by 5, i.e. 25 categories), the obtained maps are easier to interpret (due to the smaller number of categories). In the case of a 10 by 10 network (100 categories), the resulting maps show a lower uniformity of selected areas and a higher amount of data noise. This can also be seen by analysing the obtained standard deviations of indices of passability (Table 2)—in the case of a 10 by 10 map, it is higher, indicating a higher data scatter caused by the assumption of a larger number of categories. In the case of larger maps, it also turned out that an index of passability could not be assigned for all neurons ("empty" neurons in Fig. 6). This caused the resulting map to have noticeable grid squares where there is no assigned IOP.

Conclusion

The described methodology of developing passability maps is based on referring the index of passability to the primary field (in the example, measuring 1 by 1 km). In this way, it differs from previously used methods of generating passability maps, which consisted of manual or automatic (through GIS analyses) marking of areas with a specific passability on a topographic map base. The obtained passability maps can provide sufficient detail for assessing the terrain at the operational level (division, brigade). Further studies will be conducted both in terms of analysis of primary fields of different size (to meet the needs of lower and higher -level units) and shape. As a result of the research, we obtain an index of passability in a continuous range from 0 to 1. This is an advantage of the proposed methodology,

because we are not limited to three categories of passability, provided by the defensive norm. The results of the research show that SOMs can be used for terrain classification with the use of general geographic spatial data bases. The entire process is semi-automatic, which is extremely important in the process of Intelligence Preparation of the Battlefield. The only "manual" part is the preparation of a "knowledge base", which will be used to assign an index of passability to the neurons of an already-taught Kohonen network. The process of knowledge base preparation is performed only once, however. After preparation of a knowledge base for questions of a different subject, the presented methodology can be used for terrain classification in areas different than passability (e.g. soil map development or defining areas suitable for investments).

Acknowledgements This research was conducted on the basis of Vector Map Level 2 obtained from Polish Military Directorate.

This research was supported by the grant no. 801/2015 at the Military University of Technology.

References

Bagheri Bodaghabadi, M., Martinez-Casasnovas, J. A., Salehi, M. H., Mohammadi, J., Esfandiarpoor Borujeni, I., et al. (2015). Digital soil mapping using artificial neural networks and terrain-related attributes. *Pedosphere,* 25(4), 580–591. doi:10.1016/S1002-0160(15)30038-2

Bielecka, E., Pokonieczny, K., & Kamiński, P. (2014). Study on spatial distribution of horizontal geodetic control points in rural areas. *Acta Geodaetica et Geophysica, 49*(3), 357–368. doi:10.1007/s40328-014-0056-6

Campbell, L., Lotwin, A., DeRico, M. M. G., & Ray, C. (1997). *The use of artificial intelligence in military simulations*. In SMC '97 Conference Proceedings—1997 IEEE International Conference on Systems, Man, and Cybernetics, Vols. 1–5: Conference Theme: Computational Cybernetics and Simulation, Book Series: IEEE International Conference on Systems, Man, and Cybernatics (pp: 2607–2612).

Dodge, Y. (Ed.). (2003). *A dictionary of statistics*. Oxford: Oxford University Press. ISBN 0-19-850994-4.

Field manual 5-33 Terrain Analysis. (1990). Headquarters, Department of US Army.

Glinton, R., Giampapa, J., Owens, S., Sycara, K., Grindle, C., & Lewis, M. (2004). Integrating context for information fusion: Automating intelligence preparation of the battlefield, Human performance, situation awareness and automation: Current research and trends. In 2nd Conference on Human Performance, Situation Awareness and Automation (HPSAA II), Daytona Beach, FL (Vol. 2, pp: 224–229), March 22–25, 2004.

Grebby, S., Naden, J., Cunningham, D., & Tansey, K. (2011). Integrating airborne multispectral imagery and airborne LiDAR data for enhanced lithological mapping in vegetated terrain. *Remote Sensing Of Environment, 115*(1), 214–226. doi:10.1016/j.rse.2010.08.019

Han, H., Chung, W., Song, J., Seol, A., & Chung, J. (2016). A terrain-based method for selecting potential mountain ridge protection areas in South Korea, *Landscape Research, 41*(8), 906–921. doi:10.1080/01426397.2016.1173657

Hofmann, A., Hoskova-Mayerova, S., Talhofer, V., & Kovarik, V. (2014). Creation of models for calculation of coefficients of terrain passability. *Quality & Quantity, 49*(4), 1679–1691. doi:10.1007/s11135-014-0072-1

Irvin, B. J., Ventura, S. J., & Slater, B. K. (1997). Fuzzy and isodata classification of landform elements from digital terrain data in Pleasant Valley, Wisconsin. *Geoderma, 77*(2–4), 137–154. doi:10.1016/S0016-7061(97)00019-0

Kohonen, T. (1982). Self-organized formation of topologically correct feature maps. *Biological Cybernetics, 43*(1), 59–69. doi:10.1007/BF00337288

Kohonen, T., Oja, E., Simula, O., Visa, A., & Kangas, J. (1996). Engineering applications of the self-organizing map. *Proceedings of the IEEE, 84*(10), 1358–1384. doi:10.1109/5.537105

Lee, E. S., & Kim, J. B. (2014). *A utilization study of domestic thematic map for military terrain analysis cartography*. In 2014 International Conference on Information Science and Applications (ICISA): Book Series: International Conference on Information Science and Applications. doi:10.1109/ICISA.2014.6847347

Lee, S., Song, K. Y., Kim, Y., & Park, I. (2012). Regional groundwater productivity potential mapping using a geographic information system (GIS) based artificial neural network model, *Hydrogeology Journal, 20*(8), 1511–1527. doi:10.1007/s10040-012-0894-7

Medyńska-Gulij, B. (2010). Map compiling, map reading, and cartographic design in Pragmatic pyramid of thematic mapping. *Quaestiones Geographicae, 29*(1), 57–63. doi:10.2478/v10117-010-0006-5.

Miller, D., Rueter, S., Miller, D. F., & Rueter, S. P. (2013) Mission adaptable terrain analysis system used by military planner, has transform components which transform data having basic terrain evaluations to input data format. Patent Number(s): EP2554944-A2; US2013035861-A1; EP2554944-A3.

NATO Geospatial Policy (MC 296/1).

NO-06-A015:2012, Terrain—Rules of classification—Terrain analysis on operational level (2012).

Pokonieczny, K., Bielecka, E., & Kaminski, P. (2014). Analysis of spatial distribution of geodetic control points and land cover. Geoconference on Informatics, Geoinformatics and Remote Sensing, Vol II, Book Series: International Multidisciplinary Scientific GeoConference-SGEM (pp. 49–56). Published: 2014 Conference: 14th International Multidisciplinary Scientific Geoconference (SGEM), Albena, BULGARIA, June 17–26, 2014.

Richbourg, R., & Olson, W. K. (1996). A hybrid expert system that combines technologies to address the problem of military terrain analysis. *Expert Systems Applications, 11*(2), 207–225. doi:10.1016/0957-4174(96)00033-4

Shuttle Radar Topography Mission, NASA, http://www2.jpl.nasa.gov/srtm, Access: July 1, 2016.

STANAG 2259, Ed. 4: Military Geographic Documentation—Terrain. NATO standardization agreement.

STANAG 3992, Ed. 2: Military Geographic Documentation—Terrain Analysis AgeoP-1 (A). NATO standardization agreement.

STANAG 7074, Ed. 2: Digital Geographic Information Exchange Standard (DIGEST). NATO standardization agreement.

StatSoft, https://www.statsoft.com/, Access: Novenber 15, 2016.

Suzuki, K. (2013). *Artificial neural networks—Architectures and applications* (p. 264). InTech. ISBN 978-953-51-0935-8.

Dynamical Flash Flood Risk Forecast

Petr Rapant and Jaromír Kolejka

Abstract Flash floods represent very dynamical natural phenomenon. Mostly, they are the result of torrential rains which can rise suddenly in any part of a country and are tough to predict. Of course, there are many weather forecasting systems, but their spatial and temporal resolution is usually insufficient for these purposes. There are also monitoring systems which can either register precipitation over the ground (a network of rain gauge stations) or runoff in riverbeds (a network of hydrometric stations). Again, spatial (and possibly temporal) resolution is not sufficient, and in the case of runoff monitoring, there is a substantial delay between actual rainfall and registration of runoff in riverbeds. And, of course, when the hydrometric station registers higher runoff than the flash floods is running or even over. From the point of early warning, all these systems reveal disadvantages. Aside from these systems, there is one which provides us with timely information about the spatial and temporal distribution of precipitation intensity over the ground. That is weather radar. We will demonstrate possible usage of these data for dynamic prediction of flash flood risk distribution in space and time over the monitored area. Proper processing of these data in combination with soil saturation indicator established using Flash flood guidance methodology developed by the US Hydrologic Research Center can generate timely information usable for early warning with a substantially reduced level of false warnings.

Keywords Flash flood · Risk prediction · Weather radar

P. Rapant (✉)
Institute of Geoinformatics, Faculty of Mining and Geology,
VŠB-Technical University of Ostrava, 17. listopadu 15/2172,
70833 Ostrava-Poruba, Czech Republic
e-mail: petr.rapant@vsb.cz

J. Kolejka
Institute of Geonics, Czech Academy of Sciences,
Drobného 301/28, 60200 Brno, Czech Republic

I. Ivan et al. (eds.), *Dynamics in GIscience*, Lecture Notes in Geoinformation and Cartography, DOI 10.1007/978-3-319-61297-3_27

Introduction

Flash floods are a natural highly dynamical phenomenon which is hard to predict. Their random occurrence and rapid development limit the possibility to develop a reliable and efficient early warning system. However, due to changing climate conditions, the occurrence of the flash floods has become increasingly frequent. That is why the interest in flash floods is growing.

The primary cause of devastating flash floods is torrential rainfall. There are many other factors, such as the soil saturation, the terrain slope, the catchment area, geology, soil type, and the urbanisation of the territory, which also influence these floods (Březková 2011; Drbal 2009; Šercl 2015). That is why torrential rain does not necessarily cause a flash flood every time—other factors can eliminate this threat.

Because of the complexity of the process generating flash floods and the complex nature of parameters governing this process, that are moreover spatially distributed, it is hard to develop the reliable and efficient early warning system. National hydro-meteorological institutes can collect data describing rainfall and runoff distribution through precipitation gauge stations and hydrometric gauge stations, put received data to the hydrological models and obtain a probable distribution of flood in the territory, but this process is quite time-consuming. The other problem is that spatial and, in some cases, even temporal resolution of data gathered and models developed is insufficient. That is why we still do not have such the early warning system in full operation.

On the other hand, there is a method for gathering data describing a distribution of precipitation over land with sufficient spatial and temporal resolution. It is a weather radar. National hydro-meteorological institutes usually operate a system of these radars covering the whole territory of the country. In the case of the Czech Hydro-Meteorological Institute, data are provided in raster format with spatial resolution 1 × 1 km and temporal resolution 5 min. Such data are very suitable for the development of the flash flood early warning system (CZRAD 2011).

As it was mentioned above, many other factors influence the rise of the flash flood. The most important one is the soil saturation by preceding precipitation. This factor is very well described by the soil saturation indicator. The Czech Hydro-Meteorological Institute produces the soil saturation indicator established using Flash flood guidance methodology developed by the US Hydrologic Research Centre and adopted to the Czech conditions (HPPS ČHMÚ 2016). Including of this indicator to the process of a flash flood risk assessment can help to correct to some extent the assessed flash flood risk and decrease the rate of false warnings issuing.

Developed Methodology

In the last years, we have focused on the development of scenarios of geoinformation technologies applications to crisis management. One scenario was focused on a quick flash flood prediction. The first things we took into account when developing this scenario were:

- there is only a very short time interval between falling of precipitation and rise of a flash flood,
- that is why we should derive only qualitative information describing areas potentially hit by the flash flood, which can be obtained quickly,
- so we do not need a quantitative estimation of precipitation nor exact numerical rainfall-runoff modelling,
- also, data from hydrological gauge stations situated on rivers are obsolete for this purpose—they register an already existing flood.

Next, it is good to remember that:

- the greatest damage and loss of life are caused by concentrated runoff of torrential rainfall in influent watercourses, and
- residents of communities in which it does not rain, but that lay downstream and shall be thus also affected by the runoff water may be at risk too.

Based on these considerations, we have decided that (adopted from Rapant et al. 2015b):

- proposed methodology should be based on weather radar data, which provide the greatest detail both in the space and in the time dimension,
- the radar data will be processed in a raw state, without any adjustment to eliminate most of any time delay caused by the pre-processing of radar data,
- data, therefore, can be processed only qualitatively—which fits well with our entry requirements,
- qualitative assessment will be performed on individual sections of watercourses
- to minimise the number of parameters affecting the evaluation of the risk of flash floods:
  - by assuming that the runoff spreads along the watercourses at a constant speed of 10 km per hour
  - by counting the total contribution of rainfall to the runoff in sections of watercourses in last two hours
  - by supposing that the soils are fully saturated (so called the worst case scenario),
- the flash flood risk level at the watercourse sections is visualised using a five-level scale.

The proposed methodology was implemented in Python as a toolbox for ArcGIS. This toolbox continuously processes incoming weather radar data and

generate an up-to-date map of the flash flood risk distribution along the individual sections of the watercourses. Weather radar data are totalized across watersheds, sums are directly transferred to respective river sections and relayed downstream up to the distance of 20 km. All such contributions are totalized along every watercourse sections, and resulting sums are classified using five level scale (no risk–low risk–high risk–very high risk–extremely high risk).

Later, after gaining some practical experience, we included the soil saturation indicator provided by Czech Hydro-Meteorological Institute (HPPS ČHMÚ 2016) to the proposed methodology. We use it for evaluation of propensity of soils to infiltration of precipitation. With growing propensity to infiltration, the level of flash flood risk decreases. This step helped to reduce substantially false warnings.

Results

The proposed methodology was tested in many local case studies in Czechia (Rapant et al. 2015a, b, 2016). Gained results demonstrate that the proposed method is effective and also efficient in evaluating the flash flood risk and generating information suitable for early warning purposes. Two examples are shown for the events from 24.6.2009 (middle Moravia) and 7.8.2010 (north-west Bohemia).

Figure 1 demonstrates that predicted rise of the flash flood risk precedes real development in order of hours by comparing the course of the predicted risk with actual measurements done at gauge station Kozlovice on the river Ondřejnice.

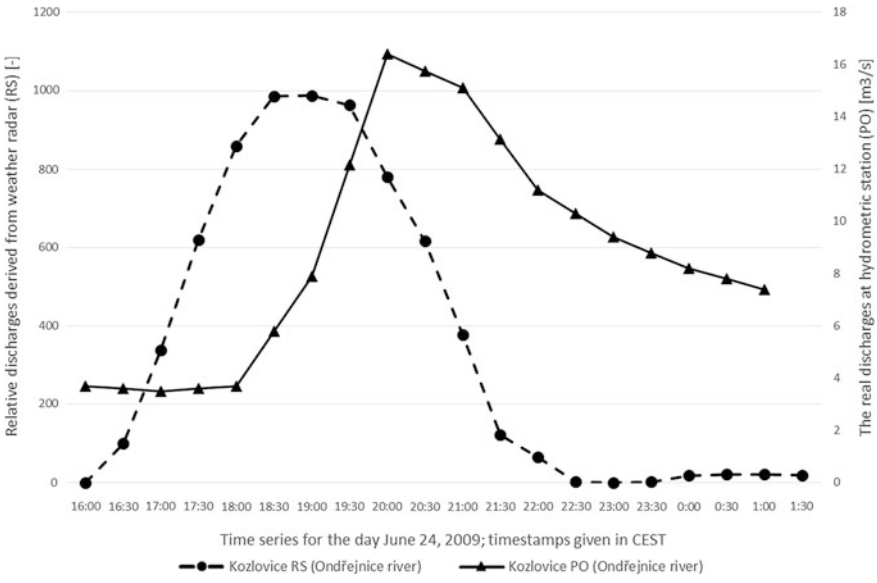

Fig. 1 Comparison of the curve of relative discharge derived from weather radar data (RS) with the curve of actual discharge (PO; data courtesy of Odra River Basin Management Company, a state enterprise) measured by a hydrometric station located in Kozlovice on the river Ondřejnice, 24.6.2009

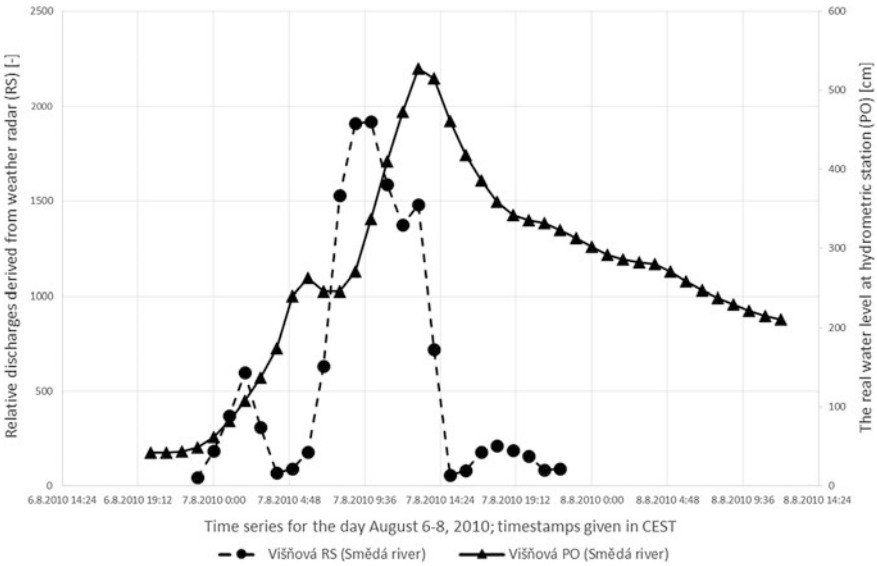

Fig. 2 Comparison of the curve of relative discharge derived from weather radar data (RS) with the curve of actual discharge (PO; data courtesy of Czech Hydro-Meteorological Institute) measured by a hydrometric station located in Višňová on the river Smědá, 7.8.2010

The similar situation is displayed in Fig. 2 for the gauge station Višňová on the river Smědá. It is necessary to mention that in both cases, the soils were highly saturated at the beginning of the respective events.

In the next step, we focused on inclusion of the soil saturation indicator to the proposed methodology. Case studies were designed to cover the whole territory of Czechia. The predicted flash flood risk was compared with real events related to flooding and registered in the database of statistical monitoring of events managed by the Fire Rescue Service (FRS) of Czechia.

The Soil Saturation Indicator

The soil saturation indicator is provided as a raster with pixel size 1 × 1 km. Values are expressed using ordered qualitative scale: extremely unsaturated–unsaturated–saturated to retention capacity–saturated–highly saturated–extremely saturated. Colour scale starts at dark red and finishes at dark green (HPPS ČHMÚ 2016).

The Fire Rescue Service Database

This database contains information about all interventions of firefighters. All records include GPS coordinates of the place of intervention, so they are well

localised. Every record contains tens of items, but we received only a subset of them, providing data necessary for identifying the event, spatially localise it and select relevant events.

Original and Improved Predictions

The soil saturation indicator is interpreted qualitatively: first three levels represent soils which can absorb at least part of the rainfall, last three levels represent regions with limited or no ability to absorb any precipitation. Simply put: Red areas are taken as they are not susceptible to flooding, the susceptibility of green areas rises with the darkness of the green colour.

Figure 3 demonstrates the maximum value of flash flood risk predicted for river sections during whole the day 25.6.2016. We can see that the entire territory of Bohemia (the western part of Czechia) should be subject to the early warning sometimes during the day. But if we compare this prediction with real events relating to flooding as they were registered in FRS database, we can also see that most of these warnings would be false. In Fig. 4 we see situation after including the soil saturation indicator: the correspondence between prediction and reality is much better. Similar results were also obtained for other days (e.g. Fig. 5).

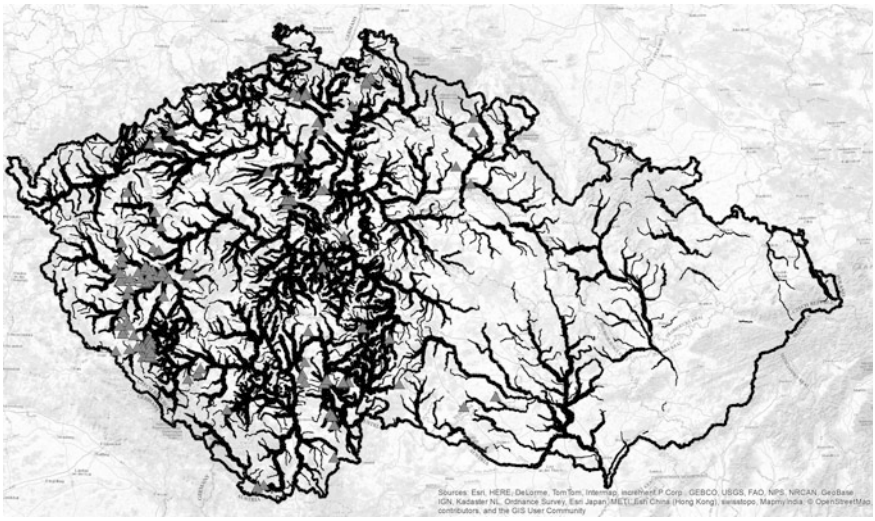

Fig. 3 Comparison of the maximum value of flash flood risk predicted for river sections during whole the day 25.6.2016 with real events relating to flooding as they were registered in FRS database (data courtesy of Fire Rescue Service, Czechia). *Grey triangle* represent events from FRS database; *black lines* represent level of flash flood risk using five level scale (no risk–low risk–high risk–very high risk–extremely high risk; coded by line thickness)

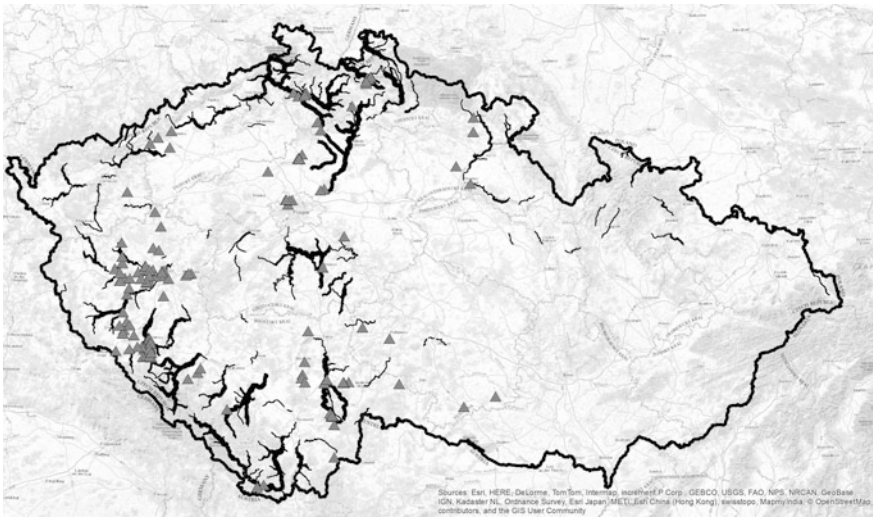

Fig. 4 Comparison of the maximum value of flash flood risk predicted for river sections during whole the day 25.6.2016, reduced by inclusion of soil saturation index to the proposed methodology, with real events relating to flooding as they were registered in FRS database (data courtesy of Fire Rescue Service, Czechia)

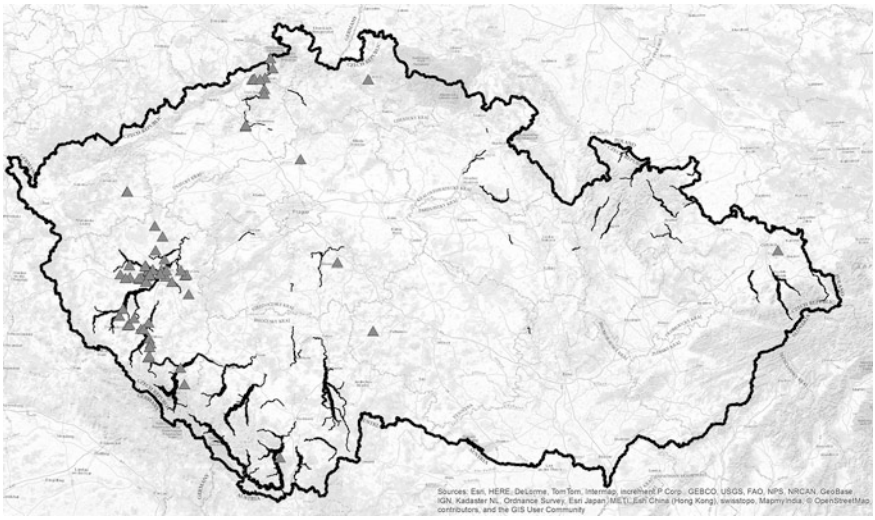

Fig. 5 Comparison of the maximum value of flash flood risk predicted for river sections during whole the day 26.6.2016, reduced by inclusion of soil saturation index to the proposed methodology, with real events relating to flooding as they were registered in FRS database (data courtesy of Fire Rescue Service, Czechia)

Discussion

Today's warning systems are typically based on mathematical models (NOAA_NWS 2010; Sene 2013; Volos 2007). Their aim is to quantify the impacts of torrential rainfall in the area. Very often they focus more on regional flooding (Alfieri et al. 2011), whose progress is not as fast. However, they are also known systems, focusing primarily on flash floods (Cosmo 2015; Dorman 2013). These are often also trying to predict the onset of heavy rains. Thus conceived systems are demanding for detailed data about areas that are not routinely available. The consequence is a paradoxical situation: predictions are the result of mathematical models (what can give us an illusion of accuracy), but they are burdened with high uncertainty (what is not always clear).

Our approach is different. It does not use the rainfall-runoff models, does not quantify the impact of torrential rains in the country and it is based on the rainfall already registered by radar measurements. With this, the time between precipitation falling and issuing a warning is very short. Residents can thus get the warning in advance before the potential development of the flash flood. FFG inclusion into the methodology significantly reduced the number of false warnings.

On the other hand, the examples also show some limitations of the proposed methodology. It does not work well for small streams (surface runoff is a predominant phenomenon here) and does not cover large regional watercourses with sufficient capacity of their riverbed. In other cases, the methodology appears to be both effective and efficient.

Acknowledgements This work was supported by the project called "Disaster management support scenarios using geoinformation technologies" No VG20132015106, program Safety Research promoted by Ministry of Interior, Czechia and by Faculty of Mining and Geology, VSB-Technical University of Ostrava, Czechia.

References

Alfieri, L., Smith, P. J., Thielen-del Pozo, J., & Beven, K. J. (2011). A staggered approach to flash flood—case study in the Cévennes region. *Advances in Geosciences*, *29*, 13–20.

Březková, L., Novák, P., & Šálek, M. (2011). Limits of flash floods forecating in the conditions of the Czech Republic. In I. Obrusník (Ed.), *Early warning of flash floods* (pp. 29–33). Český hydrometeorologický ústav: Praha.

COSMO. (2015) [online]. Accessible from: *http://www.cosmo-model.org/*. June 13, 2016

CZRAD. (2011). Český hydrometeorologický ústav. Radarová síť CZRAD, http://www.chmi.cz/files/portal/docs/meteo/rad/info_czrad/index.html (18.1.2017).

Dorman, L. I. (2013). Automated Local Evaluation in Real Time (ALERT). *Encyclopedia of Natural Hazards*, 31–31.

Drbal, K., Ošlejšková, J., Dzuráková, M., Štěpánková, P., Dumbrovský, M., et al. (2009). *Vyhodnocení povodní v červnu a červenci 2009 na území České republiky* (p. 75). Praha: Metodika mapování povodňového rizika.

HPPS ČHMÚ. (2016). Indikátor přívalových povodní (Flash Flood Guidance) [online]. Available from: http://hydro.chmi.cz/hpps/main_rain.php?mt=ffg. June 13, 2016.

NOAA_NWS. (2010). *Flash flood early warning system reference guide NOAA National Weather Service* (p. 204). Silver Spring: International Activities Office/University Corporation for Atmospheric Research.

Rapant, P., Inspektor, T., Kolejka, J., Batelková, K., Zapletalová, J., Kirchner, K., et al. (2015a). *Early warning of flash floods based on the weather radar*. In Proceedings of ICCC 2015 Conference (pp. 426–430).

Rapant, P., Lazecký, M., Kolejka, J., & Orlíková, L. (2015b). Nonparametric prediction of the onset of regional floods: Floods in North-Western Bohemia, Czech Republic, 2010. Water and Society 2015 Conference Proceedings (pp. 111–122).

Rapant, P., Kolejka, J., & Inspektor, T. (2016). Predikce rizika vzniku přívalové povodně s využitím dat meteorologických radarů (Prediction of flash flood risk using weather radar data). *Životné prostredie, 50*(3), 162–166.

Sene, K. (2013). *Flash floods. Forecasting and warning* (p. 385). Heidelberg: Springer.

Šercl, P., Janál, P., Daňhelka, J., Březková, L., Kyznarová, H., et al. (2015). *Možnosti predikce přívalových povodní v podmínkách České republiky* (p. 50). Praha: Český hydrometeorologický ústav.

Volož, B. (2007). Odvození extrémních povodňových vln v malých povodích deterministickými nástroji. Nejistoty hydraulických výpočtů na vodních tocích pro extrémní hydrologické jevy, ČVUT: Praha. http://hydraulika.fsv.cvut.cz/Hydraulika/vyzkum/nejistoty/hydrologie/odvozeni.html. January 18, 2017.

Interpolation Techniques for Predicting the Movement of Cyclists

Aleš Ruda and Ludmila Floková

Abstract Planning the development of cycling infrastructure underlines the importance of predicting the movement of cyclists inside cities. The main goal of the paper is to examine different interpolation techniques in order to estimate the most accurate predicts. The research was conducted with primarily collected data on pre-selected intersections. The data set included 30 input points measured during cyclists' rush hour in the morning, 5:30–9:00 a.m., and in the afternoon, 2:00–5:00 p.m. To choose an appropriate interpolation method IDW, EBK, RBF, Ordinary Kriging (OK) with spherical variogram, Ordinary Kriging (OK) with linear variogram, Simple Kriging (SK) with spherical variogram and Simple Kriging (SK) with linear variogram) were considered based on state of the art analysis and further examined. For selecting a suitable interpolation technique, the cross validation was taken into account comparing Mean Error (ME), Root Mean Square Error (RMSE), Root Mean Square Standardized Error (RMSSE) and Average Standard Error (ASE). The cross-validation showed that IDW and RBF have worst results although IDW was the most accurate in prediction of furthest point. Opposite, EBK and OK (spherical variogram) achieved very similar values bringing best predicts. Though kriging is very accurate interpolator, the behaviour of cyclists is determined by many other factors which can not be completely included during kriging.

Keywords Prediction · Kriging · Cycling · Regional interpolation

A. Ruda (✉)
Department of Informatics, Karel Englis College, Mezírka 775/1,
60200 Brno, Czech Republic
e-mail: ales.ruda@seznam.cz

L. Floková
Department of Undergraduate Study, College of Logistics,
Palackého 1381/25, 75000 Přerov, Czech Republic
e-mail: ludmila.flokova@vslg.cz

I. Ivan et al. (eds.), *Dynamics in GIscience*, Lecture Notes in Geoinformation and Cartography, DOI 10.1007/978-3-319-61297-3_28

Intoduction

The demand for sustainable transportation has been increasing recently so more and more authorities become interested in encouraging the use of non-motorised modes of travel such as bicycles. However, with a lack of accurate and consistence demand and usage figures it is difficult to measure the positive benefits of investments in these modes, especially comparing to other transportation modes such as the private automobile (National Bicycle and Pedestrian Documentation Project 2009). Predicting bicycle activity seems to be crucial for many purposes. Firstly, cycle network planning and the prioritisation of cycling infrastructure investments, secondly for measuring the efficiency of such investments. Last but not least, estimates of total bicycle activity can serve as the denominator for calculation of cyclist crash rates. One of the fundamental traffic engineering metrics that is often used for planning and designing purposes is the annual average daily traffic (ADDT) volume. An average annual daily bicycle (AADB) is then used as the equivalent measure for bicycle traffic (Esawey 2014; Nordback et al. 2013a, b; Lindsey 2014; Strauss 2015; Nosal 2014). Bicycle counts are an extremely useful source of basic data. Several studies and methodological documents focus on various techniques to count bicyclists and pedestrians. Counts can be conducted at mid-segment or at intersections, short-term or long-term. Nordback et al. (2013b) also concludes that counts can either be done manually or by automated technologies. Manual counts are usually binned in time periods of 2 h, whiles continuous counts 24-h per day, 365 days per year are gathered by automated counters usually using video counts, active infrared, passive infrared, inductive loops or pneumatic tubes and provide mid-segment screen line. Collected data are then combined with other sources to get cyclists volumes.

State of the Art

Few recent studies have combined short-term (manual) and long-term (automatic) counts to estimate AADB (Nosal 2014; Roll 2013; Nordback et al. 2013a; Esawey et al. 2013). Some others add more estimation factors and applied different techniques (Table 1). Strauss et al. (2015) proposed a method to estimate AABD volumes in the cycling network of Montreal combining short- and long- term bicycle counts with GPS data. Shafizadeh and Niemeier (1997), Milakis and Athanasopoulos (2014), Lundberg and Weber (2016) also involve surveys to get cyclists preferences on infrastructure which is also included in the estimation process. Salon (2016) focuses on simple small-area estimation method combining travel survey, census and land use data. K-means cluster analysis is used to categorize census tracts into neighbourhood types and estimates of travel activity for each tract are set. Also Caulfield et al. (2012) determines bicycle infrastructure preferences in Dublin based on the survey. Rybarczyk and Wu (2010) developed

Supply- and Demand-based models. Supply based model was based on BLOS index (Bicycle Level of Service) (Landis et al. 1997). Demand based model sets a 'Demand Potential Index' (DPI) of bicycle facilities incorporating six factors (crime, businesses, schools, recreation areas, parks, and population) that could potentially affect demand for cycling and cycling volume respectively. Incorporating both BLOS and DPI indexes help to generate cluster maps where there is possible to identify concentration on unsafe roads for cycling or bike friendly neighbourhood. A 'Prioritisation index' (PI) was developed by Larsen et al. (2013) for study of Montreal (Canada). It considers five factors: observed bicycle trips; potential bicycle trips (that could replace short car trips); suggestions by cyclists for specific segments of bicycle paths; bicycle-vehicle collision data; and the presence of 'dangling nodes', namely, bicycle facilities that end abruptly.

Unfortunately, there is not good spatial coverage of count data in most areas so various modelling methods employing geographic information systems (GIS) technology are used to eliminate the lack of relevant detailed information.

Table 1 Overview of applied methods in movement estimation of cyclists

Methodology	Source
Ordinary linear regression, multiple regression, spatial lag regression, logistics regression	Zhao and Chung (2001), Lowry and Dixon (2012), Mohammad et al. (1998), Strauss and Miranda-Moreno (2013), Griswold (2011), Apronti et al. (2016), Xia et al. (1999), Bagheri et al. (2012), Becker Lopes et al. (2014), Esawey (2014), Sarlas and Axhausen (2016), Cardoso et al. (2012)
Geographically weighted regression	Selby and Kockelman (2012), Sarlas and Axhausen (2016), Cardoso et al. (2012)
Travel demand modelling	Rybarczyk and Wu (2010), Landis et al. (1997), Larsen et al. (2013), Xu et al. (2016)
Origin-destination centrality based method, network analyst based method	Lowry (2014), Lowry et al. (2012), Wang and Kockelman (2009), Sarlas and Axhausen (2016)
Kernel density function, heat maps, density maps	Oksanen et al. (2015), Dongwook et al. (2014), Yu and Ai (2014), Prasannakumar et al. (2011), Mohaymany et al. (2013), Okabe (2008)
Getis Gi* method	Prasannakumar et al. (2011)
Moran's I function	Prasannakumar et al. (2011), Mitra (2009), Sarlas and Axhausen (2016)
Ripley's K-function	Yu and Ai (2014)
Kriging interpolation	Mitra (2009), Selby and Kockelman (2012), Wang and Kockelman (2009), Sarlas and Axhausen (2016)
Artificial neural network	Xu et al. (2016), Sharma et al. (2001)
Classical binomial, random parameter negative binominal model	Amoh-Gyimah et al. (2016), Mitra (2009), Sarlas and Axhausen (2016)

One attempt to estimate AADT was developed using multiple regression method utilizing aggregated data at the county level (Mohamad et al., 1998) and this method has become widely used (Xia et al. 1999; Becker Lopes et al., 2014; Zhao and Chung, 2001; Bagheri et al, 2012). Straus and Miranda-Moreno (2013) formulated a spatial lag regression model to identify the main factors associated specifically with bicycle volumes. This model stipulates that bicycle activity at intersection depends on land-use characteristics, urban form and demographics, geometric design at intersection, cyclist infrastructure and hourly weather conditions. They also include a spatial correlation component that depends on the level of bicycle activity among neighbouring intersection. Grisword et al. (2011) used longlinear ordinary least squares regression to estimate a model of bicycle intersection volume. To create this model, they used bicycle counts intersection, value of explanatory variable such as intersection site characteristics (average slopes, presence of bicycle markings), surrounding land use and transportation system characteristics (intersection density, connected node ratio). Zhao and Chung (2001) generated four regression models using six variables considering function classification of the road, number of lanes, accessibility and employment in the zone. They described strong relationship between AADT and the independent variables with no multicollinearity among them. Apronti et al. (2016) proposed estimating of traffic volume using both linear and logistics regression models. A special GIS tool compatible with ArcGIS 10 to estimate AADT based on linear regression was developed by Lowry and Dixon (2012). Another important piece of information brings using the trajectories of the vehicle which contain valuable data on real time traffic shown on the map. As the technology of the satellite tracking systems and handheld devices improved it came into wide use among cyclists too and useful information on the traffic situation and users' behaviour can be gathered (Donkwook et al. 2014). Using such data to establish cyclist activity is an issue dealt in many recent works proposing heat maps or density maps (Oksanen et al. 2015; Dongwook et al. 2014).

Besides interpolation techniques, one of the widely used estimation methods is based on a Kernel density function introduced in Silverman (1986). It is one of the most popular methods for analysing the underlying properties of point events. Kernel density estimation (KDE) enables to get a smooth output density surface from a simple input scatter plot. This method is also used for finding "hot spots" of traffic accidents in modelling pedestrian and bicycle crashes (Yu and Ai 2014, Prasannakumar et al. 2011; Mohaymany et al. 2013). Amoh-Gyimah et al. (2016) dealt with Random Parameter Negative Binomial model modelling pedestrian and bicycle crashes. Okabe (2008) formulated an unbiased discontinuous and continuous Kernel function method for network where overestimations in density around nodes were eliminated. Among other methods which measure the variation in the mean value of the spatial point pattern across the space (the first order properties) belong Quadrat analysis and Voronoi-based density. On the other hand, geostatistical methods such as Ripley's K-function, Getis's G-statistics and Moran's I function examine the spatial interaction structure of point facilities for spatial patterns (the second order properties) (Yu and Ai 2014; Prasannakumar et al. 2011).

In case of regular dispersion of counting points, real clusters cannot be considered as random distribution available for density estimation and the applicability of interpolation techniques gives more accurate results. Mostly local, exact/aproximative and stochastic interpolation methods are used. Mitra (2009) focuses on methods for identifying hot spots through the use of advanced statistical methods such as empirical Bayes technique considering AADT the most important variable explaining exposure in Safety Performance Functions. Testing done by Selby and Kockleman (2012) showed that predictive capabilities of geographically weighted regression (GWR) were significantly exceeded by kriging methods. They also propose that using network distances for kriging parameters show no enhanced performance comparing to using Euclidean distances. However, some studies deal with using network analysis and quantify the topological importance of a link in a network (Lowry 2014; Lowry et al. 2016; Wang and Kockelman 2009). The method which has been widely used across a number of transportation studies recently is Artificial Neural Network (ANN). This method is used to estimate functions that depend on a large number of inputs (Xu et al. 2016; Sharma et al. 2001). An overall comparison of various methods is presented by Sarlas and Axhausen (2016).

Previously presented interpolation techniques cover possibilities for continuous spatial data interpolation. Besides that, Shiode and Shiode (2011) examined the accuracy of network–based interpolation methods (IDW and OK). Authors found out that both network-based IDW and network-based OK are generally more accurate than their existing counterparts. The network-based methods also turn out to be more sensitive to the edge effect, and their performance improves after edge correction.

Modelling and Estimating the Movement of Cyclists

Modelling of the cycle transport load in the area belongs among current challenges, which are inseparably connected with transport infrastructure planning. Many studies (Barnes and Krizek 2005; Cardoso et al. 2012; Nordback et al. 2013a; Porter et al. 1999; Turner et al. 1999) proofed, that bicycle counts prediction at intersections cannot be generalised, mostly, not very extensive data sets have to be accepted and modelling must be adapted to outputs with high probability accurate estimation. Cycling counts data at monitored intersections can be processed basically as points with quantitatively valued attribute and hence two solutions are proposed: density estimation or fictitious surface interpolation. Density computation can be processed by density estimation methods with Kernel Density function (Silverman 1986) generating smooth density surface. In case of regular distribution of counting points, their real clusters cannot be considered as random distribution available for density estimation and the applicability of interpolation techniques gives more accurate results. Mostly local, exact/approximate and stochastic interpolation techniques might be applied (i.e. IDW—Inverse Distance Weighted, RBF

—Radial Base Function, Kriging etc.). However, some authors (Evans and Pratt 2007; Strauss and Miranda-Moreno 2015) have applied global interpolation techniques based on 'general' regression analysis in their studies. Nevertheless, not all techniques provide accurate outputs. Despite simple processing, IDW can not estimate value over maximum and below minimum. The generation of concentric lines around input points is another disadvantage of IDW (Di Piaza et al. 2011; Watson and Philip 1985). This effect can be smoothed by setting appropriate power coefficient but the smoothing effect is not linear with higher power (Ježek 1999). IDW is mostly used for primary data analysis within further sophisticated interpolation. This disadvantage is eliminated in RBF method, but this is more suitable for smooth surfaces generated from a large amount of input points (Johnston et al. 2001). Kriging methods are according to previous ones more demanding on setting up appropriate parameters in order to express the right curve of the semivariogram (Johnston et al. 2001; Krige 1951).

The diagnostic of interpolation methods as kriging can be calculated in ArcMap with Cross-validation tool. Each of the kriging methods computes the estimated prediction standard errors. In addition to making predictions, we can estimate the variability of the predictions from the true values. If the average standard errors are close to the root mean squared prediction errors, we can correctly assess the variability in prediction. If the average standard errors are greater than the root mean squared prediction errors, the model overestimates the variability of predictions. If the average standard errors are less than the root mean squared prediction errors, we underestimate the variability in predictions. Using Cross-validation results, the following error properties might be evaluated (Johnston et al. 2001).

Mean Error (ME) is the averaged difference between the measured and the predicted values (1).

$$ME = \frac{1}{n}\sum [z(x_i) - z^*(x_i)] \tag{1}$$

Root Mean Square Error (RMSE) indicates how closely the model predicts the measured values (2). The smaller, the better.

$$RMSE\sqrt{\frac{1}{n}\sum [z(x_i) - z^*(x_i)]^2} \tag{2}$$

Average Standard Error (ASE) is the average of the prediction standard errors (3).

$$ASE = \sqrt{\frac{1}{n}\sum \widehat{\sigma}^2(x_i)} \tag{3}$$

Root Mean Square Standardized Error (RMSSE) should be close to one (4), the closer, the better. If the RMSSE is greater than one, the model underestimates the variability in predictions. If the RMSSE is less than one, the model overestimates the variability in predictions.

$$RMSSE = \sqrt{\frac{1}{n}\sum \left[\left(\widehat{Z}(x_i) - z^*(x_i)\right)/\widehat{\sigma}(x_i)\right]^2}, \tag{4}$$

where z is real value and z^* represents estimated value.

Case Study: The City of Přerov

Due to a large amount of input parameters, planning the development and construction of communication lines network means a very difficult process which involves considerable subject approach. It is always important to remember that less is more. Then, it is easier to identify the dominating criteria in the output, which is determined by recognizing them. Three crucial steps were followed to obtain required results: data collection—data analysis and evaluation—output interpretation. Collecting fundamental data was accomplished via bicycle counts at 30 selected intersections. Counting took place on two business days, always on Tuesdays, specifically on May 10 and May 21, 2016. The counting methodology defined counting times both in the morning, 5:30–9:00 a.m., and in the afternoon, 2:00–5:00 p. m. Volunteer counters marked numbers of arrivals and departures of cyclists in *n*-paths intersections, then partial average numbers were computed out of this. This way of counting provides not only the total number of cyclists at intersections but also cycling intensity for each direction. Input dataset completion (road and street network) was dealt with data provided by the Municipal Government of Přerov in the scale of 1:10 000 using ArcGIS for Desktop 10.0. Further data processing was realized in WGS 1984 World Mercator coordinate system. To choose an appropriate interpolation method local, exact/approximate methods IDW, RBF, Simple Kriging, Ordinary Kriging, Universal Kriging and Empirical Bayesian Kriging were considered based on state of the art analysis as useful and examined. For selecting a suitable interpolation technique, the cross validation was taken into account comparing Mean Error (ME), Root Mean Square Error (RMSE), Root Mean Square Standardized Error (RMSSE) and Average Standard Error (ASE). For interpolation of bicycle movement estimation, data from counting points were used. This data was averaged so that an average number of cyclists per 1 h during rush hour was calculated. Six methods were tested when choosing the most suitable interpolation method and significant statistical parameters of their results were compared. Customizing other methods was done by entering parameters so that the best shape of variogram was achieved. Isotropy was also considered.

Testing Interpolation Techniques

An ordinary geostatistical data processing comprises four parts (1) data analysis, (2) structural analysis, (3) applying interpolation technique and (4) evaluation) and is being understood as an iterative procedure, especially between parts 2–4. During **data analysis** basic exploratory statistic data analysis have been completed. Figure 1 documents relatively diagonal direction with lightly significant deviation in Q-Q plot and together with featureless asymmetry (skewness: 0, 35), close mean (76, 1) and median (78, 1) values localized approximately between minimum (24, 1) and maximum (139, 5) indicate normal distribution. It was also confirmed by Shapiro-Wilk normality test that the data came from a normally distributed population. Very often IDW is used also as a primary view on interpolated surface.

Structural analysis focused on spatial correlation and computing empirical and theoretical variogram. This part is typical namely for kriging and evaluating variogram cloud (Fig. 2) is a part of it. Here we can see relatively high dissimilarity in middle distances and small density of couples near the beginning of the cloud which is very important for nugget setting. Than chosen techniques have been applied and their results were compared based on error and cross-validation parameters.

For comparative analysis, seven settings (IDW, EBK, RBF, Ordinary Kriging (OK) with spherical variogram, Ordinary Kriging (OK) with linear variogram, Simple Kriging (SK) with spherical variogram and Simple Kriging (SK) with linear variogram) for data set interpolation have been considered based on the state of the art. Although Universal Kriging (with spherical or linear variogram) is recommended as a useful tool (Ježek 1999), generated surfaces did not reflect movement of cyclists and this technique has not been applied in the study. Cross-validation

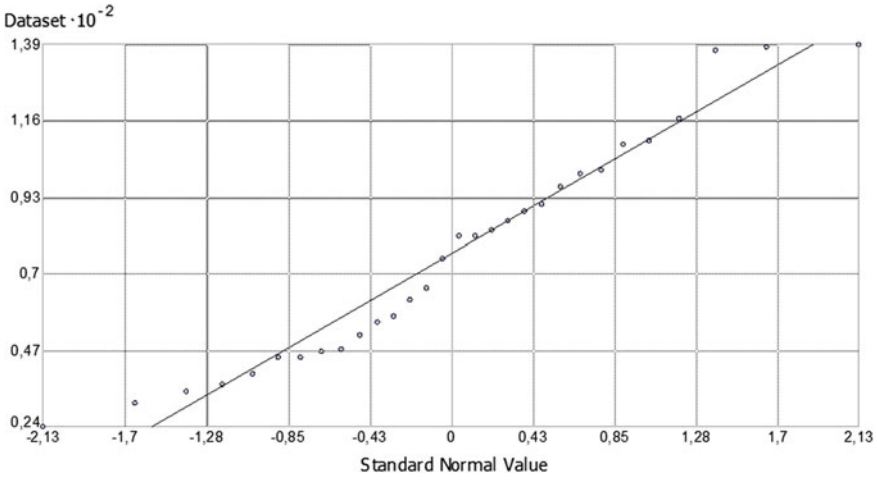

Fig. 1 Normal Q-Q plot of input data set

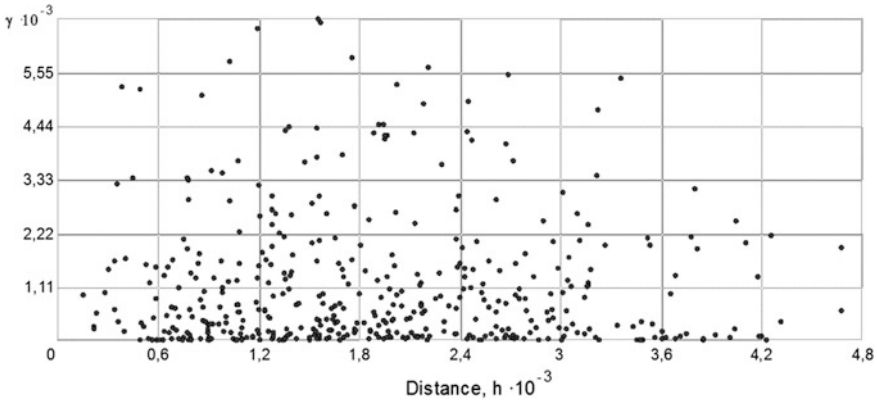

Fig. 2 Variogram cloud of input data set

Table 2 Cross-validation results

Method/error	ME	RMSE	RMSSE	ASE	ID 3 residue	ID 25 residue
IDW (coefficient = 2)	3.8673	32.9553	–	–	48.9	**0.05**
RBF (multiquadric)	2.8621	45.7472	–	–	48.91	**−38.4**
EBK	**0.7395**	32.767	**0.9684**	**33.9832**	−23.72	53.69
OK (spherical variogram)	**0.894**	32.0088	**0.9483**	**33.9183**	−21.53	43.58
OK (linear variogram)	0.9536	32.1266	0.9475	34.0735	−25.49	**42.27**
SK (spherical variogram)	2.1803	**31.8536**	0.9095	34.5406	**−19.88**	46.06
SK (linear variogram)	2.1522	**31.286**	0.9052	34.6201	**−20.27**	46.39

was followed in order to compare measured errors and two residues in two farthest points (ID 3 and ID 25) (Table 2). Two best results in evaluated criteria were typed in bold. The evaluation shows that IDW and RBF have worst results although IDW was the most accurate in prediction of point ID 25 which is caused by computing average values in predicted surface. EBK and OK (spherical variogram) achieved very similar values. Both have smallest ME and ASE is relatively close to RMSE which declares suitable variability of predicted values. These two methods will be compared in detail. Other methods gave satisfactory results but with worse errors than EBK and OK (spherical variogram).

Cross-validation results for EBK (Fig. 3) and OK (spherical variogram) (Fig. 4) shows that both method overestimate smaller values and underestimate higher values. The same was determined at both Simple Kriging methods. Opposite EBK, OK (spherical variogram) has regression line closer to theoretically needed diagonal line (compare Figs. 3 and 4).

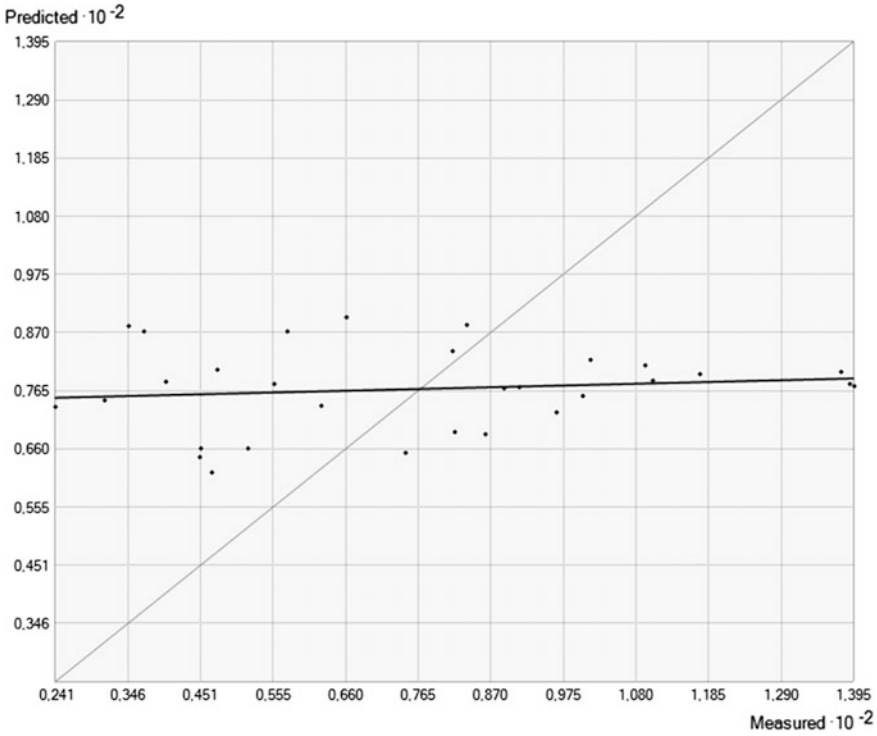

Fig. 3 Cross-validation results of RBK

Deeper analysis of individual variograms and generated prediction surfaces revealed significant differences. Variogram of EBK (Fig. 5) was set as a result of 100 simulations with standard circular neighborhood type. It is visible that empirical variogram (represented by crosses) oscillates along theoretical variogram (full line) with higher amplitude which can increase the prediction. The EBK prediction map (Fig. 6) estimates higher values in the middle of interpolated area and creates graded zones of smaller values southward from the centre of the city. The surface is relatively smooth and does not estimate enclaves of unexpected values. Farthest areas are estimated without significant changeability.

Variogram of OK (Fig. 7) was achieved with lag size of 290 m and 12 lags with nugget 936.7. Opposite EBK's variogram, theoretical variogram better fits empirical variogram. Prediction surface (Fig. 8) is less smoothed but estimates farthest input points (see ID 3 and ID 25 in Table 2) with higher accuracy. Densest area of input points is realistically graded in order to cyclists' movement. Partial uncertainty of predictions can be seen in southwest corner where values without input points are estimated not quite good for cyclists' movement.

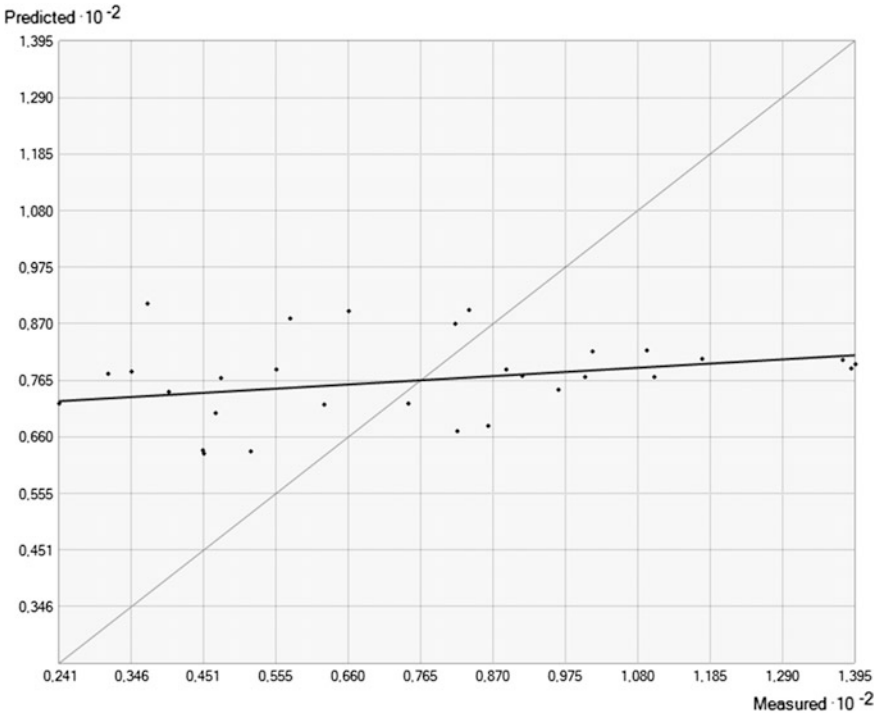

Fig. 4 Cross-validation results of OK (spherical variogram)

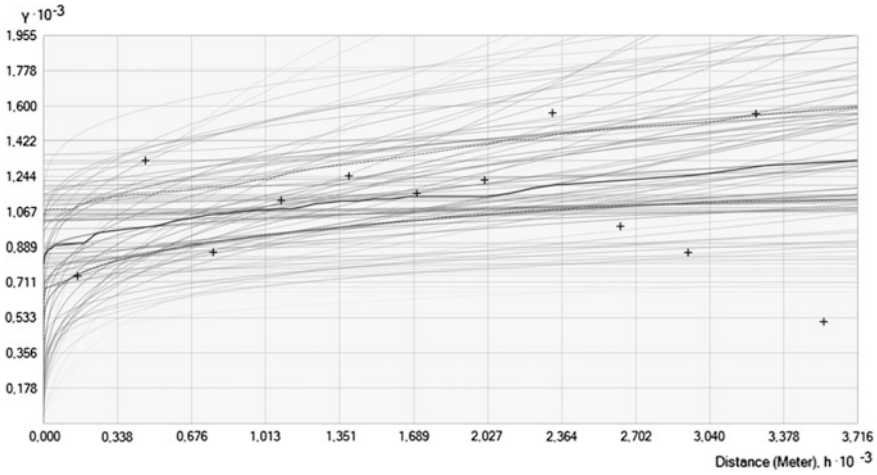

Fig. 5 Variogram of EBK

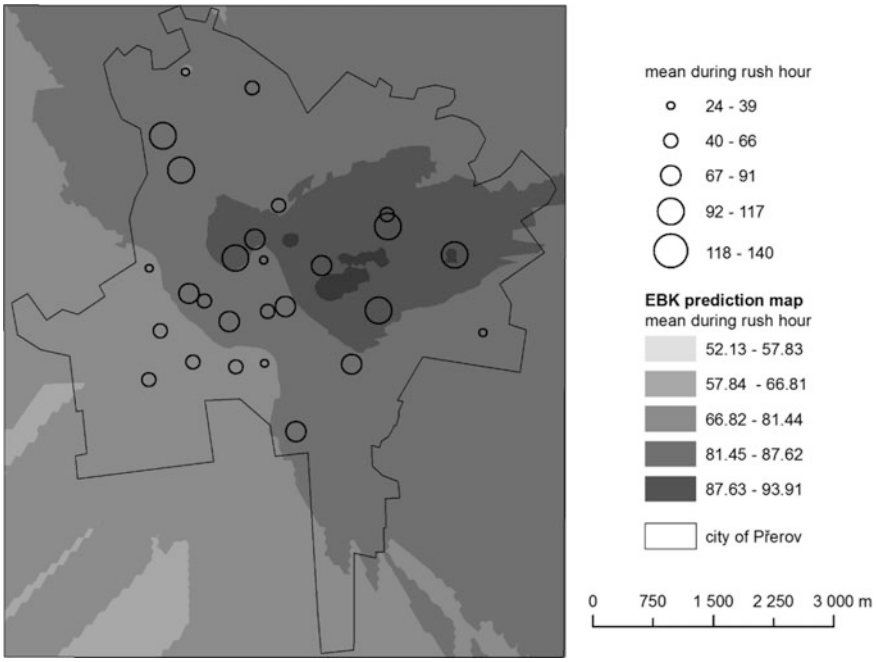

Fig. 6 Prediction map of EBK

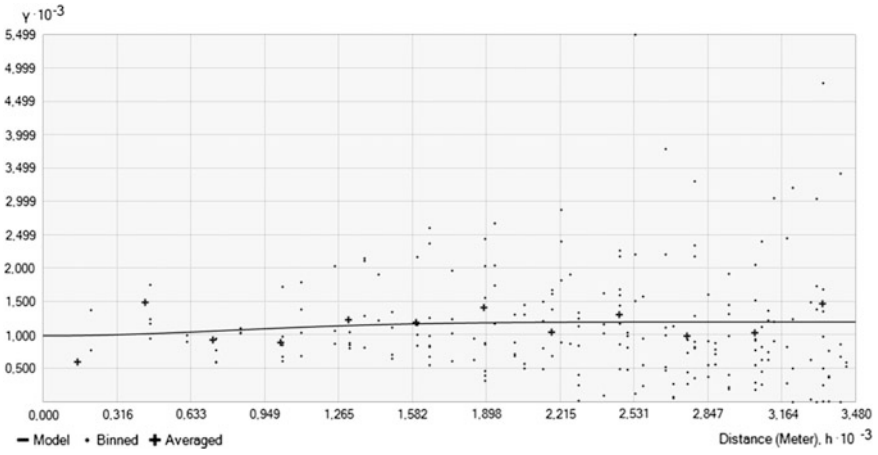

Fig. 7 Variogram of ordinary kriging (spherical variogram)

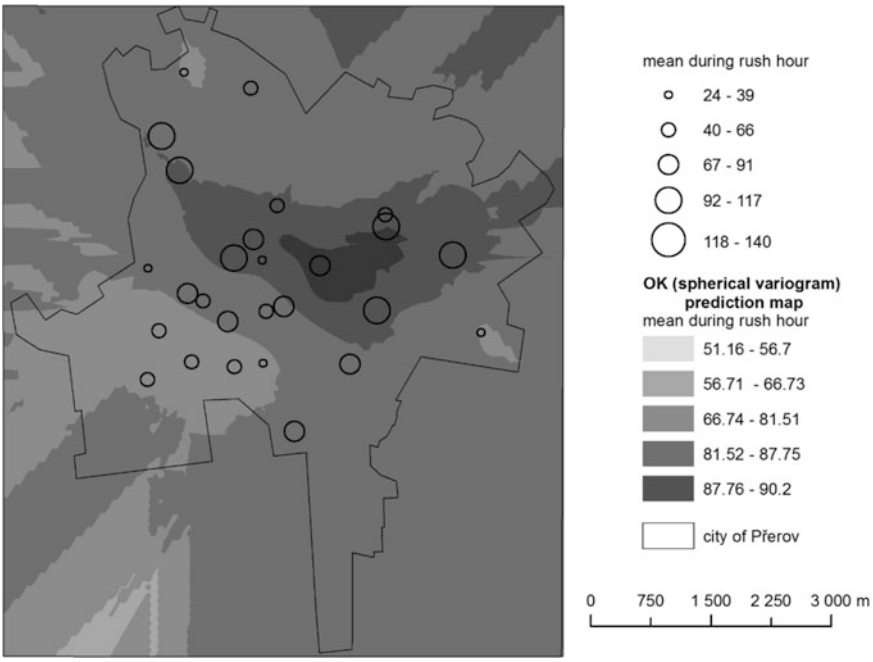

Fig. 8 Prediction map of ordinary kriging (spherical variogram)

Conclusion Remarks

Predicting cyclist's movement as an example of socioeconomic activity is very difficult but also very challenging task. This kind of activity is associated with attributes describing both the interest of cyclists and the existing infrastructure of cycle paths or any other line transport infrastructure. Counting points providing input data are irregularly distributed with prevailing clusters and vast unmeasured areas. Therefore, estimating needed values is fraught with high uncertainty.

Based on actual surveys, interpolation techniques were examined as suitable tool for predicts. Seven methods have been chosen to test their results using cross-validation parameters. Important to note that individual evaluation of these parameters does not bring satisfactory decision (e.g. ASE is fraught with existing outliers). Combination and interrelation of these errors give an opportunity for comparison and assessment.

During the evaluation two best results within each parameter were highlighted. EBK and OK (spherical variogram) reached the highest score. Next in line, simple kriging methods did not receive bad error parameters including predicts of farthest input points. On the contrary, they generated too much smoothed and simplified surface unsuitable to distinguish more details. Better fitting theoretical variogram

and smaller errors in predicts of farthest points evaluated OK (spherical variogram) as the best interpolator.

Understanding another factors determining the movement of cyclists put forward for consideration that implementation of another form of regression analysis (e.g. weighted geographical regression) completed with factor analysis could take into account those factors that significantly influence the movement of cyclists.

References

Amoh-Gyimah, R., Saberi, M., & Majid, S. (2016). Macroscopic modeling of pedestrian and bicycle crashes: Across-comparison of estimation methods. *Accident Analysis and Prevention, 93,* 147–159.

Apronti, D., Ksaibati, K., Gerow, K., & Hepner J. J. (2016). Estimating traffic volume on Wyoming low volume roads using linear and logistic regression methods. *Journal of Traffic and Transportation Engineering*. (in Print).

Bagheri, E., Zhong, M., & Christie, J. (2012). *Spatial analysis of traffic growth and variations and their implications to the operations of a traffic monitoring program.* Available from: http://conf.tac-atc.ca/english/annualconference/tac2012/docs/session18/bagheri.pdf. (cit 2016-11-16).

Barnes, G., & Krizek, K. (2005). Estimating bicycling demand. *Transportation Research Record: Journal of the Transportation Research Board, 1939*(1), 45–51.

Becker Lopes, S. B., Margarido Brondino, N. C., & da Silva, A. N. R. (2014). GIS-based analytical tools for transport planning: Spatial regression models for transportation demand forecast. *ISPRS International Journal of Geo-Information, 3,* 565–583.

Cardoso, O. D., García-Palomares, J. C., & Gutiérrez, J. (2012). Application of geographically weighted regression to the direct forecasting of transit ridership at station-level. *Applied Geography, 34,* 548–558.

Caulfield, B., Brick, E., & McCarthy, O. T. (2012). Determining bicycle infrastructure preferences —A case study of Dublin. *Transportation Research Part D, 17,* 413–417.

Di Piazza, A., Lo Conti, F., Noto, L. V., Viola, F., & La Loggia, G. (2011). Comparative analysis of different techniques for spatial interpolation of rainfall data to create a serially complete monthly time series of precipitation for Sicily, Italy. *International Journal of Applied Earth Observation and Geoinformation, 13*(3), 396–408.

Donkwook, L., Jinsul, K., & Minsoo, H. (2014). Density map visualization for overlapping bicycle trajectories. *Journal of Control and Automation, 7*(3), 327–332.

Esawey, M. E. (2014). Estimation of annual average daily bicycle traffic using adjustment factors. *Transportation Research Record: Journal of the Transportation Research Board, 2443,* 106–114.

Esawey, M., El Lim, C., Sayed, T., & Mosa, A. I. (2013). Development of daily adjustment factors for bicycle traffic. *Journal Transportation Engeneering, 139*(8), 859–871.

Evans, J. E., & Pratt, R. H. (2007). *Transit oriented development*. In TCRP Report 95, Chap. 17, 138 p.

Griswold, J. B., Medury, A., & Schneider, R. J. (2011). *Pilot models for estimating bicycle intersection volumes*. Available from: http://escholarship.org/uc/item/380855q6. (cit 2007-08-02).

Ježek, J. (1999). *Geostatisika a prostorová interpolace*. Praha: Nakladatelství Karolinum.

Johnston, K., Ver Hoef, J. M., Krivoruchko, K., Lucas, N. (2001). *Using ArcGIS® Geostatistical Analyst. 2001*. Available from: http://downloads2.esri.com/support/documentation/ao_/Using_ArcGIS_Geostatistical_Analyst.pdf. (cit. 2016-08-20).

Krige, D. G. (1951). A statistical approach to some basic mine valuation problems on the Witwatersrand. *The journal of the Chemical, Metallurgical & Mining Society of South Africa, 52*(6), 119–139.

Landis, B. W., Vattikuti, V. R., & Brannick, M. T. (1997). Real-time human perceptions: Toward a bicycle level of service. *Transportation Research Record, 1578,* 119–126.

Larsen, J., Patterson, Z., & El-Geneidy, A. (2013). Build it. But where? The use of geographic information systems in identifying locations for new cycling infrastructure. *International Journal of Sustainable Transportation., 7*(4), 299–317.

Lindsey, G., Nordback, K., & Figliozzi, M. A. (2014). *Institutionalizing bicycle and pedestrian monitoring programs in three states: Progress and challenges*. Available from: http://www.pdx.edu/ibpi/sites/www.pdx.edu.ibpi/files/14-4181_in_Compendium.pdf, (cit. 2016-07-19).

Lowry, M. (2014). Spatial interpolation of traffic counts based on origin–destination centrality. *Journal of Transport Geography, 36,* 98–105.

Lowry, M., & Dixon, M. (2012). *GIS tools to estimate average annual daily traffic*. Available from: http://ntl.bts.gov/lib/45000/45900/45948/KLK725_N12-03.pdf. (cit. 2016-11-27).

Lowry, M., Furth, P., & Haden-Loh, T. (2016). Prioritizing new bicycle facilities to improve low-stress network connectivity. *Transportation Research Part A, 86,* 124–140.

Lundberg, B., & Weber, J. (2016). Non-motorized transport and university populations: An analysis of connectivity and network perceptions. *Journal of Transport Geography, 39,* 165–178.

Milakis, D., & Athansopoulos, K. (2014). What about people in cycle network planning? Applying participative multicriteria GIS analysis in the case of the Athens metropolitan cycle network. *Journal of Transport Geography, 35,* 120–129.

Mitra, S. (2009). Spatial autocorrelation and Bayesian spatial statistical method for analyzing intersections prone to injury crashes. *Transportation Research Record Journal of the Transportation Research Board., 2136,* 92–100.

Mohamad, D., Sinha, K., Kuczek, T., & Scholer, C. (1998). Annual average daily traffic prediction model for county roads. *Transportation Research Record: Journal of the Transportation Research Board, 1617,* 69–77.

Mohaymany, A. S., Shahri, M., & Mirbagheri, B. (2013). GIS-based method for detecting high-crash-risk road segments using network kernel density estimation. *Geo-spatial Information Science., 16*(2), 113–119.

National Bicycle and Pedestrian Documentation Project. (2009). Available from: www.bikeped-documentation.org. (cit. 2016-11-16).

Nordback, K., Marshall, W. E., & Janson, B. N. (2013a). Development of estimation methodology for bicycle and Pedestrian volumes based on existing counts. Available from: http://www.coloradodot.info/programs/research/pdfs. (cit. 2007-07-28).

Nordback, K., Marshall, W. E., Janson, B. N., & Stolz, E. (2013b). Estimating annual average daily bicyclists: Error and accuracy. *Transportation Research Record: Journal of the Transportation Research Board, 2339,* 90–97.

Nosal, T. (2014). Improving the accuracy of bicycle AADT estimation: Temporal patterns, weather and bicycle AADT estimation methods. Available from: http://digitool.library.mcgill.ca/webclient/StreamGate?folder_id=0&dvs=1472369098397 ~ 876&usePid1=true&usePid2=true. (cit. 2016-07-29).

Okabe, A. (2008). A kernel density estimation method for networks, its computational method and a GIS-based tool. *International Journal of Geographical Information Science, 23*(1), 7–32.

Oksanen, J., Bergman, C., Sanio, J., & Westerholm, J. (2015). *Journal of Transport Geography, 48*, 135–144.

Porter, C., Suhrbier, J., & Schwartz, W. L. (1999). Forecasting bicycle and Pedestrian travel state of the practise and research needs. *Transportation Research Record, 1674,* 94–101.

Prasannakumar, V., Vijith, H., Charutha, R., & Geetha, N. (2011). Spatio-temporal clustering of road accidents: GIS based analysis and assessment. *Procedia—Social and Behavioral Sciences., 21,* 317–325.

Roll, J. F. (2013). Bicycle traffic count factoring: An examination of national, state and locally derived daily extrapolation factors. Available from: http://pdxscholar.library.pdx.edu/open_access_etds/998. (cit. 2016-08-02).

Rybarczyk, G., & Wu, C. (2010). Bicycle facility planning using GIS and multi-criteria decision analysis. *Applied Geography, 30*, 282–293.

Salon, D. (2016). Estimating pedestrian and cyclist activity at the neighborhood scale. *Journal of Transport Geography, 55,* 11–21.

Sarlas, G., & Axhausen, K. A. (2016). *Exploring spatial methods or prediction of traffic volumes*. In Conference Paper of 16th Swiss Transport Research Conference, STRC, Ascona, Switzerland, May 18–20, 2016

Selby, B., & Kockelman, K. M. (2012). Spatial prediction of traffic levels in unmeasured locations: Applications of universal kriging and geographically weighted regression. *Journal of Transport Geography, 29,* 24–32.

Shafizadeh, K., & Niemeier, D. (1997). Bicycle journey-to-work travel behavior characteristics and spatial attributes. *Transportation Research Record: Journal of the Transportation Research Board., 1578,* 84–90.

Sharma, S., Lingras, P., Xu, F., & Kilburn, P. (2001). Application of neural networks to estimate AADT on low-volume roads. *Journal of Transportation Engineering., 127*(5), 426–432.

Shiode, N., & Shiode, S. (2011). Street-level spatial interpolation using network-based idw and ordinary kriging. *Transaction in GIS, 15*(4), 457–477.

Silverman, B. (1986). *Density estimation for statistics and data analysis*. Available from: https://ned.ipac.caltech.edu/level5/March02/Silverman/paper.pdf. (cit. 2016-17-11).

Strauss, J., & Miranda-Moreno, L. F. (2013). Spatial modeling of bicycle activity at signalized intersections. *The Journal of Transport and Land Use, 6*(2), 47–58.

Strauss, J., Miranda-Moreno, L. F., & Morency, P. (2015). Mapping cyclist activity and injury risk in a network combining smartphone GPS data and bicycle counts. *Accident Analysis and Prevention. 83*, 132–142.

Turner, S., Hottenstein, A., & Shunk, G. (1999). *Bicycle and pedestrian travel demand forecasting: Literature review*. Available from: http://d2dtl5nnlpfr0r.cloudfront.net/tti.tamu.edu/documents/1723-1.pdf. (cit. 2016-07-19).

Wang, X., & Kockelman, K. M. (2009). Forecasting network data: Spatial interpolation of traffuc counts using texas data. *Transportation Record., 2150,* 100–108.

Watson, D. F., & Philip, G. M. (1985). A refinement of inverse distance weighted interpolation. *Geoprocessing, 2,* 315–327.

Xia, Q., Zhao, F., Chen, Z., Shen, L., & Ospina, D. (1999). Estimation of annual average daily traffic for nonstate roads in a Florida county. *Transport Research Record, 1660,* 32–40.

Xu, Y., Shaw, S., Fang, Z., & Yin, L. (2016). Estimating potential demand of bicycle tripsfrom mobile phone data—An anchor-point based approach. *ISPRS International Journal of Geo-Information, 5*(8), 131–154.

Yu, W., & Ai, T. (2014). *The visualization and analysis of urban facility pois using network kernel density estimation constrained by multi-factors*. Available from: http://www.scielo.br/scielo.php?script=sci_arttext&pid=S1982-21702014000400902&lng=en&nrm=iso&tlng=en. (cit. 2016-11-17).

Zhao, F., & Chung, S. (2001). Contributing factors of annual average daily traffic in a Florida County: Exploration with geographic information system and regression models. *Transportation Research Record, 1769,* 113–122.

New Approach to Import 3D Geodata for Remcom Wireless Insite

Jan Růžička, Libor Michálek and Kateřina Růžičková

Abstract The paper is focused on developing a new approach how automatically process 3D geospatial data for Remcom Wireless InSite. Remcom Wireless InSite is a software tool which provides efficient and accurate predictions of an electromagnetic waves propagation and a communication channel characteristics in complex urban, indoor, rural and mixed path environments. The Wireless InSite is able to import a 3D geospatial model, that consists of a DTM (Digital Terrain Model) and objects (buildings). To be able to perform any predictions, we need to import different geodata objects into Wireless InSite and run calculations in an automated way. We tested several available functions for importing geodata to Wireless InSite. All of them have some drawbacks that made us do free import/export tool that reads data from 3D GIS (Geographic Information System) database and exports them to the form that can be directly read by Wireless InSite. The main advantage of this approach is complete control over the import and export processes. For example, we can specify the LOD (Level of Detail) for import, or we can specify for each different object the type of material.

Keywords Remcom · Wireless · InSite · 3D geodata · DTM · Propagation · Import · Export

J. Růžička (✉) · K. Růžičková
Institute of Geoinformatics, Faculty of Mining and Geology, VSB-Technical University of Ostrava, 17. listopadu 15, 70833 Ostrava, Czech Republic
e-mail: jan.ruzicka@vsb.cz

K. Růžičková
e-mail: katerina.ruzickova@vsb.cz

L. Michálek
Department of Telecommunication, Faculty of Electrical Engineering and Computer Science, VSB-Technical University of Ostrava, 17. listopadu 15, 70833 Ostrava, Czech Republic
e-mail: libor.michalek@vsb.cz

I. Ivan et al. (eds.), *Dynamics in GIscience*, Lecture Notes in Geoinformation and Cartography, DOI 10.1007/978-3-319-61297-3_29

Introduction

The Wireless InSite is a powerful professional software tool for modeling an electromagnetic signal propagation in rural, urban and indoor environments. The tool performs accurate analysis of the impact of the physical environment on the performance of wireless communication systems. The Wireless Insite system allows using many propagation models. For verifying the tool accuracy, we use Remcom's X3D high fidelity ray-tracing model. X3D is a 3D propagation model, so there are no restrictions on geometry shape or transmitter/receiver height. The model includes effects from reflections, diffractions, transmissions, and atmospheric absorptions. Applications include urban, indoor, and indoor-outdoor propagation scenarios. As a result from simulation, characteristics such as a path loss, a delay, a delay spread, the direction of arrival or a complex impulse response can be obtained. Wireless InSite now supports the import and creation of KMZ (Keyhole Markup Language Zipped) (GOOGLE 2016) and COLLADA (Collaborative Design Activity) geometry files (KHRONOS 2016). These file types are imported as objects, and are particularly useful for adding single structures, such as bridges, high-resolution buildings, or new constructions, to a scene. These formats are international standards supported by much 3D DCC (Digital Content Creation) tools and 3D Geographic Information System tools (REMCOM 2016).

Despite this new support, no automatic tool for importing a larger amount of DTM object still exists. If the user wants to import many objects, it is necessary to do this manually, one after another. Our effort is, therefore, concentrated on developing a tool for automatic importing of 3D geodata objects for Wireless Insite.

The following state of art concern with methods how to import 3D models of objects into Wireless InSite. In Semkin et al. (2016), a geometrical model of the target building has been created in CAD software PTC Creo by using the outline size adopted from Google Maps. In Karner et al. (2016) an AutoCAD DXF format was used for importing the blocks with the correct heights and ground plot into Wireless InSite. In Hrovat et al. (2012), import the indoor simulation environment, including complex geometries of tunnels, from other CAD programs into Wireless InSite was proposed. In Youssef (2004), the model of the cabin was created in an AUTOCAD capable program and then imported to Wireless Insite as drawing exchange file (DXF). Unfortunately, all of these approaches use always manual import from a certain 3rd party application.

Modeled Scene

Modeled scene is a base of input dataset for modeling. It consists of DTM (Digital Terrain Model) and objects on the terrain. In general, DTM can be represented by a regular or irregular field of elevations with processing algorithm to render terrain continuously (Wilson and Gallant 2000). The most common regular structure is

square grid DEM (Digital Elevation Model). Its regularity is a significant advantage for automatic processing of the data. On the other hand, this model is often considered to be surface as DSM (Digital Surface Model) representation (El-Sheimy 2005). It means that it includes the maximum elevation everywhere (includes canopy, the roof of buildings and top of trees). However, this meaning of DEM is not clear (GIS Debaters 2016), a DSM should be used. The regular structure can also represent DSM. DSM format (also with vegetation geometry) can be imported by Wireless InSite, as a model of terrain.

However, we usually generate more detailed and genuine 3D model of buildings separately out of DSM. Therefore, it is more appropriate to process a model for terrain and buildings separately. For that reason, we use bare-earth terrain model. In this case, DTM describes morphological elements of terrain. We use 2.5D spatial dimension representation since terrain rarely contains overhang features such as crag or cave. The irregular data structure for terrain is here represented by TIN (Triangulated Irregular Network), which allows better representation of hard shapes in terrain and efficiently save disk memory. Since analytical functions over the terrain prefer regular data structures, they must often be converted into them.

Unfortunately, in simulation models, it is common that DTM formats are transformed into some internal structure. The failure to comply with format standards cause issues in the field of data transforming and proper importing into simulation models.

Level of Detail

The relationship between DTM and objects (correct location of buildings on terrain) we process as a dataset. In spatial topology, we firstly solved intersection view of objects with the terrain since the objects must have its exact footprint in terrain.

Kolbe et al. (2005) stated 5 levels of building model detail for city models for CityGML. Nowadays CityGML standard denotes (Open Geospatial Consortium 2012):

- LOD0—model contains 2.5D DTM with footprint of buildings
- LOD1—extrusion building footprints into block model without roof structures
- LOD2—building model including roof structures
- LOD3—building model including detailed architecture (detailed wall and roof structures; with doors and windows)
- LOD4—building model including interior model (interior door, stairs, furniture)

In view of building model, it makes increasing complexity: footprint > block model > coarse exterior > fine exterior > interior.

Beside CityGML, BLOM and NAVTEQ as the new approach are used (Biljecki 2013). The levels are primarily defined for multi-resolution models and a scalable digital representation, but it can also be utilized for a detail signification of

Table 1 Comparison of the accuracy of DTM data obtained by different techniques (Li et al. 2005)

Methods of data acquisition	Accuracy of data
Ground measurement (including GPS)	1–10 cm
Digitized contour data	About 1/3 of contouring interval
Laser altimetry	0.5–2 m
Radargrammetry	10–100 m
Aerial photogrammetry	0.1–1 m
SAR interferometry	5–20 m

one-scale data. We can easily construct a simple vector model (LOD0 and LOD1) of a building in traditional GIS software, or it can be derived from a remote sensing (e.g., laser scanning). This software can also transform the data into a multipatch structure and export it into the COLLADA format. However, more complex model (from LOD2) is necessary to process in CAD (Computer Aided Design) environments.

LOD is associated with data accuracy. Table 1 shows the usual accuracy of data, that can be used for building DTM and 3D objects on the surface.

Methodology

The main question of our research was to determine if we can import 3D geodata to Wireless InSite automatically and if we can specify LOD or DTM accuracy during the process of import. When possible, we can develop various scenarios, that can be used to determine the sensitivity of the model to input 3D geodata. We are mainly interested in sensitivity of models to LOD and a spatial resolution of DTM.

Common Approach

According to REMCOM (2016), we define a model by GUI (Graphical User Interface), where we import DTM and buildings from the list of supported formats. Data are transformed into internal formats, which we describe as follows.

The input format for terrain is DTM, supported by GDAL (Geospatial Data Abstraction Library), (GDAL 2016). The output format is TER, which is the TIN in any case. The input format for the object is KMZ and COLLADA. Output data format is OBJECT which is TIN in any case. For the each object, we can specify a construction material.

New Approach for Model Import

Data are stored in a 3D geodatabase which is based on PostgreSQL/PostGIS system (POSTGIS 2016). In DTM, we can reduce specified parameters, but the reduction should be heterogeneous. The output file in TER format can have areas with a high or low density of triangles. Type of the material for each triangle can be specified according to the type of ground. We export the objects to individual files in OBJECT format according to the required LOD. A different kind of material can also specify for each triangle of the building. We plan to use TIN format for input as well in the future.

We developed a tool for automatic export the geospatial data in the format which can be directly imported into Wireless InSite. The tool is developed in Java language with libraries such as Java Topology Suite or GeoTools. The software reads data from 3D geodatabase and GRID data files.

GRID processing is quite simple. The software reads GRID into memory. The software reads landuse raster into memory. Then it iterates on rows and builds for each pixel two triangles that represent GRID value according to value in pixel and according to surrounding pixels. For each triangle is specified material which is based on pixel value on landuse raster. In a case when the user wants to reduce the number of pixels in some areas, the areas must be specified with another mask raster, which holds reduction ratio. If the reduction is required, the interpolation is performed in an easy way. The average value is calculated for each reduced pixel. Output triangles are stored in TER file.

3D buildings we processed in a more complicated way. The data about objects are read from the 3D geodatabase. For each object is calculated a set of triangles, that are appropriate to object definition. For each triangle is specified material based on attributes defined in the 3D geodatabase. The definition of the building in the database relies on the definition of 2.5D elements that together form a 3D building. The building is divided into several parts. In the most simple way, the building is divided into base and roof. The database can also contain information about objects on roofs, such as solar power station blocks. The database can contain other elements that are part of the building, such as hedge or clerestory. Windows and doors are defined by 2.5D elements as well. Each of the element from the database is converted to OBJECT format.

Resulting Format Structures

TER Format

TER format is an internal format of Wireless InSite based on the definition of triangles for DTM and definition of position in space. Each triangle can include information about a material. The structure of the format is described in Fig. 1.

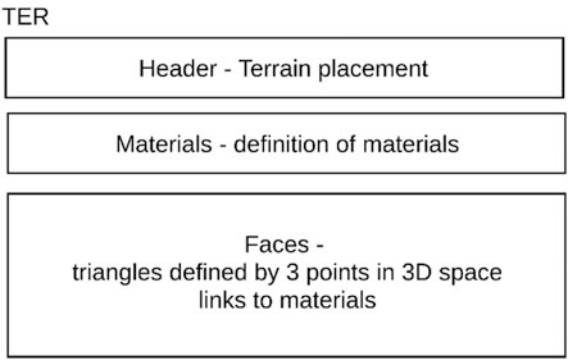

Fig. 1 TER format structure

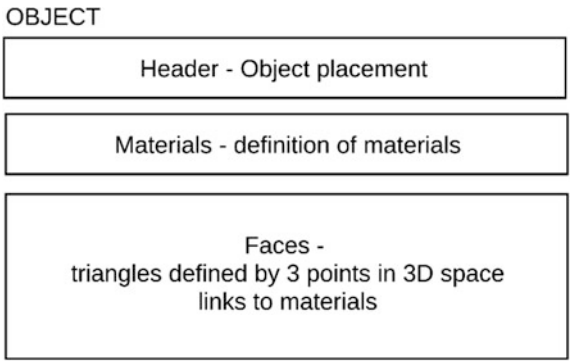

Fig. 2 OBJECT format structure

OBJECT Format

OBJECT format is an internal format of Wireless InSite based on the definition of triangles for objects on DTM and definition of position in space. Each triangle can also include information about a material. The structure of the format is described in Fig. 2.

PROJECT Format

PROJECT is an internal format of Wireless InSite based on the definition of a study area. We define in this format links to DTM, objects, the location of receivers and transmitters, study area parameters, and other parameters for simulation. The structure of the format is described in Fig. 3.

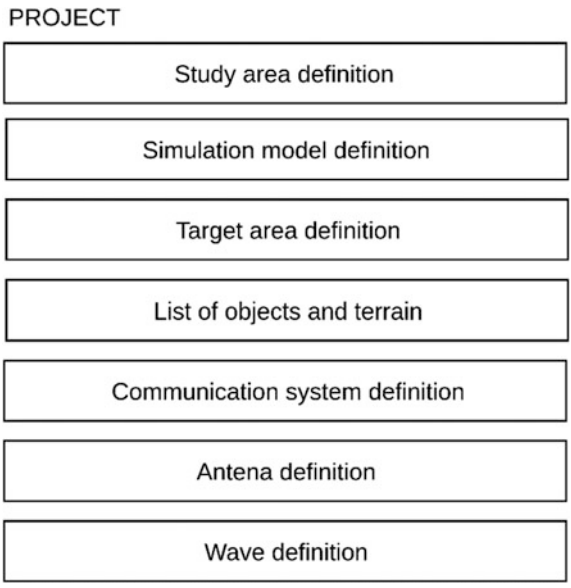

Fig. 3 PROJECT format structure

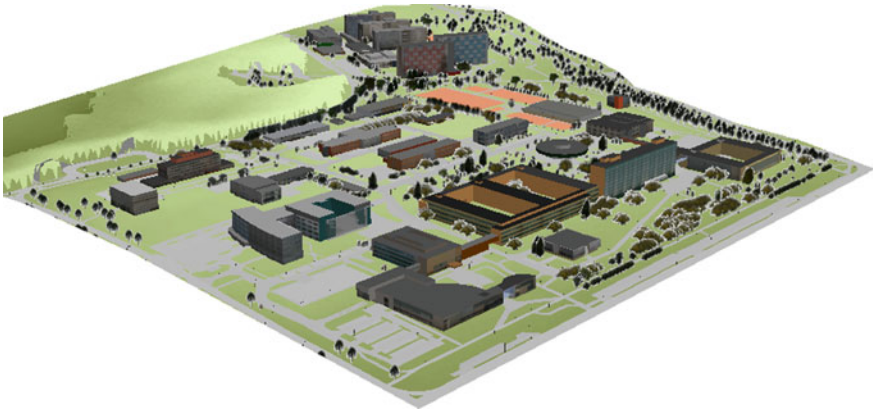

Fig. 4 VSB-Technical University of Ostrava campus

Validation and Results

We tested and validated the new approach for importing 3D geodata into Wireless InSite. For project creation, we used the geodata of university campus of VSB-Technical University of Ostrava (see Fig. 4). Using the developed tool (GIStoINSITE), we converted data from 3D geodatabase to TER, OBJECT and PROJECT file. These records were directly opened in Wireless InSite.

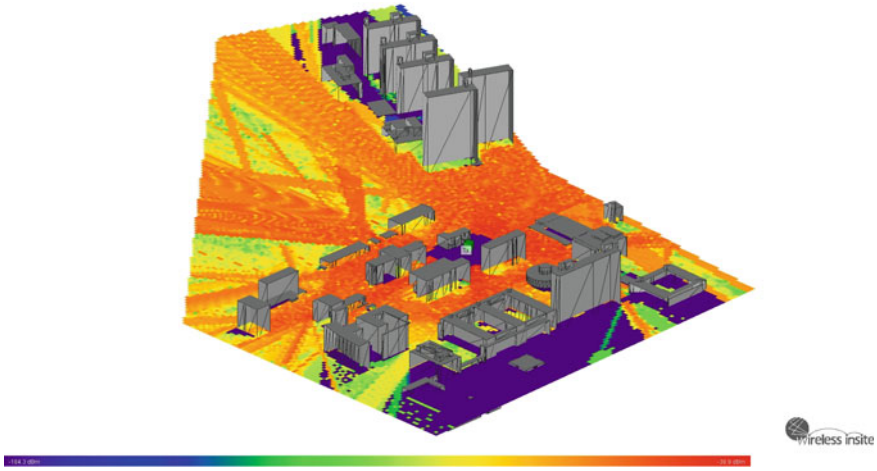

Fig. 5 Study area in wireless InSite with the requested receive level

The TER contains information about terrain profile with an accuracy of 1 m. The OBJECT file contains over 200 partial objects, which represents the concluding shape of 40 buildings on a university campus. The amount of the partial objects is based on LOD. Therefore, according to LOD, we can increase the number of partial objects to hundreds. In the PROJECT file, information about features, materials, waveforms, antennas, transmitters, receivers and study area we define. We defined calculations of the overall area by defining study area approximately 2 × 2 km wide.

In Wireless InSite, the calculations are made by shooting rays from the transmitters and propagating them through the defined geometry. These rays interact with regular features and make their way to receiver locations. Ray interactions include reflections from feature faces, diffractions around feature edges, and transmissions through features faces. At receiver location, contributions from arriving ray paths are combined and evaluated to determine predicted quantities such as received power, path loss or impulse response. Figure 5 shows an output of the study area with the requested receive level.

We observed that import of files from GIStoINSITE to Wireless InSite is correct since the series of simulations that we have performed passed successfully.

Conclusion and Discussion

We can conclude that the developed tool using a new approach for exporting and importing 3D geospatial data can correctly generate project file for Wireless InSite. The output file can differ in DTM accuracy, LOD accuracy and in essence, it is possible to modify any parameters for the whole triangular network.

Our future work focuses on sensitivity analyses which need many models with specific LOD. Presented approach help us to overcome manual importing of models into Wireless InSite and in fact, get more appropriate results. We also assume that sensitivity analyses show the new field of research using Wireless InSite tool.

Acknowledgements The research received financial support from the SGS Grant No. SP2016/170, VŠB-Technical University of Ostrava, Czech Republic.

References

Biljecki, F. (2013). *The concept of level of detail in 3D city models* (70 pp). PhD Research Proposal, TU Delft, February 2013. ISBN 978-90-77029-36-7.

El-Sheimy, N., et al. (2005). *Digital terrain modelling. Acquisition, manipulation, and applications* (257 pp). Norwood: Artech house, Inc. ISBN 1-58053-921-1.

GDAL. (2016). *GDAL—Geospatial data abstraction library* [online]. Accessed November 24, 2016. Available from: http://www.gdal.org/

GIS DEBATERS. (2016). *Geographic Information System. What is the difference between DEM, DSM and DTM*. [online]. Accessed November 24, 2016. Available from: http://gis.stackexchange.com/questions/5701/what-is-the-difference-between-dem-dsm-and-dtm

GOOGLE. (2016). *Keyhole markup language* [online]. Accessed November 24, 2016. Available from: https://developers.google.com/kml/documentation/

Hrovat, A., et al. (2012). Path loss analyses in tunnels and underground corridors. *International Journal of Communication, 6*(3), 136–144.

Karner, W., et al. (2016). *Indoor coverage prediction and optimization for UMTS macro cells* (pp. 625–630). In: 2006 3rd International Symposium on Wireless Communication Systems. IEEE.

KHRONOS. (2016). *COLLADA* [online]. Accessed November 24, 2016. Available from: https://www.khronos.org/collada/

Kolbe, T., et al. (2005). *CityGML—Interoperable access to 3D city models*. In S. Zlatonova &M. Oosterom (Eds.) Proceedings of International Symposium on Geo-information for Disaster Management. Delft: Springer, March 21–23, 2005.

Li, Z., et al. (2005). *Digital terrain modelling, principles and methodology* (p. 165). New York: CRC Press. ISBN 0-415-32462-9.

Open Geospatial Consortium. (2012). *CityGML* [online]. Accessed November 24, 2016. Available from: http://www.opengeospatial.org/standards/citygml

POSTGIS. (2016). *PostGIS* [online]. Accessed November 30, 2016. Available from: https://postgis.org/

REMCOM, Inc. (2016). *Wireless InSite* [online]. Accessed November 30, 2016. Available from: http://www.remcom.com/wireless-insite/

Semkin, V., et al. (2016) Characterization of radio links at 60 GHz using simple geometrical and highly accurate 3D models. *IEEE Transactions on Vehicular Technology*.

Wilson, P. J., & Gallant, C. J. (2000). *Terrain analysis, principles, and applications* (479 pp). New York: Wiley. ISBN 0-471-32188-5.

Youssef, M., et al. (2004). *Wireless network simulation in aircraft cabins* (pp. 2223–2226). In: IEEE Antennas and Propagation Society International Symposium. IEEE.

Floreon^{+}: A Web-Based Platform for Flood Prediction, Hydrologic Modelling and Dynamic Data Analysis

Vaclav Svatoň, Michal Podhoranyi, Radim Vavřík, Patrik Veteška, Daniela Szturcová, David Vojtek, Jan Martinovič and Vít Vondrák

Abstract The main goal of this article is to describe the overview of Floreon^{+} system, an online flood monitoring and prediction system, which was primarily developed for the Moravian-Silesian region in the Czech Republic. Moreover, the article specifies the basic processes, which are implemented for running automatic and on-demand simulations that utilize the High Performance Computing (HPC) infrastructure. The main purpose of hydrodynamic models in the disaster management context is to provide an accurate overview of hydrologic situation in a given river catchment. In the event of extreme weather conditions, such as unusually heavy rainfall, these models could provide valuable information about

V. Svatoň (✉) · M. Podhoranyi · R. Vavřík · P. Veteška · D. Szturcová · D. Vojtek · J. Martinovič · V. Vondrák
IT4Innovations, National Supercomputing Center, VSB-Technical University of Ostrava, 17. listopadu 15/2172, 70833 Ostrava, Czech Republic
e-mail: vaclav.svaton@vsb.cz

M. Podhoranyi
e-mail: michal.podhoranyi@vsb.cz

R. Vavřík
e-mail: radim.vavrik@vsb.cz

P. Veteška
e-mail: patrik.veteska@vsb.cz

D. Szturcová
e-mail: daniela.szturcova@vsb.cz

D. Vojtek
e-mail: david.vojtek@vsb.cz

J. Martinovič
e-mail: jan.martinovic@vsb.cz

V. Vondrák
e-mail: vit.vondrak@vsb.cz

D. Szturcová · D. Vojtek
Institute of Geoinformatics, Faculty of Mining and Geology, VSB-Technical University of Ostrava, 17. listopadu 15, 70833 Ostrava, Czech Republic

I. Ivan et al. (eds.), *Dynamics in GIscience*, Lecture Notes in Geoinformation and Cartography, DOI 10.1007/978-3-319-61297-3_30

imminent flood risk endangering a particular area. In the disaster management context, time plays a very significant role. Up to date and accurate results obtained in a short time can be very helpful. The availability of such results can be significantly improved by utilization of HPC resources and tools. The article describes the individual parts of the system in terms of data types, dynamic data processing, visualization, and the overall architecture.

Keywords Floreon^{+} · Hydromodelling · Geovisualization · High performance computing · Dynamic data

Introduction

Almost all large rivers in Central and Eastern Europe have experienced catastrophic flood events, e.g. the 1993 and 1995 flooding of the Rhine River, 1999 and 2002 Danube/Theiss Rivers, 1997 Oder River, 2001 Vistula River and 2002 Labe River. Each of these flood catastrophes brought damage worth several billions of euros; in some of the cases, as many as hundreds of people lost their lives (Halmo 2006). Floods, however, affect not only Central and Eastern Europe but also they represent a major problem in many regions all around the world (Knebl et al. 2005).

One of the directions contemporary world's science is taking is towards the modelling of flood catastrophes by means of available hydraulic/hydrologic modelling tools. Flood modelling, which has acquired crucial importance over the past years, is constantly enhancing its quality in connection with the development of information technologies (software, hardware). It has also considerably improved with the advent of geographic information systems, radar-based estimates using the Next Generation Radar (NEXRAD), high-resolution digital elevation models (DEMs), distributed hydrologic models and delivery systems on the Internet (Garrote and Bras 1995).

In practice hydrological models are usually coupled into platforms or systems, which are then used as a tool for flood prevention/flood control. These platforms provide similar functionality on different levels of complexity, therefore none of them carry out the process of predicting and modelling in the same way. According to provided information, flood modelling and monitoring platforms may be divided into two groups: (i) Platforms providing modelling information about flood events. Representative of the first group of platforms is eWaterCycle (Hut et al. 2016), which provides global modelling data about floods. (ii) Platforms offering information about monitoring of the current state. Such platforms mainly dispatch systems for coordinating different kinds of resources, preparing emergency plans and deploying experts and equipment. These kinds of platforms are based on exchanging information and data between them and national services (ERCC—Emergency Coordination Centre; EENA—European Emergency Number Association).

Nevertheless, the introduced Floreon+ system (Kuchar et al. 2016), which is a combination of both of the above-mentioned platform groups, is slightly different. The main objective of the Floreon+ project is to create a platform for integration and operation of monitoring, modelling, prediction and decision support for disaster management mainly in the Moravian-Silesian region. The central thematic area of the project is hydrologic modelling and prediction. The system focuses on acquisition and analysis of relevant data in real time and application of prediction algorithms with this data. The results are then used for decision support in disaster management processes by providing predicted discharge volumes on measuring stations and prediction and visualization of flood lakes in the landscape (Podhoranyi et al. 2016). Modularity of the Floreon+ system, which is developed for this science and research platform, allows for simple integration of different thematic areas, regions, and data. In addition to the flood modelling and simulation area, the Floreon+ system tackles other thematic areas—air and water pollution and environmental hazards and traffic situation. The results of these areas still focus on supporting the decision and planning disaster management processes.

Floreon+ system uses various types of static and dynamic data for operational running and therefore suitable database structure must be applied to ensure optimal and fast access to them. The database has to be prepared for storing big amount of continual data that are obtained from different geo-servers. The part of the Floreon+ system related to data and DB structures is very important for correct functionality of the entire system and thus this article tries to explain basic principles and processes inside the system database.

The major objective of the article is to present basic structure and data processing within the Floreon+ infrastructure, which covers many types of different data and DB structures. Main goal aims at heterogeneous spatial-temporal data (stored in PostgreSQL database) with a focus on describing the origin of data and the process that is optimal for storing data efficiently in a suitable form for the following spatial analysis and fast visualizations. A detailed description of the ways of publishing spatial-temporal database content in the Geoserver is the partial goal of the article that we have focused on as well.

Data and Study Area

This section provides a brief description of hydrological models used in the Floreon+ system and the structured data layer serving as a source for particular simulations.

Characteristics of Moravian-Silesian Region

The Moravian-Silesian region (see Fig. 1) is situated in the northeastern part of the Czech Republic with the Czech third largest City of Ostrava and the area of

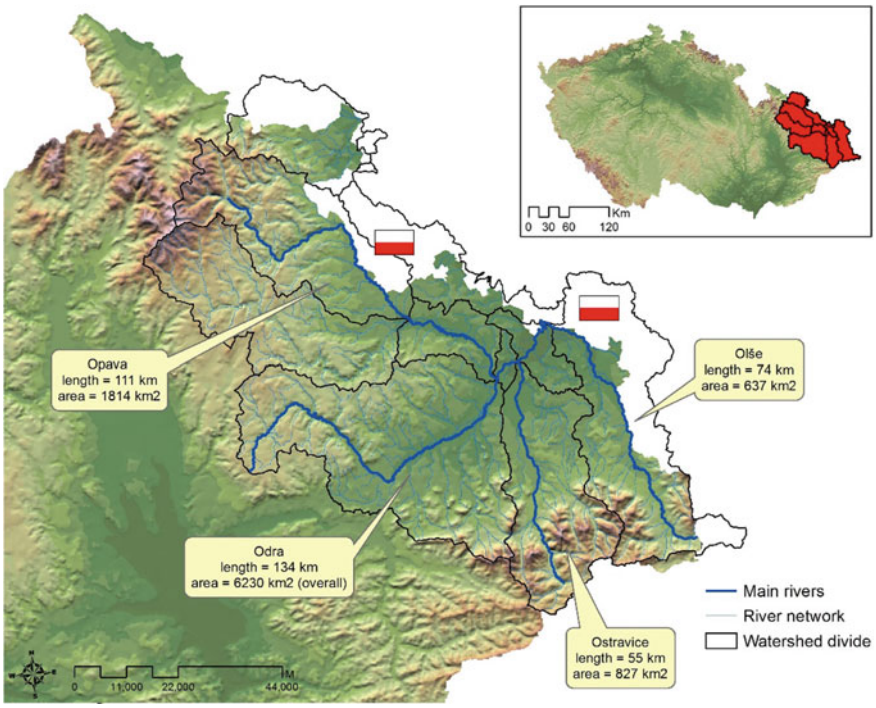

Fig. 1 Area of interest

5427 km^2. Approximately half of the area consists of farmland and another 35% is covered with forests. With its more than 1.25 million people and the average density of 240 people/km^2, the region is also home to a large number of companies.

From the hydrological point of view, the most of its area falls within the Oder River catchment. The area of the Czech part of the catchment is 6252 km^2 and is further divided into subbasins belonging to the Oder River itself (length of 134.32 km) and its largest tributaries—the Opava River (110.66 km) on the left side and Ostravice (54.79 km) and Olza rivers (73.10 km) on the right side.

The largest floods occurred on the 5th–16th July, 1997, when more than half of average annual precipitation was in the form of rain. 536 cities and villages in the Czech Republic were affected, 50 people died and 80 thousand people were evacuated. The material damage amounted to 63 billion Czech crowns.

Floreon+ System Hydrologic Models

There are two main categories of numerical hydrologic models currently used in the Floreon+ system. The first category consists of rainfall-runoff (R-R) models which allow simulating transformation of predicted precipitations from given areas into discharges in corresponding river outlets. The outputs provided by R-R models form inputs for the second category of models—hydrodynamic (HD) models. HD models enable hydrodynamic simulations of river surface and thus visualization of inundated areas in case of flood events.

HEC-HMS (Hydrologic Engineering Center—Hydrologic Modeling System)

This R-R model was originally developed by the U.S. Army in the 60s. At the beginning of 90s an independent division took over the development (HEC-HMS 2010).

The modelled catchment is represented by basin model consisting of particular elements—subbasins, channels, junctions, and sinks. Each element typically has several parameters for detailed specification of its properties and behaviour.

Several methods for each of the following categories are available: infiltration loss simulation, transformation of excess precipitation into surface runoff, representation of baseflow contributions to subbasin outflow, simulation of flow in open channels and water impoundments representation.

The schematizations and parameters are stored in text files, meteorological data and resulting hydrographs are stored in a proprietary binary format. For further Floreon+ system processing, hydrographs are exported to a CSV file using the HEC-DSSVue utility.

Math1D

Another R-R model integrated into the Floreon+ system is our in-house model internally called Math1D (Kubíček and Kozubek 2008).

It is a numerical semi-distributed R-R model that implements the unit hydrograph and SCS curve number methods and accumulates water contribution of interflow modelled by convolution integral and simplified differential equation and contribution of surface runoff using non-stationary linear and non-linear isochrones. This model uses modified schematizations exported from HEC-HMS model into XML files. The simulated hydrographs are directly stored as output CSV files.

HEC-RAS 4.1 (Hydrologic Engineering Center–River Analysis System)

HEC-RAS 4.1 is an HD model for 1D steady and unsteady flow simulations representing water movements (HEC-RAS 2010). It is based on 1D Saint-Venant equations derived from the Navier-Stokes equations. Along with the precise topographic and hydraulic data, discharge volumes for river profiles form inputs to the model. The model offers an evolution of discharge, water surface elevation, current velocity, and other statistical data.

Floreon$^+$ System Data Layer

Digital elevation models and results from HD model are stored in PostgreSQL geographical database running on the Floreon$^+$ geo-server machine. Besides this, most of the parameters of the models, their inputs and outputs, and the system management data are stored in the complex relational database structure based on Microsoft SQL.

The stored data can be divided into these two logical groups—the static and dynamic ones. The former includes all the topographic data and catchments characteristics, the latter consists of the data for monitoring, and prediction, which are continuously changing.

Topographic Data

In the Floreon$^+$ system, two types of digital elevation models differing by the data source technology are used.

The first type of DEM is created using 2007 LIDAR data from a filtered point field (cloud points) of high density (19 points per m^2). The scanning was performed from the elevation of 300 m above ground level with the resolution of 16 Mpx (4080 $\times$ 4076 px). The point field gave rise to two DEM structures, namely a raster and its triangulated irregular network (TIN) equivalent. The resolution of the raster and TIN is 0.2 m, and therefore it can be considered as very accurate.

The second type of DEM was created using a photogrammetry method in 2010. The resolution of the obtained raster is 10 m which is sufficient to capture the detail of a surface.

Catchment Parameters

Each catchment is characterised by many parameters describing particular components of the schematization. These parameters might be classified as geometric and hydrologic.

From the entered measured and interpolated cross sections, the width, depth, bank slope, channel slope, and other geometric parameters are derived.

The group of the hydrologic parameters describing attributes of flow paths includes, for example Manning's friction coefficients, base flow, curve number, land use, landcover, slope, and others.

Data for Monitoring

The data for simulation and monitoring purposes are currently provided by the Povodi Odry (the Oder River basin board) state enterprise in the 10-minute interval. Until the May 2014, the data were obtained from the Czech Hydrometeorological Institute (CHMI). The data package contains measured precipitation rates, measured water levels, measured discharge volumes, and temperatures obtained from particular hydrologic gauges.

Data for Prediction

Weather forecast data for the Floreon+ system is currently obtained from the Medard project service (ICS 2016), which is based on the Weather Research & Forecasting model. The Floreon+ system is designed to process data from multiple sources. Earlier the forecast data was also obtained from the Aladin project service (Degrauwe et al. 2016). The forecasts are composed of the predicted precipitation rates, temperatures, wind velocities, and directions. Every 6 h, the new data package containing an updated forecast for the next 72 h is available. In the first phase, the new package is downloaded by the Floreon+ system using the weather forecast downloader. This routine then launches the Floreon+ web service designed for processing the downloaded data. The process is finished by storing the new values to the Floreon+ database structure. Since our simulations provide predictions for 48 h, we do not use the second 24-hour interval of the weather forecast, which is the most inaccurate by nature.

Simulations and Dynamic Data Processing

The Floreon$^+$ system can be roughly divided into two main parts in terms of dynamic data processing (see Fig. 2). The first system part deals with automatic simulation execution. Its main task is to execute rainfall-runoff models and a hydrodynamic model for the current time and current data on hourly basis. The second part consists of user initiated simulations or computations also called on-demand simulations. These on-demand simulations are represented by modules designed specifically for HPC cluster execution (Buyya 1999). Due to the user-defined parameters, the user initiated simulations can be more computationally demanding than automated simulations, therefore they are executed directly on the HPC cluster. Thanks to the modularity of the system and properly designed architecture, which will be discussed in the following chapter, the system allows for easy integration of additional HPC modules. The Floreon$^+$ system already contains

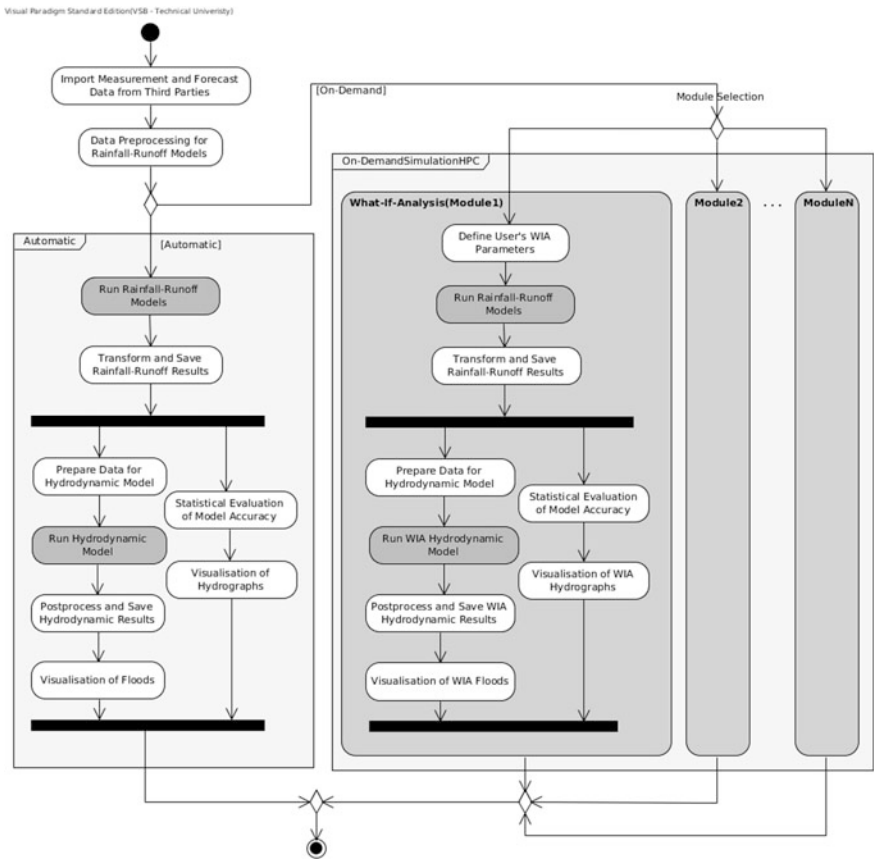

Fig. 2 Dynamic data processing

several modules, however, because the focus of this paper deals primarily with hydrology, only the module for user-defined hydrological What-if-Analysis (WIA) will be mentioned.

Automatic Simulations

Every hour, an automatic process, which includes running of rainfall-runoff simulations with hydrodynamics, is triggered on the HPC infrastructure. In this process, the data from the relational database is loaded and preprocessed according to the selected model and subsequently the simulation is run. When the calculation execution is finished, the obtained results are processed and stored in the relational database. In the next step, the process is divided into two parallel runs. Within one run, on the occasion of the user needing to visualize results of rainfall-runoff simulation, statistics evaluations of results accuracy are primarily calculated and visualized in the form of hydrographs. At the same time, hydrodynamic simulation, which pre-processes values obtained for the hydrodynamic model designed for calculation, runs and run it. Model outputs are processed and stored in the spatial-temporal database. Process finishing the possibility of visualizing the results of hydrodynamic simulation and displays it in the form of flood area.

On-Demand Simulations

Under the on-demand hydrologic simulations, the framework for running on-demand What-If Analysis (WIA) is created to simulate crisis situations. This also includes What-if hydrologic simulations. Through the web interface, users can create their own hydrologic What-if simulation running on this framework. They must choose the basic settings from the menu having the option to select river basin, schematization, and rainfall-runoff model for which the rainfall-runoff simulation and hydrodynamic model will be calculated. The framework allows the user to specify precipitation in selected precipitation stations and selected time. This type of simulation also allows the user to edit the default parameters of subbasins and channels. The next step is to run the simulation execution. Execution of What-if simulation is processed on an HPC cluster. As the result from the rainfall-runoff model is used as an input for the hydrodynamic model, the system allows the users to view the hydrographs as soon as they are available, independently of the hydrodynamic computation. As soon as the hydrodynamic model computation is completed and the result values are stored within the spatial-temporal database, the users can view the simulated flood layer within the map interface together with the hydrographs.

Postprocessing

The goal of postprocessing is to transform the results of simulation of hydrodynamic modelling into a form suitable for visualization provided by Geoserver. The result of the hydrodynamic model consists of data in SDF format and metadata. These data are considered as an input for postprocessing. The polygons for floods are calculated upon this data and stored within the PostgreSQL/PostGIS database. An important part of the postprocessing is the archiving functionality for the hydrodynamic results which vary according to the type of simulation execution.

In the case of automatic simulations, the flood prediction is calculated for the next 48 h with the last 5 h used to calibrate the model. Thus in the next hour, when another simulation with 48-hour prediction is executed, we will obtain new result values for the same 47 h (for the same time) as in the last simulation run. To archive the prediction data more efficiently considering the available storage space, only the latest result values for a specific time are archived. However, this does not apply in the case of some significant event. When the flood stage level on some measuring station exceeds the standard value, the system stores the predicted values from every simulation to be used for subsequent analysis or model calibration.

In the case of on-demand simulation, the prediction interval is part of the user's input parameters, therefore the system stores the predicted values for every simulation run.

Visualization

Publication of results of hydrological modelling via web interface (see Fig. 3) was guided mainly by an effort to visualize the current state and calculated predictions as fast as possible.

The methods used for the visualization were derived from the need to:

- show the actual state for the current time (measured data and 48-h prediction),
- visualize the different types of data (hydrographs for the rainfall-runoff models, flood lakes for the hydrodynamic models),
- be able to view the data from the past.

The above mentioned requirements were combined into the time axis widget, a part of Floreon^{+} GUI (see Fig. 3), which is the key element of the application. The users can easily change the current time within the map interface to browse the information for the selected area, no matter if it is (i) prediction of the future, (ii) the current situation based on the real data, or (iii) simulation of a situation in the past.

The time selected on the time axis by the users is passed as an input parameter for the selector of formerly prepared simulation outputs. Geoserver publishes layers corresponding to the selected parameters using the time-WMS service.

Fig. 3 Floreon+ system web interface

PostgreSQL/PostGIS is used as a storage for the precomputed layers later to be displayed within the map interface of the Floreon+ system.

Architecture of the Floreon+ System

The Floreon+ system architecture uses the high-performance computing infrastructure at IT4Innovations National Supercomputing Center in Ostrava, Czech Republic. High-performance computing (HPC), in other words, means the use of parallel processing for running advanced application programs efficiently, reliably, and quickly. The most common users of HPC systems (Younge and Andrew 2011) are scientific researchers, engineers, and academic institutions. IT4Innovations operates 2 supercomputers, namely Salomon (24,192 cores, 129 TB RAM, 2 Pflop/s) and Anselm (3344 cores, 15 TB RAM, 94 Tflop/s). The supercomputers are available to the academic community within the Czech Republic and Europe and industrial community worldwide. These two HPC clusters are currently available to use within the Floreon+ system to run on-demand simulations. The architecture of the Floreon+ system can be seen in Fig. 4.

There was need for an architecture, which would allow users to run complex and computationally demanding calculations on a supercomputer directly from the user interface of a client application without the necessity to connect directly to the HPC cluster and manage the jobs from the command line interface of the HPC scheduler. Therefore, we have developed our in-house application framework called HPC as a Service Middleware. This mid-layer, in software terminology also known as middleware, manages and provides information about submitted and running jobs and their data between a client application and the HPC infrastructure. This middleware

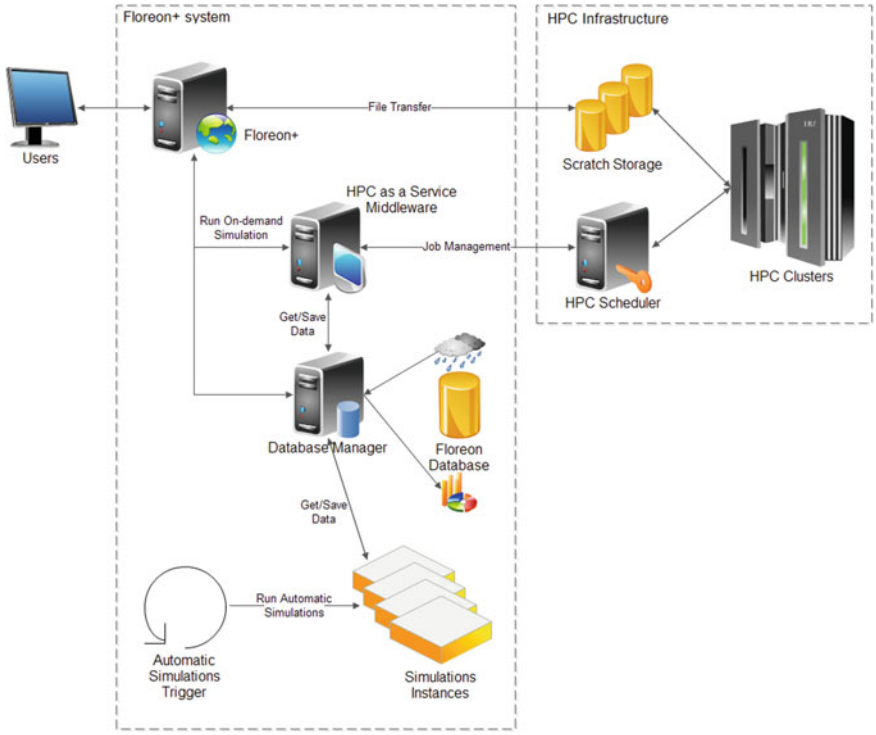

Fig. 4 Floreon^{+} system architecture

is able to submit the required computation or simulation on the HPC infrastructure, monitor the progress, and notify the user in case of need.

Middleware features

- Providing HPC capabilities as a service to client applications and their users
- Unified interface for different operating systems and schedulers
- Authentication and authorization to provided functions
- Monitoring and reporting of executed jobs and their progress
- Current information about the state of the cluster

Before running the job (What-If simulation), the users usually need to upload their input data to the application disk storage. After the job setting configuration has been chosen, specified by the cluster configuration and required computational resources, the newly created job is sent to the cluster for processing. Before the job's actual start, the input data are copied from the application storage to the HPC cluster disk storage (Scratch storage). When the copied input data are completely available on the cluster storage, the job is submitted to the HPC scheduler queue to be executed. The middleware also calls the HPC scheduler at regular intervals to acquire the status of all submitted jobs and feeds this information to the client

application. The above mentioned job execution workflow is part of the internal logic and therefore fully automated. From the user's perspective, the required steps consist of input parameter selection for the What-If simulation and simulation start only.

Conclusion

In this article, we have presented Floreon+ system, an online flood monitoring and prediction system. The main aim of the Floreon+ project is to provide detailed information about the possibility of incoming flood and its extent. In the future, Floreon+ system should estimate the possible property damage before it happens, provide recommendations about flood measures, and online decision support for emergency committees to minimize the number of casualties and property damage in case of extreme weather events.

As the Floreon+ system is very extensive, this article focuses mainly on the area of hydrology and describes the processes necessary for dynamic data processing, all the way from the initial raw data import to the visualization of floods via the map interface. The system utilizes the HPC infrastructure at IT4Innovations and enables the users to execute user-defined hydrologic What-If analyses directly on the HPC cluster. Due to the system's universally designed architecture, both in terms of infrastructure and different methods of visualization, the Floreon+ system enables an easy integration of additional modules that do not necessarily need to address the area of hydrologic modelling.

Future Work

Given that the Floreon+ system already consolidates the data from several areas of interest (hydrology, traffic modelling, mobility) the future work is mainly focused on integration of new and more accurate models and on the interconnection of these seemingly different areas of interest. We have already experimented with several use cases that are currently in the process of integration into the Floreon+ system. For example, one of these use cases is focused on traffic modelling during floods and finding alternate routes due to the traffic bottlenecks or flooded roads. Another use case is, for example, focused on analysing the arrival times of firefighting vehicles during floods, thus taking the road closures into account.

Acknowledgements This work was supported by The Ministry of Education, Youth and Sports from the National Programme of Sustainability (NPU II) project "IT4 Innovations excellence in science—LQ1602" and from the Large Infrastructures for Research, Experimental Development and Innovations project "IT4Innovations National Supercomputing Center—LM2015070" and from the SGS 2016 project "Flood and pollution modelling II—SP2016/150".

References

Buyya, R. (1999). *High performance cluster computing: Architectures and systems* (Vol. 1, p. 0130137847). Upper Saddle River, NJ, USA: Prentice Hall.

CPD-68. (2010). HEC-RAS river analysis system user's manual version 4.1. Davis, CA: U.S. Army Corps of Engineers Institute for Water Resources Hydrologic Engineering Center.

CPD-74A. (2010). Hydrologic modeling system HEC-HMS user's manual. Davis, CA: U.S. Army Corps of Engineers Hydrologic Engineering Center.

Degrauwe, D., Seity, Y., Bouyssel, F., & Termonia, P. (2016). Generalization and application of the flux-conservative thermodynamic equations in the AROME model of the ALADIN system. *Geoscientific Model Development*.

Garrote, L., & Bras, R. L. (1995). A distributed model for real-time flood forecasting using digital elevation models. *Journal of Hydrology, 167*(1–4), 279–306.

Halmo, N. (2006). *Flood protection program of Slovak Republic*. In International Conference of Flood Protection. High Tatras: Slovakia, December 4–7, 2006.

Hut, R., Drost, N., van Meersbergen, M., Sutanudjaja, E., Bierkens, M., & van de Giesen, N. (2016). eWaterCycle: A hyper-resolution global hydrological model for river discharge forecasts made from open source pre-existing components, Geoscientific Model Development. doi:10.5194/gmd-2016-225. (in Review).

Institute of Computer Science (ICS). (2016). *The Czech Academy of Sciences*. http://www.medard-online.cz, December 2016.

Knebl, M. R., Yang, Z.-L., Hutchinson, K., & Maidment, D. R. (2005). Regional scale flood modeling using NEXRAD rainfall, GIS, and HEC-HMS/RAS: A case study for the San Antonio River Basin Summer 2002 storm event. *Journal of Environmental Management, 75,* 325–336.

Kubíček, P., & Kozubek, T. (2008). *Mathematic-analytical solutions of the flood wave and its use in practice (in Czech)* (p. 150). Ostrava: VŠB-TU Ostrava.

Kuchar, S., Podhoranyi, M., Vavrik, R., & Portero, A. (2016). Dynamic computing resource allocation in online flood monitoring and prediction. *IOP Conference Series: Earth and Environmental Science, 39* (1).

Podhoranyi, M., Kuchar, S., &Portero, A. (2016). Flood evolution assessment and monitoring using hydrological modelling techniques: Analysis of the inundation areas at a regional scale. *IOP Conference Series: Earth and Environmental Science, 39*(1).

Younge, A. J., et al. (2011). *Analysis of virtualization technologies for high performance computing environments*. International Conference on Cloud Computing (CLOUD). IEEE.

Author Index

I. Ivan et al. (eds.), *Dynamics in GIscience*, Lecture Notes in Geoinformation and Cartography, DOI 10.1007/978-3-319-61297-3